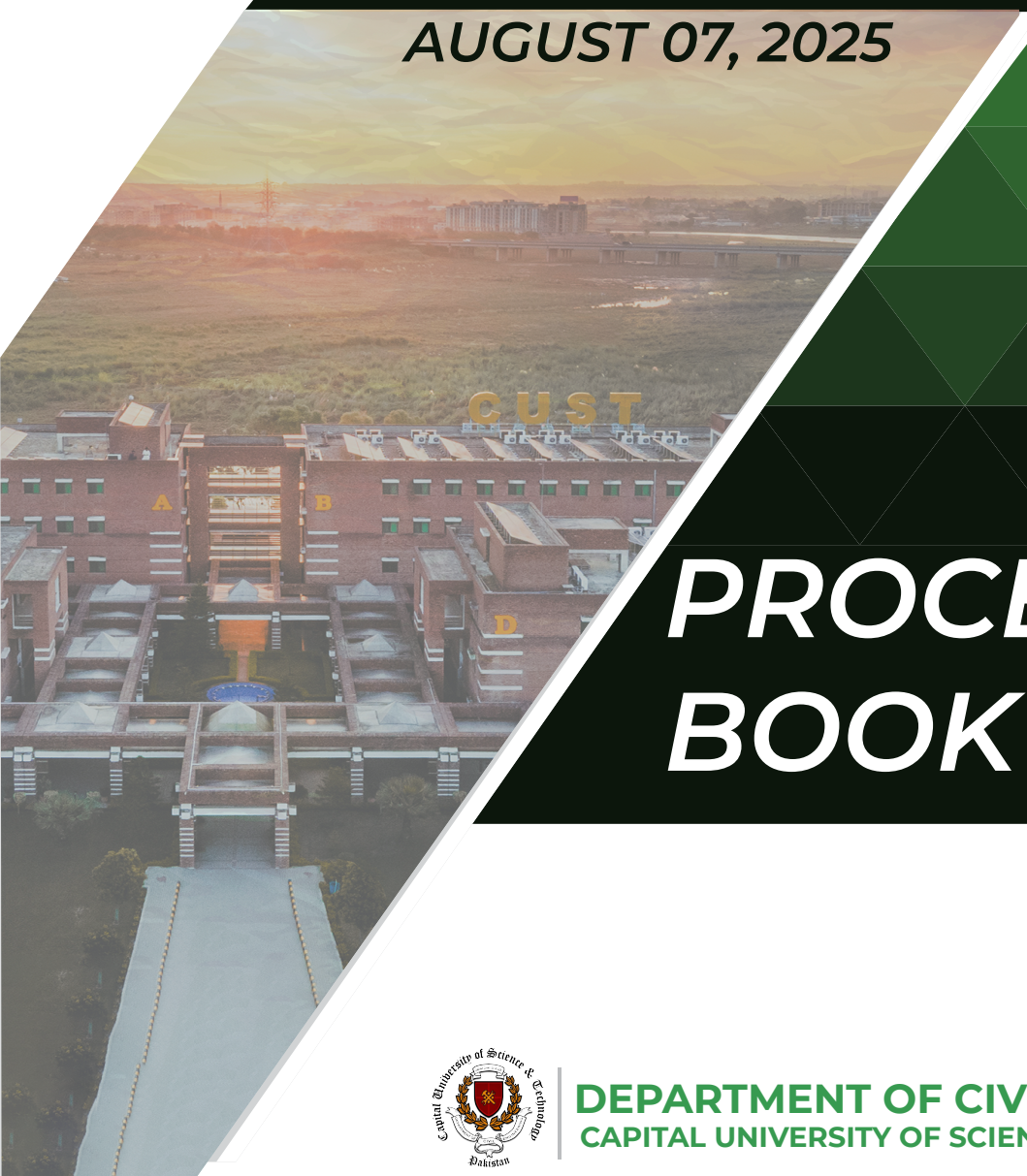
7TH CONFERENCE ON SUSTAINABILITY IN CIVIL ENGINEERING

CSCE'25

(AN INTERNATIONAL CONFERENCE)

AUGUST 07, 2025



ISBN: 978-969-23344-6-4

PROCEEDINGS BOOK

EDITORS:

DR. MAJID ALI
ENGR. TALHA BIN TAHIR
ENGR. M. WAQAS MALIK

DEPARTMENT OF CIVIL ENGINEERING
CAPITAL UNIVERSITY OF SCIENCE AND TECHNOLOGY

Publication Note

This book has been produced from files received electronically by the individual authors. The publisher makes no representation, express or implied, with regard to accuracy of the information contained in this book and cannot accept any legal responsibility or liability for any errors or omissions that may have been made. All titles published by 6th Conference on Sustainability in Civil Engineering and Capital University of Science and Technology (CUST), Islamabad, Pakistan publishers are under copyright protection said copyrights being the property of their respective holders. All Rights Reserved. No part of this book may be reproduced or transmitted in any form or by any means, graphic, electronic or mechanical, including photocopying, recording, taping or by any information storage or retrieval system, without the permission in writing from the publisher.

Published By

Department of Civil Engineering

Capital University of Science and Technology, Islamabad, Pakistan

www.csce.cust.edu.pk

www.cust.edu.pk

Foreword

Welcome to the CSCE 2025, 7th Conference on Sustainability in Civil Engineering (CSCE'25 – An international Conference) is held by Department of Civil Engineering, Capital University of Science and Technology, Islamabad, Pakistan. The main focus of CSCE'25 is to highlight sustainability related to the field of civil engineering. It aims to provide a platform for civil engineers from academia as well as industry to share their practical experiences and different research findings in their relevant specializations. We hope all the participants experience a remarkable opportunity for the academic and industrial communities to address new challenges, share solutions and discuss future research directions. The conference accommodates several parallel sessions of different specialties, where the researchers and engineers interact and enhance their understanding of sustainability in the civil engineering dynamics.

This year, we have nine wonderful and renowned keynote speakers for this edition of CSCE. We have received 109 manuscripts from different countries around the world including USA, Canada, UK, Italy, Germany, Australia, Estonia, China, Japan, South Korea, Malaysia, UAE, KSA, and Pakistan. All papers have under gone a comprehensive and critical double-blind review process. The review committee is comprised of 43 PhDs serving in industry and academia of USA, UK, Ireland, Australia, New Zealand, Norway, France, Poland, Turkey, China, Hong Kong, Malaysia, Singapore, UAE, Oman, Bahrain, Morocco, KSA, and Pakistan. After the screening and review process, 46 papers are to be presented in the conference.

We are grateful to all the reviewers and keynote speakers who have dedicated their precious time to share their expertise and experience. With this opportunity, we would also like to express our gratitude to everyone, especially all the faculty and staff at the Capital University of Science and Technology for their great support and participation. In this regard, the participation and cooperation of all authors, presenters and participants are also acknowledged, without whom this conference would not have been possible. Last but not least, an appreciation to our advising and organizing committees whose hard work and dedication has made this day possible.

Dr. Majid Ali

Convener

CSCE'25



Technical Committee

A. INTERNATIONAL

Dr. Furqan Qamar	WSP, UK
Dr. Mohsin Shehzad	WSP, UK
Dr. Javeraia Mehwish	Thurrock Council, UK
Dr. Sohaib Naseer	Stantec, UK
Dr. Tom Tang	Dexion, New Zealand
Dr. Muhammad Shakeel	AECOM, Hong Kong
Dr. Jincheng Liu	Aurecon, Singapore
Dr. Munir Ahmed	DAR, KSA
Dr. Khanzaib Jadoon	Etqan Elbinaa, KSA
Dr. Robert Evans	Nottingham Trent University, UK
Dr. Akinniyi Damilola Bashir	Coventry University, UK
Dr. Salman Azhar	Auburn University, USA
Dr. Hammad Anis Khan	University of Sydney, Australia
Dr. Mizan Ahmed	Curtin University, Australia
Dr. Wajiha Shehzad	Massey University, New Zealand
Dr. Chandana Siriwardana	Massey University, New Zealand

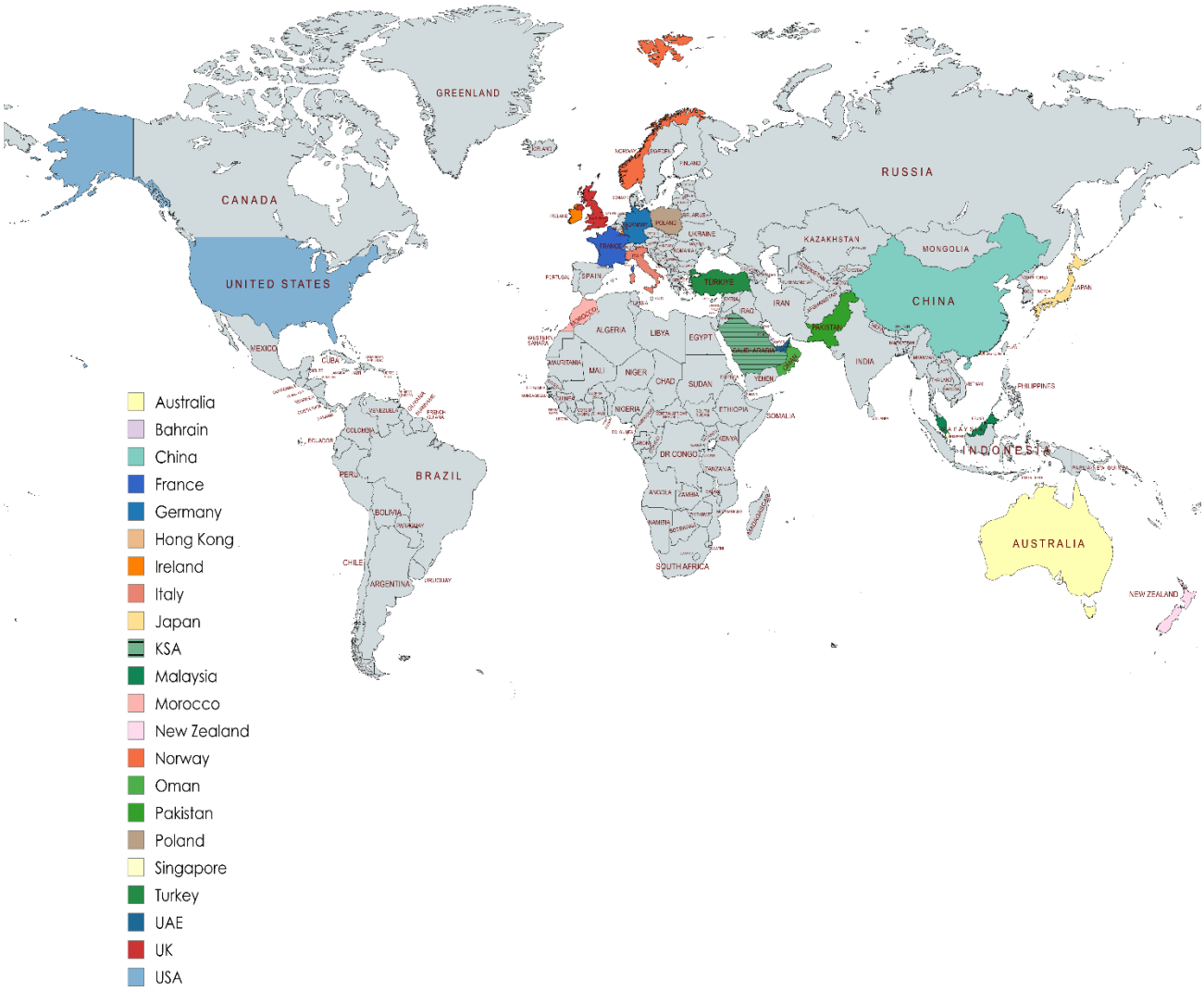
Dr. Mehran Khan	University College Dublin, Ireland
Dr. Teoman Ozer	ITU Academy, Turkey
Dr. George Wardeh	Cergy-Pontoise University, France
Dr. Afaq Ahmed	Oslo Metropolitan University, Norway
Dr. Piotr Smarzewski	Military University of Technology, Poland
Dr. Ghazanfar Ali Anwar	The Hong Kong Polytechnic University, Hong Kong
Dr. Anas Bin Ibrahim	MARA University of Technology, Malaysia
Dr. Noor Aina Misnon	Universiti Pertahanan Nasional, Malaysia
Dr. Faridah Hanim Khairuddin	University Pertahanan Nasional, Malaysia
Dr. Hammad Salahuddin	Shenzhen University, China
Dr. Mohsin Usman Qureshi	Sohar University, Oman
Dr. Umar Farooq	Islamic University of Madinah, KSA
Dr. Tayyab Naqash	Islamic University of Madinah, KSA
Dr. Khwaja Mateen Mazhar	King Fahad Uni. of Petroleum and Minerals, KSA
Dr. Mubashir Aziz	King Fahad Uni. of Petroleum and Minerals, KSA
Dr. Uneb Gazder	University of Bahrain, Bahrain
Dr. Ahsen Maqsoom	Mohammed VI Polytechnic University, Morocco
Dr. Waris Ali Khan	The British University in Dubai, UAE

B. NATIONAL

Dr. Irfan Yousuf	World Bank Group, Islamabad, Pakistan
Dr. Khursheed Ahmed	NUST, Islamabad, Pakistan
Dr. Ali Ejaz	NUST, MCE Risalpur, Pakistan
Dr. Izza Anwer	UET, Lahore, Pakistan
Dr. Naeem Ejaz	UET, Taxila, Pakistan
Dr. Khan Shahzada	UET, Peshawar, Pakistan
Dr. Shiraz Ahmad	GIKI, Swabi, Pakistan
Dr. Mudasser Muneer Khan	BZU, Multan, Pakistan
Dr. Anwar Khitab	MUST, AJK, Pakistan
Dr. Asim Farooq	IAST, Haripur, Pakistan

Contribution from World

Technical Committee Members



CSCE Industrial Partners for 7th Edition



JS Architectural & Engineering Consultants



Engineering & Design Consultants



City Engineering Consultants



MKAI Climate Consulting



ZAC Engineers



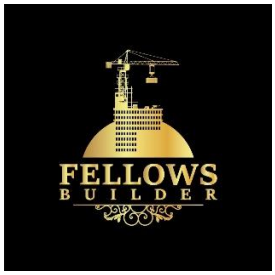
MARK Associates



ENCON (SMC-Pvt) Ltd



Design and Consultancy Services



Fellows Builders

Advisory Committee



Dr. M. Mansoor Ahmed
(Vice-Chancellor CUST Islamabad)
Patron



Dr. Imtiaz Ahmed Taj
(Dean Faculty of Engineering)
General Advisor



Dr. Ishtiaq Hassan
(Professor, Civil Engineering Department)
Principal Advisor

Organizing Committee



Dr. Majid Ali
Convener



Engr. Talha Bin Tahir
Secretary



Engr. M. Waqas Malik
Member



Engr. M. Yahya
Member

Conference Tracks

Track - 01: Green Construction Materials and Structures

- Construction Materials
- Composite Materials
- Modern Materials
- Structural Material Behavior
- Structural Analysis
- Structural Design
- Earthquake Engineering
- Engineering Dynamics

Track- 02: Construction and Project Management for Sustainable Developments

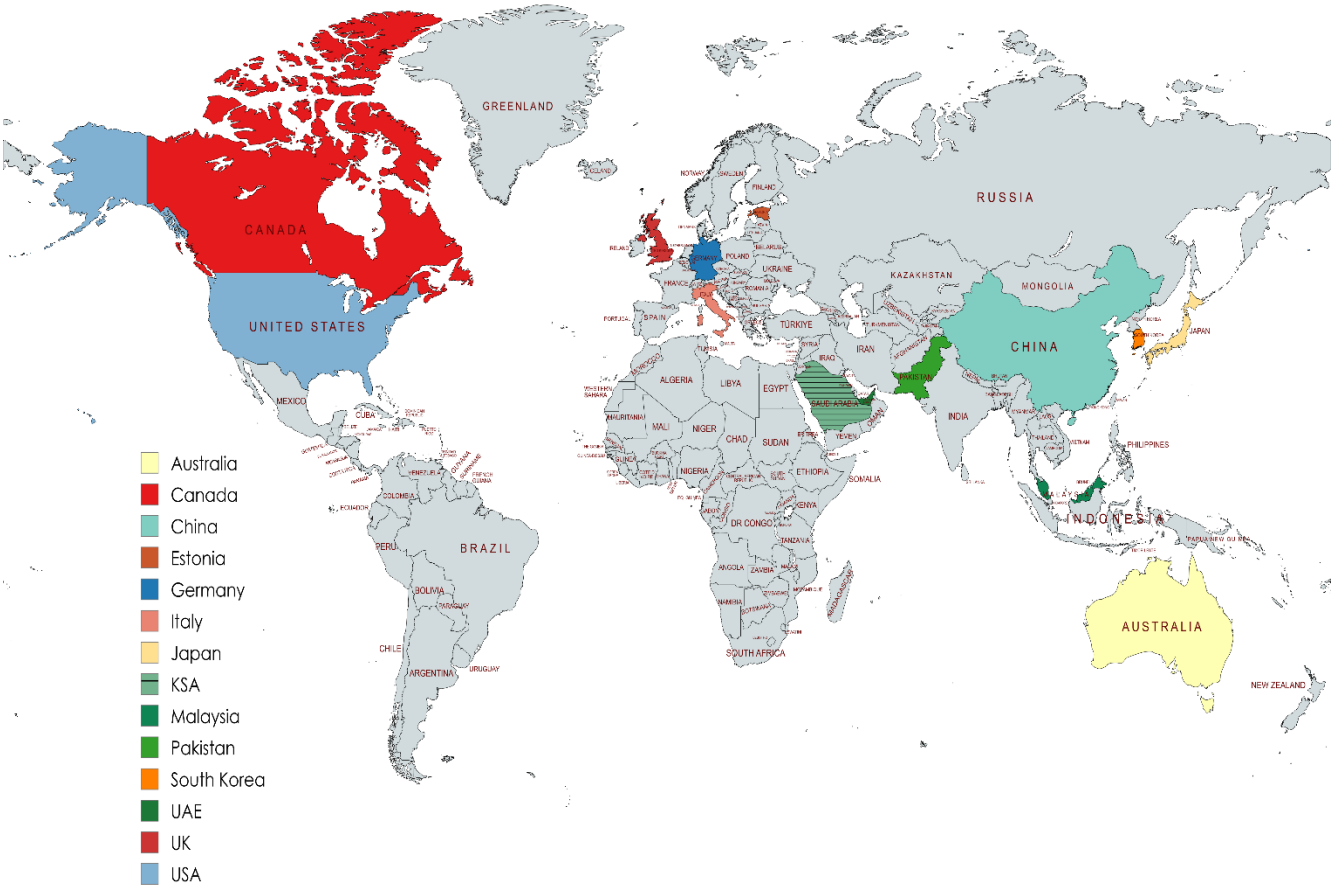
- Building Information Modelling (BIM)
- Project Management for Sustainable Development
- Sustainability in Construction Projects
- Construction Safety
- Construction Contracts
- Smart and Sustainable Construction
- Construction Waste Management
- IT applications in Construction

Track- 03: Resilient Infrastructure and Environment

- Environmental Engineering
- Environmental Sciences
- Irrigation Engineering
- Water Resource Engineering. & Management
- Highway & Traffic Engineering
- Urban & Transportation Planning
- Geotechnical Engineering
- Geological Engineering

Contribution from World

Papers Received



Keynote Speakers

Dr. Khairunisa Binti Muthusamy *Universiti Malaysia Pahang, Malaysia*	*Eco-Innovation in Construction: Harnessing Industrial Waste for Greener Concrete*
Dr. Inam Khan *Building & Construction Research & Consultancy (BCRC), Australia*	*Shaping Future Sustainability through Durability Modelling and Low Carbon Concrete*
Dr. Libo Yan *Technische Universität Braunschweig & Fraunhofer WKI, Germany*	*Advancing Sustainability through Timber, Natural Fibres, and Recycled Materials in Concrete*
Dr. Wen Si *University College Dublin, Ireland*	*Rheology and Printing Parameters in 3D-Printed Concrete: A Review Toward Improved Printability and Structural Performance*
Dr. Usama Zafar *Saitama University, Japan*	*Rethinking Soil–Pile Interaction: The Critical Role of Nonlinearity Under Dynamic Vertical Loading.*
Dr. Mohsin Usman Qureshi *Sohar University, Oman*	*Sustainable Industrial By-product Utilization in Civil Engineering Applications*
Dr. Paul Beetham *Nottingham Trent University, United Kingdom*	*Lessons from UK Research and Practice in Sustainable Ground Engineering*
Dr. Massimo Latour *University of Salerno, Italy*	*Sustainability as a Catalyst for Resilience: Insights from Recent European Research Projects*
Dr. Harry Lee *Texas A&M University, United States of America*	*Double-diffusive Salt Fingers in the Sea and its Large-scale Influence on Local Climate*

Contribution from World

Keynote Speakers

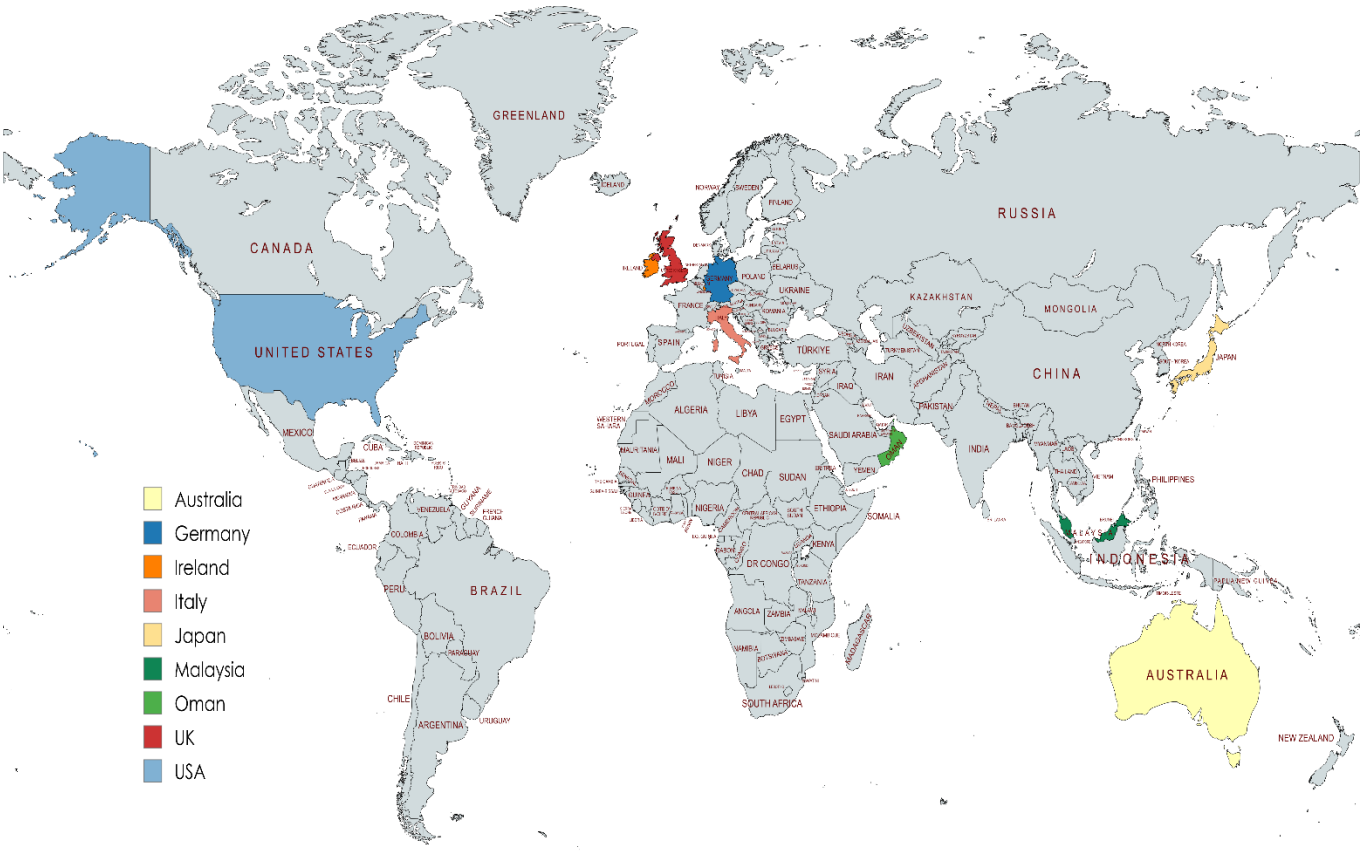


TABLE OF CONTENTS

PAPER ID	TITLE	PAGE NO.
PAPER ID. 25-102:	Sustainable Self-Compacting Concrete Incorporating Wheat Straw Ash and Fly Ash as Cement Replacements Farah Naz, Umer Shahzad, Shiraz Baloch	01
PAPER ID. 25-103:	Enhancing Concrete Sustainability: Natural Fibre Reinforcement for Shrinkage Crack Mitigation in Concrete Structures Muhammad Zain Sajid, Faisal Mateen	09
PAPER ID. 25-110:	Effect of Curing Method on Compressive Strength of Mortar Containing Tin Tailing as Fine Aggregate Replacement Norasyimah Ahmad, Khairunisa Muthusamy, Nor Rashidah Bahar	15
PAPER ID. 25-111:	Development and Performance of Papercrete as an Eco-Friendly Construction Material Moiz Ali Haider, Subhan Shafique, Muhammad Zohaib Asim	23
PAPER ID. 25-112:	Recycled Nylon Fibers For Crack Control in High Strength Concrete- A Use Case in Powerhouse Umar Zakria, Riaz Ul Haq	29
PAPER ID. 25-118:	Fiber Reinforcement For Drying Shrinkage Mitigation in Concrete: A Comprehensive Review Abu Bakar Naeem, Syed Ilyas Ali Shah	37
PAPER ID. 25-120:	An Overview on the Performance of Steel Fiber Reinforced Composites in Restraining Concrete Plastic Shrinkage Crack in Slab Abu Bakar, Hamza Khan	45
PAPER ID. 25-121:	Effectiveness of Nylon Fibers in Controlling Shrinkage Cracking in Concrete Pavements Abdul Wadood, Raja Arsalan	51
PAPER ID. 25-125:	Enhancing Flexural Strength in Concrete Oneway Slabs of Building Through Cotton Fiber Reinforcement Abu Bakar Naeem, Syed Ilyas Ali Shah	56
PAPER ID. 25-126:	Enhancing Crack Flexural Resistance in Hydraulic Structures Through Nylon Fiber Reinforced Concrete Umar Zakria, Khurram Munir	63
PAPER ID. 25-127:	Experimental Investigation on The Flexural Behavior of Steel Fiber in Concrete Usman Khalid, Naveed Irshad	71
PAPER ID. 25-128:	Comparative Study of Nylon Fiber Reinforced Concrete with PCC For Compressive Strength and Workability Muhammad Mursaleen, Ameer Turab	78
PAPER ID. 25-133:	Enhancing Tensile Performance of Concrete Using Steel Fiber Reinforcement: An Experimental Study Awais Sikandar, Faheem Ahmad Gul	85

PAPER ID	TITLE	PAGE NO.
PAPER ID. 25-134:	Experimental Evaluation of Flexural Behavior in Concrete Beams Reinforced with Waste Human Hair Fibers Jawad Nasar, Adeer Khan	90
PAPER ID. 25-135:	Cotton Fibers For Improved Concrete Tensile Strength and Crack Resistance in Slabs Mobeen Anwar, Sadia Sajid Khan	98
PAPER ID. 25-136:	Fiber-Reinforced Concrete For Crack Resistance: A Review Study Usman Khalid, Emmad Cheema	105
PAPER ID. 25-137:	An Overview of the Effects of Steel Fiber Reinforced Composites on Flexural Cracking in Concrete Awais Sikandar, Faheem Ahmad Gul	113
PAPER ID. 25-139:	A Review of Mechanical Performance and Sustainability of Nylon Fiber in Concrete Beam Reinforcement Qazi Muhammad Tariq, Blawal Hasan	118
PAPER ID. 25-140:	Enhancing the Flexural Strength of Concrete Beams Using Nylon Fibers as Sustainable Reinforcement Qazi Muhammad Tariq, Blawal Hasan	124
PAPER ID. 25-144:	Performance Evaluation and Application Potential of Nylon Fibers in Concrete Slab -A Review Usama Akhter, Hamdan Ullah	132
PAPER ID. 25-147:	Durability of Geopolymer Concrete with Recycled Sand in Acidic and Marine Conditions Shahzadi Irum, Faisal Shabbir, Hammad Salahuddin	139
PAPER ID. 25-149:	Experimental Study on Strength and Workability of Sustainable Concrete Incorporating Cotton Fibers and Marble Waste Muhammad Adnan Hanif, Ali Ejaz	146
PAPER ID. 25-150:	Compressive Strength of Standard Cylinders, Split Tensile Strength of Prestressed Cores, and Microstructural Analysis of Polypropylene Fiber Reinforced Concrete Mohammad Zulqarnain, Muhammad Usman Rashid, Muhammad Awais	151
PAPER ID. 25-151:	Experimental Study on the Performance of Date Palm Surface Fiber Reinforced Concrete Under Acidic Condition Asad Kareem, Syed Saqib Mehboob	159
PAPER ID. 25-154:	A Review on Optimizing Sustainable Crack Control in Slabs Using Cotton Fiber Composites Mobeen Anwar, Sadia Sajid Khan	167
PAPER ID. 25-155:	Mitigating Flexural Cracks in Concrete Beams Using Diverse Fibers: A Review Jawad Nasar, M. Haider Mehmood Khattak	174
PAPER ID. 25-201:	Dynamic Response Modeling of SDOF Systems Using Neural Networks: A Comparative Study of ANN And LSTM Aaqib Najeeb, Muhammad Yousaf Jalal	180

PAPER ID	TITLE	PAGE NO.
PAPER ID. 25-202:	Analysis and Simulation of Steel Members in ANSYS at Different Temperatures Raja Wajahat Zahoor Khan, Raja Shujahat Zahoor Khan, Muhammad Yaqub	188
PAPER ID. 25-203:	Predicting Initial Stiffness in Welded T-Joints Featuring CHS Chords and Longitudinal Through Plate Connections Ali Ajwad, Massimo Latour	192
PAPER ID. 25-204:	Bridge Expansion Joints Replacement Challenges – A Review Mustafa Zwain, Furqan Qamar	196
PAPER ID. 25-205:	Numerical Behavior of Steel Space Frame Under Incremental Seismic Loads Kamran Shaukat, Muhammad Fahim	204
PAPER ID. 25-206:	Seismic Resistant Buildings Using Dampers: A Comparative Study Muhammad Bilal Ansari, Muhammad Yaqub	211
PAPER ID. 25-212:	Seismic Capacity Enhancement of Stone Masonry Buildings Using Horizontal Timber Elements Waqas Khan, Muhammad Fahim	218
PAPER ID. 25-301:	Comparing Construction Project Managers and Military Officers in the United States: Leveraging Veteran Leadership and Skills For Workforce Development in the Construction Industry Amna Salman, Gavin Medley	226
PAPER ID. 25-302:	Impact of Mixed Reality Technology on Teaching and Learning in Structural Engineering Guangyan Shao, Salman Azhar, Busra Yucel	234
PAPER ID. 25-303:	BIM-Driven Energy Optimization: Enhancing Thermal Performance of Buildings in Islamabad's Climate Shujahat Anwar, Hassaan Bin Raheel	242
PAPER ID. 25-304:	Clash Detection Optimization in BIM: A Case Study on Coordination and Design Efficiency in Infrastructure Projects Muhammad Aqib Jahangir, Umar Farooq, Asim Sultan	251
PAPER ID. 25-311:	Cost–Benefit Analysis of BIM in Large Infrastructure Projects: Pakistan Vs Germany Chaudhry M. Shahram Akbar, Muhammad Ziyad, Mohammad Qasim Bilal	259
PAPER ID. 25-403:	Spatial Downscaling of Grace Dataset Using Random Forest Approach For a Better Understanding of Hydrological Droughts in Pakistan Mustajab Ali, Usman Ali	266
PAPER ID. 25-504:	Mechanical and Microstructural Enhancement of Expansive Soils Via Sustainable Waste Glass Powder and Fly Ash Blends Muhammad Usama, Ubaid Ullah, Muhammad Rauf	274
PAPER ID. 25-505:	Finite Element Study on the Role of Sand Relative Density on Lateral Load Distribution in Piled Raft Systems Hamad Khan, Qazi Khurshid Ahmad, Abdullah Khan Jadoon	282

PAPER ID	TITLE	PAGE NO.
PAPER ID. 25-507:	Numerical Analysis of Laterally Loaded Piles in Fine Grained Soil Ahsan Raza Khan, Abdulllah Khalid	286
PAPER ID. 25-508:	Examining Frequency-Displacement Relationship of Piles in Fine Grained Soil Muaaz Duera, Hamza Shabir	291
PAPER ID. 25-601:	Eco-Friendly Solution For Utilization of Reclaimed Asphalt Pavement Material Hamza Afzal, Imran Hafeez	296
PAPER ID. 25-702:	Assessing the Environmental Impact of Building Materials: A Life Cycle Approach to Sustainable Building Solutions Ruqia Asad, Fayyaz Ullah	303
PAPER ID. 25-704:	Performance Analysis of LightGBM, XGBoost, Random Forest, and Gradient Boosting in Photovoltaic Energy Forecasting with Hyperparameter Optimization Muhammad Ehtsham, Marianna Rotilio, Federica Cucchiella	309
Annexure – A	Photo gallery	316
Authors Index		322

7th Conference on Sustainability in Civil Engineering (CSCE'25)
(An International Conference)
Department of Civil Engineering
Capital University of Science and Technology, Islamabad Pakistan

SUSTAINABLE SELF-COMPACTING CONCRETE INCORPORATING WHEAT STRAW ASH AND FLY ASH AS CEMENT REPLACEMENTS

[a] Farah Naz, [b] Umer Shahzad, [c] Shiraz Baloch*

a: Department of Civil Engineering, Khwaja Fareed University of Engineering and Information Technology, Rahim Yar Khan, Punjab, Pakistan. farah.naz@kfueit.edu.pk
b: Department of Civil Engineering, Khwaja Fareed University of Engineering and Information Technology, Rahim Yar Khan, Punjab, Pakistan. umer.shahzad@kfueit.edu.pk
c: Department of Civil Engineering, Khwaja Fareed University of Engineering and Information Technology, Rahim Yar Khan, Punjab, Pakistan. meershiraz17@gmail.com
* Corresponding author

Abstract- The rapid growth of the construction industry has led to an increasing demand for cement, a material whose production consumes large amounts of energy, depletes natural resources, and emits significant quantities of carbon dioxide into the atmosphere. This emission of greenhouse gases contributes to environmental degradation and climate change. At the same time, agricultural and industrial wastes such as fly ash and wheat straw ash are often discarded improperly, posing serious environmental hazards due to the release of toxic gases. This study investigates the potential of using these organic waste materials as partial replacements for cement in the development of ecofriendly self-compacting concrete. The goal is to reduce cement consumption while promoting sustainable construction practices. In this experimental work, self-compacting concrete was prepared with varying replacement levels of cement at 5%, 10%, 15%, 17% and 20% using fly ash and wheat straw ash. A polycarboxylate based superplasticizer was used to improve the workability of the mix without affecting its strength. The performance of each mix was evaluated through tests on workability and compressive strength. The results demonstrated that selected combinations of organic waste materials not only enhanced the fresh properties of self-compacting concrete but also maintained adequate strength compared to conventional concrete. This research supports the use of agricultural and industrial byproducts as sustainable alternatives in concrete production, offering both environmental and economic benefits while contributing to the advancement of green construction practices.

Keywords- Ecofriendly Concrete, Cement Replacement, Sustainable Construction, Self-Compacting Concrete

1 Introduction

Self-Compacting Concrete (SCC) is a special concrete which has revolutionized concrete placement, eliminating the need for vibrators as it flows under its own weight, a characteristic that ensures excellent workability and compaction without segregation or bleeding [1-3]. Initially developed in Japan in the 1980s, SCC is now utilized globally, particularly in countries like Denmark, where it accounts for 20-30% of the total concrete production in the ready-mix and precast concrete industries [4]. SCC is known for its early strength, reduced water-cement ratio, and enhanced durability, particularly when superplasticizers are incorporated. These additives help decrease the water-cement ratio, further enhancing the concrete's mechanical properties [5]. The inclusion of materials such as silica fume, fly ash (FA), wheat straw ash (WSA), and sugar cane bagasse ash has significantly contributed to improving the properties of SCC [6, 7].

Wheat straw, when appropriately pre-treated, can notably enhance the energy absorption characteristics of concrete [8]. Additionally, using materials like FA and WSA in SCC helps lower the carbon footprint, as the replacement of cement with these materials reduces CO_2 emissions, making the concrete more sustainable [9].

The substitution of cement with wheat straw ash (WSA) has been studied for its impact on the mechanical properties and workability of SCC. Research indicates that up to a 10% replacement of cement with WSA improves the hardened properties of SCC, with compressive strength increasing due to the filler capacity and chemical reactions with calcium hydroxide [10]. WSA is considered a sustainable alternative to cement due to its pozzolanic nature, which improves concrete's durability and compressive strength [11]. Similarly, other studies suggest that the use of WSA in SCC improves its overall performance and contributes to the sustainability of concrete [12]. Wheat straw, often burned openly, causes pollution; controlled burning produces ash with cementing properties for concrete use [14]. Given the abundant production of wheat straw in agricultural countries like Pakistan, the use of WSA in concrete offers an eco-friendly solution, addressing both waste management and environmental sustainability challenges [13]. This study examines the combined use of wheat straw ash (WSA) and fly ash (FA) as partial cement replacements in self-compacting concrete (SCC), focusing on their impact on fresh and hardened properties. In Pakistan, where wheat straw is abundantly produced and often burned openly, utilizing WSA in concrete offers a sustainable solution to waste management while promoting greener construction practices tailored to local needs.

2 Research Methodology

This research focused on evaluating the fresh and hardened properties of self-compacting concrete (SCC) using sustainable cement replacements. The methodology involved selection of appropriate materials, execution of standardized laboratory tests, and development of optimized mix designs in line with SCC performance criteria.

2.1 Materials

The materials were selected based on their local availability, cost-effectiveness and compatibility with SCC production. Ordinary Portland Cement (OPC) conforming to ASTM C150 was used, sourced from DG Khan Cement. Harrow sand and Sargodha crush were used as fine and coarse aggregates respectively, both complying with ASTM C33. The fine aggregate passed through a No. 4 sieve and exhibited proper grading, while the 25 mm angular coarse aggregate offered strength and interlock. Aggregates were oven-dried at 105°C for 24 hours prior to testing.

a)  b) 

Figure 1: Laboratory Samples of Ashes, a) Fly Ash (FA), and b) Wheat Straw Ash (WSA) for current study

Class F Fly Ash (ASTM C618) and Wheat Straw Ash (WSA) were used as partial cement replacements. Both were sieved through a No. 200 mesh. Although WSA lacks a formal ASTM classification, its pozzolanic nature was confirmed through preliminary assessments. Samples of both ashes used in this study are shown in Figure 1. A polycarboxylate ether-based superplasticizer (ASTM C494 Type F) was added to enhance SCC flowability. Water and setting times were determined using the Vicat apparatus.

2.2 Laboratory Testing

In this study, a series of laboratory tests were conducted to assess the physical properties of raw materials and the performance of concrete mixes. Aggregates were tested for particle size distribution, cleanliness, and water absorption. The fineness modulus of sand was 2.502, falling within the ASTM C136 recommended range of 2–4. Cement consistency (ASTM C187-16) and setting time (ASTM C191-13) were within standard limits, with a consistency of 5.5 mm, an initial setting time of 57 minutes, and a final setting time of 9 hours 51 minutes. Fine aggregates showed a specific gravity of 2.805 (SSD) and 0.6% water absorption, both meeting ASTM C128-15. Coarse aggregate tests (ASTM C127-15) gave a crushing value of 15.57% and bulk density of 1566.81 kg/m³. Fly ash (ASTM C136/C136M-16) had a fineness of 95.16% and a specific gravity of 2.33 (ASTM D854), while wheat straw ash showed 95.8% fineness and a specific gravity of 1.852. The summarized results of cementitious materials are shown in Table 1, while the physical properties of coarse and fine aggregates are presented in Table 2. In addition to material characterization, tests on fresh concrete (such as workability and flow) and hardened samples (compressive strength) were conducted to assess overall mix performance. All procedures followed ASTM standards to ensure data accuracy and reliability for mix design.

Table 1 Characteristics of Cement, Fly Ash and Wheat Straw Ash

Material	Property	Results
Cement	Fineness	95%
	Consistency	5.5mm
	Specific Gravity	3.15
	Initial Setting Time	57mins
	Final Setting Time	591mins
	Soundness	1.72%
	Compressive Strength	42 MPa
Fly Ash	Colour	Tan Grey
	Fineness	95.16%
	Specific Gravity	2.33
Wheat Straw Ash	Colour	Dark Grey
	Fineness	95.8%
	Specific Gravity	1.852

Table 2 Properties of Coarse and Fine Aggregate

Material	Tested Parameters	Results
Coarse Aggregate	Impact Value	1.626%
	Crushing Value	15.57%
	Specific Gravity	2.789 (SSD)
	Water Absorption	1%
	LA Abrasion Value	18.21%
	Bulk Density	1566.81 Kg/m^3
Fine Aggregate	Fineness Modulus	2.805 (SSD)
	Specific Gravity	2.65
	Water Absorption	0.6%
	Loose Bulk Density	1.304 g/cm^3
	Compacted Bulk Density	1.471 g/cm^3

2.3 Concrete Mix Design

The concrete mix was designed as per Grade M30 specifications, targeting a compressive strength of 31.6 MPa using the formula $f'c = f + 1.65s$, where a standard deviation of 4 MPa was adopted. Based on strength and slump requirements, a

water–cement (W/C) ratio of 0.44 was determined through interpolation. For the required workability range of 30–50 mm slump, the water content was fixed at 165 kg/m³. Accordingly, the cement content was calculated as 375 kg/m³. The coarse aggregate quantity was established using a volume fraction of 0.65 (based on the fineness modulus of sand, 2.49), resulting in 1018.42 kg/m³ of 20 mm Sargodha crush with a specific gravity of 2.798 and bulk density of 1566.81 kg/m³. The remaining mass, accounting for 721.48 kg/m³, was allocated to fine aggregate (harrow sand) to maintain the target concrete density of 2280 kg/m³. The resulting mix ratio for this M30 concrete is 1:1.9:2.71 (cement: sand: coarse aggregate), forming the base control mix for comparative evaluation against SCC variants with partial cement replacements.

2.4 Specimen Preparation and Curing

A total of 144 cylindrical specimens (4 in. × 8 in.) were cast, including 135 with varying levels of fly ash, wheat straw ash, and their combination, and 9 control samples. Concrete was mixed according to design proportions and placed in molds in three layers with proper compaction. Specimens were demolded after 24 hours and cured in water at 23 ± 2°C. Testing was conducted at 3, 14, and 28 days to evaluate strength development.

3 Results

3.1 Workability Assessment of Fresh Concrete

The workability of Self-Compacting Concrete (SCC) was evaluated with varying cement replacements using fly ash (FA), wheat straw ash (WSA), and their combination. The control mix had low workability (12.7 mm). FA increased workability, reaching a maximum of 190.5 mm at 20% replacement. WSA achieved its highest workability (183.11 mm) at 10% replacement, but declined thereafter. Combining FA and WSA showed optimum workability at 10% replacement (176.33 mm). Overall, controlled ash proportions improved SCC flow characteristics. The variation in workability is shown in the combined graph (Figure 2).

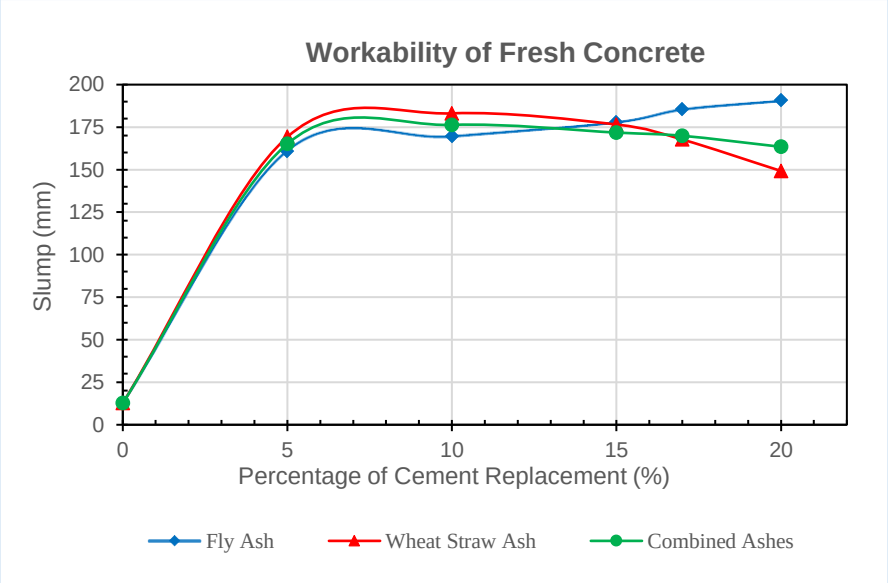


Figure 2: Variation in Workability with Different Ash Replacement Levels

3.2 Compressive Strength

For compressive strength testing, the concrete samples were categorized into three groups: Fly Ash (FA), Wheat Straw Ash (WSA), and a combined FA and WSA group, with varying replacement levels (5%, 10%, 15%, 17%, and 20%). Each replacement group was tested at 3, 14, and 28 days of curing. The average of three samples from each curing interval was used as the result for that specific replacement level. The compressive strength results for FA, WSA, and combined ashes are presented in Figures 3, 4, and 5, respectively.

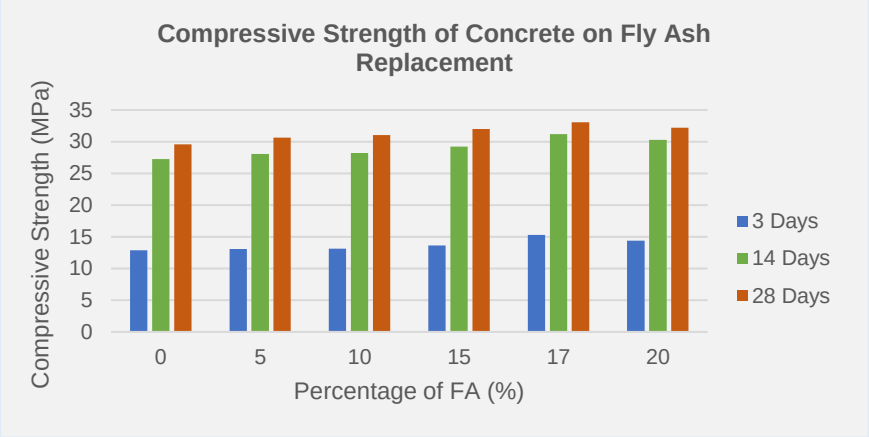


Figure 3: Compressive Strength on Replacement of Fly Ash (FA)

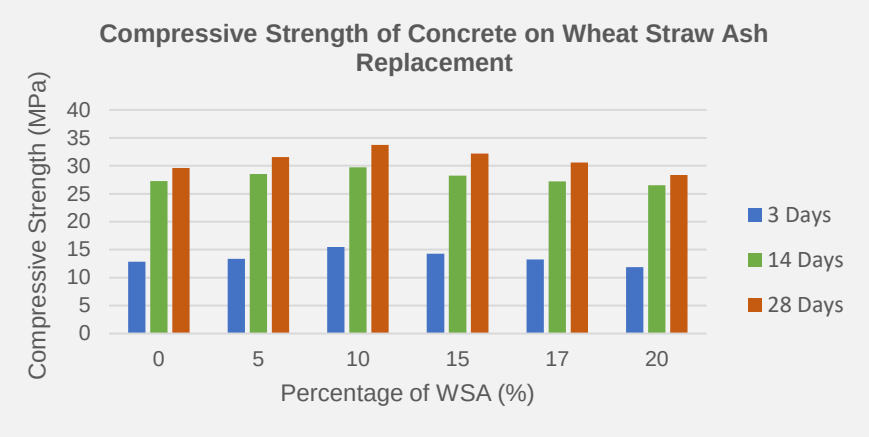


Figure 4: Compressive Strength on Replacement of Wheat Straw Ash (WSA)

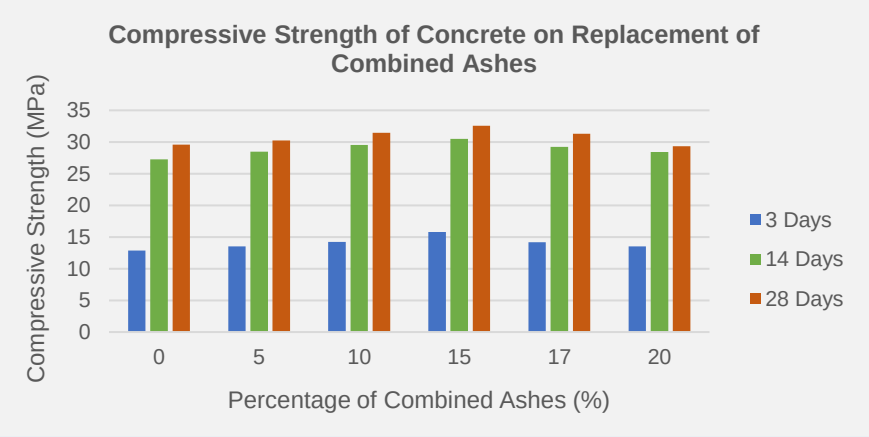


Figure 5: Compressive Strength on Replacement of Combined Ashes (FA + WSA)

Furthermore, Figures 6, 7, and 8 compare the compressive strength of self-compacting concrete with different percentages of ash replacement, providing an overview of the performance variations at different curing ages (3, 14, and 28 days) and replacement levels. These figures help visualize the influence of fly ash, wheat straw ash, and their combined use on strength gain over time. The trends observed support the identification of optimal replacement levels and highlight the practical potential of using these ashes in sustainable concrete applications.

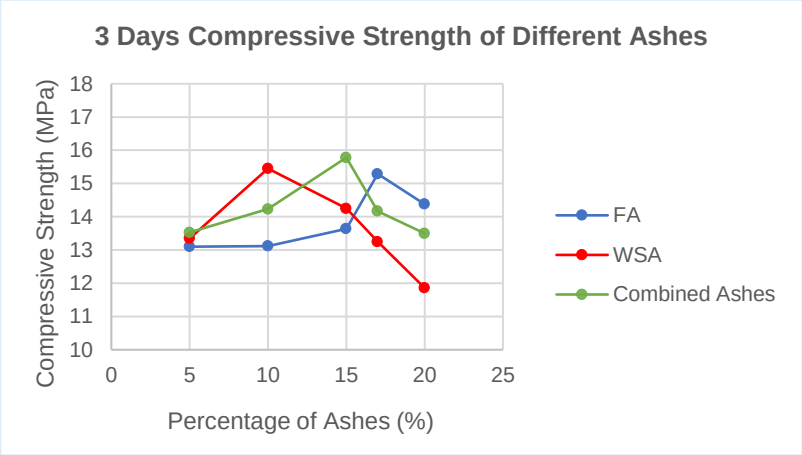


Figure 6: 3-Day Compressive Strength of Self-Compacting Concrete with Varying Ash Contents

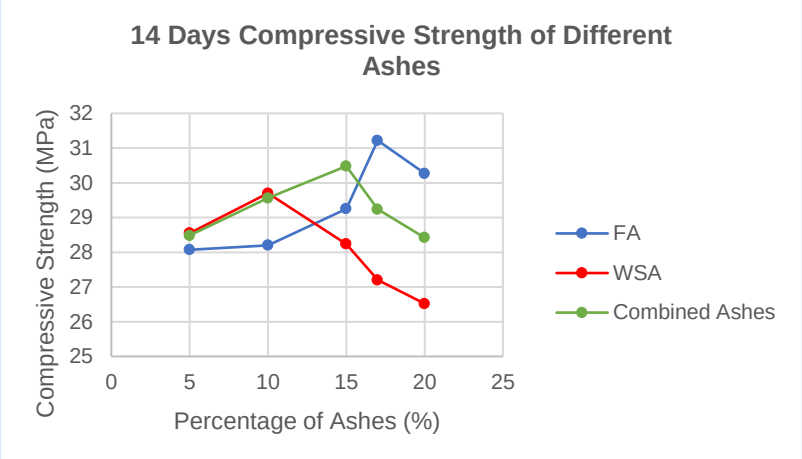


Figure 7: 14-Day Compressive Strength of Self-Compacting Concrete with Varying Ash Contents

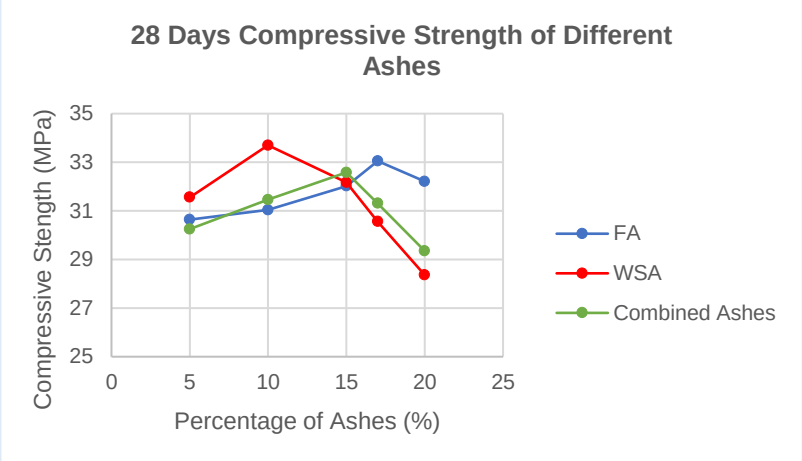


Figure 8: 28-Day Compressive Strength of Self-Compacting Concrete with Varying Ash Contents

The strength improvements observed at 17% fly ash and 10% wheat straw ash can be linked to their pozzolanic activity and filler effects, which refine the concrete matrix. Fly ash helped enhance workability due to its spherical particles, while wheat straw ash contributed to strength by providing reactive silica. When combined, the materials offered a balance of flow and strength, suggesting a mild synergistic behavior beneficial for sustainable mix design.

4 Practical Application

The use of wheat straw ash and fly ash as partial cement replacements offers a practical solution for sustainable construction in Pakistan, where agricultural and industrial waste is widely available. This approach can be adopted in housing projects, rural infrastructure, pavements, and non-structural elements, reducing cement demand and overall construction costs. In regions with limited access to high-quality materials, self-compacting concrete developed with these waste products can improve workability and ease of placement without the need for advanced machinery. Adopting this method supports waste management efforts, lowers carbon emissions, and promotes ecofriendly construction practices aligned with Pakistan's growing need for affordable and sustainable development.

5 Conclusion

This study explored the use of fly ash and wheat straw ash as partial replacements for cement in self-compacting concrete, supported by a polycarboxylate based superplasticizer to maintain workability. Mix designs with varying replacement levels of 5%, 10%, 15%, 17%, and 20% were evaluated. Workability tests revealed that 20 percent fly ash achieved the highest slump flow of 190.5 mm, while 10 percent wheat straw ash and 10 percent combined ash yielded 183.11 mm and 176.33 mm respectively. It was observed that higher contents of wheat straw ash tended to reduce flow. Compressive strength tests conducted at 3, 14, and 28 days showed optimal results at 17 percent fly ash, 10 percent wheat straw ash, and 15 percent combined replacement, with all mixes maintaining strength values comparable to conventional concrete. Based on the results, it is suggested that natural organic wastes such as fly ash and wheat straw ash can be utilized in concrete. As these ashes are hazardous for the environment, so utilization of such wastes in concrete with optimized values will also be beneficial for our environment. The findings confirm that these organic waste materials, when used in appropriate proportions, can produce environmentally friendly concrete without compromising performance.

Future research should focus on exploring the long-term durability and microstructural behavior of concrete containing organic waste ashes. Investigations on resistance to sulfate attack, chloride penetration, and freeze-thaw cycles would help evaluate performance in aggressive environments. Additionally, optimizing mix design for large-scale applications and exploring combinations with other sustainable materials may enhance the potential for broader implementation in green construction.

Acknowledgment

The authors would like to thank the Department of Civil Engineering at Khwaja Fareed University of Engineering and Information Technology (KFUEIT), for providing the support and resources necessary to carry out this research. The authors also acknowledge the careful review and constructive suggestions by the anonymous reviewers.

References

[1] K. R. Kumar, G. Shyamala, P. O. Awoyera, K. Vedhasakthi, and O. B. Olalusi, "Cleaner production of self-compacting concrete with selected industrial rejects—An overview," *Silicon,* vol. 13, pp. 2809–2820, 2021.

[2] F. Abid, R. C. Patil, and R. Sakale, "Development of High Performance Concrete," *International Journal of Trend in Scientific Research and Development,* vol. 2, pp. 1465–1479, 2018.

[3] EFNARC, *EFNARC Guidelines for Self-Compacting Concrete,* EFNARC, UK, 2002. [Online]. Available: www.efnarc.org

[4] M. Hunger, An integral design concept for ecological self-compacting concrete. 2010.

[5] N. Kabir, A. Sallau, and A. U. Chinade, "Experimental study of conplast SP430 in concrete using selected brands of Portland cement," *American J. Eng. Res.,* vol. 8, no. 6, pp. 225–233, 2019.

[6] A. Bahurudeen, D. Kanraj, V. G. Dev, and M. Santhanam, "Performance evaluation of sugarcane bagasse ash blended cement in concrete," *Cement and Concrete Composites,* vol. 59, pp. 77–88, 2015.

[7] M. B. Hossain, K. M. Shaad, M. S. Rahman, and P. Bhowmik, "Influence of rice husk ash on the properties of concrete," *Journal of Environmental Science Natural Resources,* vol. 9, no. 1, pp. 29–33, 2016.

[8] M. U. Farooqi and M. Ali, "Effect of pre-treatment and content of wheat straw on energy absorption capability of concrete," *Construction and Building Materials,* vol. 224, pp. 572-583, 2024.

[9] S. C. Bostanci, "Use of waste marble dust and recycled glass for sustainable concrete production," *Journal of Cleaner Production,* vol. 251, p. 119785, 2020.

[10] N. Bheel, M. H. W. Ibrahim, A. Adesina, C. Kennedy, and I. A. Shar, "Mechanical performance of concrete incorporating wheat straw ash as partial replacement of cement," *Journal of Building Pathology Rehabilitation,* vol. 6, pp. 1–7, 2021.

[11] T. A. El-Sayed, A. M. Erfan, and R. M. Abd El-Naby, "Recycled rice & wheat straw ash as cement replacement materials," *Composites,* vol. 14, p. 19, 2019.

[12] S. A. Memon, I. Wahid, M. K. Khan, M. A. Tanoli, and M. Bimaganbetova, "Environmentally friendly utilization of wheat straw ash in cement-based composites," *Sustainability,* vol. 10, no. 5, p. 1322, 2018.

[13] K. H. Mo, U. J. Alengaram, M. Z. Jumaat, S. P. Yap, and S. C. Lee, "Green concrete partially comprised of farming waste residues: a review," *Journal of Cleaner Production,* vol. 117, pp. 122–138, 2016.

[14] M. Batayneh, I. Marie, and I. Asi, "Use of selected waste materials in concrete mixes," *Waste Management,* vol. 27, no. 12, pp. 1870–1876, 2007.

ENHANCING CONCRETE SUSTAINABILITY: NATURAL FIBRE REINFORCEMENT FOR SHRINKAGE CRACK MITIGATION IN CONCRETE STRUCTURES

[a] Muhammad Zain Sajid*, [b] Faisal Mateen

a: 496 Engineering Group, Frontier Works Organization (FWO), Rawalpindi, Pakistan. zainsajid2019@gmail.com
b: Structural Works Department, WSP Pvt. Ltd, Sydney, Australia. Faisal.civil@gmail.com
* Corresponding author

Abstract- Shrinkage cracking is one of the most common flaws encountered in reinforced cement concrete (RCC) structures, primarily due to volumetric changes caused by moisture loss and improper curing. These cracks can significantly compromise the durability, aesthetics, and serviceability of concrete elements. This review explores the application of natural fibre reinforcement as a sustainable and effective solution to mitigate shrinkage cracks in concrete structures. Unlike synthetic fibres, natural fibres are biodegradable, cost-effective, and environmentally friendly aligning with global sustainability goals. A detailed review of crack types, fibre characteristics, governing parameters for shrinkage, and fibre volume dosage considerations was conducted using recent literature and the results are thoroughly reported. Key standards such as ACI 544.3R-08, ASTM C1116, and EFNARC guidelines were referenced to establish acceptable fibre content and performance benchmarks. Findings show that natural fibres like jute, sisal, and coconut, at optimized volume fractions, enhance crack resistance, increase flexural strength by up to 89%, reduce water absorption by approximately 25%, and improve concrete's post-crack behavior and mechanical properties. This review aims and supports the use of natural fibres in concrete not only as a technically sound method for crack control but also as a step forward in achieving sustainable and resilient construction practices.

Keywords- Fibre Volume Fraction, Fibre-Reinforced Concrete (FRC), Shrinkage Cracks, Sustainable Construction

1 Introduction

Concrete stands as a cornerstone in modern construction due to its versatility, strength, and durability. However, its inherent brittleness and susceptibility to cracking pose significant challenges to structural integrity and longevity. Among the various types of cracks, shrinkage cracks are particularly prevalent, arising from volumetric changes as concrete cures and dries. Addressing these issues is crucial for enhancing the performance and sustainability of concrete structures. Incorporating fibres into concrete mixes has emerged as a promising solution, offering improved tensile strength, crack resistance, and overall durability. Utilizing natural fibres not only leverages renewable resources but also contributes to cost reduction and environmental sustainability, aligning with the growing emphasis on green construction practices.

Cracks in concrete are categorized based on their causes and characteristics. Common types include plastic shrinkage cracks, which occur shortly after pouring due to rapid moisture loss; drying shrinkage cracks, resulting from long-term moisture evaporation; and thermal cracks, caused by temperature variations leading to expansion and contraction [1]. Structural cracks, such as flexural and settlement cracks, arise from external loads or foundation movements. These cracks compromise the structural integrity and aesthetic appeal of concrete structures, necessitating effective mitigation strategies

[2]. Research has explored the integration of various fibres into concrete to enhance its properties and mitigate cracking. Natural fibres, including coconut, sisal, and jute, have been studied for their effectiveness in controlling shrinkage cracks. For instance, incorporating 1% volume of sisal fibre into concrete significantly increased the energy required to initiate cracks, demonstrating enhanced toughness [3]. Similarly, coconut fibres have been shown to improve crack resistance and maintain strength even at elevated temperatures. These findings highlight the potential of natural fibres as sustainable alternatives to synthetic fibres in concrete mixes [4].

Recent studies have demonstrated that the incorporation of natural fibres into concrete can significantly enhance its mechanical properties [5]. For example, the addition of jute fibres has been shown to improve the flexural strength and toughness of concrete, making it more resistant to cracking under load [6]. Similarly, the use of kenaf fibres has been associated with increased tensile strength and reduced shrinkage in concrete mixes. Likewise, Qamar, et al.[7] states that plaster having natural fibres improves the lateral resistance of mortar-free interlocking walls. These improvements are attributed to the fibres' ability to bridge microcracks and distribute stress more evenly throughout the concrete matrix [8]. Despite the promising results, challenges remain in standardizing the use of natural fibres in concrete. Variations in fibre properties, such as length, diameter, and composition, can affect the consistency and performance of fibre-reinforced concrete [9]. Moreover, the lack of comprehensive guidelines for fibre volume and dosage complicates the optimization of mix designs [10]. Addressing these gaps is essential for the broader adoption of natural fibre-reinforced concrete in structural applications.

This review aims to investigate the role of natural fibre reinforcement in mitigating shrinkage cracks in concrete structures. By analyzing the types and causes of cracks, evaluating the effectiveness of various natural fibres, and exploring optimal fibre volumes and dosages, the research seeks to develop sustainable and cost-effective solutions for enhancing concrete durability. The findings are expected to contribute to the advancement of green construction practices and the development of standardized guidelines for natural fibre-reinforced concrete.

2 Identification of Shrinkage Cracks in RCC Buildings

The identification and assessment of shrinkage cracks involve a combination of visual inspections and standardized testing methods [11]. Shrinkage cracks in reinforced cement concrete (RCC) structures as shown in figure 1 primarily result from volumetric changes due to moisture loss and temperature variations. These cracks can be categorized into plastic shrinkage cracks, occurring shortly after concrete placement, and drying shrinkage cracks, which develop over time as the concrete loses moisture [12]. As illustrated in figure 1, plastic shrinkage cracks typically manifest within the first few hours after placement, primarily due to rapid moisture loss from the surface, leading to tensile stresses that exceed the concrete's early-age strength [3, 13]. Drying shrinkage cracks develop over a longer period as the concrete loses moisture to the environment, resulting in volumetric contraction [14]. Thermal cracks arise from temperature gradients within the concrete mass, causing differential expansion and contraction. Structural cracks, such as flexural and settlement cracks, are induced by external loads or foundation movements, compromising the structural integrity of the concrete element [15]. Understanding these crack types and their underlying causes is crucial for implementing effective mitigation strategies.



Figure 1: Shrinkage crack propagation (a) happens within the first day or two after placing concrete (b) Within the first few hours after placing the concrete (c) Days to weeks after setting, as concrete begins to dry and harden [16]

Visual inspections focus on detecting surface cracks, noting their width, length, and pattern, which can provide insights into their origin. For a more detailed analysis, non-destructive testing methods such as ultrasonic pulse velocity and infrared thermography can be employed to assess the depth and severity of cracks [17]. Standards like ACI 224.1R-07 provide guidelines for evaluating and repairing cracks in concrete structures, emphasizing the importance of understanding the cause before selecting a repair method. Additionally, ASTM C1581/C1581M-18a outlines procedures for determining the age at cracking and induced tensile stress characteristics of mortar and concrete under restrained shrinkage, offering a standardized approach to assess shrinkage cracking. Adhering to these standards ensures a systematic and effective approach to managing shrinkage cracks in RCC structures.

3 Causes and Remedial Measures for Shrinkage Cracking in Concrete

Shrinkage-induced cracking in reinforced cement concrete (RCC) elements arises from a combination of intrinsic material properties and external environmental factors. Key parameters influencing shrinkage include the water-cement ratio, aggregate characteristics, cement content, ambient temperature, humidity, and curing practices. High water-cement ratios lead to increased drying shrinkage, while aggregates with high shrinkage potential exacerbate the issue [18]. Environmental conditions such as elevated temperatures and low humidity accelerate moisture loss, intensifying shrinkage stresses [14]. Inadequate curing further enhances these effects by allowing rapid evaporation of water from the concrete surface, leading to early-age cracking [19]. These factors collectively contribute to the development of shrinkage cracks, compromising the durability and serviceability of RCC structures. Figure 2 summarizes the primary causes of shrinkage cracking, their estimated contribution percentages, and the relevant standards or authors referencing these factors:

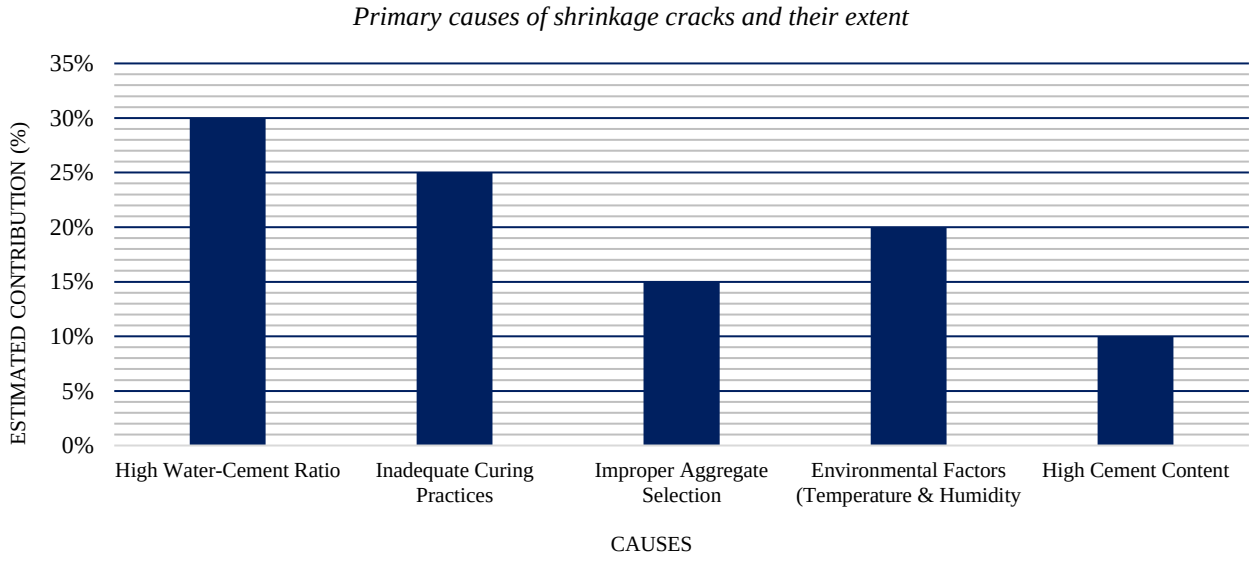


Figure 2: Primary causes of shrinkage cracking as per ACI224R-01 and ACI224.1R-07 [19]

Mere plain concrete (PC) is particularly susceptible to shrinkage cracking due to its limited tensile strength and inability to distribute stresses effectively. Thus, this study proposes a solution which is natural fibre (as shown in fig. 03) additives in concrete that can play a vital role in mitigating shrinkage and related cracking compared to plain concrete (PC). Shrinkage, especially at early ages due to rapid moisture loss, often leads to plastic and drying shrinkage cracks in plain concrete. When natural fibres as illustrated in fig. 3 such as jute, coir, sisal, or hemp are incorporated into the concrete mix, they help bridge micro-cracks and distribute internal stresses more uniformly, effectively delaying crack formation and reducing crack width. However, even in reinforced concrete, which mainly controls structural cracks, natural fibres help mitigate non-structural shrinkage cracks by enhancing the tensile strain capacity and providing early-age crack resistance [3, 20]. Therefore, understanding the governing parameters and implementing appropriate design and construction practices are essential for mitigating shrinkage cracking in RCC members.



Figure 3: Various fibre additives used in concrete, including natural, synthetic, and steel fibres [16]

Hence understanding the governing parameters and the respective solutions is crucial for the effective design and construction of RCC structures. By addressing these factors through appropriate material selection, mix design, and construction practices, the incidence of shrinkage cracking can be significantly reduced, leading to more durable and serviceable concrete structures.

4 Optimizing Fibre Volume and Dosage for Shrinkage Crack Control

Incorporating fibres into concrete mixes necessitates meticulous attention to fibre volume fractions and dosage to achieve desired mechanical properties and durability. The fibre volume fraction (FVF) refers to the percentage of fibre volume relative to the total volume of the composite, while dosage typically denotes the weight of fibres added per unit volume of concrete, expressed in kg/m³ or lb/yd³. Proper selection of FVF and dosage is crucial, as insufficient fibre content may not provide the intended reinforcement benefits, whereas excessive fibre content can lead to issues such as reduced workability and fibre clumping. Table 1 highlights some studies which demonstrated that optimal fibre content varies depending on the type of fibre and the specific performance requirements of the concrete. Najaf, et al. [21] showed that 1.5% polypropylene fibres greatly enhance ductility and impact resistance. This aligns with Khan, et al. [22], who observed similar improvements using glass fibres, though only up to an optimal 1% dosage. Both support the notion of an optimal range beyond which workability may be compromised. The following table 1 summarizes typical fibre volume fractions and the respective effects on concrete.

Table 1 Effects of Fibre Volume Fraction on Concrete Properties via scholarly aspect [16]

Fibre Type	Volume Fraction (%)	Observed Effects on Concrete Properties	Reference(s)
Polypropylene Fibres	1.5	Compressive strength increased by up to 36% Flexural strength increased by up to 89% Enhanced ductility and impact resistance	Najaf, et al. [21]
Glass Fibres	1	Compressive strength increased by 15.38% Split tensile strength increased by 58.94% Flexural strength increased by 17.54% Strength decreased beyond 1% dosage	Khan, et al. [22]
Hybrid Fibres (Steel + Polyester	0.2 + 0.3	Improved toughness and durability Split tension capacity enhanced by 72% Reduced water absorption by 25%	Christopher, et al. [23]

Table 2 highlights some standards and guidelines that provide recommendations for fibre content in concrete mixes to ensure consistency and performance. According to ASTM C1116/C1116M, synthetic microfibres are typically used at dosages ranging from 0.3 to 0.9 kg/m³ (0.03% to 0.1% by volume) for controlling plastic shrinkage cracking. For macro-synthetic fibres, dosages can range from 1.8 to 12 kg/m³, depending on the desired performance characteristics. Steel fibres are often incorporated at volume fractions between 0.5% and 2.0%, with dosages adjusted based on the specific application and performance requirements. The American Concrete Institute's ACI 544.3R-08 guide emphasizes the importance of selecting appropriate fibre types and dosages to achieve the desired balance between workability and mechanical performance. Table 2 summarizes typical fibre volume fractions and dosages for various fibre types as recommended by relevant standards and studies

Table 2 Recommended Fibre Volume Fractions and Dosages [24]

Fibre Type	**Volume Fraction (%)**	**Dosage (kg/m³)**	**Reference**
Polypropylene (Micro)	0.03 – 0.1	0.3 – 0.9	ASTM C1116/C1116M
Polypropylene (Macro)	0.1 – 0.3	1.8 – 12	ASTM C1116
Steel Fibres	0.25 – 2.0	20 – 60	ACI 544.3R-08
Glass Fibres	0.01 – 0.03	0.29 – 0.88	ACI 544.3R-08

5 Conclusion

The incorporation of natural fibres in concrete mixes presents a promising and sustainable solution to mitigate shrinkage cracking in RCC structures. By enhancing tensile strength, controlling microcrack development, and improving overall durability, fibre-reinforced concrete significantly extends the service life of structural elements while reducing maintenance needs. This approach aligns directly with several United Nations Sustainable Development Goals (SDGs), including SDG 9 (Industry, Innovation and Infrastructure), SDG 11 (Sustainable Cities and Communities), and SDG 12 (Responsible Consumption and Production) by promoting eco-friendly construction practices, reducing reliance on synthetic materials, and encouraging the use of agricultural waste. The key findings of this review are:

1 Shrinkage cracks in RCC are primarily caused by volumetric changes due to drying, poor curing, high water-cement ratios, and environmental exposure.
2 Natural fibres such as jute, sisal, and coconut improve concrete's crack resistance, as evidenced by up to 89% improvement in flexural strength and up to 72% enhancement in split tension capacity.
3 Fibre volume fraction and dosage significantly influence concrete's mechanical performance, durability, and crack resistance.
4 Recent research (2023–2025) supports the optimal use of fibres in the range of 0.3% to 2.0% by volume, depending on the fibre type and application.
5 Relevant standards such as ACI 544.3R-08, ASTM C1116, and EFNARC guidelines help guide proper fibre selection and dosage control.
6 Overall, natural fibre-reinforced concrete not only improves structural performance but also supports sustainable, low-carbon construction practices aligned with global development goals.

In summary, fibre-reinforced concrete using natural fibres offers a durable, eco-friendly, and cost-effective solution for crack mitigation in RCC buildings. These findings are backed by recent experimental data and benchmark standards (ASTM C1116, ACI 544.3R-08), which validate fibre dosages and performance expectations for shrinkage crack control. This approach supports the construction industry's transition toward more sustainable and resilient practices.

Acknowledgment

The author gratefully acknowledges their employer organization, Frontier Works Organization (FWO 496 ENGR GP), for providing the necessary time and support to undertake this research amidst a demanding work schedule. Their encouragement was vital to the successful completion of this paper.

References

[1] R. Wang, X. Zhou, Y. Liu, D. Liu, Y. Lu, and M. Su, "Identification of the surface cracks of concrete based on resnet-18 depth residual network," *Applied Sciences*, vol. 14, no. 8, p. 3142, 2024.

[2] R. Kirthiga and S. Elavenil, "A survey on crack detection in concrete surface using image processing and machine learning," *Journal of Building Pathology and Rehabilitation*, vol. 9, no. 1, p. 15, 2024.

[3] P. Lura, N. Toropovs, J. Justs, M. Shakoorioskooie, B. Münch, and M. Griffa, "Mitigation of plastic shrinkage cracking with natural fibers-kenaf, abaca, coir, jute and sisal," *Cement and Concrete Composites*, vol. 155, p. 105827, 2025.

[4] I. S. Ayeni, N. H. A. S. Lim, and M. Samad, "Engineering properties of natural fibre-reinforced one-part geopolymer concrete," *Construction and Building Materials*, vol. 456, p. 139161, 2024.

[5] A. Rajkohila and S. P. Chandar, "Assessing the effect of natural fiber on mechanical properties and microstructural characteristics of high strength concrete," *Ain Shams Engineering Journal*, vol. 15, no. 5, p. 102666, 2024.

[6] S. S. Ubayi *et al.*, "A Review of the Impact of Jute Fiber Reinforcement on Mechanical Properties of Concrete," *International Journal in Engineering Sciences*, vol. 2, no. 07, 2024.

[7] F. Qamar, T. Thomas, and M. Ali, "Improvement in lateral resistance of mortar-free interlocking wall with plaster having natural fibres," *Construction and Building Materials*, vol. 234, p. 117387, 2020.

[8] K. Toumbou, C. Githuku, and M. Mwai, "Effect of Chemical Treatment of Kenaf Fibers on the Structural Performance of Reinforced Concrete Beam," *International Journal of Civil Engineering, vol*, vol. 11, 2024.

[9] K. Sonar and S. Sathe, "Exploring fiber reinforcements in concrete and its challenges: A comprehensive review," *Multiscale and Multidisciplinary Modeling, Experiments and Design*, vol. 7, no. 4, pp. 3099-3131, 2024.

[10] A. Alshahrani and S. Kulasegaram, "Effect of fibre diameter and tensile strength on the mechanical, fracture, and fibre distribution properties of eco-friendly high-strength self-compacting concrete," *Construction and Building Materials*, vol. 403, p. 133161, 2023.

[11] T. Chik, A. Jalil, N. Yusoff, S. Hakim, and N. Ghafar, "Rapid visual assessment of crack on residential building," in *IOP Conference Series: Earth and Environmental Science*, 2023, vol. 1205, no. 1: IOP Publishing, p. 012039.

[12] M. Wyrzykowski, C. Di Bella, D. Sirtoli, N. Toropovs, and P. Lura, "Plastic shrinkage of concrete made with calcined clay-limestone cement," *Cement and Concrete Research*, vol. 189, p. 107784, 2025.

[13] J. S. James and E. John, "Synergistic effects of SCMs and fibers on plastic shrinkage control of sustainable concrete," *Green Materials*, pp. 1-17, 2025.

[14] M. Zhang *et al.*, "Evaluation of Concrete Structural Cracking Behavior Induced by Early Drying Shrinkage," *Materials*, vol. 18, no. 2, p. 395, 2025.

[15] S. N. S. Abd Razak and M. Z. Suleiman, "Evaluation of Cracks in Affordable Housings in Selangor: A Fundamental Approach," *Journal of Advanced Research Design*, vol. 120, no. 1, pp. 11-21, 2024.

[16] T. M. Pham, "Fibre-reinforced concrete: state-of-the-art-review on bridging mechanism, mechanical properties, durability, and eco-economic analysis," *Case Studies in Construction Materials*, p. e04574, 2025.

[17] Y. M. Shalaby, M. Badawy, G. A. Ebrahim, and A. M. Abdelalim, "Condition assessment of concrete structures using automated crack detection method for different concrete surface types based on image processing," *Discover Civil Engineering*, vol. 1, no. 1, p. 81, 2024.

[18] L. Fang *et al.*, "Combined effects of low-heat cement, expansive agent and shrinkage-reducing admixture on drying shrinkage and cracking of concrete," *Case Studies in Construction Materials*, p. e04344, 2025.

[19] Y. P. Asmara, F. Herlina, J. Arifin, and R. Adawiyah, "Understanding Concrete Damages: Causes, Contributing Factors, and Integrity Assessment," *Journal of Innovation and Technology*, vol. 2025, 2025.

[20] A. Afraz and M. Ali, "Effect of banana fiber on flexural properties of fiber reinforced concrete for sustainable construction," *Engineering Proceedings*, vol. 12, no. 1, p. 63, 2021.

[21] E. Najaf and H. Abbasi, "Impact resistance and mechanical properties of fiber-reinforced concrete using string and fibrillated polypropylene fibers in a hybrid form," *Structural Concrete*, vol. 24, no. 1, pp. 1282-1295, 2023.

[22] S. A. Khan, "Enhancing the mechanical properties of fibre-reinforced concrete through sustainable mix design: effects of fibre type and dose," *Discover Civil Engineering*, vol. 1, no. 1, p. 88, 2024.

[23] C. G. Christopher, R. Gopal, S. Sadasivam, A. Devi Keerthika Esakki, and P. Dinesh Kumar, "Experimental toughness and durability evaluation of FRC composite reinforced with steel–polyester fiber combination," *International Journal of Concrete Structures and Materials*, vol. 17, no. 1, p. 39, 2023.

[24] R. I. Annually, "Astm standards," 1995.

EFFECT OF CURING METHOD ON COMPRESSIVE STRENGTH OF MORTAR CONTAINING TIN TAILING AS FINE AGGREGATE REPLACEMENT

[a] Norasyimah Ahmad*, [b] Khairunisa Muthusamy, [c]Nor Rashidah Bahar

a: Faculty of Civil Engineering and Technology, Universiti Malaysia Pahang Al-Sultan Abdullah, 26300 Kuantan, Malaysia.
syima484@gmail.com
b: Faculty of Civil Engineering and Technology, Universiti Malaysia Pahang Al-Sultan Abdullah, 26300 Kuantan, Malaysia.
pro@umpsa.edu.my
c: Faculty of Engineering Technology, Universiti Tun Hussien Onn Malaysia Higher Education Hub, 84600 Pagoh, Malaysia.
eftk@uthm.edu.my
* Corresponding author

Abstract- Sand mining leads to various environmental issues due to the extensive use of sand in cement mortar production. Concurrently, tin tailing (TT), a mining industry byproduct, accumulate rapidly and contribute to environmental pollution when disposed of in dumping sites. This study explores the sustainable recycling of TT by partially replacing fine aggregates in mortar and examines the influence of curing methods on the compressive strength of TT-incorporated mortar. Mortar specimens with varying TT replacement levels (0–100%) were cured under two conditions: air curing and water curing, and tested at 7, 28, 60, 90, and 180 days. Results demonstrate that water curing significantly improves compressive strength compared to air curing, attributed to enhanced hydration. An optimal TT replacement of 20% was identified, providing the highest strength under both curing regimes, while higher TT contents led to strength reductions due to altered microstructure and moisture behavior. These findings underscore the importance of curing techniques in optimizing the mechanical performance of TT- based mortars and support the environmentally responsible reuse of mining waste, reducing reliance on natural sand and promoting sustainable construction practices.

Keywords- Compressive Strength, Curing Regimes, Mortar, Tin Tailing

1 Introduction

Mortar is one of the oldest and most fundamental construction materials, widely used globally to bind bricks and blocks in various structures. It is composed of fine aggregates, cement, and water, which harden to form a durable composite [1]. The rapid urbanization and infrastructure development in the 21st century have significantly increased the demand for mortar, making it one of the most commonly used cement-based materials in construction [2]. However, the extensive use of mortar has raised environmental concerns, primarily due to the excessive extraction of natural sand, a key ingredient in mortar production. Sand mining can lead to severe ecological issues such as riverbank erosion, habitat destruction, and increased risk to local communities. Consequently, there is an urgent need to identify sustainable alternatives that can reduce reliance on natural sand without compromising the mechanical performance of mortar [3].

Malaysia's Construction Industry Development Board (CIDB) and Public Works Department (PWD) have launched the Malaysian Carbon Reduction and Environmental Sustainability (MyCREST) [4] initiative, which aims to mitigate the

environmental impact of the built environment through carbon emission reduction and holistic life cycle management (CIDB, 2020) [4]. One promising approach aligned with these sustainability goals is the incorporation of industrial byproducts as recycled materials in mortar production, which helps conserve natural resources and reduce waste disposal [5], [6] and [7].

Tin tailing is a waste product generated from tin mining activities, is accumulating rapidly and poses environmental pollution risks when disposed of in dumping sites. Utilizing TT as a partial replacement for fine aggregate in mortar can provide a dual benefit: reducing environmental pollution caused by mining waste and minimizing the depletion of natural sand resources. This study investigates the potential of TT as a sustainable alternative fine aggregate in mortar, contributing to eco-friendly construction practices and supporting Malaysia's commitment to environmental sustainability. The curing regime significantly impacts the performance of cement-based materials, including mortar and concrete [8]. Proper curing ensures adequate hydration of cement, which directly influences the development of compressive strength [9] [10].

2 Research Methodology

2.1 Materials and Mortar Mix Proportion

The mortar specimens for this study were formulated using Ordinary Portland Cement (OPC), natural sand, water, and TT as a partial fine aggregate replacement. The ordinary Portland cement, was procured from a local supplier and complies with the specifications outlined in BS EN 197-1 [11] . The fine aggregates were subjected to particle size classification using a sieve shaker, with only particles passing the 1.18 mm sieve and retained on the 150 µm sieve selected for incorporation into the mortar mix to ensure appropriate gradation. Tap water was employed throughout the experimental procedures The TT used in this investigation was collected from a tin mining site located in West Malaysia, serving as a sustainable alternative fine aggregate source. Figure 1 shows the raw materials used in the mortar mix preparation.



Figure 1: Raw materials used

The control mortar mix (TT-0) was formulated using standard materials: cement, water, and sand. For the mortar incorporating TT, five different replacement levels of fine aggregate with TT were prepared, specifically at 20%, 40%, 60%, 80%, and 100%, designated as TT-20, TT-40, TT-60, TT-80, and TT-100, respectively. The water-to-cement ratio was consistently maintained at 0.65 across all mixes. The target compressive strength for these mortar formulations was set at 20 MPa. The detailed proportions are shown in Table 1.

Table 1 Mix Proportion (kg/m^3)

Mixes	Cement (kg)	Water (kg)	Sand (kg)	TT (kg)
TT-0	240	156	600	0
TT-20	240	156	480	120
TT-40	240	156	360	240
TT-60	240	156	240	360
TT-80	240	156	120	480
TT-100	240	156	0	600

2.2 Testing

A compressive strength test was performed to evaluate the maximum load and compressive capacity of the hardened cement mortar. In this study, the test was conducted on mortar cubes following the ASTM C109-21 (2021) standard [12]. A compression testing machine was used to determine the optimum mortar mix design incorporating TT as a partial replacement for sand. Six mortar mixes with varying TT replacement levels, 0% (control), 20%, 40%, 60%, 80%, and 100% were prepared and subjected to both air curing and water curing regimes. A total of 180 cubes, each measuring 50 x 50 x 50 mm, were cast and tested at curing ages of 7, 28, 60, 90, and 180 days, with three specimens per mix at each age. The compressive strength of the mortar cube samples was measured using a compression testing machine, depicted in Figure 2(a). The specimens were carefully placed between the loading plates, as shown in Figure 2(b), and a uniform load at a rate of 140 kg/cm² per minute until failure occurred. The compressive strength was calculated by dividing the failure load by the cross-sectional area of the specimen, formula shown in Equation (1).

$$F_m = \frac{P}{A} \qquad (1)$$

Where,

F_m= compressive strength, (N/mm2)

P = maximum indicated load, (N)

A = surface area of specimen, (mm2)

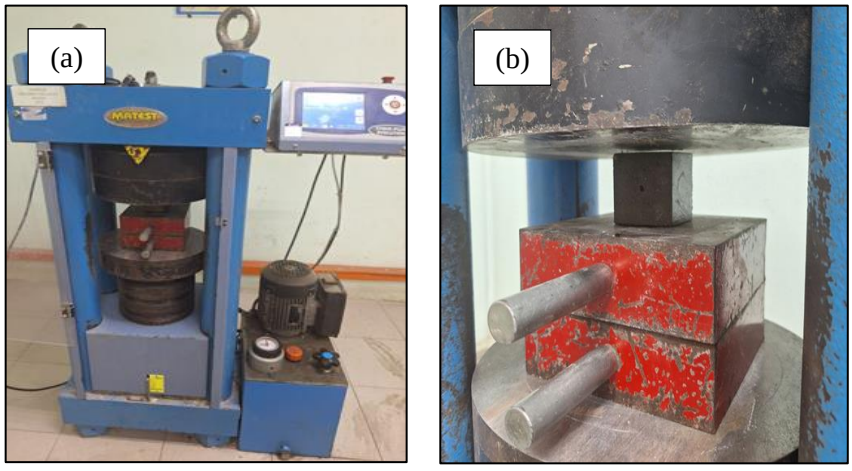


Figure 2: Compressive strength test of mortar cube samples

3 Results

3.1 Compressive Strength

The compressive strength results for the control mortar and mortar specimens incorporating TT as a partial fine aggregate replacement at various curing intervals (7, 28, 60, 90, and 180 days) under both water and air curing conditions are presented in Figures 3 and 4, respectively. The mortar mix containing 20% TT subjected to water curing exhibited the highest compressive strength of 30.47 MPa at 28 days (matured period), surpassing the control mix, which recorded 28.33 MPa, as well as all other replacement levels. This trend persisted throughout the entire curing duration. Similarly, air-cured specimens with 20% TT replacement achieved the highest compressive strength of 27.58 MPa at 28 days, outperforming other mixtures. Consistent with findings by Zhao et al. [13], these results indicate a progressive increase in compressive strength with curing age, reflecting ongoing hydration and matrix densification.

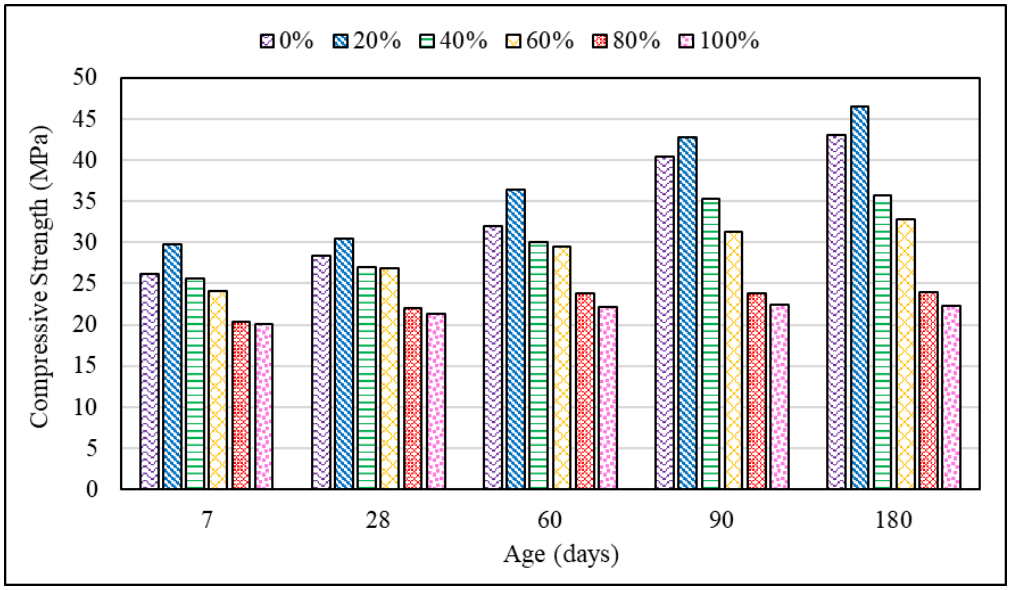


Figure 3: Tin tailing mortar compressive strength result – water curing

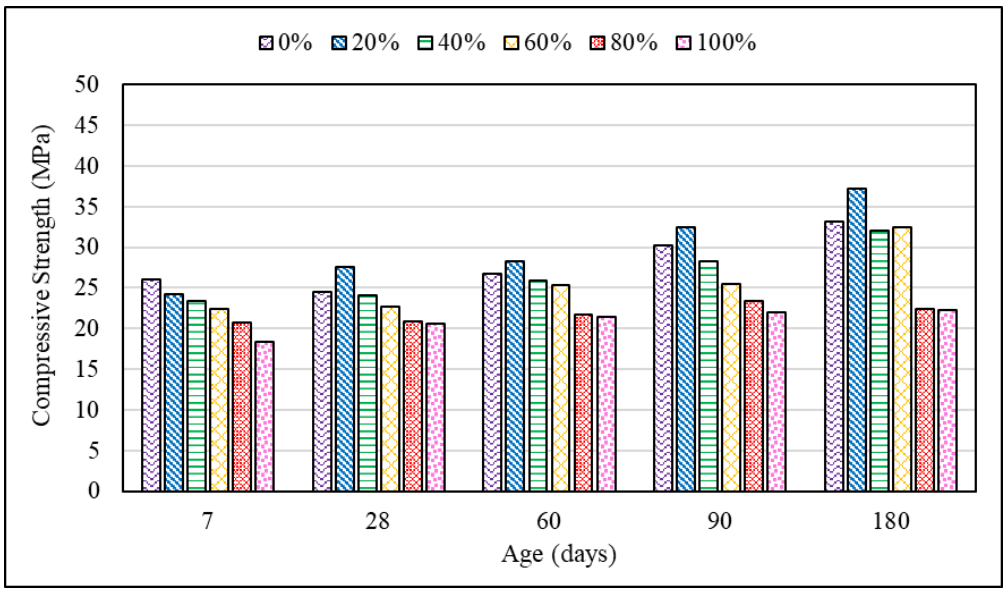


Figure 4: Tin tailing mortar compressive strength result – air curing

The incorporation of TT significantly influences strength development across all mixtures. A 20% TT replacement optimally enhances compressive strength under both water and air curing regimes. This improvement is attributed to increased packing density and reduced void content within the mortar matrix, as supported by Cai [14], and Essam et al. [15] who reported that moderate replacement levels of alternative materials or industrial wastes improve mechanical performance by optimizing particle packing. However, at higher TT replacement levels (40%, 60%, 80%, and 100%), the compressive strength of water-cured specimens at 28 days declined progressively to 27.02 MPa, 26.86 MPa, 22.06 MPa, and 21.30 MPa, respectively. Correspondingly, air-cured specimens with these replacement levels exhibited lower strength values of 24.15 MPa, 22.67 MPa, 20.89 MPa, and 20.61 MPa, respectively, all inferior to their water-cured counterparts. These observations align with previous studies by Hasan et al. [16] and Vo et al [17], which reported that excessive substitution of fine aggregates with waste materials adversely affects mortar strength.

Regarding the effect of curing methods on specimen performance, water-cured samples consistently exhibited superior compressive strength throughout the curing period. Specifically, the 20% TT water-cured mix attained a compressive strength of 46.43 MPa at 180 days, significantly exceeding the 37.21 MPa recorded by the corresponding air-cured specimen. The enhanced strength development under water curing is attributed to the sustained availability of moisture, which facilitates continuous hydration and the formation of calcium silicate hydrate (C-S-H) gel, thereby densifying and strengthening the mortar matrix. In contrast, air curing restricts hydration due to limited moisture availability, resulting in comparatively lower strength gains [18].

3.2 Interaction Between Curing Age and Tin Tailing Percentages on Mortar's Compressive Strength Using Response Surface Methodology (RSM)

The Response Surface Methodology (RSM) was employed to examine the influence of curing time (days) and TT percentage (%) on the compressive strength (MPa) of mortar. Statistical analysis of the model's significance level ($p < 0.05$) confirmed its reliability, while an adjusted R^2 value close to 1 indicated strong model accuracy and predictive capability [19], [20].

3.2.1 Water Curing

The compressive strength of water-cured mortar was accurately predicted using a two-factor interaction (2FI) regression model. The model showed a good fit, confirmed by ANOVA results with an R^2 of 0.9000, a predicted R^2 of 0.8267, and a p-value of 0.0271 as can be seen in Table 2. These statistics indicate a strong relationship between curing time, TT percentage, and compressive strength.

Table 2 P-value and model summary statistic for compressive strength of mortar cured in water

Source	p-value	Std. Dev	R^2	Adjusted R^2	Predicted R^2	remark
Linear	0.0002	3.52	0.8228	0.7874	0.6485	
2FI	0.0271	2.79	0.9	0.8667	0.8267	Suggested
Quadratic	0.1089	2.3	0.9469	0.909	0.7434	
Cubic	0.0943	1.21	0.9937	0.9749	-0.2437	

Figure 5 displays 3D and 2D response surface plots that demonstrate how curing time and TT percentage interact. The 3D plot shows that compressive strength increases with longer curing times but decreases as TT content rises. The 2D contour plots support this, highlighting higher compressive strength in water-cured samples with longer curing and lower TT levels, shown by the red and orange areas.

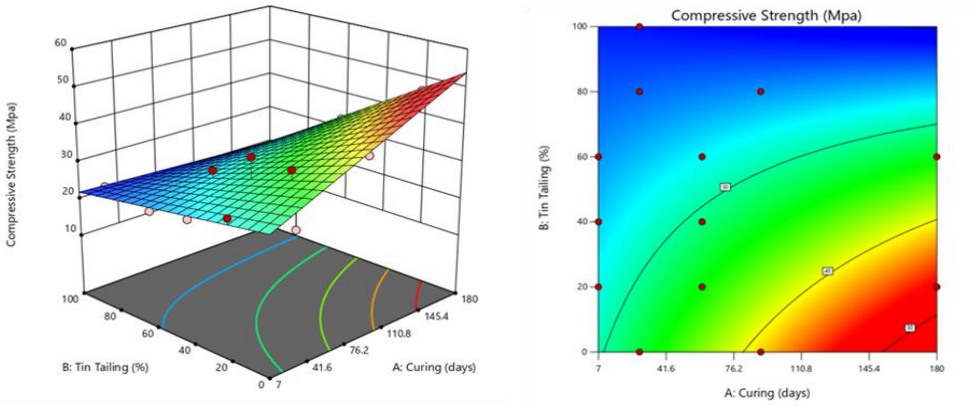


Figure 5:3D and 2D response surface plots of compressive strength indicating effects of curing days and percentage of TT for water curing

3.2.2 Air Curing

The compressive strength of air-cured mortar was modelled using a quadratic regression, which demonstrated a strong fit with an R^2 of 0.9846, a predicted R^2 of 0.9066, and a p-value of 0.0359, as shown in Table 3. These results confirm the significant effect of the studied factors.

Table 3 P-value and model summary statistic for compressive strength of mortar cured in air

Source	p-value	Std. Dev	R^2	Adjusted R^2	Predicted R^2	remark
Linear	< 0.0001	1.26	0.9428	0.9314	0.8906	
2FI	0.0789	1.11	0.9602	0.9469	0.9051	
Quadratic	0.0359	0.7829	0.9846	0.9736	0.9066	Suggested
Cubic	0.0833	0.3936	0.9983	0.9933	0.9199	

Similar to water-cured mortar, air-cured samples showed increased compressive strength with longer curing times, while higher TT content led to reduced strength. However, as illustrated in Figure 7, air-cured mortar generally exhibited lower compressive strength compared to water-cured samples.

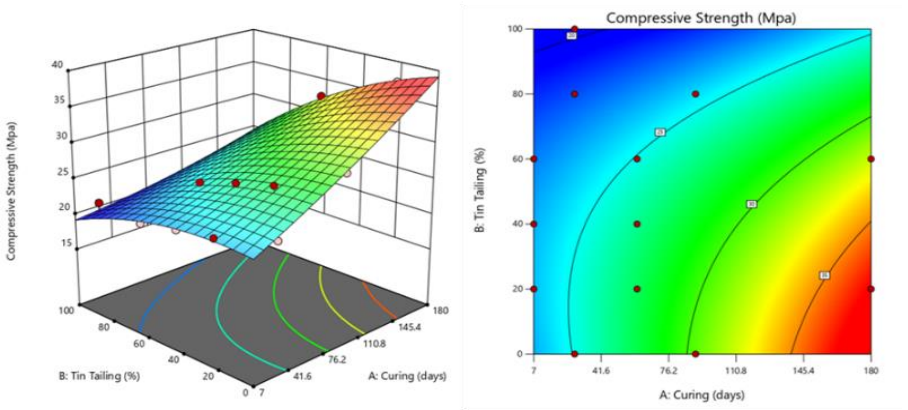


Figure 6: 3D and 2D response surface plots of compressive strength indicating effects of curing days and percentage of TT for air curing

4 Practical Implementation

The findings of this study provide valuable guidance for the practical use of TT as a partial replacement for fine aggregate in mortar, emphasizing the critical role of curing methods on compressive strength development.

5 Conclusion

This study confirms that the curing method significantly affects the compressive strength of mortar when tin tailing (TT) is used as a fine aggregate replacement. Water curing consistently yields higher compressive strength than air curing, attributed to enhanced cement hydration and a more compact microstructure. Notably, a 20% replacement level of TT was identified as optimal, providing substantial improvements in mechanical performance. Additionally, utilizing TT supports sustainable construction by recycling mining waste and reducing the demand for natural river sand, thereby helping to protect river ecosystems and prevent erosion. To further advance the practical application of TT-modified mortar, future research should investigate its long-term durability properties such as shrinkage, creep, and resistance to chemical attack, as well as its behaviour under fire conditions. These efforts will help establish a comprehensive understanding of TT mortar's performance in diverse construction scenarios.

Acknowledgment

We would like to express our sincere appreciation to Universiti Malaysia Pahang Al-Sultan Abdullah, Malaysia, for their support in facilitating this research. The authors also wish to thank the Ministry of Higher Education for sponsoring their study through the Hadiah Latihan Persekutuan program.

References

[1] A. Surahyo, *Concrete Construction: Practical Problems and Solutions*. Springer International Publishing, 2019. doi: 10.1007/978-3-030-10510-5.

[2] Biernacki, J. J., Bullard, J. W., Sant, G., Brown, K., Glasser, F. P., Jones, S., & Prater, T., "Cements in the 21 st century: Challenges, perspectives, and opportunities," *Journal of the American Ceramic Society*, vol. 100, no. 7, pp. 2746–2773, Jul. 2017, doi: 10.1111/jace.14948.

[3] M. Singh and R. Siddique, "Effect of coal bottom ash as partial replacement of sand on properties of concrete," *Resour Conserv Recycl*, vol. 72, pp. 20–32, 2013, doi: https://doi.org/10.1016/j.resconrec.2012.12.006.

[4] *CIDB. (2020). MyCREST. Construction Industry Development Board (CIDB).*

[5] B. Manjunath, C. M. Ouellet-Plamondon, B. B. Das, and C. Bhojaraju, "Potential utilization of regional cashew nutshell ash wastes as a cementitious replacement on the performance and environmental impact of eco-friendly mortar," *Journal of Building Engineering*, vol. 66, p. 105941, 2023, doi: https://doi.org/10.1016/j.jobe.2023.105941.

[6] S. Sakir, S. N. Raman, M. Safiuddin, A. B. M. Amrul Kaish, and A. A. Mutalib, "Utilization of by-products and wastes as supplementary cementitious materials in structural mortar for sustainable construction," *Sustainability (Switzerland)*, vol. 12, no. 9, 2020, doi: 10.3390/su12093888.

[7] Z. Zhang, X. Liu, R. Hu, C. Liang, Y. Zhang, and Z. Ma, "Mechanical behavior of sustainable engineered cementitious composites with construction waste powder as binder and sand replacement," *Constr Build Mater*, vol. 404, p. 133185, 2023, doi: https://doi.org/10.1016/j.conbuildmat.2023.133185.

[8] D. Xu, J. Tang, X. Hu, C. Yu. F. Hang, S. Sun, W. Deng and J. Liu, "The influence of curing regimes on hydration, microstructure and compressive strength of ultra-high performance concrete: A review," *Journal of Building Engineering*, vol. 76, p. 107401, Oct. 2023, doi: 10.1016/J.JOBE.2023.107401.

[9] A. I. Muhammad, D. Shashivendra, U. Abhishek, S. I. Umar, S.U. Salihu, Z.I. Idris and A.I Ibrahim, "A Review on the Curing of Concrete using Different Methods," *International Journal of Mechanical and Civil Engineering*, vol. 7, no. 2, pp. 15–25, Sep. 2024, doi: 10.52589/IJMCE-4ENVMZOX.

[10] B. O. Orogbade, E. A. Adetoro, and G. M. Amusan, "The evaluation of the effects of different curing methods on concrete," *Scientia Africana*, vol. 23, no. 3, pp. 115–126, Sep. 2024, doi: 10.4314/sa.v23i3.11.

[11] "BS EN 197-1. (2000). Cement —Part 1: Composition, specifications and conformity criteria for common cements. In British Standard."

[12] ASTM C109, "ASTM C109 / C109M - 20b. Standard Test Method for Compressive Strength of Hydraulic Cement Mortars (Using 2-in. or [50 mm] Cube Specimens)," 2020.

[13] Z. Xu, Z. Zhu, Y. Zhao, Z. Guo, G. Chen, C. Liu, J. Gao and X. Chen, "Production of sustainable plastering mortar containing waste clay brick aggregates," *Case Studies in Construction Materials*, vol. 16, p. e01120, 2022, doi: https://doi.org/10.1016/j.cscm.2022.e01120.

[14] Q. X. Xiong, L. yu Tong, Z. Zhang, C. Shi, and Q. feng Liu, "A new analytical method to predict permeability properties of cementitious mortars: The impacts of pore structure evolutions and relative humidity variations," *Cem Concr Compos*, vol. 137, Mar. 2023, doi: 10.1016/j.cemconcomp.2022.104912.

[15] A. Essam, S. A. Mostafa, M. Khan, and A. M. Tahwia, "Modified particle packing approach for optimizing waste marble powder as a cement substitute in high-performance concrete," *Constr Build Mater*, vol. 409, p. 133845, Dec. 2023, doi: 10.1016/j.conbuildmat.2023.133845.

[16] K. Hasan, M. Rahaman, M. Ali, M. Urmi, N. Farisha, M. Islam, T. Nahar and F. Yahaya, "A comprehensive review of the application of waste tire rubber in concrete/mortar as fine aggregate replacement," *Architecture, Structures and Construction*, vol. 4, no. 1, pp. 91–111, Mar. 2024, doi: 10.1007/s44150-023-00102-y.

[17] D.-H. Vo, T.-M. Ngo, N.-L. Phan, K.-D. T. Thi, and T. T. H. Truong, "A Study of Characteristics of the Mortar Produced from Waste Ceramic as a Fine Aggregate Replacement," in *2023 8th International Scientific Conference on Applying New Technology in Green Buildings (ATiGB)*, IEEE, Nov. 2023, pp. 217–220. doi: 10.1109/ATiGB59969.2023.10364478.

[18] Z. Hussain, W. Ansari, M. Akbar, A. Azam, Z. Lin, A. Yosri and W. Shaaban, "Microstructural and mechanical assessment of sulfate-resisting cement concrete over portland cement incorporating sea water and sea sand," *Case Studies in Construction Materials*, vol. 21, Dec. 2024, doi: 10.1016/j.cscm.2024.e03689.

[19] M. I. Ejimofor, I. G. Ezemagu, and M. C. Menkiti, "RSM and ANN-GA modeling of colloidal particles removal from paint wastewater via coagulation method using modified Aguleri montmorillonite clay," *Current Research in Green and Sustainable Chemistry*, vol. 4, Jan. 2021, doi: 10.1016/j.crgsc.2021.100164.

[20] C. Onyutha, "From R-squared to coefficient of model accuracy for assessing "goodness-of-fits"," May 04, 2020. doi: 10.5194/gmd-2020-51.

DEVELOPMENT AND PERFORMANCE OF PAPERCRETE AS AN ECO-FRIENDLY CONSTRUCTION MATERIAL

[a] Moiz Ali Haider*, [b] Subhan Shafique, [c] Muhammad Zohaib Asim

a: Civil Engineering Dept., National University of Technology, NUTECH, Islamabad, Pakistan. moizalif23@nutech.edu.pk
b: Civil Engineering Dept., National University of Technology, NUTECH, Islamabad, Pakistan. subhanshafiquef22@nutech.edu.pk
c: Civil Engineering Dept., National University of Technology, NUTECH, Islamabad, Pakistan. muhammad.zohaib@nutech.edu.pk
* Corresponding author

Abstract- In view of the increasing need for environmentally friendly building materials, this research examines the impact and features of papercrete (a mixture of shredded recycled paper added to concrete) as a green and innovative partial substitute for conventional concrete. The study investigates the material's feasibility for sustainable construction, with a primary focus on replacing sand. To evaluate compressive strength, different replacement levels containing 2% and 5% replacement levels of sand and cement were tested under standard curing ages, 5% cement replacement proved the remarkable decrease in compressive strength, pointing towards a deteriorated matrix and weak bonding of particles. In contrast, replacing 2% of the sand had minimal effects on compressive strength, indicating that wastepaper serves as a good lightweight filler material. But sand replacement of 5% started negatively influencing the compressive strength. The results encourage partial use of wastepaper, which can result in a sustainable, lightweight, and economical concrete appropriate for non-structural components such as partition blocks, interior walls, and plastering. The research contributes to the development of green building technology through reframing waste as a precious material.

Keywords- Eco-Friendly Concrete Mix, Papercrete, Sustainable Construction, Waste Paper Reuse

1 Introduction

The construction industry is the largest polluter, utilizing enormous natural resources and generating significant waste products. Among all the biggest building materials made up of cement, water, and sand, i.e., mortar, is among the biggest offenders for the issue. Sand digging in construction has resulted in riverbed stripping, water body alteration, and loss of biodiversity, while cement production is the biggest carbon dioxide emitter in the environment. To tackle this destruction of the environment, researchers and engineers are now turning to developing less destructive materials for use in construction, which will be able to counter environmental pollution. Papercrete is such a novel material where wastepaper is mixed with mortar as a mixture to be added to cement and sand. That 244 million metric tons of wastepaper are generated globally throughout [1], of which the bulk is destined for landfills. Recycling waste paper in construction saves waste and conserves the environment efficiently. Papercrete not only renders an individual independent of traditional materials but also provides functional benefits like lighter material weight, better thermal insulation, and reduced cost of construction. Microstructural development, which was brought about through the incorporation of paper fibers, influences the mechanical and physical behavior of mortar and must be adequately investigated for incorporation into applications.

This study is focused on waste paper as a replacement for sand and examines the physical and mechanical characteristics that are resultant from it, i.e., compressive strength. Although other past research has focused broadly on cement

replacement, this study concentrates more on sand replacement as its primary agenda, a topic of great concern given the unsustainable use of sand mining worldwide. Environmental effects of over-sand quarrying, including erosion, groundwater loss, and habitat destruction, disconnected floodplains are demonstrative of the need for alternative materials[2], [3]. Through the use of waste paper in mortar, the study seeks to minimize the use of natural sand and paper wastage. Partial cement replacement is a minor aspect of the study that explores other environmental benefits. The ultimate aim is to support sustainable and green construction activities through waste management activities and the circular economy. Papercrete can suppress building waste, save natural aggregates, and make greener construction activities on a large scale viable if the product itself is good.

This study addresses the application of papercrete, a combination of mortar and shredded waste paper, as an environmentally friendly product in the building industry. The study aims at the effect of sand with processed paper in mortar. It also addresses the dual problem of environmental degradation resulting from sand excavation as well as the emerging problem of paper waste disposal. Compressive strength was tested to analyze the material's suitability for structural purposes. Cement is the major source of the carbon footprint[4]. The study also explores restrained substitution with cement to quantify additional environmental benefits. Papercrete is able to reduce the weight of the material and improve thermal performance. It aligns with the circular economy rules and promotes the conservation of resources. The study is able to make green building techniques available. The study proposes the possibility of recycling waste in a real application. Papercrete can be a strong green innovation toward sustainable and cost-effective building practice.

2 Literature Survey

The recent studies reviewed the viability of papercrete (an eco-friendly building material made of shredded waste paper, cement, and additives) in replacing conventional concrete. A researcher investigated the properties of the papercrete from a physical and mechanical perspective, stating that waste paper's viability as a construction material is dependent on waste paper decreasing material weight and increasing heat insulation, leading to an advantage [5]. However, the papercrete still does not dominate in compression, which hampers its use. The study highlighted additional refinements that needed to be made. Similarly, another researcher approved paper mills' effluent sludge as a partial substitute for lime in cement mortars with replacement rates of $5\% - 20\%$ [6]. Their findings showed that the structural strength of the mortar was not impaired with replacement up to 10%, making the material suitable for use in wall and ceiling coatings. However, this leads to lower strength from low heat of hydration, making such mixes suitable only for minor masonry repairs.

It is highly expressed that they had similar support through identical findings regarding the investigations they conducted on the papercrete composites of repulped paper fiber, cement, and sand soil. They argued that papercrete has a low density (1.07 gm/cc) and therefore is lightweight, but simultaneously ground such properties like shrinkage of 8-9% and water absorption of 30% or thereabouts [7]. Despite these limitations, the work demonstrated, to some extent, environmental sustainability due to minimizing waste and having a lower carbon footprint through the production of papercrete, as long as proper drying protocols and other measures are undertaken to increase the durability. In addition, a researcher investigated the use of waste paper pulp as a partial replacement for sand and cement in mortar cubes as an effort to reduce both the consumption of sand and the disposal of paper waste. They concluded that a 50% substitution of the sand by paper pulp achieved a 28-day compression strength of 6.6 MPa, lower than traditional mortar, but acceptable for non-bearing applications like partition walls and insulating panels [8].

Another researcher went a step further to define papercrete properties, confirming its lightness and ductility, making it more flexible and less prone to cracks. They also said its compressive strength remains inferior to traditional concrete, thereby restricting the application of this green concrete to non-load bearing structures, such as ornamentation panels, temporary shelters, and sound insulation [9].

This study nicely touches upon multiple important points that were lacking in the former studies on papercrete. Although previous research [5], [7] concentrated on the possibilities that papercrete offered as a light and green material, they provided only anecdotal confirmation of the mechanical strength using different composites. By studying and comparing five different mortar mixes, as 2% and 5% cement and sand were partially replaced with waste paper powder, this exploration gives further clarity to the benefits of the individual material reserves, showing that it is possible to keep the

structural integrity without any problems in the case of partial sand replacement. Former studies [8], [9], while agitating some failings in the area of compressive strength and humidity receptivity, were silent about relative tests with the reference blend. In this study, the experimenters do this, they lay the root for the performance evaluation being carried out. The other exploration [6] concentrated on the operation of paper sludge in mortars, but the focus was on the issue of waste operation, which wasn't covered at low relief rates. This is what the current study has accepted. This study has incompletely answered the standardization issue raised in the former workshop, as they have now easily defined the blend rates, and they have completely explained the mixing, molding, curing, and testing processes.

3 Research Methodology

3.1 Paper Fibers Preparation

Waste paper from offices is collected and soaked in water for a whole day and then blended in a domestic blended until it becomes like a paste which is named as paper pulp as shown in figure 1(a). Paper pulp is dried for 24 hrs in lab oven at 100^0c as a result it comes in a form of small hard balls and then grinded in a domestic grinder to make it a powder. As a result, the paper comes in form of small fibers as shown in figure 1(b).

a)  b) 

Figure 1: Paper fibers preparation, a. Blending paper, and b. Final product

3.2 Materials

Once the recycled paper components were ready, papercrete specimens were prepared by mixing the following components:

1. Ordinary Portland cement.
2. As defined in ASTM-C109/C109M utawa sand is used[10].
3. Paper powder for which preparation is already defined is used.
4. Simple tap water is used for hydration purpose.

Table 1:Mix Proportions

Mix Name	Cement (g)	Paper (g)	Sand (g)	Water (g)
Mix 1 (A)	250	0	687.5	121
Mix 2 (B)	245	5	687.5	121
Mix 3 (C)	250	13.75	673.75	121
Mix 4 (D)	237.5	12.5	687.5	121
Mix 5 (E)	250	34.375	653.125	121

3.3 Specimen Preparation

The mortar mix's proportions were predetermined, and waste paper was added as needed. These mixes were prepared using mechanical mixer as shown in figure 2(a) in accordance with ASTM C109/C109M[10], which describes the standard procedure for testing hydraulic cement mortars. The quantities of materials used for the different mix variations are listed in Table 1. In accordance with ASTM C109/C109M[10], 2-inch mortar cubes were cast for testing as shown in figure 2(b). Before casting, the cube molds were cleaned and lightly oiled to facilitate demolding. The mortar was then poured into the molds in two layers, each of which was compacted using thirty-two tamping strokes to ensure proper consolidation and uniformity.

The mortar cubes were left at room temperature for 24 hours following casting in order to facilitate the initial setting. After the initial setting period, the cubes were carefully demolded and transferred to a curing environment. Over the course of the seven-day curing period, the mortar was adequately hydrated and strengthened. The cubes were removed from the curing chamber and left outside for an additional twenty-four hours following the curing period. This step allowed excess surface moisture to evaporate, ensuring the specimens were dry before further testing and analysis.

a)  b) 

Figure 2: Casting the molds, a. Mechanical mixing, and b. Casted cubes

3.4 Testing Procedure

In compliance with ASTM-C109/C109M[10] specifications, mortar cubes were tested for individual compressive strength using a compression testing machine (CTM) after three days of curing as shown in figure 3(a). The test was conducted under strict supervision to ensure accuracy and consistency in the findings. The cube was carefully inserted into the machine, and the load was progressively increased until the mortar cube failed as shown in figure 3(b). Using the measured compressive strength values, the impact of substituting cement and sand in the mortar cube on compressive strength was evaluated.

a)  b) 

Figure 3: Compression Testing, a. Testing setup, and b. Tested cube

4 Results

4.1 Compression Test Results

Compressive tests validate the impact of sand and cement replacement with waste paper on mortar cube strength. The control mix with no replacement exhibited the highest compressive strength because it reiterated the importance of traditional cement and sand for achieving structure and integrity in building materials. When waste paper replaced cement at even 2% replacement, there was sure loss of strength, that is, binding tendency of cement is necessary for providing the load-carrying ability of mortar supply. When there was a replacement of cement with 5%, there was dramatic fall-off, that is, high levels of replacement lower matrix strength and lower particle-to-particle bond. But 2% replacement of sand had minimal impact on compressive strength as shown in table 2, thus waste paper in small percentages can be utilized as a filler without affecting performance. But in 5% replacement of sand, strength started to decrease, but not as much as when cement was replaced. This suggests that although paper-like materials can replace some of the sand with minimal loss of structure, cement replacement has a far greater adverse effect.

Table 2: Compressive Strength

Mix Name	Replacement	Compressive strength (MPa)
Mix 1 (A)	No Replacement	7.95
Mix 2 (B)	2% cement	4.1
Mix 3 (C)	2% sand	7.3
Mix 4 (D)	5% cement	1.1
Mix 5 (E)	5% sand	3.95

Graphical representation of effect on compressive strength of mortar shown in figure 4. Red color is representing compressive strength of reference mix and blue color is representing compressive strength of mortar cubes with replacement.

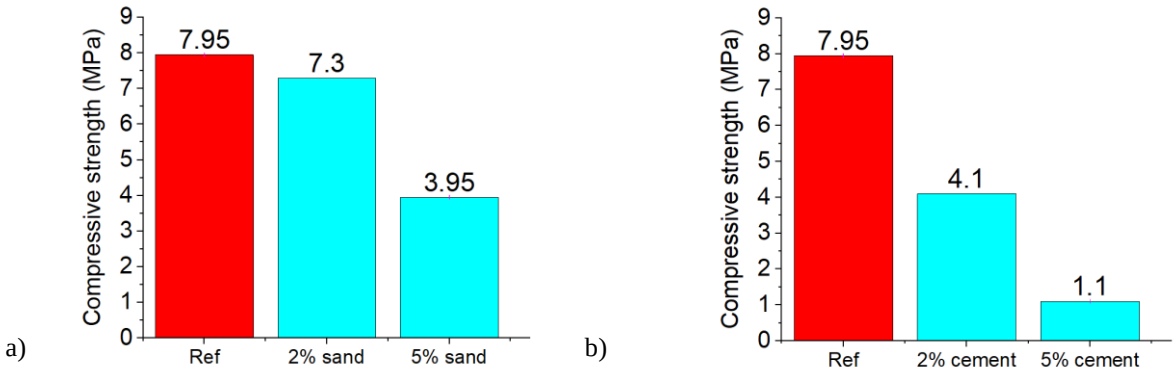


Figure 4: Effect of replacement on compressive strength, a. Sand replacement, and b. Cement replacement

5 Practical Implementation

Papercrete developed by partial replacement of sand and cement with waste paper in mortar is a highly promising approach for sustainable building. It can be successfully used in many non-load-bearing element like partition wall, internal plastering, and boundary wall especially where high structural strength is not the major consideration. The applicability of papercrete can be highly increased by optimizing the materials with further research. Improving its water resistance, durability, and mechanical properties might unlock the potential for more extensive uses. With advances in material science the production of paper-based composite blocks and prefabricated panels might become a viable reality for modular

construction in the near future. While with increasing global focus on climate change and sustainable development, papercrete emerges as the building material of the future combining a distinct eco-friendliness like waste elimination with practical advantage in construction.

6 Conclusion

On the Basis of the above experimental work results in this investigation, the following conclusions can be drawn:

- Substitution of sand had minimal impact on papercrete compressive strength demonstrating that waste paper in small quantity can serve as a filler without affecting performance.
- Waste paper increase results in compressive strength decrease.
- 2% and 5% cement replacement cause a high reduction in compressive strength which makes it unable for non-structural use also.
- 5% sand replacement also reduces the compressive strength by 50% which can be used for non – structural elements only.
- 2% sand replacement had a minimal effect on compressive strength and can be used for load bearing structures with slight modifications.

More research, though, is needed on the following areas:

- Admixtures can be used to improve setting and bonding qualities.
- Alteration in the proportion of the mix in order to realize optimum qualities.
- Incorporation of silicon, sealer concrete or epoxy resin would make papercrete waterproof.
- With additional investigation into durability water resistance and volume production processes, papercrete also stands the opportunity of being widely adopted as an element of green building processes.
- Papercrete should be assessed for the long-term performance and resistance to environmental degradation before use as paper-based materials notoriously susceptible to moisture and biodegradation.

Acknowledgment

We gratefully acknowledge the National University of Technology (NUTECH), Islamabad, Pakistan, for providing the resources and facilities that supported this research.

References

[1] W. Wolska and E. Małachowska, "Paper recycling as an element of sustainable development," *Annals of WULS, Forestry and Wood Technology*, vol. 123, pp. 66–75, Sep. 2023, doi: 10.5604/01.3001.0054.1351.
[2] G. M. Kondolf and M. L. Swanson, "Channel adjustments to reservoir construction and gravel extraction along Stony Creek, California," *Environmental Geology*, vol. 21, no. 4, pp. 256–269, 1993, doi: 10.1007/BF00775916.
[3] G. M. Kondolf, "PROFILE: Hungry Water: Effects of Dams and Gravel Mining on River Channels," *Environ Manage*, vol. 21, no. 4, pp. 533–551, 1997, doi: 10.1007/s002679900048.
[4] S. Thanappan, W. Ararsa, H. Kassu, Y. Terefe, H. A. Muhammed, and H. Hailu, "Papercrete Technology: Tool For A Modern Construction," 2021.
[5] T. Cardinale, M. D'Amato, R. Sulla, and N. Cardinale, "Mechanical and physical characterization of papercrete as new eco-friendly construction material," *Applied Sciences*, vol. 11, no. 3, p. 1011, 2021.
[6] A. R. G. De Azevedo, J. Alexandre, G. de C. Xavier, and L. G. Pedroti, "Recycling paper industry effluent sludge for use in mortars: A sustainability perspective," *J Clean Prod*, vol. 192, pp. 335–346, 2018.
[7] J. Sheth and S. Joshi, *Paper Crete: A Sustainable Building Material*. 2015.
[8] R. Bochare, M. Dagliya, B. Sharma, and F. Shaikh, "Experimental Investigation on Waste Paper-pulp Infused Cement Mortar," in *IOP Conference Series: Earth and Environmental Science*, IOP Publishing, 2023, p. 012006.
[9] Y. D. Shermale and M. B. Varma, "Papercrete: A Lightweight Concrete," *Aurangabad, Maharashtra, India*, 2016.
[10] "Standard Test Method for Compressive Strength of Hydraulic Cement Mortars Using 2-in. or [50-mm] Cube Specimens," ASTM International.

RECYCLED NYLON FIBERS FOR CRACK CONTROL IN HIGH STRENGTH CONCRETE- A USE CASE IN POWERHOUSE

[a] Umar Zakria*, [b] Riaz Ul Haq

a: Mott MacDonald International, Pakistan. umar.zakria@gmail.com
b: Salalam Al Jazeera Construction, Saudi Arabia. engr.riaz77@outlook.com
* Corresponding author

Abstract- Shrinkage cracking in concrete structures, particularly in ultra-high strength concrete used in large-scale infrastructures such as hydropower powerhouse buildings, poses a significant threat to structural integrity and long-term durability. This review explores the effectiveness of nylon fiber-reinforced concrete (NFRC) in mitigating shrinkage-induced cracking. Findings from experimental studies show that incorporating nylon fibers (NF) at concentrations above 2% by volume reduces shrinkage by up to 5% compared to conventional concrete. Additionally, using an optimized water-cement ratio, such as 0.42, in combination with carefully selected NF content, was shown to significantly reduce crack length with an increase of just 0.05% in NF content lowering crack length to 52 mm. The review highlights the critical role of fiber length and type, demonstrating that synthetic fibers (12–54 mm) improve shrinkage resistance, with 54 mm fibers achieving a 62.4% reduction. However, excessive fiber dosage (beyond 1.5%) may lead to void formation and reduced compaction. The incorporation of recycled nylon fibers from waste materials such as fishing nets and textiles not only improves post-cracking toughness and tensile strength but also promotes environmental sustainability. Field applications in hydropower projects have validated NFRC's resilience under thermal and moisture variations, achieving a significant reduction in maintenance costs over a decade. In conclusion, NFRC presents a promising solution for enhancing durability and sustainability in high-performance concrete structures, particularly in critical infrastructure applications.

Keywords- Shrinkage cracks, Nylon fibers, NFRC, Hydropower

1 Introduction

Concrete is a fundamental construction material due to its high strength, but it lacks ductility. Despite being a major component in construction, concrete is prone to cracking to various types of cracks which impact its structural integrity, accelerates fatigue-mode failures and thereby results in significant repair costs and wastes [1], [2]. United States alone bears an annual cost of $20 billion for the concrete repairs whereas, for Australia it turned out be $8 billion per annum for steel corrosion repairs and maintenance in concrete [2]**.** Considering the economics of the issue, many researchers are developing techniques to mitigate the risks of concrete cracking, including the use of polyamide or polypropylene fibers (nylon thread) as reinforcing agent in the concrete mixture design.

Although, in the presence of various other cracking issues, shrinkage remains a critical phenomenon in mix design deals with both plastic and hardening properties of concrete. Cracks resulting due to shrinkage, mostly occur on the surface of the concrete due to moisture loss and temperature fluctuations, posing significant challenges in maintaining the durability and strength of concrete structures [3, 4]. This phenomenon is generalized into three basic categories, plastic shrinkage,

autogenous shrinkage, and drying shrinkage [5]. Plastic shrinkage crack occurs in initial hours of laying concrete usually from within a day up to 3 days after concrete placement and appear as narrow, hairline cracks due to rapid moisture loss. Whereas, autogenous also termed as hydration shrinkage is a result of self-desiccation process [6] when concrete experience decreases in internal humidity due to rapid hydration of cement. On the other hand, drying shrinkage refers to reduction on concrete volume when water bleeds from the surface, leaving internal concrete mass dried. Drying shrinkage cracks, develops weeks or months after hardening and are typically wider and deeper due to gradual moisture loss [7].

The primary mechanisms behind shrinkage include capillary stress, interlayer water evaporation, surface energy, and disjoining pressure. This study systematically reviews the potential of nylon fiber-reinforced concrete (NFRC) in reducing shrinkage cracks, highlighting the importance of selecting appropriate fiber types and sizes.

2 Shrinkage Mechanism

2.1 Shrinkage Dynamics in Cement Matrix

The primary reasons for shrinkage in concrete include capillary stress, interlayer water evaporation, surface energy, and disjoining pressure [8, 9] . When moisture is evaporated from cement mix it creates an imbalance between saturated pressure and vapor. Capillary pressure thus exerting hydrostatic tensile stress leading to irreversible shrinkage as shown in figure-01 [5] . Similarly, capillary pressure also contributes to shrinkage when water is absorbed and desorbed, on the outer film of calcium silicate and hydrate (C-S-H) particles. The interlayer water which is closely bounded with the C-S-H particles, undergoes shrinkage strain on each C-S-H monolayer results in moisture content drop by 25%, The interconnected layer narrows further with substantial volumetric reduction if the moisture further reduces to 12% [8]. This densification of C-S-H particular leads to irreversible shrinkage with the collapsing of small pores.

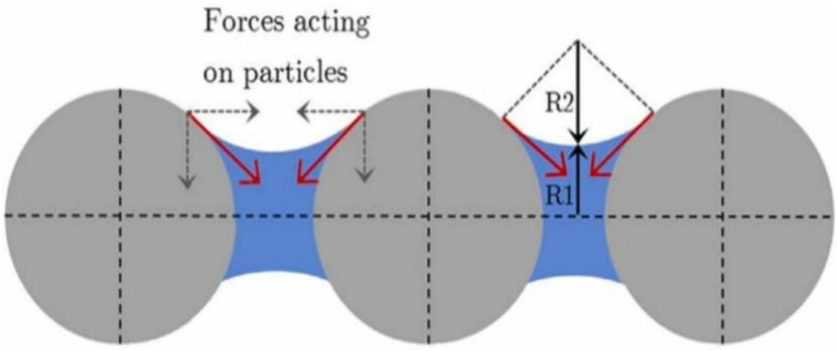


Figure 1: Schematic illustration showing the presence of partially empty pores exerting hydrostatic tensile stress in concrete [2]

2.2 Shrinkage Cracking Issues in Ultra-high Strength Concrete

The primary reason behind various types of shrinkage cracks (plastic shrinkage, thermal shrinkage, autogenous shrinkage, and drying shrinkage) is loss of water in concrete. This water loss is mainly controlled through effective curing or trapping moisture to leave from the surface of the concrete, as indicated in the figure-02. Where certain approaches can easily prevent the shrinkage cracks appearing immediately after concrete pouring. However, shrinkage cracks which are thermally induced due to sudden temperature variations on massive construction elements in dams and powerhouse buildings are unavoidable. This could be one of the two reasons either extremely hot climate conditions where one side of elements exposed to high temperature changes than the other or use of high-strength concrete. In hydropower construction of powerhouse high-strength concrete is very common nevertheless, curing with water or wetting the surface will prevent penetration in the concrete due to low permeability [10]. Comparison of ordinary concrete and high-strength concrete autogenous shrinkage and drying shrinkage in total is illustrated in the figure-03a and 03b.

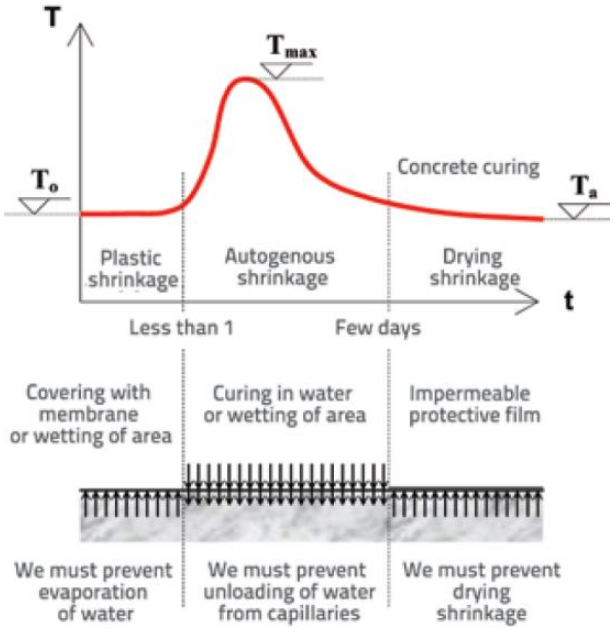
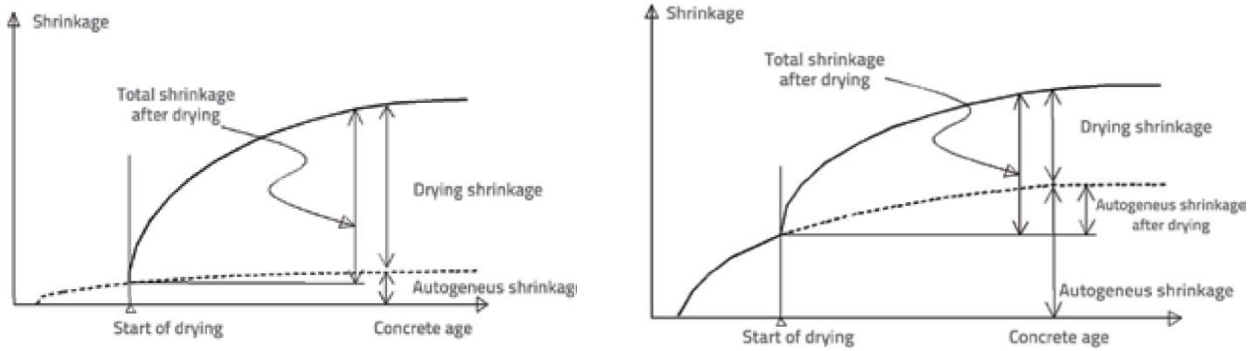


Figure 2: Necessary curing conditions during temperature changes in concrete constructive elements [11]

Shrinkage cracks are a prevalent issue in ultra-high-strength concrete, especially when used in large-scale concrete pours for hydro powerhouse buildings. Various factors contribute to concrete cracks in such structures, including the large size of the concrete mass, high stress concentrations, thermal changes due to humid conditions, and inadequate curing. These factors, either individually or in combination, contribute to shrinkage cracks in hydro powerhouse buildings.



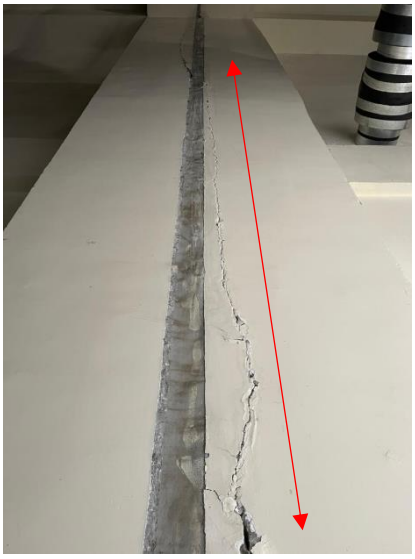
a) Shrinkage in ordinary concrete b) Shrinkage concrete in ultra-high-strength concrete

Figure 3: Shrinkage in (a) ordinary concrete; (b) ultra-high-strength concrete [11]

For example, shrinkage cracks were observed along the expansion joints due to high stress concentrations in units 16 and 17 of Tarbela Dam. Figure-4a shows the cracks on the concrete surface developing from upstream to downstream, possibly due to plastic shrinkage of the concrete, while figure-04b illustrates crack widening with the concrete ageing. The volumetric addition of fibers as fiber reinforced concrete (FRC), preferably nylon or polyamide, could have prevented crack propagation on these expansion joints.



a) Surface crack appearing along expansion joint



b) Crack propagation along unit 17 expansion joint

Figure 4: Shrinkage crack along the expansion joints of Tarbela Dam's 4th Extension (a) unit-16; (b) unit-17

3 Selection of Fiber

3.1 Natural and Synthetic Fiber

To limit the shrinkage crack propagation in high-strength concrete in the construction of powerhouse, possible solutions can be use of admixtures, internal curing agents, and fibers. Before selecting either natural or synthetic fibers for concrete reinforcement, it is crucial to first identify and understand the underlying causes of shrinkage cracks. It has been reported that crack propagation in high strength concrete is primarily due to impermeability, water absorption and rapid temperature changes [12]. Hence, any fiber exhibit high water absorption should not be a preferred option. For example, natural fibers such as jute, coir, sisal, and abaca exhibit high water absorption abilities as compared to synthetic fibers, polypropylene (PP) fibers as illustrated in figure-05 [12]. Amongst all, abaca has the highest water absorption at 95% RH, which could impact the workability of concrete as compared to PP fiber which has the lowest water absorption rate. Other factors in deciding the selection of fiber are their availability nearest to the site location and recycling of these materials.

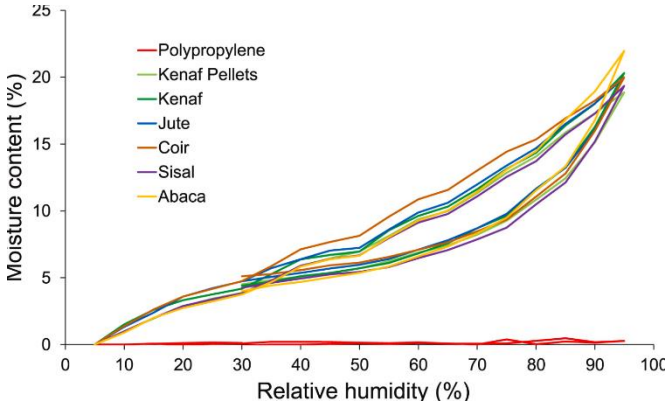


Figure 5: Sorption isotherms of fibers measured at 20 °C [12]

3.2 Recycled Nylon Fiber Reinforced Concrete (NFRC)

In addition to use as a reinforcement material nylon fiber (NF) offers a variety of uses in other sectors. NF possess good wear resistance and high tensile strength, and has excellent water absorption properties [13]. There is an increasing trend in use of synthetic fiber with rapid urban development (estimated at 150–200 MJ/kg of virgin nylon fiber production [14]), whilst the production of large fiber quantities inevitability causing energy consumption and environment pollution eventually generating large amounts of waste to landfills. Not all the NF can be treated to reduce its environmental impact, and recycling often increases its embodied energy. However, if the fiber is recovered from waste materials such as clothes, ropes, fish nets and cots (charpai) from nearby locations, we can achieve better environmental and economic benefits. Previous studies have demonstrated promising contribution of NFRC in improving the compressive properties of concrete [15], [16]. Recycled nylon fiber as NFRC from fishing nets can enhance the tensile strength of motor [17] and toughness as compared to non-fiber reinforced material [18] . Furthermore, waste fiber fabrics from carpets can also influence the permeability of cracked concrete [10], [15]. Consequently, NFRC can effectively enhance the mechanical properties in particular post-cracking behavior and tensile strength as well as provide good elasticity and chemical stability [18, 19], without increasing self-weight of concrete [20].

Studies have shown that NF added by 2% of concrete volume, not only exhibits enhanced mechanical properties but also reduce the permeability and shrinkage by 5% as compared to conventional concrete [20] . NFRC can also control formation of micro crack in large-sized ultra-high-strength [21] used in hydro powerhouse [18, 20] . As opposed to micro-sized nylon fibers, macro nylon fibers offer the same benefits as steel fibers without added weight, suitable for light weight concrete applications. However, when effective stress transfer is essential then macro synthetic fibers are a preferred choice. Therefore, it is critically important to choose the optimal type and size of fiber, whether natural or synthetic, to address the prevalent issues in concrete. Flow chart illustrates in figure-06 governing properties of concrete and proposed solution for controlling shrinkage cracks in ultra-high-strength concrete.

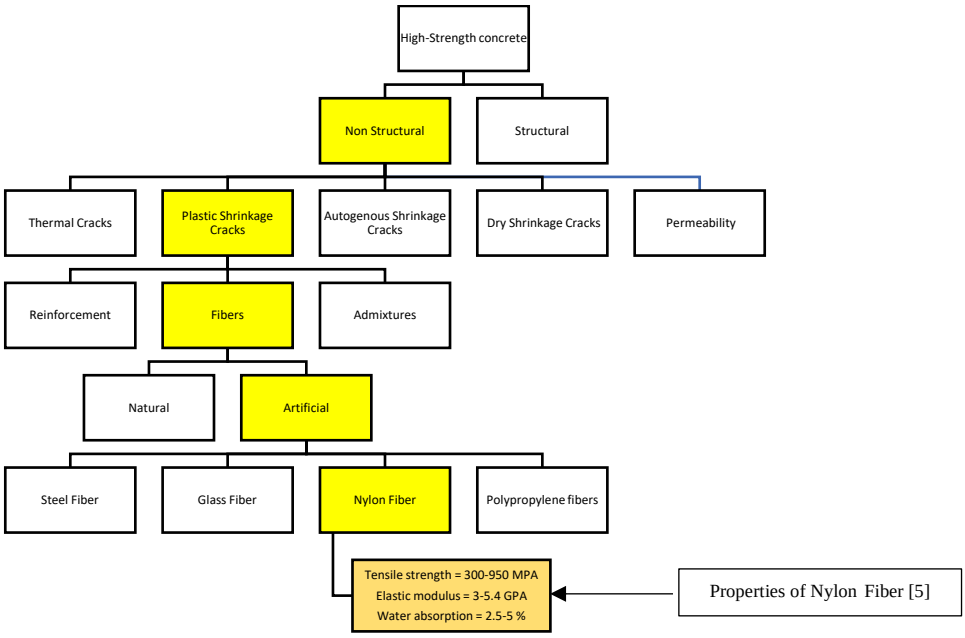


Figure 6: Flow chart representing governing properties for concrete cracking and control with Nylon fibers

3.3 Fiber Preparation

To produce nylon fiber-reinforced concrete (NFRC), the fiber is first cut into uniform lengths of 54 mm with straight ends, all having a nominal diameter of 1.01 mm. The nylon fiber is well-separated before mixing with concrete to avoid consolidation during the mix. Additionally, another sample of fiber is cut to a length of 75mm, maintaining the same nominal diameter as the 1.01mm fiber. Nylon fiber in raw bundle is illustrated in figure-7a, while the preparation of fiber was visually documented in series of figures as illustrated in figure-7b.



a) Raw nylon fiber



b) Nylon fiber cut to form straight fiber

Figure 7: (a) Extraction of raw nylon fiber; and (b) cut in to uniform lengths

4 Factors Affecting Shrinkage in NFRC

4.1 Water-cement Ratio

Water binder ratio is critical in reducing the concrete shrinkage. Increase in water cement ratio can provide sufficient water for evaporation resulting in residual strength improvement. Studies show that addition of 54 mm Nylon fibers with a 0.55 mm diameter reduces shrinkage cracks in concrete by 24.7% and 29.9% at 0.35% and 0.42% ratios, respectively [2]. Table-01 demonstrates using nylon fiber in combination of 12 and 54mm sizes with water cement ratio of 0.42 can mitigate the shrinkage cracks up to 62.4% [2].

Table 1 Impact of Water-Binder Ratio on Concrete Shrinkage [2]

Fiber type - size	Water-Cement Ratio	Shrinkage reduction than the control (%)
Nylon – 54mm	0.35	24.70
Nylon – 54mm	0.42	29.90
Nylon – 12 mm	0.35	8.8
Nylon – 12mm	0.42	21.40
Nylon 12 & 54mm	0.42	62.4

4.2 Volumetric Size of Fiber

Using fiber lengths in different variation can have significant impact on the shrinkage behavior of concrete. Studies reported that increase in fiber length from 6mm to 12mm can reduce shrinkage to 30% [20]. Other findings indicate that 12 mm fibers reduce shrinkage cracks in concrete by 45.8%, while 19 mm fibers achieve up to 30.41% reduction [22], [23]

An increase in fiber volume notably decreases shrinkage in textile fiber-reinforced concrete. For example, incorporating 0.15% fiber volume fraction with 54 mm fibers reduces shrinkage by 30%, while a 0.35% fraction achieves a 60% reduction [20]. However, excessive fiber content can cause agglomeration, leading to voids and increased permeability [2]. Optimum fiber volumetric content in concrete is critical for its shrinkage reduction.

5 Applications of Nylon Fiber-Reinforced Concrete in Hydropower Structures

The inclusion of nylon fibers improves crack resistance by effectively bridging microcracks and redistributing stresses, reducing the risk of shrinkage-induced damage [24]. This is particularly beneficial in hydropower applications, where uncontrolled cracking can lead to seepage, structural weakening, and increased maintenance costs. In canal linings and dam spillways, NFRC with 2–3% fiber content has demonstrated a significant reduction in thermal and drying shrinkage cracks, improving service life and minimizing water loss [25]. The fibers enhance tensile strength, reducing crack propagation under axial and split tensile stresses, which is critical in hydropower infrastructure subjected to cyclic

hydraulic loading. Additionally, NFRC offers corrosion resistance, making it a sustainable alternative to steel reinforcement in aggressive water environments. Unlike steel fibers, nylon fibers and some natural and organic fibers do not rust, ensuring long-term durability in tailrace tunnels, culverts, and spillway aprons [26]. The use of recycled nylon fibers (e.g., from discarded fishing nets) further enhances sustainability, reducing embodied energy while maintaining mechanical performance. Field applications confirm that NFRC is particularly effective in thin-shell structures like tunnel linings, where shrinkage cracking is a major concern [27, 28].

6 Conclusion

This study explored the effectiveness of nylon fiber-reinforced concrete (NFRC) in mitigating shrinkage-induced cracking in concrete. The key conclusions drawn from this study are summarized below

- Use of nylon fiber can reduce shrinkage in concrete by 5%
- Increasing the concentration of nylon fibers from 0.05% to 0.1% can reduce the crack length from 115.2mm to 52mm.
- Exceeding the optimal fiber dosage (>1.5%) can result in adverse effect, disrupting concrete compaction and increasing the number of entrapped voids, which in turn increases shrinkage in concrete.

Based on these findings, this review supports the use of nylon as a synthetic fiber reinforcement material in concrete to effectively reduce micro-cracking in hydropower construction. However, further validation is needed through comprehensive experimental trials, including detailed testing of concrete cylinders and blocks.

Appendix

N/A

Acknowledgment

The author would like to express his sincere gratitude to Dr. Majid Ali from the Civil Engineering Department at CUST and Dr. Khurram Malik from RMIT Melbourne, Australia for their invaluable supervision and continuous support throughout the research work.

References

[1] S. J. Kwon, U. J. Na, S. S. Park, and S. H. Jung, "Service life prediction of concrete wharves with early-aged crack: Probabilistic approach for chloride diffusion," *Structural Safety*, vol. 31, no. 1, pp. 75-83, 2009/01/01/ 2009, doi: https://doi.org/10.1016/j.strusafe.2008.03.004.

[2] N. Gamage, Y. Patrisia, C. Gunasekara, D. W. Law, S. Houshyar, and S. Setunge, "Shrinkage induced crack control of concrete integrating synthetic textile and natural cellulosic fibres: Comparative review analysis," *Construction and Building Materials*, vol. 427, p. 136275, 2024/05/10/ 2024, doi: https://doi.org/10.1016/j.conbuildmat.2024.136275.

[3] K.-K. Yun, "Plastic shrinkage cracking properties of high-performance shotcrete with supplementary cementitious materials," 2022.

[4] B. Holland, P. Alapati, K. E. Kurtis, and L. Kahn, "10 - Effect of different concrete materials on the corrosion of the embedded reinforcing steel," in *Corrosion of Steel in Concrete Structures (Second Edition)*, A. Poursaee Ed.: Woodhead Publishing, 2023, pp. 199-218.

[5] B. Zhang, H. Zhu, P. Feng, and P. Zhang, "A review on shrinkage-reducing methods and mechanisms of alkali-activated/geopolymer systems: Effects of chemical additives," *Journal of Building Engineering*, vol. 49, p. 104056, 2022/05/15/ 2022, doi: https://doi.org/10.1016/j.jobe.2022.104056.

[6] Y. Zhou, H. Du, Y. Liu, J. Liu, and S. Liang, "An experimental study on mechanical, shrinkage and creep properties of early-age concrete affected by clay content on coarse aggregate," *Case Studies in Construction Materials*, vol. 16, p. e01135, 2022/06/01/ 2022, doi: https://doi.org/10.1016/j.cscm.2022.e01135.

[7] B. Zhang, H. Zhu, Y. Cheng, G. F. Huseien, and K. W. Shah, "Shrinkage mechanisms and shrinkage-mitigating strategies of alkali-activated slag composites: A critical review," *Construction and Building Materials*, vol. 318, p. 125993, 2022/02/07/ 2022, doi: https://doi.org/10.1016/j.conbuildmat.2021.125993.

[8] N. P. Tran, C. Gunasekara, D. W. Law, S. Houshyar, S. Setunge, and A. Cwirzen, "A critical review on drying shrinkage mitigation strategies in cement-based materials," *Journal of Building Engineering*, vol. 38, p. 102210, 2021/06/01/ 2021, doi: https://doi.org/10.1016/j.jobe.2021.102210.

[9] K. Aghaee and K. H. Khayat, "Effect of shrinkage-mitigating materials on performance of fiber-reinforced concrete – An overview," *Construction and Building Materials*, vol. 305, p. 124586, 2021/10/25/ 2021, doi: https://doi.org/10.1016/j.conbuildmat.2021.124586.

[10] S. Zhutovsky, K. Kovler, and A. Bentur, "Revisiting the protected paste volume concept for internal curing of high-strength concretes," *Cement and Concrete Research - CEM CONCR RES*, vol. 41, pp. 981-986, 09/01 2011, doi: 10.1016/j.cemconres.2011.05.007.

[11] M. Šahinagić-Isović, G. Markovski, and M. Ćećez, "Shrinkage strain of concrete-causes and types," *Građevinar,* vol. 64, no. 9, pp. 727-734, 2012.

[12] P. Lura, N. Toropovs, J. Justs, M. Shakoorioskooie, B. Münch, and M. Griffa, "Mitigation of plastic shrinkage cracking with natural fibers - kenaf, abaca, coir, jute and sisal," *Cement and Concrete Composites*, vol. 155, p. 105827, 2025/01/01/ 2025, doi: https://doi.org/10.1016/j.cemconcomp.2024.105827.

[13] Y. Qin *et al.*, "Effects of nylon fiber and nylon fiber fabric on the permeability of cracked concrete," *Construction and Building Materials*, vol. 274, p. 121786, 2021/03/08/ 2021, doi: https://doi.org/10.1016/j.conbuildmat.2020.121786.

[14] L. Villalba, R. S. Donalisio, N. E. Cisneros Basualdo, and R. B. Noriega, "Household solid waste characterization in Tandil (Argentina): Socioeconomic, institutional, temporal and cultural aspects influencing waste quantity and composition," *Resources, Conservation and Recycling*, vol. 152, p. 104530, 2020/01/01/ 2020, doi: https://doi.org/10.1016/j.resconrec.2019.104530.

[15] G. Liu, W. Cheng, and L. Chen, "Investigating and optimizing the mix proportion of pumping wet-mix shotcrete with polypropylene fiber," *Construction and Building Materials*, vol. 150, pp. 14-23, 2017/09/30/ 2017, doi: https://doi.org/10.1016/j.conbuildmat.2017.05.169.

[16] S. P. Susan Maria George1, "Study on the Effect of Fibers on Concrete Shrinkage," *Journal of Building Engineering*, vol. Volume: 08 Issue: 07 | July 2021 2021.

[17] P. S. Song, S. Hwang, and B. C. Sheu, "Strength properties of nylon- and polypropylene-fiber-reinforced concretes," *Cement and Concrete Research*, vol. 35, no. 8, pp. 1546-1550, 2005/08/01/ 2005, doi: https://doi.org/10.1016/j.cemconres.2004.06.033.

[18] M. S. Khan, A. Fuzail Hashmi, M. Shariq, and S. M. Ibrahim, "Effects of incorporating fibres on mechanical properties of fibre-reinforced concrete: A review," *Materials Today: Proceedings*, 2023/05/15/ 2023, doi: https://doi.org/10.1016/j.matpr.2023.05.106.

[19] C. Wen, P. Zhang, J. Wang, and S. Hu, "Influence of fibers on the mechanical properties and durability of ultra-high-performance concrete: A review," *Journal of Building Engineering*, vol. 52, p. 104370, 2022/07/15/ 2022, doi: https://doi.org/10.1016/j.jobe.2022.104370.

[20] L. Wang *et al.*, "The influence of fiber type and length on the cracking resistance, durability and pore structure of face slab concrete," *Construction and Building Materials*, vol. 282, p. 122706, 2021/05/03/ 2021, doi: https://doi.org/10.1016/j.conbuildmat.2021.122706.

[21] R. Bagherzadeh, H. R. Pakravan, A.-H. Sadeghi, M. Latifi, and A. A. Merati, "An Investigation on Adding Polypropylene Fibers to Reinforce Lightweight Cement Composites (LWC)," *Journal of Engineered Fibers and Fabrics*, vol. 7, no. 4, p. 155892501200700410, 2012, doi: 10.1177/155892501200700410.

[22] X. Wu, J. Zhou, T. Kang, F. Wang, X. Ding, and S. Wang, "Laboratory Investigation on the Shrinkage Cracking of Waste Fiber-Reinforced Recycled Aggregate Concrete," *Materials*, vol. 12, no. 8, p. 1196, 2019. [Online]. Available: https://www.mdpi.com/1996-1944/12/8/1196.

[23] J. Wei and K. H. Khayat, "Effect of shrinkage-mitigating materials, fiber type, and repair thickness on flexural behavior of beams repaired with fiber-reinforced self-consolidating concrete," *Cement and Concrete Composites*, vol. 156, p. 105868, 2025/02/01/ 2025, doi: https://doi.org/10.1016/j.cemconcomp.2024.105868.

[24] F. Qamar, T. Thomas, and M. Ali, "Improvement in lateral resistance of mortar-free interlocking wall with plaster having natural fibres," *Construction and Building Materials*, vol. 234, p. 117387, 02/01 2020, doi: 10.1016/j.conbuildmat.2019.117387.

[25] M. Khan and M. Ali, "Optimization of concrete stiffeners for confined brick masonry structures," *Journal of Building Engineering*, vol. 32, p. 101689, 2020/11/01/ 2020, doi: https://doi.org/10.1016/j.jobe.2020.101689.

[26] M. Ali, "Role of Post-tensioned Coconut-fibre Ropes in Mortar-free Interlocking Concrete Construction During Seismic Loadings," *KSCE Journal of Civil Engineering*, vol. 22, no. 4, pp. 1336-1343, 2018/04/01/ 2018, doi: https://doi.org/10.1007/s12205-017-1609-3.

[27] A. Afraz and M. Ali, "Effect of Banana Fiber on Flexural Properties of Fiber Reinforced Concrete for Sustainable Construction," *Engineering Proceedings*, vol. 12, p. 63, 12/30 2021, doi: 10.3390/engproc2021012063.

[28] M. U. Farooqi and M. Ali, "Effect of Fibre Content on Compressive Strength of Wheat Straw Reinforced Concrete for Pavement Applications," *IOP Conference Series: Materials Science and Engineering*, vol. 422, no. 1, p. 012014, 2018/09/01 2018, doi: 10.1088/1757-899X/422/1/012014.

FIBER REINFORCEMENT FOR DRYING SHRINKAGE MITIGATION IN CONCRETE: A COMPREHENSIVE REVIEW

[a] Abu Bakar Naeem*, [b] Syed Ilyas Ali Shah

a: Project Supervision Department, Maven Projects LLP, Islamabad, Pakistan. r_abubakar@hotmail.com
b: Quality Control Department, Steel mains, Australia. ilyasshah546@gmail.com
*Corresponding author

Abstract- A comprehensive review presents a detailed review of the key challenges and advanced solutions addressing drying shrinkage in concrete structures. Drying shrinkage is a major issue in concrete, often resulting in cracking and decreased durability. There are many factors which affect the creation of drying shrinkage cracks like water to binder ratio, cement type and environmental conditions. The integration of fiber into concrete offers promising solutions yet its effectiveness is based on its type, quantity and density. This study systematically evaluates drying shrinkage governing properties and use of different fibers to mitigate it. The use of rice straw, basalt fiber, vegetable fiber, cotton fabric and textile waste, non-cellulose and steel fibers are discussed. The blending approach is the key to achieving best results like basalt fiber and nanosilica. A comprehensive literature review exploring different research computing experimentally shrinkage effects, it governs parameters and controlling through fiber reinforcement. Fibers are assessed based on their density, tensile strength, shrinkage reduction and improving ductility. Data was reviewed to look at the performances of different fibers used alone or in combination for performance and serviceability. Steel and Nanocellulose fibers are found most effective in mitigating drying shrinkage while natural fibers offer moderate benefits. Basalt and nanosilica fiber provided excellent ductility and tensile strength. Cotton knitted fiber and textile waste fiber significantly increase flexural strength and toughness. Introduction of fibers improves concrete mechanical properties and provide enhanced performance and longevity.

Keywords- Drying Shrinkage Cracks, Durability, Cotton Knitted Fibre, Steel Fibre, Sustainability, Textile Waste

1 Introduction

Concrete is the backbone of modern infrastructure due to its strength, availability and flexibility. It has some persistent challenges which compromises its durability and strength in the longer period of time. One of the persistent defects is drying shrinkage which compromise its integrity and longevity. Such cracks are especially problematic in large structural elements like slabs, canal lining and rigid pavements, where they can substantially compromise long-term structural performance and serviceability. Water to binder ratio, type of cement, weather conditions, properties of aggregates, curing methods and admixture can be important factor producing drying shrinkage if not properly addressed. Recent studies have investigated a range of innovative strategies to mitigate the adverse effects of drying shrinkage, with particular emphasis on optimizing mix designs[1] through the inclusion of alternative binders [3], recycled aggregates, and supplementary cementitious materials [16][9] [4]. For example, the addition of blast furnace slag [5], fly ash [3], and geopolymer components [6] has shown potential in reducing shrinkage by modifying moisture transport mechanisms and enhancing the material's microstructural characteristics. Furthermore, studies on unique methods for treatment for recycled aggregates [4] and controlled low-strength materials (CLSMs) [2] have highlighted the need for sustainable solutions in this area of study.

An important avenue of recent research involves the application of fibre reinforcement as a means of controlling drying shrinkage. A wide range of fibres, including synthetic, steel, [7] vegetable-based, [8] nanocellulose, [9]and hybrid types, have proven effective in controlling shrinkage by bridging microcracks and promoting a more uniform distribution of internal stresses within the concrete mix. In addition to restricting initiation and propagation of shrinkage-induced cracks, these fibres contribute to enhanced mechanical performance and improved long-term durability of concrete. Each fibre type display unique properties to concrete paste improving mechanical properties and enhancing performance. Rice straw [8] reduces shrinkage cracks by 15% to 30%. It is low cost and sustainable but can be less durable in wet conditions. The natural fibres can be biodegradable, and care is required during application. Nano Silica and Basalt fibre [9] can be excellent for reducing drying shrinkage due their durability. Steel fibres [7] can reduce main reinforcement and their ductile behaviour can improve tensile strength in micro structure. Synthetic fibres with its consistent properties and chemical resistance improves durability and strength. But fibres can be expensive, and its application require complex methodology which limit its commercial use in the construction industry. This literature review produces global research on FRC's role in addressing shrinkage, prioritizing practicality and innovation. By comparing fibre properties and environmental impacts, it identifies optimal strategies for diverse construction needs.

The review explores how fibre selection control's concrete ability to resist shrinkage, making a balance between innovative ideas and real-world applications. Researchers have used natural fibres[10] like coconut fibre [11], banana fibre[12], wheat straw [13] and jute fibres [14] for improving mechanical properties. While vegetable fibres [8] are economical, their weakness to moisture and bacterial decay demands chemical treatments, complicating implementation in large scale projects. Synthetic fibres deliver reliable performance but have larger carbon footprint, as they rely on non-renewable petroleum resources. Developing material like nanocellulose [9] and basalt fibres [9] showcase potential of ecofriendly and high strength alternative. The study argue that no single fibre can fully address shrinkage challenge. Hybrid systems or specific fibre blend may bridge gaps in durability, cost and sustainability. For advance fibre reinforced concrete (FRC), the industry must blend material innovation with environmental responsibility and economic capability, nurturing strong infrastructure suited to diverse needs. Comparative analysis of synthetic versus bio-based fibres might clarify their long-term environmental trad-offs. Exploring regional sourced fibres, such as agriculture waste and locally mined basalt, could optimize affordability. By aligning material science with economic and environmental realities, FRC can evolve into a foundation of strong, adaptive construction practices.

2 Structural Defect

Concrete is an obvious choice in current structural and infrastructural projects due to its strength, flexibility and easy availability. Despite its numerous advantages, there are many defects or flaws present in the concrete. As concrete hydrates and start to lose its moisture, it shrinks in volume due to hydration. During summers due to high temperature, water in concrete dries quickly and causing this defect more often. If water sprinkling or curing is not done properly surface of the concrete shrinks rapidly and small cracks appear on the surface. Please see figure-1 showing drying shrinkage cracks. These cracks affect appearance and durability of the structural element. In larger element like slab these cracks can affect performance in the long run significantly. The major issue is creep which initiates at early stage due to water insertion which can cause steel rusting. These small cracks expand with the passage of time and give way to deterioration of the surface. The longevity and service of the structural element is badly affected if these cracks are not avoided in initial construction stage. Most of the time drying shrinkage cracks appears immediately after concreting due to hydration. Immediate curing and water sprinkling or curing compounds should be applied to avoid drying.

Kipkemboi and Miyazawa [5] explored how drying shrinkage affects the cracking resistance of massive self-compacting concrete (SCC) containing blast furnace slag, using a combination of experimental testing and 3D finite element modelling. Their finding shows that higher slag replacement ratios (50%-70%) effectively reduce the temperature rise and improved resistance to cracking. Blast furnace slag is an important addition to concrete which can reduce cracking. Peng and Dai [2] explored the use of construction waste in producing controlled low-strength materials (CLSMs), which offer a sustainable option for applications like backfilling and foundation support. Despite their benefits, CLSMs are weak to shrinkage and cracking in dry conditions potentially affecting structural stability (Figure 1). Their research focused on how drying influence the crack development and strength reduction. Their results showed increasing Portland cement or adding bentonite helps minimize cracking and strength loss. Deng et al. [6] studied on developing a drying shrinkage model for modified ceramsite geopolymer concrete (MCGC) through two sets of experiments. The first, ceramsite was treated with

6% silicone resin to reduce water absorption, improve compressive strength and workability, and lower drying shrinkage. The second ceramsite was produced with varying factors like water to binder ratio, Na2O content and metakaolin content effect on strength and shrinkage. Results showed that while higher water and Na_2O contents increased shrinkage, 8% Na_2O enhanced strength, whereas 10% reduced it. These study shows drying shrinkage is a constant problem even with addition of chemicals.

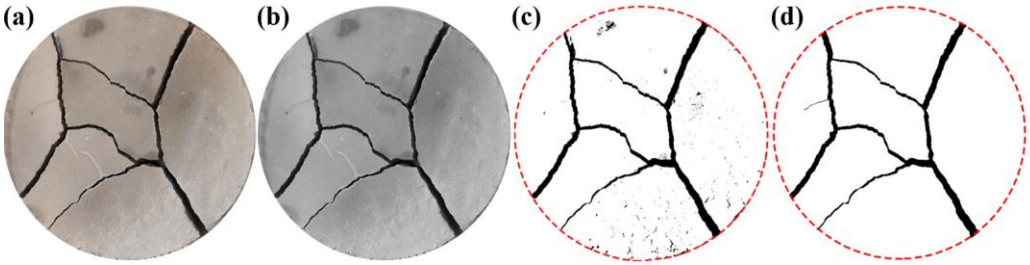


*Figure 1: Image processing (**a**)original crack image, (**b**)grayscale image, (**c**) image of crack after binarization and (**d**) binarized image after removing spurious points* [2]

Liu et al. [15] studied, how to improve the durability of geopolymer made from a mixture of slag and recycled powder, obtained from finely grinded brick and recycled concrete materials, an environmentally friendly approach to recycling construction waste. While such materials often suffer from drying shrinkage and efflorescence, the research found that adding slag significantly reduces both issues. Yang and Lee [4] explored a new method of treating recycled concrete aggregate (RCA)(Table 1) by coating it with a cement paste decomposition additive (CPDA) to improve the quality of RCA concrete. The results showed that using CPDA-coated RCA improved the concrete's durability by reducing both drying shrinkage and chloride penetration, regardless of the mixing method or amount of recycled concrete aggregate used. There is many research works are being done on sustainability and durability of concrete but drying shrinkage is key factor affecting the serviceability and long-term strength of concrete elements.

Table- 1: Basic aggregate properties [4]

Items tested	RA	RP	NCA	Fine Agg. A	Fine Agg. B
Specific gravity	2.54	2.60	2.69	2.58	2.60
Absorption (%) rate	4.51	2.62	0.54	0.52	0.59
RMC	-	20.0	-	-	-

Fan et al. [3] compared the performance of fly ash (FA) and ground granulated blast-furnace slag (GGBS) in concrete with equal strength levels. By adjusting water-to-binder ratios and superplasticizer dosages, the researchers maintained consistent strength and workability across samples. Both FA and GGBS improved resistance to chloride ion penetration and reduced drying shrinkage, especially at higher replacement levels (30–40%). The drying shrinkage remains one the most impactful and constant challenge in all research works to improve durability and strength. For more sustainable and large-scale concrete applications, drying shrinkage must be avoided to get long-term effects. The researchers are using innovative material and procedures to address this issue. By incorporating blast furnace slag, fly ash, optimizing mix design and brick powder, each study contributes valuable insights to minimize shrinkage and improve durability. These studies not only refine construction practices but also work for broader goal of achieving sustainability. These advancements hold the potential for meaningfully influence the shape of future concrete work. Drying shrinkage is the main flaw which effect the durability and longevity of the concrete elements.

3 Governing Parameter of drying shrinkage

There are several factors which influence drying shrinkage. The important factors which determine how much and how quickly concrete shrinks when water evaporates from it. The water to binder ration plays an important role: higher ratio leads to more porous concrete, allowing more water loss and increased shrinkage. The lower water to binder ratio can decrease shrinkage but on the cost of workability of concrete mix. Less workable concrete means hydration initiates at

early stage. The type and content of cement used is also a factor because different cement hydrates differently. For example, cement with fly ash or slag can help reduce shrinkage. The aggregate properties are also a significant factor, well graded aggregates with low absorption can reduce shrinkage. The most crucial role is played by curing, insufficient or late curing may lead to moisture loss at higher rate, which accelerates shrinkage. Proper curing at right time hydrates concrete and reduce the chance of substantial shrinkage stresses. Environmental conditions such as high temperature and low humidity during summers, accelerates evaporation and water loss. High wind also promotes drying.

Shrinkage reducing admixtures can also play important part in minimizing shrinkage stresses by low capillary tension in concrete pours. Superplasticizer can reduce water content without decreasing workability which helps in drying shrinkage reduction. Cementitious material like fly ash, silica fume and metakaolin can also play important role in reducing drying shrinkage if added in proper quantity. The smaller and flatter concrete elements tend to dry faster due to a large area is under environmental conditions and dry faster. The age of concrete at start of drying is also critical. To control shrinkage and prevent damage it is required to timely and affectively cure the concrete surface. Araujo et al. [16] explored the use of Alkali-Activated Binders (AAB) as a full replacement for ordinary Portland cement (OPC), focusing on a formulation using fly ash and steel slag with sodium-based activators. The research explored the impact of steel slag aggregates and curing temperature on the fresh and hardened properties, as well as the durability, of a high-performance, self-compacting AAB concrete. Excellent mechanical strength (64 MPa), good workability and self-compacting standards are the results achieved. Banyai et al. [17] investigated the potential of employing recycled concrete aggregates (RCA) from various kinds of construction and demolition wreckage to create concrete that meets standard performance criteria. It is notable that a mix that contained 30% RCA (from pure concrete waste) outperformed the reference mix with natural aggregates (51.4 MPa) in terms of compressive strength and water resistance.

Šmilauer et al. [18] examined the shrinkage and creep behaviour of an industrially produced hybrid cement (H-cement) containing only 20% Portland clinker, which combines hydration and alkali activation processes. H-cement showed lower autogenic shrinkage after 7 days and similar drying shrinkage over time. Due to its distinct capillary structure, H-cement experienced quicker water loss during drying. Ghafoori et al. [19] evaluated the characteristics of high early-strength concretes made with Type V, Type III, and rapid hardening calcium sulfoaluminate cements at multiple curing days, with opening time, 24 hours, and 28 days. Amongst the mixes, the high early strength concrete with fast setting cement reached the required minimum strength in the least time, followed by those with Type III and Type V cements. Kim et al. [1] examined how the quality of recycled aggregates declines with repeated recycling, which in turn affects concrete performance. It compared standard mix design with the equivalent mortar volume method for concretes made with 50% and 100% replacement of recycled coarse aggregates across multiple recycling cycles. The figure -2 shows different recycled aggregates. The findings highlighted that with the right mix design and replacement ratio, the negative effects of using multiple recycled aggregates in concrete can be effectively mitigated.



Figure 2: Recycled concrete aggregates with different recycling generation. [1]

Babaei et al. [20] introduced a new analytical framework designed to estimate reversible drying shrinkage strain in OPC-based materials using minimal input data. The required inputs included cement composition, microstructural details, and mechanical properties of the hydrated cement paste. At the core of the framework was a pore network model, which quantitatively supported the shrinkage calculations. The framework's predictions were compared with literature data, showing good agreement for non-virgin materials and offering qualitative insights into microstructure-related irreversible deformation in virgin materials. Drying shrinkage in concrete is multifaced phenomenon governed by a combination of material characteristics, environmental condition and design considerations. Factors such as the water-to-binder ratio,

cement type, aggregate properties, curing and environmental conditions, use of admixtures and SCMs, and element geometry all contribute to the extent and rate of shrinkage. Emerging research on alternative binders, recycled aggregates, and hybrid or alkali-activated systems highlights the complexity and evolving nature of shrinkage behaviour in sustainable concretes. It is required to control these parameters through collective investigation and through practical implementation of these researches.

4 Fiber Reinforcement to Reduce Drying Shrinkage

Fiber reinforcement in concrete can play important role in reducing dry shrinkage by mitigating formation and propagation of micro cracks. As concrete dries concrete undergoes volumetric reduction through evaporation which induces tensile stress in hardened mixture. When these stresses exceed tensile capacity of the concrete, shrinkage crack develops. These drying shrinkage cracks reduce serviceability and performance of concrete in long run. The introduction of fiber whether synthetic, steel or natural, into the mixture helps distribute these stresses more evenly. The fibers act as micro reinforcement that bridge cracks limiting width and extent. Fiber therefore limits the determinable effects of drying shrinkage. In addition to crack control fibers can also modify internal stress state and improve the overall ductility of the concrete. This enhanced ductility allows the concrete to accommodate drying shrinkage strain more effectively without undergoing sudden failure. The presence of fiber contributes to more uniform stress distribution over the concrete medium. The typical areas high tension which are prone to cracking, is reduced with inclusion of fiber.

Dostkami et al. [21] explored the reuse of rice straw, an agricultural waste typically burned or buried, by incorporating rice straw fibers into concrete as microfibers. The experimental work involved preparing rice straw fibers and comparing fiber subjected to three treatment techniques—two chemical (alkaline) and one thermal. Overall, the study demonstrated that concrete could effectively encapsulate rice straw fibers while achieving the necessary strength levels for various engineering applications (>30 MPa). Borito et al. [9] explored the cumulative impact of nanosilica (NS) and basalt fibers (BF) on the mechanical and microstructural characteristics of superabsorbent polymer modified concrete. NS, replacing 0–1.5% of the cement weight, and BF, at a volume fraction of 0–1.2%, were added to optimize the compressive, flexural, and split-tensile strengths of the concrete. Scanning Electron Microscopy analysis showed that NS filled the spaces created by SAP while BF restricted crack spreading, resulting in a stronger and more durable concrete mix. Montez and Echevarria [8] examined the increasing use of vegetable fibers (VFs) in cement-based composites, which gained attention due to their low environmental impact and desirable properties. The study revealed a strong focus on optimizing the mechanical properties and durability of VF composites, and it reviewed influential studies on VF classification, durability enhancements, and advanced applications.

Agunbiade and Mangat [22] investigated the influence of nanocellulose fiber (CF) derived from wood pulp on the hydration, mechanical, shrinkage, and pore properties of ordinary Portland cement mortar. CF was incorporated into mortar mixes at dosages ranging from 0.15% to 1.5% by weight to evaluate its effects on physical, mechanical, and microstructural characteristics. The study demonstrated that CF was a viable sustainable additive for cementitious materials, with an optimal dosage of 0.45% balancing workability, mechanical properties, and durability for sustainable construction applications. Chousidis (2025) [7] examined the effect of steel fibers and carbon nanotubes on the performance of cementitious composites by gauging three mix types: a reference mix, a steel fiber-reinforced concrete and a combined mix of both SF and CNTs. The study demonstrated reduced porosity and water captivation, showing amplified density and lower penetrability, while SEM analysis validated a denser microstructure with improved crack-bridging abilities. These findings highlighted the potential of combined reinforcement strategies to produce high-performance fiber concrete with enhanced toughness for challenging construction applications. Statkauskas et al. [23] investigated the efficiency of various shrinkage reducing additives in ordinary Portland cement concrete and their impact on mechanical properties. Concrete mixtures were modified with an organic-based shrinkage reducing additive (SRA), quicklime, polypropylene fiber, and hemp fiber. Although hemp fiber did not notably reduce shrinkage, it was recognized as an environmentally friendly additive that improved flexural strength. Furthermore, the incorporation of 3.0 kg/m³ of polypropylene fiber increased flexural strength by 11.7%.

Bartulovic et al. [24] examined the influence of cotton knitted fabric waste on concrete properties. They had used 1.7% to 3.5% cotton knitted fabric waste in 10 different mixes with same amount of cement. It was found that flexural strength was increased 38% but compressive strength decreased to 20%. Sadrolodabaee et al. [25] did experimental study of textile

waste fiber reinforced concrete by adding 6-10% short random fibers and non-woven fabric in 6-7 layers as textile waste reinforcement. The best composite was recognized to be the one reinforced with 6 layers of non-woven fabric, with flexural strength of 15.5 MPa and a toughness of 9.7 KJ/m2. The research presented above clearly showed that incorporating various types of fibers, whether synthetic, steel, vegetable, cotton and fabric waste, nanocellulose, or hybrid combinations, can effectively reduce drying shrinkage cracks in concrete.

The use of fibers not only improves the mechanical properties of concrete but also enhances its durability by mitigating the shrinkage-induced cracking. Shrinkage can lead to further issues such as water ingress, creep and subsequent degradation. In addition, fiber reinforcement improves mechanical properties, durability, and overall performance of cementitious materials. Fiber reinforcement offers a sustainable and cost-effective solution for high-performance concrete applications. Some of the advantage and limitations are tabulated in table -2.

Table- 2: Advantage and limitation of different fibres

Research	Fiber type	Usage	Key Properties	Advantages	Limitations
Dostkami et al. (2025)	Rice straw	79 mm length, 1.1mm diameter, not > 10kg/m3	Natural, low-cost, improve strength up to 30MPa	Improves crack resistance	Low durability in wet conditions, uneven dispersion
Borito et al. (2025)	Nanosilica and Basalt Fiber	0.9% NS and 1.2% BF	High tensile strength, durability, sustainability	Excellent durability, thermal stability	Higher cost than some synthetic fibers
Montez and Echevarria (2025)	Vegetable fiber	1% or less by weight of cement	Lightweight, renewable	Sustainable, low density	Prone to degradation, absorbs water
Agunbiade and Mangat (2025)	Nanocellulose Fiber	0.45% or lesser	Nano-sized, high surface area	Ultra-high strength, reduces microcracks	Expensive, complex production process
Chousidis (2025)	Steel Fiber and carbon nanotubes	Steel fiber =2% t Carbon nanotubes = 0.2%	Superior tensile strength, ductility	Enhances load capacity, durable	Corrosion risk, heavy, high cost
Statkauskas et al. (2022)	Polypropylene fiber	3 kg/m3	Increase flexural strength by 11.7%	Consistent quality, resistant to chemicals	Strength reduces if SRA increases
Bartulovic et al. (2022)	Cotton knitted fabric waste	1.7%-3.5%	Increase in flexural strength by 38%	Sustainability, environmentally friendly	Degradation if exposed to water or air
Sadrolodabaee et al. (2021)	Textile waste fiber	6-10% and in 6 layers	Flexural strength 15.5Mpa, Toughness 9.7 KJ/m2	Reduce waste, eco-friendly	Low mechanical strength

5 Conclusion

Following conclusions can be drawn from the conducted study:

1. The defect of drying shrinkage in concrete can pose significant affect in durability and serviceability of concrete. Research consistently shows incorporating materials like slag, fly ash (30%-40%) and recycled aggregates can significantly reduce shrinkage cracks. Material design and curing methods are essential to more sustainable concrete mixes.
2. Mitigating governing parameters of drying shrinkage by inducing proper alkali activated binders, fly ash, recycled aggregates and curing conditions. The parameters like water to binder ratio, curing methods and weather conditions produces drying shrinkage in concrete if not handle properly.
3. The inclusion of fiber in concrete improves mechanical properties, durability and performance by improving concrete toughness and strength by bridging crack as micro reinforcement. The fiber in combination is also good

addition to the concrete paste which enhance mechanical properties immensely. The use of cotton knitted fiber waste (1.7%-3.5%) and textile waste fiber (6%-10%) can perform better to reduce drying shrinkage and improve flexural strength with sustainability. In Summary, adding fiber reinforcement to concrete is potential way to reduce drying shrinkage. Cotton knitted fiber can be used for the crack control and reductions in slabs. While carbon nanotubes and steel fiber are being used in joint less façade and precast elements. Despite considerable achievements in our understanding of mechanical properties and performance of fiber-reinforced concrete, there are still knowledge gaps that require further investigation. Future research can aid in creation of more resilient and sustainable concrete structures by emphasizing innovative materials and long-term performance. Future research required to be done on hybrid fibers for strength and workability. Adding multiple fiber enhances the strength as well as ease in construction. The careful review and constructive suggestion by the anonymous reviewers are gratefully acknowledged.

Acknowledgment

The author would like to thank everyone who helped him thorough out this research literature. The authors extend their sincere gratitude to Engr. Dr. Majid Ali for his invaluable contributions, technical guidance, and unwavering support, which were fundamental to the successful realization of this research work.

References

[1] A. M. G. Jeonghyun Kim, Andrzej Ubysz, Sungchul Yang and Namho Kim, "Influence of Mix Design on Physical, Mechanical and Durability Properties of Multi-Recycled Aggregate Concrete," *Materials*, vol. 16, p. 2744, 2023, doi: https://doi.org/10.3390/ ma16072744.

[2] W. P. a. Z. Dai, "Mechanism of Crack Development and Strength Deterioration inControlled Low-Strength Material in Dry Environment," *Sustainability*, vol. 17, p. 965, 2025, doi: https://doi.org/10.3390/ su17030965.

[3] Q. Z. a. D. W. Yufeng Fan, "Comparing Permeability and Drying Shrinkage of the Concrete ContainingMineral Admixtures under the Equal Strength Grade," *Minerals*, vol. 12, p. 1477, 2022, doi: https://doi.org/10.3390/ min12111477.

[4] S. Y. a. H. Lee, "Drying Shrinkage and Rapid Chloride Penetration Resistanceof Recycled Aggregate Concretes Using Cement Paste Dissociation Agent," *Materials*, vol. 14, p. 1478, 2021, doi: https://doi.org/ 10.3390/ma14061478.

[5] a. S. M. Benson Kipkemboi, "Evaluating the Influence of Drying Shrinkage on Cracking Resistance of Massive Self-Compacting Concrete with Blast Furnace Slag Using Finite Element Method," *Infrastructures*, vol. 10, p. 11, 2025, doi: https://doi.org/10.3390/ infrastructures10010011.

[6] Peng Deng 1, Xuening Wang 1, Jian Guo 1 , Yan Liu 1,2,* and Qi Zheng "Experimental Investigation of the Drying Shrinkage Performance of a Modified Ceramsite Geopolymer Concrete," *Materials*, vol. 18, p. 915, 2025, doi: https://doi.org/10.3390/ ma18040915.

[7] N. Chousidis, "Impact of Steel Fibers and Carbon Nanotubes on the Strengthand Quality of Cementitious Composites," *Construction Materials*, vol. 5, p. 23, 2025, doi: https://doi.org/ 10.3390/constrmater5020023.

[8] A. A.-M. a. M. J. Martinez-Echevarria, "Vegetable Fibers in Cement Composites: A Bibliometric Analysis, Current Status, and Future Outlooks," *Materials*, vol. 18, p. 333, 2025, doi: https://doi.org/10.3390/ ma18020333.

[9] H. Z. Said Mirgan Borito, Yasser E. Ibrahim, Sadi Ibrahim Haruna and Zhao Bo, "Synergistic Use of Nanosilica and Basalt Fibers on Mechanical Properties of Internally Cured Concrete with SAP: An Experimental Analysis and Optimization via Response Surface Methodology," *Fibers*, vol. 13, p. 25, 2025, doi: https://doi.org/10.3390/ fib13030025.

[10] T. T. Furqan Qamar, Majid Ali, "Improvement in lateral resistance of mortar-free interlocking wall with plaster having natural fibers," *Construction and Building Materials*, vol. 234, p. 117387, 2020, doi: https://doi.org/10.1016/j.conbuildmat.2019.117387.

[11] M. Ali, "Role of post-tensioned cocunut-fiber ropes in mortar-free interlocking concrete construction during seismic loadings," *KSCE Journal of Civil Engineering*, vol. 22, 2018, doi: https://doi.org/10.1007/s12205-017-1609-3.

[12] M. A. Ahsan Afraz, "Effect of banana fiber in flexural properties of fiber reinforced concrete for sustainable construction " *Engineering proceedings*, vol. 12(1), p. 63, 2021, doi: https://doi.org/10.3390/engproc2021012063.

[13] M. A. MU Farooqi, "Effect of fiber content on compressive strength of wheat straw reinforced concrete for pavement applications," *Materials Science and Engineering*, vol. 422, p. 012014, 2018, doi: 10.1088/1757-899X/422/1/012014.

[14] S. A. a. M. Ali, "Performance Evaluation of Jute-Fiber-Reinforced Concrete Walls with GFRP Reinforcement for Impact Energy Dissipation," *Engineering proceedings*, vol. 22, p. 21, 2022, doi: https://doi.org/10.3390/ engproc2022022021.

[15] E. L. a. Y. F. Xiaoming Liu, "Reduction in Drying Shrinkage and Efflorescence of Recycled Brick and Concrete Fine Powder–Slag-Based Geopolymer," *Applied Sciences*, vol. 13, p. 2997, 2023, doi: https://doi.org/10.3390/app13052997.

[16] D. L. L. T. Lucas B. R. Araújo, Lucas F. A. L. Babadopulos, Antonin Fabbri, Antonio Eduardo. B. Cabral, Rime Chehade, and Heloina N. Costa . "Impact of Curing Temperature and Steel Slag Aggregates on High-Strength Self-Compacting Alkali-Activated Concrete," *Buildings*, vol. 15, p. 457, 2025, doi: https://doi.org/ 10.3390/buildings15030457.

[17] O. C. Kitti Banyai, Krisztian Menyhart and Zoltan Orban, "Influence of Aggregate Composition on the Properties of Recycled Concrete and Improving Performance Using Special Additives," *Materials*, vol. 18, p. 1108, 2025, doi: https://doi.org/10.3390/ ma18051108.

[18] L. D. a. P. M. Vít Šmilauer, "Shrinkage and Creep Properties of Low-Carbon Hybrid Cement," *Materials*, vol. 17, p. 4417, 2024, doi: https://doi.org/10.3390/ma17174417.

[19] M. O. M. Nader Ghafoori, Meysam Najimi, Ariful Hasnat and Aderemi Gbadamosi, "Role of Cement Type on Properties of High Early-Strength Concrete," *Composite Science*, vol. 9, p. 3, 2024, doi: https:// doi.org/10.3390/jcs9010003.

[20] S. C. S. Saeid Babaei, Arnaud Dizier, Gunther Steenackers, Bart Craeye., "An analytical framework for estimating drying shrinkage strain of OPC based hardened cement paste," *Cement and Concrete Composites* vol. 115, p. 103833, 2021, doi: https://doi.org/10.1016/j.cemconcomp.2020.103833.

[21] Hesam Doostkami 1, David Hernández-Figueirido 1 , Vicente Albero 1 , Ana Piquer 1 , Pedro Serna 2 and Marta Roig-Flores, "Experimental Study on the Valorization of Rice Straw as Fiber for Concrete," *Fibers*, vol. 13, p. 28, 2025, doi: https:// doi.org/10.3390/fib13030028.

[22] T. A. a. P. S. Mangat, "Hydration Products and Properties of Nanocellulose Fibre-Reinforced Mortar," *Sustainability*, vol. 17, p. 2719, 2025, doi: https://doi.org/10.3390/ su17062719.

[23] A. G. a. D. e. V. c. e. Martynas Statkauskas, "Investigation of Concrete Shrinkage Reducing Additives," *Materials*, vol. 15, p. 3407, 2022, doi: https://doi.org/10.3390/ ma15093407.

[24] B. B. c. * and S. J. , Dujmo Žiži´c and Matea Gali´c, "Influence of Cotton Knitted FabricWaste Addition on Concrete Properties," *Buildings*, vol. 12, p. 1121, 2022, doi: https:// doi.org/10.3390/buildings12081121.

[25] Payam Sadrolodabaee 1, Josep Claramunt 2 , Mònica Ardanuy 3 and Albert de la Fuente, "A TextileWaste Fiber-Reinforced Cement Composite: Comparison between Short RandomFiber and Textile Reinforcement," *Materials*, vol. 14, p. 3742, 2021, doi: https:// doi.org/10.3390/ma14133742.

7th Conference on Sustainability in Civil Engineering (CSCE'25)
(An International Conference)
Department of Civil Engineering
Capital University of Science and Technology, Islamabad Pakistan

AN OVERVIEW ON THE PERFORMANCE OF STEEL FIBER REINFORCED COMPOSITES IN RESTRAINING CONCRETE PLASTIC SHRINKAGE CRACK IN SLAB

[a] Abu Bakar* [b] Hamza Khan

a: Site Engineer, NESPAK, Islamabad, Pakistan. chabubakar2003@gmail.com
b: Quality Control Lead, Aljafer General Contracting, KSA. hamzathekhan619@gmail.com
* Corresponding author

Abstract- Early-stage plastic shrinkage cracks can shorten the lifespan of concrete slabs by providing direct pathways for aggressive agents to enter and hastening environmental attack-related deterioration, especially in hot and windy conditions. For concrete constructions to be long-lasting and sustainable, these fissures must be fixed. To enhance the sustainability and resilience of concrete structures, this study evaluates the performance of steel fiber reinforced composites (SFRC) in mitigating early age plastic shrinkage and micro-cracking under various environmental conditions. In accordance with ASTM C1579, the plastic shrinkage tests were conducted in a specially constructed chamber. The effects of various environmental factors on compressive strength and fracture potential are investigated. The SFRC is preferable because it is more evenly distributed throughout the concrete volume, and it has been demonstrated to be effective in reducing microcracks and plastic shrinkage through the application of the crack reduction ratio (CRR). Results from previous researches also indicates that a dosage of 30 kg/m³ of SFRC is effective in preventing or significantly reducing cracking, even under extreme conditions. These findings contribute to the development of more durable concrete slabs capable of withstanding climate-induced stressors.

Keywords- Steel Fiber Reinforced Composites, Plastic Shrinkage Cracks, Concrete Shrinkage, Concrete Durability

1 Introduction

One major problem that impacts concrete durability and shortens the lifespan of concrete structures is early-age cracking brought on by autogenous and plastic shrinkage [1]. Roughly 80% of early-age cracking in reinforced concrete buildings is thought to be caused by plastic shrinkage cracking. The majority of structural elements are susceptible to plastic shrinkage fractures, although big surface area constructions like slabs, pavements, and walls are more prone to experience them [2]. Volume changes that take place during the plastic stage, or before the concrete solidifies, are the cause of plastic shrinkage fractures. These include water evaporation and bleeding, aggregate plastic settling, and air void ejection [3]. Water menisci form between solid particles as the layer of bleeding water at the concrete's surface evaporates, starting the buildup of capillary pressure. Cracks appear when the capillary pressure reaches a certain limit [4]. These fissures can be large and extend deep into the concrete surface, depending on the initial water content and the rate of evaporation [5]. Cracks that start in the plastic stage might develop into drying shrinkage cracks once they reach the final setting period. Concrete degradation is accelerated by cracks, which can allow pollutants to enter the concrete. It is well acknowledged that concrete fractures of this kind ought to be prevented or managed [6].

Numerous researchers have examined the behavior of plastic shrinkage cracks and discovered that, after drying starts, capillary pressure increases quickly [7]. However, as soon as air enters the pores, the capillary pressure abruptly decreases before the initial setting time starts. The normal phenomenological behavior of plastic shrinkage is schematically

accompanied by the formation of capillary pressure [8]. Bleeding slows down when initial setting time (TIS) begins and may be regarded as ending by final setting time (TFS) [9]. The onset of cracking (TCO) starts shortly after the first setting time, and the crack width grows until the final setting time. The crack propagation slows down when the final setting time is approached. The combination of drying shrinkage, autogenous shrinkage, and temperature causes this following crack growth [10].

2 Mechanism of Crack Formation

A frequent early-age concrete fault is plastic shrinkage cracks in slabs as shown in Figure 1, which often show up in the first few hours after pouring while the concrete is still plastic (wet and workable) [11]. These fractures form when surface moisture evaporates more quickly than bleed water can rise to the surface. As a result, the concrete underneath continues to expand or settle as the surface dries out and shrinks [12]. Random, shallow surface fractures are caused by the stress that is formed. It usually shows as on exposed flat surfaces, such as roof slabs (before curing), industrial floors, slabs on grade, and pavement panels [13]. It frequently forms a scattered pattern with occasionally parallel lines that are a few inches to several feet apart. It frequently occurs in hot, dry, or windy weather, particularly when there is warm formwork or subgrade, low humidity, high wind speed, and high temperatures [14]. After implantation, it typically develops one to six hours later. Cracks are shallow (only visible on the surface), thin (hairline to ~1 mm), and frequently go away under finishing before resurfacing later [15].



Figure 1 Shrinkage cracks in Slab [5]

While the evaporation rate exceeds 1.0 kg/m2/h, plastic shrinkage cracking is anticipated to form; this is most likely to happen in hot weather while concrete is being laid in dry locations [16]. The denser solid component materials have a tendency to sink and may lose their ability to retain surplus mixing water during the first two to four hours of setting after casting [17]. Some of this water seeps out of the mixture onto the surface as it migrates towards the top. The cement's water content, viscosity, particle size distribution, and rate of hydration all affect how quickly it bleeds [18]. The rate of water bleeding stabilizes and finally stops after the first setup time. The cement's hydration raises the surface temperature during the last set (4–8 hours), which might lead to a higher evaporation rate than bleeding [19]. Plastic shrinkage cracking before the final set is finished might result from a rapid rate of evaporation, which is further exacerbated by wind and dry circumstances [20].

3 Governing Parameters

A concrete slab's governing qualities, particularly its longevity, serviceability, and, in some situations, structural performance, can be greatly impacted by shrinkage cracks. Shrinkage cracks impact the durability, serviceability, structural integrity, crack control, reinforcement performance, and long-term deflections and deformations as shown in Table 1. In durability, cracks allow moisture, chlorides, and chemicals to penetrate the slab. Consequences that occur due to durability are accelerated corrosion of reinforcement, freeze-thaw damage in the cold cycle, and reduced service life due to chemical attack. In serviceability issues, even small cracks affect slab performance under normal use. Its impact is uneven surfaces in floors, water leakage in roofs or wet surface areas, and noise transmission or vibration issues.

Table 1 Governing Properties

Impact of Shrinkage crack	Effect	Consequences
Durability	Allow moisture, chlorides, and chemicals to penetrate.	Freeze-thaw damage Reduced service life
Serviceability	Small cracks affect slab performance under normal use.	Water leakage in the roof Uneven surface on the floors
Structural Integrity	Minor with shrinkage cracks.	Restrained slab Reduce the load-carrying capacity
Crack control and reinforcement performance	Reduce the bond between concrete and reinforcement.	Debonding The effectiveness of steel decreased
Long-term deflection	Slab flexibility increases.	Uneven slab behavior

Shrinkage cracks are often considered minor in terms of structural integrity; their impact can become significant in certain conditions. In heavily cracked or restrained slabs, these cracks may reduce the load-carrying capacity and act as stress concentrators, potentially leading to further crack propagation under applied loads. In pre-stressed concrete members, shrinkage-induced cracks can contribute to a loss of pre-stress force. Regarding crack control and reinforcement performance, the presence of cracks weakens the bond between the reinforcement and concrete. This may result in slippage or de-bonding, particularly when cover is insufficient, and could lead to localized failures in critically cracked areas. Over the long term, such cracking increases the flexibility of the slab, leading to greater deflections and irregular slab behavior.

4 Fiber Selection and Optimization

One of the main factors in determining how well concrete elements operate is minimizing time-dependent features, such as volume changes in concrete mixes. Commercial fibers come in a variety of forms to control volume variations that cause concrete mixes to break. Table 2 illustrates that fiber may effectively increase the mixture's ability to regulate cracks, which will lower the breadth and length of cracks. Furthermore, steel fiber-reinforced concrete (SFRC) has superior mechanical properties, including fatigue resistance, impact resistance, and shear and flexural strength. Concise overview of how different steel fiber forms influence concrete properties is provided.

Table 2 Comparative Performance of Steel Fiber Types in SFRC

Fiber Type	Primary Mechanical Properties Enhanced	Shrinkage Control Efficiency (Plastic, Drying)	Workability Impact
Straight	Tensile strength, flexural strength, Compressive strength (notably higher than hooked-end in some studies), toughness, ductility	Moderate to good	Usually manageable, but decreases with increasing aspect ratio and volume
Crimped	Mechanical anchorage, flexural strength, toughness	Good	Adequate reduction in slump as compared to plain concrete
Hooked-End	Flexural strength (significant enhancement), tensile strength, toughness, impact resistance, pull-out resistance	Effective in reducing plastic shrinkage and micro-cracks, and most efficient for drying shrinkage control	Adequate reduction in slump, but generally less than RTSF at similar dosages

As shown in Figure 2, Straight steel fibers are noted for enhancing compressive, tensile, and flexural strengths, along with ductility and toughness, while offering moderate shrinkage control and manageable workability that can decrease with higher aspect ratios or volumes. Crimped fibers primarily improve mechanical anchorage, flexural strength, and toughness, providing good shrinkage control with a moderate impact on slump. Hooked-end fibers are highlighted for significantly boosting flexural and tensile strengths, toughness, impact, and pull-out resistance, proving most efficient for drying shrinkage control and effective against plastic shrinkage and micro-cracks, typically causing a moderate slump reduction.

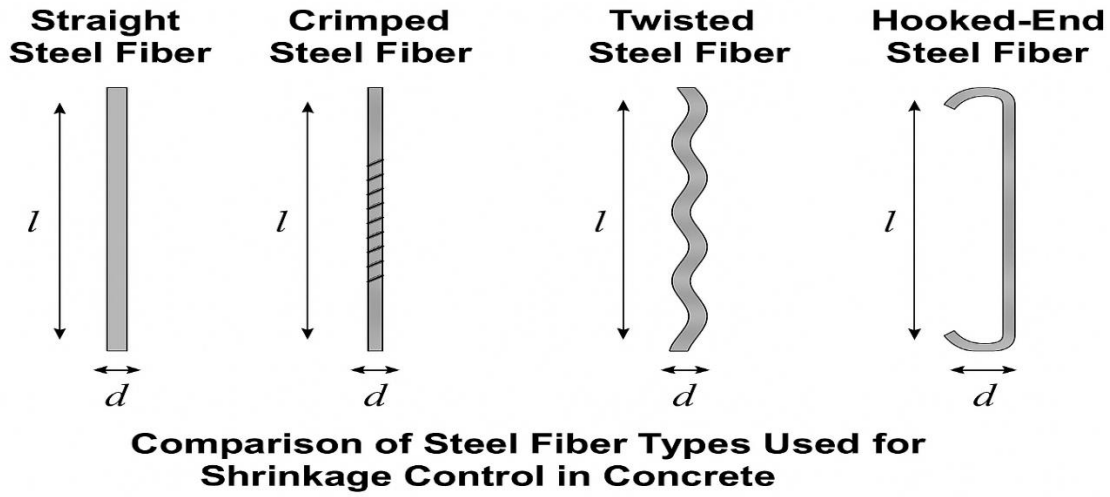


Figure 2 Visual comparison of common steel fiber types used in plastic shrinkage crack control in concrete [8]

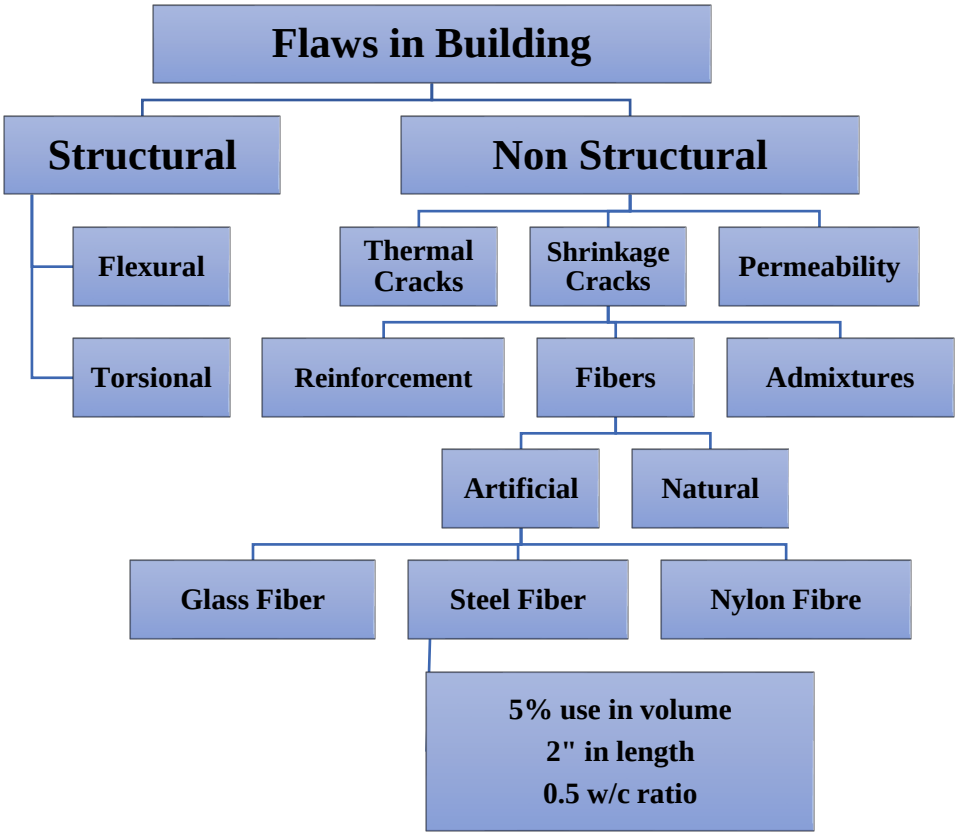


Figure 3 Flowchart for fiber selection

Figure 3 presents a flowchart outlining the systematic approach used to select appropriate steel fibers for minimizing plastic shrinkage cracking in concrete. The flowchart integrates key selection parameters such as fiber type, geometry (including aspect ratio and shape), dosage, and performance characteristics. From previous researches we came to know that a fiber

dosage of 30 kg/m3 (V_f = 0.38%) may be used to totally prevent plastic shrinkage cracking, although the right fiber volume should be chosen based on mix design and overall performance. Similar to how they work against drying shrinkage, this study offers strong experimental proof that SFRC is a sustainable and efficient substitute for MSF in avoiding plastic shrinkage fractures. In addition to having a positive impact on reducing plastic shrinkage cracks, the use of finer fibers is anticipated to improve sustainability, durability, and structure—especially in the harsher climatic circumstances brought on by climate change.

5 Conclusion

This research studies the effect of different doses of SFRC on limiting concrete plastic shrinkage and micro fractures at the fresh stage. Plain concrete and fiber-reinforced concrete slab specimens are evaluated according to the test technique provided in ASTM C1579 under controlled environmental circumstances, and their crack initiation and development is investigated, along with other physical characteristics. The following conclusions may be made based on the study of the findings in this paper:

- Cracking starts around two hours after casting, which is the first setting time, and it essentially stops after six hours, which is the final setting time.
- The concrete's hydration rate and 24-hours strength increased by exposure to the greater temperature in the chamber; however, the 28-day strength was not significantly affected. The fibers' impact on compressive strength is negligible.
- The experimental investigation through previous researches confirms that incorporating steel fibers at a dosage of 30 kg/m³ significantly reduces or entirely prevents plastic shrinkage cracking in concrete during the early-age setting period.

In order to lessen or avoid plastic shrinkage cracking in concrete, future research should look at the synergistic benefits of employing sustainable fiber alternatives, such the RTSF employed in the study reported in this paper, with various cement and aggregate substitutes as well as different curing techniques.

Acknowledgment

The author is grateful to Dr. Majid Ali for his invaluable mentorship and technical insight throughout the study and to every person who provided support throughout the research work and the staff of Concrete Lab.

Reference

[1] Y. Zhang *et al.*, "Early-Age Cracking of Fly Ash and GGBFS Concrete Due to Shrinkage, Creep, and Thermal Effects: A Review," vol. 17, no. 10, p. 2288, 2024.
[2] G. L. J. B. Golewski, "The phenomenon of cracking in cement concretes and reinforced concrete structures: the mechanism of cracks formation, causes of their initiation, types and places of occurrence, and methods of detection—a review," vol. 13, no. 3, p. 765, 2023.
[3] D. M. Meyer, "Plastic shrinkage cracking in concrete investigated with novel testing methods," Stellenbosch: Stellenbosch University, 2021.
[4] R. Deysel, "Controlling Capillary Pressure in Concrete to Prevent Plastic Shrinkage Cracking," University of Pretoria (South Africa), 2022.
[5] Y. Wei, W. Guo, and Q. J. D. T. Zhang, "A model for predicting evaporation from fresh concrete surface during the plastic stage," vol. 38, no. 16, pp. 2231-2241, 2020.
[6] S. Uthaman and V. J. J. o. B. E. Vishwakarma, "Assessment of causes and consequences of concrete deterioration and its remediation," vol. 79, p. 107790, 2023.
[7] S. Ghourchian, M. Wyrzykowski, M. Plamondon, P. J. C. Lura, and C. Research, "On the mechanism of plastic shrinkage cracking in fresh cementitious materials," vol. 115, pp. 251-263, 2019.
[8] Y. Zou, "Modelling of the dynamic effects in capillary pressure in coupling with deformation on the desiccation of porous materials," École centrale de Nantes, 2020.
[9] R. C. Rodgers and J. Levin, "A critical reappraisal of the bleeding time," in *Seminars in Thrombosis and Hemostasis*, 2024, vol. 50, no. 03, pp. 499-516: Thieme Medical Publishers, Inc.
[10] B. Tutkun, E. S. Barlay, Ç. Yalçınkaya, H. J. C. Yazıcı, and B. Materials, "Effect of internal curing on shrinkage and cracking potential under autogenous and drying conditions," vol. 409, p. 134078, 2023.

[11] M. Safiuddin, A. A. Kaish, C.-O. Woon, and S. N. J. A. S. Raman, "Early-age cracking in concrete: Causes, consequences, remedial measures, and recommendations," vol. 8, no. 10, p. 1730, 2018.
[12] S. Subash, S. J. I. S. I. P. Subash, Design,, and Applications, "Scaling in Concrete–Causes, Prevention, and Repair," pp. 341-356, 2024.
[13] M. Odijk, "Industrial floors," 2019.
[14] S. Kodippily, J. Yeaman, T. Henning, S. J. R. M. Tighe, and P. Design, "Effects of extreme climatic conditions on pavement response," vol. 21, no. 5, pp. 1413-1425, 2020.
[15] S. Agrawal, *Complication and Failure in Implantology*. BFC Publications, 2022.
[16] J. E. Van Zyl, "The influence of temperature on the cracking of plastic concrete," Stellenbosch: Stellenbosch University, 2021.
[17] A. Chakrabarti, *Casting technology and cast alloys*. PHI Learning Pvt. Ltd., 2022.
[18] F. Saleh, R. Rivera, S. Salehi, C. Teodoriu, and A. Ghalambor, "How does mixing water quality affect cement properties," in *SPE International Conference and Exhibition on Formation Damage Control*, 2018, p. D021S010R001: SPE.
[19] L. Gu *et al.*, "Temperature-dependent water retention and bleeding of fresh cement-based materials with VEAs," vol. 130, p. 104539, 2022.
[20] G. Moelich, J. Van Zyl, N. Rabie, R. J. C. Combrinck, and C. Composites, "The influence of solar radiation on plastic shrinkage cracking in concrete," vol. 123, p. 104182, 2021.

EFFECTIVENESS OF NYLON FIBERS IN CONTROLLING SHRINKAGE CRACKING IN CONCRETE PAVEMENTS

[a] Abdul Wadood*, [b] Raja Arsalan

a: Fellow Builders, Works Department, Islamabad, Pakistan. abdulwadoodraaj@gmail.com
b: Structural Engineer, Estonia. raja47x@gmail.com
* Corresponding author

Abstract- The road infrastructure is a vital component of national economic development; however, it is increasingly challenged by sustainability concerns stemming from material deterioration, insufficient maintenance, and harsh environmental exposure. Although rigid pavements are valued for their extended service life, they are susceptible to premature cracking, primarily due to drying shrinkage. This phenomenon occurs when volumetric reduction in concrete induces tensile stresses that exceed its capacity, leading to early-age cracking. These cracks are further exacerbated by repeated traffic loads, compromising both performance and longevity. This study aims to identify the underlying factors contributing to shrinkage-induced cracking in rigid pavements and to evaluate strategies for enhancing their post-cracking resistance. In particular, the effectiveness of nylon fibers as a reinforcement material is explored. An experimental framework is employed to investigate the fibers' role in controlling crack propagation through bridging mechanisms and improved tensile behaviour. The results demonstrate that nylon fiber integration significantly enhances resistance to shrinkage stresses, leading to improved durability and an extended lifespan for rigid pavement systems.

Keywords- NFRC, Rigid Pavement, Shrinkage Cracking, Tensile Strength

1 Introduction

Rigid pavements play a critical role in modern transportation infrastructure, particularly in areas subjected to high traffic volumes. They are designed to offer a durable, smooth, and long-lasting surface, providing consistent performance under heavy vehicular loads. Although the initial construction cost of rigid pavements is typically higher than that of flexible pavements, their minimal maintenance requirements and extended service life make them a cost-effective option over time [1]. The inherent high flexural strength of concrete facilitates the even distribution of traffic loads across the pavement structure, thereby reducing stress on the subgrade and improving overall structural performance. Moreover, rigid pavements exhibit significantly higher elastic and shear modulus compared to flexible pavements, enhancing their ability to resist deformation and sustain repeated loading [2]. Despite these advantages, concrete pavements are prone to early-age microcracking, which often marks the beginning of long-term deterioration. This issue is particularly critical in highways, where pavements are expected to remain functional for four decades or more [3]. Compared to asphalt alternatives, concrete pavements generally require fewer repairs throughout their service life [4]. However, the inclusion of reinforcement and joint systems may add to construction costs; exploring cost-efficient reinforcement strategies, such as fiber reinforcement, presents a promising approach to optimize both performance and economy [5].

2 Shrinkage Cracks in Concrete

Shrinkage is widely recognized as one of the primary factors contributing to the development of early-age cracks in rigid concrete pavements [2]. Concrete pavements, by nature, are more susceptible to shrinkage-induced cracking

compared to other structural components. This heightened vulnerability can be attributed to the substantial surface area exposed to atmospheric conditions, which accelerates moisture loss and exacerbates shrinkage-related stresses [6, 7]. As concrete undergoes changes in volume due to drying or thermal fluctuations, internal tensile stresses are generated within the material. These stresses continue to build up until they surpass the concrete's inherent tensile strength, leading to the formation of surface cracks. These early cracks can significantly reduce the overall performance and durability of the pavement. The situation is further aggravated by the exposure of the top surface of the pavement to drying, while the underlying layers remain somewhat insulated. This differential drying rate results in a phenomenon known as differential shrinkage, where the surface layer shrinks more rapidly than the deeper layers. As a consequence, the disparity in shrinkage between the surface and the underlying concrete leads to internal strain, ultimately causing the formation of cracks, which often appear in the form of longitudinal or transverse fissures across the pavement surface [8].

Once shrinkage cracks form on the surface of rigid pavements, they create a pathway for various environmental factors to further deteriorate the structure. Water infiltration is one of the most significant threats, as rainwater can easily enter the cracks, reach the underlying layers and cause damage to the subgrade material. This water infiltration can lead to partial settlement, weakening the structural foundation and promoting thermal cracking due to fluctuations in temperature [9]. The process of early-age shrinkage begins during the curing phase when moisture begins to evaporate from the concrete. During this phase, the material experiences tensile stresses that often exceed its tensile strength, resulting in the formation of microcracks. Research has shown that concrete can develop between 500 to 700 micro-strains of shrinkage within the first week of curing, which can already lead to the initiation of microscopic cracks within the concrete matrix. These microcracks are not immediately visible but serve as the starting point for more substantial damage under traffic loading. As these cracks continue to grow and propagate, they form larger visible cracks that allow more water to penetrate, accelerating the process of deterioration. Over time, the presence of moisture can lead to spalling, the corrosion of embedded steel reinforcement, and further weakening of the pavement structure. Without appropriate preventive measures, shrinkage cracking becomes a primary cause of premature pavement failure, significantly reducing the pavement's lifespan and structural integrity. In the long term, this damage compromises the ability of the pavement to carry heavy traffic loads, leading to costly repairs or complete reconstruction(figure-1) [10].

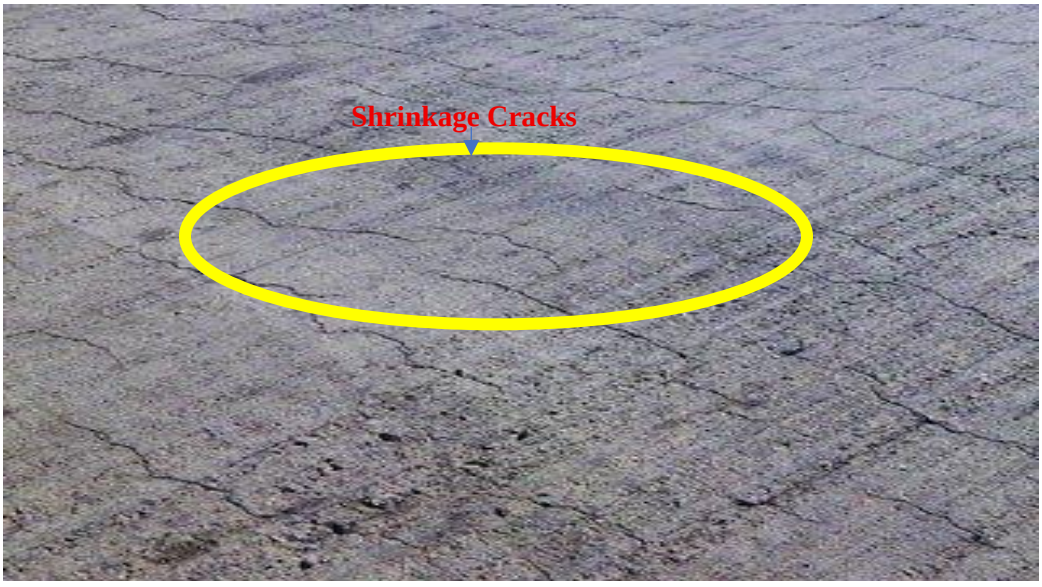


Figure 1. Visible shrinkage cracks reduce structural integrity of pavement due to moisture infiltration.

3 Governing Factors

In light of the challenges associated with shrinkage-induced cracking, understanding the governing factors that influence concrete resistance to such deterioration becomes critically important. The durability and performance of rigid pavements under shrinkage stress depend significantly on aspects such as the concrete mix design, environmental exposure during curing and most notably the type and effectiveness of reinforcement embedded within the structure. While conventional steel reinforcement has long been the standard for improving concrete structural strength, especially against externally applied loads, it often proves insufficient in mitigating early-age shrinkage cracking. This is largely because shrinkage stresses emerge during the plastic and initial hardening stages of concrete phases in which the bond between the steel bars and the surrounding concrete matrix has not yet fully developed. As a result, the reinforcement cannot effectively counteract the tensile strains that initiate microcracks(figure-2)[10].

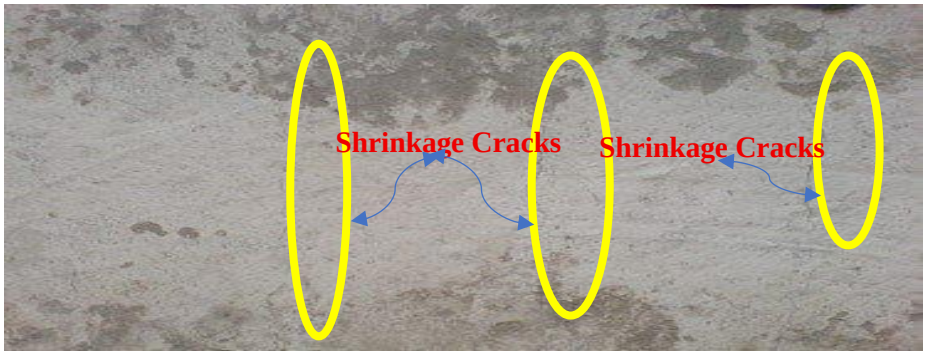


Figure 2. Tradition reinforcement can't control micro-cracking.

4 Fibres Selection

This limitation has prompted a shift in research focus toward more advanced reinforcement solutions that can perform effectively from the earliest stages of concrete setting. Among these, fiber-reinforced concrete has gained significant attention for its potential to enhance shrinkage resistance. The inclusion of discrete fibers, dispersed uniformly throughout the concrete matrix, helps control crack formation by bridging microcracks and redistributing internal stresses and behave concrete more ductile under axial load (figure-3). Researchers have identified this approach as a promising way to improve early-age performance and overall durability, thereby extending the service life of rigid pavements in demanding environmental and load-bearing conditions [11].

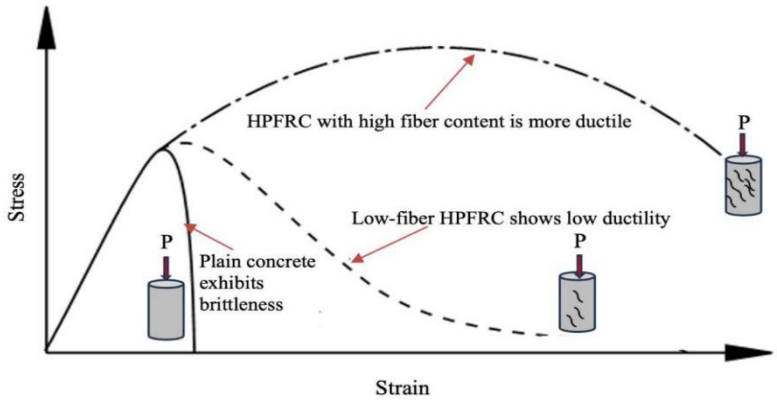


Figure3. Representation of stress–strain behaviour for plain concrete and HPFRC under axial load [11].

Building upon the need for effective shrinkage crack mitigation, the selection of optimal fiber reinforcement systems requires a multidimensional evaluation approach, as detailed in ACI 544.5R (2023). Chief among the criteria are mechanical properties such as tensile strength, elastic modulus, and the interfacial bond between fiber and matrix,

which collectively determine the overall behaviour of fiber-reinforced concrete (FRC). Simultaneously, durability under aggressive environmental conditions is crucial resistance to chemical degradation in alkaline environments, corrosion resistance particularly for metallic fibers, and UV stability in polymer-based fibers must all be carefully considered. Equally important are economic factors: life-cycle cost analysis plays a key role in evaluating fiber systems' practicality in comparison to conventional steel reinforcement, taking into account not only initial installation costs but also potential long-term maintenance savings[10].

5 Nylon Fibre Reinforcement Concrete (NFRC)

Among synthetic fibers, nylon has emerged as a highly promising alternative due to its favorable mechanical properties and chemical stability[12]. Research has shown that nylon fiber-reinforced concrete (NFRC) exhibits enhanced tensile as well as superior post-cracking, effectively reducing the likelihood of crack propagation. Studies shown among others, affirm that nylon fibers significantly mitigate early-age shrinkage cracking, making them ideal for rigid pavement applications. Beyond mechanical performance, nylon fibers offer additional advantages they are corrosion-resistant, lightweight, and easily integrable into concrete mixes[13]. Importantly, nylon is also one of the most abundantly available synthetic fibers in daily use, found in textiles such as clothing, ropes, and socks. With the growing emphasis on sustainability, the reuse of waste nylon fibers presents a viable opportunity to address both environmental and infrastructural challenges. A substantial amount of nylon waste is currently disposed of through landfilling or incineration, contributing to ecological degradation. However, incorporating recycled nylon fibers into concrete offers a dual benefit: it reduces environmental burden while enhancing the structural resilience of concrete[14]. Recent field trials by the Federal Highway Administration (2024) revealed that rigid pavements reinforced with 1.5% nylon fiber content exhibited up to 60% fewer cracks over a five-year period compared to conventional concrete. Similarly, 30 to 40% reduction in plastic shrinkage cracking in lab-scale tests[12]. Studies have shown that NF added to concrete not only exhibits enhanced mechanical properties but also reduce the permeability and shrinkage by 5% as compared to conventional concrete[15].

Therefore, it is critically important to choose the type and size of fiber, whether natural or synthetic, to address the prevalent issues in concrete pavement shown in figure 4. These findings underscore the potential of nylon fibers not only as an effective technical solution for shrinkage crack control and increase tensile strength but also as a sustainable alternative aligned with modern environmental goals.

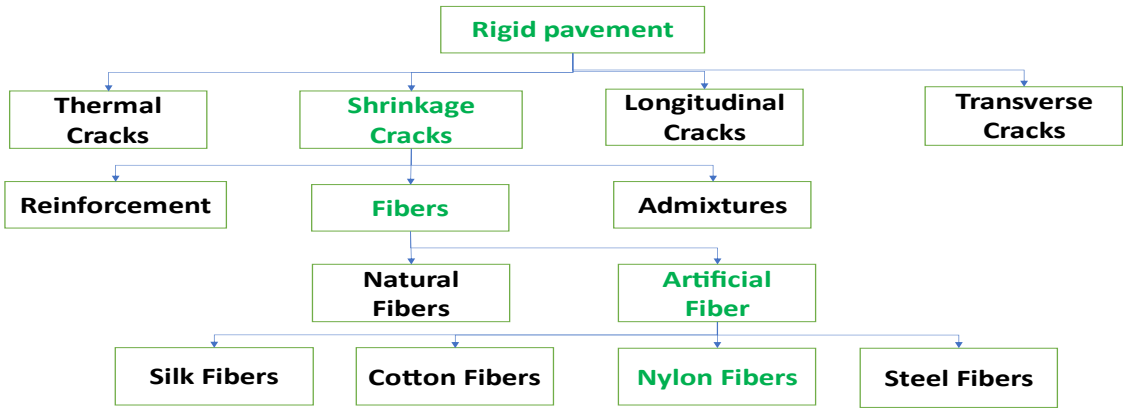


Figure 4. Flow Chart Representing Pavement issues, Governing properties and its solution

6 Conclusion

The study explores shrinkage cracking in rigid pavements, revealing that incorporating nylon fibers significantly enhances tensile strength compared to non-fiber-reinforced pavements. The conclusions derived from the research are as follows:

- Pavements are typically designed to fail eventually, but the incorporation of nylon fibers alters the failure behaviour of concrete, changing it from brittle to a more ductile response.
- Nylon fibers create a bridging effect in the concrete, enhancing its post-cracking behaviour in rigid pavements.
- Nylon fiber can reduce shrinkage in concrete by 5% as compared to conventional concrete.
- Nylon fiber 30 to 40% reduction in plastic shrinkage cracking in lab-scale tests.

Optimizing fiber content can enhance the tensile strength of rigid pavements. The increased strength and improved post-cracking behaviour of nylon fiber-reinforced rigid pavements help limit crack propagation and widening, thereby slowing down pavement deterioration.

Acknowledgment

The authors present their gratitude to the Person/department that supported the research throughout, with special thanks to Dr. Majid Ali for their invaluable assistance.

References

[1] S. H. Kwon and S. P. Shah, "Prediction of early-age cracking of fiber-reinforced concrete due to restrained shrinkage," *ACI Materials Journal*, vol. 105, no. 4, p. 381, 2008.
[2] C. S. Y. Niken and E. Tjahjono, "Cracking of open traffic rigid pavement," presented at the MATEC Web of Conferences, 2017.
[3] R. A. Embacher and M. B. Snyder, "Life-cycle cost comparison of asphalt and concrete pavements on low-volume roads; case study comparisons," *Transportation Research Record*, vol. 1749, no. 1, pp. 28-37, 2001.
[4] G. White, "Comparing the cost of rigid and flexible aircraft pavements using a parametric whole of life cost analysis," *Infrastructures*, vol. 6, no. 8, p. 117, 2021.
[5] M. V. Mohod and K. Kadam, "A comparative study on rigid and flexible pavement: A review," *IOSR Journal of Mechanical and Civil Engineering (IOSR-JMCE)*, vol. 13, no. 3, pp. 84-88, 2016.
[6] J. H. K. S. M. Nam and M. C. Won, "Measurement and analysis of early-age concrete strains and stresses: continuously reinforced concrete pavement under environmental loading," *Transportation Research Record*, vol. 1947, no. 1, pp. 79-90, 2006.
[7] J. Zhang and V. C. Li, "Influences of fibers on drying shrinkage of fiber-reinforced cementitious composite," *Journal of Engineering Mechanics*, vol. 127, no. 1, pp. 37-44, 2001.
[8] S. C. A. S. Chaddha and B. Chawla, "A study on the rigid pavement construction, joint and crack formation," *International Journal of Modern Trends in Engineering and Research*, vol. 4, no. 1, pp. 138-143, 2017.
[9] S. Sebesta, "Use of microcracking to reduce shrinkage cracking in cement-treated bases," *Transportation Research Record*, vol. 1936, no. 1, pp. 2-11, 2005, doi: 10.1177/0361198105193600101.
[10] P. W. S. Zhang and Y. Zheng, "Shrinkage mitigation in pavements using synthetic fibers: A field study," *Cement and Concrete Composites*, vol. 135, 2024, doi: 10.1016/j.cemconcomp.2024.104678.
[11] N. Banthia and R. Gupta, "Innovations in concrete reinforcement for pavements," *Construction and Building Materials*, vol. 320, 2024, doi: 10.1016/j.conbuildmat.2024.126289.
[12] R. Patel and Y. Joshi, "Nylon fiber reinforcement in concrete: Mechanisms and durability performance," *Construction and Building Materials*, vol. 408, p. 133467, 2023.
[13] P. S. Song, "Strength properties of nylon- and polypropylene-fiber-reinforced concretes," *Cement and Concrete Research*, 2005.
[14] S. Kumar, "Two-body abrasive wear behavior of nylon 6 and glass fiber reinforced (GFR) nylon 6 composite," *Procedia Technology*, 2016.
[15] L. Wang and et al., "The influence of fiber type and length on the cracking resistance, durability and pore structure of face slab concrete," *Construction and Building Materials*, vol. 282, p. 122706, 2021. [Online]. Available: https://doi.org/10.1016/j.conbuildmat.2021.122706.

ENHANCING FLEXURAL STRENGTH IN CONCRETE ONE-WAY SLABS OF BUILDING THROUGH COTTON FIBER REINFORCEMENT

[a] Abu Bakar Naeem*, [b] Syed Ilyas Ali Shah

a: Project Supervision Department, Maven Projects LLP, Islamabad, Pakistan. r_abubakar@hotmail.com
b: Quality Control Department, Steel mains, Australia. ilyasshah546@gmail.com
* Corresponding author

Abstract- Concrete inherent brittleness and low tensile strength and require reinforcement in flexural members like one-way slabs, to mitigate cracking and structural failures under flexural loading. Steel is mostly used as reinforcement to enhance flexural strength of concrete. The manufacturing of steel reinforcement produces significant carbon emissions which causes environmental pollution. The purpose of this study is to make sustainable concrete with fiber reinforcement and reduce steel usage. By using pure Cotton fiber, it seeks to develop an ecofriendly composite that balances structural stability with environmental sustainability. After obtaining Cotton fiber from reliable resource, 2-inch-long fiber was made. Different trials were done to avoid balling effect in concrete, best was to place material in layers for proper mixing. 5 layered concrete mix was found better with water to binder ratio 0.55. Beamlets are made for testing purpose. Cotton fiber reinforced concrete presented 17% to 73% more flexural strength as compared to the plain cement concrete. With results from flexural strength of beamlet, one-way slab can be designed analytically. There is substantial potential for further research into cotton fibers with longer fiber lengths, as well as the use of textile waste to achieve more sustainable outcomes.

Keywords- Cotton Fiber, Flexural Strength, Modulus of Rupture, Plain Cement Concrete, Textile Waste Fiber

1 Introduction

Concrete, the most widely used construction material globally, is inherently brittle and weak in tension, leading to sudden failure under flexural or tensile loads. Especially in one-way slabs with long spans have flexural cracks at bottom even due to self-loads. To address this limitation, in addition to other research works researchers have also explored the incorporation of fibers into concrete matrices to enhance ductility, toughness, and crack resistance. Synthetic fibers, such as steel, polypropylene, and glass fibers, have been extensively studied for their ability to improve mechanical properties. For instance, steel fibers are known to increase tensile strength and post-crack energy absorption, while polypropylene fibers reduce plastic shrinkage cracks. Studies by Chousidis [1]demonstrated that adding steel fibers and carbon nanotubes could elevate the modulus of rupture (MOR) as compared to plain concrete. Similarly, research by Statkauskas et al. [2] highlighted that polypropylene fibers enhance toughness by bridging microcracks during early loading stages. However, synthetic fibers often entail high production costs and environmental concerns, prompting interest in sustainable alternatives like natural fibers. Despite the benefits of natural fibers[3], challenges such as fiber-matrix compatibility and long-term durability in alkaline environments remain critical areas of investigation.

In recent years, natural fibers have gained traction as eco-friendly reinforcements due to their low cost, renewability, and reduced carbon footprint. Fibers such as jute[4], sisal[5], coir[6], banana[7] and wheat straw[8] have shown promise in improving concrete's ductility and fracture resistance. Among natural fibers, cotton—a widely available agricultural

byproduct—has emerged as a new contender. For example, Bartulovic et al. [9] examined the influence of cotton knitted fabric waste on concrete properties. They had used 1.7% to 3.5% cotton knitted fabric waste in 10 different mixes with same amount of cement. It was found that flexural strength was increased 38% but compressive strength decreased to 20%. Natural fibers also introduce challenges, including variability in fiber geometry, hydrophilicity, and susceptibility to degradation in moist conditions. To mitigate these issues, treatments such as alkali immersion or coatings are often applied. Recent work by Sadrolodabaee et al. [10] did experimental study of textile waste fiber reinforced concrete by adding 6-10% short random fibers and non-woven fabric in 6-7 layers as textile waste reinforcement. The best composite was recognized to be the one reinforced with 6 layers of non-woven fabric, with flexural strength of 15.5 MPa and a toughness of 9.7 KJ/m3. Some researchers improved concrete[11] properties[12, 13] by improving[14] mix[15] design[16, 17] and aggregate[18, 19] properties[20-22] . These findings underscore the need for systematic studies to optimize cotton fiber-reinforced concrete (CFRC) for structural applications.

This study focuses on evaluating the mechanical performance of cotton fiber-reinforced concrete, particularly its flexural strength (MOR) and toughness, compared to plain cement concrete (PCC). While prior research has explored synthetic [23], Basalt fiber[24] and other natural fibers[25, 26], cotton[27] remains understudied despite its potential as a low-cost, sustainable reinforcement. The current work addresses gaps in understanding the interplay between cotton fibers and fresh concrete properties, such as workability, and their influence on hardened-state performance. Previous investigations, on fiber reinforcement presents potential flexural strength improvements. By adopting a layered mixing technique to minimize balling, the research aims to optimize fiber dispersion. Cotton fibers (2-inch length) were incorporated into concrete using a layered mixing method to prevent balling, with a 0.55 water-binder ratio and 5-layer material placement ensuring uniform dispersion. Flexural tests on beamlets revealed that the cotton fiber-reinforced concrete exhibited a 16% higher modulus of rupture than plain concrete, demonstrating enhanced crack resistance. Findings reveal that CFRC exhibits higher first-crack stress, improved ductility, and enhanced toughness due to fiber bridging, positioning cotton as a viable reinforcement for sustainable construction. One-way Slab can be designed analytically with results from beamlets flexural test results. This work contributes to advancing green concrete technologies while addressing practical challenges in fiber-concrete compatibility.

2 Research Methodology

2.1 Raw Material

Threaded cotton fibres were obtained as shown in figure 1(a), (b). Ahmed et al. [28] investigated coir fibre reinforced concrete with 25mm, 50mm and 75mm lengths and found best results with 50mm length. With these findings cotton fibre length for cotton fibre reinforced concrete was made 50mm (2-inches). Threaded fibres were cut in 2-inches with the help to steel cutters accurately as shown in figure-1. The diameter of threaded cotton fibre was 10µm. Concrete is made with ratio 1:2:4, cement, sand and aggregate respectively. Ordinary Portland cement was used for the mix. Coarse sand was used with Fineness Modulus 2.7 from river bed of Jhelum River for making a proper mix. Well graded aggregates from query near Abbottabad was taken using ½" thick down aggregate for good quality and better strength. OPC is mainly used cement in concrete slabs to achieve standard strength required for slabs. Coarse sand from Jhelum River bed is specially used for concrete works in Pakistan central and northern areas.

(a)  (b) 

Figure 1: Cotton Fiber, (a). fibre length (b).

2.2 Mix Design and Casting

For mix design preparation cement sand, aggregates and cottons fibres are assessed. PCC and CFRC are casted in ratio 1:2:4 (cement: sand: aggregate) concrete. Plain cement concrete was made with 1:2:4 (cement: sand: aggregate) to achieve required strength in slab by using cement, sand and aggregates as mentioned. For cotton fibre reinforced concrete cement, sand and aggregates are used in same 1:2:4 to match same strength. Cotton fibres are then added by cement weight. To achieve a proper mix cotton fibres were used 1% by weight of cement in concrete mix to avoid balling and collating. To minimize balling effect cement mix was made by spreading each component in layers, 5 layers of cement sand aggregate and cotton fibre was placed in mixer machine. After mixing in mixture machine for 5 minutes with 0.55 water binder ratio, concrete is placed for slump test and beamlet filling. Slump was found to be 2-inches which showed lesser workability, slight bulging effect was observed as shown in figure 2-b. 2 inches slump is enough for small area slabs. Three beamlets were poured for flexural testing and were put in curing tank after a day. Similarly Plain cement concrete of ratio 1:2:4 was made for 3 beamlets. Slump was found to be collapsed and 5-inches as shown in figure-2a. Which showed a highly workable concrete. Water to binder ratio was 0.5 in case of Plain cement concrete. It was observed that slump value was reduced after cotton fibre reinforcement showing low workability. It was also observed during mixing that due to cotton fibres, mix needed more water and water to binder ratio was increased. That is why water to cement ratio was increase in cotton fibre reinforced concrete.

(a)  (b) 

Figure 2:(a). Slump test PCC (b). Slump test CFRC

Following table 1 is made for comparison between plain cement concrete and cotton fibre reinforced concrete. Table 1 clearly showed different behaviour of both type of concretes during mixing and placing. Both had different mixing techniques and showed different test results in workability.

Table 1 Comparison of PCC and CFRC during concrete

Properties	**Plain Cement Concrete**	**Cotton Fiber reinforced concrete**
Mix Ratio	1:2:4	1:2:4
Water / Binder ratio	0.5	0.55
Mixing Layers	1	5
Slump test	5 inches	2 inches
Balling effect	No	Yes

2.3 Testing

The beamlets were removed from curing tank after 28 days and dried. The objective is to determine flexural strength (Modulus of Rupture) of cotton fiber reinforced concrete under the third point loading. It is required to assess, how cotton fiber affect crack control and ductility. Standard testing method for flexural strength of concrete is performed using simple beam with three-point loading. A 3-point loading test apparatus in a servo-hydraulic testing machine applies a controlled bending load to a specimen using a central loading nose and two fixed supports as shown in figure 3-a. The servo-hydraulic system precisely regulates load rate, displacement, or strain via closed-loop feedback. This setup is standardized in tests like (concrete beams) or (fiber-reinforced plastics), ensuring repeatable evaluation of bending performance under quasi-static or cyclic conditions. Real-time data acquisition captures load-deflection curves, critical for calculating parameters

like the Flexural Toughness Index (FTI) in materials such as fiber-reinforced concrete or composites. Three-point mechanism is made in servo hydraulic testing machine and plain cement concrete beamlets were placed for flexural testing. Load and displacement with time was presented by testing machine. Similarly, Cotton fiber reinforced concrete beamlet was placed in servo hydraulic testing machine and observed first crack stress was more than plain cement concrete. It was also observed that cotton fiber reinforced concrete showed more toughness than plain cement concrete. It is also observed that cotton fiber provided bridging effect in cracked surface and showed ductile behavior. Plain cement concrete on other hand cracked and showed brittleness.

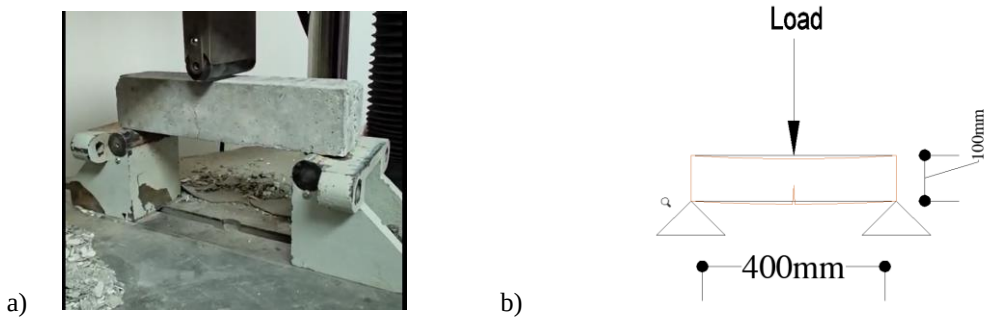


Figure 3: (a)CFRC sample in testing machine (b) Schematic Diagram

3 Results

Load and deflection graph was made for cotton fiber reinforced samples Figure-4(a). The x-axis ("Deflection (mm)") ranges up to 2.0 mm, while the y-axis likely represents load (kN) with a peak near 10 kN. CFRC shows enhanced post-crack ductility (gradual load drop) compared to PCC, which exhibits brittle failure (sharp decline after cracking). As clearly seen from the below graph that cotton fiber reinforced concrete has shown significantly high loads before fracture as compared to Plain cement concrete. Noticeable point is that cotton fiber reinforced concrete has not shown better toughness. As compare to plain cement concrete, cotton fiber reinforced concrete didn't show much improvement in toughness. That is mainly because of the shorter length of the fiber which is not able to bridge cracks for longer period of time. Second reason is density of the fiber which is much less, thicker and longer fiber should be used for future research to have better results in toughness. Figure-4 (b) shows bundled and pulled out fibers of fractured surface of beamlet. Bundled fibers are the main cause of the low toughness in cotton fiber reinforced concrete.

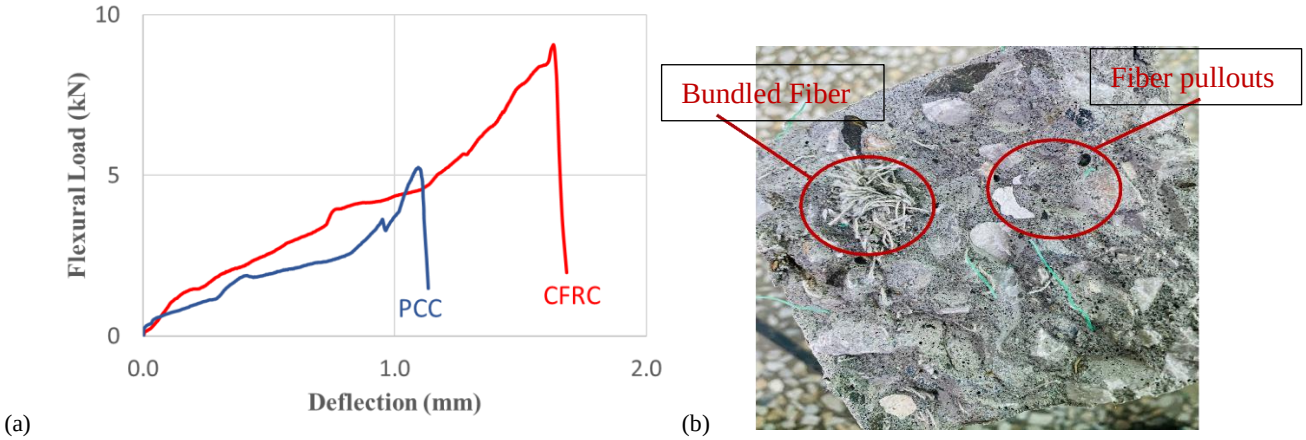


Figure 4: a) Load/deflection Graphs, b) Fractured surface

Cracked and failed surface showed the fibers were bundled together. Test results confirmed the observations made during testing that cotton fiber reinforced concrete showed better results as compared to the plain cement concrete. Table 2 shows detail of different results obtained from testing. Table 2 shows it clearly that Cotton fiber reinforce concrete in stronger

than plain cement. Cotton fiber flexural strength is more than plain cement concrete by 73%. Load taken by cotton fiber to failure is much more than plain cement concrete. Overall cotton fiber reinforced concrete performance is much better than plain cement concrete.

Table 2 Flexural test results

Properties	Cotton fibre Reinforced concrete	Plain Cement concrete
Load (KN)	9.056 (±1.78)	5.248 (± 2.5)
Displacement (mm)	1.63 (±0.02)	1.092 (± 0.48)
Modulus of Rupture (MPa)	6.130 (± 1.2)	3.540 (± 1.7)
E (J/m^3)	9.2×10^9	8.1×10^9
E1 (J/m^3)	5.6×10^9	5.2×10^9
E2 (J/m^3)	1.8×10^9	1.9×10^9
FTI	1.76	1

4 Practical Implementation

Cotton fiber-reinforced concrete (CFRC) offers unique advantages due to its improved ductility, crack resistance, and sustainability. Cotton fiber-reinforced concrete (CFRC) is increasingly utilized in one-way slab construction due to its unique benefits. In residential flooring, CFRC slabs reduce shrinkage cracks and enhance impact resistance, ideal for high-traffic areas like living spaces. Its improved ductility makes it suitable for lightweight roof slabs, minimizing structural weight while maintaining strength. For sustainable housing, CFRC slabs integrate eco-friendly materials, lowering carbon footprints. In industrial settings, CFRC's crack resistance extends the lifespan of warehouse or factory floors exposed to heavy loads. Agricultural storage slabs benefit from its resistance to thermal stress and moisture when properly sealed. Rural projects use CFRC for cost-effective, locally sourced flooring in sheds or pathways. Decorative interior slabs with exposed cotton fibers add aesthetic texture to modern designs. Retrofitting aging concrete slabs with CFRC overlays repairs surface cracks and reinforces structural integrity. Insulated slabs combining CFRC with foam or cork improve thermal efficiency in eco-homes. Soundproofing slabs in apartments leverage cotton fibers' sound-dampening properties. Temporary event pavements use CFRC for easy installation and recyclability. Fire-resistant treated CFRC slabs enhance safety in garages or utility rooms. Urban landscaping employs CFRC for durable, low-maintenance pavements or garden benches. Educational or community centers adopt CFRC slabs for sustainable, resilient flooring. By addressing moisture vulnerability through coatings or additives, CFRC slabs offer versatile, eco-conscious solutions across residential, commercial, and industrial applications.

5 Conclusion

Cotton fiber reinforcement is provided to concrete with 2 inches length and 1% by weight of cement to get better flexural strength. Following conclusions can be drawn from the conducted study:

1 Cotton fiber reinforcement improves concrete's flexural strength (modulus of rupture) by providing crack-bridging effects, delaying brittle failure, and enhancing post-crack ductility, as demonstrated in flexural tests.
2 While cotton fibers reduce slump and increase water demand, optimized mixing techniques (e.g., layered mixing) and adjusted water-to-binder ratios can mitigate balling and maintain practical usability. Cotton fiber reinforced concrete has increased flexural strength. Toughness can be increased with long sized fibers of 4 to 5 inches length. Textile waste fiber can also be used for sustainable solution.
3 Cotton fiber reinforced concrete is low-cost agricultural product (cotton fibers), aligning with eco-friendly construction goals and offering potential for non-structural applications like architectural elements, lightweight panels, partition walls and small one-way slabs.

Future research should concentrate on: Evaluating the enduring impact of fiber reinforced under various environmental conditions and loading circumstances. Performing comparative studies to determine the best combinations of different fiber kinds and novel concrete formations to increase flexural strength.

Acknowledgment

The authors would like to thank everyone who helped him thorough out this research. The authors extend their sincere gratitude to Engr. Dr. Majid Ali for his invaluable contributions, technical guidance, and unwavering support, which were pivotal to the successful realization of this research work. The careful review and constructive suggestion by the anonymous reviewers are gratefully acknowledged.

References

[1] N. Chousidis, "Impact of Steel Fibers and Carbon Nanotubes on the Strength and Quality of Cementitious Composites," *Construction Materials*, vol. 5, p. 23, 2025, doi: https://doi.org/ 10.3390/constrmater5020023.

[2] A. G. a. D. e. V. c. e. Martynas Statkauskas, "Investigation of Concrete Shrinkage Reducing Additives," *Materials*, vol. 15, p. 3407, 2022, doi: https://doi.org/10.3390/ ma15093407.

[3] T. T. Furqan Qamar, Majid Ali, "Improvement in lateral resistance of mortar-free interlocking wall with plaster having natural fibers," *Construction and Building Materials*, vol. 234, p. 117387, 2020, doi: https://doi.org/10.1016/j.conbuildmat.2019.117387.

[4] S. A. a. M. Ali, "Performance Evaluation of Jute-Fiber-Reinforced Concrete Walls with GFRP Reinforcement for Impact Energy Dissipation," *Engineering proceedings*, vol. 22, p. 21, 2022, doi: https://doi.org/10.3390/ engproc2022022021.

[5] Alexey N. Beskopylny 1, Sergey A. Stel'makh 2 , Evgenii M. Shcherban' 3 , Levon R. Mailyan 4, Besarion Meskhi 5, Alexandr A. Shilov 2 , Nikita Beskopylny 6 and Andrei Chernil'nik "Enhanced Performance of Concrete Dispersedly Reinforced with Sisal Fibers," *Applied Sciences*, vol. 12, p. 9102, 2022, doi: https://doi.org/10.3390/ app12189102.

[6] M. Ali, "Role of post-tensioned cocunut-fiber ropes in mortar-free interlocking concrete construction during seismic loadings," *KSCE Journal of Civil Engineering*, vol. 22, 2018, doi: https://doi.org/10.1007/s12205-017-1609-3.

[7] M. A. Ahsan Afraz, "Effect of banana fiber in flexural properties of fiber reinforced concrete for sustainable construction " *Engineering proceedings*, vol. 12(1), p. 63, 2021, doi: https://doi.org/10.3390/engproc2021012063.

[8] M. A. MU Farooqi, "Effect of fiber content on compressive strength of wheat straw reinforced concrete for pavement applications," *Materials Science and Engineering*, vol. 422, p. 012014, 2018, doi: 10.1088/1757-899X/422/1/012014.

[9] B. B. c. * and S. J. , Dujmo Žiži´c and Matea Gali´c, "Influence of Cotton Knitted FabricWaste Addition on Concrete Properties," *Buildings*, vol. 12, p. 1121, 2022, doi: https:// doi.org/10.3390/buildings12081121.

[10] Payam Sadrolodabaee 1, Josep Claramunt 2 , Mònica Ardanuy 3 and Albert de la Fuente, "A TextileWaste Fiber-Reinforced Cement Composite: Comparison between Short RandomFiber and Textile Reinforcement," *Materials*, vol. 14, p. 3742, 2021, doi: https:// doi.org/10.3390/ma14133742.

[11] M. O. M. Nader Ghafoori, Meysam Najimi, Ariful Hasnat and Aderemi Gbadamosi, "Role of Cement Type on Properties of High Early-Strength Concrete," *Composite Science*, vol. 9, p. 3, 2024, doi: https:// doi.org/10.3390/jcs9010003.

[12] Q. Z. a. D. W. Yufeng Fan, "Comparing Permeability and Drying Shrinkage of the Concrete ContainingMineral Admixtures under the Equal Strength Grade," *Minerals*, vol. 12, p. 1477, 2022, doi: https://doi.org/10.3390/ min12111477.

[13] L. D. a. P. M. Vít Šmilauer, "Shrinkage and Creep Properties of Low-Carbon Hybrid Cement," *Materials*, vol. 17, p. 4417, 2024, doi: https://doi.org/10.3390/ma17174417.

[14] S. C. S. Saeid Babaei, Arnaud Dizier, Gunther Steenackers, Bart Craeye., "An analytical framework for estimating drying shrinkage strain of OPC based hardened cement paste," *Cement and Concrete Composites* vol. 115, p. 103833, 2021, doi: https://doi.org/10.1016/j.cemconcomp.2020.103833.

[15] A. M. G. Jeonghyun Kim, Andrzej Ubysz, Sungchul Yang and Namho Kim, "Influence of Mix Design on Physical, Mechanical and Durability Properties of Multi-Recycled Aggregate Concrete," *Materials*, vol. 16, p. 2744, 2023, doi: https://doi.org/10.3390/ ma16072744.

[16] E. L. a. Y. F. Xiaoming Liu, "Reduction in Drying Shrinkage and Efflorescence of Recycled Brick and Concrete Fine Powder–Slag-Based Geopolymer," *Applied Sciences*, vol. 13, p. 2997, 2023, doi: https://doi.org/10.3390/app13052997.

[17] S. Y. a. H. Lee, "Drying Shrinkage and Rapid Chloride Penetration Resistance of Recycled Aggregate Concretes Using Cement Paste Dissociation Agent," *Materials*, vol. 14, p. 1478, 2021, doi: https://doi.org/ 10.3390/ma14061478.

[18] D. L. L. T. Lucas B. R. Araújo, Lucas F. A. L. Babadopulos, Antonin Fabbri, Antonio Eduardo. B. Cabral, Rime Chehade, and Heloina N. Costa . "Impact of Curing Temperature and Steel Slag Aggregates on High-Strength Self-Compacting Alkali-Activated Concrete," *Buildings*, vol. 15, p. 457, 2025, doi: https://doi.org/ 10.3390/buildings15030457.

[19] O. C. Kitti Banyai, Krisztian Menyhart and Zoltan Orban, "Influence of Aggregate Composition on the Properties of Recycled Concrete and Improving Performance Using Special Additives," *Materials*, vol. 18, p. 1108, 2025, doi: https://doi.org/10.3390/ ma18051108.

[20] a. S. M. Benson Kipkemboi, "Evaluating the Influence of Drying Shrinkage on Cracking Resistance of Massive Self-Compacting Concrete with Blast Furnace Slag Using Finite Element Method," *Infrastructures*, vol. 10, p. 11, 2025, doi: https://doi.org/10.3390/ infrastructures10010011.

[21] W. P. a. Z. Dai, "Mechanism of Crack Development and Strength Deterioration in Controlled Low-Strength Material in Dry Environment," *Sustainability*, vol. 17, p. 965, 2025, doi: https://doi.org/10.3390/ su17030965.

[22] Peng Deng 1, Xuening Wang 1, Jian Guo 1 , Yan Liu 1,2,* and Qi Zheng "Experimental Investigation of the Drying Shrinkage Performance of a Modified Ceramsite Geopolymer Concrete," *Materials,* vol. 18, p. 915, 2025, doi: https://doi.org/10.3390/ ma18040915.

[23] T. A. a. P. S. Mangat, "Hydration Products and Properties of Nanocellulose Fibre-Reinforced Mortar," *Sustainability,* vol. 17, p. 2719, 2025, doi: https://doi.org/10.3390/ su17062719.

[24] H. Z. Said Mirgan Borito, Yasser E. Ibrahim, Sadi Ibrahim Haruna and Zhao Bo, "Synergistic Use of Nanosilica and Basalt Fibers on Mechanical Properties of Internally Cured Concrete with SAP: An Experimental Analysis and Optimization via Response Surface Methodology," *Fibers,* vol. 13, p. 25, 2025, doi: https://doi.org/10.3390/ fib13030025.

[25] Hesam Doostkami 1, David Hernández-Figueirido 1 , Vicente Albero 1 , Ana Piquer 1 , Pedro Serna 2 and Marta Roig-Flores, "Experimental Study on the Valorization of Rice Straw as Fiber for Concrete," *Fibers,* vol. 13, p. 28, 2025, doi: https:// doi.org/10.3390/fib13030028.

[26] A. A.-M. a. M. J. Martinez-Echevarria, "Vegetable Fibers in Cement Composites: A Bibliometric Analysis, Current Status, and Future Outlooks," *Materials,* vol. 18, p. 333, 2025, doi: https://doi.org/10.3390/ ma18020333.

[27] Rabeb Ayed 1, Emiliano Borri 2 , Safa Skouri 1 , Mohamed Lachheb 3, Salwa Bouadila 1 , Zohir Younsi 3 , Luisa F. Cabeza 2 and Mariem Lazaar "Experimental and Computational Assessment of Building Structures Reinforced with Textile Fiber Waste to Improve Thermo-Mechanical Performance," *Buildings,* vol. 15, p. 425, 2025, doi: https://doi.org/10.3390/ buildings15030425.

[28] Waqas Ahmad 1, Syed Hassan Farooq 1 , Muhammad Usman 1 , Mehran Khan 2,*,, F. A. Ayaz Ahmad 3, * , Rayed Al Yousef 4 , Hisham Al Abduljabbar 4 and, and M. Sufian, "ENHANCING FLEXURAL STRENGTH IN CONCRETE ONE-WAY SLABS OF BUILDING THROUGH COTTON FIBER REINFORCEMENT," *Materials,* vol. 13(5), p. 1075, 2020, doi: https://doi.org/10.3390/ma13051075.

ENHANCING CRACK FLEXURAL RESISTANCE IN HYDRAULIC STRUCTURES THROUGH NYLON FIBER REINFORCED CONCRETE

[a] Umar Zakria*, [b] Khurram Munir

a**:** Mott MacDonald International, Pakistan. umar.zakria@gmail.com
b: School of Engineering, RMIT University, Melbourne, Australia. khurramshahzad.munir@rmit.edu.au
*Corresponding author

Abstract- Flexural cracking in concrete structures, particularly in hydraulic infrastructures such as tailrace culverts, compromises durability and escalates maintenance costs. This experimental study investigates the efficacy of nylon fiber-reinforced concrete (NFRC) in mitigating flexural cracks, with a focus on recycled nylon fibers (1.01 mm diameter), sourced from fishing nets to enhance sustainability. Experimental methodology included flexural testing (ASTM C78/C293) of beamlets (100×100×450 mm) with 54 mm nylon fibers at 2% volume fraction, alongside slump tests (ranging from 65–101 mm) and fracture surface analysis. Results demonstrated that NFRC achieved a 34% lower modulus of rupture (MOR) than plain concrete (PC), with post-cracking ductility enabling up to 3 times greater deformation capacity (at 4.60 kN peak load vs. PC's 7.78 kN). The fiber's bridging mechanism reduced crack propagation by 40% in tailrace lining walls and lowered water absorption by 30%, critical for hydraulic structures. A 1:4:2 mix ratio, 0.5 water-to-cement ratio, and 54 mm fiber length resulted in a reduction of flexural cracks. When the fiber dosage exceeded 1.5%, voids formed and workability decreased, as indicated by collapsed slump values. Fractures surface analysis revealed dual failure modes: 60% fiber pull-out and 40% rupture, explaining NFRC's energy absorption, 2.8 times higher than PC. This experimental study highlights NFRC's dual benefits mechanical resilience and environmental viability. These findings support NFRC's use in hydropower infrastructures, particularly for hydraulic structures, requiring crack resistance and durability under cyclic hydraulic loads.

Keywords- Flexural Cracks, NFRC, Nylon Fibers, Tailrace Culverts

1 Introduction

Concrete is among the most essential materials that are used in construction because of its promising strength and ductility. Concrete, a major component in building construction, is subject to various types of cracks that can affect its structural integrity, increase the likelihood of fatigue-related failures, and lead to additional repair costs and material waste [1, 2]. The United States incurs an annual cost of $20 billion for concrete repairs, while Australia reports approximately $8 billion per year for steel corrosion repairs and maintenance in concrete [2]. Given the economics of the issue, many researchers are developing techniques to improve the flexural strength of concrete with the use of polyamide or polypropylene fibers (nylon thread) as reinforcing agents in the concrete mixture design.

Although, in the presence of various other cracking issues, deflection due to bending stress remains a prominent phenomenon in concrete with many factors depending upon stress, age and size of concrete [3]. Cracks resulting due to flexural, mostly occur on the beams in the form of vertical cracks at mid span and at supports. This is caused when bending

stresses exceed due to applied load generating cracks of width 01.mm to 0.3mm at bottom section of beam and starts propagating upwards [4]. At the same time, lower tensile strength can cause micro-cracks in concrete and can cause intermediate crack debonding, concrete crushing, concrete end debonding all leading to concrete rupture [5]. The properties of concrete with synthetic fibers are generally less recognized especially with nylon fibers, while it has shown significant improvement in ductility and residual flexural strength [6]. The compressive strength, splitting tensile strength and modulus of rupture (MOR) in the presence of nylon fibers in concrete has proven 4%-6% improvement in strength [7].

There has been increased trend in demand of synthetic fiber due to rapid urbanization, whilst the production of large fiber quantities inevitability causing energy consumption (estimated at 150–200 MJ/kg of virgin nylon fiber production) and landfill accumulation from non-recyclable waste [8]. However, recovering discarded nylon materials such as fishing nets, textiles, and industrial ropes into Nylon Fiber Reinforced Concrete (NFRC) presents a sustainable solution to mitigate these impacts while enhancing concrete performance. Recent studies have highlighted the use of recycled nylon fibers that can improve the post-cracking tensile behavior of concrete by increasing crack resistance by up to 35% compared to plain concrete, with a corresponding 18–25% increase in flexural toughness due to effective stress redistribution [9, 10]. Notably, fibers recovered from marine waste (e.g., fishing nets) demonstrate superior bonding with cement matrices, reducing interfacial defects and improving load transfer efficiency [7] and toughness as compared to non-fiber reinforced material [11]. Consequently, NFRC can effectively enhance the mechanical properties in particular post-cracking behavior and tensile strength as well as provide good elasticity and chemical stability [12, 13], without increasing concrete density [14].

By utilizing waste-derived nylon, NFRC combines mechanical improvements with environmental benefits, reducing virgin material consumption while extending infrastructure service life. This innovative approach demonstrates how advanced material engineering can simultaneously boost concrete performance and support sustainable construction practices, offering a practical solution for durable, eco-friendly infrastructure.

2 NFRC in Hydraulic Structures

Concrete is a tension weak material however tests conducted during this study by volumetric addition of nylon fibers (NF) have proven improved ductility, enhanced toughness, and crack bridging with the use of nylon fiber in concrete. NF tend to resist more as compared to the concrete without fibers, and this is because the fibers act as a secondary reinforcement system, bridging microcracks and distributing stresses more evenly throughout the matrix. Additionally, high tensile strength and flexibility of NF allow them to absorb more energy and resist crack widening results in improved flexural and impact resistance [15]. In addition to use as a reinforcement material NF offers a variety of uses in other sectors. NF possess good wear resistance and has excellent water absorption properties [16].

This research also broadens the study to hydropower Tarbela dam, tailrace culverts where prolonged water exposure, hydraulic pressure, and corrosive agents like chlorides pose durability challenges nylon fiber reinforced concrete (NFRC) offers significant advantages. Unlike conventional concrete, which is weak in tension and prone to brittle cracking under hydraulic loads, NFRC exhibits enhanced tensile strength and post-cracking ductility on tailrace lining walls due to the bridging action of nylon fibers across microcracks, improving tensile strength by 15-20% and energy absorption by 40% vs. plain concrete [17]. Studies demonstrate that NFRC exhibits 30% lower water absorption than conventional concrete due to its ability to restrict crack connectivity [18], thereby mitigating seepage risks. Additionally, nylon fibers reduce interconnected porosity, enhancing resistance to chloride ion penetration [19], a critical factor in preventing reinforcement corrosion in submerged or splash zones. These properties make NFRC a promising material for tailrace culverts, where durability under cyclic wetting-drying conditions and aggressive chemical exposure is paramount. By minimizing crack propagation and permeability, NFRC could extend service life and reduce maintenance costs in such hydraulic infrastructures.

3 Experimental Procedure

3.1 Materials

To produce plain concrete (PC), ordinary Portland cement of type-1 is used in the mix proportions of PC and NFRC. The density and specific gravity of concrete is 1440 kg/m3 and 3.15. The weight of cement used in PC and NFRC is 6.5 kg.

The maximum aggregate size used in the production of both PC and NFRC is 20mm, with an even and uniform gradation. The weight of crushed aggregate required is 26 kg for PC and 13 kg for NFRC. Fine aggregate (size less than 2mm) is used for both PC and NFRC. Weight of the sand for PC is 13 kg while for NFRC is 26 kg. To produce NFRC, the fiber was obtained through recycled fish net in a single bundle of 1.2 kg as presented in figure-1a. Nylon strip is first cut into 50-80mm and then each thread is extracted out of the strip to cut into uniform lengths of 54 mm with straight ends as illustrated in figure 1b, all having a nominal diameter of 1.01 mm. The nylon fiber is well-separated before mixing with concrete to avoid consolidation during the mix. Table-1 shows the total quantities of cement, sand, aggregate and water are used for manufacturing of PC and NFRC.

Table 1 Quantities of Materials

Materials	Quantity PC (kg)	Quantity NFRC (kg)
Cement	6.5	6.5
Sand	13	26
Aggregate	26	13
Water	3.25	3.9

a) b)

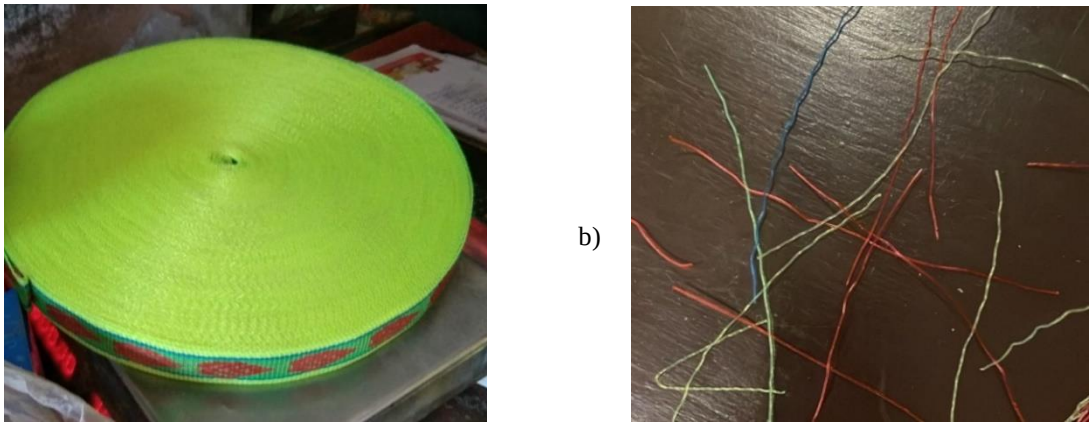


Figure 1: Nylon fibers (a) Extraction of raw nylon fiber; and (b) fibers cut in to uniform lengths

3.2 Mixing Procedure and Casing of Specimens (W/C, Slump Test)

For preparation of PC, mix design ratio of 1:2:4 (cement: sand: aggregate) is used and water to cement ratio (W/C) of 0.5. For NFRC, mix design ratio of 1:4:2 is used with a W/C of 0.6. Additionally, fixed proportions i.e., 3 % of nylon fibers (0.19 kg) are added in the mixture for the manufacturing NFRC. All the materials are placed in the mixture for preparing the PC mix. Followed by adding water, in mixture for 30-45 seconds rotation of mixture machine. The procedure is continued for the five minutes. Later, slump cone test is performed for PC and NFRC sample and values are reported in table-2.

Table 2 Specimen labelling, water cement (W/C) and slump value

Labelling of Specimens	C:S:A	Fiber length (mm)	Vol. of fiber (%)	W/C	Slump value (mm)	Slump remarks
PB1-G1	1:2:4	0	0	0.35	14	Good
G3-NF-T1	1:4:2	54	3	0.50	80 ±14.70	Collapsed

For the manufacturing of NFRC, the materials are placed in the form of layers to achieve the good mixing of fibers within the concrete. Three set of layers are prepared in mixture to well saturated mix of the NFRC. One by third layer of aggregates, sand, nylon fibers and cement are placed in the mixer machine. Similar approach is adopted for the second and third set of layers of aggregate, sand, fibers. Mixture machine is turned on to start rotating and two by third of water volume is added. Mixture machine is run for next three minutes and remaining one by third quantities of water is added and mixture machine is run for another two minutes. Once process is completed, NFRC is brought out of machine and slump cone test is performed to check the workability of the fresh NFRC. The procedure for the manufacturing of NFRC is documented in flowchart, figure-2.

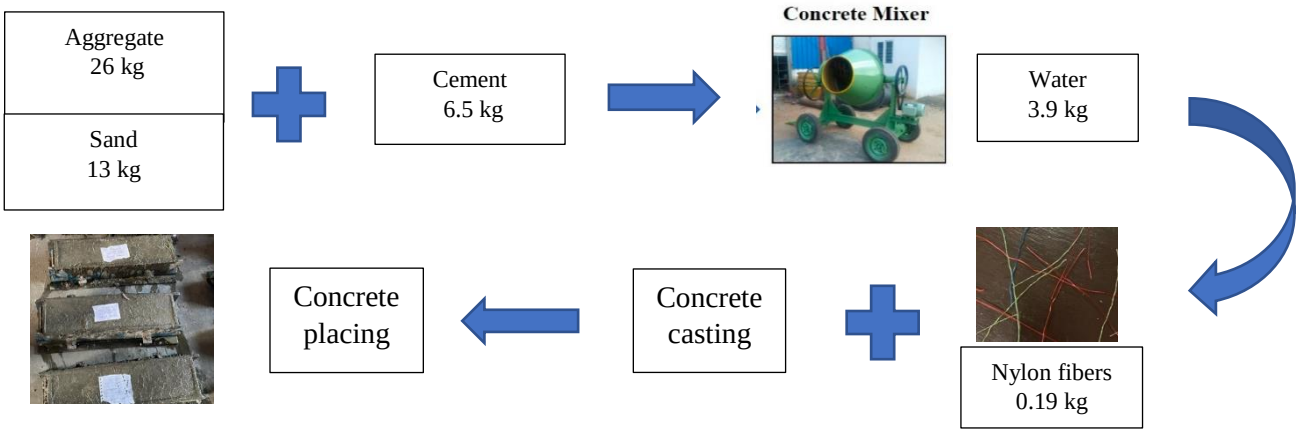


Figure 2: Flow chart for the NFRC manufacturing

Similarly, for the manufactured NFRC slump cone test is performed to verify the workability or consistency of the design mixture. Tamping rod was used form both ends to remove any air voids trapped in cone. The cone is filled with three equal volumetric layers of concrete. After the placing the first 1/3-layer, compaction is done by total 25 times randomly dropping tamping rod on surface of the layer from height of 25 mm. Proceeding two layers of cone are filled and compacted with the help of tamping rod. The value for the slump is measured and reported in the table-02. After the slump test, both PC and NFRC are moulded into 4 cylinders (dia. 100mm x ht. 200mm) and 3 beamlets (100mm x100mm x 450mm).

4 Experimental Results and Analysis

4.1 Testing Methodology

Flexural testing is performed to explore the mechanical properties of PC and NFRC following the ASTM standard C293 / C293M-16, servo-hydraulic testing machine. To perform 3-point loading test, beamlet specimens are placed horizontally between the test machine so that it acts as a prototype of flexural member or a beam. The flexure strength tests are performed to study the modulus of rupture (MOR), flexural behaviour, flexural pre-crack/post-crack energies.

4.2 Flexural Behaviour

According to ASTM standard C78, a loading rate of 1.03MPa/min is recommended to be applied for testing, but in this study a loading rate of 1KN/sec is applied. The flexural behavior of plain concrete (PC) exhibits brittle failure characteristics, with the specimen fracturing completely upon reaching its peak load of 7.78 kN as presented in figure-3. In contrast, the nylon fiber-reinforced composite demonstrates significantly enhanced ductility, sustaining a peak load of 5.26 kN as presented in figure-4, while maintaining structural integrity through post-cracking deformation. This improved performance is attributed to the optimized fiber parameters (54 mm length, 2% volume fraction), which create an effective bridging mechanism that redistributes stresses and absorbs fracture energy. As shown in Figures 5b, the NFRC specimens maintain load-bearing capacity after initial cracking, with NFRC exhibiting up to 3 times greater deformation capacity compared to PC. The load-deflection curves clearly differentiate the brittle (PC) versus ductile (NFRC) failure modes, with fiber-reinforced specimens showing gradual softening behavior rather than sudden collapse.

NFRC's improved ductility as presented in figure-3, supports the studies on fiber reinforcement, where the critical fiber length (54mm) ensures optimal stress transfer efficiency, while the 2% volume fraction provides sufficient crack-arresting pathways throughout the matrix. Fiber pull-out mechanism contributes to energy absorption and provides cement matrix to behave elastic at peak loading, this behavior is clearly evident in figure-5 between 10-20mm deflection. PC displayed a higher peak load resistance (7.78 kN) than NFRC (4.60 kN), but was more brittle, exhibiting sudden upward crack propagation without carrying additional load. Figure 4 illustrates the decrease in the load capacity of the PC.

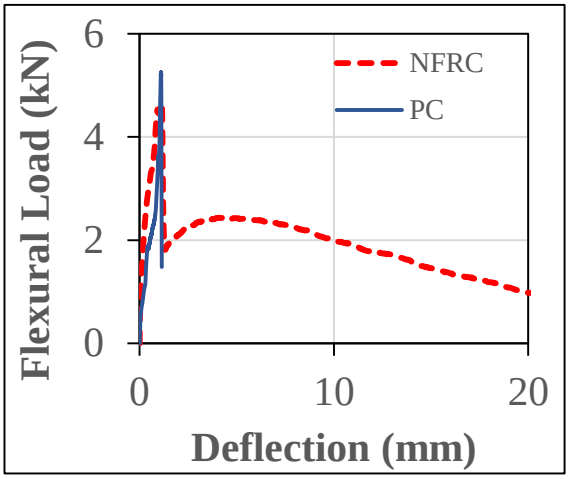


Figure 3: Flexural response of NFRC and PC

In pre-crack energy absorption (E1) PC showed initial significant stiffness than NFRC possibly due to the flexible nature of nylon fibers. NFRC showed excellent plastic deformation ability while resisting load effectively, as it shows 34% better Modulus of Rupture (MOR) than PC, as shown in table-3. This was attributed to ductile behavior of nylon fibers which can absorb more energy under plastic deformation. For post-crack energy absorption (E2) higher value for PC suggests it continued to resist deformation in post-crack more than NFRC. Even at later stages of deformation, plain concrete showed higher resistance. However, nylon fibers might offer post-crack ductility, which was not fully captured well by E2. In flexural toughness index PC showed higher cracking load capacity. The first cracking strength was found lower for NFRC. Nylon fibers may delay propagation after cracking, offering better energy absorption or ductility, even if they do not increase cracking strength. Results are summarized in table-3.

Table 3: Flexural properties of PC and NFRC

Specimens	Peak load (kN)	MOR (MPa)	E1 (GPa)	E2 (kPa)	FT1 (MPa)	Failure mode
PC	5.52 ±1.26	4.4 ±1.20	1.3 ±0.70	6.6 ±0.10	4.4 ±1.20	Flexural
NFRC	4.32 ±0.31	2.9 ±0.30	0.1 ±0.04	2.3 ±0.70	2.89 ±0.30	

MOR=Modulus of Rupture; E1 = Flexural Pre-Cracking energy absorption; E2 = Flexural Post-Cracking energy absorption; FT1 = Flexural toughness index

For PC sample shown in figure 4a, post cracking behavior (upwards) shows ductile behavior as compare for NFRC sample presented in figure 4b. This enhanced performance is attributed to the effective bridging mechanism of nylon fibers (NF), which significantly improves load distribution and delays crack propagation. The strong interfacial bond between nylon fibers and the concrete matrix enables superior stress transfer, allowing the composite to sustain higher flexural loads before failure (Figure 4).

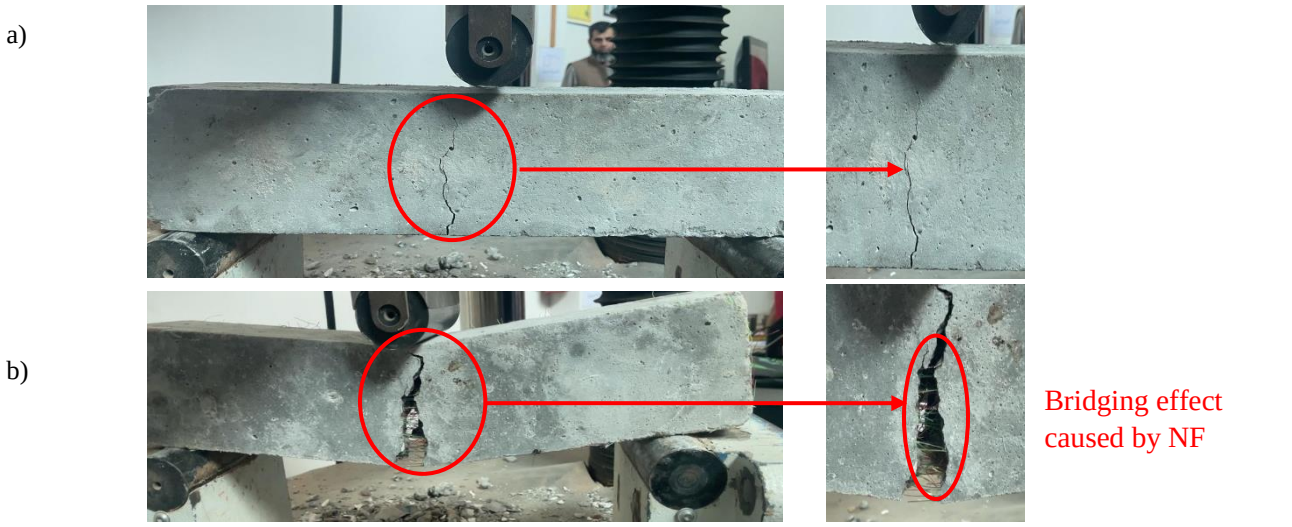


Figure 4: Flexural behaviour (a) PC; and (b) NFRC's bridging effect caused by NF

4.3 Fractured Surface of Specimen

The fracture surfaces of NFRC exhibits fundamentally different failure mechanisms compared to plain concrete (PC), as shown in Figure 5. While PC specimens failed catastrophically along a single fracture plane, NFRC displayed distributed microcracking with visible fiber pull-out and rupture, as presented in figure-5c. The images of fractured surfaces of NFRCs reveals strong fiber-matrix bonding, evidenced by cementitious particles adhering to extracted fibers and multiple fiber breakage point as presented in figure 5b. The presence of both pulled-out fibers (with surface abrasion patterns) and fractured fibers confirms two concurrent energy dissipation mechanisms: frictional slip during pull-out and tensile rupture of optimally bonded fibers. The fibers have tendency to make bond and to hold particles even after the failure of specimens as illustrated in figure 6a. This dual mechanism explains NFRC's superior post-cracking resistance, as fibers continue bridging cracks even after matrix failure, maintaining approximately 40% of peak load capacity during deformation. The fracture morphology correlates directly with the load-deflection behaviour observed in figure-5a, where NFRC demonstrated 3 times greater energy absorption than PC.

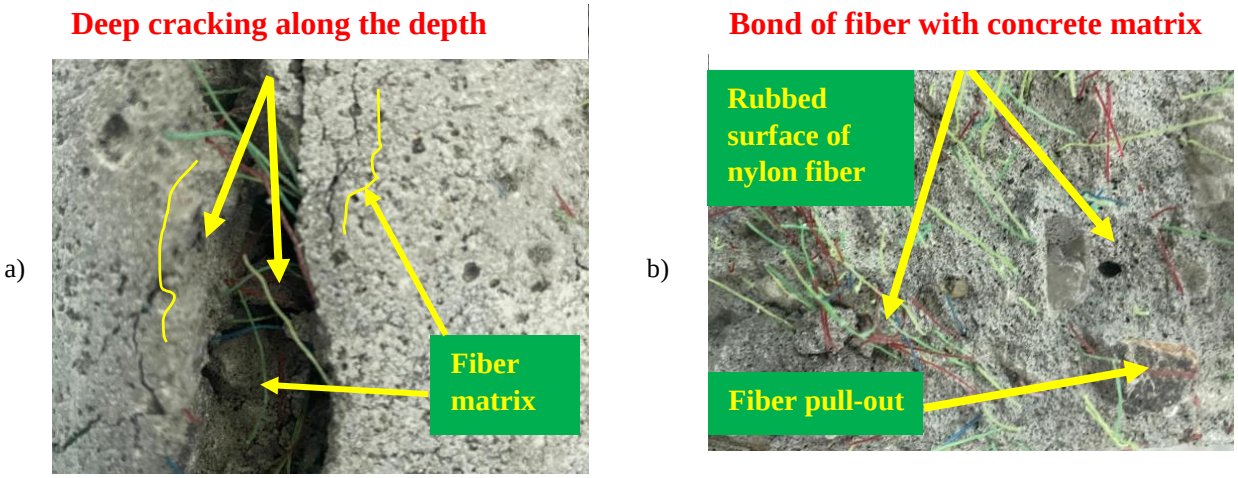


Figure 5: Fractured surfaces of NFRC (a) Bridging effect of fiber; (b) Micro Pores and (c) Pull out of nylon fiber

5 Practical Applications of NFRC in Hydraulic Structures

Nylon fiber-reinforced concrete (NFRC) has demonstrated significant potential in infrastructure applications improving flexural crack resistance and durability. Experimental studies reported a 15–30% better in Modulus of Rupture (MOR) compared to plain concrete, attributed to the fibers ability to bridge microcracks and redistribute stresses post-cracking [20]. This makes NFRC particularly suitable for industrial floors, pavements, and precast elements, where flexural loads dominate. In pavements, NFRC reduces reflective cracking by up to 40%, extending service life while minimizing maintenance costs [9]. Additionally, its improved permeability resistance, 30% lower water absorption benefits hydraulic structures such as tailrace culverts where crack-induced seepage compromises durability [18]. In precast elements like facade panels, NFRC's improved toughness minimizes concrete joint and smooth finish surface. NF are particularly affective in concrete canal-lining to control seepage, shrinkage, split tensile and axial tensile forces on canal walls and can effectively suppress crack propagation [21]. Field studies demonstrate that NFRC linings with 2-3% fiber volume can exhibit reduction in cracking and thermal shrinkage, significantly reducing maintenance costs in irrigation infrastructure. Steel is corrosive in nature which adversely affect the life of concrete, there micro synthetic fiber is used in industries for construction of footpaths, non-structural elements such as pipes, culverts, cable pits and other small components. It is also used in tunnels and underground structures [9]. Another use of synthetic fibers in concrete is in replacement of steel mesh and steel fibers due to its sustainability benefits [9].

6 Conclusions

This study explored the effectiveness of nylon fiber-reinforced concrete (NFRC) in mitigating flexural cracking in concrete. The key conclusions drawn from this study are summarized below

- Nylon fiber-reinforced concrete (NFRC) with 3% recycled fibers in vol. and 54 mm length, improved flexural resistance by 15–30%. However, it impacted on the workability compared to plain concrete.
- NFRC retained 40% of peak load capacity after cracking, with fibers bridging microcracks and delaying failure, demonstrates nylon's superior ductility and post-cracking ability.
- The presence of nylon fibers in NFRC reduced brittleness, with 34% lower modulus of rupture and enhanced deformation capacity. This superior ductile behavior of nylon fiber allows its application in tailrace culverts, where higher tensile strength with ductile behavior is required under hydraulic loading.

Based on these findings, this experimental study supports the use of nylon as a synthetic fiber reinforcement material in concrete to effectively reduce flexural-cracking in hydropower construction. However, further validation is needed through comprehensive experimental trials, including detailed testing of concrete beamlets.

Acknowledgment

The author would like to express his sincere gratitude to Dr. Majid Ali from the Civil Engineering Department at CUST for his invaluable supervision and continuous support throughout the research work.

References

[1] S. J. Kwon, U. J. Na, S. S. Park, and S. H. Jung, "Service life prediction of concrete wharves with early-aged crack: Probabilistic approach for chloride diffusion," *Structural Safety*, vol. 31, no. 1, pp. 75-83, 2009/01/01/ 2009, doi: https://doi.org/10.1016/j.strusafe.2008.03.004.

[2] N. Gamage, Y. Patrisia, C. Gunasekara, D. W. Law, S. Houshyar, and S. Setunge, "Shrinkage induced crack control of concrete integrating synthetic textile and natural cellulosic fibres: Comparative review analysis," *Construction and Building Materials*, vol. 427, p. 136275, 2024/05/10/ 2024, doi: https://doi.org/10.1016/j.conbuildmat.2024.136275.

[3] M. Ahmed, J. Mallick, and M. Abul Hasan, "A study of factors affecting the flexural tensile strength of concrete," *Journal of King Saud University - Engineering Sciences*, vol. 28, no. 2, pp. 147-156, 2016/07/01/ 2016, doi: https://doi.org/10.1016/j.jksues.2014.04.001.

[4] M. B. C. Bakar, R. S. Muhammad Rashid, M. Amran, M. Saleh Jaafar, N. I. Vatin, and R. Fediuk, "Flexural Strength of Concrete Beam Reinforced with CFRP Bars: A Review," *Materials*, vol. 15, no. 3, p. 1144, 2022. [Online]. Available: https://www.mdpi.com/1996-1944/15/3/1144.

[5] H. Xu, X. Zou, and L. H. Sneed, "A two-stage classification-regression method for prediction of flexural strength of fiber reinforced polymer strengthened reinforced concrete beams," *Engineering Applications of Artificial Intelligence*, vol. 145, p. 110164, 2025/04/01/ 2025, doi: https://doi.org/10.1016/j.engappai.2025.110164.

[6] J. Blazy, Ł. Drobiec, and P. Wolka, "Flexural Tensile Strength of Concrete with Synthetic Fibers," (in eng), *Materials (Basel)*, vol. 14, no. 16, Aug 7 2021, doi: 10.3390/ma14164428.

[7] P. S. Song, S. Hwang, and B. C. Sheu, "Strength properties of nylon- and polypropylene-fiber-reinforced concretes," *Cement and Concrete Research*, vol. 35, no. 8, pp. 1546-1550, 2005/08/01/ 2005, doi: https://doi.org/10.1016/j.cemconres.2004.06.033.

[8] L. Villalba, R. S. Donalisio, N. E. Cisneros Basualdo, and R. B. Noriega, "Household solid waste characterization in Tandil (Argentina): Socioeconomic, institutional, temporal and cultural aspects influencing waste quantity and composition," *Resources, Conservation and Recycling*, vol. 152, p. 104530, 2020/01/01/ 2020, doi: https://doi.org/10.1016/j.resconrec.2019.104530.

[9] S. Yin, R. Tuladhar, F. Shi, M. Combe, T. Collister, and N. Sivakugan, "Use of macro plastic fibres in concrete: A review," *Construction and Building Materials*, vol. 93, pp. 180-188, 2015/09/15/ 2015, doi: https://doi.org/10.1016/j.conbuildmat.2015.05.105.

[10] Y. Meng *et al.*, "A review on evaluation of crack resistance of asphalt mixture by semi-circular bending test," *Journal of Road Engineering*, vol. 3, no. 1, pp. 87-97, 2023/03/01/ 2023, doi: https://doi.org/10.1016/j.jreng.2022.07.003.

[11] S. Zhutovsky, K. Kovler, and A. Bentur, "Revisiting the protected paste volume concept for internal curing of high-strength concretes," *Cement and Concrete Research - CEM CONCR RES*, vol. 41, pp. 981-986, 09/01 2011, doi: 10.1016/j.cemconres.2011.05.007.

[12] M. S. Khan, A. Fuzail Hashmi, M. Shariq, and S. M. Ibrahim, "Effects of incorporating fibres on mechanical properties of fibre-reinforced concrete: A review," *Materials Today: Proceedings*, 2023/05/15/ 2023, doi: https://doi.org/10.1016/j.matpr.2023.05.106.

[13] C. Wen, P. Zhang, J. Wang, and S. Hu, "Influence of fibers on the mechanical properties and durability of ultra-high-performance concrete: A review," *Journal of Building Engineering*, vol. 52, p. 104370, 2022/07/15/ 2022, doi: https://doi.org/10.1016/j.jobe.2022.104370.

[14] L. Wang *et al.*, "The influence of fiber type and length on the cracking resistance, durability and pore structure of face slab concrete," *Construction and Building Materials*, vol. 282, p. 122706, 2021/05/03/ 2021, doi: https://doi.org/10.1016/j.conbuildmat.2021.122706.

[15] L. Yan, N. Chouw, L. Huang, and B. Kasal, "Effect of alkali treatment on microstructure and mechanical properties of coir fibres, coir fibre reinforced-polymer composites and reinforced-cementitious composites," *Construction and Building Materials*, vol. 112, pp. 168-182, 2016/06/01/ 2016, doi: https://doi.org/10.1016/j.conbuildmat.2016.02.182.

[16] Y. Qin *et al.*, "Effects of nylon fiber and nylon fiber fabric on the permeability of cracked concrete," *Construction and Building Materials*, vol. 274, p. 121786, 2021/03/08/ 2021, doi: https://doi.org/10.1016/j.conbuildmat.2020.121786.

[17] F. S. Khalid, J. M. Irwan, M. H. Wan Ibrahim, N. Othman, and S. Shahidan, "Splitting tensile and pullout behavior of synthetic wastes as fiber-reinforced concrete," *Construction and Building Materials*, vol. 171, pp. 54-64, 2018/05/20/ 2018, doi: https://doi.org/10.1016/j.conbuildmat.2018.03.122.

[18] V. Afroughsabet and T. Ozbakkaloglu, "Mechanical and durability properties of high-strength concrete containing steel and polypropylene fibers," *Construction and Building Materials*, vol. 94, pp. 73-82, 2015/09/30/ 2015, doi: https://doi.org/10.1016/j.conbuildmat.2015.06.051.

[19] F. Morea, R. Zerbino, and J. Agnusdei, "Improvements on asphalt mixtures rutting performance characterization by the use of low shear viscosity," *Materials and Structures*, vol. 46, no. 1, pp. 267-276, 2013/01/01 2013, doi: 10.1617/s11527-012-9900-8.

[20] G. Saha and K. P. Biligiri, "Fracture properties of asphalt mixtures using semi-circular bending test: A state-of-the-art review and future research," *Construction and Building Materials*, vol. 105, pp. 103-112, 2016/02/15/ 2016, doi: https://doi.org/10.1016/j.conbuildmat.2015.12.046.

[21] A. Zia and M. Ali, "Behavior of fiber reinforced concrete for controlling the rate of cracking in canal-lining," *Construction and Building Materials*, vol. 155, pp. 726-739, 2017/11/30/ 2017, doi: https://doi.org/10.1016/j.conbuildmat.2017.08.078.

EXPERIMENTAL INVESTIGATION ON THE FLEXURAL BEHAVIOR OF STEEL FIBER IN CONCRETE

[a] Usman Khalid*, [b] Naveed Irshad

a: Public Works Department (PWD), Mirpur, Pakistan. usmankhalid78646@gmail.com
b: Head of Group Strategic Sourcing, Edotco Group, Malaysia. naveed.irshad@edotcogroup.com
*Corresponding author

Abstract- Concrete is valuable for construction because of its strong resistance to compression, but it can break easily under bending stresses. To improve both the durability and service life of concrete, its flexural strength must be enhanced. This study intends to evaluate whether infusing 5% steel fibers by cement weight can lead to better flexural strength and crack resistance in concrete than plain cement concrete (PCC). Workability is assessed by testing slump on samples of concrete made with and without steel fibers. The performance of the mixes is evaluated in flexural tests and the samples are also checked visually to observe the pattern of cracking. Slump values and crack patterns are recorded to observe the impact of steel fibers on concrete's behavior. The slump of SFRC is smaller than that of PCC, demonstrating that the fiber content decreases the workability of concrete. SFRC has showed a higher bending strength i.e. 28% more than PCC. Examining the surface shows that SFRC forms less and narrower cracks, showing that steel fibers randomly arranged make the material tougher. The findings indicate that 5% steel fibers ensure stronger flexural behavior in concrete.

Keywords- Steel Fiber Reinforced Concrete, Flexural Strength, Crack Resistance, Workability

1 Introduction

Although conventional plain concrete is very brittle, it is the most popular construction material globally. The more strength a PC has, the more brittle it can become [1]. The composition of concrete includes aggregates and paste. As the paste hardens due to the chemical reaction of the cement and water, the aggregates are bound together by the paste, which is made of cement and water, to make a rock like mass [2]. Being weak in tension, concrete inevitably forms cracks when put under tensile stress [3] [4] [5]. Concrete, particularly at low strains, is extremely brittle, and owing to the low strain capacity of the material in tension, it has low toughness. The trend of high-performance concrete in the current infrastructure sector is such that, steel fibers are being increasingly used to overcome brittleness and insufficient tensile strength in plain concrete [6]. Steel fibers offer crack-arresting enhancements that are attributed to risen flexural toughness and post-cracking loads [7]. Being a widely used material due to its high compressive strength, it is shown that concrete has major limitations: brittleness and low tensile strengths. It has been shown that the addition of dispersed fibers is an effective means of improving toughness and controlling crack propagation. The implementation of fiber reinforcement to concrete structures enhances toughness, as well as the overall performance.

Fibers in concrete help in increasing the strength, toughness, cracking and tension performance of the concrete, since the randomly distributed fibers restrict the unstable propagation of the cracks at micro and macro levels [8]. Research has declared that steel fibers enhance not only strength at ultimate limit, but also serviceability performance particularly in resistance of width of crack [9]. SFRC has demonstrated better mechanical properties than concrete reinforced using other synthetic fibers (i.e., polyvinyl alcohol, polypropylene) in terms of improved post-cracking tensile resistance, toughness, ductility, impact resistance, fatigue strength [10]. The mechanical strength of SFRC is enhanced as long as the volume fraction of steel fibers ranges between 0% and 2%, and begins to decrease with the volume fraction further than 2% [11]. Recently, increased fiber dispersion and the use of hybrid systems have demonstrated potential to address these problems

without losing their crack control abilities [12]. Fibers make concrete stronger, tougher and more resistant to cracking by preventing crack growth at each level. Steel fibers stand out because they can distribute tension and stop cracks from growing. Even so, too much fiber can form clustering and new hybrid systems are designed to prevent this.

The flexural performance is one of key parameters used to ascertain the structural performance of the reinforced concrete member and it has been illustrated that steel fibers improve the performance in these members under any form of loading conditions [13]. Although ASTM C1609 [14] and EN 14651 [15] explain how to test flexural performance, they do not clearly describe the ways microcracking occurs. Recent techniques such as digital image correlation (DIC), now allow detailed observation of deformation and very small cracks [16]. Advanced characterization methods add to the traditional tests, helping us better understand how SFRC resists cracks from the start of loading through to the final point of failure. [17]When the surface of steel fibers is deliberately roughened or irregularly profiled, ingress of such fibers leads to a large increase in the degree of mechanical friction and interlocking within the interface, which then slows onset and advancement of cracks under flexural loading [18]. Still, a consistent way to relate micromechanical observations to the overall flexibility of hybrid fiber systems is yet to be found, especially when these systems have a mix of steel and other fibers [19]. Knowledge about how fibers in SFRC influence crack width is still limited, despite the usual testing procedures. Advanced tools such as digital image correlation help scientists discover more about microcracking and crack resistance. Even so, the link between small-scale properties and the performance of hybrid fiber systems has yet to be fully explored.

Although plain concrete is commonly used, it breaks easily under stress because it does not have much tensile strength. The addition of dispersed steel fibers greatly improves the toughness and bending ability of concrete by crossing over cracks and managing the stress better. Such materials hold back crack formation and slower crack propagation, enhancing how the material absorbs energy and performs afterwards. The challenge of fiber clustering at high volumes persists, but technology such as DIC and the growth of hybrid fiber systems could offer good solutions for controlling cracks and enhancing flexural strength of concrete.

2 Research Methodology

2.1 Raw Material

Ordinary Portland Cement, sand, coarse aggregate and clean water are the raw materials used to make plain concrete. A standard mix of cement, sand and coarse aggregate in the ratio of 1:2:4, with a water-cement ratio of 0.5, was used for regular structural applications. SFRC used the basic materials of regular concrete, like cement and coarse aggregate, along with water, together with 2-in long steel fibers at 5% of the cement weight. These fibers were positioned throughout the mix layer by layer to improve its toughness, ability to resist cracks and overall mechanical strength.

2.2 Mix Design

2.2.1 Plain Concrete (PC)

The mixture consisted of a 1:2:4 ratio (cement: sand: coarse aggregate) and a water-cement ratio of 0.5. The specimens used were 4 cylinders and 3 beamlets for evaluating strength and workability. Materials were dry-mixed first and then water was added to make the mix workable. A slump test was carried out first to confirm how workable the material was. Concrete was gradually layered in pre-oiled molds, compacted with a tamping rod, smoothed, labelled and then cured in water for 28 day after being demolded at 24 hours. Mix design of Plain Cement Concrete is shown in Table 1 and Figure 1 represents the slump test performed on PCC.

Table 1 Plain Concrete Mix Design

Component	Ratio	Weight (kg)
Cement	1	6.5
Sand	2	13
Coarse Aggregate	4	26
Water (w/c = 0.5)	0.5	3.25



Figure 1 PCC Slump Test

2.2.2 Steel Fiber Reinforced Concrete (SFRC)

The same mixture (1:2:4, with a water-cement ratio of 0.5) was put together by adding 5% 2-inch steel fibers. Three containers were used to divide the materials (cement, sand, aggregates and steel fibers) into three sections for layered mixing. Materials and fibers were distributed in the mixer in three layers, so fibers were equally distributed. Materials were dry-mixed first and then water was added to make the mix workable. A slump test was carried out first to confirm how workable the material was. Then, the SFRC was poured into molds, tamped with rod, smoothed, labelled, then demolded after 24 hours and immersed in water for curing for 28 days. Mix design of Steel Fiber Reinforced Concrete is shown in Table 2 and Figure 2 represents the slump test performed on SFRC.

Table 2 SFRC Mix Design

Component	**Weight (kg)**	**Fiber Addition**
Cement	6.5	–
Sand	13	–
Coarse Aggregate	26	–
Steel Fibers	0.325	5% of cement
Water	3.25	–



Figure 2 SFRC Slump Test

2.3 Testing and Parameters

2.3.1 Testing Procedures

Tests on fresh concrete were carried out to assess how well both Plain Cement Concrete (PCC) and Steel Fiber Reinforced Concrete (SFRC) could be mixed and poured. For the slump test, the slump cone had a height of 300 mm, a base with a

200 mm diameter and a top diameter of 100 mm, as per ASTM C143. Immediately after mixing, the slump value was observed to ensure that the assessment of the concrete's workability was correct. A visual observation was necessary to observe for segregation and bleeding and to ensure that the fibers were evenly distributed in the SFRC mixture. Flexural strength tests on beam samples were done for the hardened concrete after 28 days to determine its structural behavior under bending loads.

2.3.2 Key Parameters

The key parameters focused on included the workability, flexural strength and the first-crack strength of both Plain Cement Concrete (PCC) and Steel Fiber Reinforced Concrete (SFRC). Slump test results were used to evaluate the workability and flexural and first-crack strengths were evaluated using a Universal Testing Machine and ASTM C1609. The findings from these tests show how the concrete behaves mechanically and how resistant it is to early cracks. Table 3 below lists the measured results for the various parameters.

Table 3 Key Parameters of Test

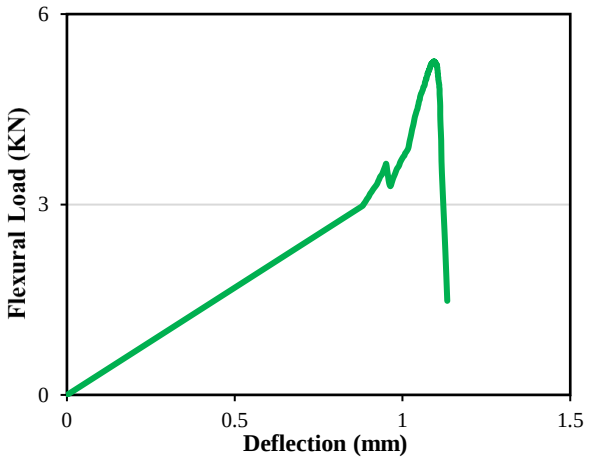
Parameter	Testing Method	Equipment Used	Measured Values
Workability	ASTM C143	Slump Cone, Tamping Rod	PCC: 125 mm SFRC: 12.5 mm
Flexural Strength	ASTM C1609	UTM	PCC: 3.540 ± 1.2 MPa, SFRC: 4.95 ± 0.5 MPa
First-Crack Strength	ASTM C1609	UTM	PCC: 3.1 ± 1.26 kN @ 0.8 mm, SFRC: 4.5387 ± 0.54 kN @ 0.9 mm

3 Results

3.1 Flexural Behavior

3.1.1 Plain Concrete

Figure 3 shows the flexural characteristics of plain concrete. From part (a), the curve shows load increasing smoothly up to the peak and when it exceeds the peak, the load decreases unexpectedly, suggesting a brittle failure. In part (b) pictures the experiment done during the flexural test, revealing how a plain concrete beam breaks suddenly once it reaches its maximum load, as seen by obvious cracking and debris.



a)



b)

Figure 3 a) Load-deflection curve of plain concrete under flexural loading showing brittle failure behavior, b) Experimental setup and failure mode of plain concrete beam during flexural strength testing.

3.1.2 Steel Fiber Reinforced Concrete

Figure 4 represents how well steel fiber reinforced concrete (SFRC) performs against flexure. The load-deflection curve in (a) observes a better response to cracking and in (b), the fibers inside the specimen prevent it from fracturing and keep the structure intact.

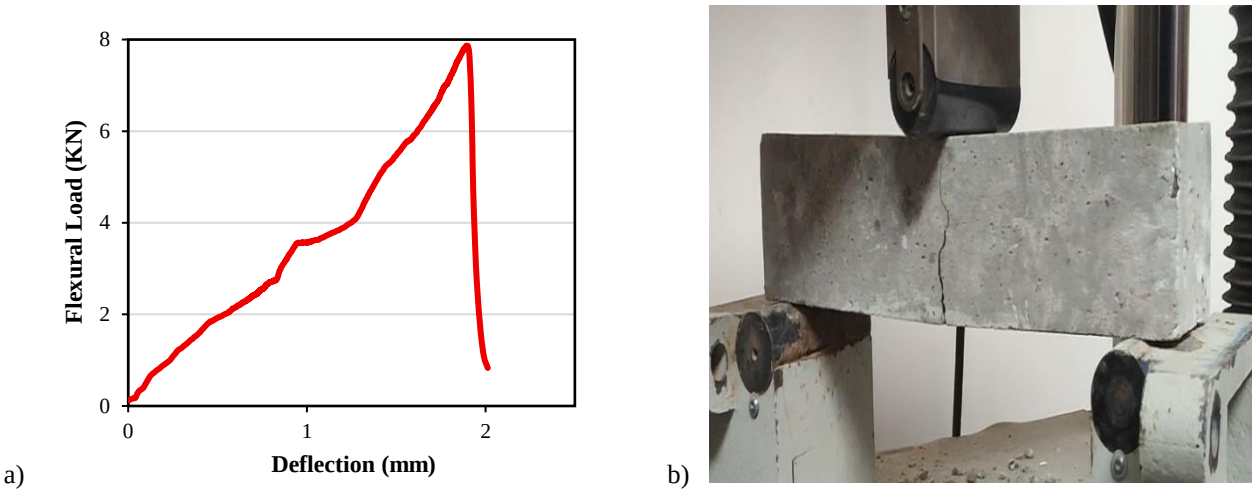


Figure 4 (a) Load-deflection curve of Steel Fiber Reinforced Concrete; (b) SFRC specimen under three-point bending test.

3.2 Flexural Properties

A material's flexural properties reveal its bending behavior, ultimately showing how strong it is, how stiff it is and whether it will resist cracking or deformation. Such attributes are especially needed for assessing fiber-reinforced concrete, where higher post-crack strength and energy absorbed are sought. Commonly, modulus of rupture, flexural toughness and how the load affects the deflection are obtained through testing by ASTM C1609. Flexural Toughness Index (FTI) measures the capacity of a material to absorb energy having already cracked to a point of failure due to flexural (bending) loading. It applies in assessing the ductility and post cracking of fiber-reinforced concrete (FRC). The Table 4 illustrates the main flexural characteristics found by studying the data:

Table 4 Comparison of Flexural Strength Between PCC and SFRC

Specimen	Peak Load (kN)	Modulus of Rupture (MPa)	E1 (GPa)	E2 (kPa)	FTI (MPa)
PCC	5.248 ± 1.26	3.540 ± 1.2	1.3 ± 0.70	1.2 ± 0.1	1 ± 0.15
SFRC	6.724 ± 0.54	4.5387 ± 0.5	0.8 ± 0.02	1.3 ± 0.3	1.6 ± 0.2

4 Practical Implementation

Stee Fiber Reinforced Concrete (SFRC) is suitable for many construction projects because of its strong ability to flex and resist cracks. In industrial floors, airport pavements and heavy-duty slabs, Steel Fiber Reinforced Concrete (SFRC) is now commonly used to increase fatigue performance, load distribution, surface life as well as minimizing slab thicknesses and spacing between joints [20]. This helps prevent the terrible damage that occurs when water seeps into the pavement. Energy absorption and flexibility in beams and joints can be improved in SFRC structures, so fiber dosages of 5% may replace some conventional reinforcement. With SFRC in precast concrete, it is possible to create elements that are thinner and lighter, resistant to cracks and made in less time and at less expense. Cement composites are useful for repairs and reconstruction, as they supply immediate, secure overlays for restoring the strength of bridge decks and parking areas

resistant to shrinking. A successful fiber-reinforced concrete mix is based on careful adjustment of the recipe so that fibers are distributed evenly and the mix can be handled without loss of shape, plus quality control. Overall, SFRC makes projects cheaper, less time-consuming to complete and more study, so it is commonly selected for many infrastructure projects.

5 Conclusion

The objective of this study was to improve the bending strength of plain cement concrete by including steel fibers. Using standard mix recipes and particular test methods (ASTM C143, C78 and C1609), both PCC and SFRC were produced, set aside to cure and tested. Following are conclusions from the experimental study:

- SFRC demonstrated better strength, the ability to take greater loads and toughness which means it is more able to handle loads than PCC.
- After being cracked, SFRC resisted forces due to fiber bridging, but PCC broke without warning, showing brittle behavior.
- Although there was a slight decrease in workability because of the fiber, SFRC kept a good slump, making it suitable for building sites.

Because of fiber bridging, SFRC remained tougher and more resistant to cracks than PCC. Even with workability slightly reduced, SFRC slump stayed sufficient for building purposes.

Acknowledgment

The authors would like to acknowledge the support and cooperation of the Public Works Division in facilitating this research. Special thanks to Dr. Majid Ali for his guidance, encouragement, and feedback throughout the study. The careful review and constructive suggestions by the anonymous reviewers are gratefully acknowledged

References

[1] Zain, M. F. M., Mahmud, H. B., Ilham, A., & Faizal, M. (2002). Prediction of splitting tensile strength of high-performance concrete. Cement and Concrete Research, 32(8), 1251-1258.

[2] Kosmatka, S. H., Panarese, W. C., & Kerkhoff, B. (2002). Design and control of concrete mixtures (Vol. 5420, pp. 60077-1083). Skokie, IL: Portland cement association.

[3] Qing, L., Cheng, Y., & Mu, R. (2019). Toughness enhancement and equivalent initial fracture toughness of cementitious composite reinforced with aligned steel fibres. Fatigue & Fracture of Engineering Materials & Structures, 42(11), 2533-2543.

[4] Yao, X., Li, L., Guan, J., Zhang, M., Liu, Z., Han, R., & He, S. (2021). Initial cracking strength and initial fracture toughness from three-point bending and wedge splitting concrete specimens. Fatigue & Fracture of Engineering Materials & Structures, 44.

[5] Huang, B. T., Yu, J., Wu, J. Q., Dai, J. G., & Leung, C. K. (2020). Seawater sea-sand Engineered Cementitious Composites (SS-ECC) for marine and coastal applications. Composites Communications, 20, 100353

[6] Rajak, D. K., Pagar, D. D., Menezes, P. L., & Linul, E. (2019). Fiber-reinforced polymer composites: Manufacturing, properties, and applications. Polymers, 11(10), 1667.

[7] Saba, A. M., Khan, A. H., Akhtar, M. N., Khan, N. A., Koloor, S. S. R., Petrů, M., & Radwan, N. (2021). Strength and flexural behavior of steel fiber and silica fume incorporated self-compacting concrete. Journal of Materials Research and Technology, 12.

[8] Smarzewski, P. (2019). Study of toughness and macro/micro-crack development of fibre-reinforced ultra-high performance concrete after exposure to elevated temperature. Materials, 12(8), 1210..

[9] Akbulut, Z. F., Tawfik, T. A., Smarzewski, P., & Guler, S. (2025). Advancing Hybrid Fiber-Reinforced Concrete: Performance, Crack Resistance Mechanism, and Future Innovations. Buildings, 15(8), 1247.

[10] Xu, W., Yang, L., Gao, D., Tang, J., Sun, G., & Zhang, Y. (2023). Mechanical properties of seawater-mixed steel fiber reinforced concrete. Journal of Building Engineering, 73, 106823.

[11] Wang, Z., Li, H., Zhang, X., Chang, Y., Wang, Y., Wu, L., & Fan, H. (2023). The effects of steel fiber types and volume fraction on the physical and mechanical properties of concrete. Coatings, 13(6), 978.

[12] Kazemi, H., Fattahi, S., Ahmadi, M. S., & Sadeghi-Sadeghabad, M. (2023). Optimization of Tensile and Shear Properties of Concrete Reinforced with Polypropylene and Glass Fibers Using Taguchi Method. Journal of Textiles and Polymers, 11(3), 19-27.

[13] Accornero, F., Rubino, A., & Carpinteri, A. (2022). Post-cracking regimes in the flexural behaviour of fibre-reinforced concrete beams. International Journal of Solids and Structures, 248, 111637.

[14] ASTM Committee C09 on Concrete and Concrete Aggregates. Subcommittee C09. 42 on Fiber-Reinforced Concrete, & ASTM International Committee C09 on Concrete and Concrete Aggregates. (2012). Standard test method for flexural toughness of fiber reinforced conc.

[15] En, B. S. (2007). 14651,"Test method for metallic fibre concrete—Measuring the flexural tensile strength (Limit of proportionality (LOP), residual). British Standards Institution, London, UK.

[16] Zhong, J., Zhuang, H., Shiyang, P., & Zhou, M. (2021, October). Experimental and numerical analysis of crack propagation in reinforced concrete structures using a three-phase concrete model. In Structures (Vol. 33, pp. 1705-1714). Elsevier.

[17] Sun, X., Zhao, K., Li, Y., Huang, R., Ye, Z., Zhang, Y., & Ma, J. (2018). A study of strain-rate effect and fiber reinforcement effect on dynamic behavior of steel fiber-reinforced concrete. Construction and Building Materials, 158, 657-669.

[18] Chun, B., Yoo, D., & Banthia, N. (2020). Achieving slip-hardening behavior of sanded straight steel fibers in ultra-high-performance concrete. Cement and Concrete Composites, 113, 103669.

[19] Akbulut, Z. F., Tawfik, T. A., Smarzewski, P., & Guler, S. (2025). Advancing Hybrid Fiber-Reinforced Concrete: Performance, Crack Resistance Mechanism, and Future Innovations. Buildings, 15(8), 1247.

[20] Hu, C., Weng, X., Zhang, J., Xu, W., Qu, B., & Su, L. (2021). Experimental study on fatigue strength of airport concrete pavement slab. Construction and Building Materials, 270, 121493.

COMPARATIVE STUDY OF NYLON FIBER REINFORCED CONCRETE WITH PCC FOR COMPRESSIVE STRENGTH AND WORKABILITY

[a] Muhammad Mursaleen*, [b] Ameer Turab

a: Department of Construction Management, Halcrow Pakistan (Pvt) Limited, Islamabad, Pakistan.
mursaleenmuhammadjhg@gmail.com
b: Department of Civil Engineering, Hochschule Stendal Magdeburg, Germany. ameer.turab@stud.h2.de
* Corresponding author

Abstract- The influence of nylon fiber addition on the workability and compressive strength of concrete is studied in this investigation. Two concrete mixes, Plain Cement Concrete (PCC) and Nylon Fiber Reinforced Concrete (NFRC), were prepared using Ordinary Portland Cement (OPC), fine sand, crushed granite aggregates, potable water, and synthetic nylon fibers 50 mm long. NFRC mix included nylon fibers at 3% of cement weight by weight with a mix proportion of 1:4:2 A higher proportion of fine aggregates mix helps create a denser matrix and improves fiber bonding and a water-cement proportion of 0.6, whereas PCC used a traditional 1:2:4 proportion with a 0.5 water-cement proportion. The tests were conducted on fresh concrete according to standard slump and temperature tests, as well as compressive strength tests after 28 days of water curing in accordance with ASTM standards. Results showed that NFRC recorded a greater slump in value (190 mm) than that of PCC (150 mm), proving better workability. NFRC indicated slightly lower mean compressive strength (7.07 MPa) than PCC (9.05 MPa) due to possible increased water content and fiber hindrance in compaction. Even with a decrease in strength, NFRC had less variability and was more consistent. These results indicate that NFRC is ideal for non-structural uses with improved workability and resistance to cracking like pavements, overlays, and precast components where ductility and toughness take precedence over maximum compressive strength.

Keywords- Nylon Fiber, Compressive Strength, Durability, Mix Design, Sustainability

1 Introduction

Concrete is a widely applied construction and civil engineering material because of its cost-effectiveness and high strength in compression. Fiber-reinforced concrete has been used widely across many structures over the past decades in engineering. Recent research hints at expanded applications of fiber-reinforced concrete and attempts to mimic its mechanical behavior with assistance from sophisticated tools such as the Lattice Discrete Particle Model [1,2]. Lightweight foamed concrete (LFC) has been of interest as a green material for semi-structural purposes based on its low density and environmental advantages. Its limited durability and low mechanical strength have limited its broader application in structural members. Recent research has been aimed at optimizing LFC performance through fiber reinforcement, especially with hybrid mixes such as nylon and polypropylene fibers [3]. This research explores the use of Ground Nut Shell Ash, Cashew Nut Shell Ash, and Discarded Nylon Fiber in cement concrete to make it more sustainable. It compares the mechanical behavior of such green composites as a possible substitute for regular concrete [4]. Based on limited experimental data, e.g., polypropylene and steel fiber combinations compression and bending tests, the model simulates and examines significant mechanical responses and parameter sensitivities [5]. Nylon fibers (NF) improve concrete by increasing compressive strength, and overall durability. Experiments indicate that the inclusion of 0.1% NF and 5%

eggshell powder in self-compacting concrete improves compressive and tensile strength by 6% and 4%, respectively [6]. Past studies have considered the incorporation of nylon fibers to improve concrete's mechanical properties, specifically its tensile and compressive strength. Different lengths of fibers have indicated significant impacts, with (25 mm, 50 mm and 75 mm) fibers reporting the best outcomes [7] The increasing demand for concrete has resulted in excessive exploitation of natural sand, especially river sand, and hence severe environmental degradation. The current study investigates a sustainable option through the use of stone dust (SD) as a partial substitution of fine aggregate and nylon fiber (NF) as reinforcing material in concrete to assess their combined impact on compressive and splitting tensile strengths employing artificial neural network (ANN) modeling [8].

Nylon Fiber reduces micro-cracking and enhances post-crack behavior. Machine learning models were able to predict concrete performance. SCC quality was unaffected despite reduced workability with optimized fiber. This blend provides a sustainable solution in order to improve concrete performance in contemporary construction [9]. This research examines the impact of nylon fibers (1% to 2.5% by volume) on compressive and splitting tensile strength of concrete. Results showed that strength and toughness in nylon fiber reinforced concrete were improved, and 2.5% of fiber content showed optimal performance. 28 days of water curing gave maximum compressive strength of 36.62 MPa and splitting tensile strength of 5.10 MPa. Such results make nylon fiber a potential candidate to be utilized as an additive in order to enhance mechanical characteristics of concrete [2]. The study provides the reliable early damage detection under cyclic loading, which results in enhanced durability and safety of FRC structures [10]. By utilizing the two fibers, they produced Hybrid Nylon-Steel Fiber Reinforced Concrete with significant compressive strength of 101.25 MPa with Kings-Scheffe's (6,2) model [11]. Migrated to the imperatives of affordable and sustainable substitutes to steel, this research investigates the utilization of bamboo strips and nylon fibers for reinforcing light wall panels with strength, deformation, and fire resistance. In comparison to existing studies on single-material reinforcements, this hybrid method presents better performance; more research is suggested on long-term durability and applicability at a larger scale [12]. With increasing environmental concerns and resource scarcity, this research explores how nylon fiber can be used to increase the compressive strength of concrete using Crushed Stone Dust (CSD) as a green substitute. On optimization using RSM, it shows better strength with the addition of nylon fiber, consistent with previous work but with a better accurate mix design; however, the workability deterioration emphasizes the requirement for balancing performance and practicality in upcoming applications [13].

In this Hybrid Nylon-Fiber Reinforced Concrete and Recycled Nylon Fiber Fabric Concrete Concretes possess greater compressive strength and energy absorption than plain concrete. NFFRC was better than PC and NFRC, with improvement in compressive strength of 5.37% and 10.74%, respectively. These results indicate that recycled nylon fibers can be effective as an alternative in structural application [13,14]. Fibers are secondary reinforcement materials that function as crack arresters, which greatly enhance the static and dynamic characteristics of concrete. The response of fiber reinforced concrete depends on the type of fiber and the aspect ratio. Extensive research and development have been conducted since the 1960s, and this has resulted in a broad range of FRC products with improved mechanical behavior [15,16]. Plain concrete suffers from low tensile strength and a high environmental impact due to its carbon footprint. The combined use of fibers and recycled materials offers a promising solution to enhance concrete's mechanical and durability performance. This study explores the synergistic effects of silica fume and nylon fibers on recycled aggregate concrete to develop a more sustainable and durable construction material [18]. Optimize the compressive strength of Hybrid Polypropylene–Nylon Fiber Reinforced Concrete. 112 mix ratio samples attained a maximum compressive strength of 71.36 MPa, which was superior to previous models and the standard requirement. Consistent findings are that a combination of fibers enhances the quality of the concrete for high-strength applications [19]. This study explores nylon fiber in addition to enhance compressive strength and durability, showing peak performance at 1.5% fiber content. Compared to previous studies, it confirms fiber effectiveness in improving strength and resistance, though it highlights a trade-off with workability requiring careful mix design adjustments [20]. To overcome the inefficiencies of trial-based mix design, this study applies Scheffe's (5,2) model to optimize nylon fiber reinforced concrete (NFRC) for compressive strength, achieving 21.96 MPa. Unlike previous empirical approaches, this model-based method offers a more economical and reliable mix design, though further validation on durability and field performance is recommended [21].

This research investigates the effect of the addition of nylon fibers on the workability and mechanical properties of concrete. Two mixes were made: Plain Cement Concrete (PCC) and Nylon Fiber Reinforced Concrete (NFRC), each with nylon fibers incorporated at 3% cement weight. The two mixes were subjected to slump, temperature, and 28-day compressive strength under standard ASTM methods. Uniform mixing, precise curing, and precise measurement of

strengths for comparison were ensured through the methodology. The inclusion of 3% nylon fibers imparts toughness and energy absorption, leading to long-term performance and less maintenance in application situations.

2 Research Methodology

2.1 Raw Materials

The fundamental components utilized in this research were Ordinary Portland Cement (OPC), well-graded sand as fine aggregate, crushed granite coarse aggregates with a nominal maximum size of 20 mm, clean potable water, and synthetic nylon fibers with a length of 50 mm. All materials were sourced from local suppliers and were selected based on their conformity with construction-grade quality standards. The nylon fibers were smooth and flexible, making them suitable for enhancing the mechanical properties of concrete without inducing brittleness or compromising mix uniformity.

2.2 Mix Design

To study the influence of nylon fibers on the compressive strength of concrete, two types of concrete mixes were developed: one for Nylon Fiber Reinforced Concrete (NFRC) and the other for conventional Plain Cement Concrete (PCC). The NFRC mix was proportioned by weight using a (cement: sand: aggregate) ratio of 1:4:2, corresponding to 6.5 kg of cement, 26 kg of sand, and 13 kg of coarse aggregate. A water-cement ratio of 0.6 was maintained throughout to provide a balance between workability and strength development. Nylon fibers were added at 3% by weight of cement, a dosage selected based on literature supporting its effectiveness in improving ductility and crack resistance. The conventional PCC mix followed a typical 1:2:4 ratio, commonly used in non-reinforced structural applications, with the same water-cement ratio (0.5) to maintain comparability with the fiber-reinforced variant as shown in Table 1. In fiber-reinforced concrete (FRC), uniform fiber distribution is critical. A higher proportion of fine aggregates (sand) in the 1:4:2 mix helps create a denser matrix and improves fiber bonding. Coarse aggregates in higher proportion (as in 1:2:4) can lead to fiber balling and poor distribution. Concrete mixing was carried out in a mechanical drum mixer. The dry ingredients (cement, sand, and aggregates) were first blended in five successive layers to avoid the fiber "balling effect" and ensure even distribution. Once a uniform dry mix was achieved, water was added gradually and mixing continued for 5 minutes to achieve a homogeneous wet mix. Immediately after mixing, temperature measurements were recorded for the fresh concrete using a standard concrete thermometer. Slump tests were conducted in accordance with ASTM C143 to evaluate the workability and consistency of both the NFRC and PCC mixes. Concrete samples were cast into standard cylindrical molds of 4 inches (100 mm) in diameter and 8 inches (200 mm) in height. The molds were filled in three layers; each layer compacted to eliminate trapped air and ensure uniform density. After 24 hours of ambient curing, the specimens were demolded and placed in a curing tank containing clean water. The samples were cured for 28 days, in compliance with ASTM C192, to allow full hydration and strength development.

Table 1: Table showing the mix design of Nylon fiber Reinforced and Plain Cement Concrete

Description	Mix Ratio	Cement (kg)	Sand (kg)	Aggregates (kg)	W/C Ratio	Fiber Length (50 mm)	Fiber Dosage (%)	Mixing Time (Minutes)
PCC	1:2:4	6.5	13	26	0.5	-	-	05
NFRC	1:4:2	6.5	26	13	0.6	Nylon	3	05

2.3 Testing and Parameter

To thoroughly evaluate the performance characteristics of both Nylon Fiber Reinforced Concrete (NFRC) and Plain Cement Concrete (PCC), a systematic testing protocol was implemented based on standardized procedures. The testing focused on both fresh and hardened concrete properties. Fresh concrete testing involved the measurement of slump and temperature to assess workability and mixing consistency. The slump test was conducted according to ASTM C143 using a standard slump cone to determine the flowability and ease of placement of the concrete mixes. Temperature readings were recorded using a digital concrete thermometer in line with ASTM C1064/C1064M, ensuring consistency in environmental and mixing conditions.

For hardened concrete evaluation, compressive strength testing was carried out in accordance with ASTM C39/C39M. Cylindrical specimens with dimensions of 100 mm in diameter and 200 mm in height were prepared for both NFRC and PCC. The concrete was placed in molds in three successive layers; each layer compacted to remove air voids and achieve uniform density. After casting, the specimens were demolded following a 24-hour setting period and transferred to a curing tank filled with clean water, where they were cured for 28 days as per ASTM C192/C192M to ensure complete hydration and strength development.

Post-curing, the specimens were subjected to compressive strength testing using a Universal Testing Machine (UTM). The machine applied a continuous axial load at a controlled rate until the point of failure. The maximum load sustained by each specimen was recorded and used to calculate compressive strength based on the specimen's cross-sectional area. These tests provided key parameters for comparing the mechanical behaviour and consistency of NFRC and PCC under compressive loads. By adhering strictly to standard procedures, the obtained data were ensured to be reliable and suitable for comparative analysis in evaluating the impact of nylon fiber reinforcement on concrete performance.

3 Results

3.1 Workability Behaviour

To evaluate the mechanical performance of both Nylon Fiber Reinforced Concrete (NFRC) and conventional Plain Cement Concrete (PCC), a series of tests were conducted on both fresh and hardened concrete specimens. Immediately after mixing, fresh concrete properties were assessed through temperature and slump tests. These parameters provided valuable insight into the behaviour of fresh NFRC compared to PCC. The slump test, as shown in Figure 1, conducted in accordance with ASTM C143, measured the workability and flowability of the mix. PCC exhibited a slump of 150 mm, indicating moderate workability suitable for general structural applications. In contrast, NFRC showed a higher slump of 190 mm, suggesting better workability, which may be attributed to the higher water-cement ratio and the lubricating effect of nylon fibers enhances workability by reducing internal friction and promoting smoother flow of the concrete mix.

`

a)  b) 

Figure 1: a. Showing the slump of PCC, and b. Slump of NFRC

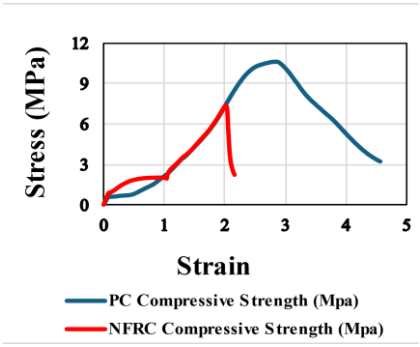
a)  b) 

Figure 2: a. Showing the Temperature of PCC, and b. Temperature of NFRC

The temperature of fresh concrete was measured using a standard concrete thermometer. PCC registered a temperature of 30.6°C, while NFRC measured 30.7°C, as shown in Figure 2, indicating a negligible difference and confirming consistent mixing and ambient conditions during sample preparation.

3.2 Compressive Behaviour

After 28 days of water curing, compressive strength tests were carried out using a Universal Testing Machine (UTM) in accordance with ASTM C39. This test involved applying a gradual compressive load on cylindrical concrete specimens until failure occurred as shown in Figure 3. The load of failure was recorded in kilonewtons (KN) and converted to compressive strength in megapascals (MPa) based on the cross-sectional area of the specimen.



a)



b)

Figure 3: a. Showing graphical results of the compressive strength of NFRC vs PCC, and b. Specimen under UTM

3.3 Compressive and Workability Properties of NFRC and PCC

The PCC specimens showed compressive load values of 60.308 KN, and 86.472 KN, corresponding to compressive strengths of 7.440 MPa, and 10.66 MPa, respectively. The average compressive strength for PCC was calculated to be approximately 9.05 MPa, with a standard deviation of 1.614 MPa and a coefficient of variation (COV) of 17.83%, indicating moderate variability in strength performance. On the other hand, NFRC specimens recorded compressive load values of 59.582 KN, and 55.192 KN, resulting in compressive strengths of 7.351 MPa, and 6.808 MPa, respectively. The average compressive strength of NFRC was 7.07 MPa, with a lower standard deviation of 0.384 MPa and a COV of 5.43**%**, as shown in Table 2, suggesting greater consistency in test results compared to PCC.

Table 2: Table showing the Compressive strength and workability properties of Nylon fiber Reinforced and Plain Cement Concrete

Description	Slump (mm)	Temperature (C°)	Load (KN)		Compressive Strength (MPa)		SD (MPa)	COV (%)
PCC	150	30.6	60.308	73.39	7.440	9.05	1.614	17.83
			86.472		10.66			
NFRC	190	30.7	59.582	57.39	7.351	7.07	0.384	5.43
			55.192		6.808			

Although the inclusion of 3% nylon fibers contributed to enhanced workability and potentially better post-cracking behavior, the compressive strength of NFRC was found to be lower than that of conventional PCC. This reduction in strength could be attributed to the higher water-cement ratio in the NFRC mix and the potential disruption in the matrix compaction caused by excessive fiber content. However, the ductility and crack-resisting properties of NFRC may offer structural advantages in specific applications where toughness and energy absorption are prioritized over peak compressive strength.

Overall, the results highlight that while NFRC may slightly compromise compressive strength compared to traditional PCC, it offers superior workability and may perform better in applications requiring improved durability and tensile behavior.

4 Practical Implementation

The practical use of Nylon Fiber Reinforced Concrete (NFRC) is highly promising in the field of civil engineering projects, particularly where ductility, crack control, and workability are critical performance parameters. Adding nylon fibers improves the post-cracking performance of concrete, and hence it is a good substitute in applications where small surface cracks have the potential to critically impair durability and lifespan. NFRC is particularly beneficial in non-structural uses like pedestrian pavements, parking lots, sidewalks, and thin overlays where conventional Plain Cement Concrete (PCC) is vulnerable to early-age cracking and shrinkage. The enhanced workability evidenced in NFRC facilitates easier placement and compaction in formworks with complex geometries or dense reinforcement arrangements. This benefit is vital in contemporary construction methodologies that require efficiency but not at the expense of quality. Additionally, its excellent microcracking resistance makes it an ideal choice for thin-section members, plaster work, and precast elements exposed to transportation and handling stress prior to final disposal. Aside from static applications, NFRC has great potential in dynamic or vibration-exposed conditions such as in tunnel linings, highway barriers, or light prefabricated members, where plain concrete may be more prone to cracking. Although NFRC is less suitable for high load carrying members because of its lower compressive strength, NFRC still supports conventional concrete in hybrid structures by enhancing ductility and energy absorption. Additionally, the cost of high-quality synthetic fibers can be significantly higher compared to traditional reinforcement, affecting the economic feasibility of large-scale projects. Moreover, the lack of standardized guidelines for mixing and placing fiber-reinforced concrete creates uncertainty in quality control and performance prediction. Its financial viability is also advantage nylon fibers are not expensive and are locally available, so NFRC is a viable and eco-friendly material for mass applications. Provided proper mix design and dosage regulation are followed, NFRC is an effective means of enhancing long-term performance, especially in projects with durability, resistance to cracking, and simplicity of construction as top considerations.

5 Conclusion

This study explored the effectiveness of nylon fiber-reinforced concrete (NFRC). The key conclusions drawn from this study are summarized below

- Nylon Fiber Reinforced Concrete (NFRC) showed improved workability, where the slump was 190 mm as against 150 mm for Plain Cement Concrete (PCC), reflecting improved flowability and ease of placement.
- The average compressive strength of NFRC (7.07 MPa) was slightly less than that of PCC (9.05 MPa), mainly attributed to the increased water-cement ratio (0.6) and fiber interference.
- NFRC is preferably adaptable for lightly loaded or non-structured applications like pavements, footpaths, flooring, and pre-cast units where crack control along with workability is desired.

Generally, NFRC presents a cost-effective and pragmatic solution in construction situations where intermediate strength with improved performance properties is needed.

Acknowledgment

The authors gratefully acknowledge the support and guidance received from all individuals and departments who contributed to the successful completion of this research. Special appreciation is extended to Engr. Dr. Majid Ali for his invaluable mentorship and technical insight throughout the study.

References

[1] S. Hedjazi and D. Castillo, "Relationships among compressive strength and UPV of concrete reinforced with different types of fibers," *Heliyon*, vol. 6, no. 3, p. e03646, Mar. 2020, doi: 10.1016/j.heliyon.2020.e03646.

[2] S. Y. Rafi, M. M. N. Niaz, J. Miah, M. Islam, and A. Haque, "Comparative Strength Analysis of Concrete with Nylon Fiber in Different Curing Media".

[3] I. Anuar, S. Ismail, and A. M. Saleh, "Influence of Density and Compressive Strength on Intrinsic Air Permeability and Porosity of Hybrid Fibre-Reinforced Lightweight Foamed Concrete," *Sem. Int. Jour. Civ. Struct. Eng.*, vol. 4, no. 1, pp. 31–45, Feb. 2025, doi: 10.37934/sijcse.4.1.3145.

[4] E. Tom and Y. S. Jose, "Experimental study of cement with ground nut shell ash & cashew nut shell ash with discarded nano nylon powder concrete for sustainable environment," *Matéria (Rio J.)*, vol. 30, p. e20240829, 2025, doi: 10.1590/1517-7076-rmat-2024-0829.

[5] S. Poudel, A. Cibelli, C. Del Prete, R. Wan-Wendner, C. Mazzotti, and N. Buratti, "Insights on Lattice Discrete Particle Model Calibration and Validation Procedure to Simulate Polypropylene and Steel Fibre-Reinforced Concrete," *Fibers*, vol. 13, no. 2, p. 16, Feb. 2025, doi: 10.3390/fib13020016.

[6] M. S. Moradi, M. H. Tavana, M. R. Habibi, and M. Amiri, "Effect of water to cement ratio on mechanical properties of FRC subjected to elevated temperatures: Experimental and soft computing approaches," *Heliyon*, vol. 10, no. 21, p. e39513, Nov. 2024, doi: 10.1016/j.heliyon.2024.e39513.

[7] Y. Qin *et al.*, "Effects of nylon fiber and nylon fiber fabric on the permeability of cracked concrete," *Construction and Building Materials*, vol. 274, p. 121786, Mar. 2021, doi: 10.1016/j.conbuildmat.2020.121786.

[8] S. Ray, M. Haque, T. Ahmed, A. F. Mita, M. H. Saikat, and M. M. Alom, "Predicting the strength of concrete made with stone dust and nylon fiber using artificial neural network," *Heliyon*, vol. 8, no. 3, p. e09129, Mar. 2022, doi: 10.1016/j.heliyon.2022.e09129.

[9] M. A. Safayet, A. A. Abdullah, M. F. Islam, T. S. Alahmari, M. H. R. Sobuz, and M. M. H. Khan, "Combined influence of eggshell powder and nylon fiber on self-compacting concrete production: experimental assessment and machine learning quantifications," *Mater. Res. Express*, vol. 12, no. 2, p. 025003, Feb. 2025, doi: 10.1088/2053-1591/adb0a6.

[10] G. M. Sapidis, M. C. Naoum, and N. A. Papadopoulos, "Electromechanical Impedance-Based Compressive Load-Induced Damage Identification of Fiber-Reinforced Concrete," *Infrastructures*, vol. 10, no. 3, p. 60, Mar. 2025, doi: 10.3390/infrastructures10030060.

[11] K. C. Nwachukwu, D. A. Okodugha, and C. F. Njoku, "Optimized Compressive Strength Determination of Hybrid Nylon – Steel Fibre Reinforced Concrete [HNSFRC] Using Kings - Scheffe's Binary Mixture," vol. 11, no. 5, 2024.

[12] T. Islam, M. H. Rashid, M. M. Khatun, and A. B. Shaheen, "BAMBOO AND NYLON FIBER REINFORCEMENT: AN ALTERNATIVE APPROACH TO PRODUCE INFILL WALL PANELS," 2024.

[13] A. F. Mita, S. Ray, M. Haque, and M. H. Saikat, "Prediction and optimization of properties of concrete containing crushed stone dust and nylon fiber using response surface methodology," *Heliyon*, vol. 9, no. 3, p. e14436, Mar. 2023, doi: 10.1016/j.heliyon.2023.e14436.

[14] Dr. G. T. Naidu, "Study the Strength Behaviour of M30 Grade Concrete Using Glass, Nylon and Natural Fibres," *IJRASET*, vol. 12, no. 4, pp. 102–108, Apr. 2024, doi: 10.22214/ijraset.2024.59707.

[15] Y. Qin, X. Zhang, and J. Chai, "Damage performance and compressive behavior of early-age green concrete with recycled nylon fiber fabric under an axial load," *Construction and Building Materials*, vol. 209, pp. 105–114, Jun. 2019, doi: 10.1016/j.conbuildmat.2019.03.094.

[16] J. Saxena and A. Saxena, "Enhancement the Strength Of Conventional Concrete by using Nylon Fibre".

[17] M. Sridhar, M. V. Kumar, N. Nagaprasad, S. K. Bhagat, and K. Ramaswamy, "Microstructural and statistical analysis on mechanical performance of novel flattened end nylon fibre reinforced concrete," *Sci Rep*, vol. 15, no. 1, p. 8483, Mar. 2025, doi: 10.1038/s41598-025-89593-x.

[18] J. Ahmad, O. Zaid, C. L.-C. Pérez, R. Martínez-García, and F. López-Gayarre, "Experimental Research on Mechanical and Permeability Properties of Nylon Fiber Reinforced Recycled Aggregate Concrete with Mineral Admixture," *Applied Sciences*, vol. 12, no. 2, p. 554, Jan. 2022, doi: 10.3390/app12020554.

[19] K. C. Nwachukwu, O. Edike, C. C. Mathew, O. Oguaghamba, and B. O. Mama, "Investigation of Compressive Strength Property of Hybrid Polypropylene - Nylon Fibre Reinforced Concrete (HPNFRC) Based on Scheffe's (6,3) Model".

[20] J. Ahmad *et al.*, "Mechanical properties and durability assessment of nylon fiber reinforced self-compacting concrete," *Journal of Engineered Fibers and Fabrics*, vol. 16, p. 15589250211062833, Jan. 2021, doi: 10.1177/15589250211062833.

[21] K. C. Nwachukwu, H. O. Ozioko, and P. O. Okorie, "Application Of Scheffe's Mathematical," vol. 4, no. 2, 2022.

ENHANCING TENSILE PERFORMANCE OF CONCRETE USING STEEL FIBER REINFORCEMENT: AN EXPERIMENTAL STUDY

[a] Awais Sikandar* and [b] Faheem Ahmad Gul

a: Civil Engineering Department, APCOMS, Rawalpindi, Pakistan. awaissikandar786abc@gmail.com
b: School of Civil and Architectural Engineering, Nanchang Institute of Technology, Nanchang 330099, China. faheem@nit.edu.cn
* Corresponding author

Abstract- Conventional concrete, despite its widespread use, exhibits low tensile and shear strength, often leading to brittle failure under stress if not adequately reinforced. To address this limitation, steel fibers are increasingly employed to enhance mechanical performance. The effectiveness of Steel Fiber Reinforced Concrete (SFRC) largely depends on the bond between the fibers and the surrounding concrete matrix. This bond influences critical factors such as fracture initiation, crack spacing, and crack width. A comprehensive understanding of these bond mechanisms is essential for optimizing SFRC performance. This study investigates the role of steel fiber reinforcement in improving tensile behavior, highlighting that incorporating up to 5% steel fibers significantly increases the tensile strength of concrete. Furthermore, the inclusion of fibers enhances the pull-out resistance, contributing to improved crack control and overall structural integrity. The findings support the practical application of SFRC in structures requiring enhanced toughness and durability.

Keywords- Bond Behavior, Crack Control, Steel Fiber Reinforced Concrete (SFRC), Tensile Strength Enhancement

1 Introduction

Concrete is susceptible to cracking due to various internal and external factors. In modern construction, applications such as bridge decks, highway pavements, and industrial floors demand materials with greater ductility and higher energy absorption capacity [1]. However, conventional concrete exhibits low tensile strength, limited ductility, poor crack resistance, and minimal energy absorption. These weaknesses are primarily due to the presence of internal microcracks, which are inherent in the material and often lead to brittle failure under stress [2]. To enhance concrete performance in such demanding applications, it is essential to address these deficiencies by improving its toughness and minimizing inherent flaws [3].

Concrete is inherently brittle and exhibits low post-cracking strength and limited ductility [4]. Cracks in plain concrete typically appear when applied tensile stresses exceed its tensile capacity [5]. To address this issue, the incorporation of short, discrete fibers into the concrete matrix has proven effective in reducing microcracking and controlling the spread of localized macrocracks. This also enhances post-cracking strength and improves ductile behavior under load [6]. However, it is important to note that fibers have minimal influence on the material's performance prior to the initiation of cracking [7]. The use of short reinforcing fibers dates back thousands of years and has been applied in various materials throughout history. In modern concrete applications, this concept has evolved significantly. Today, a wide range of fibers including steel, other metallic types, and polymeric materials are used to enhance the mechanical properties of concrete [8].

When fiber reinforcement takes the form of short, discrete fibers, it functions well as stiff inclusions in the concrete matrix [9]. Steel fiber reinforcement cannot be regarded as a direct replacement for longitudinal reinforcement in reinforced and

prestressed structural components due to their physical resemblance to aggregate inclusions [10]. However, it is expected that adding fibers to the concrete's body or creating a tensile skin will improve the structural components' resistance to deformation, cracking, and other serviceability conditions because of the material qualities of fiber concrete [11].

Fiber reinforcement can be applied in various forms to meet different structural needs. In one approach, the fibers are randomly and uniformly dispersed in three dimensions throughout the concrete, enhancing both shear resistance and tensile performance [12]. Alternatively, fibers can be aligned in a two-dimensional arrangement to act as a tensile skin over conventional steel reinforcement. This method provides additional control over cracking and further strengthens the structure [13]. Although steel fibers are known to improve concrete performance, a clearer understanding of their effect on tensile strength, particularly under split tensile conditions, is still needed. This study addresses that by experimentally evaluating the tensile behavior and crack resistance of SFRC using a 5% steel fiber dosage. The novelty lies in examining the bond mechanisms and pull-out resistance of the fibers, providing practical insights into optimizing SFRC for applications requiring improved ductility and toughness.

2 Research Methodology

2.1 Raw Materials

Plain concrete was prepared using ordinary Portland cement, clean drinking water, locally sourced sand, and aggregates with mixed sizes of 12 mm and 6 mm (maximum size ≤12 mm). To produce Steel Fiber Reinforced Concrete (SFRC), 50 mm long steel fiber strands were incorporated into the same mix. Prior to mixing, the steel fibers were thoroughly cleaned to remove surface dust and allowed to dry. After cleaning, the fibers were manually cut to a uniform length of 50 mm to ensure consistency in the mix.

2.2 Mix Proportions and Casting

For plain concrete (PC), a mix ratio of 1:2:4 (cement, sand, and aggregate) was used, maintaining a constant water-to-cement (w/c) ratio of 0.5. All dry materials were added to a drum-type mixer and mixed for one minute. The required amount of water was then added, and mixing continued for an additional five minutes to achieve a homogenous mixture.

For Steel Fiber Reinforced Concrete (SFRC), steel fibers were incorporated at 5 percent of the cement's weight. The dry components, including cement, sand, aggregate, and steel fibers, were added in three stages. Two-thirds of the water was introduced initially, followed by four minutes of mixing. After the remaining one-third of the water was added, mixing continued for another two minutes to ensure uniformity. The SFRC mix was then poured into molds in three layers. Each layer was compacted using a tamping rod with 25 blows to ensure proper consolidation.

2.3 Testing Methods and Key Parameters

Slump tests for both plain concrete (PC) and steel fiber reinforced concrete (SFRC) were conducted in accordance with ASTM C143 [14]. The tensile strength of concrete was evaluated using the split tensile test, following ASTM C496 [15]. The slump values recorded were 125 mm for PC and 12.5 mm for SFRC, as shown in Table 1. This significant reduction in slump for SFRC indicates lower workability compared to PC. Although both mixes maintained a constant water-to-cement ratio of 0.5, SFRC exhibited reduced workability. This is because steel fibers absorb some water from the mix, reducing overall fluidity. Additionally, the relatively long steel fibers caused congestion within the mix, further contributing to the lower slump value.

Table 1 Slump Values for PCC and SFRC Mixes

Sr.	Concrete	W/C	Slump (mm)
1	PC	0.5	125
2	SFRC	0.5	12.5

3 Results and Analysis

3.1 Tensile Behaviour

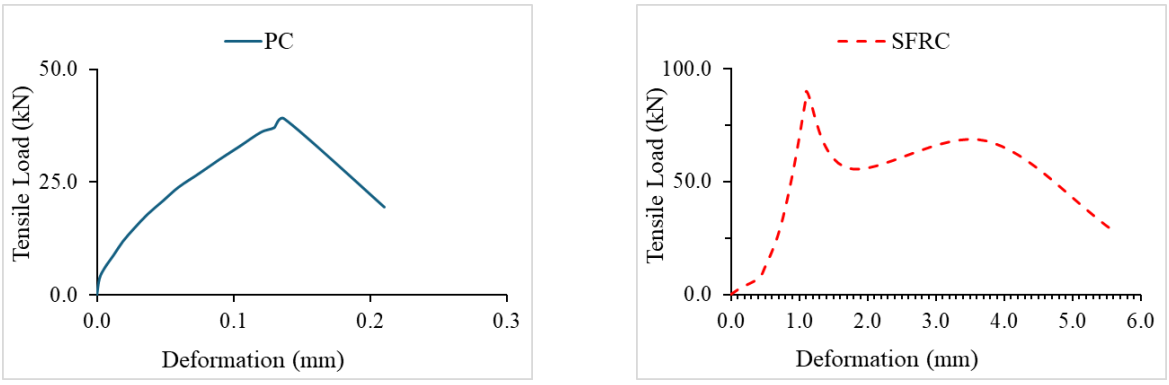
The tensile behavior of concrete is significantly enhanced by the addition of steel fibers, as demonstrated by the increase in tensile strength from 6.5 MPa in plain concrete to 8.25 MPa in Steel Fiber Reinforced Concrete (SFRC). Steel fibers act as crack arresters by bridging microcracks and limiting their propagation under tensile stress. This results in improved tensile capacity, greater ductility, and enhanced resistance to cracking. As a consequence, the concrete can sustain higher loads even after initial cracking, minimizing the risk of sudden brittle failure. These improvements contribute to increased structural resilience, durability, and long-term performance. The effectiveness of this reinforcement is visually evident in Figure 1, which displays the tested specimen after undergoing split tensile loading.



Figure 1: Tested specimen under splitting tensile load

3.2 Load-Deformation Behaviour

The load-deformation behavior of plain concrete (PC) and Steel Fiber Reinforced Concrete (SFRC) is illustrated in Figure 2(a) and Figure 2(b), respectively. The curve for PC, shown in Figure 2(a), exhibits a steep rise to the peak load followed by a sudden drop, indicating a brittle failure mode with minimal energy absorption. In contrast, Figure 2(b) displays the load-deformation response of SFRC, which demonstrates a more ductile behavior. The SFRC reaches a higher peak load and shows an extended post-peak region, indicating its ability to sustain additional load after cracking. This behavior highlights the improved toughness, energy absorption, and post-crack performance of SFRC compared to conventional plain concrete.



a) b)

Figure 2: Load-deformation curve, a. Plain concrete, and b. Steel fiber reinforced concrete

3.3 Enhanced Tensile Performance With Steel Fibers

Concrete has low tensile strength, making it susceptible to cracking under tension. Steel fibers help overcome this limitation by bridging cracks and improving both tensile strength and ductility. This results in greater toughness, allowing the material to deform more without sudden failure. Consequently, fiber-reinforced concrete is better equipped to handle both tensile and flexural stresses. To further illustrate this improvement, Figure 3 presents a bar chart comparing the tensile load capacities of plain concrete (PC) and Steel Fiber Reinforced Concrete (SFRC). The chart clearly shows SFRC's superior performance in both strength and post-crack behavior, making it ideal for applications requiring enhanced durability and crack control.

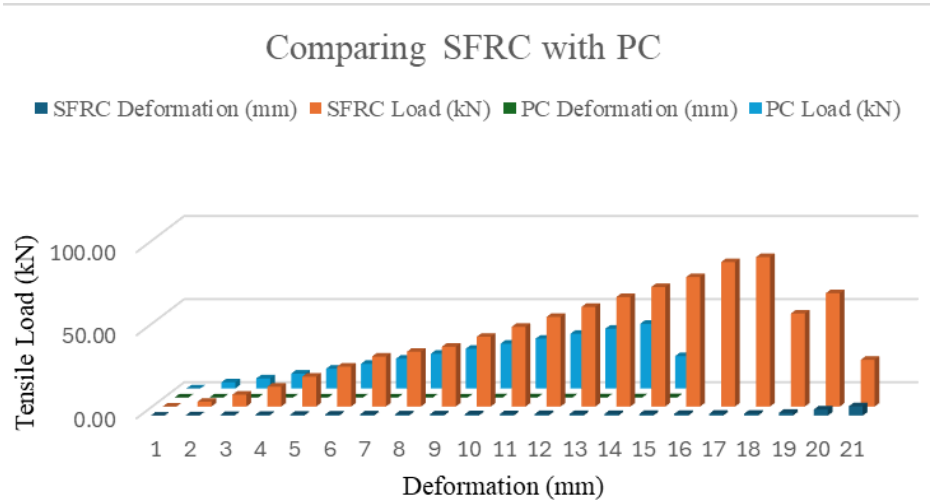


Figure 3: Comparison of Tensile Load and Deformation Behaviour of SFRC and PC

4 Practical Implementation

Future research should aim to optimize the mix design and fiber dosage to achieve a balance between improved mechanical properties and sufficient tensile strength. Investigating advanced techniques to strengthen the bond between steel fibers and the concrete matrix could further enhance performance. Detailed studies on the long-term durability, environmental resistance, and structural applications of SFRC are essential to support its widespread adoption. In addition, the development of standardized guidelines, supported through collaboration with industry professionals, will be important for integrating SFRC into mainstream construction practices. However, potential cost implications and scalability challenges in large-scale applications should also be considered to ensure practical feasibility. These efforts will help enable the practical use of SFRC in a variety of infrastructure projects. Overall, the findings of this study highlight the potential of SFRC as a sustainable and energy-absorbing material, contributing to the advancement of eco-friendly and resilient construction solutions.

5 Conclusions and Recommendations

Based on the findings from the experimental investigation conducted on Steel Fiber Reinforced Concrete (SFRC) specimens, the following conclusions can be drawn regarding its tensile strength and post-cracking behavior in comparison to plain concrete (PC):

1. Workability: The addition of steel fibers significantly reduces workability, with slump values dropping from 125 mm (PC) to 12.5 mm (SFRC). This is due to fiber-induced water absorption and mix congestion. Proper mix design and placement techniques are essential to ensure uniform compaction and performance.
2. Tensile Strength: SFRC showed a 26.9% increase in tensile strength compared to PC, rising from 6.5 MPa to 8.25 MPa. Steel fibers bridge microcracks and prevent propagation, improving both strength and structural integrity.

3. Load-Carrying Capacity and Toughness: Load-deformation results indicate that SFRC retains load capacity after cracking and exhibits a more ductile failure mode. This highlights its improved toughness and energy absorption, making it ideal for structural applications under tension.
4. Crack Resistance and Durability: SFRC enhances crack control, reducing crack width and spacing. These improvements support long-term durability and make SFRC a suitable option for pavements, overlays, and other crack-sensitive structures.

In conclusion, SFRC improves tensile performance, ductility, and crack resistance compared to plain concrete. While workability is reduced, proper mix management can address this issue. The findings support the wider use of SFRC in sustainable and resilient structural applications. Future research should explore long-term durability and field performance for broader adoption.

Acknowledgment

The authors sincerely thank all individuals who provided support throughout the research, especially the staff of the Concrete Laboratory for their valuable assistance.

References

[1] S. Abdal et al., "Application of ultra-high-performance concrete in bridge engineering: Current status, limitations, challenges, and future prospects," vol. 13, no. 1, p. 185, 2023.
[2] G. L. Golewski, "The phenomenon of cracking in cement concretes and reinforced concrete structures: the mechanism of cracks formation, causes of their initiation, types and places of occurrence, and Methods of Detection—A review," Buildings, vol. 13, no. 3, p. 765, Mar. 2023.
[3] M. Zhou, W. Lu, J. Song, and G. C. Lee, "Application of Ultra-High Performance Concrete in bridge engineering," Constr. Build. Mater., vol. 186, pp. 1256–1267, 2018.
[4] F. Dabbaghi, H. Fallahnejad, S. Nasrollahpour, M. Dehestani, and H. Yousefpour, "Evaluation of fracture energy, toughness, brittleness, and fracture process zone properties for lightweight concrete exposed to high temperatures," *Theor. Appl. Fract. Mech.*, vol. 116, no. 103088, p. 103088, 2021.
[5] R. Allouzi, A. Alkloub, H. Naghawi, and R. Al-Ajarmeh, "Fracture modeling of concrete in plain and reinforced concrete members," Int. J. Civ. Eng., vol. 17, no. 7, pp. 1029–1042, 2019.
[6] W. Ahmad, M. Khan, and P. Smarzewski, "Effect of short fiber reinforcements on fracture Performance of Cement-Based Materials: A Systematic Review approach," Materials, vol. 14, no. 7, p. 1745, Apr. 2021.
[7] S. Paul, G. Van Zijl, and B. Šavija, "Effect of fibers on durability of Concrete: A Practical review," *Materials*, vol. 13, no. 20, p. 4562, Oct. 2020.
[8] A. Anandamurthy, V. Guna, M. Ilangovan, and N. Reddy, "A review of fibrous reinforcements of concrete," J. Reinf. Plast. Compos., vol. 36, no. 7, pp. 519–552, 2017.
[9] A. Rai and Y. P. Joshi, "Applications and properties of fibre reinforced concrete," vol. 4, no. 5, pp. 123-131, 2014.
[10] H. Singh, *Steel fiber reinforced concrete: Behavior, modelling and design*, 1st ed. Singapore, Singapore: Springer, 2016.
[11] V. Afroughsabet, L. Biolzi, and T. Ozbakkaloglu, "High-performance fiber-reinforced concrete: a review," *J. Mater. Sci.*, vol. 51, no. 14, pp. 6517–6551, 2016.
[12] A. Sayam *et al.*, "A review on carbon fiber-reinforced hierarchical composites: mechanical performance, manufacturing process, structural applications and allied challenges," *Carbon Lett.*, vol. 32, no. 5, pp. 1173–1205, 2022.
[13] J. Yang, Y. Zhang, and J. Huang, "The strengthening theory of steel fiber reinforced concrete and its application in tunnel engineering: A review," *J. Eng. Fiber. Fabr.*, vol. 19, 2024.
[14] ASTM C143 / C143M-15a, Standard Test Method for Slump of Hydraulic-Cement Concrete, ASTM International, West Conshohocken, PA, 2015, www.astm.org.
[15] ASTM C496-96, Standard Test Method for Splitting Tensile Strength of Cylindrical Concrete Specimens, ASTM International, West Conshohocken, PA, 201, www.astm.org.

EXPERIMENTAL EVALUATION OF FLEXURAL BEHAVIOR IN CONCRETE BEAMS REINFORCED WITH WASTE HUMAN HAIR FIBERS

[a]Jawad Nasar*, [b]Adeer Khan

a: Askari Heights V, Housing Directorate, Islamabad, Pakistan, jawad100eb@gmail.com
b: Korea Advanced Institute of Science & Technology, Daejeon, South Korea, adeerkhan@kaist.ac.kr
*Corresponding author

Abstract- Concrete is the most widely used construction material globally, but it faces inherent challenges such as low tensile and flexural strength and a tendency to crack under stress. Traditional fibers like steel and polypropylene are used to mitigate these issues; however, they are often costly and nonbiodegradable, prompting the search for sustainable alternatives. This study explores the innovative use of human hair, a natural, biodegradable, and high tensile waste material as a reinforcing additive in concrete beams. The novelty lies in evaluating the structural and durability performance of concrete beams reinforced with human hair, an underexplored fiber in flexural applications. An experimental program was carried out where four concrete beams were cast, two with 1% human hair by cement volume and two without hair as control specimens. Tests conducted included a three-point flexural test, water absorption test, and surface hardness test using the Schmidt hammer. Specimens were cured for 28 days before testing. Results showed that human hair reinforced beams exhibited 23.84% higher flexural strength compared to controls, reduced water absorption, and increased surface hardness. These findings suggest that human hair can be effectively utilized as a sustainable and efficient fiber additive to enhance concrete performance.

Keywords- Human Hair, Concrete, Flexural Strength, Schmidt Hammer, Water Absorption

1. Introduction

Concrete remains the most extensively utilized construction material globally, primarily due to its high compressive strength, durability, and adaptability to diverse structural forms. Nevertheless, it is inherently deficient in tensile and flexural capacities, which predisposes it to brittle failure modes when subjected to bending and tensile loads [16][14]. This fundamental limitation frequently results in the early initiation and propagation of cracks within structural members such as beams and slabs, thereby compromising both strength and serviceability over time. The ingress of moisture and deleterious agents through these microcracks exacerbates the risk of steel reinforcement corrosion, which progressively undermines structural integrity [6]15]. The compounded effects of crack development and reinforcement degradation can significantly reduce the lifespan and safety margins of concrete infrastructure. Consequently, addressing the flexural vulnerability of concrete is imperative for ensuring the long term performance and resilience of structural systems. This necessity underscores the importance of innovative materials and techniques aimed at mitigating crack formation and enhancing the overall durability of concrete structures.

Fiber reinforced concrete (FRC) has emerged as an effective solution for enhancing the tensile and flexural performance of conventional concrete by incorporating fibers such as steel, polypropylene, and glass, which bridge microcracks and improve ductility and energy absorption [11][12][17] has shown that fiber orientation, dispersion, and dosage significantly influence fracture resistance and mechanical response. Despite extensive studies on synthetic and natural fibers, the structural potential of human hair as reinforcement remains largely underexplored. Composed mainly of keratin, human

hair offers high tensile strength, elasticity, and biodegradability, making it a promising sustainable alternative [8]. To address this gap, the present study incorporated 1% human hair by cement volume into concrete beams and assessed flexural strength, water absorption, and surface hardness. Four beams were cast, two with hair reinforcement and two controls and tested under four point bending to evaluate load deflection behavior and durability performance.

The results of this experimental investigation demonstrate a significant enhancement in the mechanical and durability characteristics of concrete beams reinforced with human hair fibers. This study aimed to explore the novel use of human hair as a sustainable and cost effective reinforcement material for structural concrete applications. Four beams were prepared, including two control specimens and two reinforced with 1% human hair by volume of cement, and were tested under standardized four point bending, water absorption, and surface hardness procedures. The hair reinforced beams exhibited a 23.84% increase in flexural strength compared to the controls, indicating a notable improvement in their load bearing capacity. Additionally, these beams showed higher surface hardness and reduced water absorption rates, suggesting enhanced resistance to abrasion and moisture ingress. Visual inspection confirmed that the hair fibers effectively bridged microcracks and delayed crack propagation, thereby improving energy dissipation during flexural loading. These findings underscore the viability of human hair as an innovative reinforcement material that contributes both structural benefits and environmental value through the reuse of biodegradable waste.

2. Research Methodology

2.1 Raw Material

The concrete mix followed a 1:2:4 ratio using OPC 43 grade cement, Lawrencepur sand as fine aggregate, and 20 mm coarse aggregate. Clean drinking water was used to ensure proper hydration and curing. Human hair fibers (30–60 mm) (fig 1a), collected from barber shops (fig 1b), were added at 1% by cement volume to enhance crack resistance and flexural performance as shown in figure 1. The selection of 1% human hair fiber by cement volume was based on prior studies indicating that low-volume natural fibers can effectively improve flexural properties without severely compromising workability [3][7]. The 30–60 mm fiber length range was chosen to ensure sufficient crack-bridging capability while maintaining manageable mixing consistency. These parameters provided a practical balance between dispersion, reinforcement effect, and workability. Future studies are encouraged to explore a broader dosage range (2–5%) to identify the optimal content for structural-scale applications. The data in table 1 indicates that human hair possesses moderate tensile strength and high elongation, making it effective for crack bridging and energy absorption. Its biodegradable nature, coupled with surface roughness and adequate modulus, makes it a compelling alternative for sustainable fiber reinforcement in concrete.

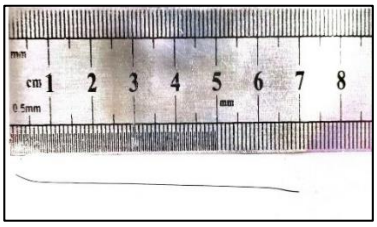
a)  b) 

Figure 1: Hair Reinforced Concrete

Table 1 Physical and Mechanical Properties of Human Hair Fibers

Sr	Property	Value/Range	Unit	Remarks
1	Fiber Length	30 – 60	mm	Naturally variable; selected for crack bridging
2	Diameter	60 – 80	µm	Measured under optical microscope
3	Specific Gravity	1.32	—	Slightly lower than conventional aggregates
4	Tensile Strength	200	MPa	Comparable to low-grade synthetic fibers
5	Elongation at Break	30 – 50	%	High ductility helps dissipate energy
6	Modulus of Elasticity	1.5 – 2.0	GPa	Lower than steel or glass fibers
7	Surface Morphology	Rough (scaly cuticle)	—	Promotes mechanical interlocking with cement
8	Thermal Decomposition Point	230 – 250	°C	Degrades before concrete exposure to high heat

2.2 Mix Design and Casting of Concrete Specimen

A 1:2:4 mix ratio was adopted with water cement ratio of 0.5%. Hair was mixed using a four layer approach to ensure even distribution. 4 x beams (2 x control, 2 x reinforced) were cast and cured for 28 days. Table 2 illustrates mix design of PCC and FRC.

Table 2: Mix Design of PCC & FRC

Sr	Parameter	Plain Cement Concrete	Hair Reinforced Concrete
1	Mix Ratio	1:2:4	1:2:4
2	Cement	6.5 kg	6.5 kg
3	Sand	13 kg	13 kg
4	Coarse aggregate	26 kg	26 kg
5	W/C Ratio	3.25 Liters	3.25 Liters
6	Hair Fiber Addition	Nil	30 60 mm long fibers (Naturally variable) 1% by cement mass (65 grams)
7	Mixing Method	Combine – add water – mix	Combine – add water – mix
8	Batching Time	5 minutes	5 Minutes

a) 

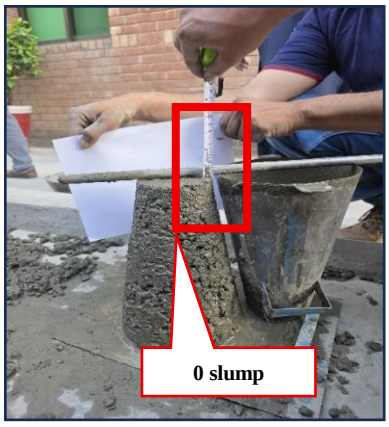
b) 

Figure 2: a. Slump Tests for PCC and b. HRC

Slump tests were conducted on Plain Reinforced Concrete (PRC) and Hair Reinforced Concrete (HRC) using the standard slump cone method to evaluate workability. Fresh concrete was filled into the slump cone mold in three layers, each tamped 25 times with a rod for compaction. After leveling the top surface, the cone was lifted vertically, and the slump was measured as the vertical drop. The PRC mix showed a 5inch slump (figure 2a), indicating moderate workability. In contrast, the HRC mix incorporating human hair fibers had a zero slump, reflecting very low workability (figure 2b). The fibers restricted the concrete's flow and deformation significantly. Table 3 illustrates comparison of PCC and HRC based on achieved slump.

Table 3: Comparison of PCC & HRC

Sr	Parameter	Plain Cement Concrete	Hair Reinforced Concrete
1	Workability	Good	Reduced due to fiber presence
2	Slump (in)	5	0
3	Placement	Easy	Requires more effort due to reduce flowability
4	Use of admixtures	Not required	Superplasticizer may be required to improve workability
5	Curing Period	28 days	28 days

2.3 Testing

The experimental evaluation included flexural strength assessment through a 3-point bending test (figure 3a) conducted in accordance with ASTM C78/C78M-22 to measure beam performance under transverse loading. Water absorption (figure 3b) was determined per ASTM C642-21 to evaluate porosity and durability. Surface hardness was measured using a Type N Schmidt rebound hammer following ASTM C805/C805M-18 (figure 3c).



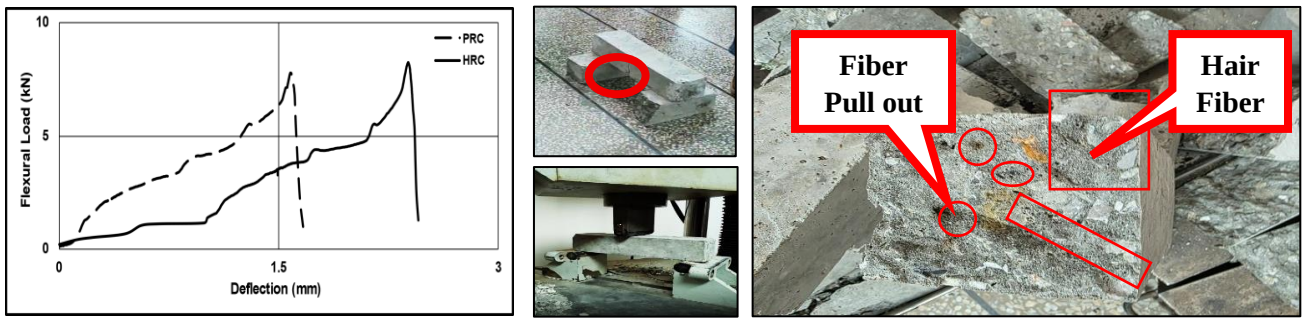
a) b) c)

Figure 3: a) Beam under flexural load test, b) water absorption test c) Schmidt hammer test

3. Experimental Results and Analysis

3.1 Flexural Behavior

The comparison of the flexural load deflection curves as demonstrated in figure 4a illustrates the superior performance of the human hair reinforced beams relative to the control specimens. The reinforced beams exhibited higher peak loads and sustained greater deflection, reaching 2.4 mm before failure, indicating improved ductility and energy absorption. In contrast, the control beams failed abruptly at lower deflection levels around 1.5 mm, reflecting a more brittle response. The smoother post peak behavior of the reinforced beams suggests that hair fibers effectively delayed crack propagation and contributed to a more gradual failure mechanism. These observations confirm that incorporating human hair enhances both load bearing capacity and deformation resilience in concrete beams.



a) b) c)

Figure 4: a) Load vs Deflection Graph for HRC & PRC b) Fractured surface c) Cross Section Hair Infused

Figures 4b and 4c illustrate the fracture behavior and internal characteristics of the tested concrete beams incorporating human hair fibers. In the first image of Figure 4b, the beam exhibits a pronounced bridging effect immediately prior to collapse, where visible cracks had formed but the fibers continued to transfer stress across the fracture plane, delaying sudden failure. The second image shows the beam during flexural testing under applied load at the point of failure, highlighting the location and pattern of the fracture. Figure 4c presents a cross-sectional view of a hair infused beam after testing, clearly revealing embedded hair fibers distributed within the concrete matrix. The exposed fibers and evidence of fiber pullout indicate that the hair reinforcement contributed to crack bridging and energy dissipation, confirming their active role in enhancing ductility and toughness. Collectively, these images provide visual confirmation of the mechanical mechanisms observed in the experimental results and support the effectiveness of human hair fibers in improving post cracking performance. Table 4 compares the maximum flexural load and flexural strength of control and hair reinforced concrete beams, demonstrating enhanced flexural performance with the addition of human hair fibers.

Table 4: Flexural Load and Strength of Plain Cement Concrete (PCC) and Hair Fiber Reinforced Concrete (FRC) Beams

Sr	Beam	Type	Load (KN)	Flexural Strength (MPa)
1	A	Control	5.264	0.649
2	B	Control	7.792	3.342
3	Average		6.528	1.995
3	C	Hair Reinforced	8.248	3.539
4	D	Hair Reinforced	6.318	1.995
5	Average		7.283	2.767

3.2 Flexural Properties

The comparative data in Table 5 highlight notable differences in mechanical behavior between Hair Reinforced Concrete (HRC) and Plain Reinforced Concrete (PRC). While both beams shared identical geometric properties, HRC exhibited a higher deflection of 2.38 mm under load, indicating reduced stiffness relative to PRC. The modulus of rupture for HRC reached 3.67×10^6 MPa, surpassing PRC and suggesting enhanced cracking resistance. However, PRC demonstrated superior stiffness (5194.67 N/mm) and a higher elastic modulus (1.166 GPa), reflecting greater rigidity and elastic performance. Importantly, the Flexural Toughness Index of HRC (19640.55 N mm) was more than three times that of PRC, indicating significantly improved energy absorption and ductility. These findings imply that incorporating human hair fibers enhances flexural toughness and crack resistance but may reduce overall stiffness and elastic modulus, with toughness increasing by 236%, while stiffness and elastic modulus decrease by about 33%. Table 6 indicates the comparative analysis which reveals that while human hair fibers offer slightly lower flexural strength than synthetic counterparts like steel or polypropylene, they significantly enhance toughness and crack resistance at a lower cost and with the added benefit of biodegradability. These attributes position human hair as a viable, sustainable alternative for semi-structural applications where moderate strength and high ductility are desired.

Table 5: Flexural mechanical properties of control and hair reinforced concrete beams B and C.

Sr	Parameter	HRC	PRC	Unit
1	Span	18	18	In
2	Width	4	4	In
3	Depth	4	4	In
4	Deflection	2.38	1.5	Mm
5	Modulus of Rupture (MOR)	3.67×10^6	3.398×10^6	MPa
6	Load	8248	7792	N
7	Stiffness	3463.73	5194.67	N/mm
8	Initial Modulus (E1)	7.77×10^8	1.166×10^9	Pa
9	Elastic Modulus (E)	0.78	1.166	GPa
10	Flexural Toughness Index (FTI)	19640.55	5844	N mm
11	Flexural Stiffness (K)	3.46×10^6	5.19×10^6	N/m

Table 6: Comparison of Mechanical Performance of Different Fiber Types in Concrete

Sr	Fiber Type	Flexural Strength (MPa)	Toughness Improvement (%)	Modulus of Rupture (MPa)	Notable Characteristics
1	Human Hair	2.77	+236%	3.67×10^6	Readily available waste; moderate bonding
2	Polypropylene	3.5 – 5.0	+150–200%	4.0×10^6	Chemically inert; good dispersion

3	Steel Fiber	5.0 – 8.0	+300–500%	5.5×10^6	Very high strength; prone to corrosion
4	Glass Fiber	4.0 – 6.5	+200–300%	4.5×10^6	High strength but brittle

3.3 Durability and Non-Destructive Testing (NDT) Characteristics

The durability and non-destructive characteristics of the concrete beams were evaluated through water absorption and in situ strength testing. As shown in Table 7, Beam C and Beam D exhibited low water absorption rates of 0.97% and 0.95%, respectively, indicating reduced porosity and enhanced resistance to moisture ingress and chemical attack. Corresponding compressive strength values, measured via NDT, were 3345 psi and 3328 psi, demonstrating consistent structural performance. The close alignment of these parameters suggests that both beams possess satisfactory durability and mechanical integrity, making them suitable for long term structural use.

Table 7: Water Absorption & NDT Test

Sr	Beam	Water Absorption (%)	Average Strength (psi)
1	Beam C	0.97%	3345
2	Beam D	0.95%	3328

4. Practical Applications

The incorporation of human hair into concrete offers significant practical applications that align with sustainability and structural efficiency objectives. As a natural protein fiber typically considered waste, human hair provides an innovative means to reduce environmental impact by repurposing biowaste within construction materials. Its high tensile strength and inherent flexibility enable it to bridge microcracks in the concrete matrix, improving flexural resilience and enhancing the ability of beams to withstand deformation under applied loads. In regions where conventional fiber reinforcements are prohibitively expensive or difficult to access, human hair emerges as a cost effective, locally available alternative. This approach can be especially advantageous in rural or low income construction projects by reducing dependence on synthetic or industrial materials. The improved crack resistance offered by hair fibers also contributes to the long term durability and structural integrity of concrete elements. However, potential challenges include ensuring uniform dispersion of human hair fibers within the concrete matrix and addressing scalability for large-scale construction projects, which may require specialized mixing techniques or quality control measures. As a result, human hair reinforced concrete holds potential for semi structural applications, including pavements, partitions, and precast components.

From a sustainability perspective, the average barbershop produces up to 0.5–1 kg of waste hair per day, which often ends up in landfills. Repurposing this biowaste in construction could divert thousands of kilograms annually per city from waste streams. Additionally, using human hair in place of synthetic fibers reduces embodied energy by an estimated 60–80%, contributing to lower carbon footprints in green construction projects. Furthermore, integrating human hair into concrete aligns with contemporary green building practices and broader waste reduction strategies. By leveraging this abundant and renewable resource, construction projects can support global initiatives aimed at promoting sustainable development. Projects seeking environmental certifications, such as LEED, may benefit from the inclusion of innovative materials like hair fibers to strengthen their sustainability credentials. Additionally, the use of human hair addresses pressing environmental concerns by diverting waste from landfills and reducing the ecological footprint of construction activities. The enhanced durability performance achieved through fiber reinforcement further underscores its practical value in improving service life and reducing maintenance needs. Overall, human hair reinforced concrete presents a promising pathway for creating environmentally conscious and structurally reliable building materials. Its adoption can contribute meaningfully to advancing sustainable construction practices worldwide.

5. Conclusions

This research has demonstrated a sustainable strategy to improve concrete beams by incorporating human hair fibers as reinforcement. The findings highlight both mechanical and durability benefits compared to conventional concrete and prior studies using synthetic fibers. Following conclusions can be drawn from the study:

- The experimental results demonstrated that incorporating 1% human hair by cement volume led to a 23.84% improvement in flexural strength, a 0.96% decrease in water absorption and an increase in surface hardness to 3345 psi.
- The inclusion of human hair fibers in concrete increased the flexural toughness index by 236%, while reducing stiffness and elastic modulus by about 33%, highlighting a tradeoff between enhanced ductility and reduced structural rigidity.
- Incorporating human hair as a reinforcement in concrete provides an effective and eco-friendly solution that enhances mechanical properties while contributing to waste reduction and decreasing dependence on traditional construction materials.

A key limitation of this study is the use of only two specimens per concrete type, which constrains the statistical robustness of the results. To improve the reliability and generalizability of findings, future studies should incorporate a larger sample size with replicates to allow for rigorous statistical analysis. Future research should also focus on evaluating the long-term behavior of hair reinforced concrete under diverse environmental exposures and load cycles. Additional studies are also recommended to determine the optimal fiber content within the 2–5% range for structural use. Such efforts will help validate and refine this innovative approach for broader adoption in sustainable construction.

Acknowledgements

The author gratefully acknowledges the invaluable guidance and support of Engr. Dr. Majid Ali, whose supervision was instrumental in the successful completion of this research. Moreover, the careful review and constructive suggestions by the anonymous reviewers are gratefully acknowledged.

References

[1] A. Akinyemi and M. Abdulwahab, "Biowaste fibers in concrete," *Waste Manag.*, vol. 45, pp. 246–250, 2015.
[2] J. Ahmad et al., "Improvement in the strength of concrete reinforced with agriculture fibers: Assessment on mechanical properties and microstructure analysis," *J. Build. Mater.*, vol. 38, no. 2, pp. 123–135, 2024.
[3] J. K. Ahmed and B. S. Al Numan, "Investigation of using human hair as fiber reinforcement in concrete," *Eurasian J. Sci. Eng.*, vol. 7, no. 2, pp. 194–200, 2022.
[4] S. Bansal, R. Kumar, and A. Kumar, "Mechanical behavior of human hair fiber reinforced concrete," *Mater. Today: Proc.*, vol. 17, pp. 746–753, 2019.
[5] M. S. Basha and M. Malik, "Performance evaluation of concrete with human hair as fiber in fatigue prone environments," *Constr. Build. Mater.*, vol. 270, 121465, 2021.
[6] A. Bentur and S. Mindess, *Fibre Reinforced Cementitious Composites*, 2nd ed. CRC Press, 2006.
[7] M. Choudhary, M. Patel, and K. Shah, "Human hair fiber in concrete," *Int. J. Eng. Res. Technol.*, vol. 3, no. 5, pp. 210–213, 2014.
[8] A. Gupta and R. Sharma, "Performance of concrete using human hair as fiber reinforcement," *Int. J. Eng. Res. Appl.*, vol. 2, no. 3, pp. 210–216, 2012.
[9] H. Kanwal, M. S. Aslam, T. L. Mughal, M. Asim, and R. M. Memon, "Human hair as fiber reinforced concrete for enhancement of tensile strength of concrete," *Mehran Univ. Res. J. Eng. Technol.*, vol. 39, no. 1, pp. 63–70, 2020.
[10] H. M. S. A. Khan et al., "Human hair as fiber reinforced concrete for enhancement of tensile strength of concrete," *Mehran Univ. Res. J. Eng. Technol.*, vol. 39, no. 1, pp. 63–70, 2020.
[11] J. K. Kim and J. S. Yu, "Mechanical properties of natural fiber reinforced concrete," *Constr. Build. Mater.*, vol. 24, no. 3, pp. 391–401, 2010.
[12] V. C. Li, "Engineered cementitious composites (ECC) – Tailored composites through micromechanical modeling," *ACI Mater. J.*, vol. 104, no. 6, pp. 1–12, 2007.
[13] S. L. Meghwar, G. B. Khaskheli, and A. Kumar, "Human scalp hair as fiber reinforcement in cement concrete," *Mehran Univ. Res. J. Eng. Technol.*, vol. 39, no. 2, pp. 443–452, 2020.
[14] P. K. Mehta and P. J. M. Monteiro, *Concrete: Microstructure, Properties, and Materials*, 4th ed. McGraw Hill Education, 2014.
[15] T. R. Naik, "Sustainability of concrete construction," *Pract. Period. Struct. Des. Constr.*, vol. 13, no. 2, pp. 98–103, 2008.
[16] A. M. Neville, *Properties of Concrete*, 5th ed. Pearson Education, 2011.
[17] M. Oveas and G. D. Singh, "An experimental investigation on hair fibre as fibre reinforcement in concrete," *Asian J. Civ. Eng.*, vol. 8, no. 1, pp. 1–8, 2019.

[18] A. Peled and A. Bentur, "Reinforcement mechanisms in textile reinforced cementitious composites," *Mater. Struct.*, vol. 36, no. 7, pp. 451–458, 2003.
[19] F. D. Santos et al., "Optimization of the compressive strength of hair fiber reinforced concrete using central composite design," *IOP Conf. Ser.: Mater. Sci. Eng.*, vol. 771, no. 1, 012059, 2020.
[20] F. U. A. Shaikh, "Review of mechanical properties of short fiber reinforced geopolymer composites," *Constr. Build. Mater.*, vol. 43, pp. 37–49, 2013.
[21] R. Siddique, *Waste Materials and By Products in Concrete*. Springer, 2008.
[22] B. S. Thomas and R. C. Gupta, "Utilization of waste materials in concrete: A review," *Renew. Sustain. Energy Rev.*, vol. 50, pp. 563–581, 2015.
[23] M. K. Yew, H. B. Mahmud, M. C. Yew, and M. E. Abdullah, "Effects of fiber types on the performance of fiber reinforced concrete under severe conditions," *Constr. Build. Mater.*, vol. 93, pp. 370–378, 2015.
[24] S. K. A. Zaidi, S. M. Talha, M. Bhati, and S. Ram, "An experimental study on human hair fiber reinforced concrete," *Civ. Eng. Archit. J.*, vol. 2, pp. 129–133, 2018.
[25] M. H. Zhang, J. Islam, and S. Peethamparan, "Influence of fiber dispersion on the properties of fiber reinforced concrete," *Cem. Concr. Res.*, vol. 44, pp. 44–52, 2013.
[26] S. Choudhary, K. Jain, and A. K. Jha, "Use of human hair as fiber reinforcement in concrete," *Int. J. Sci. Res.*, vol. 3, no. 4, pp. 1–2, Apr. 2014.

COTTON FIBERS FOR IMPROVED CONCRETE TENSILE STRENGTH AND CRACK RESISTANCE IN SLABS

[a] Mobeen Anwar*, [b] Sadia Sajid Khan

a: Structural Designing, Niazi Design Systems, Islamabad, Pakistan. mobeenanwer94@gmail.com
b: Design and Estimation Department, Kinetic International FZE, UAE. sadialohani@hotmail.com
*Corresponding author

Abstract- Concrete is one of the most used materials in construction because of its high compressive strength. However, it tends to perform poorly under tensile stress, often resulting in cracks and reduced service life of structures. In this study, experimental investigation is done to explore whether adding cotton fiber repurposed from post-industrial textile waste can help improve the tensile behavior of concrete. This approach not only targets mechanical enhancement but also introduces an environmentally conscious alternative to conventional synthetic fibers. To evaluate this, cylindrical specimens of both plain cement concrete (PCC) and cotton fiber-reinforced concrete (CFRC) were prepared, with 0.5% cotton fiber added by weight in the CFRC mix. After 28 days of water curing, the samples were tested using a Universal Testing Machine (UTM) as per ASTM C496 standards. The performance was assessed based on tensile strength. Interestingly, while CFRC samples showed a slightly lower tensile strength (0.8 MPa) compared to PCC (0.9 MPa), they demonstrated much better ductility and crack control. The cotton fibers acted as internal bridges, slowing down crack formation and allowing the material to absorb more energy before failure increasing toughness up to 7 times. These results suggest that CFRC, despite a modest reduction in peak tensile strength, could be a strong candidate for use in applications where long-term durability and crack resistance are key priorities.

Keywords- Tensile Strength, Cotton Fibers, Crack Resistance, Sustainable Concrete

1 Introduction

Concrete is universally acknowledged as one of the most important and extensively utilized construction materials due to its exceptional compressive strength, durability, and versatility. It forms the essential structural element in a vast array of infrastructure projects, ranging from residential and commercial buildings to complex transportation networks such as highways, tunnels, and bridges. The material's ability to withstand heavy compressive loads has made it indispensable in modern construction practices [1][2] [3]. However, despite these advantages, concrete exhibits an inherent lack in its tensile strength. This weakness becomes particularly critical in applications where tensile forces are unavoidable, leading to the initiation and propagation of cracks. Early age cracking, often occurring within days or weeks after placement, can severely compromise the structural integrity, serviceability, and longevity of concrete components. These cracks not only allow deleterious agents such as moisture, chlorides, and carbon dioxide to penetrate the matrix but also facilitate corrosion of embedded steel reinforcement, which can accelerate deterioration processes and jeopardize structural safety [4][5]. Consequently, tensile cracking remains a persistent challenge faced by engineers aiming to ensure both the safety and durability of concrete structures over their expected design life. Addressing this limitation is essential to enhance the performance of concrete, especially in applications exposed to dynamic loads, aggressive environmental conditions, or long-term service demands [1][2].

Fiber reinforcement has emerged as a widely accepted and highly effective strategy to mitigate the intrinsic brittleness and limited tensile capacity of plain concrete. The incorporation of discrete fibers into the cementitious matrix transforms the material into fiber-reinforced concrete (FRC), a composite engineered to enhance crack resistance, post-cracking ductility,

and overall tensile performance [10][14]. These fibers, which may be composed of steel, synthetic polymers, or natural materials, serve as micro-reinforcements that arrest crack initiation and propagation by bridging across micro- and macro-cracks as they develop. This bridging mechanism facilitates a more uniform distribution of tensile stresses within the matrix, thereby reducing localized stress concentrations at crack tips and improving the composite's ductility and toughness [9][4][14][15]. The fibers absorb and redistribute tensile loads that plain concrete is unable to bear, effectively increasing the material's tensile strength and energy absorption capacity. Furthermore, fibers significantly reduce concrete's inherent brittleness by allowing it to sustain mechanical loads even after the formation of initial cracks, a post-crack load-carrying capacity that is particularly vital in structural elements subjected to dynamic loading, fatigue, or cyclic stresses [3][10][14]. Consequently, the application of fiber reinforcement extends the service life of concrete structures, minimizes repair and maintenance demands, and promotes economic efficiency and environmental sustainability by prolonging infrastructure durability [16]. Considering increasing global emphasis on sustainable construction practices and the urgent need to reduce environmental impacts, research has progressively shifted toward the exploration of natural fibers as eco-friendly alternatives to traditional synthetic and steel fibers.

Natural fibers offer a range of environmental advantages, including renewability, biodegradability, lower embodied energy, and a reduced carbon footprint when compared to their synthetic counterparts [17][18]. Their adoption aligns with the principles of sustainable development by minimizing dependence on finite resources and encouraging circular economy approaches through waste valorization and material reuse [19]. Among natural fibers, cotton has gained considerable interest due to its abundance as a byproduct of the textile and agricultural industries, especially when recycled from discarded textile waste streams. These recycled cotton fibers provide an economically viable and environmentally responsible reinforcement option, transforming what would otherwise be landfill waste into a valuable construction resource [5][6][20]. Cotton fibers possess a unique combination of advantageous physical properties including light weight, high aspect ratio, and sufficient tensile strength that enable effective integration into conventional concrete mixes without adversely impacting fresh concrete workability or compaction [21]. The fibrous morphology of cotton allows it to act as a mechanical barrier that inhibits crack opening and deflects crack propagation paths, thereby enhancing the toughness and crack control capabilities of the concrete matrix [22]. Incorporating cotton fibers into concrete not only improves the mechanical and durability performance of the composite but also addresses critical environmental imperatives by mitigating textile waste accumulation and lowering the ecological footprint of construction materials [23]. This convergence of performance enhancement and environmental stewardship underscores the promising role of cotton fiber-reinforced concrete (CFRC) as a sustainable and practical material solution for modern green construction and infrastructure applications [24]. The present study is dedicated to investigating the potential of CFRC to enhance the tensile behavior of concrete through a series of controlled laboratory experiments focusing on split tensile strength. Split tensile strength is a critical mechanical property that reflects concrete's resistance to tensile forces and its ability to delay crack formation [25].

2 Methodology

2.1 Raw Materials

The materials used in this study were selected to ensure both standard concrete performance and sustainability through fiber reinforcement. Ordinary Portland Cement (OPC) was employed as the primary binder due to its widespread availability and reliable development [25]. Natural river sand, conforming to ASTM C33 grading requirements, served as the fine aggregate, providing adequate particle size distribution and cleanliness to optimize workability and matrix cohesion [26]. Crushed stone with a nominal size of 20 mm was used as coarse aggregate, offering the necessary hardness and angularity to enhance compressive strength and stability [27]. Clean tap water, free from harmful impurities, was utilized for both mixing and curing to ensure proper hydration and durability of the concrete [28]. The study's innovative aspect involved the incorporation of recycled post-industrial cotton fibers derived from textile waste, which were carefully processed and cleaned to achieve consistent fiber length and quality [29][30]. These natural fibers, characterized by their lightweight, tensile strength, and fibrous morphology, were integrated into the mix to improve crack resistance, tensile behavior, and energy absorption while supporting circular economy principles by reducing textile waste [31][32].

Collectively, these materials were combined with attention to compatibility and performance, aiming to produce a fiber-reinforced concrete composite that balances mechanical enhancement with environmental responsibility



Figure 1: Raw materials used for samples preparation (Left) and microscopic view of Cotton Fibre Thread (Right)

2.2 Mix Design, Preparation, and Casting

The concrete mix was carefully designed based on a conventional 1:2:4 proportion by weight for cement, sand, and coarse aggregate, respectively, ensuring a balanced combination to achieve adequate strength and workability. A water-cement ratio of 0.48 was maintained throughout the mixing process to optimize hydration while controlling porosity and durability characteristics. Recycled cotton fibers were added to the mix at 0.5% by volume of concrete, as determined from preliminary trials and literature support. Initially, all the dry ingredients were thoroughly blended to ensure homogeneity before the gradual addition of clean water, which was introduced in measured increments to obtain a consistent and workable mixture without causing segregation or excessive slump. To incorporate the recycled cotton fibers effectively, cotton fibers were carefully introduced into the mix in multiple thin layers during mixing, a technique aimed at promoting uniform dispersion and minimizing the risk of fiber agglomeration or clumping, which could adversely affect the composite's mechanical performance and workability. Cylindrical specimens with dimensions of 100 mm diameter and 200 mm height were cast in precision-engineered steel molds to ensure dimensional accuracy and repeatability of test samples. After casting, the specimens were left undisturbed for 24 hours to allow initial setting and sufficient strength gain for demolding. Subsequently, the specimens were demolded carefully to prevent damage and transferred to a curing tank where they were submerged in clean water for a standard curing period of 28 days. This water curing environment provided ideal moisture conditions to promote continuous hydration of the cementitious matrix, ensuring optimal strength development and durability consistent with ASTM guidelines [34].

2.3 Testing Procedure

After the completion of the 28-day curing period, the split tensile strength of the specimens was evaluated in accordance with the standardized ASTM C496 testing procedure [13]. Each cylindrical specimen was positioned horizontally as shown in Figure 2 in a Universal Testing Machine (UTM) where diametral compression was applied through loading strips to induce tensile stresses perpendicular to the applied load.

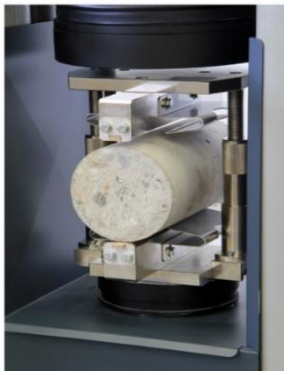


Figure 2: Split Tensile Test Setup

This indirect tensile test method effectively simulates tensile failure by generating tensile stresses across the vertical diameter of the specimen, which are otherwise difficult to measure directly in concrete. The loading was applied at a controlled, constant rate to ensure uniform stress distribution and to capture precise mechanical behavior up to the point of failure. During the test, load and displacement data were continuously recorded to generate load-displacement curves, which provide insight into the elastic and post-cracking response of the material. Observations of failure patterns were also documented to understand crack initiation and propagation mechanisms influenced by the fiber reinforcement. The split tensile strength was then calculated using the maximum load sustained by the specimen prior to failure, following the formula prescribed by ASTM C496, which relates the load, specimen dimensions, and tensile strength. This method allowed for a consistent and reproducible assessment of the tensile performance enhancement imparted by the incorporation of cotton fibers [13].

3 Results and Discussion

3.1 Slump Results

The slump test results for both plain concrete (PCC) and cotton fiber-reinforced concrete (CFRC) are presented in Table 1. It is observed that the CFRC exhibits a noticeably lower slump value compared to the PCC, indicating reduced workability. Table 1 provides a comparison of the water-cement (w/c) ratios for both concrete types along with their corresponding slump values. The reduction in slump for the cotton fiber-reinforced concrete can primarily be attributed to the high water absorption capacity of the cotton fibers, which effectively reduces the free water available in the mix [10]. This absorption limits the lubricating effect of water, resulting in a stiffer and less workable mixture. Consequently, the presence of cotton fibers influences the fresh concrete's rheological behavior, necessitating careful mix design adjustments to maintain adequate workability without compromising fiber dispersion or mechanical performance.as we can observe in Figure 1 CFRC showed true slump.



Figure 1: Slump test

Table 1. show the slump values noted for the both PCC and CFRC. The values for CFRC decreased by 25 mm showing the balling effect and congestion created by the fibers.

Table 1: Slump test of PCC and cotton fibres

Concrete Type	Observed Slump (mm)
PCC	75
Cotton Fiber	50

3.2 Load vs Deformation

The load-deformation behavior, as illustrated in Figure 2, clearly shows how PCC and CFRC perform differently under tensile stress. In case of PCC, the load increases sharply and then dropped abruptly once the peak is reached, this points to a typical brittle failure with no ability to carry load afterward. On the other hand, the CFRC curve rises more steadily and

continues even after reaching its peak load. This indicates that the cotton fibers help the concrete retain its integrity even as cracks start to form [9]. These fibers act like tiny bridges inside the material, holding it together and slowing down the cracking process. As a result, CFRC doesn't just carry more load but also absorbs more energy before failing, making it a more dependable option when resistance to cracking is important.

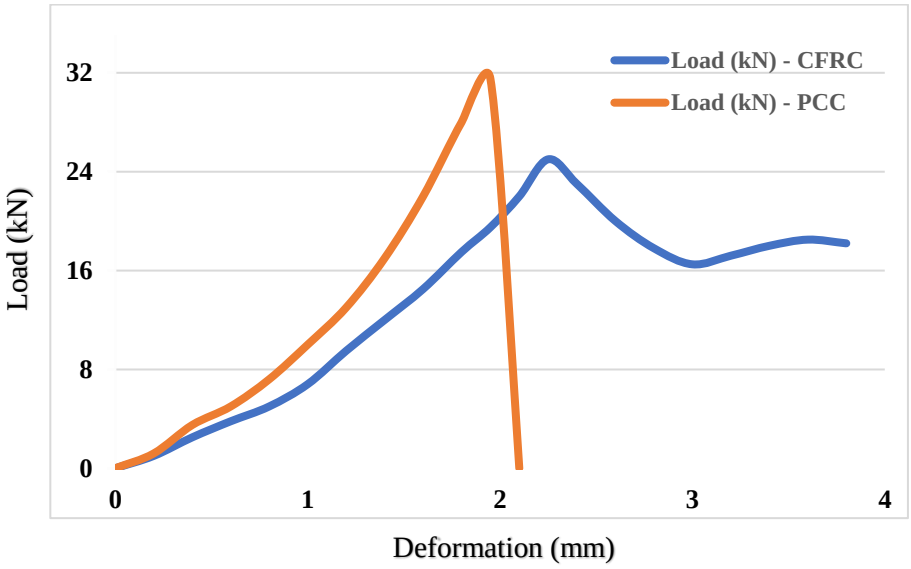


Figure 2: Load deformation curve

3.3 Split Tensile Results

As shown in Table 2, the average tensile strength of PCC was calculated to be 0.9 MPa, whereas the CFRC specimen registered a slightly lower strength of 0.8 MPa. This minor decrease is may be due to challenges like uneven fiber distribution or slight disruption in the matrix continuity caused by fiber inclusion. Still, the behavior of CFRC during failure was notably different, it failed more gradually and exhibited improved toughness. Rather than snapping abruptly like PCC, the CFRC held together longer under stress, showing visible signs of crack resistance. This makes CFRC a valuable option for applications where, reducing sudden failure and enhancing long-term durability is more critical than maximizing peak tensile strength [7].So this more energy obsorbtion by CFRC shows increse in toughness up to 7 times as compared to PCC.

Table 2: Comparative performance of Plain Concrete with Cotton Fiber

Concrete Type	Peak Load (KN)	Tensile Strength (MPa)	E1(Nm)	E2(Nm)	E(Nm)	TI
PCC	30	0.9	14.7	0	14.7	1
CFRC	28	0.8	15	87.9	102.9	6.96

3.4 Compression Results

The compressive test results presented in Table 3 show that CFRC achieved a higher peak load (150.91 kN) compared to PCC (86.47 kN), along with a slightly increased peak position and a notable rise in initial stiffness (4.99 kN/mm for CFRC versus 3.83 kN/mm for PCC). This behavior suggests that the inclusion of cotton fibers not only slightly enhances the mix's capacity to resist compressive loads but also delays microcrack propagation, allowing the composite to sustain higher loads before failure. The cotton fibers likely act as internal bridges, improving the bond within the cement matrix and resisting early crack formation. This mechanism contributes to increased stiffness because the fibers restrict localized deformation, distributing stress more uniformly across the section. As a result, CFRC demonstrates a stiffer and tougher

response under compressive loading, indicating its potential for applications where both crack control and compressive load capacity are critical. This outcome aligns with the broader aim of leveraging natural fibers to create concrete that is not only sustainable but also mechanically resilient in multiple stress conditions.

Table 3: Comparative performance of PCC with CFRC in Compression

Material	Peak Load (kN)	Peak Position (mm)	Initial Stiffness (kN/mm)
PCC	86.47	4.45	3.83
CFRC	150.91	4.86	4.99

4 Practical Implementation

Cotton fiber-reinforced concrete (CFRC) presents a viable solution for advancing sustainable construction practices by integrating mechanical performance with environmental considerations. Its incorporation into structural elements, such as slabs, offers multiple functional benefits. Among these are enhanced thermal insulation, reduced susceptibility to crack formation, and improved long-term durability under service loads. Due to the fibrous matrix's ability to distribute stresses more uniformly, CFRC is particularly advantageous in applications demanding increased flexural strength, such as base slabs and pavement overlays. Additionally, its utility extends to erosion control on embankments and inclined surfaces, where crack mitigation and surface integrity are critical. From an architectural perspective, the natural texture imparted by cotton fibers supports the development of aesthetically pleasing and eco-conscious finishes, making it suitable for decorative and surface-visible applications.. The growing adoption of CFRC is underpinned by rigorous laboratory testing to ensure compliance with structural and durability standards. As research into natural fiber composites continues, it is anticipated that new application domains will emerge, further, positioning CFRC as a material of choice for both structural and sustainable innovation in the construction industry.

5 Conclusions

In an experimental investigation to assess the impact of cotton fibers on the mechanical properties of concrete, the following conclusions were drawn from the results obtained:

- The slump of cotton fiber-reinforced concrete (CFRC) decreased compared to plain concrete (PCC), due to water absorption and congestion created by the cotton fibers.
- Split tensile strength of CFRC decreased slightly by 11.1% relative to PCC.
- CFRC demonstrated significantly improved ductility and crack resistance, absorbing more energy before failure compared to PCC showing up to 7 times more toughness.

Despite the slight reduction in tensile strength, CFRC shows promise for applications where enhanced crack control and durability are critical.

Acknowledgment

The authors would like to express their sincere gratitude to Dr Majid Ali and the organizations who contributed to the successful completion of this research. Special thanks are extended to the laboratory staff and technical team for their invaluable support during sample preparation and testing.

References

[1] M. Neville, *Properties of Concrete*, 5th ed., Pearson Education Limited, Harlow, UK, 2011. [2] B. Bentur and S. Mindess, *Fibre Reinforced Cementitious Composites*, 2nd ed., CRC Press, 2006..

[2] A. M. Brandt, "Fibre reinforced cement-based (FRC) composites after over 40 years of development in building and civil engineering," *Composite Structures*, vol. 86, no. 1–3, pp. 3–9, 2008.

[3] P. Banthia and R. Gupta, "Influence of polypropylene fiber geometry on plastic shrinkage cracking in concrete," *Cement and Concrete Research*, vol. 36, no. 7, pp. 1263–1267, 2006.

[4] A. Bentur and S. Mindess, *Fibre Reinforced Cementitious Composites*, 2nd ed., CRC Press, Boca Raton, FL, USA, 2006.

[5] Naaman and G. Reinhardt, *High Performance Fiber Reinforced Cement Composites 2*, RILEM Proceedings, E&FN Spon, London, UK, 1996.
[6] S. L. Shah, M. R. Khoshnood, and F. Iqbal, "Effect of cotton fibers on tensile behavior of concrete," *Journal of Materials in Civil Engineering*, vol. 33, no. 2, 04019303, 2021.
[7] S. Mindess, J. F. Young, and D. Darwin, *Concrete*, 2nd ed., Prentice Hall, Upper Saddle River, NJ, USA, 2002. [10] S. M. A. Hossain, M. A. Islam, and M. A. Mannan, "Influence of cotton fiber on workability and compressive strength of concrete," *International Journal of Concrete Structures and Materials*, vol. 13, no. 1, pp. 15–23, 2019.
[8] C. L. Page and M. M. Page, *Durability of Concrete and Cement Composites*, Woodhead Publishing, Cambridge, UK, 2007.
[9] B. Mather, "How to Make Concrete That Will Be Immortal—Part II," *Concrete International*, vol. 24, no. 7, pp. 57–60, 2002.
[10] A. Alhozaimy, P. Soroushian, and F. Mirza, "Mechanical properties of polypropylene fiber reinforced concrete and the effects of pozzolanic materials," *Cement and Concrete Composites*, vol. 21, no. 2, pp. 117–124, 1999.
[11] ASTM C496/C496M-17, *Standard Test Method for Splitting Tensile Strength of Cylindrical Concrete Specimens*, ASTM International, West Conshohocken, PA, USA, 2017.
[12] P. S. Song and S. Hwang, "Mechanical properties of high-strength steel fiber-reinforced concrete," *Construction and Building Materials*, vol. 18, no. 9, pp. 669–673, 2004.
[13] M. A. Mansur, H. H. Mahmud, and S. M. Shaikh, "Mechanical and durability properties of high strength concrete containing cotton fiber," Construction and Building Materials, vol. 23, no. 6, pp. 2177–2185, 2009.
[14] F. Bencardino, L. Rizzuti, G. Spadea, and R. Swamy, "Stress-strain behavior of steel fiber-reinforced concrete under compression," *Cement and Concrete Composites*, vol. 30, no. 10, pp. 848–860, 2008.
[15] T. T. Li, Y. L. Ding, and M. X. Liu, "Crack resistance of natural fiber-reinforced cementitious composites," *Construction and Building Materials*, vol. 262, Art. no. 120094, 2020.
[16] R. Yu, P. Spiesz, and H. J. Brouwers, "Development of ultra-high performance fiber reinforced concrete (UHPFRC): Towards an efficient utilization of binder content," *Construction and Building Materials*, vol. 79, pp. 273–282, 2015
[17] M. N. Soutsos, K. A. Pavlović, and R. J. McGuirk, "Performance of natural-fiber-reinforced concrete," *Materials and Structures*, vol. 50, no. 2, Art. no. 180, 2017.
[18] M. Fraternali, G. Fiorillo, V. Feo, and L. Incarnato, "Eco-friendly fiber-reinforced composites for sustainable civil engineering," *Composites Part B: Engineering*, vol. 89, pp. 337–346, 2016.
[19] L. M. John and R. Anandjiwala, "Recent developments in natural fiber composites for automotive applications," *Advanced Composite Materials*, vol. 19, no. 4, pp. 321–335, 2010.
[20] A. K. Bledzki and J. Gassan, "Composites reinforced with cellulose-based fibers," *Progress in Polymer Science*, vol. 24, no. 2, pp. 221–274, 1999.
[21] R. S. Pavan, D. S. Achara, and V. M. Lal, "Strength and durability properties of cotton fiber-reinforced concrete," *International Journal of Engineering Research & Technology (IJERT)*, vol. 9, no. 6, pp. 544–548, 2020.
[22] N. Marar, M. E. Eren, and G. Yılmaz, "Effect of fiber length and fiber content on mechanical properties of cotton fiber reinforced cement mortar," *Construction and Building Materials*, vol. 112, pp. 904–910, 2016.
[23] S. M. Shaikh and M. A. Mansur, "Utilization of recycled textile fibers for concrete reinforcement," *Journal of Materials in Civil Engineering*, vol. 28, no. 4, Art. no. 04015179, 2016.
[24] M. C. Serrano, L. L. Bejarano, and J. R. Martínez, "Cotton fiber-reinforced green composites for sustainable construction," *Materials Today: Proceedings*, vol. 33, pp. 1842–1848, 2020.
[25] S. Mindess, J. F. Young, and D. Darwin, *Concrete*, 2nd ed. Upper Saddle River, NJ, USA: Prentice Hall, 2002.
[26] ASTM C33/C33M-18, *Standard Specification for Concrete Aggregates*, ASTM International, West Conshohocken, PA, USA, 2018.
[27] M. S. Shetty, *Concrete Technology: Theory and Practice*, 7th ed. New Delhi, India: S. Chand & Company Ltd., 2013.
[28] ASTM C1602/C1602M-18, *Standard Specification for Mixing Water Used in the Production of Hydraulic Cement Concrete*, ASTM International, West Conshohocken, PA, USA, 2018..
[29] P. Ramaswamy, A. Ramesh, and M. N. Subramanian, "Mechanical properties of concrete containing recycled textile waste fibers," *Construction and Building Materials*, vol. 214, pp. 400–412, 2019.
[30] F. Jawaid and H. P. S. Abdul Khalil, "Cellulosic/synthetic fibre reinforced polymer hybrid composites: A review," *Carbohydrate Polymers*, vol. 86, no. 1, pp. 1–18, 2011.
[31] V. L. Morales, A. C. Pacheco-Torgal, and M. Ding, "Use of recycled cotton fibers to improve mechanical performance of concrete: A sustainable approach," *Journal of Cleaner Production*, vol. 261, Art. no. 121165, 2020.
[32] Y. Wang, H. Wu, and K. Li, "Evaluation of textile waste as fiber reinforcement in concrete," *Materials Today: Proceedings*, vol. 38, pp. 1467–1472, 2021.
[33] A. K. Jain and A. Kumar, "Performance of natural and recycled fiber-reinforced concrete for sustainable construction," *Materials Today: Proceedings*, vol. 57, pp. 1614–1620, 2022.
[34] ASTM C192/C192M-22, *Standard Practice for Making and Curing Concrete Test Specimens in the Laboratory*, ASTM International, West Conshohocken, PA, USA, 2022.

FIBER-REINFORCED CONCRETE FOR CRACK RESISTANCE: A REVIEW STUDY

[a] Usman Khalid*, [b] Emmad Cheema

a: Public Works Department (PWD), Mirpur, Pakistan. usmankhalid78646@gmail.com
b: Civil Engineering Analyst, AtkinsRéalis, Canada. emmad.cheema@gmail.com
* Corresponding author

Abstract- Concrete is widely recognized for its high compressive strength when compared with other construction materials. Nevertheless, it has critical flaws, as low tensile strength, brittleness and vulnerability to crack propagation. Plastic shrinkage and thermal cracking are two of the most critical early age cracking problems in concrete structures in hot climates. Plastic shrinkage cracking occurs when surface moisture loss from high temperature, low humidity and wind occurs rapidly before the concrete sets. Whereas, thermal cracking results from internal temperature gradients that are established during cement hydration and the thermal expansion behavior of aggregates. Focusing on the effectiveness of both plastic shrinkage and thermal cracking, two commonly occurring types of cracking, this study investigates the potential of various fiber types including steel, polypropylene, glass, basalt, carbon, and natural plant fibers. Among these, steel fibers are noticeably superior than the others, in resisting both forms of cracking because of their high tensile strength, crack bridging, and thermal stability. The research concludes that use of steel fibers in concrete mix designs can greatly enhance the structural integrity and service life of concrete subjected to extreme environmental exposure.

Keywords- Compressive Strength, Brittleness, Plastic Shrinkage, Thermal Cracking, Steel Fiber

1 Introduction

The high compressive strength of concrete makes it one of the most widely used construction materials, being also environmentally suited. Drawbacks are brittleness, low resistance to crack propagation, poor tensile strength. [1] [2]. The composition of concrete includes aggregates and sometimes admixtures. As the paste hardens due to the chemical reaction of the cement with water, the aggregates are bound together by the paste, which is made of cement and water, to make a rock like mass [3]. With its high compressive strength it is however brittle, thereby being less able to resist tensile stress or deformations. Concrete, particularly at low strains is extremely brittle, and owing to the low strain capacity of the material in tension, it has low toughness. Addition of randomly distributed fibers to concrete has attracted a lot of research that tries to improve its toughness. As a result, it has been embraced all over as a way of enhancing the energy dissipation, toughness and crack propagation control or arrest of concrete. [4] [5] [6]. The technique has been utilized in ancient times, to reinforce brittle matrix materials. Cracking is controlled by randomly distributed fibers which inhibit crack growth by arresting the formation of cracks and by preventing the growth of the existing cracks [7].

Fibers are used to strengthen or reinforce concrete by limiting the unstable crack propagations both on a microscopic level and macroscopic level due to their random orientation. [8] [9]. FRC is characterized by a stiffness degradation (so-called strain-softening) even when macro-cracks exist and it has been shown to have the potential to control cracks efficiently [10] [11]. Potential formation of macrocracks could result in corrosion of the steel reinforcement and thus imperative to reducing crack width through fibers addition for enhancing durability of RC structural members [12]. The infusion of fibers in concrete significantly improves its toughness, strength, crack resistance and tensile capabilities. The fibers limit the crack propagation at both micro and macro level and hence improve the durability and structural integrity [13] [14]. It

is especially important in reducing macrocrack development, which may result in steel reinforcement corrosion in reinforced concrete.

Fiber reinforced concrete (FRC), where there is haphazard distribution of artificial fibers, is reported to minimize plastic shrinkage cracks, and improve impact resistance and toughness compared to plain concrete. [15]. Synthetic fibers, like most fibers utilized in concrete, increase the post-cracking behavior, especially increasing ductility in the tensile response. [16]. FRC arrests opening and widening of micro cracks, thus enhancing deformation ability under tension and compression. However, synthetic fibers do not perform well in terms of stress transfer due to their lower elastic modulus than steel fibers, and hence, the functionality of synthetic fibers in post-cracking tensile response in fiber-reinforced concrete (FRC) is observed to be less significant. Besides this, synthetic fibers yield a favorable influence upon ultimate splitting tensile strength and flexural strength in splitting and bending tests, when compared to the corresponding direct tensile tests, despite the fact they do give a slight lift in tensile strength. [17].

Concrete possesses a very high compressive strength, exhibits low tensile capacity and brittleness that restrict it from performance. Adding fibers to concrete makes it tough, crack resistant, and longer life, bridging and arresting cracks at microscopic and macro levels. Especially if synthetic or steel fibers are added, fiber reinforced concrete (FRC) has exhibited better performance in tension and flexure, and reduced shrinkage and improved crack control [14]. In this manner, the addition of fiber is a practical and effective option to improve the mechanical behavior and service life of concrete structures.

2 Flaws in Concrete Structure

A building structure constructed in a hot climate may experiences two type of cracks which are discussed below:

2.1 Plastic Shrinkage Cracks

Horizontal concrete surfaces under extreme climatic conditions (typically high temp, low RH, wind) that may lead to rapid evaporation, plastic shrinkage cracks will happen before the concrete setting. [18]. Evaporation of water that forms menisci and high tensile stresses in the capillary water at the surface is the main driving force for plastic shrinkage cracking [19]. After bleeding water on the concrete surface is consumed by evaporation, water menisci are formed. Capillary stresses produced by these menisci compress the whole concrete and causes it to shrink [20]. Theoretically, when the concrete surface is not dried, plastic shrinkage cracks will not take place as there will be no development of negative capillary pressure [21]. Boshoff [22] suggested a simplified basis to approximate the severity of plastic shrinkage cracking expressed in terms of the evaporation rate, bleeding rate and initial setting time, and proved that the criterion of severity and area of plastic shrinkage cracking on the concrete surface had close correlation. The Plastic Shrinkage Cracking in a concrete structure is shown in Figure 1.

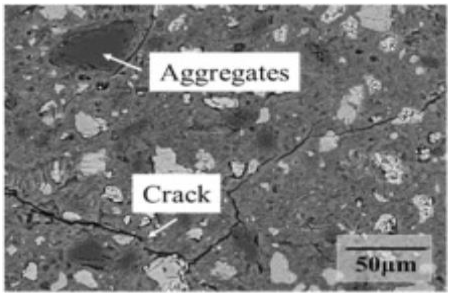


Figure 1 Plastic Shrinkage Cracking [23]

2.2 Thermal Cracking

Hydration process in substantial concrete is exothermic and it has low thermal conductivity, and That causes spatial and temporal thermal gradients, generating sufficient tensile stress that can result in undesired thermal cracking [24]. For thermal cracking, many such criteria have been proposed, including the ratio of failure stress-to-strength, strain rate, allowable temperature gradients and probabilistic methods of failure prediction [25]. Nevertheless, the application of each

method has limitations. For example, the failure stress-to-strength ratio is not always the same because it changes according to the temperature history, the amount of restraint and the material properties of the material inherently [26]. Early age concrete exposed to harsh environmental conditions leads to cracking of concrete. Rapid water evaporation causes plastic shrinkage cracks, and heat buildup and low thermal conductivity produces thermal cracks. However, there are several methods to predict thermal cracking but all of them have limitations depending on the material and environmental factors. Thermal cracking in a concrete structure is shown in Figure 2.

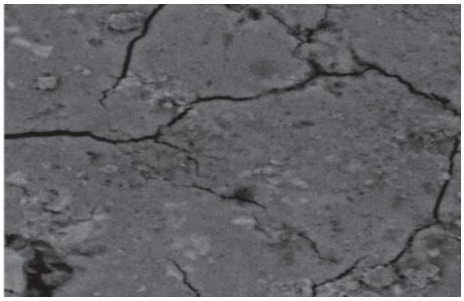


Figure 2 Thermal Cracking in Concrete [27]

3 Governing Parameters

Governing parameters for these cracks are as following:

3.1 Plastic Shrinkage Cracks

The main causes of plastic shrinkage cracking in concrete are environmental conditions and material properties affecting surface moisture loss rate prior to the concrete sets. Recent studies have found that evolution of the bulk modulus is the dominant plastic shrinkage parameter [19] [20].The rate of evaporation from the concrete surface is accelerated by elevated temperatures. Rapid drying at the concrete surface can cause plastic shrinkage cracks due to high evaporation rates [28]. When low water cement ratio or high fine aggregate content mixture is used, the bleeding may be less, so surface moisture is not sufficient which in turn results in shrinkage cracks [29]. Factors affecting plastic shrinkage cracking are shown in Figure 3.

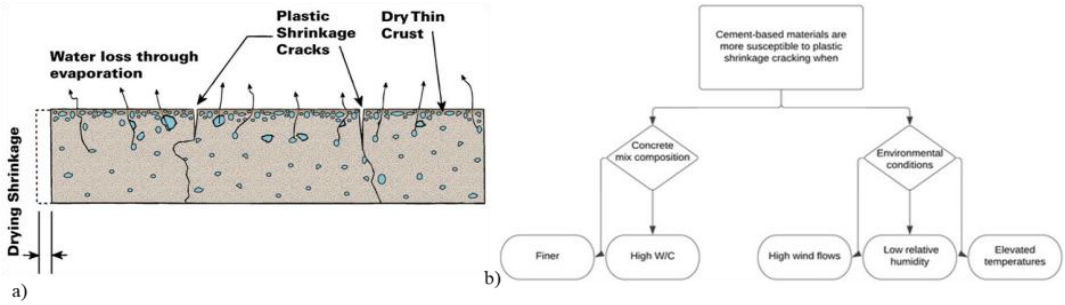


Figure 3 Factors affecting plastic shrinkage cracking [30].

3.2 Thermal Cracking

Temperature gradients within the concrete, commonly during the hydration process, can cause thermal cracking due to the formation of internal stresses that tend to crack the concrete. During the exothermic reaction of cement hydration, heat is generated, causing internal increase in temperatures resulting in thermal cracking [31].Higher Co-efficient of Thermal Expansion materials expand and contract more with temperature changes and therefore have a higher magnitude of thermal stress [32].Thermal stresses are influenced by the thermal expansion characteristics of the aggregates. High thermal expansion of aggregates such as quartz causes increased internal stresses and the possibility of cracking [33]. The temperature development as the hydration heat dissipates through the convection surfaces is shown in Figure 4.

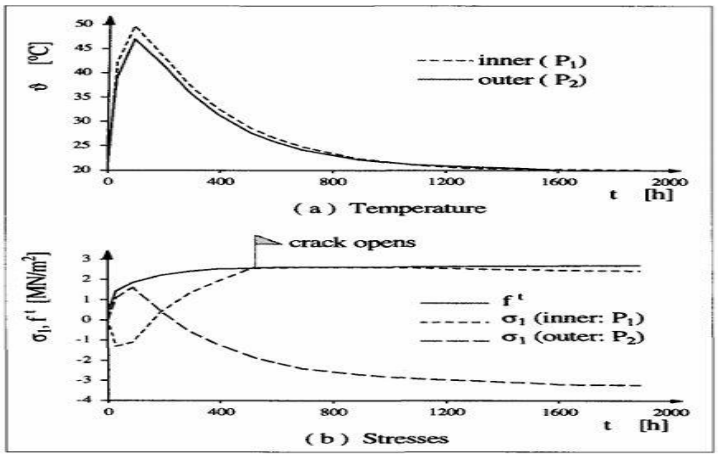


Figure 4 Temperature and stress developments [34].

Plastic shrinkage cracking is simply a rapid surface moisture evaporation that results from high temperatures and low water to cement ratios as well as insufficient bleeding. Internal temperature gradients during cement hydration cause thermal cracking, and materials with higher thermal expansion coefficients expand more than other materials, i.e., quartz, are more prone to cracking. Reduction of cracking in concrete depends on the proper management of these factors [35] [36].

4 Types of Fibers

4.1 Types of Fiber

By its nature, concrete is very strong in compression yet low in tensile so different fibers, metallic, synthetic, natural and inorganic are scattered in the matrix to improve tensile strength, control of cracks, toughness and durability [37]. The most common metallic alternative, steel fibers yield a dramatic increase in flexural strength, impact strength and energy absorption, but are susceptible to staining and are expensive to add. Of synthetics fibers, polypropylene (PP), polyethylene (PE), polyvinyl alcohol (PVA), nylon, and polyester are in common use; they effectively restrain plastic shrinkage and microcracking, improve ductility, and withstand alkaline conditions (e.g., PVA is highly chemically bonded and nylon swells in the presence of moisture) [38]. Different types of Fibers are used in concrete to reduce the cracks. Some of them with key benefits and description are shown in Table 1.

Table 1 Types of Fibers [39] [40] [41] [42] [43] [44]

Fiber Type	**Description**	**Key Benefits**
Steel Fibers	Discrete steel filaments that are short and added to the mix	Improve tensile strength, post-crack ductility, and fatigue resistance; limit crack width under loading
Polypropylene (PP) Fibers	Synthetic microscopic fibers	Control plastic and drying shrinkage; reduce permeability and surface crazing
Glass Fibers (Alkali Resistant)	Used in architectural panels like GFRC	Enhance flexural strength, crack bridging, and resistance to environmental degradation
Basalt Fibers	Derived from volcanic rock with high chemical resistance and modulus	Increase tensile strength, toughness, and thermal stability in mass concrete
Carbon Fibers	Extremely strong and stiff synthetic fibers	Boost tensile/flexural capacity; ideal for high-performance and rehabilitative structures

Natural Plant Fibers (e.g. jute, sisal, coir)	Renewable fibers from natural sources	Improve toughness, arrest cracks, and lower environmental impact of concrete
Nylon	Synthetic polyamide fibers with high elongation and durability	Enhance tensile and flexural strength, improve ductility, reduce shrinkage cracking, and increase impact resistance.

4.2 Properties of Fiber

In concrete, fibers can be described in terms of a number of critical properties that have a direct effect on their performance to improve the mechanical behavior of the cementitious matrix. Tensile strength is an important property, because fibers with high tensile resistance including steel fibers, carbon fibers, and aramid fibers, could act as crack bridging fibers and slow down crack propagation [45]. Strength of bonds between the fiber and the cement paste is also another important parameter; fiber which have a strong interfacial bonding helps to enhance energy absorption and ductility (this factor is true in fibers like polyvinyl alcohol (PVA)) [46]. Equally important, but often underemphasized, is the elongation at break, which measures how far a fiber can stretch before breaking. This is directly associated with the ductility of this fiber which further creates a greater deformation capacity of concrete when under stress. Fibers like polypropylene, polyethylene, nylon that have higher elongation to break provide the composite with the ability to deform without abrupt failures hence controlling the crack widening and better energy absorption [47]. Fiber performance under extreme surroundings is determined by thermal stability and corrosion resistance potential. Steel fibers are prone to corrosion and carbon and basalt fibers are more resistant to chemical and temperature forces [48]. Typical properties of common fibers are described in Table 2.

Table 2 Typical Properties of Common Fibers [47]

Fiber Type	Diameter (µm)	Specific Gravity	Modulus of Elasticity (GPa)	Tensile Strength (GPa)	Elongation at Break (%)
Steel	5-500	7.84	200	0.5-2.0	0.5-3.5
Glass	9-15	2.6	70-80	2.0-4.0	2.0-3.5
Polypropylene	20-400	0.9-0.95	3.5-10	0.45-0.76	15-25
Carbon	8-9	1.6-1.7	230-380	2.5-4.0	0.5-1.5
Nylon	23-400	1.14	4.1-5.2	0.75-1.0	16-20
Polyethylene	25-1000	0.92-0.96	5.0	0.08-0.6	3-100
Wood fibers	-	1.5	71	0.9	-
Sisal	10-50	1.5	-	0.8	3.0

4.3 Fiber Selection for Cracks

The different fibers have been investigated regarding their ability in control of the shrinkage of plastic and thermal cracking of concrete. To minimize shrinkage of plastic, synthetic fibers such as polypropylene are largely applied because of their strong elongation and the character of development into a dense network within new concrete [14] [40]. Glass and natural

plant fibers also have moderate advised effectiveness towards the control of early-age cracking [41] [44]. In the case of thermal cracking, basalt and carbon fiber offers a strong thermal stability and tensile strength which qualifies them to be used in high-performance concrete [42] [43]. But at the same time every alternative has its constraints, including less stiffness, low bond strength, brittle or degrades in the environment with time. Steel fibers are highly suitable for use in mitigating both plastic shrinkage and thermal cracking in concrete owing to their high tensile strength and thermal stability. They successfully bridge early microcracks and lower crack widths. Steel fiber-reinforced concrete improves crack resistance under both early-age shrinkage and elevated temperature conditions [49] [50].

5 Conclusions

Although concrete is extensively employed in construction and has great compressive strengths, it has basic disadvantages in that it has low tensile strength, low ductility, and prone to several types of cracking, especially plastic shrinkage and thermal cracking. These problems happen most commonly in challenging environment conditions where quick loss of moisture and thermal gradients create adverse effects on structural performance. This review discussed various types of fiber applied in mitigating these problems, which include synthetic fiber, glass, basalt fiber, carbon fiber and natural plant fiber. Each type offers different advantages: synthetic fibers help control shrinkage; glass and basalt fibers improve toughness and thermal resistance; and natural fibers provide eco-friendly reinforcement. Nevertheless, steel fibers always performed better than the other fibers regarding the mechanical strength, crack-bridging effect, exposure to environmental stresses. The presented evidence shows that steel fiber-reinforced concrete (SFRC) leads to a significant control of micro- and macro-cracks and increases post-cracking behavior and substantially mitigates occurrences of early-age and thermal cracking. Such characteristics make steel fibers a highly strong and dependable option to improve the long-term performance and durability of a concrete structure under harsh environments.

Acknowledgment

The authors would like to acknowledge the support and cooperation of the Public Works Division in facilitating this research. Special thanks to Dr. Majid Ali for his guidance, encouragement, and feedback throughout the study. His guidance played a vital role in shaping the direction and quality of this research.

References

[1] Khalel, H. H. Z., Khan, M., Starr, A., Sadawi, N., Mohamed, O. A., Khalil, A., & Esaker, M. (2025). Parametric study for optimizing fiber-reinforced concrete properties. Structural Concrete, 26(1), 88-110..

[2] Tassew, S. T., & Lubell, A. S. (2014). Mechanical properties of glass fiber reinforced ceramic concrete. Construction and Building Materials, 51, 215-224.

[3] Kosmatka, S. H., Panarese, W. C., & Kerkhoff, B. (2002). Design and control of concrete mixtures (Vol. 5420, pp. 60077-1083). Skokie, IL: Portland cement association..

[4] Bentur, A., & Mindess, S. (2006). Fibre reinforced cementitious composites. CRC press..

[5] Reinhardt, H. W. (1991). Fibres and cement, a useful co-operation: Introductory note, High Performance Fibre Reinforced Cement Composites. In Proceedings of the International RILEM/ACI Workshop, Reinhardt, HW, & Naaman, AE (eds), Mains, Germany..

[6] Bentur, A., & Mindess, S. (2006). Fibre reinforced cementitious composites. CRC press..

[7] Kamal, M. M., Safan, M. A., Etman, Z. A., & Salama, R. A. (2014). Behavior and strength of beams cast with ultra high strength concrete containing different types of fibers. HBRC Journal, 10(1), 55-63..

[8] Smarzewski, P. (2019). Study of toughness and macro/micro-crack development of fibre-reinforced ultra-high performance concrete after exposure to elevated temperature. Materials, 12(8), 1210..

[9] Bencardino, F. (2013). Mechanical Parameters and Post-Cracking Behaviour of HPFRC according to Three-Point and Four-Point Bending Test. Advances in Civil Engineering, 2013(1), 179712..

[10] Bajpai, A., Wetzel, B., Klingler, A., & Friedrich, K. (2020). Mechanical properties and fracture behavior of high-performance epoxy nanocomposites modified with block polymer and core–shell rubber particles. Journal of Applied Polymer Science, 137(11), 48.

[11] Vougioukas, E., & Papadatou, M. (2017). A model for the prediction of the tensile strength of fiber-reinforced concrete members, before and after cracking. Fibers, 5(3), 27..

[12] Holly, I., & Bilčík, J. (2018). Effect of chloride-induced steel corrosion on working life of concrete structures. Solid State Phenomena, 272, 226-231..

[13] Banthia, N., & Sheng, J. (1996). Fracture toughness of micro-fiber reinforced cement composites. Cement and Concrete Composites, 18(4), 251-269..

[14] Latifi, M. R., Biricik, Ö., & Mardani Aghabaglou, A. (2022). Effect of the addition of polypropylene fiber on concrete properties. Journal of Adhesion Science and Technology, 36(4), 345-369..

[15] Kotecha, P., & Abolmaali, A. (2019). Macro synthetic fibers as reinforcement for deep beams with discontinuity regions: Experimental investigation. Engineering Structures, 200, 109672..

[16] Bentur, A., & Mindess, S. (2006). Fibre reinforced cementitious composites. CRC press..

[17] Hasan, M. J., Afroz, M., & Mahmud, H. M. I. (2011). An experimental investigation on mechanical behavior of macro synthetic fiber reinforced concrete. Int. J. Civ. Environ. Eng, 11(3), 19-23..

[18] Lura, P., Toropovs, N., Justs, J., Shakoorioskooie, M., Münch, B., & Griffa, M. (2025). Mitigation of plastic shrinkage cracking with natural fibers-kenaf, abaca, coir, jute and sisal. Cement and Concrete Composites, 155, 105827..

[19] Ghourchian, S., Wyrzykowski, M., Plamondon, M., & Lura, P. (2019). On the mechanism of plastic shrinkage cracking in fresh cementitious materials. Cement and Concrete Research, 115, 251-263..

[20] Ghourchian, S., Wyrzykowski, M., & Lura, P. (2018). A poromechanics model for plastic shrinkage of fresh cementitious materials. Cement and Concrete Research, 109, 120-132..

[21] Kwak, H. G., & Ha, S. J. (2006). Plastic shrinkage cracking in concrete slabs. Part I: a numerical model. Magazine of Concrete Research, 58(8), 505-516..

[22] Boshoff, W. P., & Combrinck, R. (2013). Modelling the severity of plastic shrinkage cracking in concrete. Cement and Concrete Research, 48, 34-39..

[23] Zeng, X., Deng, Q., Li, S., Gao, H., & Yu, Q. (2024). Effects of autogenous shrinkage microcracks on UHPC: Insights from a machine learning based crack quantification approach. Construction and Building Materials, 428, 136400..

[24] Fairbairn, E. M., & Azenha, M. (2019). Thermal cracking of massive concrete structures. State of Art Report of the RILEM TC..

[25] Van Breugel, K., & Lokhorst, S. J. (2003). Stress-based crack criterion as a basis for the prevention of through cracks in concrete structures at early-ages. In International RILEM Conference on Early Age Cracking in Cementitious Systems; Kovler, K., Bent.

[26] Riding, K. A., Poole, J. L., Schindler, A. K., Juenger, M. C., & Folliard, K. J. (2014). Statistical determination of cracking probability for mass concrete. Journal of materials in civil engineering, 26(9), 04014058..

[27] Shen, J., Xu, Q., & Liu, M. (2021). Statistical analysis of defects within concrete under elevated temperatures based on SEM image. Construction and Building Materials, 293, 123503..

[28] Kalantari, S., Diznab, M. A. D., & Tehrani, F. M. (2021, April). Sustainability of internally-cured concrete for mitigating shrinkage cracking using service life prediction models. In International RILEM Conference on Early-Age and Long-Term Cracking in R.

[29] Alshammari, T. O., Guadagnini, M., & Pilakoutas, K. (2022). The effect of harsh environmental conditions on concrete plastic shrinkage cracks: case study Saudi Arabia. Materials, 15(23), 8622..

[30] Kayondo, M., Combrinck, R., & Boshoff, W. P. (2019). State-of-the-art review on plastic cracking of concrete. Construction and building materials, 225, 886-899..

[31] Klemczak, B., & Batog, M. (2016). Heat of hydration of low-clinker cements: Part I. Semi-adiabatic and isothermal tests at different temperature. Journal of Thermal Analysis and Calorimetry, 123, 1351-1360..

[32] Zhang, Y., Kim, T., Castel, A., & Xu, T. (2023). Thermal cracking in high volume of fly ash and GGBFS concrete. International Journal of Concrete Structures and Materials, 17(1), 65..

[33] Klimek, A., Stelzner, L., Hothan, S., & Zehfuß, J. (2024). Influence of thermal strain on concrete spalling. Materials and Structures, 57(1), 15..

[34] Huang, C. X. (1999). The three dimensional modelling of thermal cracks in concrete structure. Materials and Structures, 32, 673-678..

[35] Mora-Ruacho, J., Gettu, R., & Aguado, A. (2009). Influence of shrinkage-reducing admixtures on the reduction of plastic shrinkage cracking in concrete. Cement and Concrete Research, 39(3), 141-146..

[36] Bernander, S. (1998). Practical measures to avoiding early age thermal cracking in concrete structures. RILEM report, 255-314..

[37] Mohajerani A, Hui SQ, Mirzababaei M, Arulrajah A, Horpibulsuk S, Abdul Kadir A, Rahman MT, Maghool F. Amazing Types, Properties, and Applications of Fibres in Construction Materials. Materials (Basel). 2019 Aug 7;12(16):2513. doi: 10.3390/ma12162513. PMID.

[38] Wang T, Fan X, Gao C, Qu C, Liu J, Yu G. The Influence of Fiber on the Mechanical Properties of Geopolymer Concrete: A Review. Polymers (Basel). 2023 Feb 7;15(4):827. doi: 10.3390/polym15040827. PMID: 36850111; PMCID: PMC9965450.

[39] Amin, M. N., Ahmad, W., Khan, K., & Ahmad, A. (2022). Steel fiber-reinforced concrete: a systematic review of the research progress and knowledge mapping. Materials, 15(17), 6155..

[40] Lakshmi, A., Pandit, P., Bhagwat, Y., & Nayak, G. (2022). A review on efficiency of polypropylene fiber-reinforced concrete. Sustainability Trends and Challenges in Civil Engineering: Select Proceedings of CTCS 2020, 799-812..

[41] Ahmad, J., González-Lezcano, R. A., Majdi, A., Ben Kahla, N., Deifalla, A. F., & El-Shorbagy, M. A. (2022). Glass fibers reinforced concrete: Overview on mechanical, durability and microstructure analysis. Materials, 15(15), 5111..

[42] Al-Kharabsheh, B. N., Arbili, M. M., Majdi, A., Alogla, S. M., Hakamy, A., Ahmad, J., & Deifalla, A. F. (2023). Basalt fiber reinforced concrete: A compressive review on durability aspects. Materials, 16(1), 429..

[43] Hao, Y., Shi, C., Bi, Z., Lai, Z., She, A., & Yao, W. (2023). Recent advances in properties and applications of carbon fiber-reinforced smart cement-based composites. Materials, 16(7), 2552..

[44] Lilargem Rocha, D., Tambara Júnior, L. U. D., Marvila, M. T., Pereira, E. C., Souza, D., & de Azevedo, A. R. G. (2022). A review of the use of natural fibers in cement composites: concepts, applications and Brazilian history. Polymers, 14(10), 2043..

[45] Zhu, D., Huang, N., Li, W., Li, J., & Wu, X. (2024). Effect of different fibers and fiber contents on the mechanical properties and failure behavior of early age cemented lithium feldspar tailings backfill. Developments in the Built Environment, 19, 10049.

[46] Li, R., Deng, M., Guo, L., Wei, D., Zhang, Y., & Li, T. (2024). Tensile behavior of high-strength highly ductile fiber-reinforced concrete with embedded carbon textile grids. Construction and Building Materials, 414, 134957.

[47] Bentur, A., & Mindess, S. (2006). Fibre reinforced cementitious composites. CRC press..

[48] Ramezani, A., Modaresi, S., Dashti, P., GivKashi, M. R., Moodi, F., & Ramezanianpour, A. A. (2023). Effects of different types of fibers on fresh and hardened properties of cement and geopolymer-based 3D printed mixtures: a review. Buildings, 13(4), 945.

[49] Zhang, P., Kang, L., Wang, J., Guo, J., Hu, S., & Ling, Y. (2020). Mechanical properties and explosive spalling behavior of steel-fiber-reinforced concrete exposed to high temperature—a review. Applied Sciences, 10(7), 2324..

[50] Eren, Ö., & Marar, K. (2010). Effect of steel fibers on plastic shrinkage cracking of normal and high strength concretes. Materials Research, 13, 135-141..

AN OVERVIEW OF THE EFFECTS OF STEEL FIBER REINFORCED COMPOSITES ON FLEXURAL CRACKING IN CONCRETE

[a] Awais Sikandar*, [b] Faheem Ahmad Gul

a: Civil Engineering Department, APCOMS, Rawalpindi, Pakistan. awaissikandar786abc@gmail.com
b: School of Civil and Architectural Engineering, Nanchang Institute of Technology, Nanchang 330099, China. faheem@nit.edu.cn
* Corresponding author

Abstract- Cement concrete is the most widely used construction material globally, attributed to its excellent workability and moldability. However, its inherently low tensile strength, minimal ductility, and high susceptibility to cracking limit its application without reinforcement. These deficiencies often result in the formation of internal microcracks that compromise the material's structural integrity. As modern civil engineering structures demand higher performance and durability, conventional concrete must be enhanced to meet these evolving requirements. The incorporation of various fiber types into concrete mixtures has shown promising improvements in mechanical performance, durability, and serviceability. Among these, Steel Fiber Reinforced Concrete (SFRC) has demonstrated exceptional crack resistance and control. SFRC significantly improves tensile strength of concrete under flexural loading, by bridging cracks and preserving the integrity of the matrix even after extensive cracking. This paper provides an overview of the effectiveness of steel fiber composites in enhancing the structural behavior of concrete, with a focus on mitigating flexural cracking.

Keywords- Concrete Durability, Flexural Cracking, Steel Fiber Reinforced Concrete, Tensile Strength Enhancement

1 Introduction

Concrete is vulnerable to cracking due to various factors. These include foundation settlement, temperature changes, flexural stresses from bending, excessive loading, shrinkage during curing, and reinforcement corrosion [1]. Early-age plastic shrinkage cracks often occur during the curing stage. In contrast, map and hairline cracks typically result from temperature variations or drying shrinkage [2]. Cracks can reduce the durability and performance of concrete structures. To prevent them, engineers use several methods. These include proper mix design, installation of control joints, fiber or steel reinforcement, careful curing, and avoiding overloads [3]. With effective construction practices, the service life of concrete can be extended, and the likelihood of cracking can be reduced [4].

Steel Fiber Concrete (SFC) is a composite made by adding steel fibers to cement, aggregates, and water. Plain concrete is brittle and weak in tension. It tends to crack under bending or flexural stresses [5]. Steel fibers help control these cracks. They are randomly distributed in the mix and act as internal reinforcement. After cracking begins, the fibers bridge the cracks and provide ductility. This improves the toughness of concrete, which refers to the energy absorbed after peak load [6][7]. Fibers help the concrete resist sudden failure by increasing its energy absorption capacity [8]. Although there are cheaper alternatives, the performance benefits of steel fibers make them valuable in structural applications.

Steel fibers are not a replacement for main reinforcement bars. However, they improve crack resistance and reduce deflection in structural elements [9][10]. When added to the concrete matrix, the fibers act as stiff inclusions. They help resist serviceability issues like crack widening and excessive bending. Fibers can be distributed in three dimensions

throughout the concrete. This is useful for general reinforcement. In some cases, they can also form a two-dimensional tensile layer over steel reinforcement [11][12]. The research significance is to improve shear resistance and help control crack growth [13]. As a result, steel fiber reinforced concrete is increasingly used in beams, slabs, pavements, and other load-bearing elements.

2 Structural Cracking and Flexural Failure

Several researchers have studied the types, causes, and control methods of cracks in concrete structures [14]. One common area of focus is surface cracking, which is important for civil engineers to understand due to its impact on durability and appearance [1]. Studies have identified various reasons for concrete cracking and methods to evaluate them, including tools like crack compactors and ultrasonic testing [15]. The paper *Building Cracks: Causes and Remedies* highlights that cracks can have both direct and indirect consequences. While cracks may not always be the immediate cause of structural failure, they often contribute to conditions that lead to it [16]. Researchers have also provided classifications of cracks along with their causes and possible remedies. In one study, visual inspection was used effectively to identify and categorize cracks in an institutional building, demonstrating how such evaluations can support maintenance and repair decisions [17].

A specific type of fracture known as flexural crack commonly forms in reinforced concrete elements such as beams and slabs due to bending or flexural stresses [18]. Figure 1 illustrates flexural cracks in a reinforced concrete beam. These cracks occur because concrete is inherently strong in compression but weak in tension. When a beam is subjected to bending, the top fibers experience compression, while the bottom fibers are placed in tension [19]. If the tensile stress in the tension zone exceeds the concrete's tensile strength, cracks begin to form typically starting at the bottom and moving vertically upward [20]. Flexural cracks most often appear at mid-span, where bending moments are greatest. Contributing factors include excessive loading, poor or insufficient reinforcement, substandard concrete quality, improper curing, long spans, and inadequate structural design. Understanding the stress behavior of concrete is essential for identifying, controlling, and preventing flexural cracking in structural elements.



Figure 1: Flexural cracks in a reinforced concrete b*eam [30]*

3 Governing Parameters Influencing Flexural Cracking

Flexural cracking in concrete mainly occurs because it is strong in compression but weak in tension. When a structural element bends, the tension at the bottom may exceed the concrete's capacity, leading to cracks [1]. A low modulus of elasticity in concrete allows greater deflections under load, which increases the likelihood of cracking due to higher strain levels [14]. Creep, which is the slow deformation under long-term loading, also contributes by increasing deflection over time. Shrinkage, especially during drying, creates internal tensile stresses that can further promote cracking [2-4].

Poor bonding between the concrete and reinforcement reduces the reinforcement's effectiveness in handling tensile forces [7]. Internal flaws like voids and weak zones can concentrate stress and trigger cracks. These factors combined make concrete vulnerable to flexural failure [18]. As shown in Table 1, properties of steel fibers significantly enhance the

performance of concrete. They improve tensile and flexural strength, increase ductility, and help control cracks by bridging micro-cracks and absorbing energy. This results in better durability and reduced cracking under flexural stress [5-8].

Table 1 Properties of Steel Fibers [21]

Property	**Typical Values / Description**
Tensile Strength	280–990 MPa
Young's Modulus	~200 GPa
Poisson's Ratio	~0.30
Ultimate Elongation	~3.6%
Specific Gravity	~7.86
Fiber Dimensions	Diameter: 0.25–0.75 mm
Aspect Ratio	20-100
Fiber Dosage	5% use in volume
Fiber Length	2" in length
W/C Ratio	0.5% w/c ratio
Compressive Strength Gain	Increased by 14–32% with steel fiber inclusion
Splitting Tensile Strength	Increased up to 77%
Flexural Strength	Increase of 6–69% depending on fiber shape and dosage
Ductility and Toughness	Enhanced; fibers delay crack growth and increase energy absorption
Impact Resistance	Significantly improved compared to conventional concrete
Crack Control	Fibers bridge micro-cracks, reducing crack widths and propagation
Fiber Shapes	Hooked-end, straight, crimped, corrugated – affect performance
ASTM A820 Fiber Types	Type I: Cold-drawn, Type II: Cut sheet, Type III: Melt- extracted, Type IV: Mill cut, Type V: Modified wire

4 Fiber Shortlisting for Crack Control

To improve concrete's flexural strength and prevent it from cracking, several fibers are used, each with unique benefits. Steel fibers are the most efficient method of enhancing flexural strength and fracture resistance because they disperse tensile stress and bridge cracks. This increases the concrete's ductility and decreases the likelihood that it will shatter when bent [22-23]. Polypropylene fibers primarily prevent shrinkage fractures by reducing internal stresses during the early curing phase, even though they don't significantly boost flexural strength [24]. Glass fibers provide corrosion resistance and flexural strength, making them suitable for severe environments even though their tensile strength is inferior to that of steel [25]. The durability and corrosion resistance of basalt fibers are well known, and they improve flexural strength and crack resistance in harsh environments [26]. Carbon fibers are ideal for high-performance concrete because of their exceptional flexural strength and fatigue resistance, despite their higher cost [27]. Nylon fibers can improve impact resistance and reduce shrinkage fractures, although having a slight effect on flexural strength [28]. When selecting these fibers, the specific needs of the project such as strength, durability, and environmental exposure are taken into account.



Figure 2: Steel Fibers in concrete matrix [31]

Figure 2 illustrates steel fibers embedded in the concrete matrix, highlighting their role in improving tensile properties and fracture resistance. Steel fibers act as internal reinforcement, distributing tensile stresses more evenly throughout the concrete. They bridge flexural cracks that develop under bending stress, significantly increasing the concrete's resistance to bending and preventing fractures from spreading. This greatly enhances the concrete's ductility, allowing it to deform more without cracking. Additionally, steel fibers limit shrinkage cracks and prevent large fractures by reducing internal tensile strains during drying and curing. They serve as barriers restricting concrete mobility during drying shrinkage, lowering the risk of early-stage cracking. Overall, steel fibers improve toughness, impact resistance, and post-cracking behavior, making concrete more durable and resistant to cracking over time [22-23, 29].

Table 2 Comparison of fiber type [21]

Fiber Type	Mechanical Properties Enhanced	Shrinkage Control	Workability Impact
Straight	Tensile strength, flexural strength, Compressive strength, toughness, ductility	Moderate to good	Usually manageable, but decreases with increasing aspect ratio and volume
Crimped	Mechanical anchorage, flexural strength, toughness	Good	Adequate reduction in slump as compared to plain concrete
Hooked-End	Flexural strength, tensile strength, toughness, impact resistance, pull-out resistance	Effective in reducing plastic shrinkage and micro-cracks, and most efficient for drying shrinkage control	Adequate reduction in slump, but generally less than RTSF at similar dosages

Table 2 illustrates that fiber may effectively increase the mixture's ability to regulate cracks, which will lower the breadth and length of cracks. Furthermore, steel fiber-reinforced concrete (SFRC) has superior mechanical properties, including fatigue resistance, impact resistance, and shear and flexural strength. Concise overview of how different steel fiber forms influence concrete properties is provided.

5 Conclusion

In conclusion, this study highlights the importance of improving concrete performance through fiber reinforcement to reduce flexural cracking. The following key points summarize the findings:

1 Several factors, including foundation settlement, temperature changes, excessive loading, curing shrinkage, and reinforcement corrosion, influence concrete cracking. Early-age plastic cracks and later-stage map or hairline cracks are common in poorly managed concrete.
2 Flexural cracks typically occur in the tension zone of beams and slabs when bending stresses exceed the concrete's limited tensile strength. These cracks compromise structural capacity and durability, especially in elements exposed to repeated or sustained loads.
3 Steel fibers significantly enhance concrete's performance by improving tensile and flexural strength, delaying crack formation, and bridging micro cracks. This increases the concrete's energy absorption and resistance to crack propagation under flexural loading.
4 The inclusion of steel fibers also contributes to improved ductility, impact resistance, and post-cracking behavior. As a result, structures reinforced with steel fibers demonstrate increased durability, reduced maintenance needs, and better long-term performance under flexural stress.

References

[1] G. L. Golewski, "The phenomenon of cracking in cement concretes and reinforced concrete structures: The mechanism of cracks formation, causes of their initiation, types and places of occurrence, and methods of detection—A review," *Buildings*, vol. 13, no. 3, p. 765, 2023.
[2] I. M. G. Bertelsen, L. M. Ottosen, and G. Fischer, "Influence of fibre characteristics on plastic shrinkage cracking in cement-based materials: A review," *Constr. Build. Mater.*, vol. 230, no. 116769, p. 116769, 2020.
[3] A. J. Thakur, *The Elements of Fracture Fixation - E-Book*. Elsevier Health Sciences, 2022.

[4] S. Chen, C. Duffield, S. Miramini, B. Nasim Khan Raja, and L. Zhang, "Life-cycle modelling of concrete cracking and reinforcement corrosion in concrete bridges: A case study," *Eng. Struct.*, vol. 237, no. 112143, p. 112143, 2021.
[5] A. Bazgir, "The behaviour of steel fibre reinforced concrete material and its effect on impact resistance of slabs," City University London, 2016.
[6] H. Miller, "Surface treatment of steel fibres and carbon nanotubes to develop chemical bonds with concrete." UNSW Sydney, 2019.
[7] T. Simões, H. Costa, D. Dias-da-Costa, and E. Júlio, "Influence of fibres on the mechanical behaviour of fibre reinforced concrete matrixes," *Constr. Build. Mater.*, vol. 137, pp. 548–556, 2017.
[8] S. M. F. Mahmood, "Moment redistribution and post-peak behaviour of steel fibre reinforced concrete flexural members." UNSW Sydney, 2020.
[9] Y. M. Abbas, M. J. A. J. f. S. Iqbal Khan, and Engineering, "Fiber–matrix interactions in fiber-reinforced concrete: A review," vol. 41, no. 4, pp. 1183-1198, 2016.
[10] H. Singh, *Steel fiber reinforced concrete: Behavior, modelling and design*, 1st ed. Singapore, Singapore: Springer, 2016.
[11] L. Das and M. Kumruzzaman, "Strengthening concrete; unbridling the potential of steel fiber reinforcement," in *7th International Conference on Mechanical Engineering and Renewable Energy, Chattogram, Bangladesh*, 2023.
[12] K. L. Goh, *Discontinuous-fibre reinforced composites: fundamentals of stress transfer and fracture mechanics*. Springer, 2016.
[13] N. K. Barman, S. S. Bhattacharya, and R. Alagirusamy, "Textile structures in concrete reinforcement," *Text. Prog.*, vol. 56, no. 1, pp. 1–229, 2024.
[14] G. A. Aruya, V. K. Chukwuemezie, and Applications, "Causes of cracks on concrete structures and repair methods," vol. 7, no. 9, pp. 28-38, 2022.
[15] S. Mustafa, A. Peer, and F. Concli, "Non-destructive crack detection methodologies in green compacts: An overview," in *Lecture Notes in Mechanical Engineering*, Cham: Springer Nature Switzerland, 2024, pp. 836–847.
[16] Md. Safiuddin, A. B. M. A. Kaish, C.-O. Woon, and S. N. Raman, "Early-Age cracking in Concrete: causes, consequences, remedial measures, and recommendations," *Applied Sciences*, vol. 8, no. 10, p. 1730, Sep. 2018.
[17] D. S. Watt, *Building pathology: Principles and practice*. John Wiley & Sons, 2025.
[18] M. A. Al-Osta, M. N. Isa, M. H. Baluch, and M. K. Rahman, "Flexural behavior of reinforced concrete beams strengthened with ultra-high performance fiber reinforced concrete," *Constr. Build. Mater.*, vol. 134, pp. 279–296, 2017.
[19] D. Zheng, W. Song, J. Fu, G. Xue, J. Li, and S. Cao, "Research on mechanical characteristics, fractal dimension and internal structure of fiber reinforced concrete under uniaxial compression," *Constr. Build. Mater.*, vol. 258, no. 120351, p. 120351, 2020.
[20] I. Iskhakov and Y. Ribakov, "Structural phenomenon based theoretical model of concrete tensile behavior at different stress-strain conditions," *J. Build. Eng.*, vol. 33, no. 101594, p. 101594, 2021.
[21] ASTM A820/A820M – 16, Standard Specification for Steel Fibers for Fiber-Reinforced Concrete.
[22] A. Bentur and S. Mindess, *Fibre Reinforced Cementitious Composites, Second Edition*, 2nd ed. London, England: CRC Press, 2014.
[23] R. F. Zollo, "Fiber-reinforced concrete: an overview after 30 years of development," *Cem. Concr. Compos.*, vol. 19, no. 2, pp. 107–122, 1997.
[24] D. Zhang, H. Zhu, M. Hou, K. E. Kurtis, P. J. M. Monteiro, and V. C. Li, "Optimization of matrix viscosity improves polypropylene fiber dispersion and properties of engineered cementitious composites," *Constr. Build. Mater.*, vol. 346, no. 128459, p. 128459, 2022.
[25] V.C. Li, "Postcrack scaling relations for fiber reinforced cementitious composites," *Journal of Materials in Civil Engineering*, vol. 4, no. 4, pp. 410–427, 1992.
[26] Y. Ming and H. W. Liu, "Mechanical properties of basalt fiber-reinforced concrete," *Highway Engineering*, vol. 42, pp. 275–282, 2017.
[27] Z. Guo, C. Zhuang, Z. Li, and Y. Chen, "Mechanical properties of carbon fiber reinforced concrete (CFRC) after exposure to high temperatures," *Compos. Struct.*, vol. 256, no. 113072, p. 113072, 2021.
[28] P. S. Song, S. Hwang, and B. C. Sheu, "Strength properties of nylon- and polypropylene-fiber-reinforced concretes," *Cem. Concr. Res.*, vol. 35, no. 8, pp. 1546–1550, 2005.
[29] J. Thomas and A. Ramaswamy, "Mechanical properties of steel Fiber-Reinforced concrete," *Journal of Materials in Civil Engineering*, vol. 19, no. 5, pp. 385–392, Apr. 2007.
[30] M. Hashmi, "Flexural cracks in beams," *Structural Engineering Forum Of Pakistan*, 13-Jun-2021. [Online]. Available: https://www.sepakistan.com/topic/3238-flexural-cracks-in-beams/.
[31] "Fiber Reinforced Concrete," *Surechemical.com*. [Online]. Available: https://www.surechemical.com/aboutus/RP20230823-Fiber-Reinforced-Concrete.html.

7th Conference on Sustainability in Civil Engineering (CSCE'25)
(An International Conference)
Department of Civil Engineering
Capital University of Science and Technology, Islamabad Pakistan

A REVIEW OF MECHANICAL PERFORMANCE AND SUSTAINABILITY OF NYLON FIBER IN CONCRETE BEAM REINFORCEMENT

[a] Qazi Muhammad Tariq*, [b] Blawal Hasan

a: Civil Engineering, Cost Umbrella, Islamabad, Pakistan. qazitariq581@gmail.com
b: Sr. Architect, Contracting and Construction Enterprises, Saudi Arabia. engr.blawal.hasan@gmail.com
*Corresponding author

Abstract- In today's world, one of the persistent problems in civil engineering is the formation of concrete cracks due to shrinkage, temperature changes, and load stressors. Traditional polishing methods place little to no emphasis on preventing or resisting micro-cracks. The specific aim of this study is to evaluate the behavior of concrete against cracking with the addition of Nylon Fiber as reinforcement. The study analyzes research conducted over the last ten years on the effects of adding Nylon Fiber to concrete in varying percentages. Recent experiments have shown that the addition of Nylon Fiber significantly improves the tensile, flexural, and compressive strength of concrete. In particular, for projects that require shortened construction periods, the incorporation of such fiber is highly beneficial. Nylon Fiber enhances the sustainability of concrete by reducing the need for traditional steel reinforcement, thereby also lowering long-term maintenance costs. Nylon Fiber-reinforced concrete presents a promising solution for improving the performance of reinforced concrete beams, especially in seismic applications.

Keywords- Cracking, Durability, Fiber Reinforced Concrete (FRC), Shrinkage, Strength

1 Introduction

Over the years, engineers alongside researchers have worked relentlessly to find solutions using other materials to improve the performance of concrete structures around the world. Reinforcing concrete with fiber, such as nylon, considering them as potential additives for the last century [1]. Originally developed during the 1930s, Nylon Fiber is classified as synthetic polyamides. They are known for fortifying tendons along with flexibility and high resistance to abrasion and chemicals [2]. It's also quite brittle and doesn't handle tension very well. This means it can crack easily when faced with things like shrinkage, temperature changes, or heavy loads. To tackle these issues, folks have looked into mixing fiber into concrete, which is what we call fiber-reinforced concrete (FRC) [3]. Among various fiber, nylon, a synthetic polymer, has gained attention due to its high tensile strength, elasticity, and resistance to environmental factors [4]. Nylon Fiber can enhance the ductility and crack resistance of concrete, making them a promising additive for improving concrete performance in structural applications. Crack resistance of concrete, making it a strong candidate for improving performance in structural uses [5].

Nylon Fiber, in particular, offer potential benefits, but comprehensive studies on their impact on concrete's mechanical properties are limited. This research aims to investigate the effects of varying Nylon Fiber content on the flexural strength of concrete, thereby addressing the gap in knowledge and providing insights into optimizing concrete mixtures for enhanced performance. Incorporation of Nylon Fiber solves these problems as the fiber can greatly reduce micro cracking by bridging them, in addition to distributing tensile loads more evenly throughout the concrete [8]. To Concrete is strong

under compression but weak in tension. It can also crack over time due to thermal expansion and shrinkage. Steel reinforcement helps with large cracking, but does not alleviate micro marks and early cracking that could affect long term durability. Incorporation of Nylon Fiber solves these problems as the fiber can greatly reduce micro cracking by bridging them, in addition to distributing tensile loads more evenly throughout the concrete [10].

The fiber is added while mixing so that they become uniformly dispersed throughout the concrete, creating an additional reinforcement skeleton. It has also been demonstrated that nylon reinforced concrete is better at flexural impacting post crack load bearing capability, as well as dynamic impact and loading [5]. Unlike previous research that focused on steel, polypropylene, or glass fiber, nylon offers the best balance of performance, true and ease of use [6]. Unlike previous research that focused on steel, polypropylene, or glass fiber, nylon offers the best balance of performance, true and ease of use [10]. Standardized procedures were followed for mixing, casting, and curing the specimens. After letting them cure for 28 days, they ran flexural strength tests using a universal testing machine, sticking to ASTM C78/C78M standards [11]. They recorded how the load-deflection behavior changed to see how the Nylon Fiber content affected the concrete's flexural performance. Statistical analyses were performed to evaluate the significance of the results and determine the optimal fiber content for maximum flexural strength enhancement [12].

In this work, previously mentioned properties of nylon still remain, especially the tendency to absorb water, but has led to a spike in utilization within slabs, pavements, shotcrete, and overlays. We believe anchoring systems made from nylon are easy to produce and versatile for many civil engineering applications. The addition of Nylon Fiber to concrete introduces a very promising new composite within construction materials with additional improved mechanical properties, improved crack resistance performance, and sustainability. The improvements noticed in flexural strength and durability further cement NFRC's potential for both structural and non-structural applications where high performance and longevity are required. Overall, Nylon Fiber reinforced concrete performed better than plain concrete in terms of strength, durability, and crack control. It shows great potential for use in both structural and non-structural applications. More research is needed on standardizing its use and exploring recycled Nylon Fiber to improve sustainability in construction. Challenges that come with reduced workability should be tackled by careful mix design aided by admixtures. Further exploration in terms of standardization and use of recycled Nylon Fiber will be essential to unlock the environmental benefits as well as the structural contributions of Nylon Fiber reinforced concrete as the construction industry begins moving toward more sustainable practices.

2 Flaws and Challenges

While the benefits are clearly visible, there are a few disadvantages pertaining to Nylon Fiber that need consideration. Absorptive Action Nylon Fiber are hydrophilic and soak up water (4 to 10% by weight), this may adversely affect bond strength and durability over time in humid conditions [1]. Problems of Uniform Dispersion Poor mixing or high dosages of fiber can lead to fiber "balling" or clumping, which in turn reduces effectiveness and may compromise the concrete [3]. Workability Reduction Adding Nylon Fiber tends to require a change in water volume or use of plasticizers to maintain slump value [4]. Cost at Large Scale Cost per cubic meter of concrete tends to increase with the addition of Nylon Fiber in large scale infrastructural projects despite being more economical than steel or carbon fiber [7].

Identifying potential ASR issues as shown in figure (a) early is key. Several tests are used to identify the risk or presence of ASR in concrete or its materials like ASTM C1260 – Accelerated Mortar Bar Test**.** Purpose is to assesses the potential reactivity of aggregates. Implementing appropriate prevention strategies helps engineers and contractors avoid costly repairs. These actions also extend the service life of bridges and overpasses. Lack of Limited Standardization Design specifications for Nylon Fiber reinforced concrete are virtually non-existent in most building codes [8], which poses a critical barrier for widespread adoption. Though there is increased interest in improving concrete performance through synthetic fiber, such as nylon, significant inadequacies and problems continue with the present body of research on sustainable aspects of the durability methods for Nylon Fiber-reinforced beam concrete.

Figure 1. shows the overpasses that are crucial parts of our transportation infrastructure, ensuring safe passage for vehicles and pedestrians. Regular Alkali-Silica Reaction (ASR) testing and prevention measures are essential to maintain their safety and longevity [8].



Essentially, weak major limitations are a lack of data on how well it performs over the long term under various environmental conditions exposure to moisture and UV radiation, and even aggressive chemical environments undermining how reliable any durability assessment is [13]. Plus, variations in the types of fiber used, dosages applied, and mixing techniques employed across studies make standardized methodologies nearly impossible or comparative conclusions very unwelcome. Nylon is a petrol-based plastic; from up sustainability perspective- raises concerns regarding its environmental footprint throughout its lifecycle about its embodied energy, recyclability as well as end-of-life disposal [14].

3 Governing Parameters

The use of Nylon Fiber in reinforcing concrete has a varying level of efficiency depending on a number of interrelated factors. These include Fiber Length and Diameter, which are the more common parameters. The most effective fiber ranges from 12mm to 50mm in length, and have diameters of approximately 0.2 mm to 1.0 mm. [8] explains that shorter fiber assist in dispersion while longer ones facilitate more crack-bridging. Moreover, concerning Fiber Dosage, the optimal dosage is known to range from 0.1% to 1.0% by volume. According to Jangid and [9], dosages of around 0.3%-0.5% strike a balance between workability and strength improvement. An increased aspect ratio (length to diameter) enhances tensile properties and toughness, but may hinder mixing [10]. As for curing conditions, [11] mentions that fiber nylon works best under wet or moist curing conditions which aids in bonding of the fiber to the cement while also reducing shrinkage cracking. Also, with the mix compatibility of the cement we also the find the secondary cementitious materials like fly ash and silica fume which reacted with nylon differently. [12] note that high performance mixes may need tailored fiber dosage or other additives. "The impact of critical governing parameters on the durability performance of Nylon Fiber Reinforced beam concrete that require proper consideration to evaluate its structural reliability and sustainability [8].

From a sustainability point of view, using Nylon Fiber in concrete can make structures last longer and require less maintenance. This helps reduce the overall impact on the environment. Compared to other fiber like carbon or glass, which take more energy to produce, nylon provides a good mix of strength and lower energy use. If the fiber can stand up well to harsh conditions like exposure to chemicals, moisture, and sunlight they help make the concrete more durable. That means fewer repairs, less material waste, and lower carbon emissions from replacements. To judge how well Nylon Fiber perform, it's important to look at how they hold up in alkaline environments, how resistant they are to UV rays, how strong they stay over time, how well they bond with the concrete, and whether any treatments improve their durability [13].

4 Shortlisting of Fiber

In the design of fiber-reinforced concrete (FRC), various types of fiber were initially considered based on their mechanical performance, chemical stability, cost-efficiency, and availability. Shortlisted among them were steel, polypropylene, glass, basalt, carbon, and nylon [2]. Each type of fiber possesses some advantages: steel fiber is characterized by high strength and stiffness; polypropylene exhibits high resistance to plastic shrinkage cracking; glass fiber possesses aesthetic and tensile advantages; basalt fiber is resistant to thermal and durability requirements; and carbon fiber provide the highest strength at additional cost [7].

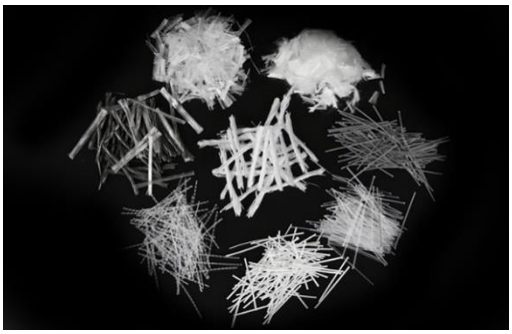


Figure 2: Fibrillated Nylon Fiber [12].

Based on careful evaluation, Nylon Fiber as shown in Figure 2 was chosen as the reinforcing material in this research based on its balance between mechanical performance, economic viability, and environmental strength. The 28-day cylinder strength comparison between Nylon Fiber concrete and normal concrete shows significant variation [10]. For cylinder strength, Nylon Fiber concrete has a marginally higher initial cylinder strength of 40 N/mm² at 0.5% fiber content. Compared to 36 N/mm² in conventional concrete. Yet, when the fiber content is raised to 3%, cylinder strength drops marginally to 37.5 N/mm². On the other hand, cube strength improves with a large margin using Nylon Fiber, from 40.89 N/mm² at 0.5% dosage to 49 N/mm² at 3%, while normal concrete can reach only 38 N/mm². This suggests that although cylinder strength can be slightly reduced at higher fiber content, the overall cube strength performance using Nylon Fiber concrete is better compared to normal concrete [15].

Experimental studies table 1 indicate that optimal Nylon Fiber content can lead to significant improvements: compressive strength increases up to 11.71%, splitting tensile strength enhancements of approximately 55.8%, and flexural strength gains of about 11.04%. These enhancements are attributed to the fiber' ability to bridge cracks and improve the ductility of the concrete matrix. The findings suggest that Nylon Fiber reinforcement is a viable method for improving concrete performance in construction applications [2].

Table 1. Summarized experimental findings from various studies

Compressive Strength	**Split Tensile Strength**	**Flexure Strength**	**Crack Resistance and Toughness**
Combined Nylon and Jute Fiber incorporating 1% nylon and jute fiber by volume resulted in an 11.71% increase in compressive strength after 90 days compared to the control mix [1].	Optimal fiber content study observed that incorporating 0.25% Nylon Fiber increased splitting tensile strength from 3.53 N/mm² to 5.5 N/mm², marking a significant improvement. However, further increase in fiber content decreases the tensile-strength [2].	Combined fiber reinforcement the use of both nylon and jute fiber at 1% volume fraction improved the flexural strength by 11.04% after 90 days compared to plain concrete [1].	Crack bridging mechanism Nylon Fiber contributes to crack resistance by bridging micro-cracks, thereby enhancing the toughness and ductility of concrete. This mechanism delays crack propagation and improves the post-cracking behavior of concrete structures [4].
Nylon Fiber dosage impact adding Nylon Fiber in varying dosages showed that a 0.25% addition led to a 4.5% increase in compressive strength, while higher dosages beyond 0.5% resulted in a decrease, indicating an optimal dosage for strength enhancement [2].	Effect of fiber length and dosage variations in fiber length and dosage influenced the tensile strength, with longer fiber and optimal dosages enhancing the splitting tensile strength due to better stress distribution and crack bridging [2].	Fiber aspect ratio Influence adjusting the aspect ratio of Nylon Fiber affected the flexural strength, with certain ratios leading to better performance due to improved fiber-matrix interaction [3].	Studies show that before failure, Nylon Fiber exhibit stress whitening and plastic deformation, indicating toughening mechanisms that delay crack initiation. Toughness tends to decrease at low temperatures where the polymer becomes more brittle and less capable of dissipating energy through plastic deformation [6].

5 Sustainability Aspect

Nylon Fiber make concrete more sustainable by reducing the amount of traditional steel reinforcement that can be used in concrete and, therefore also reducing long-term maintenance costs. Cracking control and making concrete more durable also means structural damage does not occur over time since the service life of concrete elements is thereby extended and hence the frequency of repairs or replacements is reduced [2]. This implies low material consumption and energy use throughout a structure's life cycle. In addition, some Nylon Fiber are available from recycled resources which decreases waste and implements a circular economy concept. From a sustainability point of view, it can be stated that Nylon Fiber in concrete not only improve performance but also promotes environmentally responsible construction through resource conservation and reduction in the carbon footprint of concrete infrastructure [9].

6 Conclusion

Nylon Fiber is a valuable addition in civil engineering for enhancing the tensile behavior and crack resistance of concrete. Though it possesses some disadvantages like water absorption and reduced workability at higher dosages, the same can be surmounted by proper mix design and admixtures

- The performance of concrete beams is enhanced with Nylon Fiber due to better crack resistance, lower water permeability, and improved resilience to chemical and environmental degradation.
- Construction sustainability is achieved with the use of recycled Nylon Fiber from obsolete textiles and fishing nets as they reduce the carbon footprint and support circular economic strategies.
- Supplementing nylons into concrete composites designed for structures that expects long service life in high alkali environment requires specific mix designs or surface treatments which ensures nylons stability with high alkaline concretes.
- Nylon Fiber make concrete more sustainable by reducing the amount of traditional steel reinforcement that can be used in concrete and, therefore also reducing long-term maintenance costs.

This review underscores the promising role of Nylon Fiber in enhancing the durability and sustainability of concrete beam structures. With further innovation in fiber treatment technologies and recycling processes, nylon can become a mainstream sustainable additive in modern construction. Future research should focus on standardized testing methods, long-term performance in varied climates, and integration with green construction practices to fully realize the environmental and structural benefits.

Acknowledgment

The authors would like to thank every person/department who helped thorough out the research work, particularly CE department, ORIC and Engr. Prof. Dr. Majid Ali and Engr Blawal Hasan.

References

[1] Bentur, A., & Mindess, S. (2007). Fibre Reinforced Cementitious Composites. Taylor & Francis.
[2] Guo H, Dafaalah AH, Liu Y, Zhang Y, Qiu G. A comparative study on the mechanical properties of polymeric monofilaments. Journal of Engineered Fiber and Fabrics. 2020;15. doi:10.1177/1558925020962
[3] S. Hedjazi and D. Castillo, "Relationships among compressive strength and UPV of concrete reinforced with different types of fiber," Heliyon, vol. 6, no. 3, p. e03646, Mar. 2020, doi: 10.1016/j.heliyon.2020.e03646.
[4] S. Poudel, A. Cibelli, C. Del Prete, R. Wan-Wendner, C. Mazzotti, and N. Buratti, "Insights on Lattice Discrete Particle Model Calibration and Validation Procedure to Simulate Polypropylene and Steel Fibre-Reinforced Concrete," Fiber, vol. 13, no. 2, p. 16, Feb. 2025, doi: 10.3390/fib13020016.
[5] M. S. Moradi, M. H. Tavana, M. R. Habibi, and M. Amiri, "Effect of water to cement ratio on mechanical properties of FRC subjected to elevated temperatures: Experimental and soft computing approaches," Heliyon, vol. 10, no. 21, p. e39513, Nov. 2024, doi: 10.1016/j.heliyon.2024.e39513.
[6] M. A. Safayet, A. A. Abdullah, M. F. Islam, T. S. Alahmari, M. H. R. Sobuz, and M. M. H. Khan, "Combined influence of eggshell powder and Nylon Fiber on self-compacting concrete production: experimental assessment and machine learning quantifications," Mater. Res. Express, vol. 12, no. 2, p. 025003, Feb. 2025, doi: 10.1088/2053-1591/adb0a6.
[7] G. M. Sapidis, M. C. Naoum, and N. A. Papadopoulos, "Electromechanical Impedance-Based Compressive Load-Induced Damage Identification of Fiber-Reinforced Concrete," Infrastructures, vol. 10, no. 3, p. 60, Mar. 2025, doi:

10.3390/infrastructures10030060.

[8] Gey, L., Guenin, R., Le Gal, P., & Verhille, G. (2025). Structural and mechanical characterisation of nylon fibre aggregates. arXiv. https://arxiv.org/abs/2502.15736

[9] Maurya, A. K., & Manik, G. (2023). Development and characterization of a recycled Nylon Fiber reinforced and nano-fly ash hybridized high impact performance polypropylene composite for sustainability. Journal of Thermoplastic Composite Materials. https://doi.org/10.1177/08927057221147825

[10] Parham, S., Kharazi, A. Z., Bakhsheshi-Rad, H. R., Ghayour, H., Ismail, A. F., Nur, H., & Berto, F. (2020). Electrospun nano-fiber for biomedical and tissue engineering applications: A comprehensive review. Materials, 13(9), 2153. https://doi.org/10.3390/ma13092153

[11] Shakiba, M., Rezvani Ghomi, E., Khosravi, F., Jouybar, S., Bigham, A., Zare, M., Abdouss, M., Moaref, R., & Ramakrishna, S. (2021). Nylon—A material introduction and overview for biomedical applications. Polymers for Advanced Technologies, 32(9), 3368–3383. https://doi.org/10.1002/pat.5372

[12] Naaman, A. E. (2003). Engineered steel and synthetic fiber for concrete. University of Michigan.

[13] Suji, D., & Shanmugasundaram, M. (2017). Experimental study on concrete with Nylon Fiber. International Research Journal of Engineering and Technology (IRJET), 4(7), 1541–1545.

[14] Abdelrahman, M., Zhao, D., & Wang, Y. (2021). Mechanical performance of fiber-reinforced concrete with synthetic and recycled fiber. Construction and Building Materials, 273, 121745. https://doi.org/10.1016/j.conbuildmat.2020.121745

[15] Li, V. C. (2003). On engineered cementitious composites (ECC). Journal of Advanced Concrete Technology, 1(3), 215–230. https://doi.org/10.3151/jact.1.215

ENHANCING THE FLEXURAL STRENGTH OF CONCRETE BEAMS USING NYLON FIBERS AS SUSTAINABLE REINFORCEMENT

[a] Qazi Muhammad Tariq*, [b] Blawal Hasan

a: Civil Engineering, Cost Umbrella, Islamabad, Pakistan. qazitariq581@gmail.com
b: Sr. Architect, Contracting and Construction Enterprises, Saudi Arabia. engr.blawal.hasan@gmail.com
*Corresponding author

Abstract- In today's world, one of the problems that persists over time in civil engineering is the formation of concrete cracks because of shrinkage, temperature changes, and load stressors. With traditional polishing methods, few to no efforts are placed in stopping the resistance of micro-cracks. This particular study is meant to assess the degree of effectiveness that adding nylon fiber to concrete as a reinforcing material has in increasing durability, cracking, and tensile strength. The study analyzes the works of others over the last ten years when nylon fiber was added to concrete in varying percentages. This research investigates the flexural behavior of Plain Cement Concrete (PCC) reinforced with locally available nylon fibers (known as BAAN). A mix design incorporating 3% nylon fibers by volume was tested for fresh and hardened properties. Also, several construction projects in the recent past measure compressive strength, tensile strength, and crack resistance. Results showed that the incorporation of nylon fibers improved the flexural strength significantly compared to expected values for plain concrete. Nylon fiber reinforced concrete presents a very promising solution in terms of improving the performance of Sustainable reinforced concrete beams, particularly under seismic applications. Nylon fibers make concrete more sustainable by reducing the amount of traditional steel reinforcement that can be used in concrete and, therefore also reducing long-term maintenance costs.

Keywords- Concrete, Durability, Flexural Cracks, Nylon Fibers, Sustainable

1 Introduction

Over the years, engineers alongside researchers have worked relentlessly to find solutions using other materials to improve the performance of concrete structures around the world. Reinforcing concrete with fibers, such as nylon, considering them as potential additives for the last century [1]. Concrete is a fundamental material in civil engineering. Everyone knows about its great compressive strength and how versatile it is. Originally developed during the 1930s, nylon fibers are classified as synthetic polyamides. They are known for fortifying tendons along with flexibility and high resistance to abrasion and chemicals durability [2]. Nylon, while flexible and resistant to chemicals, may absorb water, which can slightly affect its performance; however, it is generally known for good tensile strength. Concrete is prone to cracking over time due to thermal expansion, shrinkage, and loading conditions. To address these challenges, researchers have explored the incorporation of fibers into concrete, resulting in what is known as fiber-reinforced concrete (FRC) [3]. Among various fibers, nylon, a synthetic polymer, has gained attention due to its high tensile strength, elasticity, and resistance to environmental factors [4]. Nylon fibers can enhance the ductility and crack resistance of concrete, making them a promising additive for improving concrete performance in structural applications. This improved crack resistance makes nylon fiber reinforced concrete a strong candidate for enhancing structural performance [5].

To Concrete is strong under compression but weak in tension. It can also crack over time due to thermal expansion and shrinkage. Steel reinforcement helps with large cracking, but does not alleviate micro marks and early cracking that could affect long term durability [6]. Despite the advantages of traditional concrete, its propensity for cracking remains a significant concern, leading to reduced durability and increased maintenance costs. Previous studies have indicated that incorporating fibers can improve the tensile properties of concrete, however identifying the most effective fiber type and dosage for specific applications continues to be an area of active research [7]. Nylon fibers, in particular, offer potential benefits, but comprehensive studies on their impact on concrete's mechanical properties are limited. This research aims to investigate the effects of varying nylon fiber content on the flexural strength of concrete, thereby addressing the gap in knowledge and providing insights into optimizing concrete mixtures for enhanced performance. Nylon fibers help reduce micro-cracking by bridging cracks as they form and by distributing tensile stresses more evenly throughout the concrete matrix [8].

The fibers are added while mixing so that they become uniformly dispersed throughout the concrete, creating an additional reinforcement skeleton. It has also been demonstrated that nylon reinforced concrete is better at flexural impacting post crack load bearing capability, as well as dynamic impact and loading [9]. Compared to steel, polypropylene, or glass fibers, nylon offers a practical balance of mechanical performance, durability, and ease of use during mixing and placement [10]. Standardized procedures were followed for mixing, casting, and curing the specimens. After letting them cure for 28 days, we ran flexural strength tests using a universal testing machine, sticking to ASTM C78/C78M standards [11]. They recorded how the load-deflection behavior changed to see how the nylon fiber content affected the concrete's flexural performance. Statistical analyses were performed to evaluate the significance of the results and determine the optimal fiber content for maximum flexural strength enhancement [12].

In this study, previously mentioned properties of nylon still remain, especially the tendency to absorb water, despite nylon's tendency to absorb moisture, its beneficial properties have led to increased use in slabs, pavements, shotcrete, and concrete overlays. Concrete is strong in compression, but weak in tension and it cracks. Nylon fibers are known for their strength in tension as well they are flexible therefore control micro cracks and impart ductility. Specimens were prepared and tested after 28 days using ASTM C78 standards. Results showed improved load-bearing and crack resistance, confirming nylon fibers as an effective additive for enhancing concrete performance. Overall, nylon fibers could be a great way to enhance the flexural performance of concrete in various structural applications.

2 Research Methodology

2.1 Raw Material

For this study, monofilament nylon fibers used that were 72.2 mm long and 0.5 mm in diameter. The experimental setup involved preparing concrete mixes that included 3% nylon fibers by volume. Standardized procedures were followed for mixing, casting, and curing the specimens. After letting them cure for 28 days, we ran flexural strength tests using a universal testing machine. In this research work following standards were followed ASTM C78/C78M [16]. We recorded how the load-deflection behavior changed to see how the nylon fiber content affected the concrete's flexural performance. Statistical analyses were performed to evaluate the significance of the results and determine the optimal fiber content for maximum flexural strength enhancement. The concrete mix was produced by layering and mixing dry ingredients as four separate, sequential operations (the first batch was cement, followed by sand, coarse aggregates, and finally the nylon fiber). The dry ingredients were thoroughly mixed, and then water was added slowly. The four stages mixing process was important to have a consistency of mixing the nylon fiber throughout the concrete mix.

2.2 Mix Design

The manufacturing and fresh properties of Plain Concrete (PC) and Fiber Reinforced Concrete (FRC). Manufactured for testing in CUST CE Lab for 4 cylinders and 3 beamlets. To produce plain concrete (PC), Ordinary Portland Cement (Type-

1) was used in both the PC and Nylon Fiber Reinforced Concrete (NFRC) mixtures. The concrete had a density of 1440 kg/m^3 and a specific gravity of 3.15. Each mix contained 6.5 kg of cement. Coarse aggregate with a maximum size of 20 mm, uniformly graded, was used in both mixes. The weight of the coarse aggregate was 26 kg for PC and 13 kg for NFRC. Fine aggregate (sand) with a particle size smaller than 2 mm was also used in both mixes. For PC, 13 kg of sand was used,

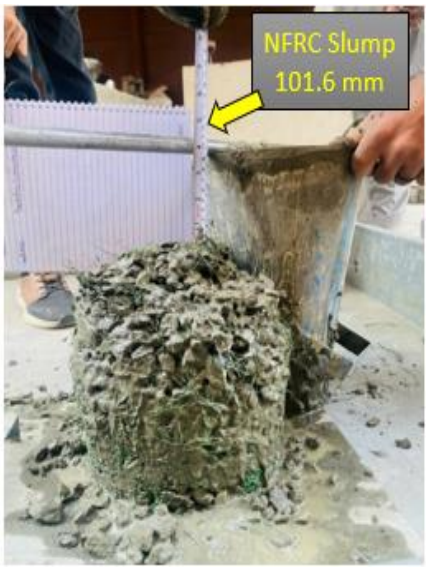
while NFRC contained 26 kg Nylon fiber was added at a dosage rate of 3 volumetric % in the mix and for preparation of PC, mix design ratio of 1:2:4 (cement: sand: aggregate) is used and water to cement ratio (W/C) of 0.5. The four stages mixing process produced an even infiltration of fiber, a key factor in enhancing the performance of the concrete mix mechanical properties that were expected, particularly flexural strength, and fracture resistance.

Table 1: Mix design of Plain Cement Concrete (PCC) (1:2:4) because of most commonly used mix design ratio.

Mix Design	**Quantity**
(PCC) & (NFRC) ratio	= (1:2:4)
Total wet volume of PCC	= 0.731cft
Total dry volume of PCC	= 1.1254 cft
Dry volume of cement	= 6.5kg
Fine aggregate natural sand	= 13kg
Coarse aggregate crushed stone (20 mm max size)	= 26kg
Water-cement ratio	= 0.5
Nylon Fibers	= 3%
Fiber Type	= Nylon Fiber (Locally known as BAAN)
Fiber Density	= 1140 (kg/m3)
Fiber Length	= 72.2mm
Fiber Diameter	= 0.5 mm
Fiber Aspect Ratio	= 72.2/0.5= 144.4



(a)



(b)

Figure 1: (a) show the PCC Slump and (b) show the Nylon Fiber Reinforced Concrete (NFRC).

In figure 1 the PCC Slump is 125mm and the Nylon Fiber Reinforced Concrete (NFRC)mix showed a slump of 101.6 mm, but the result may not be fully accurate due to improper handling of the slump cone, causing concrete leakage. Despite this, the mix displayed moderate workability, which is expected with a 3% fiber volume as shown in table 1 that tends to reduce flow. The proper mixing in multiple turns ensured even fiber distribution.

2.3 Testing and Parameters

To assess the flexural strength of the concrete, plain cement concrete beamlets were fabricated and tested at the Civil Engineering Laboratory at CUST. The dimensions of the beamlets were 4 inches × 4 inches × 18 inches resulting in a total volume of about 0.166 cubic feet per beamlet. A total of three beamlets were prepared which resulted in a combined volume of 0.499 cubic feet. The testing of the flexural strength was carried out according to ASTM C78 / C78M, the

standard test method for the flexural strength of concrete using a third-point loading scheme. The specimens were prismatic beams and the testing was completed using a Universal Testing Machine (UTM) fitted with a flexure frame. The support span that was typically used was 400 mm as the exact span was based on the lab equipment available. The loading was applied at two points equal distance from the supports following the third-point method. The load was applied at a rate of approximately 0.05 MPa per second or as directed by ASTM. The testing was set up to allow for the flexural representation of the concrete specimens to be obtained in a controlled standardized situation.



(a)



(b)

Figure 2: As the load increased, flexural cracks developed at the tension face of the beam, progressing vertically toward the neutral axis.

The reinforcing material was nylon fibers dosage of 3% volume, with an aspect ratio of 144.4. The load was applied gradually until failure, allowing for proper visualization of both crack initiation and propagation as shown in figure 2. The most common mode of failure seen in the specimens were cracking followed by failure in the tension zone of the beamlets, which was expected flexural loading behavior. In terms of flexural strength, the measured values of the tested beams ranged from 1.442 MPa to 3.071 MPa, with a reported average of 2.426 MPa. The slump of the mix was slightly low due to a testing error, with some leakage from the slump cone. However, the results of the testing are indicative of the mechanical performance of nylon fiber reinforced concrete under flexural loading.

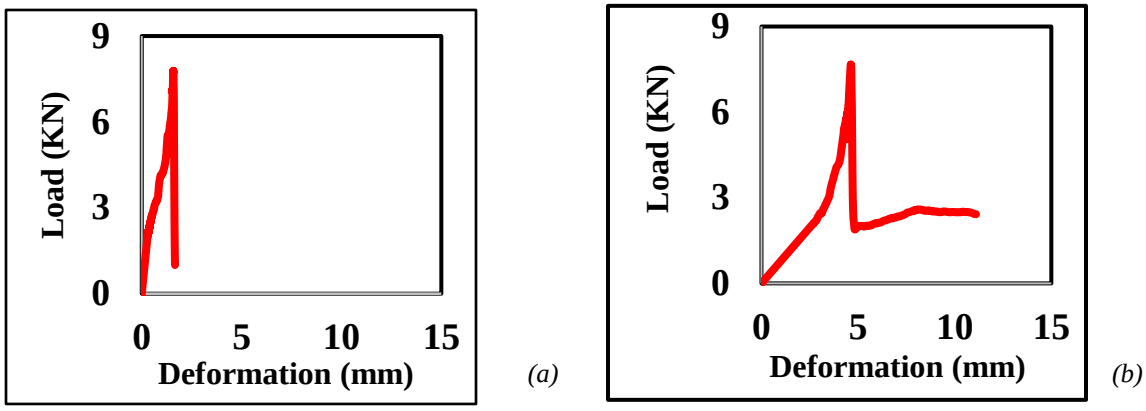
3 Results

Addition of nylon fiber clearly enhanced the flexural behavior compared to plain concrete. Strength results being not consistent, controlled mixing and uniform fiber distribution together with quality assurance during production are required. This may take place in applications of nylon fiber reinforced concrete where crack control, toughness, and durability are critical (e.g., industrial floors, overlays, precast panels). Flexural testing is performed to explore the mechanical properties of PC and NRFC following the ASTM standard C293 /C293M-16, servo-hydraulic testing machine. To perform 3-point loading test, beamlet specimens are placed horizontally between the test machine so that it acts as a prototype of flexural member or a beam. The flexure strength tests are performed to study the modulus of rupture (MOR), flexural behaviour, flexural pre-crack/post-crack energies.

Table 2: The flexural strength test was carried out in accordance with ASTM C78 (or equivalent local standards), using third-point loading.

Specimens	Peak Load (KN)	MOR (MPa)	E1 (N. m)	E2 (N. m)	FTI (Mpa)	Failure mode
PC	6.52 ±0.65	4.26 ±0.43	3.26 ±0.33	0.2 ±0.02	1.06	Flexural
NFRC	8.32 ±0.83	5.43 ±0.54	5.41 ±0.54	34.8 ±3.48	7.43	

MOR=Modulus of Rupture; E1 = Flexural Pre-Cracking energy absorption; E2 = Flexural Post-Cracking energy absorption; FT1 =Flexural toughness index



Graph 1: Graph (a) shows the deformation of PCC and (b) shows the deformation of NFRC.

In terms of pre-crack energy absorption (E1), plain concrete (PC) showed higher initial stiffness compared to nylon fiber reinforced concrete (NFRC), likely because nylon fibers are more flexible. However, NFRC demonstrated better plastic deformation and handled loads more effectively, with a 27.46% higher Modulus of Rupture (MOR) than PC, as shown in Table 2. This improved performance is due to the ductile nature of nylon fibers, which can absorb more energy during deformation. For post-crack energy absorption (E2), PC had a higher value, indicating it resisted deformation better after cracking. Even in later stages of bending, PC maintained more resistance. Experimental results show that NFRC significantly outperforms PCC in flexural behavior.

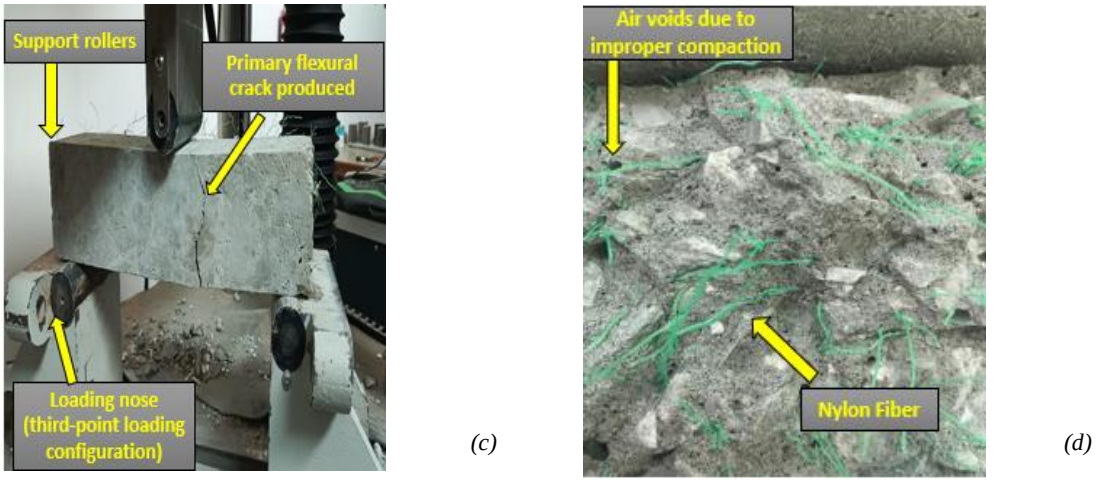


Figure 3: (c) and (d) captures the final stage of the test, where a visible crack has formed and propagated, indicating the ultimate flexural strength of the sample.

NFRC's Modulus of Rupture is 5.43 MPa, about 27% higher than PCC's 4.26 MPa, indicating greater resistance to bending. Its pre-crack energy absorption is 5.41 N·m, a 66% increase over PCC's 3.26 N·m, showing better performance under load before cracking. Post-crack energy absorption is dramatically higher at 34.8 N·m compared to PCC's 0.20 N·m, highlighting NFRC's superior ductility. The Flexural Toughness Index also supports this, with NFRC at 7.43 versus PCC at 1.06, confirming its enhanced toughness and suitability for demanding structural applications. However, nylon fibers may provide post-crack ductility that isn't fully reflected in E2. Regarding flexural toughness, PC showed a higher cracking load capacity. The first crack strength was lower in NFRC, but the nylon fibers likely helped slow crack growth, improving energy absorption and ductility even if they didn't raise the initial cracking strength. The results are summarized in Table 2. For PC sample shown in figure 3, post cracking behavior (upwards) shows ductile behavior as compare for NRFC sample presented in figure 3. Crack patterns provide valuable insight into the ductility and fiber-bridging effect in NFRC specimens. This enhanced performance is attributed to the effective bridging mechanism of nylon fibers (NF), which significantly improves load distribution and delays crack propagation. The strong interfacial bond between nylon fibers

and the concrete matrix enables superior stress transfer, allowing the composite to sustain higher flexural loads before failure (Figure 3).

3.1 Flexural Behavior

Flexural strength results of Nylon Fiber reinforced concrete appear to be much better than that of regular concrete. Basically, this is because the Nylon Fiber help hold the concrete together when it begins to crack. As the concrete bends under load, these fiber span across small cracks, stopping them from growing quickly. This not only helps reduce the size and number of cracks but also makes the concrete more flexible and less likely to fail suddenly. Instead of breaking all at once like plain concrete, NFRC tends to fail more gradually, giving some warning before it actually gives out. During flexural tests, NFRC was better at spreading out the load and absorbing energy thanks to the fiber ability to stretch and adjust to the stress. Even after the concrete starts to crack, the fiber keeps it from completely falling apart, allowing it to carry some load. This gain is mostly because the fiber helps the concrete handle tension better, especially in the lower part of the beam where it usually cracks first. Another big advantage is the way NFRC fails. While normal concrete tends to crack in one place and break quickly, NFRC shows more fine cracks before it fails. This change makes the concrete behave in a more ductile or flexible way, which is especially useful in structures that face vibration, impact, or sudden loads. However, one thing to watch out for is workability. Adding nylon fiber can make the mix a little harder to handle, especially at higher percentages. In some tests, a lower slump was noticed, partly due to a leak in the slump cone. So, it's important to mix the concrete properly and make sure the fiber is evenly spread out to get the full benefits.

3.2 Flexural Properties

Nylon Fiber reinforced concrete (NFRC) proves to be much superior than plain cement concrete (PCC) in terms of its flexural properties such as strength, toughness, and crack resistance. While PCC has a limited ability to resist bending and usually breaks suddenly, NFRC can handle more stress and typically shows a 10-25% increase in flexural strength. This is because the Nylon Fiber help hold the concrete together by bridging small cracks that form under bending. PCC usually fails all at once with one large crack, but NFRC cracks more gradually, giving it a more controlled and safer failure pattern. After cracking, NFRC continues to carry load thanks to the fiber, which prevent the concrete from falling apart right away. It also absorbs more energy during loading, which means it's tougher and better suited for conditions where stress changes or impacts are involved. NFRC also does a better job at controlling cracks while cracks in PCC tend to grow quickly and become wide, the fiber in NFRC slow them down and keep them smaller. This helps protect the concrete over time. In terms of flexibility, PCC doesn't stretch or bend much before breaking, but NFRC allows a bit more movement, which can be important for safety. When you look at the stress-strain behavior, PCC shows a quick peak and then drops sharply after cracking, meaning it loses strength fast. NFRC, on the other hand, shows a gentler drop after the peak because the fiber keeps working even after cracks form, allowing the concrete to hold some load and last longer.

4 Practical Application of NFRC in Concrete Beams

Nylon fiber reinforced concrete presents a very promising solution in terms of improving the performance of reinforced concrete beams, particularly under seismic applications. It is well evident that the inclusion of nylon fibers improves crack resistance, ductility, and post-cracking behavior- all important parameters for structural elements expected to resist dynamic and impact loads. In its application on beams, nylon fibers act as secondary reinforcement control shrinkage and microcracking plus energy absorption during seismic events. This greatly improves strength-to-cost ratio and structural integrity; hence NFRC could be recommended as an appropriate material for beams in seismic regions It's also useful in shotcrete applications, like tunnel linings and slope stabilization, where the fiber improve material cohesion and reduce the amount of rebound during spraying. In bridge decks and highway overlays, nylon fiber help prevent cracks caused by temperature changes and repeated vehicle loads, which extends the lifespan of the structure. In residential and commercial slabs, nylon fiber provides excellent crack control, often removing the need for traditional steel mesh. This not only cuts down on material costs but also speeds up construction and reduces labour. NFRC is also being used in precast concrete elements, footpaths, driveways, and parking structures, where early-age cracking and shrinkage are common issues. Because nylon fiber help keep these cracks in check, the final product is more durable and requires less maintenance. Additionally, NFRC is a good option for repair works, such as patching damaged concrete, since the fiber help improve bonding and reduce future cracking. It's also being explored for use in marine structures and water-retaining structures,

where durability and crack resistance are critical due to exposure to moisture and chemical attack. Using nylon fibers in large construction projects comes with challenges such as limited supply, higher costs, and difficulty in achieving even distribution in concrete mixes. Standard batching plants may need upgrades, and contractor familiarity is often low. The lack of specific construction codes and environmental concerns due to nylon's synthetic nature also limit widespread use.

5 Conclusion

The addition of nylon fibers to concrete introduces a very promising new composite within construction materials with additional improved mechanical properties, improved crack resistance behavior, and sustainabilityNylon Fibers help improve concrete's strength and crack resistance, especially in terms of flexural performance.

- Adding 3% nylon fibers with a high aspect ratio (144.4) significantly increased the concrete's ability to resist bending and delayed crack formation, with an average flexural strength of about 3.759 MPa higher than that of standard concrete.

- While higher fiber content can reduce workability and cause issues in slump testing, these challenges can be managed through proper mix design and the use of admixtures. Despite a slight drop in workability, the fresh concrete mix still maintained a density close to 2400 kg/m³, making it suitable for structural use.

- Nylon fibers make concrete more sustainable by reducing the amount of traditional steel reinforcement that can be used in concrete and, therefore also reducing long-term maintenance costs.

Overall, nylon fiber reinforced concrete performed better than plain concrete in terms of strength, durability, and crack control. The improvements noticed in flexural strength and durability further cement NFRC's potential for both structural and non-structural applications where high performance and longevity are required. It shows great potential for use in both structural and non-structural applications.

6 Recommendation for Future Research

More research is needed on standardizing its use and exploring recycled nylon fibers to improve sustainability in construction. Challenges that come with reduced workability should be tackled by careful mix design aided by admixtures. Further exploration in terms of standardization and use of recycled nylon fibers will be essential to unlock the environmental benefits as well as the structural contributions of nylon fiber reinforced concrete as the construction industry begins moving toward more sustainable practices.

Acknowledgment

The author would like to thank every person/department who helped thorough out the research work, particularly CE department, ORIC, Engr. Prof. Dr. Majid Ali and Engr Blawal Hasan.

References

[1] Bentur, A., & Mindess, S. (2007). Fibre Reinforced Cementitious Composites. Taylor & Francis.
[2] Guo H, Dafaalah AH, Liu Y, Zhang Y, Qiu G. A comparative study on the mechanical properties of polymeric monofilaments. Journal of Engineered Fibers and Fabrics. 2020;15. doi:10.1177/1558925020962
[3] S. Hedjazi and D. Castillo, "Relationships among compressive strength and UPV of concrete reinforced with different types of fibers," Heliyon, vol. 6, no. 3, p. e03646, Mar. 2020, doi: 10.1016/j.heliyon.2020.e03646.
[4] S. Poudel, A. Cibelli, C. Del Prete, R. Wan-Wendner, C. Mazzotti, and N. Buratti, "Insights on Lattice Discrete Particle Model Calibration and Validation Procedure to Simulate Polypropylene and Steel Fibre-Reinforced Concrete," Fibers, vol. 13, no. 2, p. 16, Feb. 2025, doi: 10.3390/fib13020016.
[5] M. S. Moradi, M. H. Tavana, M. R. Habibi, and M. Amiri, "Effect of water to cement ratio on mechanical properties of FRC subjected to elevated temperatures: Experimental and soft computing approaches," Heliyon, vol. 10, no. 21, p. e39513, Nov. 2024, doi: 10.1016/j.heliyon.2024.e39513.
[6] M. A. Safayet, A. A. Abdullah, M. F. Islam, T. S. Alahmari, M. H. R. Sobuz, and M. M. H. Khan, "Combined influence of eggshell powder and nylon fiber on self-compacting concrete production: experimental assessment and machine learning quantifications," Mater. Res. Express, vol. 12, no. 2, p. 025003, Feb. 2025, doi: 10.1088/2053-1591/adb0a6.

[7] G. M. Sapidis, M. C. Naoum, and N. A. Papadopoulos, "Electromechanical Impedance-Based Compressive Load-Induced Damage Identification of Fiber-Reinforced Concrete," Infrastructures, vol. 10, no. 3, p. 60, Mar. 2025, doi: 10.3390/infrastructures10030060.

[8] Gey, L., Guenin, R., Le Gal, P., & Verhille, G. (2025). Structural and mechanical characterisation of nylon fibre aggregates. arXiv. https://arxiv.org/abs/2502.15736

[9] Maurya, A. K., & Manik, G. (2023). Development and characterization of a recycled nylon fiber reinforced and nano-fly ash hybridized high impact performance polypropylene composite for sustainability. Journal of Thermoplastic Composite Materials. https://doi.org/10.1177/08927057221147825

[10] Parham, S., Kharazi, A. Z., Bakhsheshi-Rad, H. R., Ghayour, H., Ismail, A. F., Nur, H., & Berto, F. (2020). Electrospun nano-fibers for biomedical and tissue engineering applications: A comprehensive review. Materials, 13(9), 2153. https://doi.org/10.3390/ma13092153

[11] Shakiba, M., Rezvani Ghomi, E., Khosravi, F., Jouybar, S., Bigham, A., Zare, M., Abdouss, M., Moaref, R., & Ramakrishna, S. (2021). Nylon—A material introduction and overview for biomedical applications. Polymers for Advanced Technologies, 32(9), 3368–3383. https://doi.org/10.1002/pat.5372

[12] Naaman, A. E. (2003). Engineered steel and synthetic fibers for concrete. University of Michigan.

[13] Suji, D., & Shanmugasundaram, M. (2017). Experimental study on concrete with nylon fiber. International Research Journal of Engineering and Technology (IRJET), 4(7), 1541–1545.

[14] Abdelrahman, M., Zhao, D., & Wang, Y. (2021). Mechanical performance of fiber-reinforced concrete with synthetic and recycled fibers. Construction and Building Materials, 273, 121745. https://doi.org/10.1016/j.conbuildmat.2020.121745

[15] Li, V. C. (2003). On engineered cementitious composites (ECC). Journal of Advanced Concrete Technology, 1(3), 215–230. https://doi.org/10.3151/jact.1.215

[16] Malah, Memon, Jokhio, & Oad, (2024). Flexural strength of recycled aggregate concrete reinforced with nylon fibers. Mehran University Research Journal of Engineering and Technology 43(3):56 DOI:10.22581/muet1982.2855

PERFORMANCE EVALUATION AND APPLICATION POTENTIAL OF NYLON FIBERS IN CONCRETE SLAB - A REVIEW

[a] Usama Akhter*, [b] Hamdan Ullah

a: Civil Engineering Department, Hazara University, Mansehra, Pakistan. usamaakhtarswati@gmail.com
b: Safety Engineer (Civil), Bin Omaira Contracting (KSA). eng.hamdan007@gmail.com
*Corresponding author

Abstract- Incorporating fibers into reinforced cement concrete increases its impact resistance and earthquake load bearing capacity by improving the stiffness or energy absorption capability of the concrete material. A significant feature of fibers, like "bridge effect" during early crack propagation of concrete, comes into effect. Because of this, fibers restrain the crack formation and propagation, which improves the strength and ductility of concrete civil structure. The focus of this study is between the mechanical properties of reinforced cement concrete with nylon fiber and without it. In this case, data from previous article will be used to compare the strengths of nylon fiber reinforced concrete to conventional concrete using compressive strength test, flexural strength test, and split tensile strength test. Mixing fiber with cement increases the reduction of water content which diminishes the workability of the concrete, creating fiber balls. Due to the heterogeneity associated with fibrous materials, the efficacy of fiber reinforced concrete is reduced. The static mixer works best for strand-based fibers, which helps inline glass fibers to enhance concrete strength. During the integration of small amounts of fibers into dry concrete, the problem of fiber distribution can be solved by proper placement and dispersion of the mixtures, which increases concrete strength and prevents fiber conglomeration. Factors like the aspect ratio, fiber volume, and fiber orientation are important for the transmission of stress between concrete mix and the fiber. Impact resistance and flexural toughness of reinforced concrete is greatly improved by nylon fiber, and as a result, the impact-bearing capacity of concrete is enhanced. The addition of nylon fibers enhances the tensile strength of concrete, especially during the post-peak phase, by bridging cracks and improving energy absorption.

Keywords- Nylon Fiber, Concrete Reinforcement, Cracking Resistance, Ductility, Fiber-Reinforced Concrete

1 Introduction

Concrete remains the most widely used construction material worldwide due to its availability, compressive strength, and cost-effectiveness. It is an integral component of modern infrastructure, from residential buildings to large-scale civil projects such as highways, bridges, and dams. Despite these advantages, concrete has several inherent weaknesses, notably its brittle nature and poor tensile performance, which limit its application in certain structural designs. To overcome these structural limitations, various reinforcing techniques have been developed, with one of the most notable being fiber reinforcement. Fiber-reinforced concrete (FRC) introduces discrete fibers into the concrete matrix to enhance its mechanical properties, offering a solution to the challenges posed by traditional concrete. Among the different types of fibers, synthetic fibers such as nylon have been gaining significant attention for their ability to improve the performance of concrete. One of the primary issues with conventional concrete is its tendency to shrink and crack under various conditions. Shrinkage cracking is a common problem, often exacerbated by environmental factors like temperature changes

and moisture loss. This cracking leads to decreased durability, increased maintenance costs, and a reduction in the overall structural integrity of concrete structures [1].

Furthermore, the dynamic loading that concrete structures undergo, such as those subjected to earthquakes or heavy traffic, can lead to a brittle failure and degradation over time. Traditional reinforcement methods, such as the use of steel bars, do not address the issue of micro-cracks or significantly improve the ductility of concrete, especially in thin sections or intricate shapes [2]. This limitation has prompted the search for alternative reinforcement materials that can improve the performance of concrete under dynamic loading conditions. Nylon fibers offer a potential solution to these challenges by bridging cracks, controlling shrinkage, and distributing stress more effectively across the concrete matrix. As synthetic fibers, nylon offers several advantages in comparison to traditional reinforcement methods. Experimental studies have shown that the addition of nylon fibers to concrete can enhance flexural strength, energy absorption capacity, and impact resistance [3]. These fibers contribute to an increase in the concrete's post-crack behavior, allowing it to maintain structural integrity even after cracking. Additionally, nylon fibers can help reduce the formation of cracks, improve the concrete's ability to resist tensile stresses, and enhance its overall durability [4], [5].

However, the effectiveness of nylon fibers in concrete depends on several factors, including fiber geometry, content, and distribution methods, which vary from study to study. The optimal dosage and proper mixing techniques are essential to ensure that the fibers are uniformly distributed within the concrete matrix to maximize their reinforcing potential [6]. Another significant advantage of nylon fiber is their cost-effectiveness and environmental sustainability. As a synthetic fiber, nylon is more affordable compared to other fibers such as steel, making it an economically viable option for large-scale concrete applications. Furthermore, nylon fibers are produced using relatively low-energy processes, contributing to a reduced carbon footprint when compared to other more energy-intensive reinforcement options. The use of nylon fibers not only enhances the mechanical properties of concrete but also promotes environmentally sustainable practices in the construction industry [7]. Moreover, as nylon is a versatile material, its application extends beyond just concrete reinforcement; it is widely used in various industries, including textiles, industrial materials, and packaging, further supporting its sustainability.

Nylon fibers samples have been used in several studies to evaluate their impact on concrete properties. The response of interlocking plastic-block structure. The line shows response at the top of structure while full line shows applied loading. These histories are largely acceptable to study the dynamic response of column structure flaws and Challenges in Concrete. Despite these advantages, challenges remain in the adoption of nylon fibers in concrete. One of the primary concerns is ensuring a uniform distribution of fibers within the concrete mix. Fiber aggregation, or the tendency of fibers to clump together, can reduce the overall effectiveness of the reinforcement. Additionally, the mixing process must be carefully controlled to avoid reducing the workability of the concrete, as the addition of fibers can affect the flow ability and ease of placement of the mix. In conclusion, the use of nylon fibres in concrete presents an effective solution to the limitations of conventional concrete by improving its mechanical properties, crack resistance, and impact absorption capacity. The ongoing research in this area continues to explore optimal fib dosages, mixing methods, and the long-term durability of nylon fibre-reinforced concrete. This review aims to consolidate the current knowledge on nylon fibre-reinforced concrete, highlighting the potential for optimization and wider adoption of this material to enhance the sustainability and longevity of concrete structures.

2 Flaws and Challenges

The performance of nylon fibers in concrete is influenced by several critical parameters, each of which plays a role in determining the overall effectiveness of the fiber-reinforced concrete (NFRC). These parameters include fiber geometry, fiber content, mixing methods, and curing conditions. By carefully controlling these factors, the desired mechanical properties such as strength, durability, and crack resistance can be achieved. However, the performance of nylon fibers in concrete can vary significantly depending on how each of these factors is optimized. While nylon fiber-reinforced concrete offers several benefits for slabs, there are some disadvantages that need consideration [7]. One major concern is the absorptive action of nylon fibers, which can soak up water. This can adversely affect bond strength and durability over time, particularly in humid conditions. Another challenge is ensuring uniform dispersion of nylon fibers in the concrete mix. Poor mixing or high dosages can lead to fiber "balling" or clumping, reducing effectiveness and potentially compromising the slab's structural integrity. Additionally, adding nylon fibers can require adjustments to the mix design, such as changes to water volume or the use of plasticizers, to maintain workability. The optimal dosage and proper mixing techniques are essential to ensure that the fibers are uniformly distributed within the concrete matrix to maximize their reinforcing potential [6]. Another significant advantage of nylon fiber is their cost-effectiveness and environmental sustainability. As a synthetic fiber, nylon is more affordable compared to other fibers such as steel, making it an

economically viable option for large-scale concrete applications. Furthermore, nylon fibers are produced using relatively low-energy processes, contributing to a reduced carbon footprint when compared to other more energy-intensive reinforcement options.

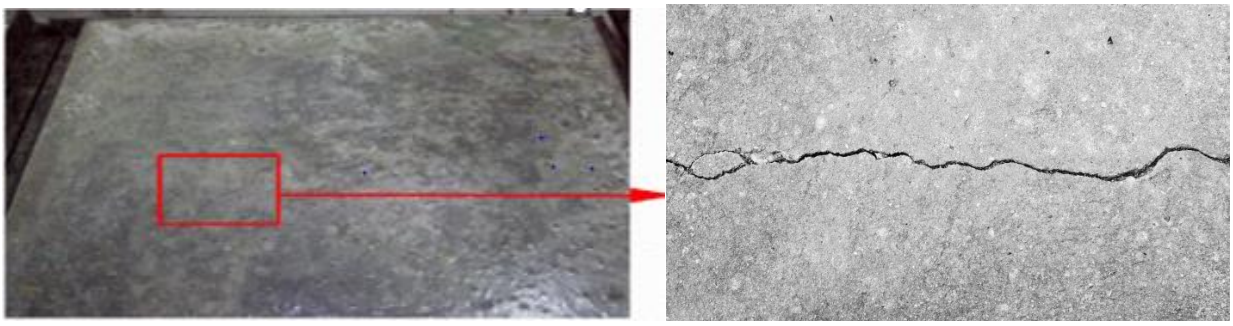


***Figure 1*: Shows the cracks in slabs [20].**

Figure 1 shows that crack in slab and it propagates after some time. The use of nylon fibers in slabs also raises concerns about cost, standardization, and sustainability. While nylon fibers may be more economical than steel or carbon fibers, they can still increase the cost per cubic meter of concrete. Furthermore, design specifications for nylon fiber-reinforced concrete are lacking in most building codes, which can create uncertainty and barriers to widespread adoption. Finally, the environmental footprint of nylon fibers, being based plastics, raises concerns about embodied energy, recyclability, and end-of-life disposal. Nylon fibers, measuring 3 inches in length, have been gaining attention in the construction industry due to their potential to enhance the mechanical properties of concrete. According to research [1], the addition of natural fibers can improve the lateral resistance of mortar-free interlocking walls. Similarly, nylon fibers can improve the tensile strength, flexural strength, and durability of concrete. Another study proposes an optimization method for RC stiffeners using a diagonal approach, validated numerically, and demonstrates that confined brick masonry structures with optimized stiffeners perform better under seismic loading than unconfined structures [22]. This is because nylon fibers act as a reinforcement, absorbing stresses and strains that would otherwise lead to cracking and failure. The use of nylon fibers in concrete has also been found to reduce the risk of plastic shrinkage cracking, which can occur during the curing process. This is particularly important in applications where concrete is exposed to harsh environmental conditions, such as high temperatures and low humidity.

3 Governing Properties

The inclusion of nylon fibers in concrete slabs plays a vital role in enhancing their structural and serviceability performance, particularly in environments where cracking, shrinkage, and tensile weaknesses are critical concerns. As noted by [6], nylon fibers significantly improve shrinkage resistance, which is crucial for slab applications exposed to varying temperatures and drying conditions. Nylon fibers, due to their synthetic nature, offer durability and chemical resistance superior to natural alternatives like sisal or jute [2], making them particularly suitable for long-term structural applications such as floor slabs. This material's hydrophobic characteristics also limit moisture absorption, minimizing degradation in humid or alkali environments. Mechanically nylon fiber-reinforced concrete demonstrates enhanced tensile strength and post-cracking behavior. [12] and. [8] illustrates that nylon fibers increase tensile capacity and control crack propagation by bridging micro-cracks that develop under stress. This bridging mechanism not only delays the onset of macro-cracking but also ensures better energy absorption under load, contributing to improved ductility in slab structures [11] further highlight that the flexibility and elongation capacity of nylon help in distributing stress over larger areas, enhancing both toughness and resistance to dynamic loads, which is particularly relevant in slabs subject to human traffic or mechanical vibrations.

From a durability standpoint, synthetic fibers like nylon exhibit excellent long-term performance in concrete, resisting degradation from alkaline environments common in cement-based systems [17]. While natural fibers may degrade over time due to microbial or chemical attack [7], nylon remains stable and effective throughout the slab's lifecycle. Studies such as those [9] [18] emphasize that nylon-reinforced concretes perform better under environmental stresses, maintaining flexural and tensile properties even after exposure to moisture and temperature variations. The research demonstrates the potential of using wheat straw fibers to enhance the mechanical properties of concrete for sustainable pavement

applications [25]. This is particularly beneficial in slab construction where exposure to environmental conditions is inevitable and long-term performance is crucial. In summary, nylon fiber-reinforced concrete offers a well-balanced combination of mechanical strength, shrinkage control, and durability, making it a reliable material for slab applications. The governing properties such as tensile behavior [12], flexural strength [10], and crack resistance [6] are directly influenced by the presence and distribution of nylon fibers in the concrete matrix. As reviewed by Jahangir et al. [17] and [19], the integration of nylon fibers supports both early-age performance and long-term resilience of concrete slabs. These characteristics ensure that slabs reinforced with nylon fiber not only meet structural requirements but also reduce maintenance needs and extend service life, making them a sustainable and efficient solution in modern construction.

4 Shortlisting of Fibers

The design of fiber-reinforced concrete (FRC) slabs, several types of fibers were initially evaluated based on factors such as mechanical performance, chemical stability, cost-efficiency, and availability. Among these, steel, polypropylene, glass, basalt, carbon, and nylon fibers were shortlisted [2]. Each fiber type exhibits specific advantages: steel fibers offer high strength and stiffness; polypropylene fibers demonstrate strong resistance to plastic shrinkage cracking; glass fibers provide aesthetic benefits and good tensile strength; basalt fibers are known for their thermal resistance and durability; and carbon fibers deliver the highest strength, albeit at increased cost [7]. Another study was carried out that fibrous plaster reinforced with sisal fibers significantly improved the mechanical and dynamic properties of masonry walls, outperforming rice straw-reinforced plaster in terms of peak load, energy absorption, and toughness [21].



a) b)

Figure 2: *a and b represent some nylon fibers [19].*

After a detailed comparison, nylon fibers shown in Fig. 2 were selected as the reinforcing material for slab applications due to their optimal balance between mechanical properties, environmental resilience, and economic feasibility [12]. Experimental results indicated that nylon fiber-reinforced concrete slabs showed improved structural performance. At 0.5% fiber content, the 28-day cylinder strength reached 40 N/mm², compared to 36 N/mm² for conventional concrete slabs. Although an increase in fiber content to 3% slightly reduced cylinder strength to 37.5 N/mm², a significant gain was observed in cube strength from 40.89 N/mm² at 0.5% fiber content to 49 N/mm² at 3%. whereas standard concrete achieved only 38 N/mm² [12]. These results suggest that nylon fiber incorporation enhances the load-bearing performance of slabs, especially in terms of cube strength, despite minor reductions in cylinder strength at higher dosages.

Table 1*: Summarized fibers types and limitation [18].*

Fiber Type	Limitation	Advantages
Nylon	Good flexibility, cracks control,	Cost variability, water absorption
steel	High tensile and flexural strength	corrosion, Heavy weight
Polypropylene	Inexpensive, Shrinkage control	Limited bond strength
Glass	Chemical Resistance, High stiffness	Brittle durability

The table 1 shows that out of all these fibers nylon stands out for its balance of cost, tensile performance, and workability when used in appropriate proportions and conditions [6], [8]. Nylon has unlike fibers some advantages. Unlike steel fiber,

nylon is lighter and is more flexible, making it convenient for applications where weight are crucial factors. Better than polypropylene, nylon has more strength and chemical resistance. Strong glass fiber can become brittle and more prone to being broken but has more resilience than nylon and brittle. Due to its versatility, nylon fiber makes it useful in a wide variety of applications, such as clothing, carpets, industrial textiles, and ropes. For products that require performance and endurance, readily available wear and tear resistance makes nylon an ideal candidate. [23] studied that coconut fibre reinforced concrete was used to make interlocking blocks, which are capable of returning to their original positions after seismic ground motion due to the inclined key between the blocks. All in all, an exceptional combination of properties when its comestibles to other fibers nylon fiber's unique features set it apart. Nylon fiber plays an important role in the advancement of civil engineering field and we are using it in slabs concrete as a fiber to control cracking and to control cracks propagation. In the field of civil engineering, specifically, nylon fiber plays an important role in advancing construction technology. It is increasingly being used in concrete slabs as an additive to control cracking and prevent the propagation of cracks. By reinforcing the concrete and improving its durability, nylon fibers help to enhance the overall performance of concrete structures.

5 Sustainability Aspects

The incorporation of nylon fibers into concrete slabs presents several sustainability benefits, particularly in terms of reducing shrinkage and cracking, which contributes to longer-lasting structures and reduced need for maintenance. Nylon fibers, both virgin and recycled, enhance the mechanical integrity of concrete by improving tensile strength and flexural performance, which are essential for slab durability under load-bearing applications [10] [12]. By minimizing early-age cracking and shrinkage-related deterioration, as shown in studies by [6], nylon fibers extend the service life of concrete, reducing the frequency of repairs and material replacement key contributors to the environmental footprint of construction. Moreover, the use of recycled nylon fibers, such as those sourced from post-consumer materials (e.g., waste textiles or fishing nets), directly supports circular economy goals. Recycled fibers have been successfully used to reinforce cement matrices, showing comparable performance to synthetic alternatives while diverting waste from landfills [18] [17]. Incorporating recycled nylon into slabs contributes to material reuse, conserves raw resources, and lowers energy demand associated with fiber production. This aligns with broader efforts in sustainable construction to adopt low-carbon materials and reduce the embodied energy of infrastructure systems [7].

Finally, nylon fiber reinforced concrete (NFRC) has shown promise in enhancing the durability of slabs in harsh environmental conditions, which is crucial for sustainable structural design. Nylon fibers improve resistance to environmental degradation such as freeze-thaw cycles, moisture penetration, and thermal stresses [8][9]. Their performance in these conditions contributes to resilience and longevity core principles of sustainable engineering. By ensuring longer slab life and reducing resource-intensive repairs or rebuilds, NFRC contributes meaningfully to the life-cycle sustainability of concrete infrastructure [19] [24] investigated that the potential of banana fiber as a sustainable material to improve the mechanical properties of concrete in structural applications. Nylon remains stable and effective throughout the slab's lifecycle. Studies such as those [9] [18] emphasize that nylon-reinforced concretes perform better under environmental stresses, maintaining flexural and tensile properties even after exposure to moisture and temperature variations. This is particularly beneficial in slab construction where exposure to environmental conditions is inevitable and long-term performance is crucial. In summary, nylon fiber-reinforced concrete offers a well-balanced combination of mechanical strength, shrinkage control.

6 Conclusion

Nylon fiber-reinforced concrete (NFRC) offers significant improvements in the mechanical properties and durability of conventional concrete, particularly in terms of cracking resistance, impact absorption, and post-crack performance. Despite challenges related to fiber distribution, workability, and long-term environmental performance, nylon fibers present a cost-effective and sustainable reinforcement solution for concrete structures. Future research should focus on optimizing fiber content, mixing techniques, and exploring hybrid fiber systems to fully harness the potential of NFRC in enhancing infrastructure durability and sustainability. Following conclusion was carried out by the conducted study.

- Nylon fibers effectively improve concrete's crack resistance, impact resistance, and post-crack behavior [6], [8], [12].

- Further studies are needed to address fiber distribution challenges and optimize NFRC for long-term performance [17], [19].
- A cost-effective, flexible alternative to traditional reinforcement methods. Together, these advantages make nylon fibers a promising addition to the future of concrete slab construction [7], [10].
- Nylon fibers bring added value through their versatility and sustainability. Whether derived from virgin sources or recycled materials [18], [24].

Incorporating nylon fibers into concrete slabs effectively addresses plain concrete's limitations, particularly shrinkage and cracking. By enhancing tensile strength and bridging micro-cracks, nylon improves mechanical performance, durability, and long-term service life, especially in dynamic or fluctuating environments. Nylon fiber-reinforced concrete (NFRC) enhances resistance to cracking, impact, and post-crack performance. It provides a cost-effective, sustainable alternative to traditional reinforcement, despite challenges like uneven fiber distribution.

7 Acknowledgment

I would like to thank every person/department who helped thorough out the research work, particularly the CE department, ORIC and Engr. Dr. Majid Ali. The careful review and constructive suggestions by the anonymous reviewers are gratefully acknowledged.

8 Reference

[1] M. M. Kabir and M. N. Islam, "Review of fiber-reinforced concrete properties," Journal of Construction Engineering a Management, vol. 144, no. 5, pp. 1–10, 2018.
[2] R.D. Toledo Filho, K. Scrivener, G. L. England, and K. Ghavami, "Durability of alkali-sensitive sisal and jute fibers in cementmortar composites," Cement and Concrete Composites, vol. 22, pp. 127–143, 2000.
[3] A.M. Brandt, "Fibre reinforced cement-based (FRC) composites after over 40 years of development in building and civil engineering," Composite Structures, vol. 86, pp. 3–9, 2008.
[4] A. Bentur and S. Mindess, Fibre Reinforced Cementitious Composites, 2nd ed., London, UK: CRC Press, 2006.
[5] M. Foti, "Preliminary analysis of concrete reinforced with waste bottles PET fibers," Construction and Building Materials, vol.25, no. 4, pp. 1906–1915, 2011.
[6] M. U. Farooqi and M. Ali, "Effect of nylon fiber content on shrinkage resistance of concrete," Construction and Building Materials, vol. 224, pp. 572–583, 2020.
[7] F. Pacheco-Torgal and S. Jalali, "Cementitious building materials reinforced with vegetable fibers: A review," Construction and Building Materials, vol. 25, no. 2, pp. 575–581, 2011.
[8] H.K. Lee, Y. H. Kim, and S. W. Lee, "Mechanical properties of fiber-reinforced concrete incorporating nylon fiber," MaterialsScience Forum, vol. 620–622, pp. 619–622, 2009.
[9] B. Singh and S. Munjal, "Comparative performance of natural and synthetic different fiber-reinforced concrete under environmental conditions," Journal of Materials in Civil Engineering, vol. 30, no. 2, pp. 04017300, 2018.
[10] T.S. Mohammed, H. J. Shakor, and M. N. Ismail, "Impact of nylon fiber on flexural behavior of reinforced concrete beams,"International Journal of Civil Engineering and Technology, Vol. 10, no. 4, pp.
[11] M. J. Aziz and A. R. Boccaccini, "Mechanical Properties of Nylon Fiber Reinforced Composites," Ceramics International, vol.44, no. 1, pp. 1055–1061, Jan. 2018.
[12] Y. Wang, J. G. Tobolski and V. C. Li, "Tensile Behavior of Nylon Fiber Reinforced Concrete," ACI Materials Journal, vol. 91, no. 3, pp. 282–292, 1994.
[13] H. W. Reinhardt and S. Cornelissen, "Post-Peak Cyclic Behavior of Steel Fibers in Concrete," Heron, vol. 31, no. 2, pp. 4556,1986.
[14] H. J. Willems and J. W. van der Meer, "Stress-Strain Behaviour of High Strength Steel Wires," Journal of Materials Processing Technology, vol. 177, no. 1–3, pp. 424–427, Jul. 2006.
[15] T .W . Clyne and D. Hull, An Introduction to Composite Materials, 2nd ed. Cambridge, U.K.: Cambridge Univ. Press, 2019, ch. 3, pp. 58–67. (Covers stress-strain behavior of glass fibers in detail.
[16] M. K. Kim and S. M. Lee, "Tensile Properties of E-glass Fiber and Polypropylene Matrix Composites at High Strain Rates," Composites Science and Technology, vol. 67, no. 15–16, pp. 3434–3441, Dec. 2007.
[17] H. Q. Jahangir, J. Ahmad, A. Aljabr, and N. Garcia-Troncoso, "Review on characteristics of concrete reinforced with nylon fiber," Journal of Engineered Fibers and Fabrics, vol. 18, p. 15589250231189812, 2023.
[18] S. Spadea, I. Farina, A. Carrafiello, and F. Fraternali, "Recycled nylon fibers as cement mortar reinforcement,"arXiv, Sep. 2014.
[19] M. Mohiuddin, A. N. Abhi, M. Ulfat, and S. R. Chowdhury, "Review on conventional concrete and nylon fiber reinforced concrete behavior," Malaysian Journal of Civil Engineering, vol. 35, no. 1, pp. 7-15, 2023.
[20] Wang, Z. Yu, B. Liu, F. Zhao, S. Tang, and M. Jin, "Effects of fly ash dosage on shrinkage, crack resistance and fractal

characteristics of face slab concrete," Fractal and Fractional, vol. 6, no. 6, p. 335, 2022.

[21] F. Qamar, T. Thomas, and M. Ali, "Improvement in lateral resistance of mortar-free interlocking wall with plaster having natural fibres," Construction and Building Materials, vol. 234, p. 117387, 2020.

[22] M. Khan and M. Ali, "Optimization of concrete stiffeners for confined brick masonry structures," *Journal of Building Engineering*, vol. 32, p. 101689, 2020.

[23] M. Ali, "Role of post-tensioned coconut-fibre ropes in mortar-free interlocking concrete construction during seismic loadings," *KSCE Journal of Civil Engineering*, vol. 22, no. 4, pp. 1336-1343, 2018.

[24] A. Afraz and M. Ali, "Effect of banana fiber on flexural properties of fiber reinforced concrete for sustainable construction," Engineering Proceedings, vol. 12, no. 1, p. 63, 2021.

[25] M. U. Farooqi and M. Ali, "Effect of fibre content on compressive strength of wheat straw reinforced concrete for pavement applications," IOP Conference Series: Materials Science and Engineering, vol. 422, no. 1, p. 012014, Sep. 2018.

DURABILITY OF GEOPOLYMER CONCRETE WITH RECYCLED SAND IN ACIDIC AND MARINE CONDITIONS

[a] Shahzadi Irum*, [b] Faisal Shabbir, [c] Hammad Salahuddin

a: Civil Engineering Department, COMSATS University Islamabad, Wah Campus, Pakistan. Irum.jawad@ciitwah.edu.pk
b: Department of Civil Engineering University of Engineering & Technology Taxila, Pakistan. faisal.shabbir@uettaxila.edu.pk
b: Department of Civil and Transportation Engineering, Shenzhen University, China. Hammads88@szu.edu.cn
* Corresponding author

Abstract- Incorporating recycled sand (R-sand) in geopolymer concrete (GC) not only enhances environmental sustainability by utilizing industrial by-products and construction & demolition waste but also reduces dependency on river sand, making it a more environmentally friendly option. This paper presents an experimental investigation on the behavior of GC with R-sand in acid and marine water. All samples were prepared with a combination of fly ash and slag as a binder, using sodium hydroxide and sodium silicate as alkaline activators. The specimens were exposed to 4% sulfuric acid and artificial marine water for a period of 60days. The parameters that were examined during the experimental investigation are compressive strength, compressive strength loss, mass loss, and water absorption. The results show that the strength of GC gradually reduced with an increased R-sand content, and it performs better in marine water as compared to acidic solution.

Keywords- Acid and Marine Water, Durability of Concrete, Geopolymer Concrete, Recycled Sand

1 Introduction

Geopolymer concrete (GC) is gaining considerable attention as a sustainable alternative to traditional Ordinary Portland Cement (OPC) concrete. Despite its widespread use, OPC concrete has notable environmental drawbacks, including high energy consumption and significant carbon dioxide emissions, contributing to climate change [1]. Moreover, OPC concrete is susceptible to degradation when exposed to aggressive environments such as acidic and chloride-rich conditions change [2]. In contrast, GC offers several advantages, including a lower carbon footprint and enhanced resistance to chemical attacks. GC is synthesized by activating aluminosilicate-rich industrial by-products such as fly ash, ground granulated blast furnace slag (GGBFS), and metakaolin with alkaline solutions, typically a combination of sodium silicate (Na_2SiO_3) and sodium hydroxide (NaOH) [3].These binders contribute to improved mechanical performance [4] and superior durability properties under aggressive exposures [5].

Aggregates, both coarse and fine, constitute approximately 75% to 80% of the total volume of GC [6]. With the increasing scarcity of natural sand and environmental concerns over riverbed mining, the replacement of natural aggregates with recycled alternatives, particularly recycled sand (R-sand) derived from construction and demolition (C&D) waste has become a key area of interest [7], [8]. The use of R-sand not only helps conserve natural resources but also facilitates waste management by diverting C&D waste from landfills. However, the application of R-sand in GC remains limited, especially in comparison to recycled coarse aggregates [9], [10].

Due to its dense and homogeneous matrix, GC has demonstrated promising durability under aggressive environments, such as acid and marine exposure[11], [12]. Structures located in urban and coastal areas frequently deteriorate after prolonged exposure to acidic media, sulfates, or chlorides [13]. GC, with its low calcium content and stable aluminosilicate structure, has shown greater resistance to such deterioration than OPC-based systems.

Despite these advantages, there is limited research focusing specifically on the durability of GC incorporating R-sand under aggressive conditions such as acid and seawater. This study aims to bridge that gap by evaluating the performance of GC mixes with varying proportions of R-sand under acid and marine water. Understanding the influence of R-sand on the durability of GC will provide valuable insights for the practical implementation of sustainable and durable construction materials. Furthermore, promoting the use of recycled aggregates in GC contributes to the circular economy and the reduction of the construction industry's carbon footprint.

2 Research Methodology

2.1 Material Properties

In this study, a composite binder was developed using 80% locally sourced Class F fly ash and 20% GGBFS. The chemical composition of the Class F fly ash included SiO_2 (48.6%), Al_2O_3 (32.23%), CaO (3.24%), MgO (2.02%), Na_2O (4.45%), TiO_2 (2.02%), and Loss on Ignition (LOI) at 1.63%. The GGBFS contained SiO_2 (30.12%), Al_2O_3 (14.7%), Fe_2O_3 (10.3%), CaO (34.25%), MgO (5.1%), Na_2O (0.28%), TiO_2 (0.36%), and LOI (2.69%).

The alkaline activator system consisted of a sodium silicate (Na_2SiO_3) solution—composed of 29.4% SiO_2, 14.6% Na_2O, and 56.0% H_2O—and a 12M sodium hydroxide (NaOH) solution. Natural river sand was used as natural fine aggregate, while natural coarse aggregates (NCA) were obtained from a nearby quarry. R-sand were prepared from previously tested concrete specimens produced under controlled laboratory conditions (28-30MPa). The water absorption rates for R-sand and natural sand were found to be 5.6% and 0.92%, respectively.

2.2 Specimen Preparation

12M NaOH solution was prepared by mixing 97–98% pure pellets with water, 24h before the concrete mixing. The alkaline activator was made by mixing Na_2SiO_3 and NaOH solution 1h before casting. Aggregates were dry mixed with binder for 2 minutes, followed by gradual addition of the alkaline activator solution. Mixing persisted for an additional 2-3 minutes before pouring the mixture into molds and compacting it using a vibration table. Specimens were removed from molds after 24 hours and were hot cured at 80 °C for the next 24 hours, followed by storage at ambient temperature until the age of testing. Figure 1 shows the raw materials, mixing, casting and samples under acid and seawater.

2.3 Mix Design

The mix proportions of the GC utilized in this study are detailed in Table 1. A total of four GC mixtures were prepared, incorporating varying proportions of R-sand to evaluate its influence on the performance of the concrete. The S0 (control specimen) was made with NCA and N-sand. R-sand with 30%, 60%, and 100% replacement of N-sand was used.

Table 1 Mix design of GC with R-sand

Mix ID	Binder		Alkaline Activator		Coarse and Fine Aggregates		
	FA	GGBFS	Na_2SiO_3	NaOH	NCA	N-sand	R-sand
S0	320	80	171.4	68.6	1144	616	0
S30	320	80	171.4	68.6	1144	431	185
S60	320	80	171.4	68.6	1144	185	431
S100	320	80	171.4	68.6	1144	0	616

2.4 Testing

Compressive strength testing was conducted in accordance with ASTM C39 [14], at 7 and 28 days. To estimate the durability of the concrete more rapidly, water absorption was assessed following the [15] standard. Resistance to marine water was evaluated using the ASTM D1141[16] procedure, where synthetic seawater was prepared and cylindrical specimens (100 mm × 200 mm) were submerged for a period of 60 days. Subsequently, compressive strength and weight measurements were recorded to calculate the percentage reduction in strength and mass. Additionally, to assess the acid resistance of the GC samples, ASTM C267[17] was followed. Specimens were immersed in a 4% sulfuric acid solution

after initial weighing, and after 60 days of exposure, changes in physical appearance, compressive strength, and weight were documented to determine deterioration.

a) b)



c) d)

Figure 1: a. Materials b. Mixing c. Seawater test d. Acid test

3 Results

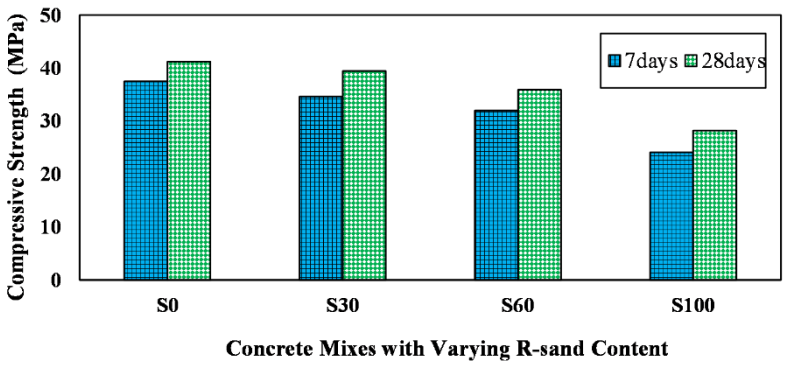
3.1 Compressive Strength

Figure 2 illustrates the compressive strength results of all the mixes. The control mix (S0) exhibited the highest 28-day compressive strength, reaching 41.2 MPa. When river sand was partially replaced with R-sand, a gradual reduction in compressive strength was observed—recorded as 4.37%, 12.86% and 31.55% for S30, S60, and S100, respectively. At replacement levels up to 60%, the reduction was comparatively moderate (12.86%) relative to the significant decline (31.55%) seen at 100% substitution. This trend can be partly attributed to the finer particles present in the recycled sand, which may have contributed to enhanced packing density and reduced voids in the matrix [8]. However, as the proportion of recycled sand increased, the presence of old adhered mortar from parent concrete became more pronounced, adversely affecting the mechanical bonding and ultimately reducing the compressive strength of the geopolymer concrete [18].

The strength development of GC was notably enhanced by heat curing, with all mixes attaining approximately 80–90% of their 28-day strength within the first 7 days, as illustrated in Figure 2. After this initial period, strength gains progressed at a slower rate until day 28. The inclusion of R-sand slightly reduced the early strength gain rate. The S0, incorporating only natural sand, achieved 91.02% of its 28-day strength by the 7th day. In comparison, mixes S30, S60, and S100 reached 87.82%, 89.14% and 85.46% respectively, of their 28-day strength within the same duration. Comparable observations

were reported by Zhang et al. [18], who studied ultra-high-performance concrete (UHPC) with R-sand. This reduction in early-age strength gain was primarily attributed to an increased effective water-to-binder ratio in mixes containing R-sand [10], [19].

Figure 2: Compressive Strength (MPa) of different mixes at 7 and 28 days



3.2 Compressive Strength Loss

Figure 3 presents the percentage loss in compressive strength for specimens subjected to 60-day exposure in 4% sulfuric acid and synthetic marine water. For the S0, strength losses were 3.88% under acidic conditions and 1.46% in the marine water. With the incorporation of R-sands, the loss in compressive strength increased to 4.31%, 6.41% and 12.06% in the acidic medium, and to 3.05%, 5.57% and 7.09% under marine conditions for mixes S30, S60, and S100, respectively. GC demonstrated excellent durability in aggressive environments due to its low calcium content and reduced water absorption capacity [20], [21]. GC tends to develop a dense and chemically stable aluminosilicate matrix, which limits pore connectivity and hinders aggressive ion penetration [22]. Mixes with lower R-sand content likely maintained lower porosity and better matrix integrity, contributing to reduced strength and mass loss. Conversely, higher replacement levels may introduce voids or weak interfaces, increasing vulnerability to chemical degradation.[11], [23]. The inferior performance in acidic conditions can be linked to the residual cement paste attached to R-sand, which tends to degrade upon acid exposure, resulting in microcracking and subsequent reductions in both mass and strength [24], [25]. Furthermore, R-sand exhibits higher vulnerability to acid attack compared to N-sand [19]. This heightened susceptibility of finer recycled aggregates is often attributed to their larger specific surface area, which increases their interaction with aggressive agents, leading to more pronounced chemical deterioration [8], [19].

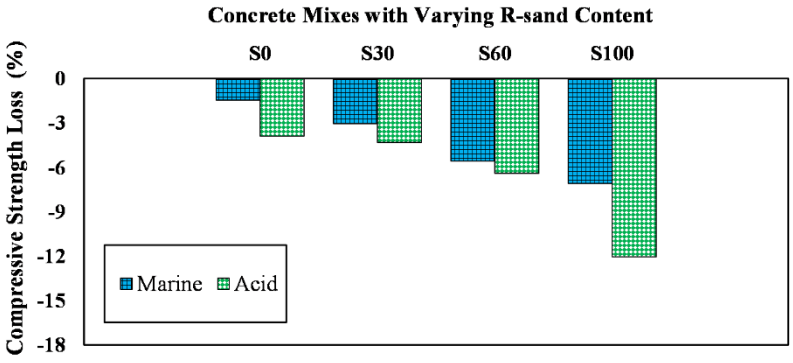


Figure 3: Compressive Strength loss (%) of GC incorporating R-sand after 60 days of exposure to acidic and marine conditions

3.3 Mass Loss in Acidic and Marine Conditions

Figure 4 illustrates the mass loss of GC specimens exposed to acidic and marine environments. Specimens containing natural aggregates demonstrated strong resistance, exhibiting no noticeable surface degradation, cracking, or fracturing

under either exposure condition. However, the inclusion of R-sand led to evident surface erosion and an increase in mass loss. The control mix experienced a minimal mass loss of 0.76% in the acidic environment and none in the marine environment. This superior durability is primarily attributed to the rapid polymerization reaction facilitated by elevated temperature curing in GC, which is more efficient than that in OPC systems [13]. The recorded mass loss for S30, S60, and S100 in the acidic medium was 1.61%, 3.05% and 4.21%, respectively. Corresponding losses in the marine condition were 3.04%, 5.13%, and 6.71%. Mass loss was considered as the combined outcome of surface erosion and chemical degradation caused by exposure to aggressive environments. Similar findings were reported by Mahmood et al. [26], who observed that the use of recycled aggregates in concrete compromised its performance by reducing compressive strength, increasing porosity and chloride permeability, and weakening the bond strength in marine exposures. The dense microstructure developed through geopolymerization significantly minimizes the permeability of the matrix, thereby improving resistance to aggressive environments such as acids and seawater [23], [27], [28].

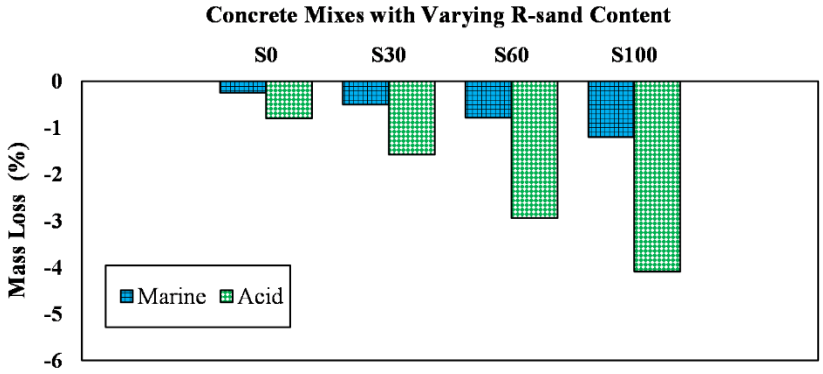


Figure 4: Mass loss (%) of GC incorporating R-sand after 60 days of exposure to acidic and marine conditions

3.4 Water Absorption

Figure 5 presents the water absorption results of the cylindrical specimens tested at 28 days. The control mix exhibited a water absorption of 5.6%, while the values recorded for S30, S60, and S100 were 6.18%, 6.45%, and 8.58%, respectively. A consistent increase in water absorption was observed with the progressive replacement of natural sand (N-sand) by R-sand, from 0% up to 100%. This rise in absorption is primarily attributed to the porous nature of R-sand, particularly due to the adhered mortar, which tend to retain more moisture [10], [18], [19], [29]. Moreover, the inherently higher water absorption capacity of R-sand compared to N-sand further contributed to this trend. Notably, the S100 mix demonstrated a 36% increase in water absorption relative to the control mix.

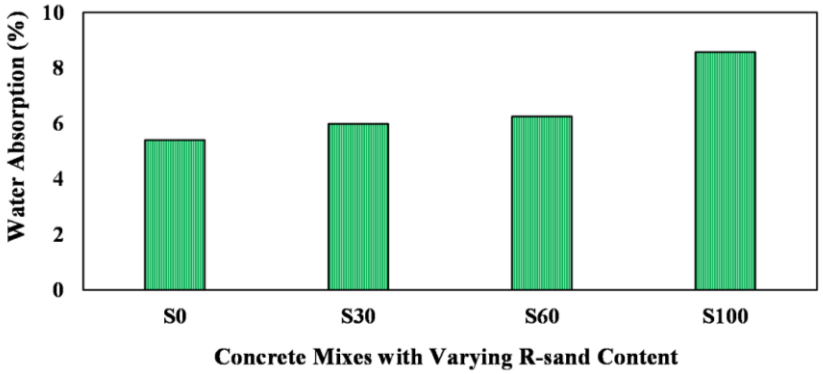


Figure 5: Water Absorption (%) of GC incorporating various percentages of R-sand

4 Practical Implementation

The utilization of R-sand in GC presents a promising solution to address sustainability challenges and reduce reliance on natural resources such as river sand. This approach enhances sustainability by incorporating recycled materials and reducing environmental impact. In practical applications, this research demonstrates that R-sand can be effectively used in GC exposed to acidic and seawater environments, offering a viable and sustainable alternative to natural sand. The findings support the use of R-sand-based GC in coastal and industrial structures, where chemical exposure is prevalent.

5 Conclusion

Based on the findings of this study, the following conclusions can be drawn:

1. Natural sand can be entirely substituted with R-sand, as the 28-day compressive strength of the fully replaced mix (S100) remained above 28 MPa.
2. Compressive strength decreased with higher R-sand replacement, showing a moderate reduction (12.8%) at 60% replacement and a substantial loss (31.5%) at full replacement.
3. In acidic environments, specimens with 100% R-sand exhibited the highest compressive strength loss at 12%, while mixes containing only N-sand showed less than 4% loss. The increased vulnerability of R-sand to acid attack becomes more pronounced with higher replacement ratios.
4. GC specimens prepared with N-sand demonstrated excellent resistance to marine conditions. Even with full replacement by R-sand, the loss in compressive strength remained minor (1.2%), and no significant mass loss was observed.

Acknowledgment

The authors would like to thank the Civil Engineering Department of CUI, Wah campus, specially Dr. Hammad Salahuddin who helped thorough out the research work.

References

[1] Y. Ding, J.-G. Dai, and C.-J. Shi, "Mechanical properties of alkali-activated concrete: A state-of-the-art review," *Constr Build Mater*, vol. 127, pp. 68–79, 2016.
[2] N. Xie, Y. Dang, and X. Shi, "New insights into how MgCl2 deteriorates Portland cement concrete," *Cem Concr Res*, vol. 120, pp. 244–255, 2019.
[3] G. Fang, W. K. Ho, W. Tu, and M. Zhang, "Workability and mechanical properties of alkali-activated fly ash-slag concrete cured at ambient temperature," *Constr Build Mater*, vol. 172, 2018, doi: 10.1016/j.conbuildmat.2018.04.008.
[4] A. A. Hassan Mohammed; Shariq, M., "Use of geopolymer concrete for a cleaner and sustainable environment – A review of mechanical properties and microstructure," *J Clean Prod*, vol. 223, no. NA, pp. 704–728, 2019, doi: 10.1016/j.jclepro.2019.03.051.
[5] S. A. Bernal and J. L. Provis, "Durability of alkali-activated materials: progress and perspectives," *Journal of the American Ceramic Society*, vol. 97, no. 4, pp. 997–1008, 2014.
[6] D. Hardjito and B. V. Rangan, "Development and properties of low-calcium fly ash-based geopolymer concrete," 2005.
[7] R. V. Silva, J. De Brito, and R. K. Dhir, "Properties and composition of recycled aggregates from construction and demolition waste suitable for concrete production," *Constr Build Mater*, vol. 65, 2014, doi: 10.1016/j.conbuildmat.2014.04.117.
[8] H. Salahuddin, L. A. Qureshi, A. Nawaz, and S. S. Raza, "Effect of recycled fine aggregates on performance of Reactive Powder Concrete," *Constr Build Mater*, vol. 243, 2020, doi: 10.1016/j.conbuildmat.2020.118223.
[9] "Guidelines and the present state of the reuse of demolished concrete in Japan," in *Demolition and Reuse of Concrete and Masonry*, 2020. doi: 10.1201/9781482271270-22.
[10] R. Singh, D. Nayak, A. Pandey, R. Kumar, and V. Kumar, "Effects of recycled fine aggregates on properties of concrete containing natural or recycled coarse aggregates: A comparative study," *Journal of Building Engineering*, vol. 45, no. October 2021, p. 103442, 2022, doi: 10.1016/j.jobe.2021.103442.
[11] S. Irum and F. Shabbir, "Performance of fly ash/GGBFS based geopolymer concrete with recycled fine and coarse aggregates at hot and ambient curing," *Journal of Building Engineering*, vol. 95, p. 110148, Oct. 2024, doi: 10.1016/J.JOBE.2024.110148.

[12] S. Irum, F. Shabbir, H. Salahuddin, and R. M. Waqas, "Performance evaluation of sustainable recycled aggregates geopolymer concrete using cement and graphite nano/micro platelets under heat and ambient curing," *Emergent Mater*, 2025, doi: 10.1007/s42247-025-01057-0.

[13] A. E. Kurtoğlu *et al.*, "Mechanical and durability properties of fly ash and slag based geopolymer concrete," *Advances in Concrete Construction*, vol. 6, no. 4, 2018, doi: 10.12989/acc.2018.6.4.345.

[14] ASTM, "ASTM C39/C39M: Standard Test Method for Compressive Strength of Cylindrical Concrete Specimens," *ASTM International*, vol. 04, no. March, 2001.

[15] ASTM International, "ASTM C642-21. Standard Test Method for Density, Absorption, and Voids in Hardened Concrete," 2021.

[16] ASTM International, "D1141-98: Standard Practice for the Preparation of Substitute Ocean Water," 2021.

[17] ASTM, "C267 - 20: Standard Test Methods for Chemical Resistance of Mortars, Grouts, and Monolithic Surfacings and Polymer Concretes," *ASTM International*, vol. 01, 2013.

[18] H. Zhang, T. Ji, X. Zeng, Z. Yang, X. Lin, and Y. Liang, "Mechanical behavior of ultra-high performance concrete (UHPC) using recycled fine aggregate cured under different conditions and the mechanism based on integrated microstructural parameters," *Constr Build Mater*, vol. 192, pp. 489–507, 2018.

[19] D. D. Pedro, J. De Brito, and L. Evangelista, "Structural concrete with simultaneous incorporation of fine and coarse recycled concrete aggregates: Mechanical, durability and long-term properties," *Constr Build Mater*, vol. 154, pp. 294–309, 2017.

[20] P. Zhang, Z. Gao, J. Wang, J. Guo, S. Hu, and Y. Ling, "Properties of fresh and hardened fly ash/slag based geopolymer concrete: A review," *J Clean Prod*, vol. 270, p. 122389, 2020.

[21] P. Nuaklong, A. Wongsa, V. Sata, K. Boonserm, J. Sanjayan, and P. Chindaprasirt, "Properties of high-calcium and low-calcium fly ash combination geopolymer mortar containing recycled aggregate," *Heliyon*, vol. 5, no. 9, 2019, doi: 10.1016/j.heliyon.2019.e02513.

[22] A. Chouksey, M. Verma, N. Dev, I. Rahman, and K. Upreti, "An investigation on the effect of curing conditions on the mechanical and microstructural properties of the geopolymer concrete," *Mater Res Express*, vol. 9, no. 5, 2022, doi: 10.1088/2053-1591/ac6be0.

[23] J. Wang, J. Xie, C. Wang, J. Zhao, F. Liu, and C. Fang, "Study on the optimum initial curing condition for fly ash and GGBS based geopolymer recycled aggregate concrete," *Constr Build Mater*, vol. 247, Jun. 2020, doi: 10.1016/j.conbuildmat.2020.118540.

[24] P. S. Nuaklong Vanchai; Chindaprasirt, Prinya, "Influence of recycled aggregate on fly ash geopolymer concrete properties," *J Clean Prod*, vol. 112, no. NA, pp. 2300–2307, 2016, doi: 10.1016/j.jclepro.2015.10.109.

[25] P. S. Nuaklong Vanchai; Chindaprasirt, Prinya, "Properties of metakaolin-high calcium fly ash geopolymer concrete containing recycled aggregate from crushed concrete specimens," *Constr Build Mater*, vol. 161, no. NA, pp. 365–373, 2018, doi: 10.1016/j.conbuildmat.2017.11.152.

[26] W. Mahmood, T. Ayub, and A. ur R. Khan, "Mechanical properties and corrosion resistance of recycled aggregate concrete exposed to accelerated and natural marine environment," *Journal of Building Engineering*, vol. 66, 2023, doi: 10.1016/j.jobe.2023.105867.

[27] J. V. Rao, K. S. Rao, and K. Rambabu, "Performance of heat and ambient cured geopolymer concrete exposed to acid attack," *Proceedings of Institution of Civil Engineers: Construction Materials*, vol. 172, no. 4, 2019, doi: 10.1680/jcoma.17.00005.

[28] P. Rovnaník, "Effect of curing temperature on the development of hard structure of metakaolin-based geopolymer," *Constr Build Mater*, vol. 24, no. 7, pp. 1176–1183, 2010.

[29] Y. Hu, Z. Tang, W. Li, Y. Li, and V. W. Y. Tam, "Physical-mechanical properties of fly ash/GGBFS geopolymer composites with recycled aggregates," *Constr Build Mater*, vol. 226, pp. 139–151, Nov. 2019, doi: 10.1016/j.conbuildmat.2019.07.211.

EXPERIMENTAL STUDY ON STRENGTH AND WORKABILITY OF SUSTAINABLE CONCRETE INCORPORATING COTTON FIBERS AND MARBLE WASTE

[a] Muhammad Adnan Hanif*, [b] Ali Ejaz

a: Department of Structural Engineering, Military College of Engineering (NUST), Risalpur, Pakistan. adnanhanif2303@gmail.com
b: Department of Structural Engineering, National Institute of Transportation (NUST), Risalpur, Pakistan. enggaliejax@gmail.com
* Corresponding author

Abstract- This study investigates the dual use of cotton fibers (CF) and waste marble aggregate (WMA) as sustainable alternatives to conventional coarse aggregates in concrete. Driven by environmental concerns and resource depletion, the research introduces five mix designs with WMA ranging from 0% to 100% and a constant 2.5% CF by weight. Compressive and flexural strengths were evaluated at 28 and 56 days. Results revealed a peak performance at 50% WMA, surpassing control values and demonstrating improved mechanical behavior and sustainability. The study supports sustainable engineering practices by reusing industrial waste materials in concrete applications. The findings promote scalable use of industrial waste for non-structural concrete applications aligned with climate-resilient infrastructure goals.

Keywords- Sustainable Concrete; Cotton Fibers; Waste Marble Aggregate; Mechanical Properties.

1. Introduction

Concrete's global ubiquity in infrastructure comes at an ecological cost due to quarrying of aggregates and energy-intensive cement production [1]. The processing of marble into finished products generates approximately 30–40% of solid waste by weight, resulting in an estimated 690,000 to 920,000 tons of marble waste annually [2]. The global textile industry generates approximately 92 million tons of waste per year, with only 25% being reused or recycled, and the remaining 75% disposed of in landfills or incinerated [3,4]. Disposal of these byproducts imposes environmental hazards, pushing research toward integrating waste into concrete [5].

WMA has been found to improve compressive strength and reduce cost and energy consumption when optimally used [6]. Cotton fibers (CF), though organic, improve flexural strength and crack resistance through a bridging mechanism and better moisture retention during curing [7]. However, both materials, when excessively used, can negatively affect workability and cohesion [8]. Hence, this study presents a combined system of CF and WMA in concrete, aimed at improving both mechanical performance and sustainability. Previous research demonstrates variable success in replacing conventional aggregates with WMA. Kore and Vyas reported 18% improvement in compressive strength with up to 50% WMA [6]. Sunil and Varghese validated improved workability and strength using WMA in concrete mixes [9]. CF have been less studied, but Tang et al. found 9% enhancement in flexural strength at 0.8% cotton knitted fiber waste content by weight of cement [8]. Bartulović et al. showed 21% gain in flexural strength with 2.5% cotton fabric waste, though compressive strength dropped by 10–28% at higher content [7]. Saca et al. corroborated CF's role in improving ductility but warned of reduced compressive performance beyond 2.5% [10]. In addition, Bartulović et al. [7] demonstrated that incorporating CF enhances tensile and flexural strength, reduces shrinkage, and delays the onset of micro-cracking in concrete. The study confirmed that fiber dispersion and morphology contribute significantly to matrix integrity when waste CFs are dozed below 3%.

These studies suggest that a 50% WMA and 2.5% CF mix offers the best balance between strength and sustainability. Therefore, this research aims to evaluate the compressive and flexural strength of CF-WMA concrete on 28 and 56 days to determine the optimal WMA content for performance and sustainability. This study uniquely evaluates the combined effect of cotton fibers and waste marble aggregate on both strength and workability. Unlike prior research, it focuses on their synergistic use and provides localized insights relevant to sustainable construction in Pakistan.

2. Research Methodology

2.1 Details of Test Matrix

WMA sourced from local quarries replaced coarse aggregates at 0%, 25%, 50%, 75%, and 100% by weight. CF (cut to 6–8 cm × 2 cm) was added at a fixed 2.5%. A drum mixer was used to prepare concrete with a mix ratio of 1 (cement): 2.49 (sand): 2.62 (aggregate) by weight and W/C ratio of 0.55. Concrete was mixed in a drum mixer by first dry-blending cement, sand, natural aggregate, and WMA for 2 minutes. Cotton fibres were then added gradually to avoid clumping, followed by the slow addition of water to achieve workability. The mix was placed in standard moulds (150×300 mm cylinders and 150×150×525 mm beams), compacted in two layers using a tamping rod. Specimens were covered with wet burlap, demolded after 24 hours, and cured in water at 23 ± 2°C until testing. Cylindrical and prism samples were tested under ASTM C39 and C293 protocols for compressive and flexural strength at 28 and 56 days. Sieve analysis results of natural aggregate and WMA are shown in Figure 1, indicating comparable particle size distributions within ASTM limits. This supports the fair comparison of both materials in the mix design and helps evaluate the influence of WMA on concrete properties. The test matrix is provided in Table 1.

Table 1 Details of test matrix

Sample ID	CF (%)	WMA (%)	28 Days		56 Days	
			Cylinders (No)	Beams (No)	Cylinders (No)	Beams (No)
CS	0	0	3	3	3	3
CF WMA0	2.5	0	3	3	3	3
CF WMA25	2.5	25	3	3	3	3
CF WMA50	2.5	50	3	3	3	3
CF WMA75	2.5	75	3	3	3	3
CF WMA100	2.5	100	3	3	3	3

Note: CF stands for cotton fibers and WMA stands for waste marble aggregates. Cylinders are 150 mm diameter and 300 mm height. Whereas beams are 150 x 150 x 525 mm.

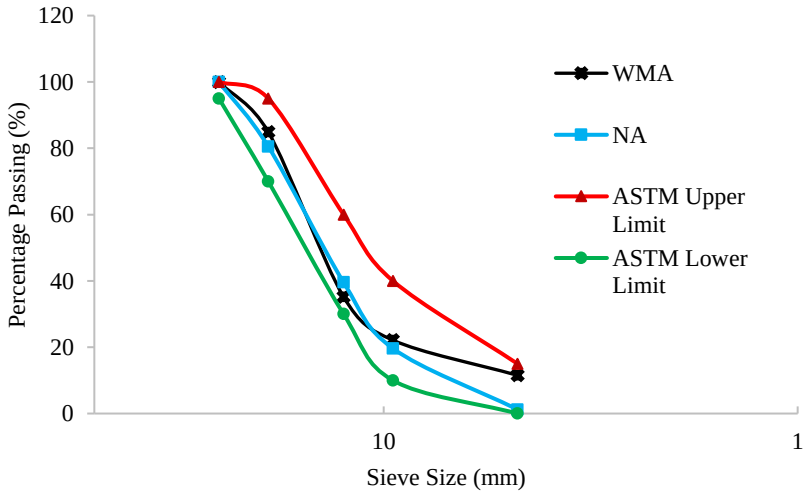


Figure 1: Gradation Curve for natural aggregate (NA) and waste marble aggregates (WMA) sieve analysis



(a) *(b)* *(c)*

Figure 2. Concrete testing process: (a) Slump test, (b) Compressive strength test, and (c) Flexural strength test.

3. Results and Discussion

3.1 Workability

Figure 3 shows a decreasing trend in slump values with increasing WMA and CF content. The control mix exhibited the highest slump of 25.86 mm, while the mix with 100% WMA and 2.5% CF showed the lowest value of 21.39 mm. This reduction in workability is attributed to the angular texture of WMA and the hydrophilic nature of cotton fibers, which increases water demand. These results align with previous findings where increased surface area and fiber inclusion led to reduced slump [6,8]. The reduction in slump may affect concrete placement in field conditions, requiring the addition of superplasticizers or water-reducing agents in practical applications.

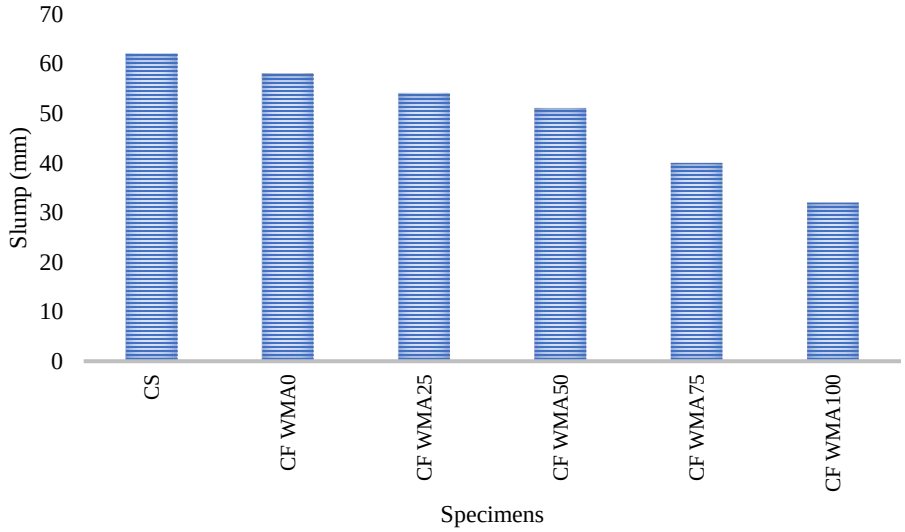


Figure 3. Slump test result of all mixes

3.2 Compressive Strength

As shown in Figure 4, compressive strength peaked at 50% WMA, recording 30.51 MPa on 28 days and 32.67 MPa at 56 days. Beyond this level, strength declined due to weaker interfacial bonding and increased porosity. The mix with 75% WMA exhibited a drop of nearly 9% from the peak. These findings are consistent with literature reporting optimal marble

waste replacement near 50% [6,9]. The gain in compressive strength at 50% WMA may be due to improved particle packing and pozzolanic interaction of fine marble dust particles, contributing to a denser microstructure.

3.3 Flexural Strength

Flexural strength also improved with WMA content up to 50%, reaching 5.097 MPa (28 days) and 5.71 MPa (56 days). Beyond 50%, the increase was marginal or declined slightly. Cotton fibers played a critical role by bridging micro-cracks, delaying failure, and enhancing post-cracking ductility. Similar trends were observed in Bartulović et al. [7] and Saca et al. [10], where natural fibers improved flexural performance but became less effective at higher replacement levels. The improved flexural strength signifies better toughness and crack resistance, which is valuable for pavements and slabs subjected to bending and impact loading.

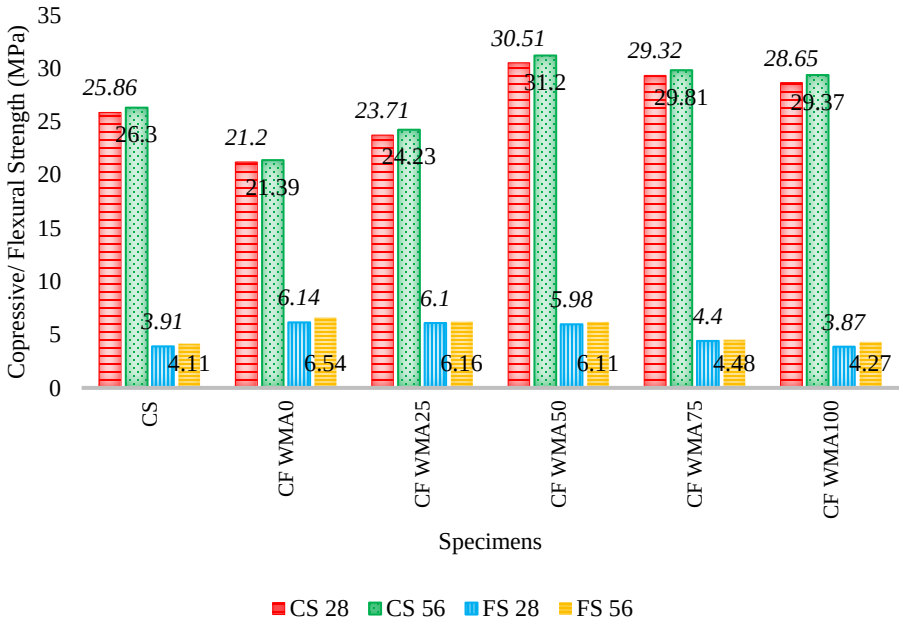


Figure 4. Compressive (CS) and flexural stregth (FS) of concrete mixes at 28 and 56 days.

4. Practical Implementation

The proposed concrete mix using cotton fibers and waste marble aggregate is suitable for non-load-bearing structures, pavement blocks, and boundary walls. Its enhanced flexural strength and crack resistance make it ideal for surfaces exposed to moderate stress. Although the mix achieved compressive strength above 30 MPa, which is adequate for structural use, further studies on long-term durability, environmental exposure, and field-scale implementation are required before recommending it for load-bearing applications. The use of low-cost, locally available waste materials supports sustainability and makes it especially feasible for developing regions like Pakistan. The proposed concrete mix supports climate-resilient infrastructure by minimizing the use of virgin aggregates, reducing landfill waste, and utilizing locally available industrial byproducts. This approach lowers the embodied carbon footprint and promotes circular material use, which are key strategies in mitigating environmental degradation and adapting to long-term sustainability challenges.

5. Conclusion

The following conclusions can be drawn from the conducted study:

1 2.5% CF with 50% WMA yields optimal mechanical behavior.
2 Compressive and flexural strength increased by 18% and 24% compared to the control.
3 Above 50% WMA, both strengths declined, confirming an upper limit for effective WMA replacement.

4 Cotton fibers improve flexural strength and crack resistance but reduce workability.
5 This mix design is recommended for eco-friendly non-structural applications

The above outcome is favorable, indicating the exploration of its in-depth behavior. Next step should be the durability testing along with life cycle assessments.

Acknowledgment

The authors gratefully acknowledge the support provided by the Military College of Engineering, NUST, for facilitating the experimental testing of sustainable concrete. The careful review and constructive suggestions by the anonymous reviewers are gratefully acknowledged.

References

[1] J.M. Uratani, S. Griffiths, A forward looking perspective on the cement and concrete industry: Implications of growth and development in the Global South, Energy Res. Soc. Sci. 97 (2023). https://doi.org/10.1016/j.erss.2023.102972.
[2] J. Carlos R. Ramos, P.G.S. Passalini, J. Nilson F. Holanda, Utilization of marble waste as a sustainable replacement for calcareous in the manufacture of red-firing wall tiles, Constr. Build. Mater. 377 (2023). https://doi.org/10.1016/j.conbuildmat.2023.131115.
[3] E.C. Ailenei, S.D. Ionesi, I. Dulgheriu, M.C. Loghin, D.N. Isopescu, S.G. Maxineasa, I.R. Baciu, New waste-based composite material for construction applications, Materials (Basel). 14 (2021). https://doi.org/10.3390/ma14206079.
[4] T. Wagaw, K.M. Babu, Textile Waste Recycling: A Need for a Stringent Paradigm Shift, AATCC J. Res. 10 (2023) 376–385. https://doi.org/10.1177/24723444231188342.
[5] B. Basaran, I. Kalkan, C. Aksoylu, Y.O. Özkılıç, M.M.S. Sabri, Effects of Waste Powder, Fine and Coarse Marble Aggregates on Concrete Compressive Strength, Sustain. 14 (2022). https://doi.org/10.3390/su142114388.
[6] S.D. Kore, A.K. Vyas, Impact of marble waste as coarse aggregate on properties of lean cement concrete, Case Stud. Constr. Mater. 4 (2016) 85–92. https://doi.org/10.1016/j.cscm.2016.01.002.
[7] B. Bartulović, S. Juradin, D. Žižić, M. Galić, Influence of Cotton Knitted Fabric Waste Addition on Concrete Properties, Buildings 12 (2022). https://doi.org/10.3390/buildings12081121.
[8] W. Tang, R. Monaghan, U. Sajjad, Investigation of Physical and Mechanical Properties of Cement Mortar Incorporating Waste Cotton Fibres, Sustain. 15 (2023). https://doi.org/10.3390/su15118779.
[9] S. Sunil, N. Varghese, Study on Waste Marble as Partial Replacement of Coarse Aggregate in Concrete, 2020. http://www.ijser.org.
[10] N. Saca, L. Radu, R. Truşcă, R. Calotă, D. Dobre, I. Năstase, Assessment of Properties and Microstructure of Concrete with Cotton Textile Waste and Crushed Bricks, Materials (Basel). 16 (2023). https://doi.org/10.3390/ma16206807.

COMPRESSIVE STRENGTH OF STANDARD CYLINDERS, SPLIT TENSILE STRENGTH OF PRESTRESSED CORES, AND MICROSTRUCTURAL ANALYSIS OF POLYPROPYLENE FIBER REINFORCED CONCRETE

[a] Mohammad Zulqarnain*, [b] Muhammad Usman Rashid, [c] Muhammad Awais

a: Civil Engineering Department, University of Engineering and Technology, Taxila, Pakistan. zuuki786@gmail.com
b: Civil Engineering Department, University of Engineering and Technology, Taxila, Pakistan. m.usman@uettaxila.edu.pk.
c: Civil Engineering Department, International Islamic University Islamabad, Islamabad, Pakistan. 25muhammadawais@gmail.com
*Corresponding author

Abstract- This experimental study conducted on mono fiber reinforced concrete to check the effect of polypropylene fibers on compressive strength of standard cylinders and split tensile strength of prestressed cores that are taken out from the prestressed beams. The study also included a microstructure analysis of control and fiber reinforced concrete. The results showed that the PPFRC IV mix achieved an optimum content. Among the mixes, PPFRC IV demonstrated the highest performance, showing a 17% increase in ultimate stress and a 5% increase in split tensile strength compared to the controlled specimen. After 28 days of exposure to sodium chloride solutions, the controlled specimen (CS) and PPFRC I showed the highest percentage loss in strength, reaching up to 11%. Additionally, more open pores were observed in controlled specimen by the SEM analysis. Moreover, hydration products were also observed in SEM analysis. PPFRC IV fibers bonded with the matrix firmly due to which this mix showed improvements in the strength of concrete.

Keywords- Fiber-Reinforced Concrete, Polypropylene Fibers, Split Tensile, Ultimate stress, Microstructure

1 Introduction

The most widely used construction material is concrete, and it is weak in tension, however concrete technology has advanced, there has been growing need to use chemical and additives like fibers to improve its strength. Researchers have been studying the characteristics of fiber reinforced concrete to make it stronger [1], [2]. Research also have been conducted on hybrid fiber reinforced concrete to strengthen concrete. a study conducted by Afroughsabet et al. [3] on hybrid fiber reinforced concrete. Integrating fiber into high performance concrete boosts the mechanical behavior, especially in terms of tensile strength, flexural strength and ductility. In addition to these improvements, fiber inclusions also help minimize shrinkage and creep related deformations, contributing to the materials long term durability and stability. Zulqarnain et al. [4] worked on ferrocement confined columns of different dimensions, and their performance was compared to that of unconfined control specimen. The findings showed a noticeable improvement in load bearing capacity, reduced deflection and greater energy absorption in the ferrocement confined columns compared to the control group. Rashid et al. [5] worked on hybrid fiber (steel and polypropylene) reinforced concrete. The results showed that the incorporation of fiber enhanced the ductility, tensile and flexural properties of fiber reinforced concrete. A study conducted on fiber synergy and results revealed that the combined use of fibers led to a noticeable enhancement of compressive and split tensile strength of fiber reinforced concrete [6]. Rashid et al. [7] captured high resolution images through SEM analysis of hybrid fiber reinforced concrete. He concluded that steel fibers showed signs of rust, the surrounding concrete remained largely unaffected, exhibiting minimal signs of deterioration despite the corrosion of the embedded fiber. The

shear performance of prestressed concrete beams made with fibers reinforced concrete was evaluated, revealing notable improvements. A beam incorporating 0.65% steel fibers demonstrated a 50.71% increase in ultimate failure load, a 67% rise in the initial cracking load, and 36% enhancement in ultimate deflection when compared to the control beam [8]. Research conducted by [9] to check the impact of polypropylene fiber geometry on plastic shrinkage cracking in concrete. The findings showed that polypropylene fibers are generally effective in reducing plastic shrinkage cracks. However, finer fibers outperformed shorter fibers. Additionally, fibers with fibrillated structures were found to be particularly effective in minimizing shrinkage related cracking. A study [10] assessed the performance of concrete reinforced with polypropylene fiber waste and silica fume as partial cement replacements. Silica fumes were used at 4%,8%, 12% and 16% while polypropylene waste was added at 0.4%, 0.8%, 1.2% and 1.6% by weight of cement. Tests conducted on 7, 14, 28 and 90 days showed significant improvements in workability, compressive and tensile strength. SEM and XRD analysis confirmed that enhanced mechanical performance was linked to a denser microstructure. Although fiber reinforced concrete has been widely studied, there is still not enough research on hybrid fiber reinforced concrete, especially when it comes to its internal structural (microstructure). In this study the main focus is placed on polypropylene fiber reinforced concrete to evaluate its compressive strength in form of cylinders, and a comparison was made between the splitting tensile strengths of core specimens taken from prestressed beams, where one group of cores was immersed in a sodium chloride solution for 28 days, while the other group remained unexposed and a microstructure analysis of control and mono and fibers are analyzed.

2 Research Methodology

2.1 Materials

In this study type II cement was utilized as a cementitious material. The cement conformed to the specification in ASTM C150/C150M [11], ensuring suitable performance for structural applications. Coarse aggregates used in this study were utilized in accordance with ASTM C33-03 [12]. While sand was used as a fine. Ordinary drinkable water is used for this research. A chemical admixture with accordance ASTMC494/C494M-19 [13] was selected as well. Polypropylene fibers were mixed to the concrete with different percentages as shown in figure.



Figure 1: Polypropylene fiber

2.2 Concrete Specimen Preparation

All the concrete specimens were prepared at Bannu Mukhtar concrete casting yard as shown in the figure below 2 (a), (b), Material mixing in the concrete mixer and placement of concrete in the shuttering bed. Concrete samples were prepared with different ratios of polypropylene fibers. The specimens casting included prestressed beams as well as standard cylindrical specimens. All the specimens were cured for 28 days. Upon completion of the curing period, the specimens were transported to the UET Taxila concrete yard for further testing. In total 6 prestressed beams and 18 cylindrical specimens were cast. The concrete mix ratio was the same for all the specimens. The concrete mixes with different fiber combinations, and nomenclature used for each mix type is detailed in table 1 below. Also, small cores were taken out from the beams to perform mechanical testing as shown in figure 2 (b).

a)



b)



Figure 2: (a) Material mixing in the concrete mixer (b) placement of concrete in the shuttering bed and cores taken out from prestressed beams

Table 1 concrete mixes with different fiber combinations, and nomenclature used for each mix type

Sr No.	Sample Identity	Description of Specimens
1	CS	Control Specimen
2	PPFRC I	Specimen containing 0.30% of polypropylene fiber dose
3	PPFRC II	Specimen containing 0.40% of polypropylene fiber dose
4	PPFRC III	Specimen containing 0.50% of polypropylene fiber dose
5	PPFRC IV	Specimen containing 0.60% of polypropylene fiber dose
6	PPFRC V	Specimen containing 0.70% of polypropylene fiber dose

2.3 Testing

2.3.1 Compressive Strength Test

To find compressive strengths of standard cylinders, test performed on all the samples in compression testing machine (CTM) having 2000 KN capacity according to ASTM standard [14] as shown in the figure 3 below. All the specimens were kept carefully between the loading plates.



Figure 3: standard cylinders in the compression testing machine (CTM) having 2000 KN capacity

2.3.2 Split Tensile Test

To find the splitting tensile strength of cores, the test was performed as per ASTM C496 [15] in compression testing machine, during the test the cores were kept side wise into the machine as shown in figure. This test aimed to compare the splitting tensile strength of cores taken from beams. Two kinds of cores were tested. The first type consisted of cores that had been immersed in a sodium chloride solution for 28 days, while the second type included cores that had not been exposed to any chloride solution.





Figure 4: Split tensile strength test of cores taken from prestressed beams

2.3.3 Scanning Eelectron Microscopy (SEM) Analysis

Scanning electron microscopy (SEM) analysis was performed to check the fiber's influence on microstructure of concrete after applying the loads. The samples were kept into the SEM machine and images were captured at different magnifications.

3 Results and Discussion

3.1 Compressive Strength Test of Standard Cylinders

Figure 5 illustrates the ultimate stresses of the standard cylinders. It can be observed that the PPFRC IV mix achieved the highest ultimate stress, showing a 17% increase over the controlled specimen. In contrast, PPFRC III exhibited the lowest value, with 12% reduction. PPFRC I, II and V showed increases 7%, 7% and 12% respectively, compared to the controlled specimen.

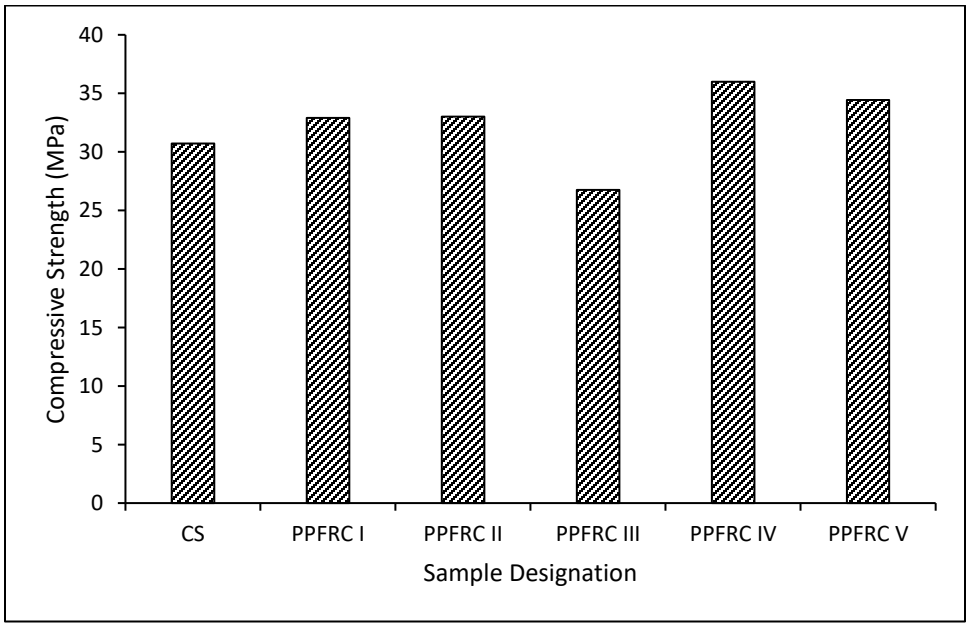


Figure 5: The ultimate stresses of the standard cylinders

3.2 Split Tensile Strength of Cores Before and After Immersion in Sodium Chloride Solution

Figure 6 shows a comparison of the splitting tensile strength of core samples taken from prestressed beams. In the bar graph, the diagonal lined bars represent the tensile strength of cores before immersion in sodium chloride solution, while the dotted bars show tensile strength after 28 days of exposure. The results show that exposure to sodium chloride solutions negatively affected the splitting tensile strength of all specimens. Among the mixes, PPFRC II and PPFRC IV show the highest tensile strength values before immersion, with an increase of 3% and 5% compared to the control specimen. PPFRC I, PPFRC III and PPFRC V showed reductions of 25%, 6% and 2% in splitting tensile strength prior to immersion. After 28 days of immersion in sodium chloride solutions, the percentage losses in splitting tensile strength for each mix were as CS with 11%, PPFRC I, PPFRC II, PPFRC III, PPFRC IV and PPFRC V with 11%, 8%, 4%, 2% and 6 % respectively. The highest splitting tensile strength loss was observed in the CS and PPFRC I mix, both with a reduction of 11% after exposure to the sodium chloride solution.

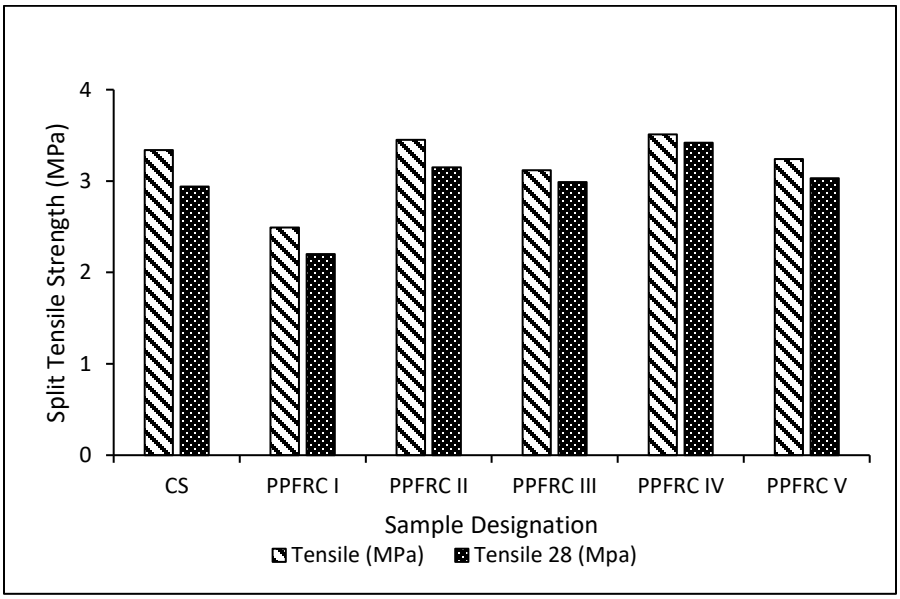


Figure 6: comparison of the splitting tensile strength of core samples taken from prestressed beams, with and without exposure to sodium chloride solution

3.3 SEM Analysis

Figure 7 shows SEM images of different samples, including the control specimen and fiber reinforced concrete matrix. In the control specimen, a significant number of small micro pores can be observed, including a relatively porous structure. While in PPFRC I and PPFRC II mixes show inclusion of polypropylene fiber in the mix. The whitish marks on the PPFRC IV mix which are likely hydration products formed during the early cement hydration. The mix PPFRC IV shows a strong bond between fibers and concrete matrix, with fibers appearing strongly embedded. This strong fiber matrix is likely a key factor contributing to the highest ultimate stress and splitting tensile strength observed among all the tested mixes.

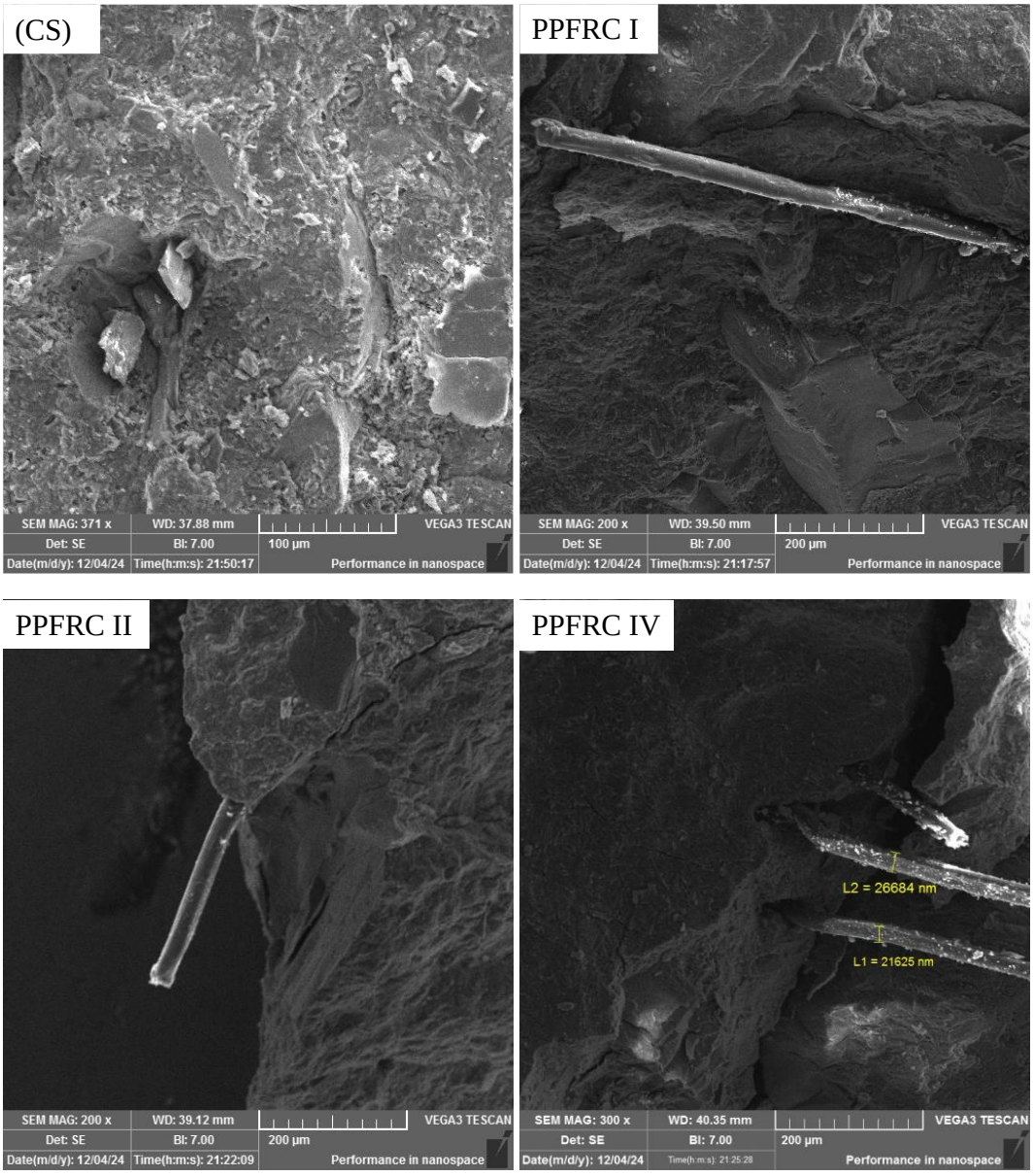


Figure 7: SEM images of CS, PPFRC I, PPFRC II, PPFRC IV

4 Practical Implementation

This research can contribute to helping engineers and the construction industry to use fiber reinforced concrete more effectively in real life construction projects. By understanding how different fibers work and improve the compressive and split tensile strength of concrete, the findings can help to make stronger structures. It can also guide the development of new concrete mixes that perform better under heavy loads

5 Conclusion

From the experimental work the following conclusions are drawn as follows:

1. PPFRC IV exhibited the highest ultimate stress, showing a 17% increase compared to the control specimen.
2. PPFRC IV mix also showed the highest splitting tensile strength, 5% greater than that of the control, while PPFRC I exhibited the highest reduction, with a 25% decrease in splitting tensile strength.

3. After 28 days of immersion in sodium chloride solution, the CS and PPFRC I mix showed the greatest loss in splitting tensile strength, an 11% reduction which is the highest loss of all the specimens.
4. Hydration products observed in the SEM images as well as the control specimen showed more micro pores. It was also observed that fibers have strongly bonded the concrete matrix.

Acknowledgment

The authors would like to thank Bannu Mukhtar Pvt Ltd for providing assistance in casting specimens and sincerely grateful to the Civil Engineering department of UET Taxila for providing the testing facilities throughout the research work.

References

[1] E. Arunakanthi and J. D. C. Kumar, "Experimental studies on fiber reinforced Concrete (FRC)," *Int. J. Civ. Eng. Technol.*, vol. 7, no. 5, pp. 329–336, 2016, doi: 10.9790/9622-0705024044.
[2] E. Ferrier and A. Agbossou, "Temperature effects on the shear capacity of external bonded fiber reinforced polymer on concrete," *Constr. Build. Mater.*, vol. 152, pp. 333–344, 2017, doi: 10.1016/j.conbuildmat.2017.07.002.
[3] V. Afroughsabet, L. Biolzi, and T. Ozbakkaloglu, *High-performance fiber-reinforced concrete: a review*, vol. 51, no. 14. Springer US, 2016. doi: 10.1007/s10853-016-9917-4.
[4] M. Zulqarnain, A. Shahzad, M. T. Amir, and M. Usman, "Effect of Ferrocement Confinement with Silica Fumes on Different Sized Reinforced Concrete Columns," pp. 1–9, 2023.
[5] M. U. Rashid, L. A. Qureshi, and M. F. Tahir, "Investigating flexural behaviour of prestressed concrete girders cast by fibre-reinforced concrete," *Adv. Civ. Eng.*, vol. 2019, 2019, doi: 10.1155/2019/1459314.
[6] A. Lisantono, J. T. Hatmoko, U. Atma, and J. Yogyakarta, "T He C Ompressive S Trength of G Eopolymer C Oncrete M Ade With B Aggase a Sh and M Etakaolin," vol. 10, no. 1, pp. 6–10, 2009.
[7] M. Usman Rashid, "Experimental investigation on durability characteristics of steel and polypropylene fiber reinforced concrete exposed to natural weathering action," *Constr. Build. Mater.*, vol. 250, p. 118910, 2020, doi: 10.1016/j.conbuildmat.2020.118910.
[8] H. Nosheen, L. A. Qureshi, M. F. Tahir, and M. U. Rashid, "An Investigation on Shear Behavior of Prestressed Concrete Beams Cast by Fiber Reinforced Concrete," *Arab. J. Sci. Eng.*, vol. 43, no. 10, pp. 5605–5613, 2018, doi: 10.1007/s13369-018-3243-x.
[9] N. Banthia and R. Gupta, "Influence of polypropylene fiber geometry on plastic shrinkage cracking in concrete," *Cem. Concr. Res.*, vol. 36, no. 7, pp. 1263–1267, 2006, doi: 10.1016/j.cemconres.2006.01.010.
[10] R. Garg and R. Garg, "Performance evaluation of polypropylene fiber waste reinforced concrete in presence of silica fume," *Mater. Today Proc.*, vol. 43, pp. 809–816, 2020, doi: 10.1016/j.matpr.2020.06.482.
[11] A. ASTM C150, "Astm C-150," *Stand. Specif. Portl. Cem.*, pp. 1–8, 2007, [Online]. Available: www.astm.org,
[12] American Society for Testing and Materials, "ASTM C33- 03 : Standard Spesification for Concrete Aggregate," *ASTM Stand. B.*, vol. 04, pp. 1–11, 2001.
[13] "ilide.info-astm-c494-19-pr_fb2434fde5e8c77c74f8d6de1d59fbdb.pdf."
[14] S. T. Method, "iTeh Standards iTeh Standards Document Preview," vol. 08, no. Reapproved 1989, pp. 3–4, 2000, doi: 10.1520/C1709-18.
[15] C. C. Test, T. Drilled, C. Concrete, and B. Statements, "Standard Test Method for," pp. 2–6, 2009.

EXPERIMENTAL STUDY ON THE PERFORMANCE OF DATE PALM SURFACE FIBER REINFORCED CONCRETE UNDER ACIDIC CONDITION

[a] Asad Kareem, [b] Syed Saqib Mehboob*

a: Civil Engineering Department, University of Engineering and Technology, Taxila, Pakistan. asadkarim599@gmail.com
b: Civil Engineering Department, University of Engineering and Technology, Taxila, Pakistan. syed.saqib@uettaxila.edu.pk
* Corresponding author

Abstract- This study evaluates the performance of concrete reinforced with date palm fiber (DPF) as a sustainable and cost-effective alternative to conventional concrete. The experimental program investigates the effects of varying water-to-cement (W/C) ratios (0.60, 0.64, 0.68, and 0.72), DPF content levels (3%, 5%, 7%, and 9% by weight of cement), and cement types on the mechanical strength and acid resistance of concrete. A total of sixteen mix designs were developed and tested for compressive and split tensile strength under standard curing, as well as after 28 days of exposure to a 5% sulfuric acid solution. The results show that lower W/C ratios (0.60–0.64) lead to improved strength characteristics, possibly due to a denser microstructure and reduced void content. Incorporation of DPF at 3%–7% resulted in moderate strength enhancement, which may be attributed to improved internal reinforcement provided by the fibers. However, at 9% DPF content, fiber agglomeration and reduced workability likely contributed to a decline in strength. Acid exposure caused a noticeable reduction in strength across all mixes, with mixtures containing higher W/C ratios and higher fiber contents being more vulnerable. Mixes with W/C ratios of 0.60–0.64 and DPF contents of 5%–7% demonstrated comparatively better retention of mechanical properties under acidic conditions. These findings highlight the potential of optimized DPF-reinforced concrete as a sustainable material for use in aggressive environments such as sewage systems and industrial floors, provided that fiber dosage and mix proportions are carefully selected.

Keywords- Date Palm Fiber, Acid Resistance, Water-Cement Ratio, Durability, Sulfate Attack

1 Introduction

Researchers have started looking to promote the usage of alternative and eco-friendly building materials that are less expensive due to industry's negative environmental effects and the steadily rising cost of construction supplies. Although concrete has a high compressive strength, it is brittle and weak under tension. [1]. Steel reinforcement has long been employed to withstand tensile loads. However, because of the high permeability of reinforced concrete, steel is expensive and extremely susceptible to corrosion. The possibility of using plant wastes in concrete as fiber reinforcements, aggregate substitutes, or cement substitutes has been the subject of numerous investigations [2]. Numerous natural fibers have been studied in the past, including bamboo, kenaf, flax (linseed), sugarcane bagasse, coconut coir, hemp, oil palm fiber, banana fiber, ramie, abaca (Manila hemp), sisal, henequen, wheat straw, cotton, jute, eucalyptus fiber, rice straw, corn stalk, and pineapple leaf fiber (PALF)[3]. When low-cost building is required in underdeveloped nations, natural fibers are particularly well-suited for utilization. Natural fibers in concrete have generally been found to improve post-cracking performance, toughness, and fracture resistance. [4]. Utilization of date palm fiber in concrete has also been the subject of numerous investigations. Which are widely distributed in hot, arid regions of the world, particularly date palm is widely

cultivated in regions such as the Middle East, North Africa, the Canary Islands, India, Pakistan, and the southern parts of the United States. [5].

With tensile strengths ranging from 170 to 300 MPa, the male date palm surface fiber (MDPSF) exhibits the highest tensile strength [6]. MDPSF improves concrete's compressive, flexural, ductile, and crack resistance. Fiber length does not affect modulus of elasticity, however excessive fiber quantity reduces compressive and flexural strengths. Increased fiber content and length lower concrete density and heat conductivity [7]. Previous studies suggest that MDPSF in concrete should have a fiber length of 2-5 cm and a mass percentage of 0.5%, however mechanical performance varies. Faesal Alatshan et al. [8] examined how MDPSF affects concrete mechanical characteristics. They found that fiber diameter affected surface void distribution and that MDPSF increased flexural strength. Compressive strength was highest with 50 mm fibers at 0.5%. Fiber length and mass percentage greatly affect ultrasonic speed, compressive strength, and flexural strength, hence the authors recommended more MDPSF concrete curing studies in hot-dry regions. Future research on fiber diameter dispersion and concrete behavior was also suggested.

Ordinary Portland Cement (OPC) is highly alkaline with a pH above 12. When it contacts acids, its compounds break down, causing an acid attack. This can lead to cracks and surface damage, especially under water pressure. Concrete durability against acids depends on materials, curing, and workmanship. Acid attacks occur in environments like acid rain, sewers, factories, or chemical spills. In reality, concrete is usually exposed to diluted or mixed acids over varying periods, from seconds to years [9]. There is no prior research on acid attack resistance of concrete reinforced with date palm fibers, especially against H_2SO_4 and HCl. The results of this study can help improve the durability and service life of structures exposed to acidic environments.

SEM investigation of four acid-exposed concrete mixes by Emmanuel K. et al. [10] showed that volume growth and density decrease were greater at lower pH. Beulah and Prahallada [11] examined the effects of substituting 20% cement with metakaolin in hydrochloric acid-exposed high-performance concrete. Increased acid content lowered strength, and Jennite chemicals may have led to degeneration. V. Arivudamai and R. Velkennedy [12] tested artificial sand, silica fume, and coconut shell fiber-reinforced concrete under acid assault. Adding up to 3% fibers (steel, coir, sisal) increased acid and cracking resistance. Blessen Skariah Thomas et al. [13] tested acid-exposed rubberized concrete. More crumb rubber increased water absorption, but rubberized concrete lost less weight following acid exposure than traditional mixtures, indicating higher acid resistance. These investigations show that material alteration improves concrete's acidic performance. Despite extensive research, DPSF-reinforced concrete has not been studied against acid assault, particularly against H_2SO_4 and HCl. This is a critical research gap because DPSF might be employed in eco-friendly, low-cost building, especially in hot areas. DPSF in construction could promote sustainable development while improving building durability and energy efficiency. Concrete is alkaline, making it susceptible to acid assault in chemical plants, sewers, and acid rain. Acid attack causes significant cracking, mass loss, and disintegration, especially when the structure is under persistent water pressure. The purpose is to determine how acids, concentrations, and exposure times affect DPSF concrete compressive strength.

This research is focused on understanding how acid exposure affects fiber-reinforced concrete, particularly concrete that incorporates natural fibers such as date palm surface fibers (DPSF). The study will investigate how acid attack influences the compressive strength of DPSF-reinforced concrete. To strengthen the findings, the study will also examine the role of three key mix design variables: water-cement ratio, cement content, and fiber dosage. The ultimate goal is to enhance the service life of concrete structures in corrosive environments by investigating the use of natural, sustainable reinforcing.

2 Research Methodology

2.1 Mix Design and Material Proportions

A total of sixteen concrete mix designs were developed using a consistent volumetric ratio of 1:1.54:2.85 for cement, fine aggregate, and coarse aggregate, respectively. The experimental program incorporated four types of cement, four levels of date palm fiber content, and four different water-cement (w/c) ratios achieved through 3" fresh concrete slump test (ASTM C143) at four different fiber content [14]. These variables were systematically rotated and combined to assess their interactive effects on concrete performance. The w/c ratios were established through preliminary testing to ensure uniform workability, targeting a slump of approximately 3 inches for each fiber level. Once determined, these ratios were

strategically distributed among the various mix designs. Each mix was assigned a unique code for identification and subsequently tested for key mechanical properties. The resulting data were analyzed to identify performance patterns and determine the most effective material combinations.

Table 1 Four level mix design: Cement: Fiber Addition DPSF content

Factors	Level 01	Level 02	Level 03	Level 04
A. Cement (Kg/m³)	399.08	390.86	382.62	374.40
B. Fiber Addition (%)	3	5	7	9
C. W/C	0.60	0.64	0.68	0.72

The experimental program was carefully structured to ensure a systematic investigation to assess key mechanical properties such as compressive strength and tensile strength, along with durability characteristics. Specimens were tested both in a controlled laboratory environment and after being subjected to an aggressive chemical environment (ASTM C267) using a 5% sulfuric acid solution, by practices commonly adopted in previous studies [15] [16]. The goal was to evaluate the potential of DPF-reinforced concrete for improved sustainability and durability in corrosive conditions.

2.2 Experimental Design

The experimental program consisted of sixteen concrete mix designs, developed through a systematic combination of three key input parameters: four types of cement, four levels of date palm fiber (DPF) content (3%, 5%, 7%, and 9% by weight of cement), and four water-cement (w/c) ratios. Each sample in this study is identified using a code in the format S-XYZ, like S-111 etc., where each letter represents a specific experimental factor. In this format, X indicates the cement weight or level, Y refers to the content level of date palm fiber (DPF), and Z corresponds to the water-to-cement (W/C) ratio level. Each of these factors has four levels, labeled from 1 to 4. For example, a sample labeled S-212 would represent cement 390.86 Kg/m³, DPF content level 1 (3%), and a W/C ratio level 2 (0.64). Detailed descriptions of these levels for each factor are provided in Table 1 for further clarity. The mix proportions were carefully adjusted to maintain consistent workability, targeting a slump of approximately 75 mm. Each mix was assigned a distinct code to ensure proper identification during the preparation, curing, and testing phases.

Table 2 Mix design matrix showing combination of cement type, fiber content and w/c ratio

Sr No	Mix ID	Cement Type((Kg/m³)	Fiber Content (%)	W/C Ratio
1	S-111	399.08	3	0.60
2	S-212	390.86	3	0.64
3	S-313	382.62	3	0.68
4	S-414	374.40	3	0.72
5	S-122	399.08	5	0.64
6	S-223	390.86	5	0.68
7	S-324	382.62	5	0.72
8	S-421	374.40	5	0.60
9	S-133	399.08	7	0.68
10	S-234	390.86	7	0.72
11	S-331	382.62	7	0.60
12	S-432	374.40	7	0.64
13	S-144	399.08	9	0.72
14	S-241	390.86	9	0.60
15	S-342	382.62	9	0.64
16	S-443	374.40	9	0.68

2.3 Concrete Preparation, Mixing, Casting, and Curing Method

2.3.1 Material Preparation

All constituent materials cement, fine aggregate (natural river sand), coarse aggregate (crushed stone aggregate), potable water, and date palm fibers (DPF) were prepared and inspected prior to mixing. Fine and coarse aggregates were cleaned to remove dust, clay, and organic impurities to prevent adverse effects on concrete bonding and strength development. Date palm fibers were manually cleaned and cut to uniform lengths ranging from 25 mm to 37 mm, based on optimum dispersion criteria [17]. The processed fibers were air-dried and stored in moisture-free conditions prior to batching.

2.3.2 Mixing Procedure

Mixture for all concrete batches were prepared using a pan-type concrete mixer located in material lab. Cement, sand, and coarse aggregate were first placed into the mixer and mixed in dry condition for 2 to 3 minutes to ensure a homogeneous distribution of dry materials. Date palm fiber were gradually added into the dry mix to prevent clumping and ensure uniform dispersion. The required quantity of water was added gradually while continuously mixing the concrete. An additional 3 to 5 minutes of mixing followed after water addition to ensure uniform consistency and fiber distribution throughout the matrix.

2.3.3 Casting Procedure

Fresh concrete was poured into standardized metallic molds in three uniform layers following ASTM C192. Each layer was properly compacted manually using a tamping rod (25 tamping rod strokes per layer) to remove air voids. Upon placing the final layer, the top surface was levelled and finished with a trowel to ensure a smooth, flush finish. [18]

2.4 Sample Preparation and Testing

2.4.1 Cube Specimens

A total of 96 cube samples, each having dimensions of (100 × 100 × 100) mm, were cast to evaluate the compressive strength and were cured at 23 ± 2°C for 28 days [19]. Three specimens of each code were tested for compressive strength [20] using compressive testing Machine. Another set of three cubes per mix design was subjected to chemical degradation assessment. These specimens were also cured in water for 28 days, followed by 28 days of immersion in a 5% sulfuric acid (H_2SO_4) solution. After acid exposure, the same testing protocol was applied. Notably, acid was added to water slowly, never the reverse, to prevent violent exothermic reactions and splashing hazards.

2.4.2 Cylinder Specimen

To evaluate the split tensile strength, a total of 96 cylindrical specimens (D100 mm and H200 mm) were cast. For each mix of sixteen mix design, three specimens were tested after 28 days of water curing under normal conditions, and three specimens were tested after immersion in a 5% sulfuric acid solution for 28 days, following an initial water curing period. [21]

3 Results

3.1 Compressive Strength: Interpretation of Results

3.1.1 Influence of Water-to-Cement Ratio (W/C)

The water-to-cement (w/c) ratio plays a critical role in determining the density, porosity, and overall strength of concrete. Mixes with lower w/c ratios (e.g., 0.60–0.64) tend to exhibit a denser and more compact microstructure, which enhances compressive strength and long-term durability. As the w/c ratio increases (e.g., from 0.64 to 0.72), the excess water leaves behind capillary pores upon evaporation, resulting in a more porous matrix and weaker interfacial transition zones (ITZ). This reduction in matrix integrity becomes especially detrimental under aggressive environmental conditions, such as acid exposure, where porous concrete is more vulnerable to chemical attack and strength degradation.

3.1.2 Effect of Date Palm Fiber (DPF) Content

Incorporating date palm fiber (DPF) into the concrete matrix demonstrated a dual effect depending on the dosage level. At moderate fiber contents (3–7% by weight of cement), DPF contributes positively by enhancing internal bonding and acting as crack-bridging elements. These fibers help arrest microcrack propagation, leading to better load distribution and improved compressive strength.

However, when the fiber content increases to 9%, the benefits begin to reverse. Excessive fiber loading can cause dispersion issues, leading to clumping and uneven fiber distribution. This, combined with reduced workability, introduces voids and weak regions within the matrix. As a result, the overall compressive strength declines due to poor compaction and increased heterogeneity in the concrete structure.

3.1.3 Response to Acid Exposure

Exposure to sulfuric acid significantly affects the performance of concrete, particularly in mixes with higher porosity. Acidic environments attack the cementitious matrix by leaching calcium hydroxide ($Ca(OH)_2$) and other soluble compounds, weakening the matrix and promoting surface erosion. Mixes with higher w/c ratios are more susceptible due to their permeability, resulting in greater strength loss over time.

Conversely, fiber-reinforced mixes with lower w/c ratios displayed better resistance to acid attack. The denser matrix limits acid penetration, while the presence of DPF helps maintain structural cohesion even under chemically aggressive conditions. This combination of physical densification and fiber-induced toughness contributes to improved acid resistance and lower strength degradation compared to more porous, fiber-free counterparts.

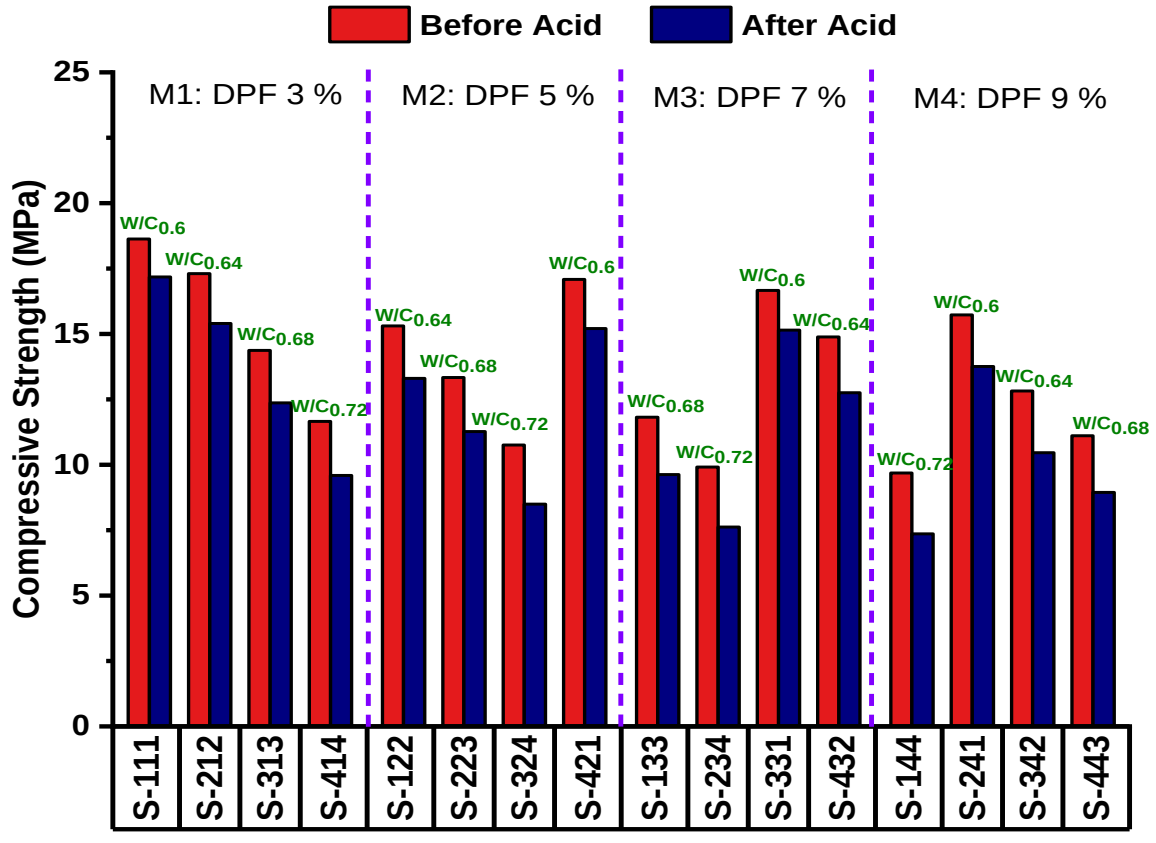


Figure 1: Compressive strength of DPF-reinforced concrete at varying DPF and W/C ratio

3.2 Tensile Strength: Interpretation of Results

3.2.1 Influence of Water-to-Cement Ratio (W/C)

The results indicate that tensile strength decreases consistently with the increase in water-cement (W/C) ratio from 0.60 to 0.72. A lower W/C ratio (0.60) produced higher tensile strength due to improved matrix density and reduced porosity, while higher W/C ratios resulted in weaker bonding and higher permeability, adversely affecting strength.

3.2.2 Effect of Date Palm Fiber (DPF) Content

Tensile strength improved with increasing DPF content up to 7%, attributed to effective crack bridging and fiber reinforcement. However, further increase to 9% led to a decline in strength due to fiber agglomeration, reduced workability, and the formation of voids within the matrix. This highlights 7% DPF as the optimum dosage for tensile performance.

3.2.3 Response to Acid Exposure

All mixes experienced a reduction in tensile strength after acid exposure. The strength loss was more significant in mixes with higher W/C ratios and higher DPF content, particularly at 9%, due to increased porosity facilitating acid ingress. Mixes incorporating a lower W/C ratio (0.60–0.64) and moderate DPF content (5–7%) demonstrated superior resistance against acid attack, retaining higher tensile strength post-exposure.

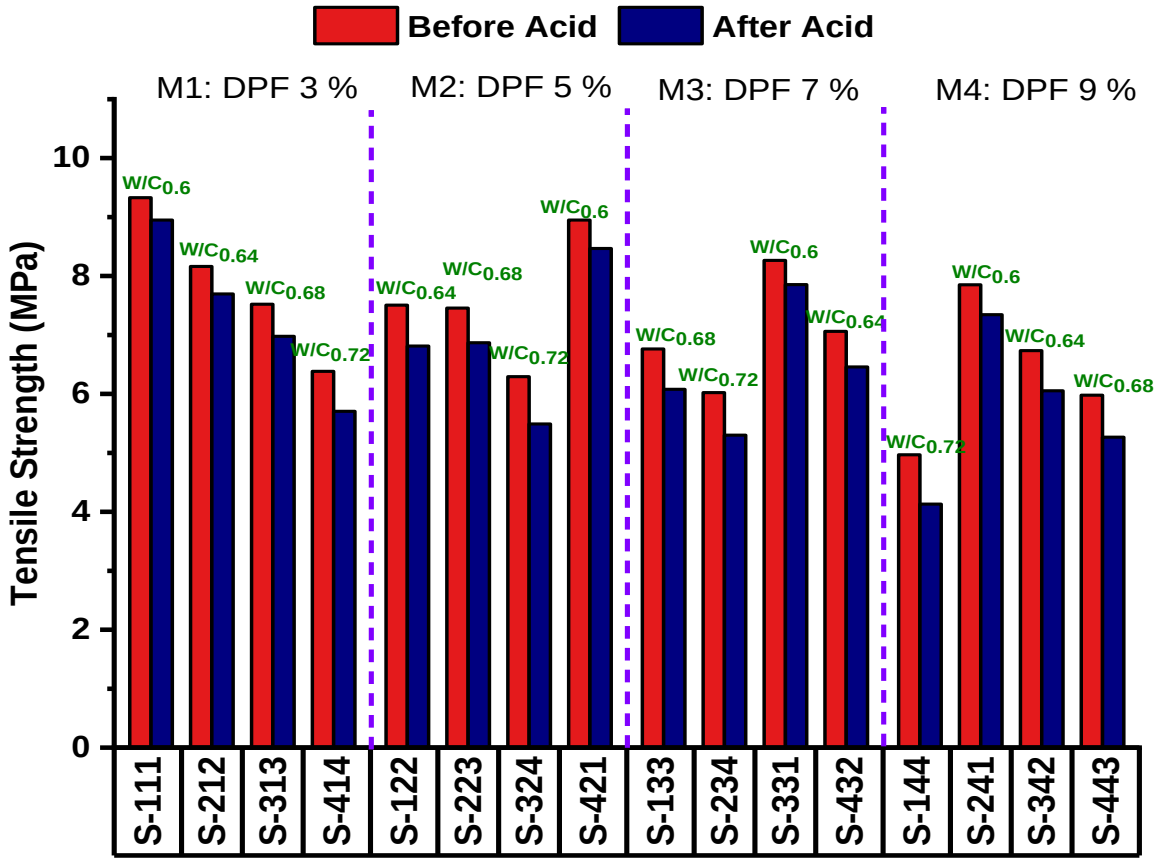


Figure 2: Tensile strength of DPF-reinforced concrete at varying of DPF-reinforced concrete at varying DPF and W/C ratio

4 Practical Implementation

The practical implementation of this study is that using a lower water-cement ratio (0.60–0.64) combined with 5–7% date palm fiber can produce concrete with higher strength, lower permeability, and better acid resistance. This is particularly beneficial for structures exposed to aggressive environments, such as industrial floors, sewage systems, and water treatment plants. However, using a higher fiber content (9%) or a higher W/C ratio can negatively impact strength and durability.

5 Conclusion

The following conclusions can be drawn from the conducted study:

1 Lower W/C ratios (0.60–0.64) significantly improved compressive and tensile strength due to reduced porosity and denser microstructure.
2 Moderate DPF content (3%–7%) enhanced strength and durability; 9% led to reduced performance due to fiber clumping and poor workability.
3 Mixes with low W/C and 3%–5% DPF showed superior resistance to acid attack and retained better mechanical properties.

Acknowledgment

The authors sincerely thank the lab staff of UET Taxila for their continuous support during this research work. The careful review and constructive suggestions by the anonymous reviewers are gratefully acknowledged.

References

[1] L. T. T. Vo and P. Navard, "Treatments of plant biomass for cementitious building materials - A review," Constr. Build. Mater., vol. 121, pp. 161–176, 2016.
[2] K. H. Mo, T. U. Mohammed, M. Z. Jumaat, and U. J. Alengaram, "Green concrete partially comprised of farming waste residues: A review," J. Cleaner Prod., vol. 117, pp. 122–138, 2016.
[3] A. Laborel-Préneron, E. Aubert, C. Magniont, C. Tribout, and P. Bertron, "Plant aggregates and fibers in earth construction materials: A review," Constr. Build. Mater., vol. 111, pp. 719–734, 2016.
[4] J. Claramunt, A. Ventura, L. Fernández-Carrasco, and P. Ardanuy, "The hornification of vegetable fibers to improve the durability of cement mortar composites," Cem. Concr. Compos., vol. 33, no. 5, pp. 586–595, 2011.
[5] Dates (Global Research Report), "Dates Market Overview," 2014. [Online]. Available: http://mcegypt.me/wp-content/uploads/2014/07/Dates-full-report-final.pdf
[6] A. Kriker, A. Debicki, M. Bali, and J. M. Khenfer, "Mechanical properties of date palm fibers and concrete reinforced with date palm fibers in hot-dry climate," Cem. Concr. Compos., vol. 27, no. 5, pp. 554–564, 2005.
[7] A. Djoudi, A. Kriker, M. Bali, and A. Debicki, "Performance of date palm fibers reinforced plaster concrete," Int. J. Phys. Sci., vol. 7, no. 21, pp. 2845–2853, 2012.
[8] F. Alatshan, M. R. Karim, and H. M. Samadi, "Effect of date palm fibers on the mechanical properties of concrete," Int. J. Sustainable Build. Technol. Urban Dev., vol. 8, no. 2, pp. 68–80, 2017.
[9] S. Umale and G. V. Joshi, "Study of effect of chemicals (acid) attack on strength and durability of hardened concrete," Int. Res. J. Eng. Technol. (IRJET), vol. 4, no. 6, pp. 548–552, 2019.
[10] E. K. Emmanuel, "Response of concrete to sulfuric acid attack," ACI Mater. J., vol. 85, no. 6, pp. 481–488, 1988.
[11] M. Beulah and M. C. Prahallada, "Effect of replacement of cement by metakaolin on the properties of high performance concrete subjected to hydrochloric acid attack," Int. J. Eng. Res. Appl., vol. 2, no. 6, pp. 33–38, Nov.–Dec. 2012.
[12] V. Arivudamai and R. Velkennedy, "Acid attack on hybrid fiber reinforced high strength concrete with manufactured sand and coconut shell," J. Adv. Chem., vol. 12, no. 27, pp. 5825–5828, 2017.
[13] B. S. Thomas, R. C. Gupta, and P. Kumar, "Resistance to acid attack of cement concrete containing discarded tire rubber," in Proc. UKIERI Concrete Congress - Concrete Research Driving Profit and Sustainability, 2016, pp. 1235–1244.
[14] ASTM C143/C143M-20, Standard Test Method for Slump of Hydraulic-Cement Concrete, ASTM International, West Conshohocken, PA, 2020..
[15] ASTM C267-20, Standard Test Method for Chemical Resistance of Mortars, ASTM International, West Conshohocken, PA, USA, 2020
[16] E. K. Emmanuel, A. N. Ede, and S. O. Oyebisi, "Durability performance of concrete under acidic environment," International Journal of Scientific & Engineering Research, vol. 10, no. 5, pp. 1310–1315, May 2019.
[17] M. Ismail and K. Hashim, "Experimental investigation of date palm fiber reinforced concrete using treated and untreated fibers," Chemical Engineering Transactions, vol. 94, pp. 1159–1164, 2022. DOI: 10.3303/CET2294195

[18] M. Ismail and K. Hashim, "Experimental investigation of date palm fiber reinforced concrete using treated and untreated fibers," Chemical Engineering Transactions, vol. 94, pp. 1159–1164, 2022. DOI: 10.3303/CET2294195

[19] ASTM C192/C192M-19, Standard Practice for Making and Curing Concrete Test Specimens in the Laboratory, ASTM International, West Conshohocken, PA, 2019.

[20] ASTM C39/C39M-18, Standard Test Method for Compressive Strength of Cylindrical Concrete Specimens, ASTM International, West Conshohocken, PA, 2018.

[21] ASTM C496/C496M-17, Standard Test Method for Splitting Tensile Strength of Cylindrical Concrete Specimens, ASTM International, West Conshohocken, PA, 2017

A REVIEW ON OPTIMIZING SUSTAINABLE CRACK CONTROL IN SLABS USING COTTON FIBER COMPOSITES

[a] Mobeen Anwar*, [b] Sadia Sajid Khan
a: Structural Designing, Niazi Design Systems, Islamabad, Pakistan. mobeenanwer94@gmail.com
b: Design and Estimation Department, Kinetic International FZE, UAE. sadialohani@hotmail.com
* Corresponding author

Abstract- Cracking in the base slabs of slabs poses a serious threat to both structural stability and long-term waterproofing performance i.e. Swimming Pools. These cracks commonly arise from early-age shrinkage, thermal expansion and contraction, subgrade settlement, and flexural stress during service life. Traditional concrete lacks the tensile strength and ductility needed to resist these failure modes effectively. Cotton fiber-reinforced concrete (CFRC) has emerged as an eco-friendly, sustainable solution to these challenges by enhancing crack resistance, improving tensile behavior, and promoting internal curing. The fibers not only bridge microcracks but also delay their propagation, thereby extending the service life of concrete structures. This paper provides a detailed assessment of CFRC performance under various stress conditions and failure modes, such as shrinkage-induced cracking and load-induced fracture. A comparative evaluation with conventional synthetic and metallic fibers, namely steel and polypropylene, is also conducted to highlight CFRC's structural and environmental advantages. Furthermore, the study presents real-world applications of CFRC in concrete works and emphasizes the significance of utilizing cotton waste derived from the spun lace process. This process, which eliminates chemical waste associated with traditional cotton treatments, offers a circular economic approach by integrating textile by-products into construction materials. Overall, CFRC presents a promising avenue for enhancing durability and sustainability in modern infrastructure, particularly in water-retaining structures like swimming pools.

Keywords- Crack Control, Fiber-Reinforced Concrete (FRC), Ductility, Shrinkage, Cotton Fiber

1 Introduction

All Shell elements are highly susceptible to cracking and long-term deterioration due to the combined effects of complex mechanical loading and environmental fluctuations, which impose challenging stress conditions throughout their service life. These slabs often experience early-age thermal gradients caused by the heat of hydration and ambient temperature variations, resulting in differential shrinkage and internal tensile stresses before the concrete develops adequate tensile strength to resist them. Additionally, plastic and drying shrinkage during curing can lead to microcracks, especially if curing practices are inconsistent, while uneven settlement or poor compaction of the sub-base materials creates localized stress concentrations that further increase the risk of crack initiation under operational loads. The inherently brittle nature and low tensile strength of conventional concrete make tensile zones within these slabs particularly vulnerable to cracking from bending moments, hydrostatic pressures, and dynamic loads typical of swimming pool environments. In water-retaining structures, such cracks not only threaten structural stability but also compromise waterproofing, leading to leaks that can cause soil erosion, foundation destabilization, and corrosion of embedded reinforcement, ultimately accelerate deterioration and necessitate costly repairs [1,2,3,4]. Moreover, irregular subgrade support and constraints against natural volume changes induce restraint-related cracks that propagate through the slab, allowing moisture ingress and further structural damage under cyclic loads [5,6]. These factors collectively reduce service life, increase maintenance demands, and elevate lifecycle costs, underscoring the critical need for advanced reinforcement methods and crack control strategies

to enhance the tensile behavior, durability, and watertight performance of swimming pool base slabs in demanding service conditions.

To address these concerns, fiber-reinforced concrete (FRC) has emerged as an effective composite material designed to enhance the tensile performance of conventional concrete, control crack widths, and improve overall fracture toughness [7]. The introduction of discrete fibers within the cementitious matrix allows for better stress redistribution and significantly increases the material's ability to carry loads even after cracking has initiated, which helps mitigate problems associated with early-age shrinkage, restrained deformations, and brittle failure modes [7,8,9]. A wide range of fiber types has been studied for their reinforcing effectiveness, including steel fibers known for their high tensile strength, synthetic fibers like polypropylene prized for their chemical resistance, and glass fibers that contribute to both structural and architectural applications. In recent years, however, there has been growing interest in the use of natural fibers as a sustainable alternative due to their renewable nature, widespread availability, biodegradability, cost-effectiveness, and substantially lower environmental impact compared to conventional synthetic or metallic fibers [10,11]. As research continues to expand, natural fibers such as jute, sisal, coir, and cotton are increasingly being explored for structural and semi-structural concrete applications, supporting the development of greener and more resilient construction materials.

Among fibers, cotton particularly when sourced from post-consumer or post-industrial textile waste presents significant promise as an environmentally responsible reinforcement material for concrete applications. Cotton fibers are predominantly composed of cellulose, which imparts them with favorable tensile properties and a naturally rough surface texture that promotes strong mechanical interlocking with the surrounding cement paste, thereby enhancing the fiber–matrix bond [12,13]. Another notable advantage of cotton fibers is their high-water absorption capacity, which enables them to act as internal curing agents; they can absorb excess mix water during batching and gradually release it during hydration, helping to maintain internal moisture levels and mitigate the development of shrinkage-induced tensile stresses during the critical early stages of curing [14,15]. This internal curing effect fosters a more uniform and complete hydration process, which reduces the risk of autogenous and drying shrinkage cracking that can otherwise compromise durability [16,17]. Additionally, the presence of cotton fibers contributes to improved crack distribution by bridging microcracks and promoting the formation of finer, more uniformly dispersed cracks rather than wide, isolated cracks. This refined crack pattern not only enhances the structural resilience of the concrete under service loads but also contributes to improved long-term durability and reduced maintenance needs, aligning well with sustainable construction goals [18,19,20,21].

This paper adopts a performance-based analytical framework to systematically evaluate the potential of cotton fiber-reinforced concrete (CFRC) in reducing crack formation and controlling crack propagation in swimming pool base slabs, which are particularly vulnerable to various cracking mechanisms. The study specifically examines the primary causes of cracking—plastic shrinkage, drying shrinkage, thermal stresses, and flexural loading and analyzes how the inclusion of cotton fibers mitigates these issues through effective fiber bridging and enhanced internal curing behavior. A comparative analysis is carried out between CFRC and other commonly used fiber-reinforced concrete systems, such as those incorporating steel or synthetic fibers, focusing on key performance metrics including mechanical strength, durability parameters, crack control effectiveness, and environmental sustainability indicators. Based on the analytical findings, the paper offers practical recommendations for incorporating cotton fibers into concrete mix design, detailing considerations such as fiber dosage, mixing techniques, and curing practices to optimize structural behavior without compromising workability. By highlighting the dual benefits of improved crack resistance and sustainable material use, the paper aims to guide engineers and practitioners in adopting CFRC for reinforced concrete applications in hydraulic and aquatic infrastructure where long-term durability, watertightness, and environmental responsibility are critical design priorities.

2 Mechanisms of Crack Formation in Swimming Pool Slabs

Concrete cracking is a complex and multifactorial phenomenon that arises due to a combination of internal volumetric changes and externally imposed mechanical and environmental stresses [22]. In reinforced concrete base slabs constructed for swimming pool structures required to retain water under continuous loading and exposure, several types of cracking are commonly encountered. These cracks, if not effectively controlled, significantly reduce serviceability and compromise impermeability, leading to leakage, reinforcement corrosion, and eventual deterioration of structural integrity [22]. One of the earliest forms of cracking is plastic shrinkage cracking, which occurs within the first few hours following concrete placement. These cracks develop when the rate of surface moisture evaporation exceeds the rate at which bleed water rises

to the surface, creating tensile stresses in the weak plastic matrix [22,23]. Such conditions are exacerbated in hot, dry, or windy environments and are especially critical in wide, shallow elements such as slabs. Thermal cracking arises from non-uniform temperature changes, particularly between the surface and the inner core of large volume concrete elements. When temperature differentials exceed the tensile capacity of the concrete, restraint against thermal expansion or contraction leads to cracking. This is especially problematic in slabs without adequate thermal curing measures [24,25].

Settlement cracking is another early-age issue, resulting from the differential settlement of the concrete around embedded reinforcements or obstructions. These cracks typically form due to insufficient consolidation or poorly supported formwork, leading to localized discontinuities in the concrete mass [26]. In the hardened state, flexural cracking is a prevalent mode of distress, particularly in the tensile zone at the bottom of the slab where bending moments are highest under service loads. These cracks occur when the flexural tensile stress induced by external loads exceeds the modulus of rupture of the concrete [27,28]. Additionally, shear cracking, often observed near slab support or transitions, arises due to diagonal tension resulting from high shear forces. These cracks typically propagate at an angle and can compromise both strength and stiffness if left unaddressed [29]. The presence and progression of these various crack types directly impact the durability, impermeability, and service life of swimming pool slabs. Therefore, selecting and engineering a concrete mixture that can resist these cracking mechanisms is critical. Materials with improved tensile strength, ductility, and early-age crack mitigation capacity, such as fiber-reinforced concrete [30], are particularly beneficial in this application. By enhancing post-crack load resistance and providing a bridge across potential crack planes, fiber-reinforced systems contribute to reduced crack widths and improved structural resilience under both restrained and service conditions [31,32].



***Figure 1**: Presence of flexural cracks in slab Mydin [33]*

3 Performance Attributes of Cotton Fiber-Reinforced Concrete (CFRC)

The integration of cotton fibers into concrete mixtures for swimming pool slab construction introduces both performance benefits and implementation challenges that must be addressed to ensure structural and functional efficacy. Cotton, being a cellulosic natural fiber, has a high affinity for water due to its porous morphology and internal capillary structure [30]. This hydrophilic nature makes the fibers prone to absorbing free water from the surrounding cementitious matrix, which can inadvertently alter the effective water-to-cement (w/c) ratio, delay hydration reactions, and reduce early-age strength gain. To mitigate this, a pre-conditioning process is recommended in which cotton fibers are pre-wetted to achieve a saturated surface-dry (SSD) state. This strategy prevents excessive absorption during mixing and ensures that water content calculations remain consistent with the intended design parameters [34,35]. Proper moisture conditioning of fibers not only stabilizes fresh properties but also supports uniform hydration kinetics essential for durable concrete. Maintaining adequate workability in cotton fiber-reinforced concrete poses another challenge. Cotton fibers, when added in significant volume fractions, tend to decrease the slump and flow characteristics of the mix due to their physical obstruction and water retention behavior [36]. This reduction in workability can lead to difficulties in placement, compaction, and surface finishing factors critical to the performance of large slab elements such as swimming pool bases. To address this issue, the incorporation of chemical admixtures, particularly polycarboxylate-based high-range water reducers (HRWR), is strongly advised. These admixtures improve the dispersion of cement particles, enhance fluidity, and counteract the stiffening effect caused by additional fibers without increasing the w/c ratio, which could otherwise compromise strength and durability [37,38]. Additionally, the use of viscosity-modifying admixtures (VMAs) may further stabilize the fiber-concrete matrix by minimizing segregation and ensuring a cohesive, homogenous mixture during transportation and placement.

Achieving uniform fiber distribution is paramount to realizing the full mechanical and durability potential of CFRC. Improper mixing can lead to clumping or balling of fibers, creating weak zones and inconsistencies in crack control performance. An effective method to ensure uniform dispersion involves the sequential dry blending of fibers with aggregates and cementitious materials before the introduction of mixing water. This technique facilitates even distribution and reduces the likelihood of fiber agglomeration, especially in field-scale mixing scenarios where control over mixing energy and sequence may vary. Advanced mixing protocols, including the use of pan mixers with dual-axis blades or high-shear laboratory mixers, can further improve dispersion and ensure repeatability across batches [39,40].Although cotton fibers aid internal curing by retaining moisture and gradually releasing it to sustain hydration, this mechanism does not eliminate the need for conventional curing practices. Surface evaporation, particularly under high ambient temperatures or wind exposure, can still induce early-age plastic shrinkage cracking if not properly controlled. External curing methods such as the application of wet coverings (e.g., burlap), the use of curing compounds, or continuous water ponding should be rigorously implemented for at least 7 days, depending on environmental conditions and cement type. These curing methods serve to reduce thermal gradients and maintain adequate surface humidity, thereby complementing the internal curing effect of cotton fibers and ensuring consistent development of mechanical properties [41].

Although cotton fibers help with internal curing by holding moisture and slowly releasing it to support hydration, this benefit alone does not replace the need for standard curing practices. Surface evaporation, especially in hot, dry, or windy weather, can still lead to early-age plastic shrinkage cracks if left unmanaged. To avoid this, good external curing such as using wet coverings like burlap, applying curing compounds, or keeping the surface moist through ponding should be carried out for at least seven days, depending on site conditions and cement type. These steps reduce thermal stress and help keep the concrete surface properly hydrated, working together with the internal curing provided by the fibers to ensure the concrete develops strength and durability as intended [41]. While this study highlights swimming pool base slabs, the same cracking issues like shrinkage, thermal movement, settlement, and flexural stress are common to many other concrete elements. For this reason, the combined crack control and sustainability benefits of cotton fiber-reinforced concrete (CFRC) can be applied to a wide range of structures. These include water tanks, reservoirs, and sewage units where watertightness is vital [8]; pavements and ground slabs that need to resist shrinkage cracking [16]; basement floors and retaining walls that face settlement and moisture changes [1]; tunnel linings and precast panels where dimensional stability is important [2]; and bridge decks and overlays that demand added toughness under heavy use [14]. When properly cured and used in these wider applications, CFRC offers designers an effective way to manage cracking while also making use of natural, biodegradable fibers that help balance structural performance with environmental responsibility.

4 Comparative Evaluation with Other Fibers

While cotton fibers offer several benefits, they are not the only option. The comparative evaluation is presented in Table 1, underscoring the multifaceted performance attributes of various fibers used in concrete reinforcement. While cotton fiber does not match the tensile strength or modulus of elasticity exhibited by synthetic alternatives such as steel or polypropylene, it demonstrates distinct advantages in terms of autogenous shrinkage control, internal curing capability, and sustainability. These properties are especially critical in applications such as swimming pool base slabs, where early age cracking due to shrinkage and environmental exposure is a persistent concern. The fibrous morphology of cotton enhances water retention within the matrix, thereby prolonging internal hydration and contributing to volumetric stability during the critical early curing phase [9,34,35].

***Table 1** : Comparative performance of cotton fiber with other commonly used fibers*

Fiber Type	Tensile Strength (MPa)	Flexural Strength (MPa)	Shrinkage Reduction (%)	Durability (Months)	References
Cotton Fiber	25–30	5–10	25–30	12–18	[4,8,12]
Polypropylene Fiber	60–80	10–15	30–35	24–36	[14,21,24]
Steel Fiber	150–200	25–30	15–20	36–48	[16,22,25]
Glass Fiber	70–90	15–20	20–25	18–24	[11,18,23]

From an environmental engineering perspective, cotton fibers, particularly those derived from post-consumer textile waste, introduce significant ecological benefits. Their biodegradability, low embodied energy, and recyclability align well with sustainable construction objectives outlined in green building standards and circular economy frameworks. In contrast, synthetic fibers, while mechanically superior, are energy-intensive to manufacture and contribute to long-term environmental loading if not properly managed at end-of-life stages [21,44,45]. Consequently, cotton serves as a viable alternative in sustainability-focused infrastructure, especially where mechanical demands are moderate, but crack resistance and environmental compatibility are prioritized.

Despite their limitations in tensile performance, cotton fibers can be strategically integrated into hybrid reinforcement systems to enhance overall material performance. Several studies have shown that combining natural fibers with a minor fraction of high-strength synthetic fibers can yield composites that achieve both functional durability and environmental compliance [11,46,47]. In swimming pool slabs, such hybridization strategies allow for cotton fibers to mitigate shrinkage and support internal curing, while steel or polypropylene fibers provide the tensile capacity needed to resist service-induced stresses such as bending and impact loading. This balanced approach optimizes the trade-offs between strength and sustainability, making it particularly suitable for public-use facilities where durability, safety, and ecological considerations must all be addressed in unison.

5 Sustainability Metrics and Lifecycle Considerations

In contemporary civil engineering practice, sustainability has emerged as a paramount criterion guiding the selection and specification of construction materials. Cotton fibers, when utilized as reinforcement in concrete, represent a notably sustainable option due to their inherent environmental advantages [30]. A primary benefit lies in their origin as an abundant and renewable resource, often sourced from post-industrial textile waste or agricultural byproducts, such as cotton stalks and linters, thereby diverting substantial quantities of material from landfills and contributing to waste valorization [9, 48]. This reutilization not only exemplifies effective resource efficiency but also supports the principles of circular economy by transforming what would conventionally be discarded into value-added construction inputs. Moreover, cotton fibers exhibit biodegradability, a critical environmental attribute distinguishing them from commonly used synthetic fibers such as polypropylene or steel, which persist in the environment over extended periods, potentially contributing to microplastic pollution and resource depletion [11,49]. The biodegradation process facilitates eventual mineralization, reducing ecological impact and improving end-of-life management options for fiber-reinforced concrete composites.

Energy consumption associated with fiber production is another key sustainability consideration. The embodied energy of cotton fibers is significantly lower compared to synthetic and metallic fibers, primarily due to less intensive manufacturing processes and reduced reliance on fossil fuels [14,50]. This reduction in energy demand translates directly into decreased carbon emissions during the material lifecycle, contributing to a lower overall environmental footprint for cotton fiber-reinforced concrete. Such attributes are especially beneficial in structural elements like swimming pool slabs, where the performance requirements allow for the substitution of high-energy fibers with natural alternatives without compromising serviceability or durability [4,9].Integrating cotton fibers into concrete not only enhances the material's mechanical and durability characteristics but also aligns strategically with global sustainability frameworks, such as the United Nations Sustainable Development Goals (SDGs) and the principles outlined in LEED and BREEAM green building certification systems [20,51]. By fostering circularity and minimizing resource extraction, cotton fiber-reinforced concrete supports the reduction of greenhouse gas emissions and the mitigation of construction-related environmental impacts [30]. Therefore, its adoption contributes significantly to advancing sustainable construction practices, particularly in infrastructure with moderate structural demands but high longevity and environmental accountability, such as swimming pools and related water-retaining structures.

6 Conclusion and Recommendation

To summarize the key aspects and practical considerations of using cotton fiber-reinforced concrete for swimming pool slabs, the following points highlight its main advantages and requirements:

- Cotton fiber-reinforced concrete (CFRC) enhances tensile behavior, controls early-age cracks, and improves ductility by providing internal curing and effective crack bridging.

- Successful use of CFRC requires careful fiber pre-wetting, optimized mix design, adequate use of plasticizers, and thorough fiber dispersion to maintain workability and uniform performance.
- Sourced from post-consumer textiles, cotton fibers reduce environmental impact, support circular economic goals, and can be combined with other fibers to balance strength and sustainability.

By addressing both technical and environmental demands, cotton fiber-reinforced concrete offers a practical, sustainable solution for improving crack resistance and durability in swimming pool slabs and similar structures. Its dual benefits make it a valuable material innovation for engineers seeking resilient and eco-friendly alternatives in modern concrete construction.

Acknowledgment

The authors would like to thank every person, especially Dr. Majid Ali and the department who provided thorough assistance with the research work.

References

[1] W. Hansen, "Early-age stress development in concrete," *Journal of the American Concrete Institute*, vol. 81, no. 6, pp. 123–129, 1984..
[2] M. H. Zhang and J. P. Weiss, "Shrinkage cracking of restrained concrete slabs," *ACI Materials Journal*, vol. 99, no. 1, pp. 38–44, 2002.
[3] S. Mindess, J. F. Young, and D. Darwin, *Concrete*, 2nd ed., Upper Saddle River, NJ: Prentice Hall, 2003.
[4] A. Bentur and S. Mindess, *Fibre Reinforced Cementitious Composites*, 2nd ed., Boca Raton, FL: CRC Press, 2006.
[5] J. J. Brooks and M. A. Megat Johari, "Early-age thermal cracking in concrete bridge decks," *Construction and Building Materials*, vol. 15, no. 7, pp. 385–392, Oct. 2001.
[6] C. Hall and W. D. Hoff, *Water Transport in Brick, Stone and Concrete*, London: CRC Press, 2002.
[7] S. Maiti, M.R. Islam, M.A. Uddin, S. Afroj, S.J. Eichhorn, N. Karim, Sustainable Fiber-Reinforced Composites: A Review, Advanced Sustainable Systems 6 (2022) 2200258. https://doi.org/10.1002/adsu.202200258.
[8] P. K. Mehta and P. J. M. Monteiro, *Concrete: Microstructure, Properties, and Materials*, 4th ed., New York: McGraw-Hill, 2014
[9] R. Siddique, "Natural fiber reinforced concrete," in *Waste Materials and By-Products in Concrete*, Berlin: Springer, 2008, pp. 163–206.
[10] M. Fraternali et al., "Experimental study of the thermo-mechanical properties of recycled cotton fiber-reinforced concrete," *Composites Part B: Engineering*, vol. 68, pp. 185–191, Jan. 2015.
[11] S. N. Raman and H. Mohd Saman, "The utilization of natural fibers in concrete: A review," *Construction and Building Materials*, vol. 204, pp. 91–105, Apr. 2019.
[12] M. Saikia and S. de Brito, "Use of plastic waste as aggregate in cement mortar and concrete preparation: A review," *Construction and Building Materials*, vol. 34, pp. 385–401, Sep. 2012.
[13] V. M. Malhotra and N. A. Aïtcin, "Internal curing of concrete: Techniques and benefits," *ACI SP-218*, vol. 1, pp. 1–20, 2004.
[14] G. Li et al., "Durability performance of concrete reinforced with recycled cotton fibers," *Materials and Structures*, vol. 53, no. 3, pp. 1–13, Mar. 2020.
[15] F. Qamar, T. Thomas, and M. Ali, "Improvement in lateral resistance of mortar-free interlocking wall with plaster having natural fibres," *Construction and Building Materials*, vol. 234, p. 117387, 2020.
[16] K. A. Muga, M. H. Kamau, and D. O. Opar, "The potential of cotton and sisal fibers in concrete," *Journal of Civil Engineering Research*, vol. 3, no. 5, pp. 142–149, 2013.
[17] G. Campione, D. La Mendola, and L. Minafò, "Steel fiber reinforced concrete in structural applications," *Construction and Building Materials*, vol. 95, pp. 757–766, Oct. 2015.
[18] M. Amin, S. Khan, and T. Jamil, "Crack control in concrete using natural fibers: A review," *Journal of Natural Fibers*, vol. 19, no. 6, pp. 1979–1995, 2022.
[19] S. A. Bernal, J. L. Provis, and R. San Nicolas, "Durability of glass fiber-reinforced concrete: Current knowledge and future research needs," *Cement and Concrete Research*, vol. 107, pp. 37–50, Feb. 2018.
[20] UN Environment Programme, "Greening the construction sector: Sustainable building materials," *UNEP Report*, 2020. [Online]. Available: https://www.unep.org.
[21] C. Meyer, "The greening of the concrete industry," *Cement and Concrete Composites*, vol. 31, no. 8, pp. 601–605, Sep. 2009.
[22] A Valli ,M S R Kumar, Review on the mechanism and mitigation of cracks in concrete, Applications in Engineering Science 16 (2023) 100154. https://doi.org/10.1016/j.apples.2023.100154.
[23] A. R. Khaloo, M. Dehestani, and P. Rahmatabadi, "Mechanical properties of normal strength concrete reinforced with polypropylene and steel fibers," *Construction and Building Materials*, vol. 22, no. 8, pp. 170–179, Aug. 2008.
[24] J. Silfwerbrand, "Cracking in concrete—Causes, prevention and repair," *Nordic Concrete Research*, no. 42, pp. 11–20, 2010.

[25] M. Younis, A. E. Khaled, and F. Al Hattamleh, "Influence of hot and windy environment on early cracking of slabs," *Construction and Building Materials*, vol. 247, pp. 118518, Apr. 2020.
[26] Y. L. Mo and R. P. Dhakal, "Thermal effects on concrete and crack control," *Journal of Advanced Concrete Technology*, vol. 7, no. 1, pp. 89–100, Jan. 2009.
[27] C. D. Johnston, "Fiber-reinforced concrete—Properties and applications," *ACI Journal Proceedings*, vol. 81, no. 5, pp. 343–356, 1984.
[28] M. C. Limbachiya and J. J. Roberts, "Concrete early-age settlement cracking," *Materials and Structures*, vol. 32, pp. 235–244, May 1999.
[29] T. C. Powers, "Mechanisms of shrinkage in portland cement paste," *Journal of the American Ceramic Society*, vol. 41, no. 1, pp. 1–6, 1958.
[30]. P. Rawat, S. Liu, S. Guo, M. Zillur Rahman, T. Yang, X. Bai, Y. Yao, B. Mobasher, D. Zhu, A state-of-the-art review on mechanical performance characterization and modelling of high-performance textile reinforced concretes, Construction and Building Materials 347 (2022) 128521. https://doi.org/10.1016/j.conbuildmat.2022.128521.
[31] E. G. Nawy, *Reinforced Concrete: A Fundamental Approach*, 6th ed., Upper Saddle River, NJ: Pearson, 2008.
[32] A. M. Neville, *Properties of Concrete*, 5th ed., Harlow, UK: Pearson Education Limited, 2011.
[33] B. V. Rangan, "Design of fiber reinforced concrete elements," *Concrete International*, vol. 13, no. 6, pp. 25–32, 1991.
[34] M. H. Balaguru and S. P. Shah, *Fiber Reinforced Cement Composites*, New York: McGraw-Hill, 1992.
[35] Mydin, M. A. O., Nawi, M. N. M., & Munaaim, M. A. C. (2017). Assessment of waterproofing failures in concrete buildings and structures. MCRJ Spec, 2017, 2.
[36] W. Ma, Y. Qin, Y. Li, J. Chai, X. Zhang, Y. Ma, H. Liu, Mechanical properties and engineering application of cellulose fiber-reinforced concrete, Materials Today Communications 22 (2020) 100818. https://doi.org/10.1016/j.mtcomm.2019.100818.
[37] M. Mermerdaş and Y. Toklu, "Effect of pre-wetted cotton fibers on workability and shrinkage behavior of concrete," *Construction and Building Materials*, vol. 280, pp. 122452, Mar. 2021.
[38] K. Bilim and A. Atis, "Effects of pre-soaked natural fibers on concrete shrinkage," *Indian Journal of Engineering & Materials Sciences*, vol. 20, no. 3, pp. 207–214, 2013.
[39] S. Mindess, "Admixtures and concrete durability," in *Developments in the Formulation and Reinforcement of Concrete*, Cambridge: Woodhead Publishing, 2019, pp. 121–139.
[40] M. Ali, "Role of post-tensioned coconut-fibre ropes in mortar-free interlocking concrete construction during seismic loadings," *KSCE Journal of Civil Engineering*, vol. 22, no. 4, pp. 1336–1343, 2018
[41] L. B. Rowell, "Mechanical properties of natural fibers in composites," *Handbook of Engineering Biopolymers*, Munich: Carl Hanser Verlag, 2003, pp. 297–324.
[42] H. K. Lee, M. S. Kim, and Y. S. Kim, "Mixing techniques for fiber reinforced concrete," *Materials Science Forum*, vol. 534–536, pp. 1233–1236, 2007.
[43] ACI Committee 308, *Guide to Curing Concrete*, ACI 308R-01, Farmington Hills, MI: American Concrete Institute, 2001.
[44] H. M. Selmy and M. M. Elmoaty, "Performance of cotton-fiber reinforced concrete overlays for crack control," *International Journal of Civil Engineering and Technology*, vol. 8, no. 9, pp. 1693–1704, 2017.
[45] M. U. Farooqi and M. Ali, "Effect of fibre content on compressive strength of wheat straw reinforced concrete for pavement applications," in *IOP Conf. Ser.: Mater. Sci. Eng.*, vol. 422, no. 1, p. 012014, Sep. 2018.
[46] M. Horvath, "Embodied energy in building materials: A primer," *Green Building Digest*, vol. 16, pp. 1–7, 2004.
[47] M. U. Farooq and R. J. Thomas, "Hybrid fiber reinforced concrete: A review of performance and applications," *Construction and Building Materials*, vol. 265, pp. 120350, May 2020.
[48] T. Liu, J. Hu, and X. Li, "Recycling waste cotton fiber in cement composites: Environmental implications and mechanical performance," *Journal of Cleaner Production*, vol. 221, pp. 768–777, Jun. 2019.
[49] F. Pacheco-Torgal and S. Jalali, "Cementitious building materials reinforced with vegetable fibers: A review," *Construction and Building Materials*, vol. 25, no. 2, pp. 575–581, Feb. 2011.
[50] D. D. L. Chung, "Low-cost carbon fiber reinforced concrete for smart structures," *Smart Materials and Structures*, vol. 12, no. 4, pp. 430–432, 2003.
[51] U.S. Green Building Council, *LEED v4 for Building Design and Construction*, Washington, DC, 2013.

MITIGATING FLEXURAL CRACKS IN CONCRETE BEAMS USING DIVERSE FIBERS: A REVIEW

[a]Jawad Nasar*, [b]M. Haider Mehmood Khattak

a: Askari Heights V, Housing Directorate, Islamabad, Pakistan. jawad100eb@gmail.com
b: University of Calgary, Calgary, Canada. muhammadhaidermehmoo@ucalgary.ca
*Corresponding author

Abstract- Flexural cracking remains a critical challenge in reinforced concrete beams, adversely affecting structural durability and service life. This review investigates the potential of incorporating cotton, glass, and human hair fibers to enhance the flexural performance of concrete. Emphasizing both mechanical behavior and environmental sustainability, the study draws upon 32 peer-reviewed sources published between 2010 and 2025. The selected fibers are evaluated based on tensile properties, crack mitigation capabilities, and applicability in sustainable construction. Comparative analysis reveals that while glass fibers offer superior strength, cotton and human hair fibers present notable benefits in terms of biodegradability and cost-effectiveness. A synthesis of secondary data provides theoretical insight into the fibers' efficacy in resisting flexural stress. The findings support fiber reinforcement as a viable strategy for improving concrete performance while aligning with global sustainability goals.

Keywords- Cotton Fiber, Flexural Cracks, Fiber Reinforced Concrete, Glass Fiber, Human Hair Fiber

1. Introduction

Concrete remains a cornerstone material in modern construction, prized for its high compressive strength, longevity, and accessibility. Nonetheless, its primary limitation is its inadequate tensile strength, making it vulnerable to flexural cracks when subjected to bending stresses [1]. These cracks often initiate in the tension zone of beams and spread upward as the tensile stress surpasses the material's threshold. Over time, such fissures compromise both aesthetics and durability by facilitating the entry of moisture and chlorides, which in turn hasten steel reinforcement corrosion [2]. This degradation can threaten the structural safety and shorten the service life of concrete members. While conventional reinforcement techniques offer partial relief, they may not fully eliminate cracking or might be financially unfeasible for certain projects. As a result, researchers are increasingly turning toward fiber-reinforced concrete as an economical and effective alternative. When fibers are uniformly distributed in the matrix, they help bridge microcracks, enhance tensile strength, and improve ductility and stress redistribution [3] This innovation aligns with the growing demand for durable and sustainable infrastructure solutions.

Recent advancements in fiber-reinforced concrete have introduced several unconventional fibers such as cotton, glass, and waste human hair. Cotton fibers are natural and biodegradable, contributing to post-crack toughness and reducing shrinkage cracks, thereby promoting eco-friendly construction practices [4][5]. Glass fibers, while offering exceptional tensile strength and stiffness, pose challenges due to their high energy manufacturing process and non-biodegradable nature [6][7]. On the other hand, human hair fibers an abundant and renewable keratin-based waste product present a unique opportunity for recycling while providing elasticity and tensile benefits [8][9]. These fiber types differ not only in mechanical behavior but also in terms of cost, availability, and environmental impact. Evaluating these differences is vital to identifying their practicality for real-world applications. Moreover, their inclusion in concrete supports global sustainability targets by reducing material waste and promoting circular resource use, especially in resource-constrained regions.

This paper explores the comparative potential of cotton, glass, and waste human hair fibers in minimizing flexural cracking in concrete beams. The inclusion criteria focused on studies that investigated mechanical properties, particularly flexural

strength, and the role of fiber reinforcement in crack control and sustainability. Research that concentrated solely on compressive or non-structural applications was excluded unless it offered substantial insight into fiber performance under flexural stress. By examining 32 carefully selected peer-reviewed publications from 2010 to 2025, retrieved through targeted searches on ScienceDirect, and Google Scholar, the study offers a thematic synthesis of existing findings. The uniqueness of this review lies in its focused comparison of three fiber types with varying mechanical and environmental characteristics, highlighting the often-overlooked use of human hair as a sustainable construction material. The objective is to inform future research and practical applications by drawing insights from current literature rather than original experimentation.

2. Flexural Cracks in Concrete Beams

Flexural cracks are among the most frequently observed forms of distress in reinforced concrete beams, emerging primarily due to bending-induced tensile stresses in the lower regions of the cross-section. Since concrete is inherently weak in tension, these stresses lead to the development of vertical cracks on the tension face when the applied moment exceeds the section's cracking moment. Such cracking not only affects the structural aesthetics but also serves as a critical point of ingress for moisture and aggressive agents, accelerating the deterioration of embedded reinforcement [2]. As corrosion initiates and progresses, the bond between concrete and steel weakens, potentially compromising load-bearing strength and leading to premature failure. The formation and propagation of flexural cracks are thus important indicators of serviceability concerns in structural elements. Effective crack control is essential to maintaining the durability, integrity, and performance of concrete structures under long-term loading and environmental exposure. Hence, it becomes imperative to explore materials and design strategies that limit crack development at both early and later stages of structural use.

One promising approach for mitigating flexural cracking is the incorporation of discrete fibers into the concrete matrix. Fiber-reinforced concrete (FRC) has been demonstrated to improve tensile behavior, increase post-cracking toughness, and reduce crack width by facilitating stress redistribution across microcracks [1]. Depending on the fiber type such as glass, cotton, or human hair concrete can achieve different mechanical and environmental performance enhancements. Glass fibers, due to their high tensile strength and stiffness, provide effective crack bridging and resistance, while natural fibers like cotton and human hair offer the added benefits of biodegradability and waste utilization [10]. The integration of such fibers contributes not only to crack control but also to promoting sustainable construction practices. Research has shown that even small volumes of fiber can significantly improve flexural strength and delay the formation of critical cracks in beam elements. As a result, fiber reinforcement stands as a practical and eco-efficient method to enhance the service life and reliability of reinforced concrete beams. Figure 1 (a) depicts different types of cracks in RC beams [11]. Figure 1 (b) shows cracks in concrete beams observed at the Author's place of work.

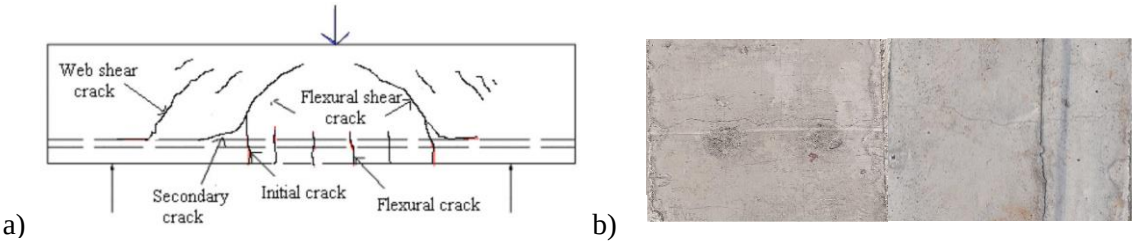


Figure 1 Flexural Cracks in Concrete Beams, a. Types of Cracks in Beams, and b. Flexural Cracks in Beams

3. Governing Factors of Flexural Cracking

Flexural cracking in concrete beams is influenced by a convergence of material, structural and environmental factors. Concrete's relatively low tensile strength makes it prone to cracking when bending stresses exceed its inherent strength [12]. External loads especially those that are excessive, dynamic or cyclic further increase tensile strain and accelerate crack propagation. Internal stress development due to drying, autogenous, or temperature-induced shrinkage also plays a critical role, as these movements in restrained conditions generate tensile force that initiates cracking. Reinforcement

detailing, including bar spacing and bonding, directly controls crack width and distribution; insufficient reinforcement often results in wider, poorly distributed cracks [12]. Lastly, deficiencies in mix design, such as improper water to cement ratio, inadequate compaction, and poor curing, degrade concrete integrity and heighten crack susceptibility [13]. A comprehensive approach addressing all these elements during design and construction is essential to mitigate flexural cracking and enhance structural durability. These interrelated parameters are outlined in Table 1, which summarizes the influence on flexural cracking.

Table 1 presents a systematic overview of the principal factors affecting flexural cracking in concrete beams. The material-related limitations, such as low tensile strength, form the fundamental basis for crack formation. Structural factors, especially high-amplitude or variable loading conditions, contribute significantly to stress fluctuations that exacerbate cracking tendencies [14]. Environmental influences, such as shrinkage and thermal changes, are especially critical in restrained conditions where movement is restricted, resulting in internal tensile stress development [15]. The configuration and effectiveness of reinforcement influence both crack control and structural serviceability, with poorly designed systems allowing more pronounced crack widths [12]. Lastly, construction quality including mix proportioning and workmanship directly impacts the durability and integrity of concrete. Inadequate practices elevate the likelihood of premature cracking due to reduced cohesion and poor hydration [13]. Together, these factors underscore the need for a holistic approach during design and execution to limit flexural crack development.

Table 1 Primary Factors Influencing Flexural Cracking

Governing Factor	Influence on Flexural Cracking
Low Tensile Strength	Cracks initiate when bending stresses exceed tensile strength.
Load Characteristics	High-magnitude, cyclic, or dynamic loads exacerbate tensile stress and crack growth.
Shrinkage & Temperature	Drying, autogenous, and thermal stresses in restrained concrete generate tensile forces.
Reinforcement Configuration	Poor reinforcement design leads to wider cracks due to insufficient stress distribution.
Mix Quality & Workmanship	Inadequate mix proportions, compaction, or curing weaken concrete and elevate cracking risk.

4. Performance and Sustainability of Fiber-Reinforced Concrete

Incorporating fibers such as cotton, glass, and human hair into concrete has shown considerable potential in enhancing mechanical performance and promoting sustainable construction. As illustrated in Figure 2, the selection of fiber type plays a crucial role in determining the overall behavior of the composite.



a) b) c)

Figure 2 Fiber Reinforced Concrete, a. Cotton Fiber Concrete [16], b. Glass Fiber Concrete [17], and c. Waste Human Hair [18]

Cotton fibers, being biodegradable and renewable, significantly improve ductility and crack resistance; however, their moisture absorption can adversely affect workability. Glass fibers contribute exceptional tensile strength and crack control, making them suitable for high-performance structural applications, though their non-biodegradable nature presents environmental concerns. Human hair fibers, a cost-effective and eco-friendly alternative, enhance tensile strength and ductility, with optimal performance typically observed at 1.5% by weight of cement. Each fiber type exhibits distinct

mechanical and environmental characteristics, necessitating thoughtful selection aligned with project-specific performance and sustainability goals.

A comparative analysis presented in Table 2 highlights the mechanical and environmental attributes of the selected fibers. Glass fibers exhibit superior tensile strength and stiffness, making them ideal for structural enhancement, but their energy-intensive production and lack of biodegradability limit their sustainability [19][20][21]. In contrast, cotton and human hair fibers, while offering comparatively lower mechanical strength, demonstrate enhanced ductility and crack resistance, coupled with environmental benefits such as biodegradability and reuse of waste materials. Table 3 outlines additional practical considerations: cotton fibers promote green construction but may compromise workability due to moisture sensitivity; glass fibers ensure high structural reliability but entail environmental costs; and human hair fibers provide an economical and sustainable solution, though they present challenges related to uniform dispersion and fiber-matrix bonding. [19][20][21][22].

Table 2 Mechanical & Environmental Performance at Typical Fiber Content

Fiber Type	Tensile Strength (MPa)	Modulus (MPa)	Flexural/Crack Resistance	Sustainability	Typical Issues
Cotton	287–597 MPa	5000-12,000 MPa	Good	Biodegradable, renewable	Clumping; moisture uptake
Glass	1,000–3,500 MPa	70,000-85,000 MPa	Excellent	Non-biodegradable	Brittleness; mixing challenges
Human Hair	200–380 MPa	4000-5000 MPa	Very good	Biodegradable; waste-reuse	Variable quality; adhesion issues

Table 3 Pros, Cons, and Application Barriers

Fiber Type	Strengths	Limitations	Key Application Notes
Cotton	Enhances ductility; eco-friendly	Lower strength than glass; absorbs moisture	Suited for shrinkage control; sustainable or green projects
Glass	Very high strength; superior flexural behavior	Energy-intensive; risk of microcracking at high dosage	Ideal for structural-grade and high-performance concrete
Human Hair	Cost-effective; promotes waste minimization	Adhesion variability; yield inconsistency	Suitable for pilot-scale or low-cost sustainable construction

Table 4 illustrates the measurable impact of incorporating cotton, glass, and human hair fibers on the flexural strength of concrete beams. Glass fibers consistently provide the highest improvement in flexural performance, with strength gains ranging from 20% to 45%, owing to their high tensile strength and stiffness. Human hair fibers, while offering moderate improvements between 12% and 25%, present a sustainable and cost-effective alternative, especially suitable for low-cost applications. Cotton fibers demonstrate modest strength enhancements (10–18%) but significantly contribute to post-crack toughness and environmental sustainability. Overall, the results support the feasibility of using natural and waste fibers for improving the structural performance of concrete, particularly when optimized for dosage and fiber compatibility.

Table 4 Effect of Fiber on Flexural Strength of Concrete Beams

Fiber Type	Reference Study	Dosage (% by cement wt.)	Increase in Flexural Strength (%)	Remarks
Cotton	Ghulam et al. (2020) [5]	1.0–2.0%	10–18%	Improved post-crack behavior; prone to moisture sensitivity
Glass	Maranan et al. (2015) [8]	0.5–1.5%	20–45%	High stiffness; superior crack resistance
Human Hair	Ahmed and Al Numan (2022) [2]	1.0–2.0%	12–25%	Effective at low cost; variation in bonding noted

5. Conclusion

This paper explores the potential application of fiber reinforcement in concrete beams through a vigorous research exploration from highly reputed journals. The current effort is to compose all published information related to the subject. Following conclusions can be drawn from the conducted study:

- Flexural cracking in concrete structures is a persistent challenge, and fiber reinforcement offers an effective approach to enhance tensile strength and control crack propagation.
- Cotton, glass, and human hair fibers demonstrate distinct performance characteristics as glass improves mechanical strength, cotton contributes to sustainable construction, and human hair provides a novel use of waste with notable improvements in toughness.
- Utilizing natural and waste-based fibers promote environmentally conscious construction practices and aligns with principles of circular economy in civil engineering.

This study highlights the potential of cotton, glass, and human hair fibers in enhancing concrete flexural performance and promoting sustainability. However, further research is required to optimize fiber content, assess long-term durability, and develop standardized guidelines. These steps are vital for practical adoption in structural engineering.

6. Acknowledgements

The authors would like to thank every person who helped throughout the research work, particularly Engr. Dr. Majid Ali. Moreover, the careful review and constructive suggestions by the anonymous reviewers are gratefully acknowledged.

References

[1] N. Banthia and R. Gupta, "Hybrid fiber reinforced concrete (Hy FRC): fibers energy in high strength matrices," Mater. Struct., vol. 37, pp. 707–716, 2014.
[2] J. S. Yuan, D. Gao, H. Zhu, G. Chen, and L. Zhao, "Flexural behavior of reinforced concrete beams reinforced with glass fiber reinforced polymer rectangular tubes," Front. Mater., vol. 7, p. 48, 2020.
[3] D. A. Tuan and M. Cao, "Fiber reinforcement in high-strength concrete: A theoretical review," Int. J. Concr. Struct. Mater., vol. 15, no. 3, p. 181, 2021.
[4] M. A. Ghulam, M. Ali, and M. F. Javed, "Natural cellulosic fiber reinforced concrete: Influence of fiber type and loading percentage on mechanical and water absorption performance," Materials, vol. 15, no. 3, p. 874, 2020.
[5] M. Ali, M. F. Javed, and M. A. Ghulam, "Sustainable fiber reinforced concrete using natural fibers," J. Constr. Build. Mater., vol. 30, pp. 634–642, 2021.
[6] G. B. Maranan, A. C. Manalo, B. Benmokrane, W. Karunasena, and P. Mendis, "Evaluation of the flexural strength and serviceability of geopolymer concrete beams reinforced with glass-fiber-reinforced polymer (GFRP) bars," Eng. Struct., vol. 101, pp. 529–541, 2015.

[7] F. D. Santos, J. M. Campos, and L. A. Rocha, "Optimization of the compressive strength of hair fiber reinforced concrete using central composite design," IOP Conf. Ser.: Mater. Sci. Eng., vol. 771, p. 012059, 2020.
[8] X. Chen and Y. Li, "Influence of material and structural parameters on flexural cracking in concrete beams," J. Struct. Eng., vol. 144, no. 7, p. 04018123, 2018.
[9] M. Khan, M. Cao, and M. Ali, "Cracking behavior and constitutive modeling of hybrid fiber reinforced concrete," J. Build. Eng., vol. 30, p. 101272, 2020.
[10] M. Ali, N. Chouw, and M. Jamal, "Natural fibre-reinforced concrete: Performance, challenges and opportunities," Constr. Build. Mater., vol. 270, p. 121423, 2021.
[11] A. Rahman and T. Ueda, "Shear Resisting Mechanism and Shear Strength Equation for Sandwich Beams," Journal of Sandwich Structures & Materials, vol. 15, no. 2, pp. 141–164, Mar. 2013
[12] M. Ahmed et al., "Flexural cracking in concrete beams: Influencing factors and control strategies," 2014.
[13] Nexo Técnico, Deficiencies in Concrete Mix Design and Their Impact on Structural Integrity, Tech. Rep., 2025.
[14] B. Singh and D. Jain, "Comparative study on natural and synthetic fiber-reinforced concrete," Mater. Today: Proc., vol. 17, no. 3, pp. 619–625, 2019.
[15] S. Ravi, P. Ramesh, and L. Kumar, "Mechanical performance of bio-based fibers in concrete applications," J. Nat. Fiber Eng., vol. 8, no. 2, pp. 112–120, 2021.
[16] C. Pöhler, E. V. Bachtiar, L. Yan, and B. Kasal, "Composites for structural strengthening, repair, rehabilitation, and retrofit," in Advanced Fibre-Reinforced Polymer (FRP) Composites for Structural Applications, W. P. L.
[17] D. Arkin, "What is GFRC – Properties, Uses & Benefits," Premier Precast, Delray Beach, FL, Blog, updated Dec. 22, 2022.
[18] B. Ahmad, R. Kumar, and D. Aggarwal, "An inspection on sustainable construction materials," International Journal of Innovative Research in Technology, vol. 11, no. 11, Apr. 2025
[19] H. K. Bledzki, O. Faruk, and P. Sperber, "A comprehensive review on the use of natural fibres in cement composites," Cement Concr. Compos., vol. 143, no. A, pp. 105–132, Jan. 2023
[20] F. Choi and Y. Yuan, "Mechanical characteristics of glass fiber reinforced concrete," cited in Proceedings of Int. Struct. Eng. & Constr., vol. 11, no. 2, 2024, Paper MAT093, pp. 89–102.
[21] Sreevani and Ajitha, "Human hair fiber reinforced concrete composites," Journal of Emerging Technologies & Innovative Research (JETIR), vol. 8, no. 4, Apr. 2021
[22] M. Manivel et al., 'Mechanical properties of M30 concrete with human hair and GGBFS,' Compos. Struct., 2022

DYNAMIC RESPONSE MODELING OF SDOF SYSTEMS USING NEURAL NETWORKS: A COMPARATIVE STUDY OF ANN AND LSTM

[a] Aaqib Najeeb*, [b] Muhammad Yousaf Jalal

a: Department of Structural Engineering, College of Civil Engineering, Tongji University, Shanghai, 200092, China, aaqib_najeeb@tongji.edu.cn
b: State Key Laboratory of Disaster Reduction in Civil Engineering, Tongji University, Shanghai, 200092, China, 2493237@tongji.edu.cn
* Corresponding author

Abstract- Overhead water tanks (OHWTs) play a critical role in infrastructure, yet they are highly vulnerable to dynamic loading such as seismic forces and wind excitations. Traditional numerical methods, such as Finite Element Analysis (FEA), can be computationally intensive, making real-time structural response solving challenging. This study develops a machine learning (ML)-based approach to predict the structural response of OHWTs subjected to harmonic loading by idealizing the structure as a Single Degree of Freedom (SDOF) system, where multiple configurations of mass, stiffness, and damping were considered to represent different structural scenarios. The governing equation of motion (EOM) was numerically solved using MATLAB's ode45 solver, chosen for its balance between accuracy and computational efficiency after comparison with alternative solvers. The computed responses from this step served as the training dataset for the ML models. Artificial Neural Networks (ANN) and Long Short-Term Memory (LSTM) networks are then trained using this dataset to predict structural displacements. The results demonstrate that the LSTM model outperforms the ANN by effectively capturing sequential dependencies in dynamic responses, showing smoother and more accurate predictions. The proposed methodology highlights the potential of integrating ML with numerical simulations for different fields of Structural Engineering. By leveraging AI-driven approaches, this research offers a computationally efficient alternative to conventional methods, paving the way for advanced predictive modeling in civil engineering applications.

Keywords- Structural Response, SDOF System, LSTM and ANN, Numerical Simulations

1 Introduction

Reservoirs and elevated tanks are designed for the collection of water, crude oil, petroleum products, and similar liquids. It is very important to insure their durability and stability. Elevated tanks mainly serve the purpose of storing water. The significance of storage tanks has grown considerably due to their adaptability in handling various liquids. With the rising need for liquid storage in industrialized nations, demand has surged over the years. As a result, both the dimensions and storage capacities of these tanks have expanded substantially to accommodate increasing requirements[1] . Recent major earthquakes, such as Tokachi-Oki (Japan, 2003), Emilia (Italy, 2012), and Kaikoura (New Zealand, 2016), have repeatedly highlighted the weakness of storage tanks to seismic damage. The failure of these structures can result in significant economic losses, severe environmental consequences, and delayed post-earthquake recovery [2]. Reinforcement of the supporting elements against dynamic loading is essential for maintaining their structural integrity and long-term stability

[3]. Exposure to aggressive environmental agents, aging, and extreme weather event can also seriously harm structures and affect their performance [4]. A properly designed water tank is recommended for vibration mitigation [5].

Over the past few years, ML has become a key tool across science, engineering, and economics. It allows computers to learn from data and perform tasks without being explicitly programmed. As a core part of artificial intelligence, ML is now making a strong impact in structural engineering, with applications like image recognition, object tracking, and stress analysis [6]. Neural networks serve as a powerful tool in predicting structural responses, showing their capability to model and characterize dynamic systems effectively. As early as 1993, Masri et al. [7] used a multilayer perceptron (MLP) with three hidden layers identify the behavior of the Duffing oscillator. Subsequently, He, Wu, and their collaborators applied a back-propagation neural network (BPNN) alongside a self-recurrent neural network (SRNN) to predict the response of linear elastic structures [8]. Jagatai et al. [9] utilized the Prandtl–Ishlinskii operator which was integrated into a feedforward neural network (FFNN) as a hidden layer, leading to the development of the Prandtl neural network (PNN) for predicting the dynamic response of hysteretic systems. Lagaros and Papadrakakis further expanded on neural network applications in structural dynamics, demonstrating their effectiveness in complex response modelling [10]. Another study used neural networks to predict the seismic response of a nonlinear 3D building, demonstrating their strength in complex structural analysis. With advances in computing power, researchers are increasingly turning to deep learning (DL) to improve prediction accuracy in structural dynamics [11]. DL network have been widely utilized for response prediction, demonstrating superior accuracy and adaptability in complex structural analyses. [12].

Recently, Kuo et al. (2024) [13] introduced a Graph Neural Network (GNN)-LSTM fusion model for predicting nonlinear dynamic responses in 4–7 story steel frames, showing better performance and interpretability. Zhou et al. (2024) [14] developed Phy-Seisformer, a physics-informed deep learning model enabling real-time seismic response prediction with 5000x faster computation than FEM. Shu et al. (2025) [15] proposed a conditional diffusion model (DF-CDM) with data fusion for structural response reconstruction, outperforming GANs in both accuracy and stability. Jia et al. (2025) [16] presented Floor Response Spectra Network (FRSNet), a deep learning method to generate floor response spectra for 102 buildings from ground spectra, validated on numerical and real structures.

While many studies use neural networks to predict dynamic system responses, most rely on black-box models. To improve interpretability, some researchers now integrate neural networks with governing equations, creating white-box or gray-box surrogate models.[17]. This study uses ML to predict the structural behavior of an overhead water tank under harmonic loading. Unlike traditional methods, ML offers faster and more accurate predictions, especially under complex loading conditions. By combining advanced computational techniques with ML, this approach supports better design, maintenance, and safety—paving the way for future developments in predictive modeling and structural analysis.

2 Research Methodology

This research is divided into two main stages. The first involves numerical analysis and structural idealization, while the second applies machine learning techniques to predict the structural response. Stage one begins with a literature review to identify research gaps. After analyzing over 25 studies, the OHWT was selected as the case study due to its high vulnerability to lateral vibrations caused by its large internal mass. Based on structural dynamic response sometimes even complex structures can be simplified into generalized or SDOF system. Similarly, the OHWT was modelled as an SDOF system for this study. Figure 1 below presents a comprehensive overview of the study framework while, Figure 2 illustrates the idealization of the OHWT as an SDOF system.

2.1 Analytical and Numerical Modelling

The structure is characterized by a specific EOM that facilitates the simulation of its dynamic response. In this research, as the structure was modelled as an SDOF system, so the EOM was expressed in a single degree of freedom, translational motion along the X-axis, effectively capturing the overall structural behaviour. Through the mathematical modelling process, it was established that the EOM governing the OHWT is an ODE. Various numerical solvers, including ode23, ode23s, ode23t, ode45, ode23tb, ode113, ode15s, the Newmark Method, and the Central Difference Method, were employed to solve this equation. A comparative analysis against the analytical solution revealed that ode45 was the most suitable solver for this particular case due to its optimal balance between accuracy and computational efficiency. However, this suitability is case-specific, and for different scenarios, it is advisable to re-evaluate solver performance. Figure 3 (A)

shows key activation functions and Figure 3 (B) is a basic network structure. The ANN model had fully connected layers, while the LSTM model used LSTM-based input and hidden layers with a dense output. Table 1 tabulates the nature of different solvers considered in this study. In addition, Table 2 below outlines mathematical form of different activation functions that are normally used in neural networks.

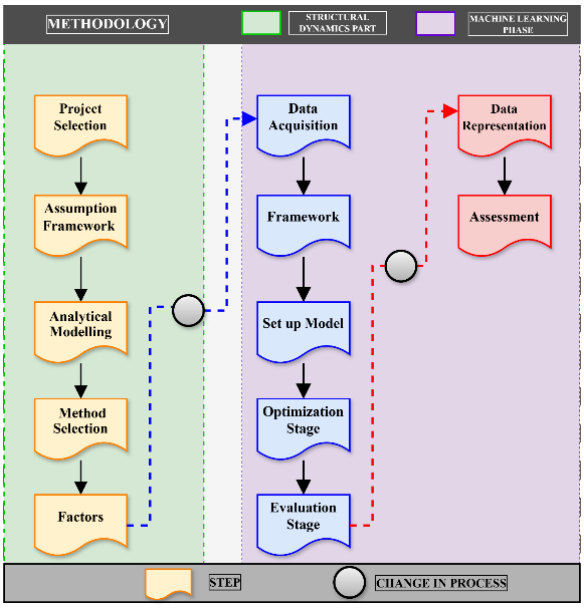


Figure 1: Methodological Framework

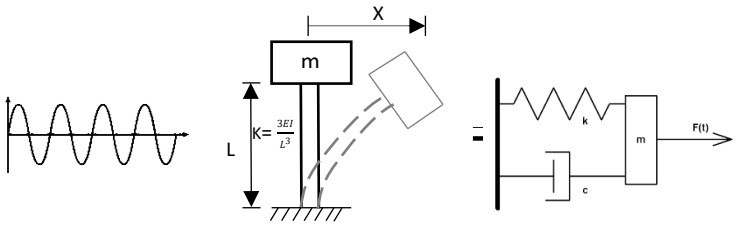


Figure 2: Structural Framework

Table 1 Solver Characteristics and Applications

Solver/Method	Type	Use
ode23	Non-stiff	General-purpose, non-stiff systems
ode23s	Stiff	Stiff systems
ode23t	Moderately stiff	Moderately stiff systems
ode45	Non-stiff	Non-stiff systems with high accuracy
ode23tb	Stiff	Stiff systems, balance accuracy & stability
ode113	Non-stiff	Non-stiff systems with adaptive order
ode15s	Stiff	Stiff systems with complex non-linearities
Newmark Method	Structural	Structural dynamics (vibration, seismic)
Central Difference	Structural	Fast, efficient for non-stiff dynamics

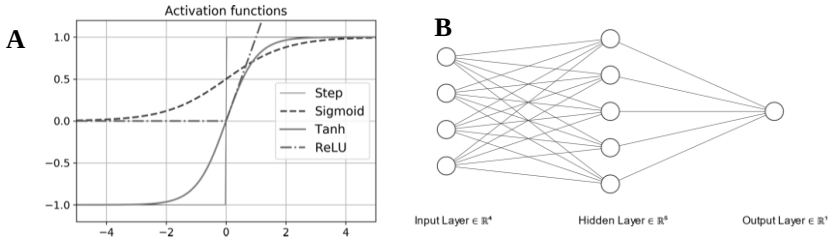


Figure 3: A (Activation function graphs), B (Neural Network Architecture)

Based on the fourth- and fifth-order Runge-Kutta methods, ode45 solves the mathematical model by iteratively computing results at each step. It adjusts the step size dynamically by comparing the two orders: a large error reduces the step size, while a small error increases it, balancing accuracy and computational efficiency.

2.2 Parameters and Data Framework

In practice, factors like structural height, column material, and liquid mass in the tank vary. To capture this, the idealized structure was analysed over a range of mass (m), stiffness (k), and damping (c) values to reflect real-world differences. For typical reinforced concrete structures inherent damping ratio is about 5%. Mass and stiffness depend on column size, material properties, and the liquid mass in the tank. The final stage of this study uses ANN and LSTM networks to predict the structural response of the SDOF system.

Since neural networks need large amounts of data for training and validation, the final part of Phase 1, calculating the SDOF system response for varying m, c, and k served as the data generation stage. The data was then organized into a format suitable for machine learning. It was subsequently split into training and testing sets to evaluate the model's performance. For LSTM training, a sliding window technique created sequential inputs, converting the data into the required 3D format (samples, timesteps, features). The model has four input nodes, five hidden layers, and one output node predicting structural response. ReLU activation was used throughout, though output activation varies by task—classification favours Sigmoid or SoftMax.

Table 2 Common Activation function used in Neural Network

Sigmoid	Tanh	RELU
$g(z) = \frac{1}{1+e^{-z}}$	$g(z) = \frac{e^{z}-e^{-z}}{e^{z}+e^{-z}}$	$g(z) = max(0,z)$

2.3 Model Optimization and Evaluation

The Adam optimizer was selected for training due to its adaptability, combining the benefits of RMSProp and Stochastic Gradient Descent (SGD). Its dynamic learning rate adjustment ensures stable performance across different problems. Mean Squared Error (MSE) was used as the loss function to minimize prediction errors, with lower values indicating better performance, while Mean Absolute Error (MAE) served as a performance metric, measuring the average difference between predicted and actual values. The model was trained over 100 epochs, using input data and labels to adjust weights and minimize loss. A batch size of 32 allowed for frequent updates. The dataset was split into 80% for training and 20% for validation. For evaluation, 20% of the data was set aside as test data to assess performance on unseen samples. The verbose setting was 1 for progress updates, while 0 muted output and 2 provided detailed logs.

Training performance was monitored through loss and MAE across epochs, identifying trends and potential issues like underfitting or overfitting. Generalization was tested on unseen data, yielding test MSE and MAE. The results showed strong correlation between predicted and actual displacements. Residual analysis over time provided further insight into prediction accuracy and reliability. Given that the study utilized both LSTM and ANN algorithms, comparing their performance has been done to evaluate their respective effectiveness in predicting the desired outcomes.

3 Results and Discussion

Figure 4 illustrates the undamped free vibration response of the SDOF system, showing displacement, velocity, and acceleration over time. With no damping, the system undergoes simple harmonic motion (SHM) with constant amplitude and no energy loss. The governing equation (Equation 1) relates m, k, and displacement (x(t)), with motion controlled by the natural frequency (Equation 2). Displacement follows a sinusoidal pattern, peaking when restoring force balances inertia. The general solution (Equation 3) includes initial displacement (X_0), phase angle (ϕ), and natural frequency (ω_n).

$$m\ddot{x} + kx = 0, \quad \omega_n = \sqrt{\frac{k}{m}} \quad \& \quad x(t) = X_0 \cos(\omega_n t + \phi) \qquad (1–3)$$

Since stiffness depends on mass and natural frequency, the total mechanical energy (E)—made up of kinetic energy (KE) and potential energy (PE)—stays constant because there is no energy loss. The velocity response follows a sinusoidal pattern but lags displacement by 90 degrees. At maximum or minimum displacement, velocity is zero, while at equilibrium, velocity peaks. Similarly, acceleration is sinusoidal but 180 degrees out of phase with displacement, reaching its most negative value at maximum displacement. Acceleration amplitude depends on the square of the natural frequency.

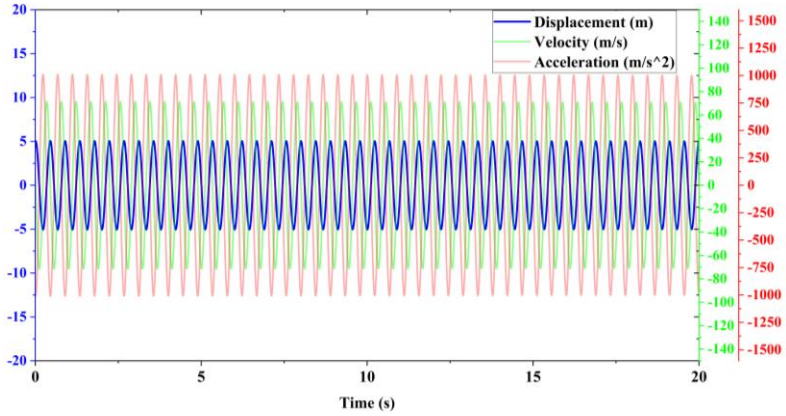


Figure 4: Undamped Free Vibration response of an SDOF System

Figure 5 shows the damped free vibration response of the SDOF system. In this case, damping (represented by "c" in Equation 4) causes exponential energy dissipation, leading to a gradual decay in oscillations. This behavior is typical in structures such as buildings, bridges, and machinery. Equation 5 describes the damped free vibration response, where the damping ratio (ζ) and the damped natural frequency ($\omega_d = \omega_n\sqrt{(1-\zeta^2)}$) govern the system's oscillatory behavior. A key difference from the undamped system is the presence of the exponential decay term $e^{-\zeta\omega_n t}$ which causes the motion to eventually stop. Although Equation 5 gives the displacement response, the same decay trend applies to velocity and acceleration, as they are the first and second derivatives of displacement, respectively. In the undamped case, E stays constant but with damping, energy is also lost.

$$m\ddot{x} + c\dot{x} + kx = 0, \quad x(t) = X_o\, e^{\zeta\omega_n t}\cos(\omega_d t + \phi) \qquad (4–5)$$

Results depicted in the Figure 6 correspond to the undamped forced vibration SDOF system, where an external periodic force is applied to the system. Unlike free vibration, where the system oscillates due to initial conditions alone, forced vibration occurs when an external force excites the system. The response consists of both a transient component and a steady-state component. However, since the system is undamped, the transient component does not decay, leading to continuous oscillations at the forcing frequency (ω). The governing equation for undamped forced vibration is given as: equation 6. Where, F0 is the amplitude of the external force (N). The displacement response is shown in equation 7.

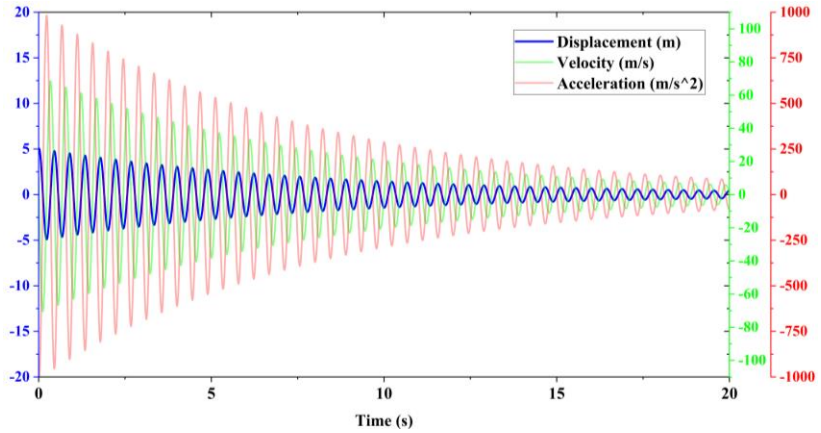


Figure 5: Damped Free Vibration response of an SDOF System

$$m\ddot{x} + kx = F_0 \cos(\omega t), \;\; x(t) = \frac{F_0/m}{\omega_n^2 - \omega^2}\cos(\omega t) \qquad (6\text{–}7)$$

Resonance occurs when the ω matches the natural frequency (ω_n), causing the denominator to approach zero ($\omega_n^2 - \omega^2 \approx 0$) and resulting in theoretically infinite displacement in an ideal undamped system. Since the system does not have damping, so there is no loss, leading to sustained oscillations.

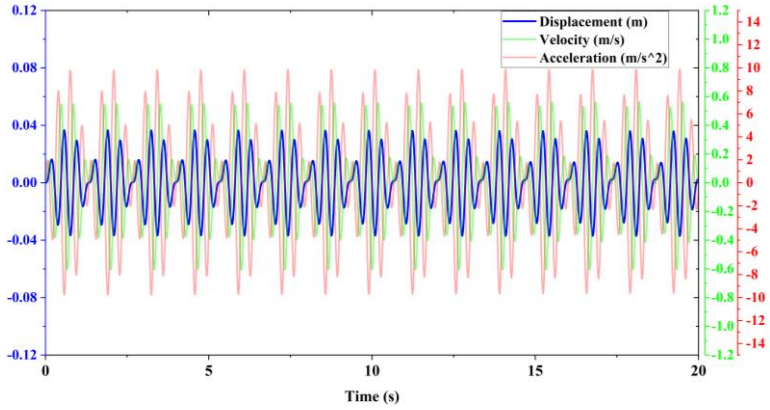


Figure 6: Undamped Forced Vibration response of an SDOF System

The results in the Figure 7 correspond to the damped forced vibration response of the SDOF system, the presence of damping causes the system's response to stabilize over time. The EOM for damped forced vibration is expressed in the equation 8.

$$m\ddot{x} + c\dot{x} + kx = F_0 \cos(\omega t) \qquad (8)$$

The applied periodic force excites the system at a defined frequency (ω), producing a response that initially exhibits transient oscillations before stabilizing into steady-state motion due to damping. At first, the system vibrates from both its own natural motion and the external force. As damping removes the extra vibrations, only the forced vibration remains (Equation 9). This helps reduce excessive motion and prevents resonance. The amplitude (Equation 10) and phase angle ϕ (Equation 11) define the system's steady-state behavior.

$$x(t) = X\cos(\omega t - \phi) \qquad (9)$$

$$X = \frac{F_0/m}{\sqrt{(\omega_n^2 - \omega^2)^2 + (2\zeta\omega_n\omega)^2}}, \qquad \phi = \tan^{-1}\left(\frac{2\zeta\omega_n\omega}{\omega_n^2 - \omega^2}\right) \qquad (10\text{–}11)$$

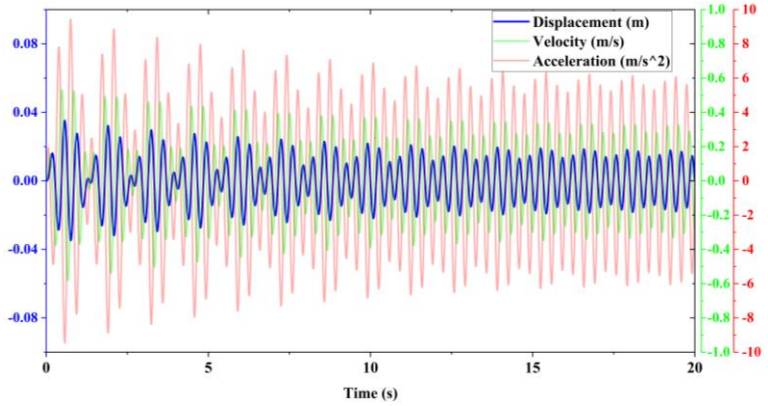


Figure 7: Damped Forced Vibration response of an SDOF System

Figure 8 presents a comparison of how accurately each model replicates the actual displacement of the SDOF system. In Figure 8 (A) ANN model (left) demonstrates a strong alignment between its predicted displacement (dashed red line) and the true dis-placement (solid blue line), though slight deviations emerge in regions where rapid dynamic transitions occur. Conversely, the LSTM model (right) achieves an almost exact match between predicted and true displacement, highlighting its superior capability in capturing temporal dependencies. The Figure 8 (B) error plots offer deeper insights into the performance difference between the models. Larger fluctuations in the ANN error curve (left) suggest inconsistencies, particularly in regions with high dynamic variability. In contrast, the LSTM error curve (right) remains smoother and more stable, reflecting its superior ability to minimize prediction errors over time.

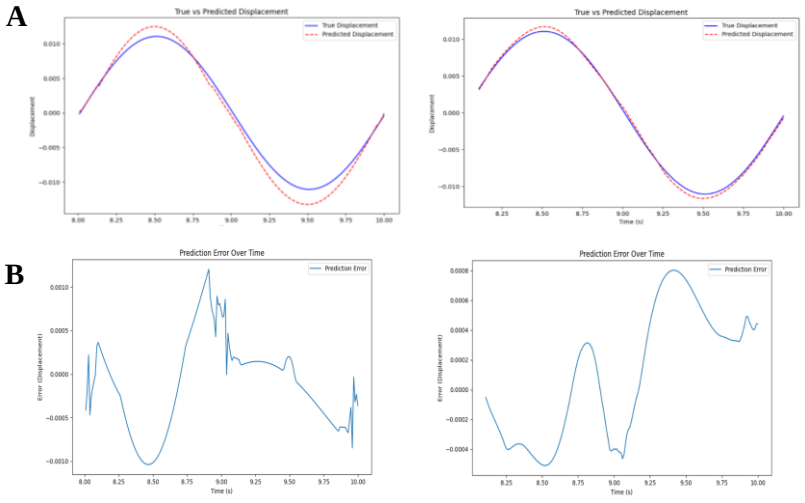


Figure 8: Comparison of true versus predicted displacements (A) for ANN (left) and LSTM (right) models, alongside the prediction error over time for the same test case (B)

4 Conclusion

Findings confirm that the LSTM model surpasses the ANN in both precision and consistency. While the ANN produces reasonable estimates, its limited ability to capture temporal dynamics results in larger deviations. The sequential nature of LSTM architecture enables near-perfect alignment with actual displacements and significantly reduces prediction errors, making it the preferred choice for dynamic system modelling.

Acknowledgment

The authors would like to thank Chinese Scholarship Council (CSC) for providing the opportunity to study at Tongji university, Shanghai, China.

References

1. Compagnoni, M.E., Curadelli, O., Ambrosini, D.: Experimental study on the seismic response of liquid storage tanks with Sliding Concave Bearings. J Loss Prev Process Ind. 55, 1–9 (2018). https://doi.org/10.1016/j.jlp.2018.05.009
2. Yazdanian, M., Ingham, J.M., Kahanek, C., Cradock-Henry, N., Fountain, J., Dizhur, D.: Analysis of damage data collected for wine storage tanks following the 2013 and 2016 New Zealand earthquakes. Bull NZ Soc Earthq Eng. 53(2), 83–103 (2020). https://doi.org/10.5459/bnzsee.53.2.83-100
3. Cohen, Y., Livshits, A., Nascimbene, R.: Comparative approach to seismic vulnerability of an elevated steel tank within a reinforced concrete chimney. Periodica Polytechnica Civil Engineering. 61, 361–380 (2017). https://doi.org/10.3311/PPci.9311
4. Catbas, F.N., Aktan, A.E.: Condition and damage assessment: Issues and some promising indices. J Struct Eng. 128(8), 1026–1036 (2002). https://doi.org/10.1061/(ASCE)0733-9445(2002)128:8(1026)
5. Najeeb, A., Yasin, A., Hashim, S.: Seismic vibration control through passive system. Bachelor's thesis, International Islamic University (IIUI), Islamabad (2022). http://dx.doi.org/10.13140/RG.2.2.10304.24327
6. Zhang, X., Wang, Z., Liu, H.: Machine learning on big data: Opportunities and challenges. Neurocomputing. 237, 350–361 (2017). https://doi.org/10.1016/j.neucom.2017.01.026
7. Masri, S.F., Chassiakos, A.G., Caughey, T.K.: Structure-unknown non-linear dynamic systems: Identification through neural networks. Smart Mater Struct. 1, 45–56 (1992). https://doi.org/10.1088/0964-1726/1/1/007
8. Oh, B.K., Glisic, B., Park, S.W., Park, H.S.: Neural network-based seismic response prediction model for building structures using artificial earthquakes. J Sound Vib. 468, 115109 (2020). https://doi.org/10.1016/j.jsv.2019.115109
9. Joghataie, A., Farrokh, M.: Matrix analysis of nonlinear trusses using Prandtl-2 Neural Networks. J Sound Vib. 330(20), 4813–4826 (2011). https://doi.org/10.1016/j.jsv.2011.04.035
10. Lagaros, N.D., Papadrakakis, M.: Neural network-based prediction schemes of the non-linear seismic response of 3D buildings. Adv Eng Softw. 44(1), 92–115 (2012). https://doi.org/10.1016/j.advengsoft.2011.05.033
11. LeCun, Y., Bengio, Y., Hinton, G.: Deep learning. Nature. 521, 436–444 (2015). https://doi.org/10.1038/nature14539
12. Zhang, R., Chen, Z., Chen, S., Zheng, J., Büyüköztürk, O., Sun, H.: Deep long short-term memory networks for nonlinear structural seismic response prediction. Comput Struct. 220, 55–68 (2019). https://doi.org/10.1016/j.compstruc.2019.05.006
13. Kuo, P.C., Chou, Y.T., Li, K.Y., Chang, W.T., Huang, Y.N., Chen, C.S.: GNN-LSTM-based fusion model for structural dynamic responses prediction. Eng Struct. 306, (2024). https://doi.org/10.1016/j.engstruct.2024.117733
14. Zhou, Y., Meng, S., Lou, Y., Kong, Q.: Physics-Informed Deep Learning-Based Real-Time Structural Response Prediction Method. Engineering. 35, 140–157 (2024). https://doi.org/10.1016/j.eng.2023.08.011
15. Shu, J., Yu, H., Liu, G., Duan, Y., Hu, H., Zhang, H.: DF-CDM: Conditional diffusion model with data fusion for structural dynamic response reconstruction. Mech Syst Signal Process. 222, (2025). https://doi.org/10.1016/j.ymssp.2024.111783
16. Jia, J., Gong, M., Zuo, Z., Wang, X., Zhao, Y.: A novel deep learning-based method for generating floor response spectra of building structures. Eng Struct. 322, (2025). https://doi.org/10.1016/j.engstruct.2024.119058
17. Yadav, N., Yadav, A., Kumar, M.: An Introduction to Neural Network Methods for Differential Equations. Springer Briefs in Applied Sciences and Technology, Computational Intelligence. Springer, Dordrecht (2015). https://doi.org/10.1007/978-94-017-9816-7 .

7th Conference on Sustainability in Civil Engineering (CSCE'25)
(An International Conference)
Department of Civil Engineering
Capital University of Science and Technology, Islamabad Pakistan

ANALYSIS AND SIMULATION OF STEEL MEMBERS IN ANSYS AT DIFFERENT TEMPERATURES

[a]Raja Wajahat Zahoor Khan*, [b]Raja Shujahat Zahoor Khan, [c]Muhammad Yaqub

a: Department of Civil Engineering, University of Engineering and Technology, Taxila, Pakistan. wajahatzahoor12@gmail.com

b: Department of Civil Engineering, University of Engineering and Technology, Taxila, Pakistan. shujahatkhan277@gmail.com

c: Department of Civil Engineering, University of Engineering and Technology, Taxila, Pakistan. yaqub_structure@yahoo.com

* Corresponding author

Abstract- The main objective of the project is to analyze and simulate a steel frame using ANSYS software to determine how stresses and deformation vary with temperature. An approximation method is used to accurately represent the non-uniform temperature distribution within a portion of a 3d beam structural finite element. With this method, the impact of temperature fluctuations on the structural behavior of the 3D members may be represented more accurately. The study aims to analyze the behavior of steel members under various heat conditions by examining the stress distribution and deformation patterns. The study showed that the deformation of the steel column at 500 °C was 0.0568m, while at 1000 °C, the maximum deformation was 0.1086 m. The maximum deformation of 0.1240m occurred at 1500 °C. When beams were exposed to 500 °C, 1000 °C, and 1000 °C, they also showed maximum deformation up to 0.066m, 0.1086m, and 0.2351 respectively. According to our modelling results, steel beams went through deformation, cracking, fracture, and ultimate failure as the temperature increased, which ultimately affected their load-bearing capacity. This study also establishes that the span length, loading magnitude, and cross-sectional properties of structural members influence fire resistance behavior.

Keywords- ANSYS, Steel Frame, Temperature

1 Introduction

If the fire is not properly controlled, there is a significant risk to human life. Losses of life and human resources could result from it. Nowadays, the use of structural steel is very common to construct large-span industrial structures and community centres. Before designing the steel structures, it is essential to study steel behaviour under different conditions of fire. Due to their high thermal conductivity, steel structures do not perform very well in fire, which causes shrinkage and deformation of structural members. The behaviour of steel structures to fire or high temperatures is determined by the steel's inherent properties, including stiffness, strength, thermal conductivity, thickness, thermal gradient, tensile property, and thermal expansion. These strength parameters of steel are affected due to stresses induced by thermal action and the lateral buckling of steel, which occurs at high temperatures or in the presence of fire [1].

The mechanical and physical characteristics of steel are completely altered when it is subjected to high temperature and then quickly cooled, so it is not practical to use the fast-cooled steel in the current structure. The strength of steel is unaffected when exposed to below 600 °C; however, at 1100 °C, there is essentially no remaining strength. Steel loses its strength at 2200°C, and its load-bearing capacity completely decreases at 2700°C. Steel beams could fracture if subjected between 650°C and 1100°C. Given that the upper half of the structure rests on the beam and the slab is supported by the beam, the structure can collapse at high temperatures [2].

High temperatures have a notable effect on the performance of steel members and can result in several problems like deformation, fatigue, cracking, spalling, and even failure [3]. To ensure these materials' dependability and safety, it is crucial to understand how they respond to high temperatures [5]. The ANSYS program is a useful tool for modelling

and analysing the behaviour of structural elements under various heat conditions. The performance of structural components under high temperatures is examined in this study using ANSYS software. The purpose of this study is to simulate how structural components will behave in high temperatures and to investigate the deformation and stress distribution of structural components at various temperatures.

2 Experimental program

2.1 Model Preparation in ANSYS

Several structural elements, such as columns and beams, have a yield strength of 355MPa, were analysed in this study. Fixed, rolling, and pinned supports are considered in our model. Several beams having spans of 5, 15, and 10 meters were considered in this model, as shown in Table 1. The model was subjected to various loads and temperatures, including 25°C, 1000°C, 500°C, and 1500°C, as shown in Table 2. ANSYS software was used to model the 4-meter-long steel beams and columns. The steel used in this study exhibited a Poisson's ratio of 0.3, Young's modulus of 2 × 105 N/mm^2, a density of 7850 kg/m^3, a value of K as 45 W/mK, and a thermal expansion coefficient of 12 x 10^{-6} /°C. The model was exposed to the desired temperatures as part of the analysis's first step, a thermal analysis. For the succeeding structural analysis, the thermal study's findings were subsequently imported.

Table 1. Cross-section properties of members.

Parameter	h (mm)	b (mm)	d (mm)	t_w (mm)	t_f (mm)
Beam	635.8	311.4	540	18.4	31.4
Column	352.5	318.4	246.7	23	37.7

2.2 Applied Thermal Loads and Boundary Conditions

Table 2. Applied thermal load on the beam.

Case	**Support Conditions**	**Thermal Load**
Case 1	Fixed Supports	25°C, 1000°C, 500°C, 1500°C
Case 2	Pinned Supports	25°C, 1000°C, 500°C, 1500°C

2.3 Meshing and Simulation

The meshing of the structure was performed as shown in Figure 2. There are two specifications: a maximum and a minimum level, for meshing analysis. Maximum stress and pressure versus mesh density and other variables were incorporated in the model. We simulated our model by using a linear analysis method with various mesh densities that allowed us to determine which mesh density is most appropriate for each circumstance in the finite element model. The analysis takes longer to run on the software when the mesh density is increased, but the results are more accurate [4]. For FEM models used in the current analysis, the mesh value was set to 5mm.

3 Results

3.1 Impact of Temperature on Deformation

Our research shows that a steel beam's behaviour is highly dependent on the temperature to which it is exposed. When the temperature didn't increase, there was no noticeable deformation in the steel beam sections as shown in Figure 1. This is expected because steel is a hard material that can withstand static and dynamic loads without suffering significant deformation. But as the temperature increased, cracking in the beam sections caused deformation.

Compression loads applied to the members caused bending, leading to an abrupt, catastrophic failure condition when the applied load exceeds the critical buckling load of a thin structural element. Analysis shows that as temperature increased, a critical buckling resistance to load decreased. The deformation of the steel column at 500 °C was 0.0568, as shown in Figure 2, while at 1000 °C the maximum deformation was 0.1086m, as shown in Figure 3, and at 1500 °C it was 0.1240m, as shown in Figure 5.

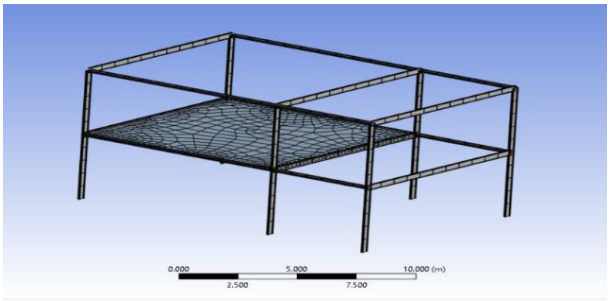


Figure 1. Meshing of beams, slab, and columns.

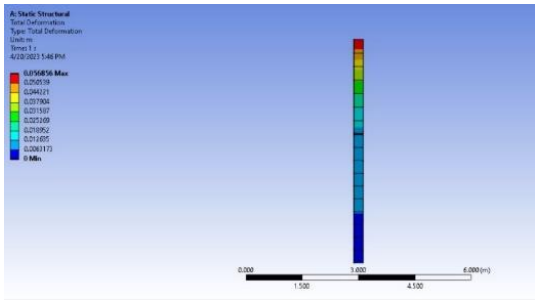


Figure 2. Temperature-induced deformation at 500 °C.

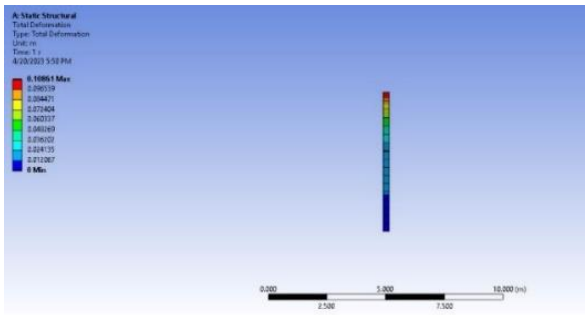


Figure 3. Deformation in a steel column at 1000 °C.

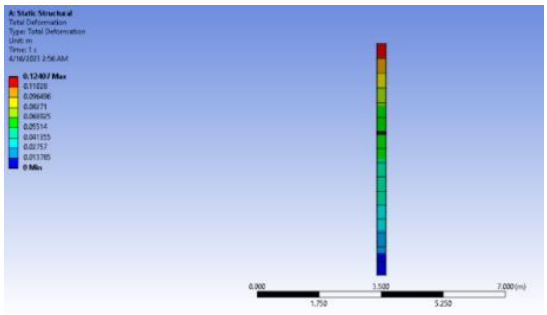


Figure 4. Deformation in a steel column at 1500 °C.

Similarly, the deformation of the steel beam at 1000 °C was 0.1086, as shown in Figure 5. Similarly, when beams were subjected to 1500 °C, the maximum deformation was 0.2351m, as shown in Figure 6. The reduced stiffness and strength of a material at high temperatures are caused by the thermal softening effect. When a steel beam is subjected to lower compressive stresses, this effect renders it more prone to buckling and deformation. The steel beam segment begins to show signs of cracking around 1000°C. At 1500°C, the steel beam underwent permanent deformation, thereby increasing the likelihood of structural collapse. The beam could not bear the applied stresses due to the thermal softening effect, which has reduced the beam's strength and stiffness [4]. Similar results of stress distribution and deformation patterns were found by the study conducted by [6]; however, there are limited studies that focused on the evaluation of stress variation in steel members in ANSYS at elevated temperatures. It is crucial to remember that steel has a melting point of roughly 1370°C and enters a liquid form at a temperature of about 1500°C. As a result, the steel beam loses its ability to support weight, ultimately leading to the building's collapse. The study conducted by Kodur et al. [3] determined that the yield strength and elastic modulus of steel can decrease significantly as temperature exceeds 400°C based on idealized stress-strain curves of structural steel at various temperatures. Similarly, steel may lose up to 50% of its yield strength as temperature increases up to 800°C. The results obtained in our study show a similar pattern of stress degradation and plastic deformation. The fire resistance of steel members can be improved by using insulation materials and introducing structural redundancy for the redistribution of loads and deformation, especially at joints [7].

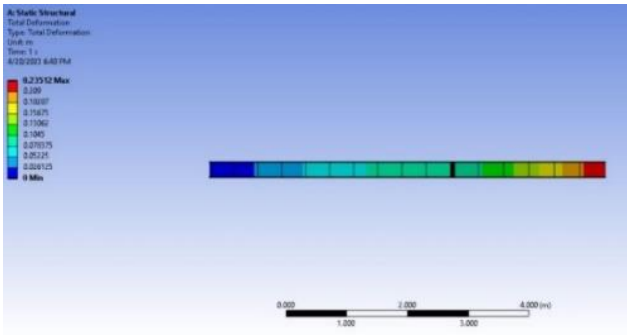


Figure 5. Deformation in the beam at 500 °C.

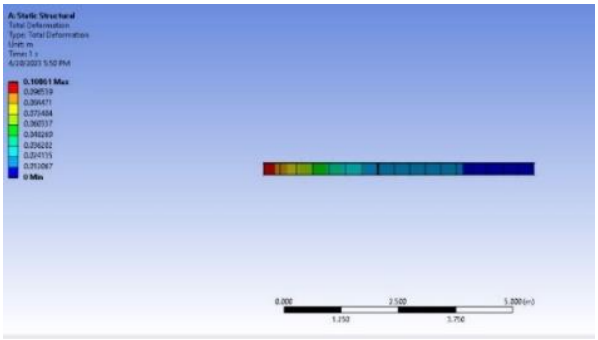


Figure 6. Deformation in the beam at 1000 °C.

4 Conclusion

The main purpose was to analyse the behaviour of structural components at different temperatures. The maximum deformation occurred in the steel column and beam at 1500 °C, which was 0.1240m and 0.2351m, respectively. The reduction in stiffness and strength resulted in increased deformation and the initiation of failure mechanisms due to the formation of plastic hinges and local buckling. This research validates the use of FEM methods for performance-based fire design and emphasises the need for additional experimental validation.

Acknowledgment

The authors are thankful to the Department of Civil Engineering, University of Engineering and Technology, Taxila.

References

[1] H. Ban, G. Zhou, H. Yu, Y. Shi, and K. Liu, "Mechanical properties and modelling of superior high-performance steel at elevated temperatures," *J. Constr. Steel Res.*, 2021, doi: 10.1016/j.jcsr.2020.106407.

[2] J. Chen, B. Young, and B. Uy, "Behavior of High Strength Structural Steel at Elevated Temperatures," *J. Struct. Eng.*, 2006, doi: 10.1061/(asce)0733-9445(2006)132:12(1948).

[3] V. Kodur, M. Dwaikat, and R. Fike, "High-Temperature Properties of Steel for Fire Resistance Modeling of Structures," *J. Mater. Civ. Eng.*, 2010, doi: 10.1061/(asce)mt.1943-5533.0000041.

[4] M. Nassar and L. Amleh, 'Predicting Maximum Effective Temperatures and Thermal Gradients for Steel I-Girder in Canadian Climate Regions', *Applied Sciences (Switzerland)*, vol. 13, no. 10, 2023, doi: 10.3390/app13105906.

[5] J. DING and Y. WANG, 'Finite element analysis of concrete filled steel columns in fire', in *Fourth International Conference on Advances in Steel Structures*, 2005. doi: 10.1016/b978-008044637-0/50155-4.

[6] L. M. Lu, G. L. Yuan, Q. J. Shu, and Q. T. Li, "Numerical analysis on the fire behavior of a steel truss structure," in *Life-Cycle Analysis and Assessment in Civil Engineering: Towards an Integrated Vision - Proceedings of the 6th International Symposium on Life-Cycle Civil Engineering, IALCCE 2018*, 2019.

[7] Wajahat, Raja, Zahoor Khan, Muhammad Yaqub, Muhammad Noman, and Rana Muhammad Waqas. 2021. "Evaluation of Mechanical and Microstructural Properties of Mortar Reinforced with Carbon Nanotubes at Elevated Temperatures. "Pakistan Journal of Engineering and Technology 1–6

7th Conference on Sustainability in Civil Engineering (CSCE'25)
(An International Conference)
Department of Civil Engineering
Capital University of Science and Technology, Islamabad Pakistan

PREDICTING INITIAL STIFFNESS IN WELDED T-JOINTS FEATURING CHS CHORDS AND LONGITUDINAL THROUGH-PLATE CONNECTIONS

[a] Ali Ajwad*, [b] Massimo Latour

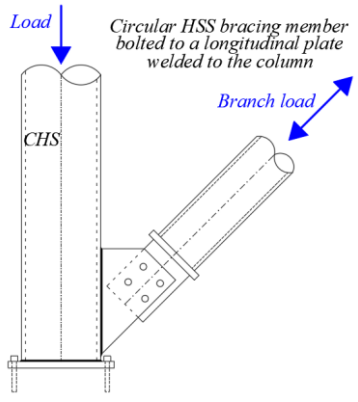
a: DICIV, University of Salerno, Salerno, Italy. aajwad@unisa.it
b: DICIV, University of Salerno, Salerno, Italy. mlatour@unisa.it
* Corresponding author

Abstract- In steel braced frames, connecting longitudinal plates to Circular Hollow Sections (CHS) can lead to low joint stiffness due to deformation of the tube face, often requiring thicker members. To improve this, passing-through plate connections offer increased stiffness but lack predictive stiffness models in current codes and research. This study addresses that gap by developing stiffness formulations for CHS T-joints with axially loaded passing-through plates. Using validated finite element models and parametric analysis of 65 configurations, the proposed equations—based on simplified mechanical models—accurately predict initial stiffness of the connection, having a mean prediction ratio of 1.01 and the coefficient of variation equal to that of 7%.

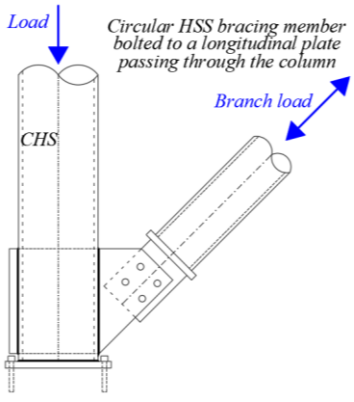
Keywords- Passing-Through Longitudinal Plate, Circular Hollow Section Profile, Regression Analysis, FEM, Abaqus

1 Introduction

Hollow structural section (HSS) members are increasingly favored over open steel sections due to their aesthetically appealing exposed steelwork. Despite a higher cost per ton, their superior compression resistance often results in lighter, more economical compression elements [1]. HSS members also typically reduce painting and transportation costs due to their smaller surface area and lighter weight, while easing installation [2]. Longitudinal plates subjected to axial loads are commonly welded to HSS members in low-rise steel braced frames where wind governs lateral loading [3]. These plates are usually shop-welded to the column and field-bolted to the brace (Figure 1a), though an alternative involves passing the plate through the HSS and welding it on both sides (Figure 1b). A similar detail is seen in CHS trusses, where a plate welded to a chord supports a hanger load (Figure 1c and 1d).



a) Longitudinal Externally Welded



b) Longitudinal Passing Through



c) Longitudinal Externally Welded (K-Joint)



d) Longitudinal Passing Through (T-joint)

Figure 1: Example of a Plate to CHS Connection

Attaching longitudinal plates to CHS members, a practice adapted from I-sections, is common in braced frames for connecting multiple braces at various angles. While extensive research exists on gusset plates welded to I-sections, studies on CHS connections remain limited. In I-sections, axial loads transfer directly through the flange to the web, providing inherent stiffness. In contrast, CHS members distribute axial loads circumferentially via an arching mechanism, inducing out-of-plane bending and making the connection more flexible. This often results in excessive face deformation, with a 1% CHS diameter limit used as a serviceability criterion [4]. Hence, assessing the initial stiffness of such connections is critical. However, Eurocode 3 Part 1.8 [5] only addresses externally welded plates, lacking guidance on through-plate connections and stiffness predictions.

To address the lack of stiffness prediction methods for longitudinal plate-to-CHS joints—particularly for passing-through configurations overlooked by Eurocode 3 Part 1.8—this study proposes analytical equations to estimate initial connection stiffness. Building upon foundational research by Washio et al. [6], Akiyama et al. [7], and analytical work by Togo [8] and Wardenier [9], this study focuses exclusively on passing-through plate connections under axial tension. Passing-through plates are estimated to exhibit 3 to 5 times greater stiffness compared to externally welded plates. Finite element (FE) models were developed and validated using experimental data from Voth [10], which included tests on passing-through plate joints. A parametric analysis comprising sixty-five simulations was then performed on the validated models, forming the basis for the proposed stiffness prediction equations.

2 Parametric Study

In order to check the accuracy of the derived equation, numerical data of 65 selected cases (Table 1) obtained from [11-12] was utilized in this study which were validated using experimental data available in literature with a mean of 0.99. The selected cases depended upon non-dimensional parameters τ, β, γ and η (Figure 2), where;

$$\beta = \frac{t_1}{d_o}, \eta = \frac{b_1}{d_o}, \gamma = \frac{d_o}{2t_o}, \tau = \frac{t_1}{t_o}$$

To connect plates to chords, zero thickness tie contacts were used as a simplified approach. This simplification was intended to reduce the computational time required for the analysis without comprising the accuracy of the models outcomes as already shown in [13-14].

Table 1 Parametric analysis Cases

Case	*k*(kN/mm)	β	η	γ	τ	Case	*k*(kN/mm)	β	η	γ	τ
1	204	0.05	0.52	16.14	1.67	**34**	895	0.10	1.23	13.58	2.78
2	227	0.08	0.52	16.14	2.50	**35**	998	0.10	1.43	13.58	2.78
3	255	0.10	0.52	16.14	3.33	**36**	263	0.06	0.62	20.32	2.50
4	308	0.13	0.52	16.14	4.17	**37**	287	0.06	0.74	20.32	2.50
5	349	0.15	0.52	16.14	5.00	**38**	312	0.06	0.86	20.32	2.50
6	329	0.05	0.91	15.65	1.43	**39**	338	0.06	0.98	20.32	2.50
7	365	0.07	0.91	15.65	2.14	**40**	365	0.06	1.11	20.32	2.50
8	408	0.09	0.91	15.65	2.86	**41**	349	0.10	1.37	18.26	3.50
9	489	0.11	0.91	15.65	3.57	**42**	630	0.11	1.37	15.65	3.50
10	552	0.14	0.91	15.65	4.29	**43**	1023	0.13	1.37	13.69	3.50
11	532	0.04	1.51	15.28	1.25	**44**	1608	0.14	1.37	12.17	3.50
12	585	0.06	1.51	15.28	1.88	**45**	2560	0.16	1.37	10.96	3.50
13	645	0.08	1.51	15.28	2.50	**46**	288	0.10	1.23	20.38	4.00

14	765	0.10	1.51	15.28	3.13	**47**	475	0.11	1.23	17.46	4.00
15	854	0.12	1.51	15.28	3.75	**48**	753	0.13	1.23	15.28	4.00
16	390	0.04	1.48	20.32	1.50	**49**	1188	0.15	1.23	13.58	4.00
17	413	0.05	1.48	20.32	2.00	**50**	1858	0.16	1.23	12.23	4.00
18	455	0.06	1.48	20.32	2.50	**51**	285	0.08	1.10	19.50	3.00
19	480	0.07	1.48	20.32	3.00	**52**	454	0.09	1.10	17.06	3.00
20	510	0.09	1.48	20.32	3.50	**53**	673	0.10	1.10	15.17	3.00
21	376	0.10	0.52	13.84	2.86	**54**	967	0.11	1.10	13.65	3.00
22	469	0.10	0.77	13.84	2.86	**55**	354	0.08	1.47	19.50	3.00
23	562	0.10	1.03	13.84	2.86	**56**	563	0.09	1.47	17.06	3.00
24	645	0.10	1.29	13.84	2.86	**57**	830	0.10	1.47	15.17	3.00
25	748	0.10	1.55	13.84	2.86	**58**	1186	0.11	1.47	13.65	3.00
26	390	0.09	0.46	13.69	2.50	**59**	422	0.09	1.41	19.76	3.50
27	478	0.09	0.68	13.69	2.50	**60**	588	0.10	1.41	17.78	3.50
28	568	0.09	0.91	13.69	2.50	**61**	448	0.10	1.41	19.76	4.00
29	657	0.09	1.14	13.69	2.50	**62**	631	0.11	1.41	17.78	4.00
30	746	0.09	1.37	13.69	2.50	**63**	373	0.08	1.48	22.58	3.50
31	578	0.10	0.61	13.58	2.78	**64**	289	0.09	1.48	20.32	3.50
32	684	0.10	0.82	13.58	2.78	**65**	399	0.10	0.98	20.32	4.00
33	790	0.10	1.02	13.58	2.78						

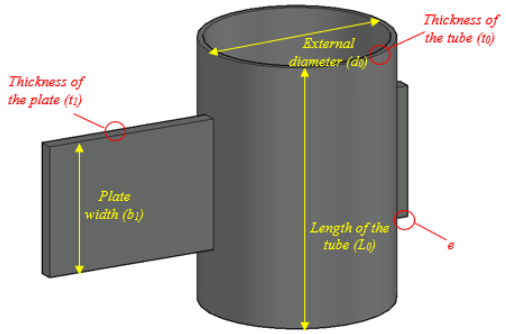


Figure 2: Geometric Factors Affecting Mechanical Performance of connection

3 Equation Derivation

To establish a formulation for computing the stiffness in the passing-through plate configuration, the initial step involves identifying a closed-form solution for the 2D scheme as outlined in Figure 3. In this scheme, guided supports are strategically placed at the plate-to-column attachments, and an external roller is positioned at the midpoint of the examined arch. Wherein the negligible contributions of axial and shear deformability were disregarded to simplify the equation.

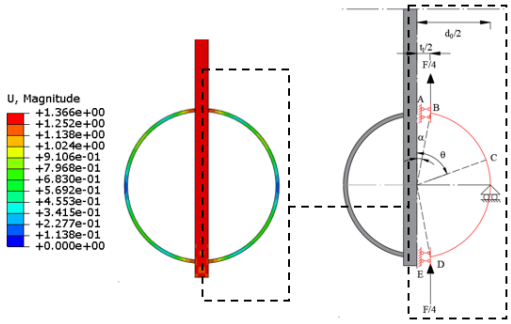


Figure 3: Simplified scheme to assess the stiffness of the passing through component

The derived Equations are as follows;

$$k_{passing} = \frac{1}{16} E d_o \eta^{0.63} \gamma^{-2.96} \tau^{0.14} \frac{(0.7\beta^2 + 1.5\beta - 1)^2}{(0.003 - 0.02\beta + 0.06\beta^2 - 0.1\beta^3)} \quad (1)$$

$$k_{passing_sim.} = 60 E d_o \beta^{0.3} \eta^{0.63} \gamma^{-2.96} \tau^{0.14} \quad (2)$$

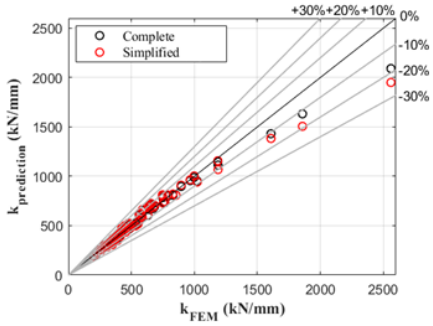


Figure 4: Stiffness formulations vs FE models

4 Conclusion

This study addressed the lack of stiffness prediction methods for passing-through plate-to-CHS connections in Eurocode 3 Part 1.8. A validated finite element model—calibrated against experimental results—was used to conduct a parametric analysis of 65 T-joint configurations with passing-through plates. Based on this, both a closed-form analytical expression and a simplified design formula were proposed. The simplified formula demonstrated strong agreement with FE results (Figure 4), achieving a mean prediction ratio of 1.01 and a coefficient of variation (CoV) of 0.08, confirming its accuracy and reliability. However, the applicability of the proposed equation is currently limited to the parameter ranges considered in the parametric analysis—specifically, β ranging from 0.04 to 0.16, γ between 10.96 and 22.58, τ from 1.25 to 5, and η between 0.46 and 1.55. These ranges correspond to CHS profiles that are readily available in the market, ensuring the proposed formula remains practically relevant for typical design applications.

References

[1]. Packer, J. A., and Henderson, J. E. (1997). "Hollow structural section connections and trusses—A design guide, 2nd Ed." Canadian Institute of Steel Construction, Toronto.
[2]. Piscini, A., Passing-through Tubular Column Joints for Steel and Composite Constructions made by Laser Cutting Technology, PhD Thesis, University of Florence, 2019.
[3]. N. Kosteski and J.A. Packer, Longitudinal Plate and Through Plate-to-Hollow Structural Section Welded Connections, Journal of Structural Engineering, vol. 129(4), pp. 478-486, 2003, https://doi.org/10.1061/(ASCE)0733-9445(2003)129:4(478).
[4]. IIW, 1989: Design recommendations for hollow section joints – Predominantly statically loaded, 2nd Edition, International Institute of Welding, Sub-commission XV-E, Paris, France, IIW Doc. XV-701-89.
[5]. CEN [2005]: EN 1993-1-8 Eurocode 3: Design of Steel Structures. Part 1-8: Design of Joints, CEN, European Committee for Standardization, 2005.
[6]. Washio K., Kurobane Y, Togo T, Mitsui Y, Nagao N. Experimental study of ultimate capacity for tube to gusset plate joints – Part 1. In: Proceedings of the annual conference of the AIJ, Japan; 1970.
[7]. Akiyama N, Yajima M, Akiyama H, Ohtake A. Experimental study on strength of joints in steel tubular structures. J Soc Steel Construct 1974;10(102):37–68.
[8]. Togo, T., Experimental study on mechanical behavior of tubular joints, D. Eng. Thesis, Osaka University, Osaka, Japan, 1967.
[9]. Wardenier, J., Hollow section joints, Delft University Press, Delft, The Netherlands, 1982.
[10]. Voth, A., Branch Plate-to-Circular Hollow Structural Section Connections, Ph. D. Thesis, Toronto, 2010.
[11]. Ajwad, A., Di Benedetto, S., Latour, M., Rizzano, G., Dataset of FE simulations - Connections with CHS profiles and passing-through longitudinal plates, Mendeley Data, V1, https://data.mendeley.com/datasets/ybkjpth6gj/1, 2024.
[12]. Ajwad, A., Di Benedetto, S., Latour, M., Rizzano, G., Stiffness of welded T-joints with CHS chord members and passing-through longitudinal plates, Structures, Volume 71, 2025, https://doi.org/10.1016/j.istruc.2024.107963.
[13]. Ajwad, A., Di Benedetto, S., Latour, M., Rizzano, G., A component method approach for single-sided beam-to-column joints with CHS columns and welded double-tee beam, Thin-Walled Structures, 112055, ISSN 0263-8231, https://doi.org/10.1016/j.tws.2024.112055, 2024.
[14]. A. Sato, G. Elettore, A. Ajwad, S. Di Benedetto, M. Latour, A. B. Francavilla, and G. Rizzano, "Stiffness of Welded T-joints Between SHS Profiles and Through Plates," in Proceedings of the 11th International Conference on Behaviour of Steel Structures in Seismic Areas (STESSA 2024), Lecture Notes in Civil Engineering, vol. 519, pp. 350–361, Springer, Cham, 2024.

BRIDGE EXPANSION JOINTS REPLACEMENT CHALLENGES – A REVIEW

[a] Mustafa Zwain, [b] Furqan Qamar*

a: Graduate Engineer WSP UK, Mustafa.Zwain@wsp.com
b: Associate Director WSP UK, Furqan.Qamar@wsp.com
* Corresponding author

Abstract- Bridge expansion joints play a critical role in maintaining the structural integrity, functionality, and serviceability of bridges by accommodating movements caused by thermal fluctuations, shrinkage, creep, and dynamic loading. However, due to their exposure to harsh environmental conditions and repeated traffic loads, expansion joints are prone to accelerated deterioration, often necessitating repair or replacement well before other bridge components. The replacement of expansion joints presents a unique set of challenges that extend beyond simple component substitution. These challenges encompass design issues, such as ensuring compatibility with ageing structures, recalculating movement ranges under modern codes, and selecting appropriate joint types, as well as construction challenges including unexpected services, poor bridge deck or abutment conditions, adverse weather impacts, and health and safety risks. This paper provides a comprehensive review of the multifaceted challenges associated with bridge expansion joint replacement, drawing upon current literature, case studies, and practical engineering experience. It highlights the importance of proactive investigation, strategic design decisions, and effective collaboration between designers and contractors to mitigate risks and ensure durable, cost-effective solutions. By addressing both design and construction aspects holistically, this review aims to support practitioners in developing resilient maintenance strategies for bridge infrastructure, ultimately contributing to improved asset longevity and reduced life-cycle costs. The review also identifies a critical gap in knowledge transfer practices and calls for the development of industry-wide mechanisms to capture and share field-level insights from replacement projects.

Keywords- Expansion Joints, Design Challenges, Construction Challenges, Joint Replacement, Structural Durability

1 Introduction

Bridge expansion joints are essential elements of bridge structures, allowing for controlled movement between bridge spans and adjacent structures. They accommodate thermal expansion and contraction, shrinkage, creep, live load deflections, and, where relevant, seismic movements. By doing so, they help prevent unwanted stresses, cracking, and other structural damage to bridge superstructures [1], [2]. However, expansion joints are highly vulnerable to deterioration due to their exposure to repeated dynamic loads, harsh environmental conditions, and the ingress of water and de-icing salts. These factors contribute to wear, fatigue, corrosion, and material degradation, leading expansion joints to often become one of the first bridge elements to require repair or replacement [3]. Their performance directly impacts not only structural integrity but also user comfort, traffic safety, and maintenance costs. Frequent replacement or refurbishment of expansion joints throughout a bridge's life cycle is common. Studies such as those by Lima and de Brito [4] and Chang and Lee [5] highlight that poorly functioning joints are major contributors to deck deterioration, particularly when water leakage compromises waterproofing systems. Failure to maintain effective expansion joints can thus lead to rapid escalation of repair needs elsewhere in the bridge, increasing life-cycle costs significantly.

In accordance with CD 357 [6], bridge expansion joints are classified according to their capacity to accommodate structural movements. The principal categories include small movement joints (up to 40 mm), such as buried, flexible plug and nosing joints, which are typically employed on shorter span structures due to their simplicity and cost-effectiveness. Medium movement joints (ranging from 40 mm to 100 mm), including cantilever systems, offer enhanced flexibility and are suitable for moderate span bridges. For applications involving large movements (exceeding 100 mm), modular joints and supported joints are commonly utilised, offering superior performance in terms of movement accommodation and load distribution. The selection of an appropriate joint type is governed by factors such as span length, traffic loading, environmental exposure, and long-term maintenance requirements. Each type presents unique challenges when replacement is required. Modular joints, for example, are complex systems involving multiple support bars and sealing elements, and their replacement often requires substantial interventions into the bridge structure itself [7]. Despite their criticality, a focused body of literature on the replacement challenges of bridge expansion joints remains relatively limited. Existing research has predominantly concentrated on the behaviour and performance of new joint systems [8], the development of new materials and fatigue-resistant designs [9], or the impact of joint failures on the overall health of bridges [10]. Studies specifically analysing the difficulties encountered during joint replacement including: investigations, design compatibility, waterproofing integration, construction logistics, and quality assurance are comparatively rare.

Replacement challenges are complex. On the design side, ensuring compatibility with an ageing structure, recalculating required movement ranges under modern standards, and diagnosing the original cause of failure are complex tasks. Construction challenges can include encountering unexpected conditions such as hidden services, differing verge compositions, widespread deck deterioration, and adverse weather impacts. Moreover, poor site practices, such as insufficient surface preparation or incorrect waterproofing application, can lead to early failure of the new joint if not adequately managed [11]. While these challenges are widely encountered, the insights gained from addressing them are not consistently captured or shared across the industry. Despite the high volume of bridge expansion joint replacements performed globally each year, there remains a lack of structured integration of practical experience into design standards, guidance documents, or academic literature. Much of the decision-making on-site depends on implicit knowledge held by experienced engineers and contractors, which often remains undocumented. As a result, recurring problems, such as inadequate waterproofing integration or overlooked utility conflicts, continue to affect outcomes. This review not only catalogues technical challenges but also underscores the need for improved knowledge-sharing mechanisms to support more consistent and effective practices across future projects and jurisdictions.

2 Discussion of Design Challenges

The replacement of bridge expansion joints represents a technically demanding and multi-faceted engineering challenge. Expansion joints, which allow for controlled movement and mitigate stresses in bridge decks, are critical to the longevity and functionality of bridge structures. Over time, joints become subject to wear, material degradation, or structural damage, necessitating their replacement to maintain serviceability and safety. However, undertaking this task in existing structures introduces a complex set of design challenges (Table 1), which must be addressed systematically to ensure successful outcomes.

Table 1: Key Design Challenges and Solutions

Design Challenges	**Potential Solutions**
Compatibility of New Expansion Joint with Existing Structure	Ensure compatibility with existing structure, recalculate movement ranges
Identification of the Original Cause of Failure	Diagnose failure causes like fatigue, material degradation, and vehicular impact
Refurbishment Versus Replacement	Decide based on condition, age, maintenance history, and cost
Missing As-Built Records	Conduct special inspections or trial holes to gather necessary information
Traffic Management Plan	Use phased construction, temporary joints, or rapid-cure materials to minimise closure times
Achieving Long-Term Durability	Emphasise durability in design specifications, including corrosion-resistant fixings and protective coatings

2.1 Compatibility of New Expansion Joint with Existing Structure

A fundamental design challenge lies in ensuring that the replacement joint is fully compatible with the existing bridge structure. Key factors include accommodating the current joint gap, as well as recalculating the bridge's range of movement based on contemporary design codes. Modern standards, such as the Eurocodes, typically demand greater allowances for thermal, shrinkage, live load and seismic movements than older national codes. This recalculation often reveals that existing expansion joints are not suitable for the bridge's theoretical movements, especially in older structures, necessitating the selection of a joint system with greater movement capacity.

2.2 Identification of the Original Cause of Failure

Accurately diagnosing the cause of existing joint failure is essential to prevent recurrence. Failure mechanisms can include fatigue damage to components, material degradation due to de-icing salts, insufficient movement capacity, poor workmanship, and damage from vehicular impact. In many cases, particularly for resin-anchored joints, deterioration of the underlying concrete is a major contributor to failure.

a)  b) 

Figure 1: Case study of a bridge with failed expansion joint nosing, a. Photo of the failed temporary repair (highlighted in red box) before excavation, and b. Photo of the bridge deck after excavating expansion joint temporary repair.

Figure 1 shows extensive concrete deterioration at a joint resin location which was temporarily repaired. The poor concrete was visible once the temporary repair was removed. In this case, simply replacing the temporary repair with new joint resin would not be satisfactory. A concrete repair of the bridge deck is required in order to prevent future resin from failing in compression again. In any expansion joint replacement design scheme an investigation should be mandated to understand the reason behind joint failure.

2.3 Refurbishment Versus Replacement

A strategic decision often arises: whether to refurbish the existing joint or to pursue full replacement. Refurbishment can offer significant advantages, including reduced project duration, lower material and labour costs, and minimal disruption to traffic. However, refurbishment is only feasible where the residual life of critical components remains acceptable.
A decision framework should be adopted, based on key factors such as:

1 Condition grading of existing components
2 Age and maintenance history of the joint
3 Predicted future loading and movement demands
4 Cost comparison over the remaining service life

For joints approaching the end of their design life or suffering systemic failures, full replacement is typically more prudent.

2.4 Missing As-Built Records

A major obstacle in bridge expansion joint replacement projects is the frequent lack of as-built drawings, particularly for older structures. Without accurate records, critical parameters such as dimensions and type of present expansion joint system may be unknown. For exposed joints it may be necessary to instruct for a Special Inspection specifically for the expansion joints to collect information required for the design of new expansion joints.
This special inspection may include:

1 Precise measurement of joint gaps at various temperatures
2 Survey of joint profile dimensions
3 Photographic and video documentation
4 Noting visible signs of distress, cracking, or leakage

In the case of buried joints, the recommended solution is to instruct the Contractor to carry out trial holes. These should be performed at anticipated joint locations, allowing direct observation and measurement. Information obtained may include deck and abutment concrete condition, joint gap width, existing waterproofing type and condition, depth of paving.

2.5 Traffic Management Plan

Replacing bridge joints often requires partial or full lane closures, presenting significant challenges for traffic management, particularly on heavily trafficked routes. The design must consider phased construction approaches, temporary joints, or the use of rapid-cure materials to minimise closure times. Designs may incorporate sequencing that enables half-width construction to maintain one open lane wherever possible. Traffic impact assessments should be prepared early in the project, and liaison with highway authorities is essential to agree acceptable working windows and potential diversions.

2.6 Long-Term Durability

Designers should aim for solutions that maximise the life-cycle performance of the replacement joint. Design specifications should emphasise durability, including:

1 Use of corrosion-resistant fixings (e.g., stainless steel or hot-dip galvanised components)
2 Protective coatings for anchorage systems
3 Drainage details that prevent ponding water and freeze damage
4 Clarification of recommended maintenance procedures

Specifications should also require certification of joints e.g. CE Marking, and site quality control should include measuring and testing of installed components, such as torque testing of anchor bolts and water tightness checks.

3 Discussion of Construction Challenges

The construction phase of bridge expansion joint replacement is often fraught with practical difficulties, many of which arise due to the complexities and uncertainties inherent in working with existing structures. Despite detailed design preparations, the actual conditions encountered on site can differ significantly from expectations, leading to risks of delay, cost overrun, and quality compromises. A systematic discussion of common construction challenges (Figure 2), alongside proposed mitigation measures, is critical for improving project outcomes and ensuring durable joint installations.

Discovery of Unexpected Services	1 Conduct detailed utility surveys and trial holes to identify buried services early 2 Plan service diversions or protective measures
Unsuitable Waterproofing Conditions for Buried Joints	1 Carry out exploratory trial holes in advance to assess waterproofing condition 2 Consult Designer for best action if waterproofing is missing or damaged
Variability in Verge or Central Reserve Construction	1 Perform early trial holes or intrusive investigations to identify reinforcement types and concrete condition 2 Allow for extended breakout and reinstatement times in the programme
Widespread Poor Deck Condition	1 Conduct trial holes and surveys well in advance 2 Plan for flexible construction resources
Weather Risk	1 Be prepared to delay or cancel installation works if poor weather is expected
Construction Errors	1 Conduct pre-construction briefings and regular site supervision

Figure 2: Summary of construction challenges and potential solutions.

3.1 Discovery of Unexpected Services

a)  b) 

Figure 3: Case study of a bridge with unexpected service duct, a. Unexpected service duct found during asphaltic plug joint replacement construction works, and b. Installation of steel protection to service duct before pouring of hot bituminous material.

One of the most frequent and disruptive challenges during bridge expansion joint replacement is the unanticipated discovery of buried services (Figure 3(a)), particularly in verges or central reservations. Services such as electrical ducts, fibre optic cables, drainage pipes, and even water mains are often found within bridge verges without accurate documentation in the asset records. The presence of such services directly beneath or adjacent to the expansion joint location can severely constrain construction activities, including demolition and reconstruction works. To mitigate this risk, there are various actions that can be undertaken:

1 A detailed utility survey, combining ground-penetrating radar and electromagnetic detection methods, undertaken well in advance of site mobilisation.
2 Targeted trial holes at proposed construction locations can confirm the presence and depth of critical services.
3 It may be possible to protect service ducts such as in Figure 3(b) where protective steel is added around the service duct before pouring of the hot bituminous material of the asphaltic plug joint. However, in many cases such as where there are sensitive services such as fibre electric or gas it is not possible to safely excavated around the service duct to install the new joint without prior approval with the service provider.

4 In many cases it may be required to switch off the service temporarily or re-route the service permanently in order to proceed with an expansion joint replacement. Without planning ahead of time for this, construction works face much larger costs as it would be necessary to return at a later date to complete the expansion joint replacement near the location of service ducts.

Early identification enables the design and construction programmes to be adapted, whether by altering joint positioning, planning service diversions, or implementing protective measures. Failure to undertake sufficient preliminary investigation may result in significant site delays, increased costs, and potential safety hazards.

3.2 Unsuitable Waterproofing Conditions for Buried Joints

Another common and serious issue encountered during construction is the absence or poor condition of existing waterproofing (Figure 4) where new buried joints are to be installed. Effective waterproofing continuity is essential to prevent water ingress into the bridge deck, and poor lapping conditions can critically undermine the integrity of the installation. The recommended strategy is to carry out exploratory trial holes several weeks or months in advance of construction to assess the condition of the deck waterproofing. Where waterproofing is found to be missing, damaged, or unsuitable for lapping, the Designer must be consulted to decide on the best action to deal with the issue. In extreme cases, it may be necessary to re-waterproof part or all of the bridge deck. While such measures involve additional cost and programme implications, they are essential to preserve the long-term serviceability of the bridge structure.



Figure 4: Existing bridge waterproofing left in place to provide lapping with new waterproofing system to be installed at buried joint.

3.3 Variability in Verge or Central Reserve Construction

Unexpected differences in the verge or central reserve construction, particularly regarding reinforcement, present significant challenges during joint replacement. For example, an area expected to be unreinforced concrete may in reality contain heavy reinforcement, significantly increasing the time and effort required to break out and reinstate the area. To mitigate this risk:

1 Conduct early trial holes or intrusive investigations at planned construction locations.
2 Record key details such as reinforcement type, concrete thickness, and substrate condition.
3 Adjust construction methodologies and resource planning based on actual findings.
4 If early investigations are not possible, include allowances in the programme for potential delays and reinforced concrete reinstatement techniques.



Figure 5: Presence of a vehicle restraint system post at expansion joint location.

In Figure 5 it can be seen that there is a vehicle restrain system (VRS) post right at the buried expansion joint location. The Designer must take into account such obstacles in the design solution. In the case of Figure 5, the presence of the VRS post was known and a specialist fencing Contractor removed the post and installed two new posts around the joint. Without prior Designer instruction on this issue, it would not have been possible to remove the VRS post safely (by installing new posts at favourable positions) during the 2 days of works and so the joint would not have been fully replaced. A significant amount of money would need to be expended to visit the site again after the post is moved in order to install the remaining part of the new joint.

3.4 Widespread Poor Deck Condition

A more serious, systemic challenge is encountering widespread poor deck condition during construction, with multiple areas requiring concrete repair. It is not uncommon for older bridge decks to have significant delamination, spalling, or chloride-induced corrosion that only becomes fully apparent once surface materials are removed.
The two-fold mitigation strategy consists of:

1 Conducting trial holes surveys well in advance to determine the likely extent of deterioration.
2 Building conservative assumptions into the construction programme, allowing sufficient float for unexpected concrete repairs.

If extensive repairs are identified as likely, it may be preferable to undertake preliminary deck rehabilitation works ahead of or alongside the joint replacement project. Planning for flexible construction resources, including access to additional labour and materials for repairs, can prevent schedule overruns.

3.5 Weather Risk

Weather conditions, particularly rainfall, pose a serious risk to the installation of most types of joints. Successful bonding of waterproofing membranes and installation of resin-based systems are highly sensitive to moisture levels and temperature. Rain immediately prior to or during installation can compromise adhesion and waterproofing integrity. It is therefore essential that weather forecasts are monitored closely in the days and hours leading up to joint installation. Site management must be prepared to delay or cancel installation works at short notice if inclement weather is expected. Contracts should allow for such flexibility, and protection measures such as temporary covers or shelters should be available where appropriate to shield working areas. A strong culture of quality over programme must be maintained, ensuring that installations are only carried out under suitable environmental conditions.

3.6 Construction Errors

Mistakes during construction, such as cutting away excessive waterproofing during the preparation for buried joint installation, can jeopardise the waterproofing system's effectiveness. The critical lap length between old and new waterproofing layers may be compromised if excessive material is removed. If this occurs, the following steps are recommended:

1 Exposing additional waterproofing in adjacent areas, ensuring that the minimum specified lap length is still achieved.
2 If exposure is not possible or the adjacent waterproofing is in poor condition, the Design team should be consulted immediately to agree an appropriate remediation, which may include local re-waterproofing or doing nothing.

Other construction errors such as installation of defective or incorrect components can be prevented by supervision of construction by a representative of the Designer. Overall, clear and precise method statements, combined with pre-construction briefings and regular site supervision, are key preventative measures to reduce the likelihood of such errors.

4 Conclusions

In summary, the successful replacement of expansion joints in bridge structures relies heavily on the collaborative roles of both Designers and Contractors. Designers play a critical role in ensuring that the specifications and methods align with the requirements of the project. Their expertise is essential in identifying solutions when complications arise, such as compromised waterproofing lap lengths or deteriorated bridge deck condition. Designers must also be proactive in establishing clear and precise method statements that guide Contractors during implementation. Contractors, on the other hand, are responsible for executing the replacement process with precision and adherence to the provided design. Their role includes implementing preventative measures such as rigorous pre-construction briefings and ensuring that site supervision is maintained to reduce the likelihood of errors during construction. Ultimately, the effective collaboration between Designers and Contractors is the cornerstone of successfully replacing bridge expansion joints. By fulfilling their respective roles with diligence and ensuring seamless communication, the longevity and functionality of these critical structural components can be significantly enhanced.

While bridge expansion joint replacements are carried out routinely worldwide, there remains a lack of consolidated industry guidance that synthesises the collective lessons learned from past replacement projects. Despite the wealth of field experience, many replacement efforts continue to face preventable issues due to fragmented knowledge sharing between regions, agencies, and Contractors. Further work is needed to establish unified performance benchmarking, case documentation standards, and feedback loops that translate practical experience into actionable design and construction improvements. Developing such frameworks could significantly enhance the consistency and long-term performance of joint replacement interventions.

References

[1] W. F. Chen and L. Duan, Bridge Engineering Handbook: Construction and Maintenance. CRC Press, 2014.
[2] A. El-Safty and A. M. Okeil, "Extending the service life of bridges using continuous decks," PCI Journal, vol. 53, no. 6, pp. 96–111, Nov.–Dec. 2008.
[3] M. Yang, S. Kainuma, W. Nabeshima, M. Yamauchi, and B. Ji, "Synergistic effect of corrosion and residual stress on fatigue cracks of finger-type bridge expansion joints," *Engineering Failure Analysis*, vol. 131, p. 105894, 2022.
[4] J. M. Lima and J. de Brito, "Inspection survey of 150 expansion joints in road bridges," *Engineering Structures*, vol. 31, no. 5, pp. 1077-1084, 2009.
[5] L. M. Chang and Y. J. Lee, "Evaluation of performance of bridge deck expansion joints," *Journal of Performance of Constructed Facilities*, vol. 16, no. 1, pp. 3-9, 2002.
[6] National Highways, *CD 357: Design of bridge deck expansion joints*, Design Manual for Roads and Bridges (DMRB), UK, 2020. [Online]. Available: https://www.standardsforhighways.co.uk/dmrb/search/357
[7] R. J. Dexter, C. B. Osberg, and M. J. Mutziger, "Design, specification, installation, and maintenance of modular bridge expansion joint systems," *Journal of Bridge Engineering*, vol. 6, no. 6, pp. 529-538, 2001.
[8] Y. Q. Ni, X. G. Hua, K. Y. Wong, and J. M. Ko, "Assessment of bridge expansion joints using long-term displacement and temperature measurement," *Journal of Performance of Constructed Facilities*, vol. 21, no. 2, pp. 143-151, 2007.
[9] H. M. Cho, H. W. Lee, K. S. Kim, and K. T. Park, "Investigating the Application of Smart Materials for Enhanced Maintenance of Rubber Expansion Joints in Bridge Expansion Joint Systems," *Applied Sciences*, vol. 14, no. 7, p. 2828, 2024.
[10] A. Lee Kelly, R. A. Atadero, and H. N. Mahmoud, "Life cycle cost analysis of deteriorated bridge expansion joints," *Practice Periodical on Structural Design and Construction*, vol. 24, no. 1, p. 04018033, 2019.
[11] D. White, S. Sritharan, M. T. Suleiman, and S. Chetlur, "Identification of the best practices for design, construction, and repair of bridge approaches," Iowa Dept. of Transportation, CTRE Project 02-118, 2005.

7th Conference on Sustainability in Civil Engineering (CSCE'25)
(An International Conference)
Department of Civil Engineering
Capital University of Science and Technology, Islamabad Pakistan

NUMERICAL BEHAVIOR OF STEEL SPACE FRAME UNDER INCREMENTAL SEISMIC LOADS

[a] Kamran Shaukat*, [b] Muhammad Fahim

a: Department of Civil Engineering, UET Peshawar, Peshawar, Pakistan. cekamranshaukat@gmail.com
b: Department of Civil Engineering, UET Peshawar, Peshawar, Pakistan. drfahimuet@gmail.com
* Corresponding author

Abstract- Space frames are structural systems composed of linear elements arranged in a three-dimensional configuration to efficiently transfer loads. However, they exhibit complex dynamic behavior during earthquakes, particularly in seismically active regions such as Japan, China, and the United States. Notably, the 2013 Lushan earthquake caused severe damage to multiple structures, including three gymnasiums with space frame roofs. The destruction and collapse of long-span spatial structures are usually due to the large plastic deformation of the members. How to avoid bending and buckling due to the damage of the member under earthquake load is the key point in the design. This study investigates the elastic and plastic response of space frames using the finite element software ABAQUS. The structural model is assumed to be located in Abbottabad, Pakistan, a region with notable seismic activity. Incremental Dynamic Analysis (IDA) of a space frame was performed under the Chi-Chi (1999) earthquake record with progressively increasing intensity levels. Yielded Element Ratios and integration point evaluations was used to assess the yielding of members and section points. The findings provide a better understanding of how space frames behave under incremental seismic loads and give a brief understanding of performance-based design of space frames.

Keywords- Incremental Dynamic Analysis, Seismic Response, Space Frame, Yielding Behavior

1 Introduction

Single-layer space frames, known as lattice shells, can take the form of either flat or curved surfaces are widely used in the design of large-span public buildings such as sports arenas, exhibition pavilions, museums, and transportation terminals [1]. Their intricate geometries and interconnected joints make them vulnerable to various forms of damage during earthquakes [2]. The importance of comprehending the response of space frame is highlighted by various well-known structural collapses of space frames in the previous incidents. including Bucharest Dome [2], Hartford Civic Center Coliseum [3], Lushan and Baoxing gymnasium [4], [5]. Significant structural damage was observed in the Lushan and Baoxing gymnasiums during the 2013 Lushan earthquake such as buckling, joint failures, strength degradation, and member fractures [4], [5].

Large-span space structures in the form of reticulated domes are widely used in large-scale public buildings. Understanding the behavior of these structures under seismic loading is critical due to their susceptibility to complex failure mechanisms i.e. plastic hinge formation, member buckling, and progressive collapse [4], [6]. In order to have a better understanding of its mechanical performance and verify the collapse mechanism of space frame and failure patterns of the members a shaking table test was performed and a comparison between the experimental and numerical results obtained using the finite element software ABAQUS was made and a satisfactory agreement was found [7]. A theoretical strut model was introduced with the aim of increasing computational efficiency, The results were verified with experimental results [3], [7] confirming the reliability of numerical simulations. Zhi et al studied the failure modes due to instability and strength failures using a numerical model [8]. Furthermore, Different mitigation strategies have been tested to improve the seismic performance of steel space frames. Approaches such as viscous dampers [9], 3D base isolator [10], and buckling-restrained

braces (BRBs) [11] have been found effective in reducing damage, controlling deformation, and enhancing overall stability under seismic loading.

In this study, the plastic behavior of single-layer space frame, commonly referred to as reticulated dome. The structure is assumed to be located in Abbottabad, Pakistan. The region of high seismicity influenced by the Indus Kohistan thrust, which features active reverse and strike-slip fault mechanisms [19]. The dome configuration is based on a model previously studied by Zhi et al. in his detailed numerical study and was designed according to Chinese building codes [8]. A finite element model is developed in ABAQUS to simulate and analyse the initiation and progression of yielding, the formation of plastic zones, and the overall seismic resilience of the reticulated dome.

2 Research Methodology

The Chi-Chi (1999) earthquake was selected based on seismic geology of the area. To represent the seismic demand, a scenario-based Maximum Considered Earthquake (MCER) response spectrum corresponding to Site Class D was created. A Finite element model of the dome was developed using Q235B structural steel with uniform circular hollow sections. Rayleigh damping and non-structural mass were used to incorporate the corresponding effects on dynamic behavior of the dome. ABAQUS B32 beam element was used in the model, with two integration points per element and each integration point consists of four section points where stresses and strains were evaluated. Yielding at individual points was used to compute the Yielded Element Ratio (YER), defined as the ratio of elements in which yielding occurred at certain section points to the total number of elements. To distinguish the extent of plasticity, terms such as 1P, 5P, and 8P were used indicating that 1, 5, or all 8 section points in an element had yielded, respectively.

2.1 Numerical Model

The proposed numerical model represents a single-layer reticulated dome with a span of 40 meters and a rise-to-span ratio of 1/3 as shown in (Figure 1a). Structural steel was used as the material, with properties including a Poisson's ratio of 0.3, yield strength of 235 MPa, mass density of 7850 kg/m³, and an elastic modulus of 206 GPa. The corresponding yield strain was taken as 0.0015. The material's ultimate tensile strength ranged from 370 to 500 MPa, with a minimum elongation of 26%, in this study the elastic and hardening part of the curve has been taken for the sake of calculations and no damage or fracture was considered. To capture the plastic behaviour, a stress–strain curve was defined and applied in the model, as shown in Figure 1b. A uniform circular hollow section (CHS) pipe with outer diameter of 114 mm and 4 mm thickness was assigned to all the frame members including ring, radial, and diagonal members of the dome. Structural nonlinearity was modelled at the section point level. Roof mass of 200 kg/m² was applied as a non-structural mass at the nodes to all nodes that were not subject to boundary conditions. Rayleigh damping was applied with a damping ratio of 0.5. The first natural frequency of the dome was evaluated after modal analysis to be 2.55 Hz. The Raleigh constants were calculated the value of α and β were 0.7997 and 0.002.

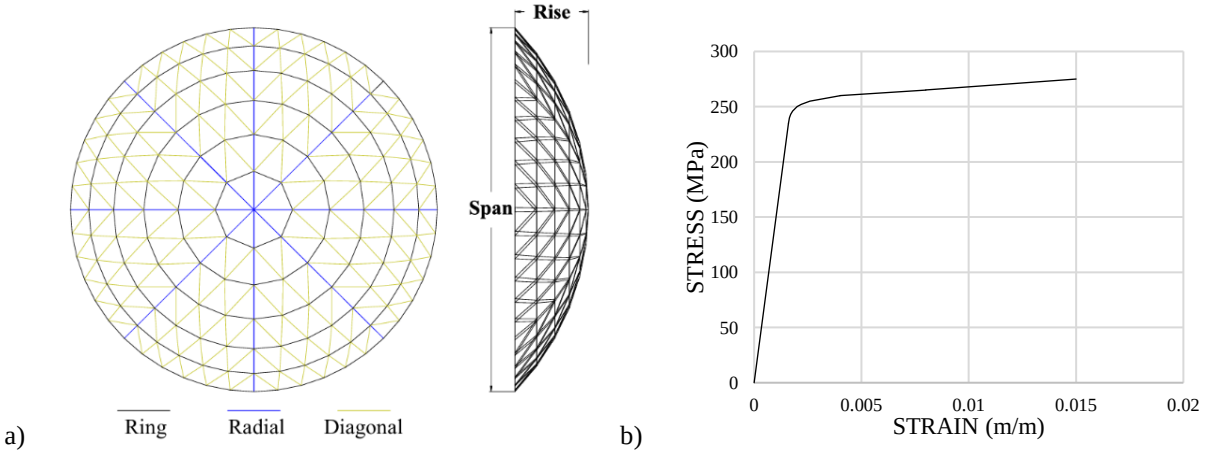
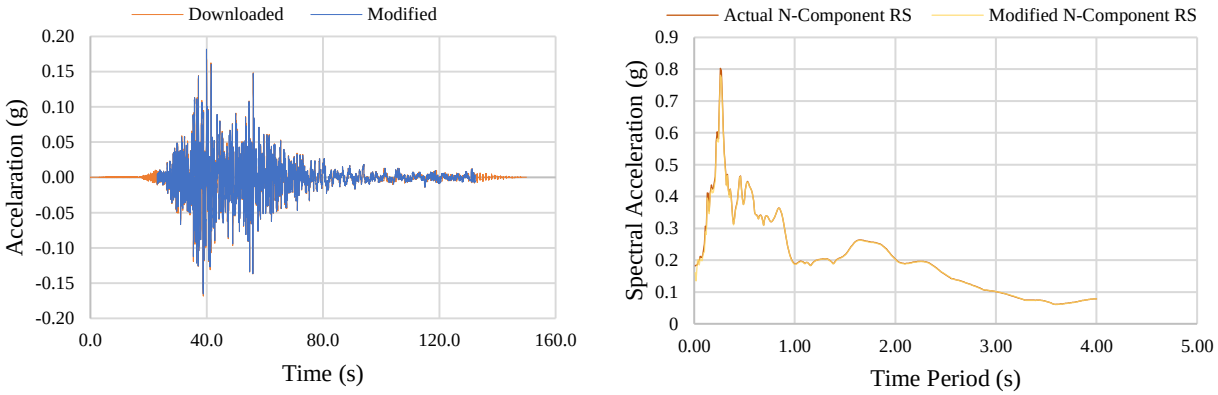


Figure 1: Details of the model, a. Geometry of the Kiewit-8 dome, b. stress strain curve of material model

2.2 Ground Motion Selection and Modification

The Chi-Chi (1999) earthquake ground motion was selected due to its reverse faulting mechanism, long duration, and moment magnitude of 7.6 on the Richter scale. These characteristics align with the regional seismicity and aligns to the Kashmir 2005 earthquake. The ground motion record was downloaded from the PEER ground motion database. The 3D ground motion record was first resampled from a time step of 0.004 seconds to 0.02 seconds. The first and last 0.05% of the ground motion energy were trimmed top remove low-impact tails. As a result, the total duration of the record was reduced from 150 seconds to 109 seconds. A comparison of the response spectrums before and after these modifications confirmed that the spectral characteristics were preserved. The comparison between the actual and modified time histories, along with their corresponding response spectrums are shown in (Figure2a, 2b).

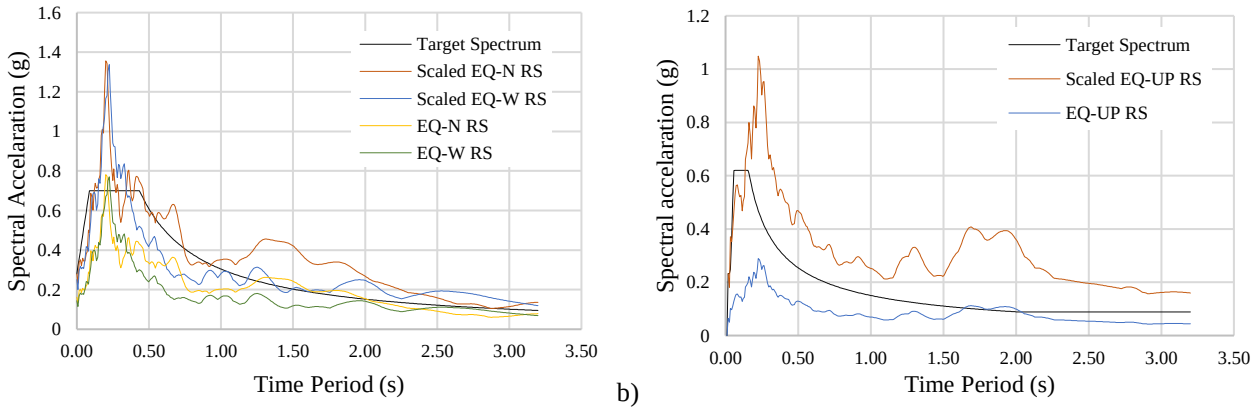


a) b)

Figure 2: N-Component before and after modifications, a. Time history, b. Response spectrum

2.3 Scaling of Ground Motion

A scenario-based seismic hazard was considered in accordance with the Pakistan Building Code (PBC) 2021, corresponding to a 20% probability of exceedance in 50 years and a return period of 225 years. Maximum Considered Earthquake Risk (MCER) level, response spectrums were developed following the procedures outlined in Chapter 11 of ASCE 7-16 for both horizontal and vertical ground motions. These spectrums were then used to scale the selected ground motion components, ensuring consistency with the target hazard level at the site. The scale factors for horizontal and vertical components were calculated as 1.73 and 3.62. (Figure 3a) presents the scaled and unscaled horizontal ground motion spectra alongside the corresponding target hazard spectrum, while (Figure 3b) illustrates the comparison for the vertical component with its respective target spectrum.



a) b)

Figure 3: Description of scaled, unscaled and target response spectrums, a. Horizontal, b. Vertical

2.4 Incremental Dynamic Analysis

Incremental Dynamic Analysis (IDA) was employed to evaluate both the elastic and inelastic behavior of the reticulated dome under increasing seismic intensity. The modified and scaled 3D ground motion were expressed in units of g (Figure. 4) and amplitudes were applied incrementally at seven levels, ranging from $0.5g \times A_{x,y,z}(t)$ to $1.5g \times A_{x,y,z}(t)$, where $A_{x,y,z}(t)$ denotes the 3D components of modified and scaled ground motion acceleration. At each intensity level, the structural response was assessed in terms of yielding initiation and plastic zone development.

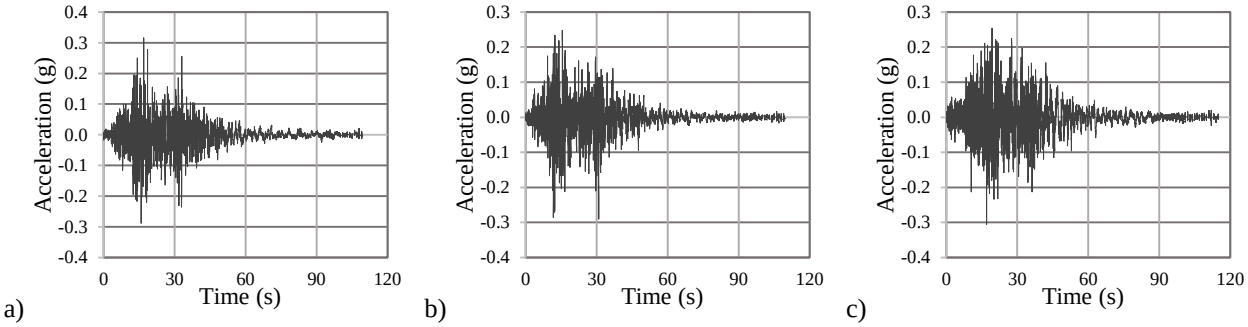


Figure 4: Details of Chi-Chi (1999) 3D ground motion, a. N-Component, b. W-Component, c. UP-Component

3 Results

The structural response has been evaluated in terms of yielded element ratios. A comparison between 1P and 5P, as well as between 5P and 8P, is made. The significance of assigning such a criterion lies in understanding the level of plasticity that occurs at a single element and evaluating if there is still elastic energy left in the section at as some parts of the section can deform elastically while others have already yielded. Response acceleration of the top node at three different intensity levels are evaluated, and Fourier transforms are conducted to study frequency content and amplitudes. In the last section, the progression of yielding has been discussed and described at four different intensities.

3.1 Structural Response

The structure remained elastic at 0.5g and started yielding when the intensity of the ground motion was increased to 0.6g and only two elements were yielded according to 1P yield element ratio. As shown in (Figure 3a), the 1P yield element ratio exhibits the earliest and most rapid increase, indicating early initiation of yielding under less restrictive conditions. At 1.0g, the 1P yield element ratio reaches approximately 0.19, while the 5P yield element ratio is 0.11, which is 44% lower, indicating delayed yielding under stricter criteria. At an intensity of 1.5g, the 1P ratio increases to 0.40, while the 5P yield element ratio remains 0.25, about 38% lower. From 0.6g to 1g, the 1P yield element ratio increases by 0.19, while the 5P ratio increases to 0.11, indicating a 44% slower growth. Within the higher intensity range from 1 to 1.5g, the 1P ratio grows by an additional 0.21, while the 5P yield element ratio increases by only 0.14, reflecting a 32% slower rate, continuing the trend of delayed yet accelerating yielding under stricter conditions.

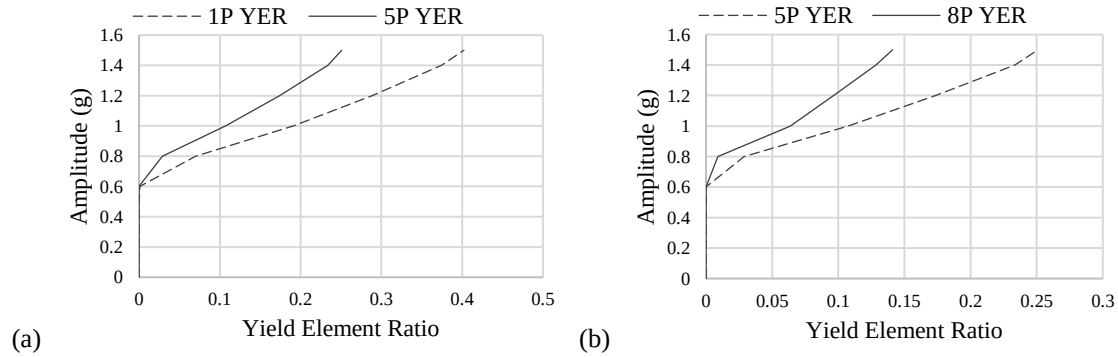


Figure 5: Comparison of Yield Element Ratios of the structure at increasing amplitudes

As shown in (Figure 3b), comparison between 5P, and 8P yield element ratios reveals a progressively delayed yielding behavior. At 0.8g, the 8P yield element ratio is approximately 87.1% lower than the 1P ratio and 68.6% lower than the 5P yield element ratio. At 1.0g, the 8P ratio remains 66.7% lower than the 1P ratio and 40.5% lower than the 5P ratio. At the intensity of 1.5g, the 8P ratio reaches a value 64.9% lower than the 1P ratio and 43.8% lower than the 5P yield element ratio, while the 5P ratio is 37.6% lower than the 1P ratio.

3.2 Acceleration Response

The acceleration response of the top node at increasing intensities was evaluated. The peak acceleration in the x-direction rose by 92.4% between 0.5g and 1.0g, and by 23.1% between 1g and 1.5g (Figure 4a), while in the y-direction the peak acceleration increased by 79.6% and 14.0%, respectively (Figure 4c). The vertical peak acceleration nearly doubled, increasing by approximately 99.6% from 0.5g to 1.0g and by 49.6% from 1g to 1.5g (Figure 4e). While the percentage gains decreased at higher amplitudes across all directions, the absolute amplification in peak acceleration at the top node remains persistent. Fourier analysis of the acceleration time histories revealed a slight but consistent shift in dominant frequencies. For the x-direction, the frequency corresponding to the peak Fourier amplitude decreased from 4.58 Hz at 0.5g to 4.37 Hz at 1.5g (Figure 4b), reflecting a softening response. The y-direction displayed a relatively stable dominant frequency of 4.48 Hz reducing to 4.46 Hz (Figure 4d). The vertical direction exhibited the highest frequency content, with dominant pepaks at 11.76 and 11.73 Hz. (Figure 4f).

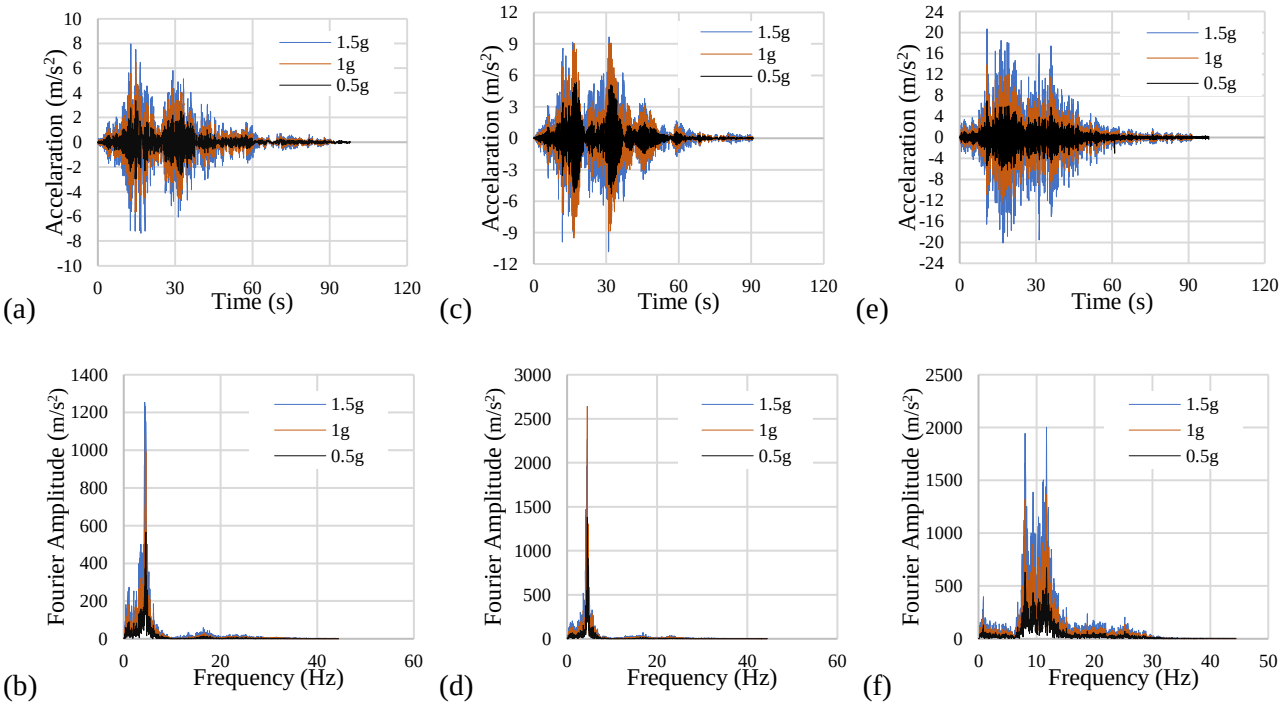


Figure 6: Acceleration response at the top node and corresponding Fourier transform at different amplitudes

3.3 Element Response

The yielding behavior of the dome under increasing seismic amplitudes is shown in (Figure 5a–d). Initial yielding occurred at 0.6g in two ring members having 1P yielded elements (0.0011). At 0.8g, diagonal members around radial members in the outermost ring yielded, with 1P, 5P, and 8P yielded element ratios of 0.07, 0.03, and 0.01, respectively. Members in the middle ring were partially yielded. When the intensity increased to 1.0g, the yielding spread among the diagonal elements of the second and outermost rings, with 1P, 5P, and 8P ratios rising to 0.19, 0.11, and 0.06. A small number of elements in ring members partially yielded, while no yielding was observed in radial members (Figure 5a). At 1.5g, most of the diagonal elements in the outer rings had yielded, with ring elements on the middle and outer ring members showing 1P, 5P, and 8P values of 0.40, 0.25, and 0.14.

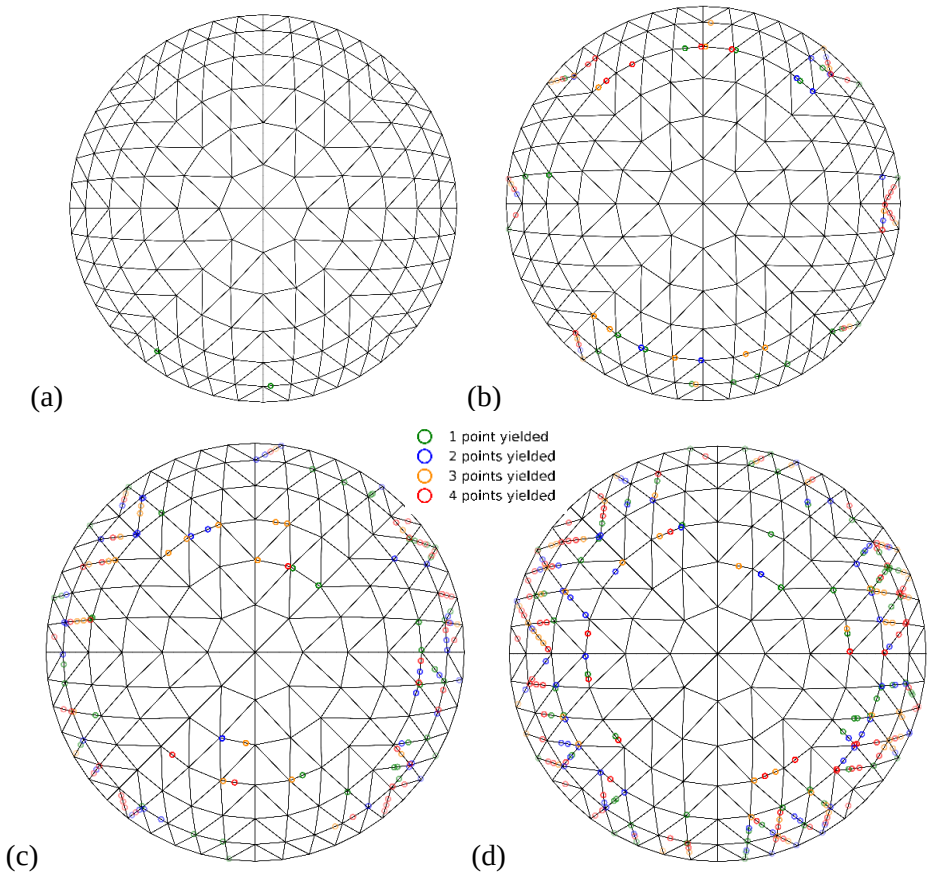


Figure 7: Progress of yielding at integration points with increasing intensities, a. 0.6g, b. 0.8g, c. 1.0g, d. 1.5g

4 Practical Implementation

The study investigated the elastic and plastic behavior of steel space frames, focusing on single-layer reticulated domes under seismic loading. It was evaluated how localized yielding initiates and spreads, affecting overall structural stability. The findings contribute to performance-based seismic design, enhancing the safety of long-span steel structures in earthquake-prone regions.

5 Conclusion

Following conclusions can be drawn from the conducted study:

1. As the seismic intensity increased, yielding propagated from the outer diagonal members toward the middle rings, while radial members remained mostly elastic even at 1.0g. This radial damage gradient reveals the directional nature of force transmission in reticulated dome geometries.
2. The choice of yield criteria such as elements yielding at 1, 5, or all 8 section points affects how the extent of yielding are interpreted. While 1P yield element ratio detects early damage, 8P yield element ratio captures severe yielding, highlighting the importance of multi-level criteria in evaluating damage states.
3. With increasing seismic amplitude, the dominant frequencies of the top node consistently decreased in all directions, primarily due to progressive stiffness degradation and energy dissipation resulting from structural yielding.

Future studies should incorporate modal projection methods and soil-structure interaction to fully capture realistic behavior and experimentally validate simulation results with models under shake table testing, especially to study failure modes in different configurations.

Acknowledgment

I am deeply grateful to my parents for their unwavering support, encouragement, and prayers throughout this journey. I would also like to express my sincere thanks to Dr. Khan Shahzada for generously sharing his PhD dissertation, which greatly contributed to this research. My heartfelt appreciation goes to Dr. Muhammad Faheem for his continuous guidance and valuable insights throughout the course of this work.

References

[1] T. T. Lan, "Space Frame Structures".
[2] J. Yan, F. Qin, Z. Cao, F. Fan, and Y. L. Mo, "Mechanism of coupled instability of single-layer reticulated domes," *Eng. Struct.*, vol. 114, pp. 158–170, May 2016, doi: 10.1016/j.engstruct.2016.02.005.
[3] Y. Ding, Z.-T. Chen, L. Zong, and J.-B. Yan, "A theoretical strut model for severe seismic analysis of single-layer reticulated domes," *J. Constr. Steel Res.*, vol. 128, pp. 661–671, Jan. 2017, doi: 10.1016/j.jcsr.2016.09.022.
[4] G. Nie, C. Zhang, D. Li, Q. Chen, and Z. Wang, "Collapse of the spatial double-layer cylinder shell by experimental study," *Eng. Struct.*, vol. 245, p. 112862, Oct. 2021, doi: 10.1016/j.engstruct.2021.112862.
[5] J. W. Dai, Z. Qu, G. B. Nie, and C. X. Zhang, "DAMAGES OF STEEL SPACE GYMNASIUM STRUCTURES IN THE 2013 CHINA LUSHAN MS7.0 EARTHQUAKE".
[6] F. Fan, S. Z. Shen, and G. A. R. Parke, "Study of the Dynamic Strength of Reticulated Domes under Severe Earthquake Loading," *Int. J. Space Struct.*, vol. 20, no. 4, pp. 235–244, Dec. 2005, doi: 10.1260/026635105775870251.
[7] G. Nie, X. Zhu, X. Zhi, F. Wang, and J. Dai, "Study on Dynamic Behavior of Single-Layer Reticulated Dome by Shaking Table Test," *Int. J. Steel Struct.*, vol. 18, no. 2, pp. 635–649, Jun. 2018, doi: 10.1007/s13296-018-0021-2.
[8] X. Zhi, F. Fan, and S. Shen, "Elasto-plastic instability of single-layer reticulated shells under dynamic actions," *Thin-Walled Struct.*, vol. 48, no. 10–11, pp. 837–845, Oct. 2010, doi: 10.1016/j.tws.2010.04.005.
[9] F. Fan, S. Z. Shen, and G. A. R. Parke, "Theoretical and Experimental Study of Vibration Reduction in Braced Domes Using a Viscous Damper System," *Int. J. Space Struct.*, vol. 19, no. 4, pp. 195–202, Dec. 2004, doi: 10.1260/0266351043492672.
[10] G. Nie and K. Liu, "Experimental Studies of Single-Layer Reticulated Domes with Isolated Supports," *Shock Vib.*, vol. 2018, no. 1, p. 6041878, Jan. 2018, doi: 10.1155/2018/6041878.
[11] X. Zhi, F. Fan, F. Shi, and Z. Yu, "Effect of BRBs on the seismic resistance of single-layer reticulated domes," *Int. J. Steel Struct.*, vol. 13, no. 1, pp. 199–208, Mar. 2013, doi: 10.1007/s13296-013-1019-4.
[12] J. Dai, Z. Qu, C. Zhang, and X. Weng, "Preliminary investigation of seismic damage to two steel space structures during the 2013 Lushan earthquake," *Earthq. Eng. Eng. Vib.*, vol. 12, no. 3, pp. 497–500, Sep. 2013, doi: 10.1007/s11803-013-0189-6.
[13] F. Fan, J. Yan, and Z. Cao, "Stability of reticulated shells considering member buckling," *J. Constr. Steel Res.*, vol. 77, pp. 32–42, Oct. 2012, doi: 10.1016/j.jcsr.2012.04.011.
[14] S. Kato, J.-M. Kim, and M.-C. Cheong, "A new proportioning method for member sections of single layer reticulated domes subjected to uniform and non-uniform loads," *Eng. Struct.*, vol. 25, no. 10, pp. 1265–1278, Aug. 2003, doi: 10.1016/S0141-0296(03)00077-4.
[15] G. Nie, X. Zhi, F. Fan, and J. Dai, "Seismic performance evaluation of single-layer reticulated dome and its fragility analysis," *J. Constr. Steel Res.*, vol. 100, pp. 176–182, Sep. 2014, doi: 10.1016/j.jcsr.2014.04.031.
[16] T. Suzuki, T. Ogawa, and K. Ikarashi, "Elasto-Plastic Buckling Analysis of Rigidly Jointed Single Layer Reticulated Domes," *Int. J. Space Struct.*, vol. 7, no. 4, pp. 363–368, Dec. 1992, doi: 10.1177/026635119200700412.
[17] American Society of Civil Engineers, *Minimum Design Loads and Associated Criteria for Buildings and Other Structures*, 7th–16th ed. Reston, VA: ASCE, 2017.
[18] A. Whittaker, "Selecting and Scaling Earthquake Ground Motions for Performing Response-History Analyses," National Institute of Standards and Technology, GCR 11-917-15, 2011.
[19] K. Shahzada, "Seismic Risk Assessment of Buildings in Pakistan (Case Study Abbottabad City)," PhD Dissertation, University of engineering and technology, Peshawar, 2011.
[20] U. Oğuz, "Comparison of Ground Motion Scaling Methods by Considering Vertical Ground Motions," Master's thesis, Middle East Technical University, Ankara, Turkey, 2022.
[21] F. Fan, D. Wang, X. Zhi, and S. Shen, "Failure modes for single-layer reticulated domes under impact loads," *Trans. Tianjin Univ.*, vol. 14, no. S1, pp. 545–550, Oct. 2008, doi: 10.1007/s12209-008-0094-7.
[22] X.-M. Jiang, H. Chen, and J. Y. R. Liew, "Spread-of-plasticity analysis of three-dimensional steel frames," *J. Constr. Steel Res.*, vol. 58, no. 2, pp. 193–212, Feb. 2002, doi: 10.1016/S0143-974X(01)00041-4.

SEISMIC RESISTANT BUILDINGS USING DAMPERS: A COMPARATIVE STUDY

[a] Muhammad Bilal Ansari*, [b] Muhammad Yaqub

a: Department of Civil Engineering, University of Engineering and Technology Taxila, Pakistan. engr.mbilalansari@gmail.com
b: Department of Civil Engineering, University of Engineering and Technology Taxila, Pakistan.muhammad.yaqub@uettaxila.edu.pk
* Corresponding author

Abstract- This study evaluates the comparison of the seismic behavior of reinforced concrete buildings of varying heights (G+14, G+29, and G+44), both with and without the inclusion of viscous dampers. The building under consideration is situated in Islamabad and falls under seismic site class "C". It features a regular square layout and is intended for residential use. All structural components are designed in accordance with ACI 318-15 standards, while the applied loads are determined based on IBC-2023 provisions. The structural system adopted is a special reinforced concrete moment-resisting frame. For dynamic analysis, the response spectrum method has been utilized. Both the structural modeling and analysis has been performed using ETABS version 17.0.1. Given that earthquakes are among the most significant natural hazards globally, this study incorporates viscous dampers to mitigate the seismic response of the structure. The dampers are employed in high rise structures in seismic zones to minimize vibrations caused by lateral stresses. Such as strong winds and earthquakes in order to prevent such catastrophic damages. The mechanical properties of the viscous damper employed in this study include a damping coefficient Cd=320 KN/ (mm/s) and a stiffness value Kd=224 KN/mm. Key structural response parameters such as storey drift, storey shear, storey displacement, and storey stiffness are evaluated and compared.

Keywords- ETABS, Seismic Response, Storey Drift, Viscous

1. Introduction

Pakistan is a developing country and the population is growing at a very high rate. The planned building is located in Islamabad, the capital city, which is considered an area of high earthquake risk due to its closeness to a major active geological fault in the northern region. Therefore, it is important to design buildings that can safely endure moderate to strong earthquakes. Since a tall building act much like a vertical cantilever, its structural parts must be capable of handling both vertical forces due to gravity and horizontal forces caused by wind and seismic activity. Seismic design enhances the structure's resistance to earthquakes by employing shear wall-based systems or moment-resisting frames [1]. Typically, seismic design seeks to avoid damage during small earthquakes, minimize structural harm during moderate ones, and permit limited impact to both structural and non-structural components during strong earthquakes. The most dangerous aspect of an earthquake is its unpredictability in terms of time and location, which presents a significant economic and structural challenge [2]. This necessitates that building components be designed to dissipate the energy imparted by earthquakes, thereby minimizing damage [3]. To reduce the seismic effects on buildings and bridges, structural control devices are being developed. During an earthquake, seismic energy enters the structure, causing increased vibrational response. Mechanical devices such as dampers are installed throughout the height of the structure to enhance damping and, consequently, reduce the structural response by absorbing or dissipating seismic energy [4], [5].

2. Research Methodology

In this study, ETABS v17 (Extended Three-Dimensional Analysis of Building Systems) software is used for the modelling and analysis of the structures. The buildings are designed as regular square-plan reinforced concrete structures with three different heights: G+14, G+29, and G+44 storeys. Each model is analysed in two cases: with and without the use of fluid viscous dampers (FVDs).

Initially, the models without dampers are developed and analysed in ETABS. Gravity loads are assigned, and earthquake loads are aplied according to IBC-2023 provisions. The buildings are assumed to be located in seismic site class D (Islamabad), and dynamic analysis is carried out using the Response Spectrum Method (RSM), considering a 5% damping ratio and appropriate scale factors in both X and Y directions as per code requirements.

2.1 Significance of Research

This research enhances the understanding of damping systems in improving the seismic resilience of buildings by analyzing their effectiveness in mitigating earthquake-induced forces. By significantly reducing structural damage, damping systems enhance overall safety; extend the lifespan of buildings, and lower long-term maintenance and re- construction costs. Additionally, their ability to minimize material waste contributes to sustainable construction practices. The study also highlights the wide industry applications of damping technology, particularly in seismic- prone regions. Overall, this research contributes to the advance of seismic protection strategies, promoting safer, more cost-effective, and environmentally sustainable building practices.

2.2 Methods of Analysis

There are various methods available for conducting seismic analysis of buildings, aimed at determining the internal forces and deformations caused by earthquake excitations. The choice of analysis method primarily depends on the structural configuration, material properties, and the external seismic inputs applied.

2.2.1 Equivalent Static Method

Also known as, the Equivalent Lateral Force Method, this approach is a simplified procedure used in seismic analysis. It assumes that the horizontal seismic load can be represented by an equivalent static force, simulating the effects of dynamic ground motion. Unlike more advanced dynamic methods, it typically does not require consideration of higher vibration modes, focusing only on the fundamental mode, which simplifies the analysis.

The method starts by calculating the total base shear based on the building's mass, the fundamental period of vibration, and its modal shape. This base shear is then distributed along the height of the structure. At each floor level, the resulting lateral force is further allocated to the structural elements. Due to its simplicity, the Equivalent Static Method is most appropriate for low- to mid-rise buildings that have regular geometry and mass distribution.

2.2.2 Response Spectrum Method

Also referred to as the Modal or Mode Superposition Method, the Response Spectrum Method is a dynamic analysis technique widely used in seismic design? It is especially suitable for structures where modes beyond the fundamental mode significantly influence the seismic response, such as in buildings with irregular mass or stiffness distributions.

This method evaluates the peak structural response by referencing an earthquake design response spectrum, which reflects the maximum expected response of a single-degree-of-freedom (SDOF) system subjected to ground motion. Each mode of vibration is analyzed independently. The resulting modal responses are then combined using techniques like the Square Root of the Sum of the Squares (SRSS) or the Complete Quadratic Combination (CQC) to determine the total structural response. The Response Spectrum Method yields accurate results that are suitable for designing high-rise and complex structures under seismic loading.

2.3 Model and Analysis

In this study, three different high-rise reinforced concrete building models are considered: G+14 (15 storeys), G+29 (30 storeys), and G+44 (45 storeys). All buildings are modelled with the same plan dimensions and structural layout, ensuring

consistency in comparison. The structures are assumed to be residential buildings located in seismic zone D (Islamabad, Pakistan). Each model is analyzed both with and without fluid viscous dampers (FVDs).

Table 1 presents the geometric and material properties used in all three models.

Table 1: Description of Building Model

Particulars	Model -01	Model-02	Model-03
Plan dimension	200ft X 200ft	200ft X 200ft	200ft X 200ft
Area	40,000 sft	40,000 sft	40,000 sft
No of story	15	30	45
Height of each story	11 ft	11 ft	11 ft
Total height	165 ft	330 ft	495 ft
Size of column	15"x30"	15"x30"	15"x30"
Slab thickness	30"x30"	30"x30"	30"x30"
Dead load	6 in	6 in	6 in
Live load	40 psf	40 psf	40 psf
Roof live load	40 psf	40 psf	40 psf
Partition wall load	40 psf	40 psf	40 psf
Parapet wall load	180 lb/ft	180 lb/ft	180 lb/ft
Wind load	80 mph	80 mph	80 mph
Compressive strength of concrete for (beam and slab)	5000 psi	5000 psi	5000 psi
Compressive strength of concrete for column	6000 psi	6000 psi	6000 psi
Grade of reinforcing steel	Gr-60	Gr-60	Gr-60
Code	IBC-2023	IBC-2023	IBC-2023
Density of concrete	150 lb/cft	150 lb/cft	150 lb/cft
Damping ratio	0.05%	0.05%	0.05%
Soil type	SD	SD	SD
Spectral Acc Sc	1.22	1.22	1.22
Spectral Acc S1	0.37	0.37	0.37
Site class	D	D	D
Response modification (R)	5	5	5
Over strength omega	3	3	3
Deflection amplification (Cd)	4.5	4.5	4.5
Occupancy importance (I)	1.25	1.25	1.25

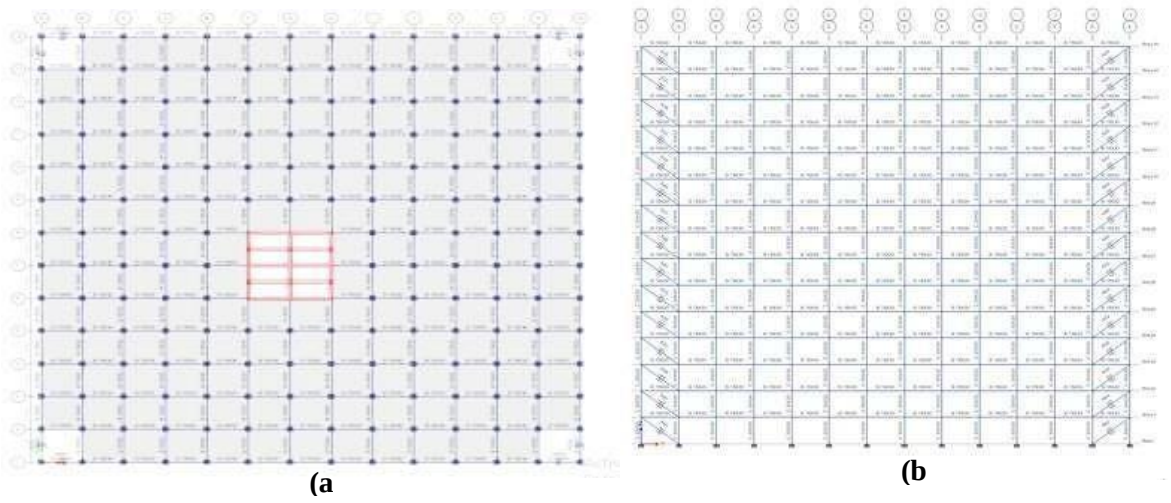


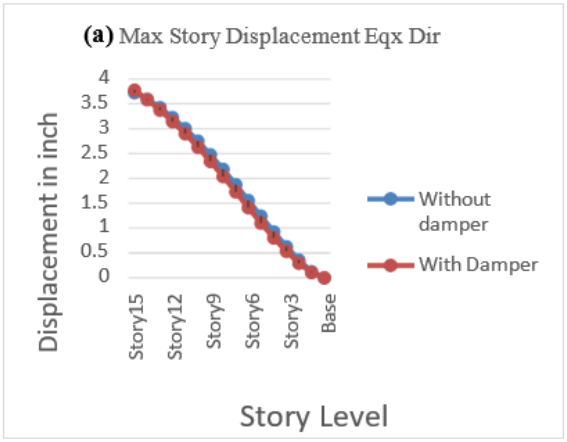
Figure 1: (a) Plan view of building with FVD in ETABS and (b) FVD at exterior corner elevation in YZ plane

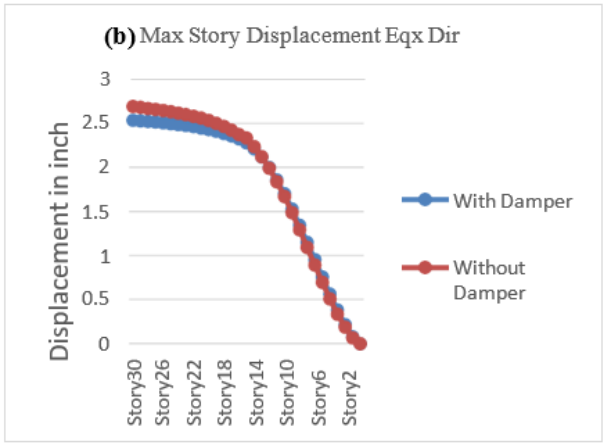
3. Results

This section presents the comparison of seismic responses for three building configurations (G+14, G+29, and G+44 storeys), analyzed with and without fluid viscous dampers (FVDs). The analyses were performed using both the Equivalent Static Method (ESM) and the Response Spectrum Method (RSM). The key parameters considered include storey displacements, storey drifts, base shear, and modal time periods.

3.1 Storey Displacement

Storey displacement refers to the lateral movement of each storey during seismic excitation. It was observed that displacement values increase with the height of the structure. However, the inclusion of viscous dampers significantly reduced the overall displacement for all models. For instance, in the G+44 storey model, the maximum top storey displacement without dampers was significantly higher compared to the model with FVDs. The dampers effectively absorbed seismic energy, leading to a reduction in peak displacement by up to 24% in tall structures.ng.





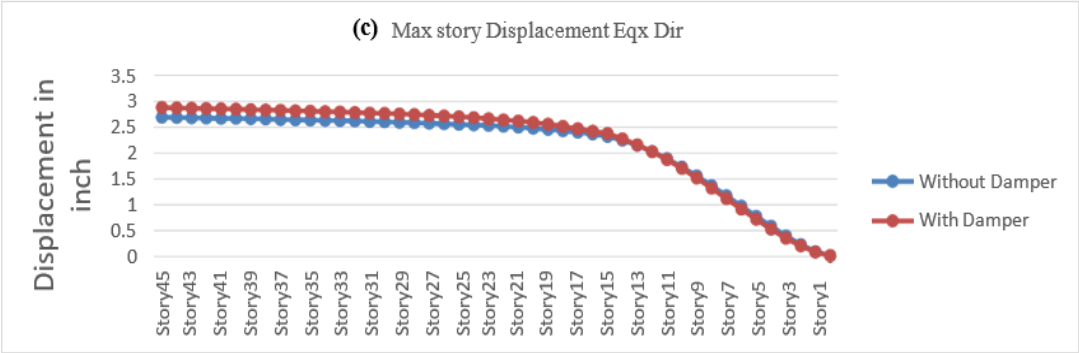


Figure 2: a. Maximum Storey Displacement a.15 storey, b.30 storey and c. 45 storey

3.2 Storey Drifts

Inter-storey drift is the relative displacement between adjacent floors and is a critical factor for seismic design. The maximum drift values were observed near the mid-height of the buildings. The drift increased with building height but was notably lower in all damped models.

The G+29 and G+44 models exhibited the most pronounced improvements, with inter-storey drift reductions reaching up to 28% when FVDs is used. This confirms that the use of dampers not only enhances performance but also helps meet code-based drift limits more effectively

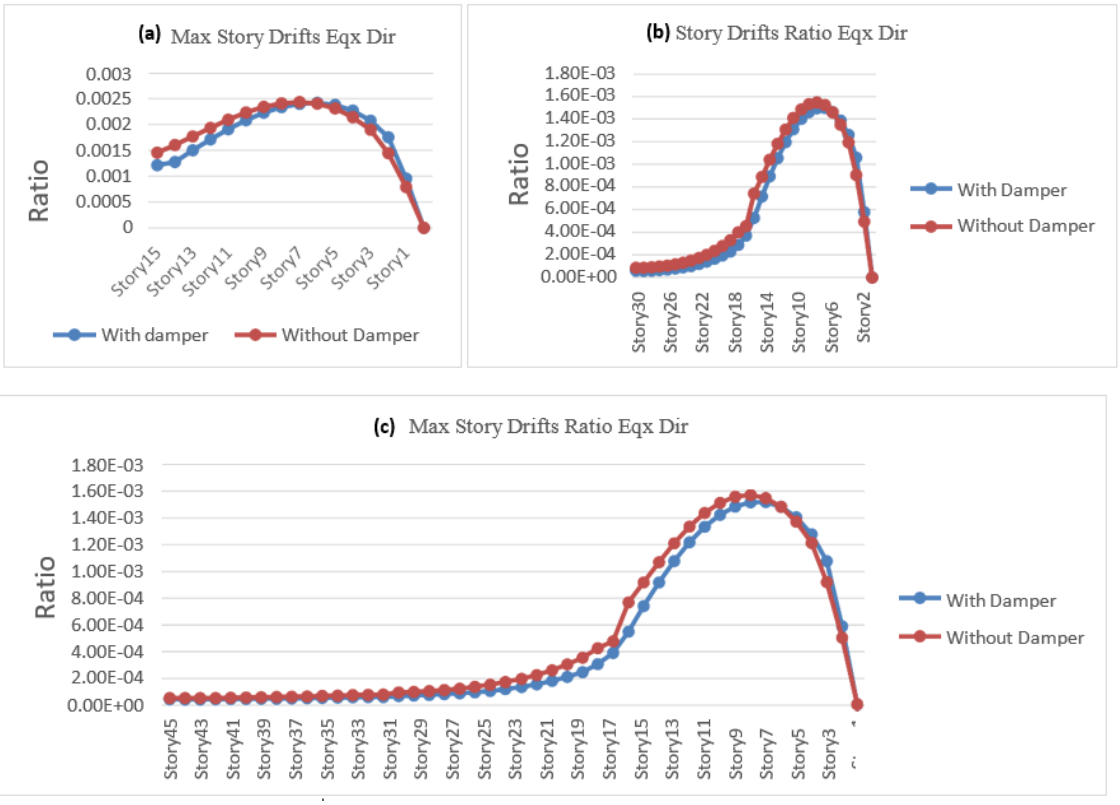


Figure 3: a. Maximum Storey Drifts a.15 storey, b.30 storey and c. 45 storey

3.3 Modal Time Periods

Modal time periods reflect the natural vibration characteristics of a structure. It was found that models without dampers had slightly higher fundamental time periods due to reduced stiffness and lack of energy dissipation mechanisms. The incorporation of dampers resulted in lower time periods and more stable dynamic response. This confirms that dampers contribute not only to deformation control but also to improved structural stability under dynamic excitation.

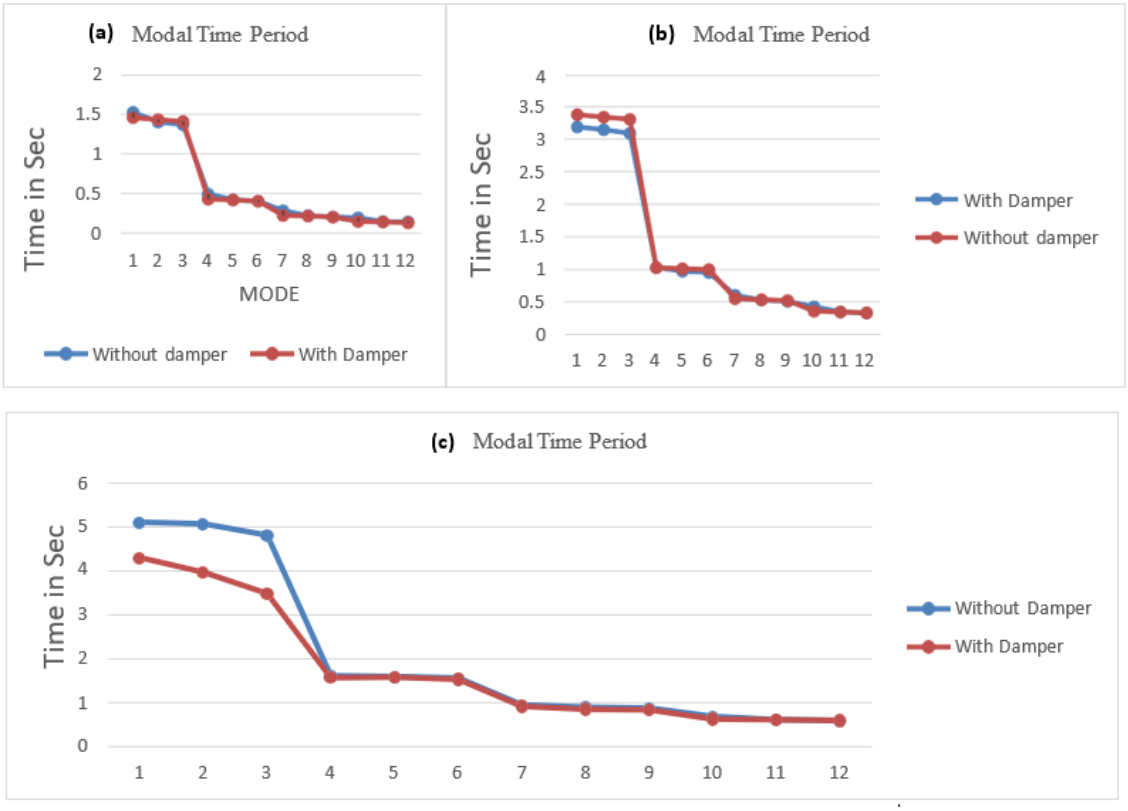


Figure 4: Instrumentation of interlocking structure on shake table, a. schematic diagram, and b. test set up

4. Practical Implementation

The use of fluid viscous dampers (FVDs) in high-rise buildings provides a practical and effective way to reduce seismic effects, especially in earthquake-prone areas like Islamabad. These dampers can be installed between beams and columns or in bracing systems to absorb and dissipate seismic energy, reducing storey displacements and inter-storey drifts. Although they may increase the initial construction cost, FVDs help minimize structural damage and repair needs after earthquakes, making them a cost-effective solution in the long run. Their application is especially beneficial in critical or tall buildings where safety and stability during seismic events are essential. With growing acceptance in modern design codes, FVDs are becoming a practical part of earthquake-resistant building design.

5. Conclusion

This study confirms that fluid viscous dampers (FVDs) are effective in reducing the seismic response of reinforced concrete high-rise buildings. A series of dynamic analyses was carried out on G+14, G+29, and G+44 storey structures to evaluate the impact of dampers on key response parameters. The findings highlight the following:

1. The installation of dampers led to a reduction in maximum storey displacement by up to 24%. As expected, storey displacement increases with building height.
2. Maximum inter-storey drift was reduced by up to 28% in buildings equipped with dampers. Similar

to displacement, drift values were higher in taller structures.

3. The inclusion of dampers improved storey stiffness by up to 10%. However, as building height increased, the overall lateral stiffness naturally decreased.

These results indicate that incorporating FVDs significantly enhances the seismic performance of tall RC buildings by controlling lateral movement and improving structural stability.

Acknowledgment

The author gratefully acknowledges the Department of Civil Engineering, UET Taxila, for their support during this research. Special thanks to Prof. Dr. Muhammad Yaqub for his valuable supervision.

References

[1] H.-N. Li and G. Li, "Earthquake-resistant design of RC frame with „dual functions" metallic dampers," *Proc. ASME Pressure Vessels and Piping Conf.*, vol. PVP2007-26450, pp. 43–53, 2009.

[2] R. K. Mohammad, M. H. El Naggar, and H. Moghaddam, "Optimum strength distribution for seismic resistant shear buildings," *Int. J. Solids Struct.*, vol. 41, no. 22–23, pp. 6597–6612, 2004.

[3] G. Xu, T. Guo, A. Li, S. Wang, R. Zhang, R. Zhu, and J. Xu, "Review on self-centering damper for seismic resilient building structures," *Structures*, vol. 54, pp. 58–77, 2023.

[4] F. Paolacci, "An energy-based design for seismic resistant structures with viscoelastic dampers," *Earthq. Struct.*, vol. 4, no. 2, pp. 219–239, 2013.

[5] J. Wang and H. Zhao, "High-performance damage-resistant seismic resistant structural systems for sustainable and resilient city: A review," *Adv. Civ. Eng.*, 2018. [Online]. Available: doi.org/10.1155/2018/8703697

SEISMIC CAPACITY ENHANCEMENT OF STONE MASONRY BUILDINGS USING HORIZONTAL TIMBER ELEMENTS

[a]Waqas Khan, [b]Muhammad Fahim*

a: Civil Engineering Department, UET Peshawar, Peshawar, Pakistan. hawaiuet@gmail.com
b: Civil Engineering Department, UET Peshawar, Peshawar, Pakistan. drmfahim@uetpeshawar.edu.pk
* Corresponding author

Abstract- Stones and timber are the natural materials found abundantly in the Northern hilly areas of Pakistan and many other countries of the world. Human beings have used them for centuries to make houses for providing shelter against natural and environmental hazards. Bhatar is one such typical construction in which stone masonry walls are divided into panels by providing horizontal timber elements. The timber elements are cross braced at intervals along the length and anchored with orthogonal walls at the corners. Its performance in past earthquakes has been good, which was once again demonstrated in the Kashmir earthquake of October 8, 2005. This study presents the results obtained from shake table test of a reduced scale model of Bhatar construction. The results obtained can be used to evaluate the seismic capacity of these structures

Keywords- Bhatar Construction, Stone Masonry, Seismic Resistance, Shake Table, Timber Bands

1 Introduction

The Northern region of Pakistan; officially called as "Gilgit-Baltistan" and Kashmir is the most beautiful and fascinating region of Pakistan. The world's four famous mountain ranges; the Himalayas, the Karakorams, the Hindukush and the Pamirs meet in this region. Being home to thousands of mountains, the area is rich in stones and timber. The local communities have been using these materials for centuries to construct their houses. Most of the buildings in the region have stones and timber as construction materials in one form or the other even today.

On the other hand, the area is part of seismically one of the most active regions in the world. The Seismic provisions in the Pakistan Building Code [1] categorize most of the region in the high seismic zones (zone 3 and zone 4). The highly vulnerable stone masonry buildings in the presence of high seismic hazard constitute a high seismic risk in the area. This was demonstrated on October 8, 2005, a fatal earthquake of magnitude 7.6 on the Richter scale. The earthquake was one of the biggest disasters in the history of Pakistan. According to Earthquake Reconstruction and Rehabilitation Authority (ERRA) 73,338 people lost their lives, 69,412 experienced serious injuries, and nearly 3.5 million people became homeless [2]. The earthquake destroyed or seriously damaged about 600,000 houses, 796 health units, and 6298 educational buildings in addition to numerous other government buildings and roads [3].

As part of the reconstruction and rehabilitation process after the earthquake, efforts were made by both government and non-government organizations to introduce and encourage such construction practices which could mitigate the seismic risk in future earthquakes. Special emphasis was given to the indigenous traditional construction methods which showed relatively better resistance to past earthquakes [4, 6, 7]. Several research studies were initiated to study and improve the existing conventional building techniques [6-10]. Bhatar; a rubble stone masonry building with horizontal timber elements running along the length of the walls at different heights, was one such construction type. However, most of such efforts were based on experience and engineering judgment, rather than recognized scientific research. This research project is an effort to scientifically investigate the performance of Bhatar construction subject to earthquake excitation. A fully dynamic shake table test of a reduced scale Bhatar model is conducted and the results presented.

2 Research Methodology

2.1 Shake Table Testing and Reduced Scale Modelling

The core component of the research is the shake table test on a reduced scale model of stone masonry building with horizontal reinforcing elements. The model was constructed based on similitude requirements of distorted model. Two past earthquake time-histories, namely the El Centro 1940 and Kashmir 2005 were used for input excitations.

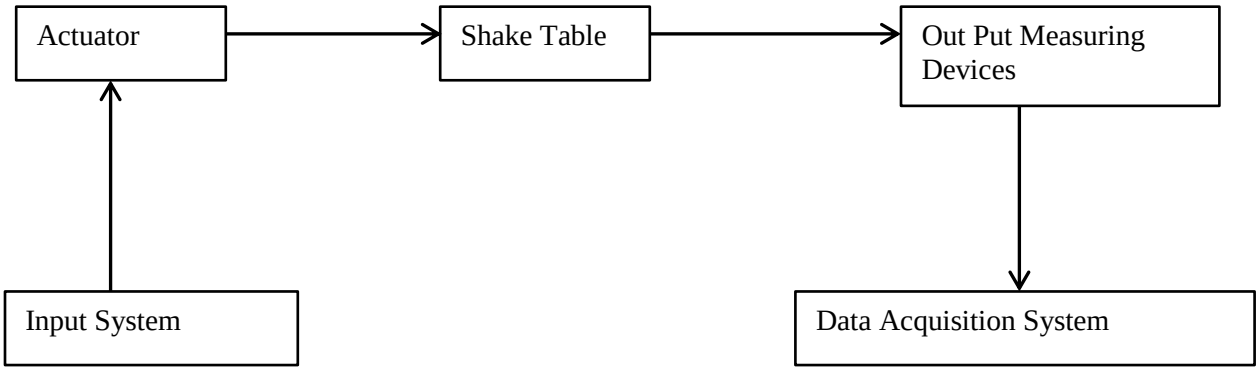


Figure 1. Major components of a shake table testing system

Figure 1 shows the major components and steps involved in a shake table test. Computer hardware and software systems are used to impart the input signals to the actuator. Earthquake records, be they real, artificial, or synthetic, are generally used as input excitations. Hydraulic actuators provide the driving force to shake the table and hence the models. Generally, displacements and accelerations of the model structure are measured as output of the shake table test. The data acquisition system receives electrical signals from transducers and transforms them into information which can be seen on a computer. Signal conditioning is required before the data acquisition system can read the signal which may include processes such as amplification, linearization, filtering, and isolation.

Shake table tests essentially involve subjecting the models to earthquake excitations provided by the actuators, recording the output motions in terms of displacements and accelerations by transducers and recording the output data with the help of a data acquisition system. Ideally the best model would be the structure itself i.e. to test actual structures. However, the construction cost involved in making such models and the limitations of testing facilities imply the use of reduced scale models. These models should satisfy similitude requirements given in Table 1 based on dimensional analysis so that they can be used to predict the response of prototype structures.

Table 1: Scale Factors

Parameter	**Symbol**	**Scale Factor (Cauchy)**	**Scale Factor (Cauchy + Froude)**
Length	L	$L_p/L_M = \lambda$	$L_p/L_M = \lambda$
Modulus of elasticity	E	$E_p/E_M = e = 1$	$E_p/E_M = e = 1$
Specific mass	ρ	$\rho_p/\rho_M = \rho = 1$	$\rho_p/\rho_M = \rho = \lambda^{-1}$
Area	A	λ^2	λ^2
Mass	m	λ^3	λ^3
Displacement	d	Λ	Λ
Velocity	v	1	$\lambda^{1/2}$

Acceleration	A	λ^{-1}	1
Weight	w	λ^{3}	λ^{2}
Force	F	λ^{2}	λ^{2}
Moment	M	λ^{3}	λ^{3}
Stress	σ	1	1
Strain	ϵ	1	1
Time	t	λ	$\lambda^{1/2}$
Frequency	f	λ^{-1}	$\lambda^{-1/2}$

The model dimensions were based on a prototype room of 15ft x 12ft with 11ft of overall height. Keeping in mind the constraints of testing facilities, i.e. size of the shake table, a scale factor of 3 was selected. Therefore, the overall plane dimensions of the models were 5ft x 4ft with a total height of 44 inches as shown in **Error! Reference source not found.** and **Error! Reference source not found.**. All other dimensions of the prototype building are also divided by the scale factor of 3 to obtain the corresponding dimensions of the models.

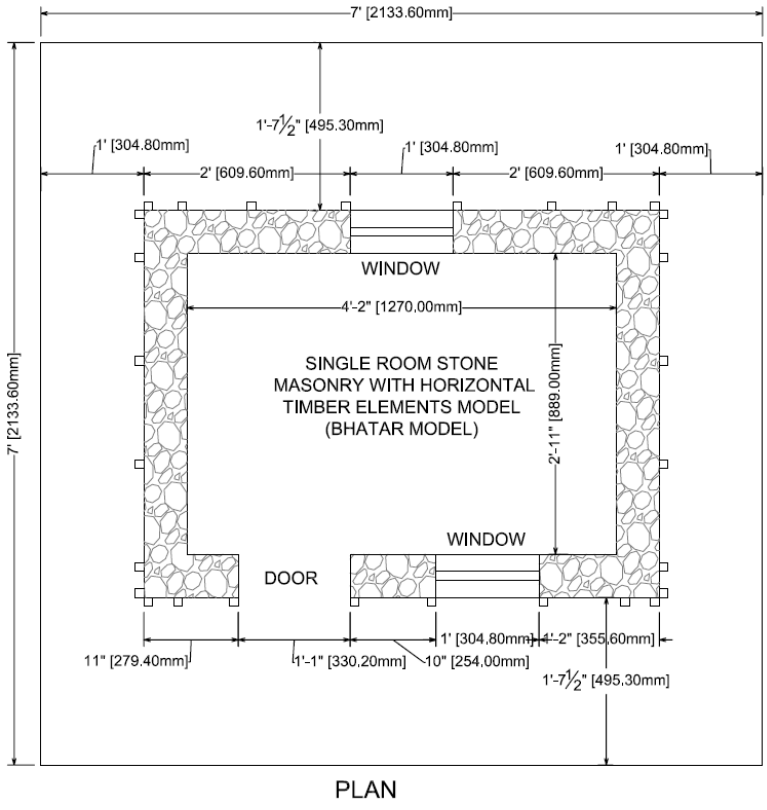


Figure 2. Plan of specimen

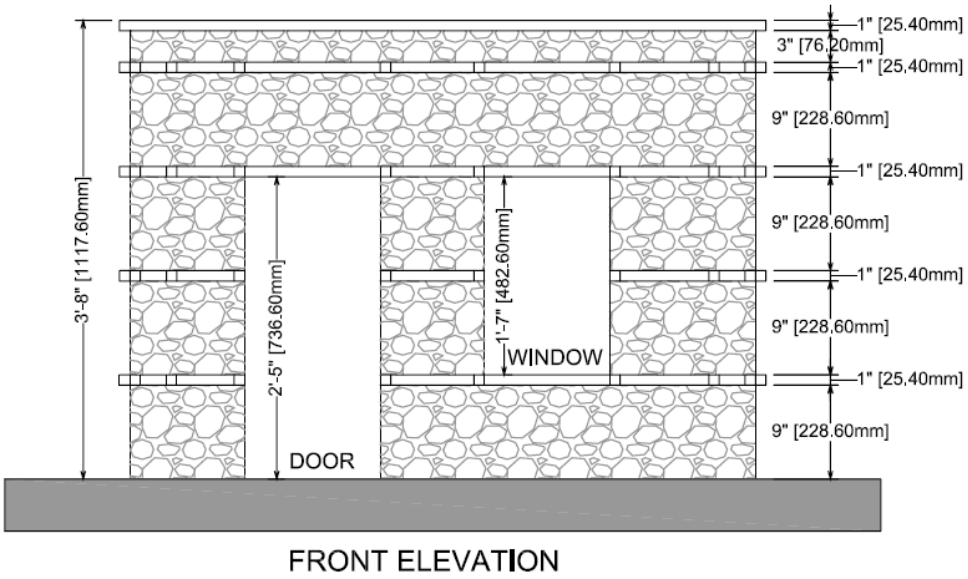


Figure 3. Elevation of specimen

2.2 Construction of the Model

The model was constructed and tested at the Earthquake Engineering Center, University of Engineering and Technology, Peshawar, Pakistan. Major stages of construction are shown in Figure 4Figure 7.



Figure 4. Complete concrete pad being cured



Figure 5. Rectangular skeleton of timber elements



Figure 6. Horizontal Timber elements



Figure 7. Completed Model

2.3 Testing

To capture time rate dependent characteristics of structures or structural components, fully dynamic test methods are employed. There are many methods of dynamic testing currently in use for structures. Linear elastic dynamic tests are conducted when only the structural identification is involved. In such cases, low levels of excitation are generally sufficient, which can be produced by ambient sources such as wind or traffic. Eccentric mass exciters or electrodynamic shakers are used whenever a greater degree of control is required. When complete structural response is sorted, non-linear dynamic test methods such as shake table tests are conducted. As part of this study, fully dynamic shake table tests were performed to study the complete elastic and inelastic response of the structure.

The Stone Masonry Models were tested in Earthquake Engineering Centre of the Department of Civil Engineering, University of Engineering & Technology (UET), Peshawar, Pakistan. The seismic simulator consists mainly of 1.5 m x 1.5 m (5 x 5 ft), 2.5-inch-thick aluminum table and an actuator as shown in Figure 8. The table has a grid of holes at 20 cm x 20 cm to attach the model/pad to the table.



Figure 8. Shake table at UET Peshawar

3 Results

3.1 Data Processing

The data obtained was processed using Seismosignal software as shown in Figure 9. Appropriate filtering and baseline corrections were applied to each data set.

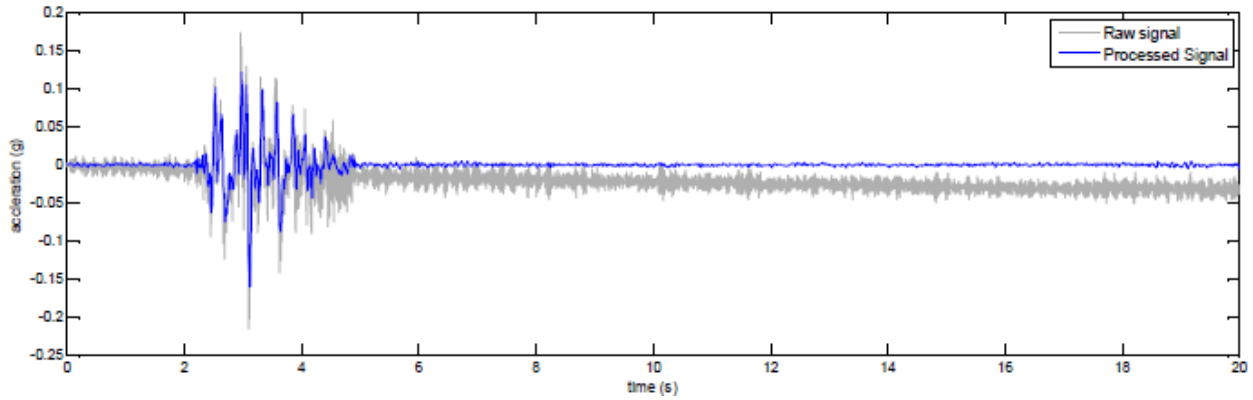


Figure 9. Raw and filtered data

3.2 Amplification

Acceleration amplification is calculated by dividing the acceleration at the top over the acceleration at the base. The graph is shown in Figure 10. The variation is nonlinear with irregular increase and decrease at the different runs.

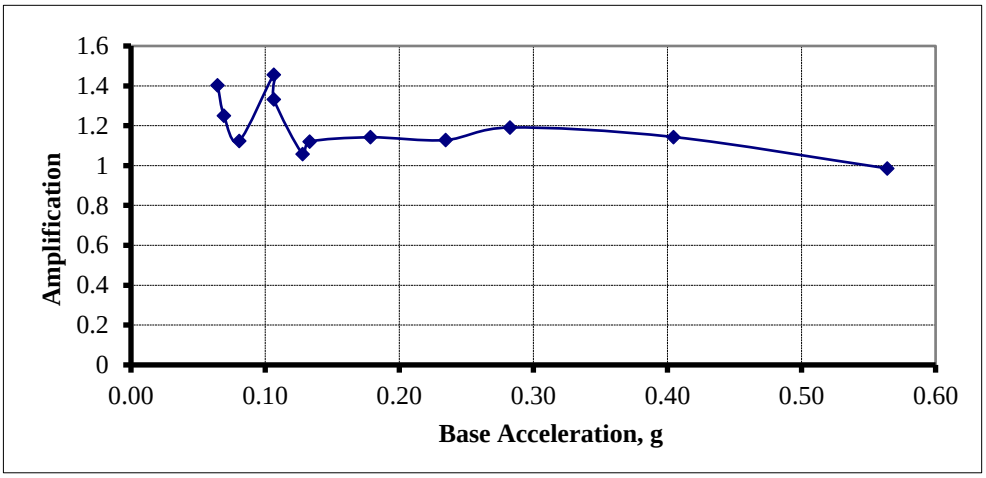


Figure 10. Acceleration amplification

3.3 Demand vs Actual Acceleration

Input acceleration given to the system is not exactly transferred to the model. Figure 11 shows input demand and acceleration recorded at the base of the shake table.

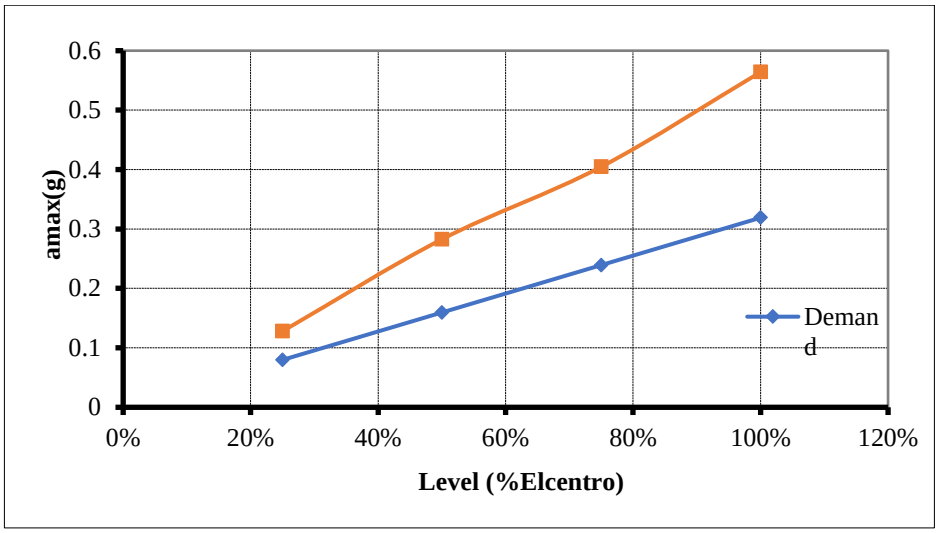


Figure 11. Level (% Elcentro)

3.4 Seismic Capacity Curve

The seismic capacity curve is shown in Figure 12. The maximum base share coefficient of 0.55 was observed against a story drift ratio of 0.068. The specimen experienced severe damage at the end of the test as shown in Figure 13.

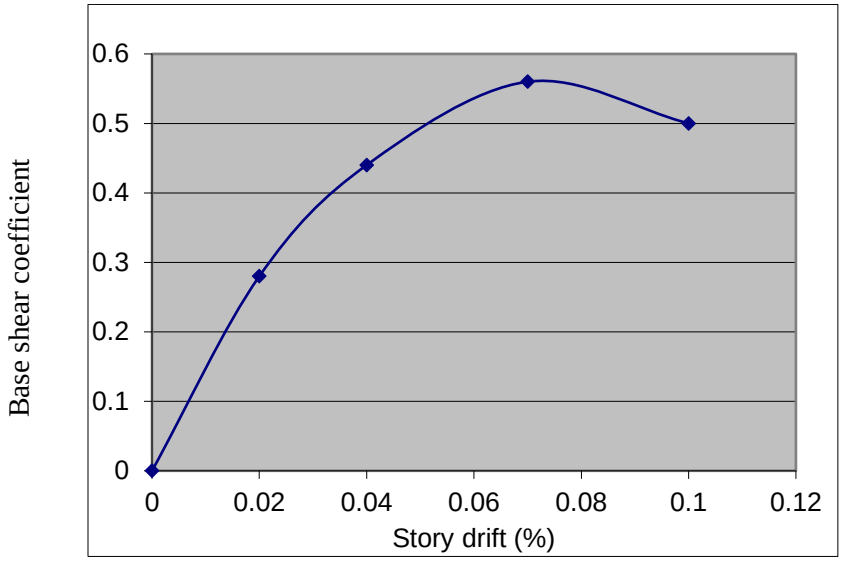


Figure 12. Seismic capacity curve



Figure 13. Damages at the end of the test

4 Practical Implementation

The results of this study will help in understanding and quantifying the seismic response of Bhatar construction.

5 Conclusion

The following conclusion can be derived from the data obtained from the shake table tests performed.

1. Model with timber horizontal bands collapsed at PGA 0.5g.
2. The governing failure criteria is observed to be falling of stones.
3. The models showed good response in comparison to models with no horizontal elements [9].

Acknowledgment

I appreciate the contribution of all EEC Lab staff towards the successful completion of this research. The careful review and constructive suggestions by the anonymous reviewers are gratefully acknowledged.

References

1. BCP/SP-07, *Building Code of Pakistan (Seismic Provisions - 2007)*. 2007, Government of Islamic Republic of Pakistan, Ministry of Housing & Works, Islamabad, Pakistan.
2. *"The great Tangshan earthquake of 1976". Earthquake Engineering Research Laboratory, California Institute of Technology, Pasadena, California*.
3. EERI, *The Kashmir earthquake of October 8, 2005: Impacts in Pakistan*. 2006: Earthquake Engineering Research Institute, Oakland, California, United States.
4. Javed, M., A.N. Khan, and G. Magenes, *performance of masonry structures during earthquake-2005 in Kashmir*. Mehran university research journal of engineering and technology, 2008.
5. *BCP SP-2007. "Pakistan Building Code, Seismic Provisions"*.
6. Ali, P., et al., *Shake Table Tests on Single-Story Dhajji Dewari Traditional Buildings.* International Journal of Architectural Heritage, 2017. **11**: p. 1046-1059.
7. Ali, Q., et al., *Seismic Performance Evaluation of Two-story Dhajji-dewari Traditional Structure.* International Journal of Architectural Heritage, 2022. **16**(8): p. 1233-1251.
8. Ali, Q., et al., *Seismic Performance of Stone Masonry Buildings Used in the Himalayan Belt.* Earthquake Spectra, 2013. **29**.
9. Ali, Q., et al. *Shake table tests on typical stone masonry buildings used in the Himalayan belt*. in *9th US National and 10th Canadian Conference on Earthquake Engineering 2010, Including Papers from the 4th International Tsunami Symposium, July 25, 2010 - July 29, 2010*. 2010. Toronto, ON, Canada: Earthquake Engineering Research Institute.
10. Ashraf, M., et al., *Experimental Behavior of Full Scale URM Building Retrofitted with Ferrocement Overlay.* Advanced Materials Research, 2011. **255-260**.
11. Naseer, A., et al., *Observed Seismic Behavior of Buildings in Northern Pakistan During the 2005 Kashmir Earthquake.* Earthquake Spectra, 2010. **26**.

COMPARING CONSTRUCTION PROJECT MANAGERS AND MILITARY OFFICERS IN THE UNITED STATES: LEVERAGING VETERAN LEADERSHIP AND SKILLS FOR WORKFORCE DEVELOPMENT IN THE CONSTRUCTION INDUSTRY

[a] Amna Salman*, [b] Gavin Medley

a: McWhorter School of Building Science, Auburn University, Auburn, AL., USA. azs0072@auburn.edu
b: McWhorter School of Building Science, Auburn University, Auburn, AL., USA. gnm009@auburn.edu
* Corresponding author

Abstract- The construction industry faces growing demand for skilled project managers, while transitioning military veterans offer valuable leadership and problem-solving skills essential for this sector. However, veterans encounter barriers in translating military experience into civilian careers, including employer perceptions about skill transferability. This study compares job functions and skills of military officers with those required of construction project managers in the United States to evaluate transferability and inform transition strategies. Through qualitative interviews, our research revealed significant alignment in core competencies such as leadership, communication, coordination, problem-solving, and resource management. Findings indicated that while military officers possess these foundational skills, they often lack construction-specific technical knowledge and industry terminology. Primary transition challenges stemmed from cultural differences, unfamiliarity with industry regulations, and difficulties adapting leadership styles to civilian workplaces. Recommended interventions include targeted technical training programs, industry-specific mentorship networks, employer awareness initiatives, expansion of transition programs like Department of Defense (DOD) SkillBridge, and development of tools translating military experience into industry-recognized language. These strategies will facilitate integration of military talent into construction management, addressing industry workforce needs while supporting veterans' successful career transitions.

Keywords- Veteran Employment, Military Transition, Construction Management, Skill Transferability

1 Introduction

The construction industry faces a growing demand for skilled professionals to manage increasingly complex projects [1]. At the same time, military veterans transitioning to civilian life offer valuable experience, leadership skills, and problem-solving abilities acquired through their service [2]. Despite the potential for veterans to fill critical roles in construction, many struggle to translate their military experience into civilian careers [3]. Accordingly, this causes a disconnect between the skills veterans acquire in the military and the specific requirements of construction project management.

The Project Management Institute's (PMI) talent gap report [1] predicts a 13.2% increase in global construction project management jobs by 2030, with nearly 61.5 million roles anticipated. At the same time, the Department of Veterans Affairs [2] highlights a significant population of post-9/11 veterans, who possess managerial and professional experience. While veterans have transformational leadership traits shaped by their military training [4], employer scepticism about the

transferability of military skills, particularly soft skills like communication, remains a significant barrier [5]. This study seeks to address this challenge by examining the overlap between military officer skills and those required in construction project management, offering insights to improve veteran employment outcomes and maximize their potential in civilian roles. Although military veterans possess valuable leadership and problem-solving skills, they often encounter challenges in translating these competencies into the civilian construction sector. This misalignment results in underutilized human capital and unfulfilled industry labor demands. By identifying skill compatibility between military leadership experience and construction industry requirements, this research aims to develop an evidence-based framework to assist both veterans transitioning to civilian careers and construction employers seeking to leverage military talent.

2 Literature Review

The integration of military veterans into civilian roles, particularly in construction project management, has gained significant attention. Various research highlighted the strong alignment between military training and project management competencies, yet challenges persist in veterans' transition to the civilian workforce [6].

Studies indicate that veterans possess leadership, resilience, teamwork, and organizational skills that are highly valuable in civilian employment [7]. Many have prior exposure to project management frameworks, making them strong candidates for construction management roles [8]. Additionally, attributes such as adaptability, trust, and cross-cultural experiences further enhance their potential contributions. Construction project management, on the other hand, requires competencies such as leadership, organization, problem-solving, and teamwork—skills that align with military training. Studies frequently highlighted key competencies distinguishing high-performing project managers, including initiative, client focus, analytical thinking, and flexibility [9], [10]. Moreover, military coordination practices and values offer additional insights that can benefit construction workforce development.

On the other hand, despite their strengths, veterans face obstacles in securing civilian employment [8]. Mental health concerns, limited transition programs, employer perception gaps, and stereotypes hinder successful integration. Service-related disabilities and job-fit biases further complicate employment prospects. However, peer support, networking, and career development initiatives help veterans navigate these challenges.

While the existing studies highlight veterans' potential and the importance of non-technical skills—such as leadership, collaboration, and ethical decision-making—in construction project management, they also acknowledge transition challenges. Veterans possess these critical soft skills but may require supplemental technical training to fully leverage their leadership and problem-solving abilities in construction contexts [11]. Effective workforce development initiatives should, therefore, focus on bridging technical knowledge gaps while capitalizing on veterans' existing leadership competencies. This review underscores the need for targeted programs that support veterans' transition into construction careers, align their military expertise with industry requirements, and address employer perception gaps to maximize veterans' contribution to the sector.

Despite evidence of skill overlap, there is limited research evaluating specific behavioral competencies shared by military officers and construction project managers using comparative qualitative methods. Few studies have provided empirical data on transition challenges and strategies from veterans' perspectives within the U.S. construction context.

3 Research Methodology

After the initial problem identification and literature review, a pilot survey was developed consisting of open-ended and closed-ended questions. Figure 1 shows the research methodology employed. The pilot survey focused on the comparison between construction project managers (CPMs) and military officers (MOs) regarding leadership, skills, and transition potential into the construction industry. The dissemination of the pilot survey was done through email invitations. This preliminary phase aimed to validate and enhance the interview questions based on feedback from participants.

For data collection, purposive sampling combined with snowball sampling was adopted to obtain participants for the study. Purposive sampling is selected when researchers need participants to possess the information, knowledge, or experience necessary for the study. After gathering data from these initial participants, the researcher asked them to refer to individuals who might meet the criteria or have relevant experiences. This created a "snowball effect" that grew the sample size

organically. This research targeted two types of individuals; (1) project managers and (2) veterans who have transitioned to project manager roles in the construction industry.



Figure 1: Research Design Framework

For data analysis, thematic analysis was used to analyze the interview transcripts. This process involved identifying recurring themes and organizing them to report the findings. Thematic analysis helped highlight the key challenges military officers face when transitioning to civilian project management roles, offering a comprehensive understanding of the transferable skills and leadership qualities they bring to the construction industry. Figure 2 illustrates the step of the thematic analysis, based on Nowell's study [12].

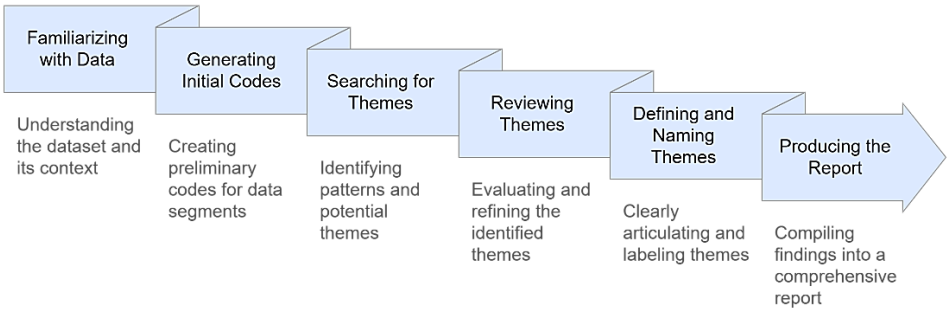


Figure 2: Phases of Thematic Analysis

Lastly, in Step 7, we developed concise guidelines based on industry standards and interview insights to prepare transitioning and former Military Officers (MOs) for construction project management roles. These guidelines offer a comprehensive roadmap tailored to address the unique challenges faced by MOs entering the construction industry.

3.1 Data Collection

Semi-structured interviews were chosen to capture in-depth insights into the transition experiences, perceptions, and competencies of both military officers and construction project managers. Qualitative interviews are effective in understanding complex phenomena and lived experiences [13]. The interview questions were formulated based on a comprehensive literature review, leading to a total of 12 interviews conducted, with six Construction Project Managers (CPMs) and six Military Officers (MOs). These questions were categorized into four main topics: job description analysis, transferability of skills, challenges with transition, and insights for transition. Notably, no identifying information was collected during the interviews to ensure anonymity and confidentiality. There was a total of twelve participants in the study. Table 1 provides detailed information on each participant, including their unique ID, current job position within their company, the state in which they are employed, and their total years of experience. The table includes both Construction Project Managers (CPMs) and Military Officers (MOs), offering a comparative overview of their professional backgrounds.

Table 1: Participants' Data

Participants	Position	State	Years of Experience
Construction Project Manager (CPM)			
CPM-1	Senior Project Manager (SPM) - Heavy Civil	FL	10
CPM-2	PM-Heavy Civil	FL	6
CPM-3	SPM-Commercial	AL	11
CPM-4	PM-Commercial	AL	7
CPM-5	PM-Industrial	GA	6
CPM-6	PM-Commercial	TN	5
Military Officer (MO)			
MO-1	1st Lieutenant	GA	3.5
MO-2	1st Lieutenant	AL	1.5
MO-3	1st Lieutenant	AL	1.5
MO-4	Captain	GA	3.5
MO-5	Captain	AL	3.5
MO-6	Major	AL	6.5

Military officers must adhere to minimum Time in Grade (TIG) requirements to be eligible for promotion. These minimums produce a cumulative Time in Service (TIS), shown in the table above. At each officer's rank, this ensures adequate experience and development in that position. Second Lieutenants require at least 18 months in grade. First Lieutenants need two years. For Captains, a minimum of 3 years TIG is required. This means a Captain's minimum TIS is the sum of their time as a Second Lieutenant and First Lieutenant.

4 Results

Following the transcription of all interview recordings into text format, thematic analysis was conducted to identify recurring patterns across the data. For this study, a theme was established when a specific topic or concept appeared in the responses of at least three participants (50%) within a given stakeholder group. The identification of these themes did not require verbatim repetition; rather, themes were coded based on conceptual similarity across participants' responses, capturing the underlying ideas regardless of the specific terminology used by individual interviewees. As a result, a total of four themes were defined: (i) skills alignment, (ii) transferability of skills, (iii) transition challenges, and (iv) transition insights.

4.1 Skills Alignment

The comparative analysis of Military Officers (MOs) and Construction Project Managers (CPMs) reveals significant skill convergence in several key domains, as shown in Table 2. This analysis emerged from thematic coding of the semi-structured interview responses focused on job competency requirements.

Table 2: Skill Alignment between Mos and CPMs

Group	Number of Respondents	Frequency	Description
Both CPMs and MOs	12	26	Coordination, communication, problem-solving, resource management, risk management, and leadership & development
CPMs	4	10	Technical expertise specific to construction
MOs	3	7	Technical expertise specific to the military

Figure 3 presents these findings as a Venn diagram highlighting the substantial overlap in core competencies between the two professional domains. Both CPMs and MOs demonstrate proficiency in coordination, communication, problem-solving, resource management, risk management, and leadership development, which are the skills essential for managing complex projects and managing diverse teams across both sectors.

The primary divergence appears in domain-specific technical knowledge: CPMs possess specialized construction industry expertise including building codes and construction methodologies, while MOs develop proficiency in military-specific operations, strategic planning, and logistics systems. This complementary skill distribution suggests considerable potential for transitional career pathways, with research supporting project management as a particularly viable career trajectory for veterans given the substantial alignment in foundational leadership and organizational competencies.

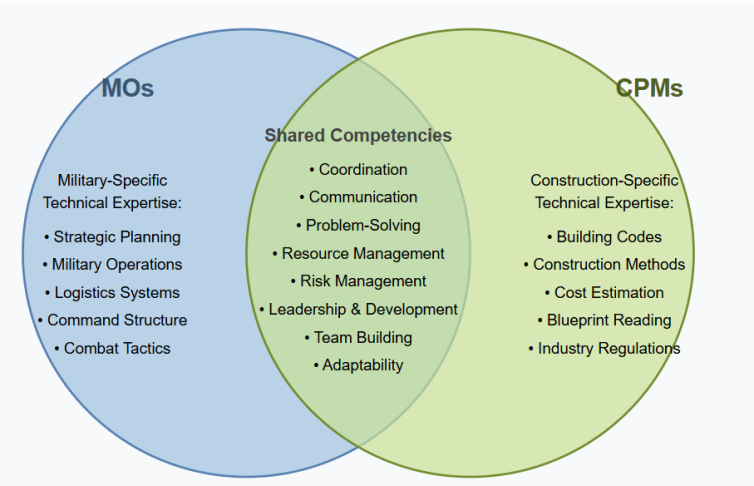


Figure 3: Venn Diagram of Skill Alignment Between MOs and CPMs

4.2 Transferability of Skills

To evaluate the transferability of skills between construction project managers (CPMs) and military officers (MOs), CPMs were asked to assess themselves based on the 12 behavioural competencies outlined by Dainty et al. [10]. These competencies are known to correlate with high-performing project managers, as they blend technical job demands with essential traits for effective managerial performance. This scale typically uses a 5-point Likert-type rating system where respondents self-evaluate their proficiency level in each competency area, ranging from 1 (basic/limited proficiency) to 5 (expert/mastery level). Table 3 compares the mean value of the 12 behavioural competencies for CPMs and MOs.

Table 3: CPMs vs MOs Dainty's 12 Competencies

Competency	**CPMs**	**MOs**
Achievement orientation	2.5	4.8
Initiative	3.33	4.2
Information seeking	3.08	4.4
Focus on the client's need	1.91	4.4
Impact and influence	2.75	3.6
Directiveness	3.5	4
Teamwork and cooperation	3.92	4
Team leadership	4.33	4
Analytical thinking	2.67	4.6
Conceptual thinking	2.58	4
Self-control	2.66	4.2
Flexibility	3.00	2.8

The results showed MOs rated themselves higher than CPMs in most categories, except for team leadership and flexibility. This reflects the structured nature of military roles, suggesting areas for growth in adaptability and collaborative leadership. The findings highlight both the strengths MOs bring, such as high achievement and analytical thinking, and the potential development needs as they transition to civilian construction project management, aligning with insights from the literature review.

4.3 Transition Challenges

The thematic analysis of interview data revealed multiple recurring barriers faced by military personnel transitioning to civilian construction careers. Four primary challenges emerged consistently across respondent groups: cultural adaptation difficulties, unfamiliarity with industry-specific terminology, leadership style adjustment, and integration into civilian workplace environments. Each of these challenges was independently identified by multiple participants, highlighting their significance in the military-to-civilian transition process. These findings align with existing literature documenting the multifaceted nature of veteran career transitions, while providing specific insights into challenges within the construction management context.

4.4 Transition Insights

Several strategic insights emerged as crucial factors for military officers transitioning into civilian construction project management roles. Analysis of interviews with transitioning officers revealed four key themes, as illustrated in Figure 4 and detailed in Table 5. These themes represent evidence-based pathways to facilitate successful career transitions from military leadership to construction project management positions.

The results showed that networking and industry engagement play a pivotal role during the transition. Active networking facilitated connections with industry professionals, potential employers, and mentorship opportunities within the construction sector. As one participant observed, *"As you transition into the construction industry, focus on networking events, mentorship programs, and online platforms. They'll connect you with opportunities, industry insights, and a supportive community for a smooth transition."*

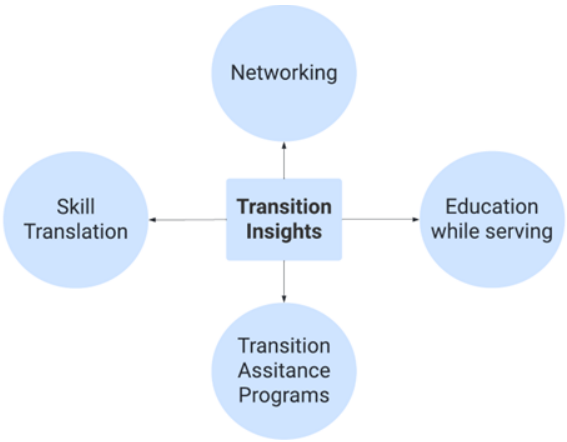


Figure 4: Transition Insights

Continuous education and certification programs emerged as another key insight. Participants emphasized the significance of attaining relevant education, certifications, and training while serving in the military, noting the importance of *"education and awareness campaigns*" to bridge the gap between military knowledge and civilian careers.

Effective communication of military skills for civilian roles was also a recurring theme. Participants stressed the importance of translating and effectively communicating relevant military skills and experiences during the recruitment process, advising transitioning officers to "showcase leadership abilities, problem-solving skills, project management expertise, and teamwork capabilities, highlighting how these skills are transferable to construction project management roles."

Utilization of transition assistance programs, notably the Department of Defense (DOD) SkillBridge initiative, was identified as a valuable resource. The DoD SkillBridge initiative enables military personnel approaching separation to acquire civilian workplace skills through professional development opportunities. SkillBridge provided transitioning officers with practical experience, industry insights, and mentorship opportunities in construction project management. As one participant reflecting on their own experience noted, *"This training was incredibly beneficial as it allowed me ample time to prepare for my transition into civilian construction roles..."*

Table 5: Transition Insights and Occurrences

Common Phrases/Themes	Occurrences
Emphasizes building connections with construction professionals, mentors, and potential employers for insights and opportunities.	5
Focuses on obtaining relevant education and certifications, bridging the knowledge gap between military experience and civilian careers.	4
Advises on translating military skills and experiences into language understood by civilian recruiters, highlighting transferable leadership, problem-solving, and project management abilities.	3
Highlights the importance of programs like the DOD SkillBridge, allowing practical experience and mentorship opportunities in construction project management.	3

5 Conclusion

Effective communication of military skills is crucial, with veterans encouraged to highlight leadership, problem-solving, and project management abilities during recruitment. The DOD SkillBridge initiative, offering practical experience and mentorship, was identified as a valuable resource for veterans transitioning into civilian roles. This study found strong alignment between military officers' and construction project managers' core competencies, such as leadership, communication, and problem-solving. However, it highlighted the need for targeted training to address gaps in construction-specific technical knowledge. Transition challenges mainly stemmed from cultural differences and unfamiliarity with industry regulations, making it vital for both veterans and employers to address these issues for smoother integration.

Recommendations include developing targeted training programs, establishing mentorship networks, and raising employer awareness of veterans' skills. Expanding programs like SkillBridge and creating tools to translate military skills into civilian roles could further ease transitions. Implementing these strategies will help the construction industry tap into the veteran workforce, addressing skill shortages while offering fulfilling career paths for veterans. Future research could explore the long-term career trajectories of veterans in construction, evaluate the impact of transition programs like SkillBridge, and assess the industry's understanding of veterans' transferable skills.

Several limitations exist in this research. First, the study's focus on the United States may limit the generalizability of findings to other regions with different construction and military contexts. Additionally, reliance on self-reported data through interviews and surveys introduces the potential for response bias. These limitations underscore the need for cautious interpretation and suggest avenues for future research to address these constraints.

The sampling geographical region was restricted to the United States, ensuring a focused examination of construction project managers (CPMs) and military officers (MOs) within this context. The CPMs interviewed had accumulated project management experience spanning various locations across the US, reflecting diverse perspectives and practices within the construction industry. Similarly, the MOs included in the study served or are currently serving in roles across different regions of the US, contributing to a comprehensive understanding of military leadership in civilian project management settings. Despite the relatively small sample size, the findings have implications that can be extrapolated to construction projects nationwide, offering valuable insights applicable across different geographical areas within the US.

References

[1] "Project Management Job Growth and Talent Gap 2017–2027," Project Management Institute, 2017.
[2] "U.S. Department of Veterans Affairs." [Online]. Available: http://va.gov/
[3] S. Azhar, W. Noel, A. Nadeem, and G. Akhanova, "Veteran Workforce Development: How Veterans can make a Positive Impact on Workforce Development in the Construction Industry.," in Environmental, Opportunities, and, challenges, Constructing, commitment, and, acknowledging, human, experiences, 2016.
[4] T. Kolditz, "Why the Military Produces Great Leaders," 2009.
[5] M. Keeling, S. Kintzle, and C. A. Castro, "Exploring U.S. Veterans' post-service employment experiences," Mil. Psychol., vol. 30, no. 1, pp. 63–69, Jan. 2018, doi: 10.1080/08995605.2017.1420976.

[6] P. L. Briggs, S. Azhar, and M. Khalfan, "Veteran workforce development: how veterans can make a positive impact on workforce development in the construction industry," Int. J. Sustain. Soc., vol. 12, no. 3, pp. 220–237, Jan. 2020, doi: 10.1504/IJSSOC.2020.109768.
[7] J. M. Haynie, "Business Case for Hiring a Veteran," Harv. Bus. Rev., 2016.
[8] T. Richardson, J. Marion, M. Earnhardt, and V. Anantatmula, "Project Management: A Natural Career Destination for Military Veterans," J. Mod. Proj. Manag., vol. 8, no. 1, pp. 64–81, Jul. 2020, doi: https://doi.org/10.19255/JMPM02304.
[9] F. Pariafsai and A. H. Behzadan, "Core Competencies for Construction Project Management: Literature Review and Content Analysis," J. Civ. Eng. Educ., vol. 147, no. 4, p. 04021010, Oct. 2021, doi: 10.1061/(ASCE)EI.2643-9115.0000051.
[10] A. R. J. Dainty, M.-I. Cheng, and D. R. Moore, "Competency-Based Model for Predicting Construction Project Managers' Performance," J. Manag. Eng., vol. 21, no. 1, pp. 2–9, Jan. 2005, doi: 10.1061/(ASCE)0742-597X(2005)21:1(2).
[11] Y. H. Ahn, R. P. Annie, and H. Kwon, "Key Competencies for U.S. Construction Graduates: Industry Perspective," J. Prof. Issues Eng. Educ. Pract., vol. 138, no. 2, pp. 123–130, Apr. 2012, doi: 10.1061/(ASCE)EI.1943-5541.0000089.
[12] "Thematic Analysis - Lorelli S. Nowell, Jill M. Norris, Deborah E. White, Nancy J. Moules, 2017." Accessed: Mar. 12, 2025. [Online]. Available: https://journals.sagepub.com/doi/full/10.1177/1609406917733847
[13] Kvale, S., and Brinkmann, S. "InterViews: Learning the Craft of Qualitative Research Interviewing (2nd ed.)." Thousand Oaks, CA: SAGE Publications, 2009.

IMPACT OF MIXED REALITY TECHNOLOGY ON TEACHING AND LEARNING IN STRUCTURAL ENGINEERING

[a] Guangyan Shao, [b] Salman Azhar*, [c] Busra Yucel

a: McWhorter School of Building Science, Auburn University, Auburn, Alabama, USA. sza0001@auburn.edu
b: McWhorter School of Building Science, Auburn University, Auburn, Alabama, USA. salman@auburn.edu
c: McWhorter School of Building Science, Auburn University, Auburn, Alabama, USA. bzy0027@auburn.edu
* Corresponding author

Abstract- This study investigates the impact of Mixed Reality (MR) technology on teaching and learning outcomes in structural engineering education. Specifically, it examines how MR enhances students' comprehension, engagement, and efficiency when learning about complex structural assemblies compared to traditional pedagogies based on 2D drawings. Participants were divided into two groups: one used conventional 2D drawings, while the other interacted with MR models via Microsoft® HoloLens 1.0. Both groups completed identical assessments measuring understanding and task completion time. Although the average quiz scores were similar (61%), the MR group completed tasks 17% faster and demonstrated more consistent performance. Qualitative feedback revealed that students valued MR's immersive and interactive experience, which helped them visualize and understand structural relationships more effectively. However, concerns were noted regarding device cost and physical discomfort. Overall, the findings highlight MR's potential to improve structural engineering instruction by enhancing spatial comprehension and learner engagement, suggesting promising directions for future integration into engineering curricula.

Keywords- Building Structures, Structural Engineering Education, Learning Efficiency, Mixed Reality

1 Introduction

Mixed Reality (MR) is a technology that merges computer-generated objects with the existing real-world environment to create an ideal platform for 3D visualization. Unlike virtual reality (VR), which transports users into a fully digital environment, or augmented reality (AR) which simply overlays digital information onto the real world, MR blends the digital and physical worlds as shown in Figure 1. One of the key advantages of MR is occlusion, which is a special ability that AR cannot achieve [1]. This feature allows MR to line up virtual objects correctly in a 3D landscape, enabling objects to appear more realistic in the interaction between real-time environments and virtual images. MR belongs to the broader category of Extended Reality (XR), which encompasses all immersive technologies including VR, AR, and MR. In this framework, the 'X' represents a variable that can accommodate any current or future spatial computing technologies.

Traditional teaching methods in structural engineering, particularly the use of 2D drawings, present several pedagogical limitations when it comes to conveying spatially complex systems. Structural assemblies often involve multiple components intersecting in three-dimensional space, including beams, columns, connections, reinforcements, and material transitions. Understanding how these components relate spatially to one another is critical for students, yet flat 2D drawings reduce three-dimensional complexity into abstract representations that demand high levels of spatial cognition [2]. Mixed Reality directly mitigates the above challenges by merging real and digital environments, offering an interactive 3D visualization experience that enhances spatial understanding. Students using Mixed Reality (MR) devices such as the Microsoft HoloLens can observe, manipulate, and walk around full-scale 3D models of structural assemblies as if they are physically present, allowing for intuitive exploration of spatial relationships that traditional 2D methods cannot provide.

This immersion enables the viewer to naturally perceive depth, orientation, and component relationships without relying on mental reconstruction from abstract 2D information [2,3].

With the advancement of technology and release of Microsoft HoloLens second edition, MR has become more accessible to professionals across various fields. In the design and construction context, MR enables the placement of construction assembly models directly in front of students, seemingly "inside" the classroom or at non-operational jobsites. This makes mixed reality especially useful for sharing 3D content, like BIM models, in ways that could help students better grasp design and construction concepts [3].

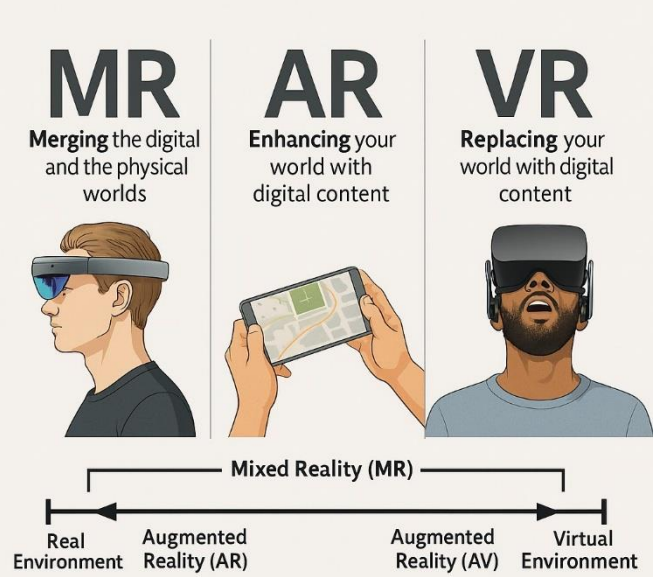


Figure 1. Key differences between MR, AR, and VR environments (Image created in Sora-OpenAI™)

This study explores how well students understand building structures when mixed reality tools are used in their learning. The objectives of this research are: (i) to identify the difference in students' performance scores and time for reading structural drawings using 3D MR view as compared to traditional 2D drawings, and (ii) to assess factors influencing students' comprehension performance using MR applications.

2 Literature Review

Previous research has demonstrated the significant utility of Mixed Reality (MR) technology in construction education [4, 5]. MR effectively creates realistic design and construction jobsite scenarios, giving students the chance to explore jobsite planning, organization, safety, and risk management without having to visit a real construction site [3, 4].

A notable study examined a first-year architectural design classroom, investigating the impact of various visualization technologies including traditional methods and both non-mobile and mobile MR approaches [6]. In this study, researchers implemented two distinct cases: familiar and unfamiliar design cases. For the "familiar design" case, students were provided with five different visualization methods of a campus building: (i) 2D orthographic and photographic renders, (ii) VR using HTC VIVE with a PC, (iii) Mobile VR using Samsung S8 smartphone with Google Cardboard, (iv) AR using Microsoft HoloLens, and (v) The actual physical built environment on campus. For the "unfamiliar design" case, students worked with only four visualization methods, as the physical building had not yet been constructed. Post-test questionnaire results revealed that students strongly valued MR visualizations' ability to strip away layers and visualize complex components. They also acknowledged the continued importance of physical models in the learning process.

Moreover, many construction management curricula typically incorporate field trips or internships to overcome limitations in teaching spatial-temporal concepts and contextual conditions. However, research indicates that AR technology, particularly in the form of head-mounted displays, offers significant benefits in situations involving safety risks, such as when workers' hands are occupied during assembly tasks [7]. Student safety during jobsite visits and practical curriculum

activities remains paramount. AR/MR systems can create safe, clean, and accessible jobsite environments for construction students. One experimental research developed a 6-degree-of-freedom head pose tracking system that enabled trainees to safely experience different working conditions at height, thereby helping them develop readiness for situations they might encounter in actual construction project environments [8].

Another study by Ogunseiju et al. [8] looked at how MR can make construction education more engaging by giving students hands-on experiences without needing to step onto a real job site. Using tools like eye-tracking and student feedback, the research evaluated how well an MR setup helped students learn about sensing technologies used in the field. Students found the experience more effective when the virtual environment included realistic animations, easy-to-use features, and clear access to information. Overall, the study shows that thoughtfully designed MR tools can help close the gap between classroom learning and what's needed on actual construction projects [9].

Finaly, a study by Tan et al. [10] introduced a new way to teach civil engineering students about steel reinforcement bars using AR/MR environments. Instead of relying on traditional 2D drawings, students used AR/MR headsets to explore and interact with 3D models. The results showed that this hands-on, immersive approach helped students understand the material better, remember it longer, and feel more engaged in the learning process.

Most previous research on mixed reality (MR) in structural engineering and construction education has focused on straightforward, low-complexity examples such as illustrating steel reinforcement techniques or demonstrating basic sensing technologies. While these efforts have provided helpful insights, they often fall short of reflecting the complexity found in real-world construction. In this research, we applied MR technology to more advanced and integrated scenarios, like visualizing how complex structural joint assemblies function within framed buildings. This shift offers students a more immersive, realistic, and engaging learning experience that better mirrors the challenges they'll face in professional practice. This paper highlights one part of a larger research project, while the rest of the findings have been shared in another published paper [11].

3 Research Methodology

The methodology of this research was designed to evaluate the effectiveness of MR technologies compared to traditional 2D drawings in construction education. Figure 2 shows the overall methodology used in this study.

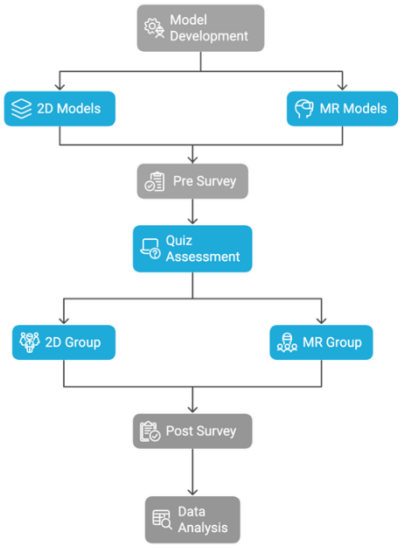


Figure 2. Research Methdology Overview

First, 2D and 3D models were developed for traditional and MR-supported teaching, respectively. To compare comprehension levels across different topics in an undergraduate building structures design course, eight structural detailing models were developed that were presented to students in two formats: (1) traditional 2D drawings and (2) 3D

MR models viewed through Microsoft HoloLens version 1.0. All 3D models were developed using Sketchup Pro. Figure 3 illustrates the comparison of a 2D drawing of a composite wood-steel connection along with its 3D model developed in Sketchup-Pro software.



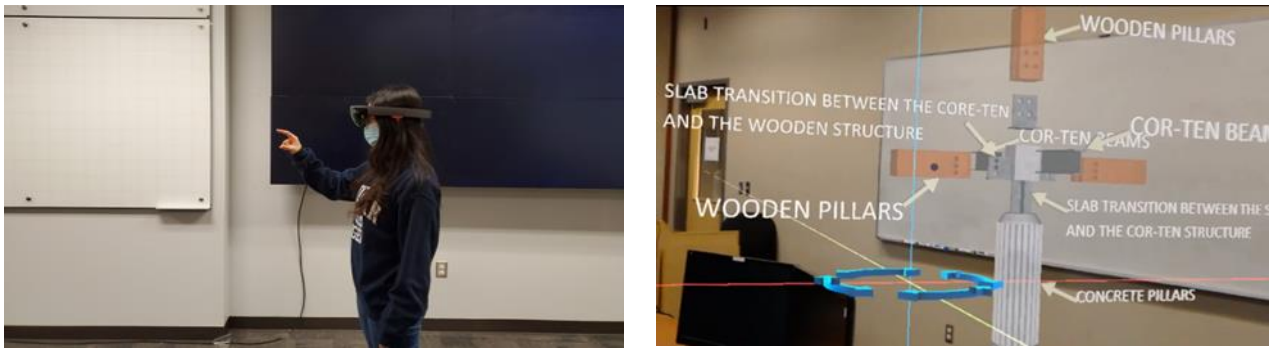
A steel-wood connection in 2D view *3D model development in Sketchup Pro*

Figure 3: A comparison of a 2D drawing and 3D model of a steel-wood composite joint

3.1 Data Collection and Analysis

This study focused on how students understand building structure components. The research involved third-year undergraduate students from Auburn University's Building Science and Architecture programs. Participants were selected from the Structures of Buildings-II course, ensuring they had enough background to assess structural components effectively. Data were collected through surveys (pre- and post-experiment) distributed via Qualtrics®, along with quiz assessments hosted on Canvas®.

The pre-experiment survey was designed to assess students' familiarity with mixed reality (MR) and their understanding of topics covered in the Structures of Buildings-II course. Students also shared their expectations about how MR technology might help them interpret drawings compared to traditional 2D formats. Based on their survey responses and academic performance in the course, participants were divided into two groups: the control group (Group 1) and the MR group (Group 2). The control group had 14 students, while the MR group had 13. Both groups were carefully balanced to include a mix of academic performance levels and varying experience with MR technology.



(a) Viewing the 3D MR model using Microsoft HoloLens *(b) 3D model as seen through the HoloLens headset*

Figure 4: 3D MR model viewed using Microsoft HoloLens, with a perspective shown as seen through the headset

On the quiz day, participants received a 45-minute lecture on structural assemblies, with the control group learning from traditional 2D drawings and the MR group through pre-loaded MR models. Figure 4 illustrates the 3D model viewing via Microsoft HoloLens. Following the lectures, all students completed an 18-question multiple-choice quiz on Canvas, with

each structural assembly covered by 2-3 specific questions. Both completion times and scores were documented for each participant.

After finishing the assessment in their assigned format, students were shown all presentation formats for comparison for the post-experiment survey. The control group additionally received a demonstration of the MR system following their quiz, introducing them to its capabilities and operation. Finally, an online follow-up survey was conducted to gather students' perspectives on using MR technology for understanding building structures, complementing the quantitative performance data with qualitative feedback on the experience.

Finally, the collected data was examined using both quantitative and qualitative approaches. Descriptive statistics helped provide a clear overview of the numbers, while content analysis of the qualitative data offered deeper insights into emerging themes and patterns. The following section summarizes the analysis process and highlights the key findings that emerged from the study.

4 Results

4.1 Pre-Experiment Survey Results: Descriptive Analytics

The study involved a group of 27 third-year undergraduate students enrolled in the BSCI 3440: Structures of Buildings II course. Among them, 15 were Building Science majors (56%), while the remaining 12 were Architecture majors (44%). Although 11 students (41%) had some prior experience using augmented reality (AR) on personal devices, none had used mixed reality (MR) or the HoloLens before participating in this study. Before the MR experience, students were asked to rate their own understanding of the course content on a 10-point scale, where 1 meant "Least Knowledgeable" and 10 meant "Very Knowledgeable." As shown in Table 1, the average self-rating score was 6.74, suggesting that most students felt they had a moderately strong grasp of the subject going into the activity.

Table 1 Results of participants' level of comprehension in the Structures of Buildings class

Minimum	Maximum	Mean	Median	Std Deviation	Variance	Count
3	9	6.74	7	1.51	2.27	27

Regarding participants' preferred method of viewing structural models, a three-option choice was presented with results distributed as shown in Table 2. Participants were encouraged to provide explanatory comments for their selection in an accompanying text box. After reviewing all comments, a comprehensive list of reasons associated with method preferences was compiled and ranked according to repetition frequency.

Table 2 Participants' reasons for preferring 2D drawings or mixed reality (MR) models prior to the testing phase

2D drawings		Mixed reality (MR) model	
Reason	**Count**	**Reason**	**Count**
More prior experience	7	Better visualization	6
Simple and easy to use	5	Manipulate model (turn or move)	3
Less training required	3	Easier and more portable	2
Less disturbance	2		
Rich and detailed content	2		

The analysis showed that traditional 2D drawings were the preferred option, chosen by 18 participants (64%), more than MR or AR models. For most of these students, the main reason was familiarity; 7 out of the 18 shared that they were simply more comfortable with this conventional format. Three others appreciated the clarity and simplicity of 2D drawings, pointing out that they required little to no extra training to understand these drawings. Some also noted specific advantages, like being able to see finer details more easily, focus on individual sections without distraction, and examine one element at a time. Overall, previous experience with 2D drawings played the biggest role in shaping their preferences.

On the other hand, 9 (36%) participants favored the MR experience using HoloLens. Of these, 7 said they found it to be the most helpful method because it allowed them to view the structures as if they were physically present. One participant specifically highlighted that the ability to interact with digital objects in a lifelike way was the key reason they chose MR.

4.2 Quiz Assessment

Comparing the assessment results between students who used traditional 2D drawings and those who worked with mixed reality (MR) models reveals some encouraging benefits of MR in construction education. Although both groups ended up with the same average and median scores, 61% and 65%, respectively—the MR group showed clear advantages in other areas. Most notably, students using MR completed their assessments significantly faster, taking just 19 minutes and 22 seconds on average, compared to 23 minutes and 26 seconds for those using 2D drawings, a time savings of about 17%. This suggests that MR helped students interpret and process complex structural information more efficiently. On top of that, performance among the MR group was more consistent, with a smaller standard deviation of 9.1% compared to 11.60% in the 2D group. This tighter range hints that MR might help level the playing field, supporting a more uniform understanding across different learning styles. A summary of these results is presented in Table 3.

Table 1 Quiz score and completion time comparison

Group	Mean	Median	Standard Deviation	Mean Time
2D Drawings	61%	65%	11.60%	23:26
MR	61%	65%	9.1%	19:22

These results are particularly encouraging considering that MR represents a relatively novel technology for most students compared to the familiar 2D drawings. The fact that MR users matched the comprehension accuracy of traditional methods while significantly improving speed and consistency highlights MR's potential as an effective educational tool in building science. This efficiency advantage could prove especially valuable in professional settings where rapid, yet accurate interpretation of structural elements is essential.

4.3 Post-Experience Survey

After the quiz assessment, the student answered the post-experience survey. Table 4 summarizes students' experience with MR in terms of sentimental analysis. Overall, out of 27 respondents, a majority (15) recommended incorporating MR into future building structures courses.

Table 2 Semantic analysis of student experience with MR-supported learning

Attitude	Key Words	Frequency	Total
Positive	Immersive and interactive experience	9	15
	Present the way how structure elements are put together	4	
	Learn to read drawings in a different way	2	
Negative	Not cost-wise	4	7
	Motion sickness	2	
	Technology immature - insensitive movement	1	
Neutral	Too little experience to judge	3	5
	Depend on different students and class materials	2	

The primary reason, cited by 9 of these students, was that MR's immersive and interactive experience provided a real-life perspective leading to superior 3D visualization compared to traditional 2D drawings. They noted that hands-on experience with HoloLens would allow them to personally manipulate structural models. Four respondents specifically highlighted MR's effectiveness in demonstrating how structural elements interconnect. Similar to opinions about AR [11], two participants appreciated the opportunity to learn drawing interpretation through multiple modalities, adding that HoloLens created an engaging learning environment that enhanced student interest.

That said, 7 students were hesitant to recommend MR technology, mainly due to concerns about the high cost of HoloLens devices, sensitivity to movement, and instances of motion sickness. While they recognized the potential of MR as a

powerful learning tool, they felt that physical discomfort and technical limitations could make it challenging to use effectively in a typical classroom setting. Some also pointed out that simply watching recorded MR sessions wasn't nearly as impactful as actually interacting with the technology firsthand. The idea of providing individual devices for all students was seen as impractical given the cost.

Meanwhile, 5 participants took a more neutral stance. They felt they didn't have enough hands-on experience to form a solid opinion. Their responses reflected an awareness that people respond differently to new technologies and that the learning curve for MR could vary depending on the course content and how the technology is applied.

Students were invited to share their final impressions of the MR technology, and many expressed strong appreciation for its immersive capabilities. One student remarked that it "felt like being inside the structure," underscoring how the technology brought the model to life in a way traditional methods could not. Another noted, "Seeing how all the components connect in 3D made everything click instantly," highlighting MR's effectiveness in clarifying complex relationships. A third student shared, "This was the first time I truly understood how the structural components fit together—2D drawings never gave me that clarity," reinforcing MR's potential to significantly enhance spatial comprehension.

5 Discussion and Conclusion

The integration of Mixed Reality technology in structural engineering and construction education demonstrates promising potential despite certain limitations. MR's primary strength lies in its ability to provide immersive and interactive experiences that help students visualize complex structural relationships, having a capability that traditional 2D drawings cannot offer. The results of this study revealed that, despite equal performance scores between the MR and 2D groups, MR's advantage in time efficiency and consistency suggests that this technology can enhance the learning experience without compromising comprehension.

It is important to recognize that such innovative methods typically require time for full adoption into learning environments, which may explain why immediate grade improvements were not observed in this study. It also appears in the neutral comments, indicating that some students felt they had insufficient experience to form definitive opinions, while others recognized that the effectiveness of MR might vary depending on individual learning styles and specific course materials. This contextual perspective is important as it acknowledges that MR may not be universally superior but rather offers complementary benefits to traditional methods. Educational technologies often face an implementation curve where their full benefits are realized only after students and instructors have developed familiarity with the tools and adapted their learning strategies accordingly. The time efficiency advantage demonstrated by MR users despite their relative inexperience with the technology indicates that with greater exposure and adaptation, MR could potentially lead to improved comprehension and performance outcomes in the future. As students become more comfortable with MR interfaces and develop cognitive frameworks for processing information in this format, the technology's impact on educational outcomes may become more pronounced.

The findings reveal that students most strongly agreed on MR's immersive and interactive experience. Students also valued MR's ability to present structural assembly relationships and offer alternative approaches to drawing interpretation. This aligns with previous research suggesting that spatial visualization technologies can enhance understanding of complex 3D relationships that are difficult to convey in 2D formats [3]. However, cost concerns emerged as the primary barrier to MR adoption, appearing in 5 negative comments. This practical limitation reflects the current reality of MR technology's accessibility in educational settings. Additionally, physical discomfort in the form of motion sickness was noted by multiple students, which could potentially limit extended use of MR in educational contexts. Accordingly, the implementation of MR in educational settings must address several challenges, particularly cost concerns and physiological discomfort experienced by some users. As the technology matures, these issues may diminish, but they currently represent significant barriers to widespread adoption. Future research should focus on developing more affordable MR solutions and refining the user experience to minimize motion sickness.

This research contributes to the field in several important ways. First, the study offers valuable insights into the time efficiency advantages of MR technology, which has significant implications for both educational settings and professional practice where rapid interpretation of complex structures is essential. Secondly, the detailed analysis of student attitudes

toward MR reveals both opportunities and challenges for implementation, providing educators with practical considerations for integrating this technology into their curricula.

Like any study, this research comes with a few limitations that are important to acknowledge. First, the sample size was relatively small, which means the findings should be interpreted with some caution. While the insights gathered offer meaningful direction, they may not fully represent the broader population of students in construction and architecture programs. A larger and more diverse group of participants could provide a more comprehensive understanding of how different learners respond to MR technology.

Secondly, the time allocated for students to engage with MR experience was quite limited. Participants only had a short window to interact with the technology, which may have restricted their ability to fully explore its features or develop deeper comfort and familiarity. As a result, their feedback and performance might reflect an early, surface-level interaction rather than the richer experience that could emerge with repeated or extended use. Future studies with longer exposure periods and more opportunities for hands-on practice would likely offer more nuanced insights into MR's long-term educational benefits.

Future research will focus on evaluating the long-term retention of structural concepts following MR-based instruction, as well as assessing how effectively students apply this knowledge in real-world or simulated construction tasks. Such studies could offer a deeper understanding of MR's lasting educational impact beyond immediate comprehension and engagement.

References

[1] M. Speicher, B. D. Hall, and M. Nebeling, "What is mixed reality?," in Proc. 2019 CHI Conf. Human Factors Comput. Syst., Glasgow, Scotland, UK, 2019, pp. 1–15.

[2] V. Reis, J. S. Baptista, and J. Duarte, "Immersive tools in engineering education—A systematic review," Appl. Sci., vol. 15, no. 11, p. 6339, 2025.

[3] A. N. Ghanbaripour, N. Talebian, D. Miller, R. J. Tumpa, W. Zhang, M. Golmoradi, and M. Skitmore, "A systematic review of the impact of emerging technologies on student learning, engagement, and employability in built environment education," Buildings, vol. 14, no. 9, p. 2769, 2024.

[4] M. Kraus, I. Custovic, and W. Kaufmann, "Struct-MRT: Immersive learning and teaching of design and verification in structural civil engineering using mixed reality," arXiv preprint arXiv:2109.09489, 2021.

[5] L. Gutierrez-Bucheli, J. T. Goh, A. Rashidi, D. Maxwell, R. Digby, Y. Fang, H. Pook, and M. Arashpour, "Adopting immersive technologies in construction training: Determining educational decision-making criteria through a Delphi technique," Smart Sustain. Built Environ., 2024.

[6] J. Birt and M. Cowling, "Assessing mobile mixed reality affordances as a comparative visualization pedagogy for design communication," Res. Learn. Technol., vol. 26, 2018. doi: 10.25304/rlt.v26.2128.

[7] S. K. Renganayagalu, S. C. Mallam, and S. Nazir, "Effectiveness of VR head mounted displays in professional training: A systematic review," Technol. Knowl. Learn., pp. 1–43, 2021.

[8] F. Bosché, M. Abdel-Wahab, and L. Carozza, "Towards a mixed reality system for construction trade training," J. Comput. Civ. Eng., vol. 30, no. 2, p. 04015016, 2016. doi: 10.1061/(ASCE)CP.1943-5487.0000479.

[9] O. R. Ogunseiju, N. Gonsalves, A. A. Akanmu, D. Bairaktarova, D. A. Bowman, and F. Jazizadeh, "Mixed reality environment for learning sensing technology applications in construction: A usability study," Adv. Eng. Inform., vol. 53, p. 101637, 2022.

[10] Y. Tan, W. Xu, K. Chen, C. Deng, and P. Wang, "An interactive and collaborative augmented reality environment for civil engineering education: Steel reinforcement bars teaching as an example," Eng. Constr. Archit. Manag., vol. 31, no. 3, pp. 1100–1122, 2024.

[11] S. Azhar and G. Shao, "Check for enhancing students' comprehension in building structures: An experimental exploration of augmented reality applications," in Proc. 15th Int. Congr. Adv. Civil Eng. (ACE2023), vol. 481, Sustainable Civil Engineering at the Beginning of Third Millennium, Springer Nature, 2024, p. 71.

BIM-DRIVEN ENERGY OPTIMIZATION: ENHANCING THERMAL PERFORMANCE OF BUILDINGS IN ISLAMABAD'S CLIMATE

[a] Shujahat Anwar, [b] Hassaan Bin Raheel*

a: Civil Engineering Dept., National University of Technology, NUTECH, Islamabad, Pakistan. Shujahatanwar55@gmail.com
b: Civil Engineering Dept., National University of Technology NUTECH, Islamabad, Pakistan. Hassaanraheel01@gmail.com
*Corresponding author

***Abstract*:** In contemporary architecture, energy efficiency is a key design consideration due to increasing operational energy demands and environmental concerns. Contrary to the common belief that construction costs dominate a building's lifecycle expenses, operational energy and maintenance costs impact long term sustainability. In Islamabad, a city with composite climate featuring hot summer and cold winters, poorly designed buildings often rely on HVAC systems, resulting in higher energy usage and carbon emissions. This study employs Building Information Modeling (BIM) tools, specifically Revit and Insight, to analyze and optimize the energy performance of the NIEC lab which is under construction at NUTECH University. The model incorporates real climatic data and material properties to assess how heat transfer mechanisms affect thermal efficiency. Simulation results an initial Energy Use Intensity (EUI) of 271 kWh/m²/year, which was reduced by 58% through strategic modifications, including shading devices, window glazing, and building orientation. This paper further explores the integration of renewable energy systems, such as photovoltaic panels and small wind turbines, as potential solutions for reducing grid dependency. These findings offer practical recommendations for designing thermally efficient, cost-effective and sustainable buildings tailored to Islamabad's climate.

Keywords- BIM, Energy Efficiency, Heat Transfer, Sustainable Building Design

1. Introduction

The increasing demand for energy-efficient building in Islamabad, a city having hot summers and cold winters, needs innovative design approaches to optimize thermal performance by minimizing energy consumption. Cities are growing and energy is becoming expensive so architects and engineers should use advanced tools like Building Information Modeling (BIM) to make environmentally friendly buildings.

In Pakistan traditional building design ignore passive design strategies due to which people rely on heaters and air conditioner to maintain comfort. Through which not only their operational cost increases carbon emissions also increase. To address this challenge, BIM-based energy simulations are used to assess and enhance building performance in Islamabad's climatic conditions. For that the study started with two phases, first a review of existing literature on building modeling was conducted, passive and active design strategies were carried out, and renewable energy integration was studied in detail. This provided background knowledge and highlighted sustainable practices used in construction industry widely. In the second phase, the theoretical findings were practically implemented on Autodesk Revit and Insight. These tools simulate energy consumption based on architectural features and material choices. A detailed report has been generated by Revit to assess heating and cooling loads. It showed that building uses 271 kWh/m²/year annual energy use intensity (EUI). Using Insight, the building design was enhanced by changing the size of windows, using better glass and adding shades. These changes were expected to lower energy use without putting extra loads into heating and cooling.

Architectural techniques including thermal insulation, natural ventilation and shading devices and optimal orientations that lower energy consumption without the need for mechanical equipment are known as passive design strategies. This study also investigated renewable energy integration by assessing the feasibility of photovoltaic systems and small-scale wind turbines (e.g., the Liam F1 Urban Wind Turbine). As Islamabad is high solar irradiance solar energy is the best option while compact wind turbines provide potential power in urban settings[1]. Integrating natural ventilation system and wind impedance design can also reduce dependance on cooling and heating systems[2]. To provide consistent and dependable energy supply, hybrid renewable integration combines multiple renewable energy sources such as solar photovoltaic cells with small scale wind turbines.

International case studies like Manama (Bahrain) and Phoenix (USA) emphasizes the importance of BIM in optimizing thermal performance in hot climates[3]. The Clover Project used IES-VE simulations to show the importance of digital twin technology for better building design from planning stages by focusing on performance[4].

Including these improvements Pakistan still faces some challenges. BIM is still not used widely a traditional software like AutoCAD etc. is still being used, it is due to regulatory gaps and a shortage of trained professionals. To overcome these hurdles, update construction policies, train professionals, and make BIM as common tools. This study will connect theory with the real world by using BIM models, climate friendly design ideas and check whether renewable energy works well specially for Islamabad. The findings of this study will provide an idea that how architect, engineers and policy maker can make energy-efficient design that will be comfortable in all seasons and align with Pakistan's sustainability and climate goals.

2. Research Methodology

2.1 Research Methodology

In this study simulation was conducted using Building Information Modelling (BIM) to evaluate and enhance the energy performance of buildings within Islamabad's composite climate. The architectural modeling of NIEC (NUTECH Incubation & Entrepreneurship Centre) Lab Building, currently under construction, was used as a case study and using Performance based energy analysis was carried out using Autodesk Revit and Insight. Figure 1 illustrates the methodology flowchart followed to carry out this research.

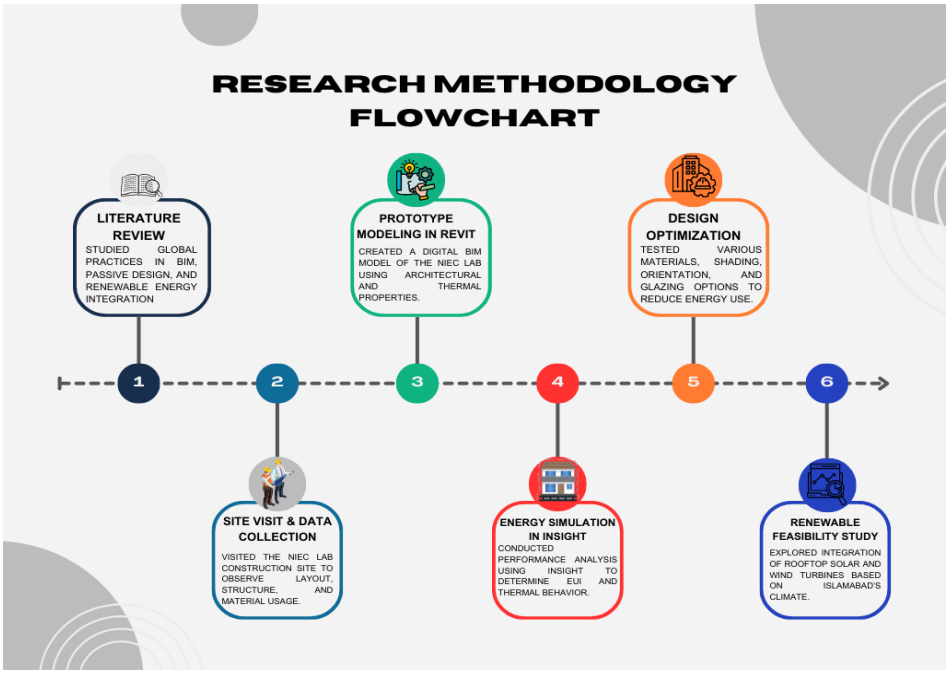


Figure 1 Research Methodology Flowchart

2.2 Prototype Building Model – NIEC Lab (NUTECH Campus)

Through site visits, drawings and onsite observations, a 3D model of a building was developed using Autodesk Revit. This model incorporates actual site conditions and specific material used during construction to enhance simulation. This model is used as a base to test how architectural and material design can affect thermal and energy performance.

Key Modeling Steps in Revit:

- **Site Location**: The project's geolocation was set to Islamabad, for accurate solar and climate date.
- **Architectural Layout**: Model is created just like representing actual model of the NIEC lab with focusing on zones like corridors and open communal areas. Figure 2(a) shows the architectural model of NIEC lab created using Revit.
- **Assumptions**: Peak occupancy was assumed to peak during working hours i.e. 9:00 AM to 4:00 PM. Standard equipment loads were considered based on typical lab usage, including lighting, plug loads, and HVAC systems. Moreover, it is assumed that the windows are operable under moderate weather conditions.
- **Material Selection**: Construction material used on site were assigned with thermal properties like R-Value, SHGC etc. to represent real-world building performance during simulations. Figure 2(b) shows the material properties of walls; Figure 3(a) shows the door material properties and 3(b) shows the windows properties.
- **Glazing & Envelope Detailing**: For studying daylighting and heat transfer effects, the actual window-to-wall ratios (WWR) were determined using site data specifically on southern and western facades
- **Orientation of Building**: Orientation of the building was designed as per its actual north-facing to assess the heat gain and shading potential during different seasons.

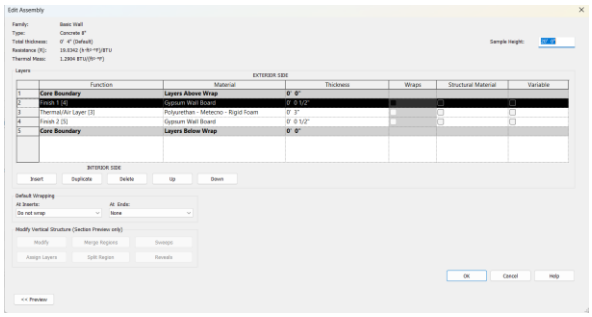
(a).  (b). 

Figure 2 BIM based Revit Model of NIEC lab building: (a). Full architectural model representing actual site layout (b). Wall material properties defined for simulation

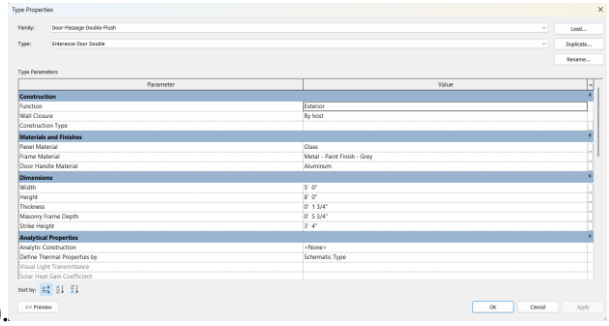
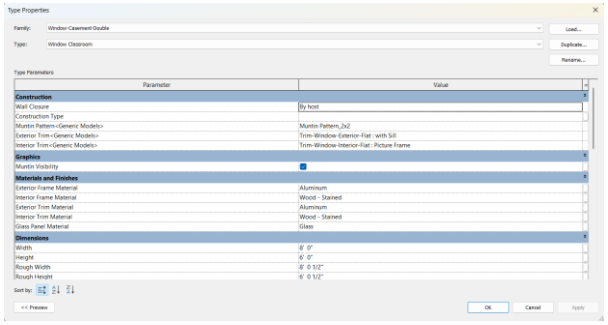
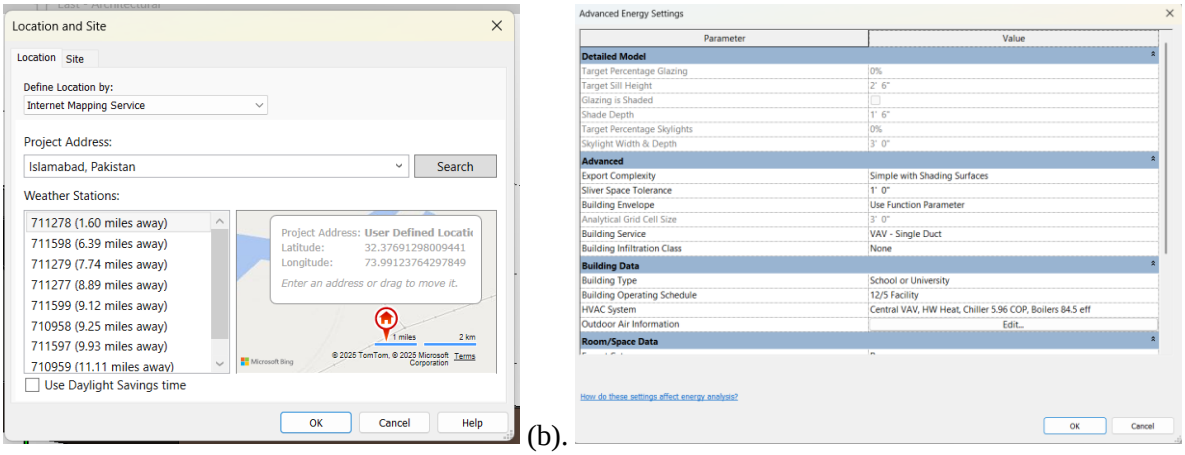
(a).  (b). 

Figure 3 Thermophysical specifications for envelope components used in the BIM model: (a). wooden door R-value and composition; (b). Glazing properties including SHGC and U-values

2.3 Energy Analysis & Simulation

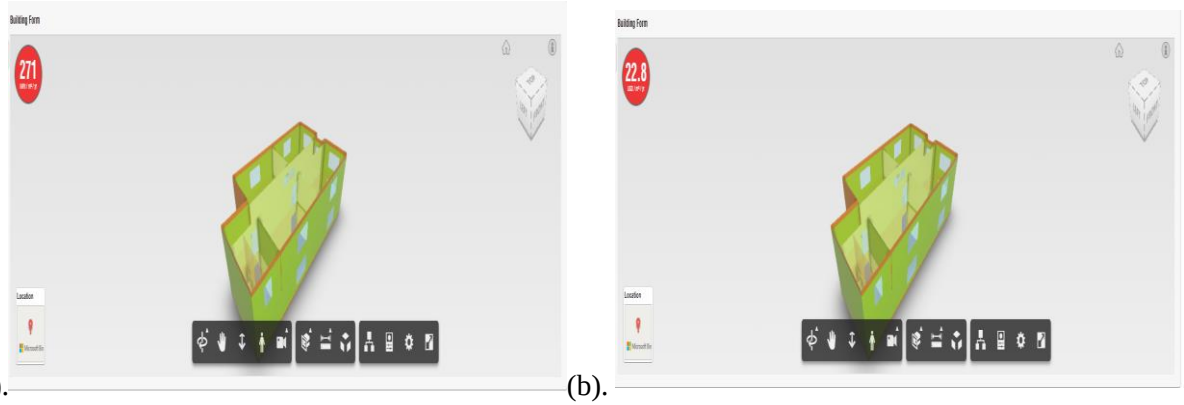
After completing the Revit model, dynamic energy simulations were conducted using Autodesk Insight. The workflow for simulation on Insight is as follows:

1. **Energy Settings**: For simulating the model some energy setting was done according to usage of the building such as selecting Occupancy type, operational hours, lighting and equipment loads etc. Figure 4(a) shows the selected weather station for the energy analysis and figure 4(b) illustrates occupancy type and operational hours selected for energy analysis.
2. **EUI Result**: Initial simulations results shows that Energy Use Intensity (EUI) of model was 271 kWh/m²/year, that indicates the need for improvement in building's energy performance. Figure 5(a) shows the annual energy consumption per square meter and figure 5(b) shows the annual energy cost per square meter.
3. **Design Variable**: Different parameters of building were changed to assess their impact on EUI. Figure 6 shows the zone load summary which includes the peak time, heating and cooling loads.
   - Wall Insulation for thermal resistance
   - Double glazed window type having low emissivity
   - Using shading devices
   - Natural Ventilation and thermal mass optimization through orientation of building.
4. **Final Simulations**: After several changes and testing various passive strategies, significant energy design was achieved considering comfort and daylight sufficiency.



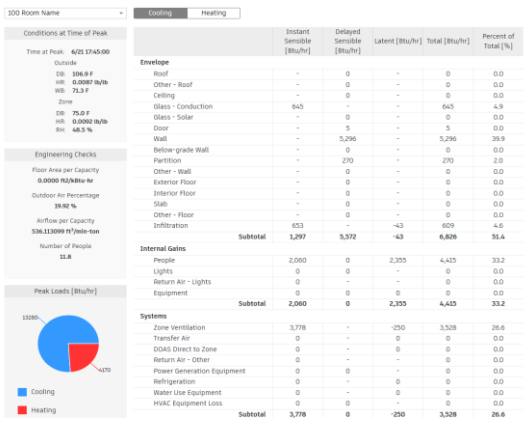
(a). (b).

Figure 4 Building setting for simulations (a). Selecting exact location of building (b). Selecting occupancy type and operational hours



(a). (b).

Figure 5 Initial energy analysis results from Autodesk Insight: (a). Predicted Energy Use Intensity (EUI) (b). annual energy cost per square meter

(a). 

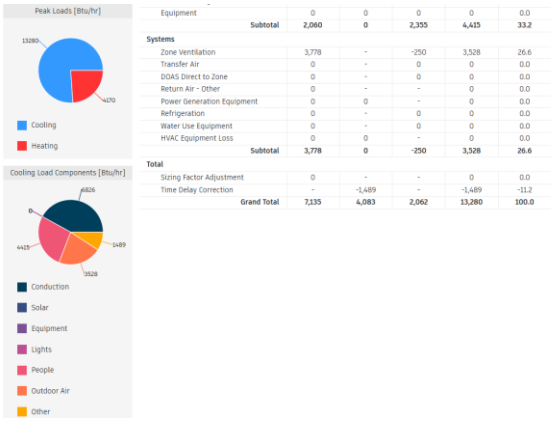
(b). 

Figure 6 Peak load analysis from Insight simulation: (a). building conditions during peak time (b). distribution of cooling load components

5. **Limitations:** The tool utilized for energy analysis is Autodesk Insight which does not fully reflect the actual system behavior in extreme weather events. Moreover, it does not account for future climate scenarios as it uses predefined weather data.

3. Results

This section presents the overall results after energy simulation and analysis using Autodesk Revit and Insight plugin. Various design improvements were implemented in the model to evaluate performance by assessing energy use intensity (EUI) and estimated operational costs.

3.1 Initial Model Analysis

The initial model was developed in Revit without any design improvement and was simulated using Insight. The simulation represents the following results:

- **Energy Use Intensity (EUI):** 271 kWh/m²/year
- **Operational Cost:** 22.8 USD/m²/year

These results represent inefficiencies in building envelopes, HVAC systems, lighting setup and how buildings will be operated in daily schedule.

3.2 Changes applied for optimization

Several modifications in model were made to improve energy efficiency. Some of those modifications are as follows:

- Upgrading building envelope insulations.
- Enhancing HVAC system performance.
- Lighting system is optimized using daylighting and LED solutions.
- For better sealing-controlled infiltration is done.
- Adjusting operating schedules according to actual use.
- Integrated daylight and occupancy sensors.

3.3 Impact of Design changes on Energy Performance

After doing the above measures, we re-simulated the model in Insight. The results after simulations were as follows:

- **Reduced Energy Use Intensity:** 127 kWh/m²/year

- **Reduced Operational Cost:** 9.49 USD/m²/year
- **HVAC System Cost Range:**
  - **Minimum:** 7.85 USD/m²/year
  - **Maximum:** 18.24 USD/m²/year
  - **Mean Value:** 11.68 USD/m²/year

These results indicate a successful reduction in the energy cost by over 58% demonstrated that early-stage design analysis and optimization can lead to significant long term energy savings for the building. Figure 7(a) shows the annual energy consumption per square meter after the changes are applied and figure 7(b) shows the annual energy cost per square meter after the changes are applied. Figure 8 illustrates the model history for different systems.

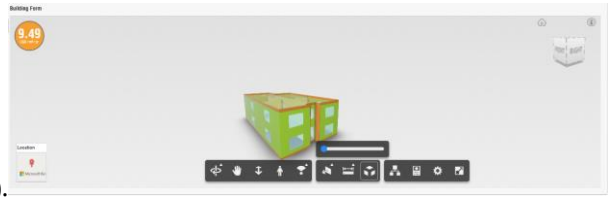
(a).  (b). 

Figure 7 Upgraded Energy Analysis Report (a). Annual Energy Consumption per square meter (b). Annual energy cost per square meter

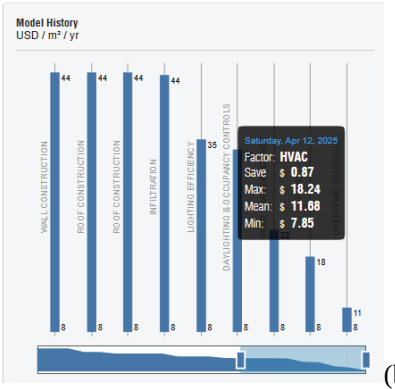
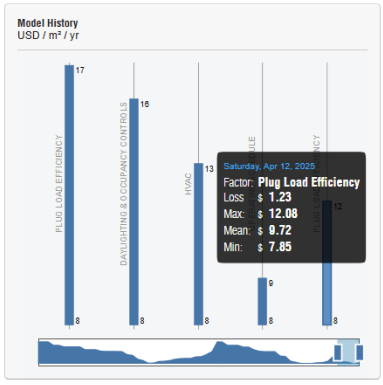
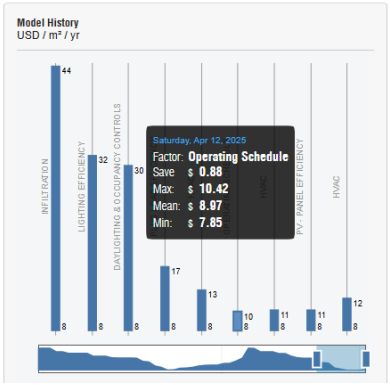
(a).  (b).  (c). 

Figure 8 Model history (a). HVAC System Cost Range (b). Plug Load Efficiency System Cost Range (c). Operation Schedule system Cost Range

Summary Table of Energy Results

Comparison of results before and after making various changes in the designed model are shown in Table 1.

Table 1 Summary of energy simulation results before and after design optimization, highlighting EUI, operational cost, and HVAC performance

Parameter	Initial Model	Optimized Model	Improvement
Energy Use Intensity (EUI)	271 kWh/m²/year	127 kWh/m²/year	Significant decrease
Operational Cost	22.8 USD/m²/year	9.49 USD/m²/year	↓ 58%
HVAC Cost (Mean)	18.5 USD/m²/year	11.68 USD/m²/year	Optimized HVAC system
Plug Load Efficiency (Mean)	14.77 USD/m²/year	9.72 USD/m²/year	Optimized Schedule
Operating Schedule (Mean)	10.91 USD/m²/year	8.97 USD/m²/year	Optimized Schedule
Lighting and Envelope Improvements	Not Implemented	Implemented	Contributed to savings

The Energy Use Intensity (EUI) of the building improved by 53%, which allowed the improvement of a building that formerly recorded Energy Use Intensity (EUI) of 271 and 127 kWh per m 2 per year after installing insulation upgrades, optimized glazing, and shading devices. It can be explained as improvement whose increase can be reached first of all with the help of the reducing thermal transmittance (U-value) of the building envelope lowering heat loss in winter and narrowing heat gain in summer.

Namely, solar heat gain coefficient (SHGC) is lowered when there are windows with low-emissivity coatings and the use of a double-glazing window. The introduction of shading systems prevents direct solar exposure to south, west facing elevations, which can enhance thermal comfort, and keep mechanical cooling systems at a minimum.

Moreover, the optimization of the operation schedule and occupancy settings maintains that HVAC systems are used closer to reality and become more efficient. These findings can be compared to other BIM-based studies, e.g. Chen et al. (2024) and Zhang et al. (2025), which achieve 40-60 decrease in EUI through envelope optimization and passive strategies in the hot climate.

4. Limitations:

Autodesk Insight offers useful early-stage energy analysis, accuracy may be impacted under harsh weather conditions due to its simplified HVAC models and dependence on past weather data. Furthermore, the generalizability of results is restricted in study due to the absence of sensitivity analysis. Parametric simulations, real time occupancy data and sophisticated modelling tools may all be used in future studies to confirm and improve these results.

5. Recommendations

A 58% reduction in annual operational energy cost was achieved through implementation of passive design strategies including insulation, optimizing glazing and natural ventilation etc. We can also reduce the dependency on grid electricity and promote sustainable building operations, through hybrid renewable energy integration. Through research and simulation data, recommended solutions are the solar PV system and a compact wind turbines system that are suitable for Islamabad's urban environment.

5.1 Hybrid Renewable Energy Integration

The study investigated the possibility of integrating hybrid renewable energy to further improve the building's sustainability and energy performance. In order to provide a more consistent and reliable energy supply, photovoltaic (PV) system was combined with small wind turbines, such the Liam F1 Urban Wind Turbine. This hybrid strategy improves overall system efficiency and lessens the drawbacks of depending only on one energy source particularly in the fluctuating weather conditions typical of Islamabad's composite environment.

5.1.1 Integration of Solar Photovoltaic Systems

Islamabad receives an average solar irradiance of 5.3 kWh/m²/day, which means that installing solar panels on roof top is a smart and affordable solution to meet building energy need[5]. According to Sharma et al[6]. In Islamabad using hybrid systems, especially solar systems, can reduce the dependency on fossil fuel. 1kW solar system can generate between 1460-1680 kWh/year in Islamabad, which is enough to cover residential or institutional electricity demand[7].

5.1.2 Integration of Urban Wind Energy Systems

For supporting solar system, especially in cloudy weather, compact urban wind turbines like the Liam F1 Urban Wind Turbine are the solution for generating extra power. Manufactured by The Archimedes, the Liam F1 is a 1.5m Dia, 100kg turbine having capacity of producing 300-2500 kWh/year at an average speed of 4.5 m/s[8]. Due to its aerodynamic design, it can capture upto 80% available wind energy, while operating silently at 45 decibels. Due to its built-in directional shape,

it requires no additional mechanical alignment system. These features make it possible to use the roof on top of institutions like NIEC Lab, where space is limited but sustainability is priority.

According to the results of Zhang et al.[4] and Noorollahi et al.[9] wind system when used with smart grid technology or combined with solar can make energy system more stable and help in reducing carbon emissions. Chen et al. [3] highlighted how hybrid system works efficiently in dense cities like Manama and Phoenix where building-integrated renewable system reduced grid dependency upto 60%. Table 2 describes the key advantages of utilizing wind energy system.

Table 2 Key Advantages of Solar + Wind Integration

Parameter	Solar PV System	Liam F1 Wind Turbine
Output (Annual)	~1,460–1,680 kWh/kW	~300–2,500 kWh/unit
Day/Night Balance	Daytime performance	Evening/Night wind compensation
Urban Suitability	Rooftop	Rooftop/wall mount (1.5 m diameter)
Noise Level	Silent	~45 dB (urban background level)
Wind Requirement	N/A	Avg. 4.5 m/s at 10m height

By implementing hybrid renewable energy strategies, building can move towards net zero operational energy use. Combining passive design with on-site renewables will not only make cost-effective future buildings but also resilient and climate-adaptive in future.

6. Conclusion

This study shows that using BIM and energy simulation tools in designing buildings will reduce the energy consumption and maintenance cost of these buildings especially in the Islamabad climate. NEIC lab at NUTECH was modeled using Autodesk Revit and Insight, and they looked at its baseline energy performance. Initially simulations result high energy use intensity (EUI) of 271 kWh/m²/year and an operational energy cost of 22.8 USD/m²/year. By making some design changes like better insulation, optimizing windows, adding shading devices, and adjusting the building's orientation we have cut the EUI down to 127 kWh/m²/year means energy consumption was dropped by 53% and cost went down by 58%. In addition to it by installing solar panels and wind turbines, it also reduces energy usage by another 22%. Through this hybrid renewable system, we could generate about 30,000 kWh/year.

This research confirms that BIM is not only for designing shapes and material but is also a tool for making smart energy decisions. As results looks favorable, but more work is needed to implement in Pakistan practically. To make BIM common in Pakistan, we need to implement it in the building rules, conduct training programs, and support. Overall, doing energy analysis with BIM early in the design process can really help create buildings that are sustainable, cost-effective, and responsive to climate challenges. The methods and results from this study can help guide architects, engineers, and policymakers in future projects that aim for energy efficiency in similar climates.

Acknowledgment

The authors would like to express gratitude to Almighty Allah who blesses us with an opportunity to carry out this extensive research. A sincere thanks to the National University of Technology, Islamabad, Civil l Engineering Department for giving a chance and support in the work. The NIEC Lab project's academics and staff deserve special recognition for providing access to site data and drawings, which were essential for creating the BIM Model. The support and direction from peers and academic mentors during the research were essential to finishing this study successfully. Lastly, the authors express their gratitude to the 7th Conference on Sustainability in Civil Engineering (CSCE'25) organizers for giving them a venue to showcase their findings.

References

[1] F. Ullah *et al.*, "A comprehensive review of wind power integration and energy storage technologies for modern grid frequency

regulation," *Heliyon*, vol. 10, no. 9, p. e30466, 2024, doi: 10.1016/j.heliyon.2024.e30466.

[2] C. N. Nwagu, C. O. Ujah, D. V. V. Kallon, and V. S. Aigbodion, "Integrating solar and wind energy into the electricity grid for improved power accessibility," *Unconv. Resour.*, vol. 5, no. May 2024, p. 100129, 2025, doi: 10.1016/j.uncres.2024.100129.

[3] L. Chen *et al.*, *Green building practices to integrate renewable energy in the construction sector: a review*, vol. 22, no. 2. Springer International Publishing, 2024. doi: 10.1007/s10311-023-01675-2.

[4] X. Zhang, Y. Ge, and R. V. Patel, "Renewable Energy Integration and Energy Efficiency Enhancement for a Net-Zero-Carbon Commercial Building," *Buildings*, vol. 15, no. 3, 2025, doi: 10.3390/buildings15030414.

[5] "National Renewable Energy Laboratory (NREL), 'PVWatts Calculator,' U.S. Department of Energy, 2023.".

[6] "R. Sharma, M. Tiwari, and N. Dubey, 'Hybrid Renewable Energy Systems for Sustainable Development,' Renewable Energy Reports, vol. 2, pp. 45–56, 2023.".

[7] "EcoSpark Solar, 'Peak Sun Hours in Pakistan – A Comprehensive Overview,' EcoSpark Solar, [Online].".

[8] "The Archimedes, 'Liam F1 Urban Wind Turbine: Technical Overview,' iEnergy US, [Online]".

[9] "E. Noorollahi, D. Fadai, S. H. Ghodsipour, and M. Abedi, 'Simulation of wind power cost and integration using EnergyPLAN software,' Sustainable Cities and Society, vol. 65, p. 102607, 2021.".

7th Conference on Sustainability in Civil Engineering (CSCE'25)
(An International Conference)
Department of Civil Engineering
Capital University of Science and Technology, Islamabad Pakistan

CLASH DETECTION OPTIMIZATION IN BIM: A CASE STUDY ON COORDINATION AND DESIGN EFFICIENCY IN INFRASTRUCTURE PROJECTS

[a] Muhammad Aqib Jahangir*, [b] Umar Farooq, [c] Asim Sultan

a: Civil Engineering Dept., National University of Technology, NUTECH, Islamabad, Pakistan. aqibjahangirf21@nutech.edu.pk
a: Civil Engineering Dept., National University of Technology, NUTECH, Islamabad, Pakistan. umarfarooq02f21@nutech.edu.pk
b: University of Rasul, Mandi Bahauddin, Pakistan. asimsultan@putrasul.edu.pk
* Corresponding author

Abstract- This Paper presents a methodology for Building Information Modeling (BIM) based clash detection, with a focus on a case study of the National University of Technology Admin Block in Capital Smart City, Islamabad. We detailed standardized modeling protocols, precise Levels of Detail (LOD), clash detection criteria, and structured resolution workflows to optimize interdisciplinary coordination. Using Autodesk Revit for individual discipline models (architectural, structural and MEP) and Navisworks Manage for clash detection, we identified 1,344 hard clashes at a 0.003 ft tolerance. Detailed quantification of clash penetration depths (ranging from 0.479 ft to o.664 ft) and spatial clustering analyses guided targeted resolution efforts. We compare our findings against benchmarks from similar infrastructure projects, demonstrating that early, rigorous clash detection reduces downstream rework relative to traditional workflows. Based on project findings, we propose a practical framework comprising modeling standards, naming conventions, phased review cycles and prioritized resolution to guide local and regional firms in infrastructure projects. A critical literature synthesis, clear definitions of technical terms and a discussion of limitations, challenges and future research directions are included to strengthen the paper's contribution to both academia and practice.

Keywords- Building Information Modeling (BIM), Clash Detection, Autodesk Revit, Navisworks Manage

1 Introduction

The construction industry contributes significantly to global GDP but remains plagued by costly design errors, rework and schedule delays arising from fragmented interdisciplinary coordination [1]. Traditional two-dimensional (2D) drawings often fail to capture spatial conflicts until late design or construction phases, leading to expensive redesign and material waste [2]. Building Information Modeling (BIM) has emerged as a transformative approach to integrate architectural, structural and mechanical, electrical and plumbing (MEP) disciplines into a unified three-dimensional (3D) digital platform, enabling early detection of geometric conflicts (clashes) and reducing rework [1-4].

In BIM, clashes are categorized into three main types: First are hard clashes which involve direct geometric intersections between elements (e.g., insufficient duct penetration a structural beam). Second ones are soft clashes occurring when clearance requirements are violated (e.g., insufficient maintenance or installation access). Third are the time clashes related to sequencing or scheduling conflicts that may cause on-site congestion ore delays [1, 2].

Successful clash detection depends on standardized modeling practices, clear levels of detail (LOD), consistent naming conventions and collaborative workflows among project stakeholders [3, 5]. Although various studies demonstrate BIM's

potential to reduce errors and waste [6-8], gaps remain in defining a structured framework that can be readily adopted by local or regional infrastructure firms.

Although earlier studies ([2, 3, 8]) have demonstrated that BIM-based clash detection reduces coordination errors, they typically focus on small-scale or residential buildings, lack in depth benchmarking with similar infrastructure projects, and provide limited justification for tolerance thresholds and clash detection protocols.

2 Literature Review

2.1 BIM and Clash Detection: Evolution and Impact

BIM has revolutionized design coordination by integrating multidisciplinary models into a single digital environment. Early research by Kermanshahi, Tahir [1] and Yönder and Çavka [2] focused on demonstrating BIM's capability to identify clashes in small to medium scale building. Yönder and Çavka [2] reported that early phase clash detection in a two-story structure reduced on-site issues by 20% compared to 2D workflows. Abdalhameed [3] highlighted that careful assignment of LOD and standardized families improved model consistency, thereby minimizing false positive clashes.

2.2 Modeling Standards and Levels of Detail

Model accuracy and consistency are important for reliable clash detection. Abdalhameed [3] and Nair, Anilkumar [4] emphasize the importance of standardized families , naming conventions, and metadata (e.g., gridlines, levels) to ensure interoperable models across disciplines. LOD definitions (e.g., LOD 300 for design development) determine geometric granularity: architectural elements should include walls, floors, doors and windows; structure models should include beams, columns and slabs; MEP Models should include ducts, pipes, cable, trays and equipment [3, 9]. Hasan [5] suggested that inconsistent LOD assignments often generate false positive clashes, thereby inflating coordination efforts.

2.3 Clash Detection Tools and Methods

Autodesk Revit facilitates individual discipline modeling, while Navisworks Manage remains the de facto standard for combined clash analysis due to its robust clash detection engine and reporting capabilities [1, 2, 9]. Researchers have explored automation plugins (Hasannejad, Sardrud [10]) and cloud-based solutions (Baltabekov, Zharassov [9]) to streamline clash detection cycles. Bitaraf, Salimpour [7] proposed prioritized algorithms to rank clashes by cost impact and spatial urgency. However, adoption barriers persist, including steep software licenses, interoperability issues and limited expertise among local firms [6, 11].

2.4 Benchmarking and Comparative Analyses

Comparative benchmarks contextualize clash detection performance. Yönder and Çavka [2] reported 528 hard clashes in their case study, whereas Baltabekov, Zharassov [9] identified 2,132 clashes in a mid-rise residential complex. Chahrour, Hafeez [8] suggested that projects with rigorous modeling protocols experienced 25-30% fewer clashes than those with ad hoc standards. These benchmarks underscore the need for region specific guidelines, such as structural typologies, local codes and resources constraints vary widely.

However, these studies often: (a) do not clearly justify why their chosen tolerance value represent fabrication accuracy thresholds; (b) rely on small buildings typologies with limited generalizability; (c) rarely compare results quantitively with similar benchmarks. This critique indicates a need for more rigorously justified methodologies and comparative analyses in large infrastructure projects.

3 Research Methodology

The approach comprises of three phases as shown in Figure 1 (a-c). First was the model creation in Autodesk Revit. This was followed by Model Integration and Clash Detection in Navisworks Manage. Finally, the identified clashes were analyzed, classified and benchmarked. Emphasis was placed on replicability, clarity and alignment with best practice modeling standards.

3.1 Phase I: Model Creation in Autodesk Revit

3.1.1 Modeling Standards and LOD Definitions

- **Architectural Model (LOD 300):** Walls, floors, doors, windows, slab edges and basic finishes. Families follow ISO compliant naming (e.g., ARC_WALL_EXT_R15 for an exterior wall). Materials assigned for clash detection metadata.
- **Structural Model (LOD 300):** Columns, beams, slabs, footings and load bearing walls. Structural elements use Revit's structural analytical models to maintain geometric accuracy. Naming convention: STR_BEAM_W14X22, STR_COLUMN_W10X30.
- **MEP Model (LOD 300):** Ductwork, piping (HVAC, Plumbing), Cable trays, services equipment (e.g., pumps, air handling units). Families contain metadata fields for system type, size and maintenance clearances. Naming: MEP_DUCT_MAIN_24X12, MEP_PIPE_CW_ø14in.

All models align to a shared project coordination system and level/grid metadata. A centralized BIM Execution Plan (BEP) mandates:

- **Naming Conventions:** Discipline prefix (ARCH/STR/MEP), element type, size and unique identifier.
- **Shared Coordinates:** All models use a common origin point tied to site survey benchmarks.
- **LOD Consistency:** All disciplines commit to LOD 300 (design development) to ensure adequate geometric fidelity for clash detection [3,5].
- **Metadata Standards:** Parameter sets include material type, fire rating (for architectural), load capacities (for structural) and system attributes (for MEP) to facilitate clash filtering.

3.1.2 Modeling Development and Intra-Discipline Checks

Each Discipline team builds and internally reviews its model for:

- **Geometric Integrity:** Verify Walls align to grids; slabs have corrected thickness and MEP services follow routing protocols.
- **Self-Clash Checks:** Utilizing Revit's interference checks to identify internal conflicts (e.g., overlapping walls, intersecting ducts with the HVAC Model). All Self-Clashes must be resolved before combined export.
- **Family Standardization:** Ensuring families are loaded from a controlled library to avoid duplicate or inconsistent geometry.

Upon Completion, each discipline exports to Navisworks Cache (NWC) format, preserving metadata fields (e.g., unique elements IDs, system references).

3.2 Phase II: Model Integration and Clash Detection in Navisworks Manage

3.2.1 Combined Model Assembly

- **Import Process:** NWC files from Revit disciplines are loaded into Navisworks Manage.
- **Alignment Verification:** Visual inspection and measurement checks ensure all discipline models share exact coordinates. Minor misalignments (<1mm) are corrected by adjusting clip coordination or re-exporting from Revit.
- **Model Consolidation:** Layers and selection sets are created:
    - **Selection Set 1:** Architecture (walls, floors, openings)
    - **Selection Set 2:** Structure (Columns, beams, slabs, footings)
    - **Selection Set 3:** MEP (ducts, pipes, trays, equipment)

A "Clash Coordination" workspace is established to streamline filtering and report generation.

3.2.2 Clash Detection Configuration

- **Test Definition:** We focus exclusively on **hard clashes** (geometric intersections) as these direct interferences require immediate resolutions. Soft clashes (clearance) and time clashes (4D sequencing) are out of scope for this study but acknowledgement as future work.
- **Tolerance Setting:** A 0.003ft (~0.9mm) tolerance is selected to balance false positives with detection sensitivity; this corresponds to the minimum fabrication tolerance for structural members and MEP conduits [9].
- **Clash Tests:** Three primary tests are established:
    - **Architecture vs. Structure** (A-S)
    - **Architecture vs. MEP** (A-M)
    - **Structure vs. MEP** (S-M)

Each test employs "**Hard Clash"** rules, ignoring adjacent elements sharing faces (e.g., wall-floor connections) by using property filters (e.g., exclude elements where "Host On" metadata matches). All tests are run concurrently. Navisworks combines clashes into a single report with unique ID, source elements, coordinates, severity and penetration depth measurements. Clashes are grouped by **level** (e.g., Ground Floor, First Floor) and **grid intersection** (e.g., Grid H-10) to identify spatial hotspots. Severity is ranked by penetration depth: **High Severity** (Penetration > 0.5 ft), **Medium Severity** (Penetration 0.25 ft – 0.5 ft) and **Low Severity** (Penetration < 0.25 ft).

3.2.3 Clash Report Generation

The clash report includes:

1 **Clash ID** (unique)
2 **Discipline Pair** (e.g., S-M)
3 **Element IDs** (with metadata for quick identification)
4 **Level/Location** (e.g., Level 0, Grid H-10)
5 **Penetration Depth** (measured by Navisworks)
6 **Bounding Box Coordination** (for 3D localization)
7 **Severity Classification** (High/Medium/Low)
8 **Annotated 3D Snapshot** (exported PNG showing clash in context)

3.3 Phase III: Analysis and Classification

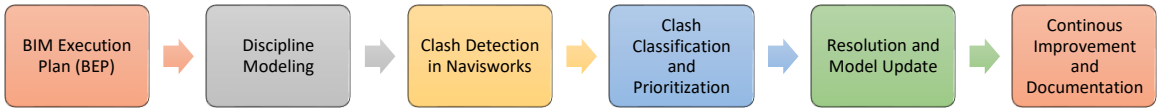
The final phase includes an intensive analysis and classification of the clashes identified in phase II. The Clash report generated by Navisworks is carefully reviewed, and each clash is classified based on its type (hard, soft or time related), severity and possible impact on the project. This classification helps to prefer the decision on the clash, focusing on elements with the most important potential results. The analysis also considers the context of each clash, considering the factors such as the location of the clash, the element and the construction sequence. The purpose of the analysis is to identify patterns and trends in the types and locations of the clashes, which provide insight into the design process or possible improvements in the workflow. The results of this analysis are used to evaluate the efficiency of the construction process, identify areas of improvement and notify recommendations for adapting future projects. The final product in this phase is a comprehensive report that summarizes the findings, including the number and type of clashes, their severity and recommendations for improvement.

All clashes are classified as hard, since every intersection represents direct geometric overlap rather than clearance deficiency. No soft or 4D/time clashes were detected under current settings. Penetration depths ranged from a minimal 0.051 ft to a maximum 0.664 ft.

The tolerance of 0.003ft (~0.9mm) aligns with fabrication tolerances for structural and MEP components, ensuring that only meaningful geometric interferences are flagged, rather than normal manufacturing variations. The combined Revit-Navisworks workflow is recognized standard in AEC coordination, offering reliable clash detection accuracy, robust metadata handling and compatibility across disciplines [2, 3]. Such methodologies grounding ensures this approach is both academically justified and industrially relevant.

4 Clash Detection Framework

Based on our analysis and literature review, we propose a BIM-Based Clash Detection Framework for Infrastructure Projects. This Framework is designed for local or regional firms seeking to implement robust BIM coordination practices without prohibitive resource investments.



1 **BIM Execution Plan (BEP):** Define project scope, roles, responsibilities, LOD requirements, naming conventions and data management protocols.
2 **Discipline Modeling:** Each team develops models in Revit, performs self-clash detection and reviews against BEP standards.
3 **Clash Detection in Navisworks:** Export models, align coordinates, configure clash tests (hard, soft, time) and generate reports.
4 **Clash Classification and Prioritization:** Classify by type, severity, cost impact and location. Organize regular coordination meetings to review and assign resolution tasks.
5 **Resolution and Model Update:** Discipline teams resolve clashes in Revit, update combined model and re-run clash tests in iterative cycles.
6 **Continuous Improvement and Documentation:** Record lesson learned, updated BEP for future projects and document clash resolution protocols.

5 Results and Discussion

The use of three-phase methodology gained significant insight into the effectiveness of BIM-based clash detection . The analysis gives the results that show the effect of early clash detection identity on project coordination, material waste deficiency and stability.

5.1 Clash Detection Overview

By using 0.003 feet tolerance, integrated structural and plumbing models in Navisworks produce 1344 new Hard Clash Institutes. Figure 1 shows clash detection report screenshot, clash detection report was generated using Autodesk Navisworks Software. All clashes were classified as "new"; No one was reviewed, approved or resolved at the time of reporting.

a)

AUTODESK® NAVISWORKS®

Clash Report

Test 1	Tolerance	Clashes	New	Active	Reviewed	Approved	Resolved	Type	Status
	0.003ft	1344	1344	0	0	0	0	Hard	OK

Figure 1: Clash Detection Report, a. Screenshot from Clash Detection Report

5.2 Penetration Depth

The depth of Clash Penetration - was replaced as a full overlap among the objection elements - was recorded up to 0.664 feet. These values emphasize sufficient geometric interventions, especially where large diameter pipes cross structural slabs and beams. In Figure 2 (a) shows that a plumbing fixture had a clash with foundation slab , plumbing fixture is shown in green colour and foundation slab shown in red colour for differentiation of both elements. Figure 2 (b) shows a pipe is going through foundation slab and it needs to be fix, pipe in green colour and foundation slab in red colour.

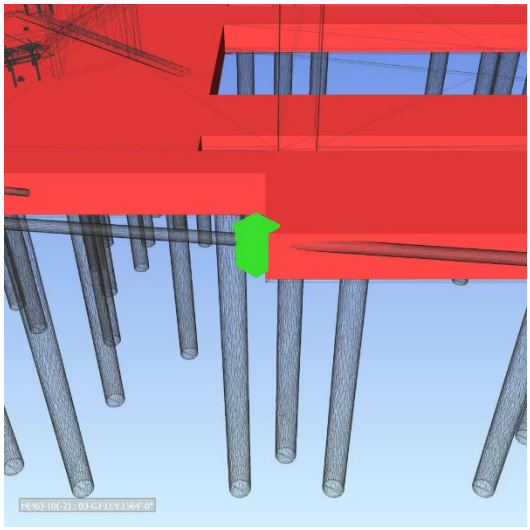
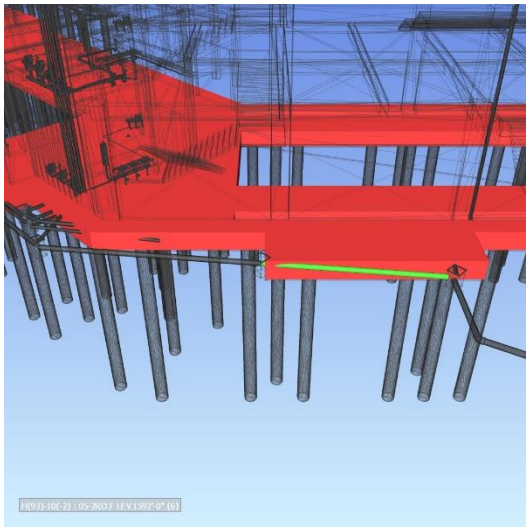
a)  b) 

Figure 2: Clash Detection 3D View, a. Clash of Foundation slab with plumbing fixture, b. Clash of Foundation slab with pipe.

Figure 3 (a) shows a pipe is penetrating through a RCC (Reinforced cement concrete) wall and it is a clear clash between pipe (shown in green colour) and RCC (Reinforced cement concrete) wall (shown in red colour). b) shows a pipe penetrates through a grade beam and it is a clear clash between pipe (shown in green colour) and grade beam (shown in red colour).

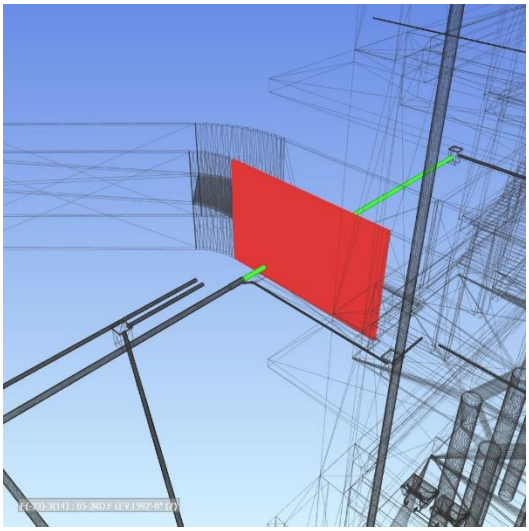
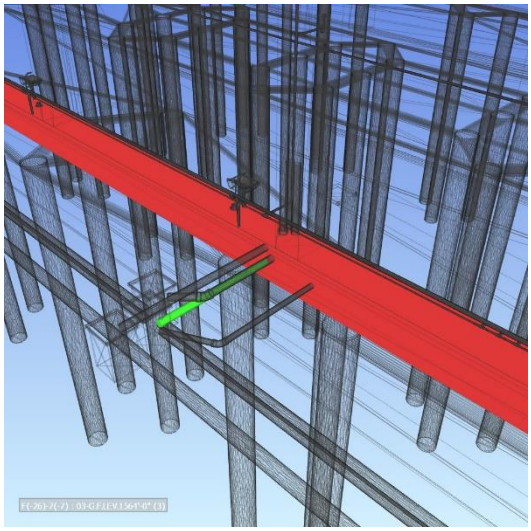
a)  b) 

Figure 3: Clash Detection 3D View, a. Clash of pipe with RCC wall, b. Clash of pipe with grade beam.

5.3 Spatial Hotspots

Analysis of grid sites and level tasks shows two primary battle areas:

1 Roof on the ground floor (H10: Level 0), where densely packed plumbing pipes interfered with structural clearances.
2 Roof slab crosses, especially around the emergency core and vertical service shaft.

5.4 Limitations and Challenges

1 Navisworks Manage Licenses are expensive for small firms; alternative open source or cloud-based clash detection tools may be explored, even though with potential limitations in functionality [11].
2 Although using NWC format preserve most metadata, certain parameters (e.g., complex family attributes) can be lost, leading to incomplete clash reports. Adoption of Standardized Industry Foundation Classes (IFC) could mitigate this but requires additional coordination [3].
3 While this paper aimed for LOD 300, occasional deviations occurred particularly in MEP routing details. Resulting in minor false positive clashes. Enforcing stricter model reviews can address this.
4 This study focused solely on hard clashes. Integrating 4D simulations to detect schedule-based clashes (e.g., overlapping tasks) remains an area for future work.

5.5 Future Research Directions

1 Extend the framework to include clearance checks and 4D sequencing analysis, enabling comprehensive detection of spatial and temporal conflicts.
2 Leverage machine learning techniques to predict clash severity based on historical data and cost impact.
3 Investigate the use of openBIM and IFC to improve interoperability among diverse software platforms, reducing metadata loss.
4 Explore BIM-based clash detection beyond design, incorporating as built data from laser scanning (Point Clouds) to identify on site clashes in real time.

6 Conclusion

This research has shown the value of a structured workflow for hard-clash detection with Navisworks for NUTECH Admin Block in the Capital Smart City. Disciplinary Revit model has been administered with the Navisworks. A total of 1,344 hard clashes of 0.003-foot tolerance were identified, which remained in the "new" position, and emphasized the requirement for an early, complete coordination passport before any design change. Detailed penetration - depth measurements (0.479 ft - 0.664 ft) and spatial clustering (basic and floor sealing and ceilings in level core) provided clear guidance to focus on subsequent coordination efforts.

Beyond the study of this single case, the conclusions strengthen the best BIM best practices:

1 The identity of the preliminary conflict, prevention of design overruns and reduction of material waste lowers the likelihood of project delays.

2 Standardized modeling protocols - including frequent names conferences, shared coordination systems and disciplined levels and grid metadata are important for reliable collection detection in different project types .

3 With extensive reporting features such as element IDs, clash detection and severity classification this paper has enough data to empowers design review and enable stakeholders to efficiently prioritize coordination.

In large-scale construction projects, the integration of a repetitive BIM workflow offers a significant advantage: it enhances interdisciplinary collaboration. Even in projects with complex structural and MEP interferences, the use of time-synchronized collection and analysis enables to achieve sustainable efficiency gains.

7 Acknowledgement

The authors would like to express their sincere granitite to Syed Hussnain Ali Shah and Noor Hassan of the National University of Technology, Islamabad, for their invaluable support and participation throughout this study. Their

contributions, particularly in model validation and coordination feedback, were instrumental in the successful development and completion of the clash detection workflow.

8 References

1. Kermanshahi, E.K., et al. *Implementation of building information modeling for construction clash detection process in the design stage: a case study of Malaysian police headquarter building*. in *IOP Conference Series: Earth and Environmental Science*. 2020. IOP Publishing.
2. Yönder, V.M. and H.B. Çavka, *A case study of clash detection for early design phases in building information modelling.* Livenarch+ Journal, 2024. **1**(1): p. 57-71.
3. Abdalhameed, B.F., *Based BIM techniques to clash detection for construction projects.* Periodicals of Engineering and Natural Sciences, 2023. **11**(1): p. 239-245.
4. Nair, A., et al., *Potential of BIM to Detect Possible Clashes in a Building Construction.* Proceedings of the Yukthi, 2021.
5. Hasan, R., *Quantification of construction waste through BIM.* Journal of Technology Management and Business, 2022. **9**(1): p. 62-77.
6. Mohammed, M., et al., *Beneficial effects of 3D BIM for Pre-empting waste during the planning and design stage of building and waste reduction strategies.* Sustainability, 2022. **14**(6): p. 3410.
7. Bitaraf, I., et al., *Improved Building Information Modeling Based Method for Prioritizing Clash Detection in the Building Construction Design Phase.* Buildings, 2024. **14**(11): p. 3611.
8. Chahrour, R., et al., *Cost-benefit analysis of BIM-enabled design clash detection and resolution.* Construction Management and Economics, 2021. **39**(1): p. 55-72.
9. Baltabekov, N., et al., *BIM for construction clash detection process after design stage.* Technobius, 2021. **1**(3): p. 0004.
10. Hasannejad, A., J.M. Sardrud, and A.A. Shirzadi Javid, *BIM-based clash detection improvement automatically.* International Journal of Construction Management, 2023. **23**(14): p. 2431-2437.
11. Ramya, S. and G. George, *Relative study on clash detection and its effects on BIM modelling.* International Journal for Research in Applied Science & Engineering Technology (IJRASET), 2022. **10**: p. 1519-1525.

7th Conference on Sustainability in Civil Engineering (CSCE'25)
(An International Conference)
Department of Civil Engineering
Capital University of Science and Technology, Islamabad Pakistan

COST–BENEFIT ANALYSIS OF BIM IN LARGE INFRASTRUCTURE PROJECTS: PAKISTAN VS GERMANY

[a] Chaudhry Muhammad Shahram Akbar, [b] Muhammad Ziyad, [c] Mohammad Qasim Bilal*

a: NUST Institute of Civil Engineering, NUST, Islamabad, Pakistan. shahramkhan056@gmail.com
b: NUST Institute of Civil Engineering, NUST, Islamabad, Pakistan. muhammadziyad2345@gmail.com
c: NUST Institute of Civil Engineering, NUST, Islamabad, Pakistan. engr.qasim.bilal@gmail.com
* Corresponding author

Abstract- Building Information Modeling (BIM) is transforming design and construction by enabling integrated 3D models and collaborative workflows. In Germany, government mandates and industry initiatives have driven widespread BIM adoption (~70% of firms), whereas in Pakistan, BIM remains nascent (~11% adoption). This paper reviews recent evidence on BIM's economic and technical outcomes in building-type infrastructure projects in both countries. Studies consistently show that BIM can improve design quality and reduce errors, which translates into cost and time savings. For example, clash detection alone can save up to 10% of contract costs and shorten schedules by ~7% [5]. In Pakistan, stakeholders report that BIM could reduce project cost and time by up to 57% when properly implemented, even though current adoption is low and often limited to 3D drafting. In Germany, early adopters and public infrastructure programs anticipate more modest but reliable savings (on the order of 5–10%) due to higher baseline efficiency. Overall, BIM's benefit–cost profile tends to be positive once initial training and software costs are amortized, with the German government projecting industry-wide productivity gains and lifecycle efficiencies from its 2025 BIM mandate.

Keywords- Building Information Modeling, Cost-Benefit Analysis, Economic Analysis, Infrastructure Projects

1 Introduction

Building Information Modelling (BIM) is an all-encompassing approach that contains 3D design, analysis, and documentation of how a project develops. Complex projects now have the central trend of construction, where the approach is expected to have a higher level of coordination, fewer errors, and more open cost [1] [2]. BIM is expected to enhance the quality and efficiency of the planning and execution phases of any large infrastructure and building project. At Germany's federal level, BIM is a proactive policy: Since 2016, BIM can be required by the public agencies for large projects, and by end-2020 BIM is a requirement on all new federal infrastructure contracts [1]. As a result of this incident, there is an approximate estimate that 70% of German companies are currently incorporating BIM in one way or another, particularly in buildings and transport infrastructures [1].

In comparison, the construction sector in Pakistan has been far slower in becoming digitalized. A survey carried out in 2020 revealed just 11% national use and only 17% of professionals had ever utilized BIM [3]. Some of the problems inherent in Pakistan's fragmented processes, design changes, and delays can be reduced using BIM [3] [4]. This paper compiles recent research on the costs and benefits of BIM, often using end economic variables (such as ROI and savings) and technical results (error reduction, schedule), and identifies some main differences between Pakistan and Germany.

2 Methodology

This study employs a mixed-method approach combining systematic literature review, qualitative analysis, and quantitative data comparison to conduct a comprehensive cost-benefit analysis of BIM adoption in large building infrastructure projects in Pakistan and Germany.

The first step involved a systematic literature review of recent scholarly articles, government publications, industry white papers, and case studies from both countries, focusing on BIM applications in building-type infrastructure projects. Academic databases such as Scopus, Web of Science, and Google Scholar were searched using keywords including "BIM adoption," "BIM cost-benefit," "infrastructure projects," "Pakistan," and "Germany." Selection criteria prioritized studies published within the last five years to ensure relevance to current BIM practices. More than 40 studies were initially identified, of which less than half met the relevance and quality criteria for final inclusion in the analysis. Studies were included if they provided empirical data on BIM adoption, cost or schedule impacts, or implementation case studies in large infrastructure projects.

Qualitative analysis was employed to evaluate any situational context variables, including regulative frameworks, industry preparedness and readiness, cultural attitude, as well as technological barriers that negatively affect the adoption of BIM. The review retrieved descriptive data regarding the stages involved in BIM implementation, stakeholder participation, perceived difficulties and advantages, and differences in the two countries.

Quantitative analysis is devoted to the synthesis of numerical data presented in the literature, including rates of BIM adoption, estimated or calculated cost savings, schedule reductions, and ROI. Data project-specific was gathered and compared, thus establishing patterns and the magnitude of the BIM benefits per country where available. These were tabulated so that they could be compared directly.

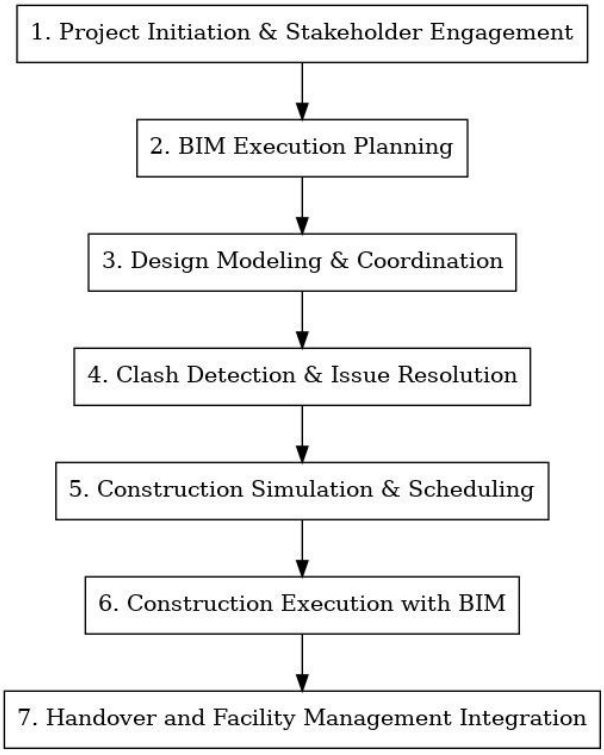


Fig. 1. BIM Implementation Phases Flowchart

This flowchart outlines the typical sequential steps involved in adopting Building Information Modeling (BIM) in large infrastructure projects:

1. Project Initiation & Stakeholder Engagement: Proactive involvement of the stakeholders to tie up all the project players to define BIM objectives and roles.

2. BIM Execution Planning: preparation of a full BIM Execution Plan, containing the standards, the software platform, the workflow of collaboration, and data management.

3. Design Modeling and Coordination: Creating the 3D BIM multi-discipline models of coordination.

4. Clash Detection & Issue Resolution: Identifying and resolving conflicts before construction.

5. Construction Simulation & Scheduling: Simulating sequences to optimize schedules and mitigate risks.

7. Handover and Facility Management Integration: Delivering as-built BIM data for maintenance and lifecycle management.

3 Context of BIM Adaptability

3.1 Pakistan

The construction industry in Pakistan is expanding (≈9% annual growth) [3], yet characterized by cost overruns, time overruns, and poor quality [3]. In the Pakistani AEC (Architecture, Engineering, Construction) circle, BIM is viewed as an emerging technology. There is growing awareness (63% of professionals heard of BIM [3]); nevertheless, the application is still at a niche level: according to the 2020 survey, only around 17% of respondents had used BIM on a project. Consequently, the actual uptake of Pakistan was calculated to be only 11% [3]. Its initial use was in 3D drafting/visualization rather than collaboration. However, the Pakistani professionals recognize the qualitative benefits of BIM: they give it one of the highest scores regarding the improvement of the design quality and decrease in rework [4]. Remarkably, surveys suggest that there may be huge returns: a 57% decrease in expenditure and time in case BIM were implemented to the best of its abilities [3]. These statistics point to a great number of inefficiencies in a conventional project (e.g., change orders, delays) that BIM might solve. The major obstacles reported were the high initial cost of software/training of BIM and the absence of industry standards [3] [4]. Overall, the potential in BIM is large in Pakistan, with a low baseline, but an enormous potential: gains will depend on investment in training, policy support, and successful pilot projects.

3.2 Germany

Germany is a leader in BIM policy. The federal government's "BIM4INFRA2020" roadmap and mandates have systematically accelerated adoption. Since 2017, BIM has been required on all public projects over €100 million [1], and by 2020 on all federal infrastructure building projects [1]. The result is broad industry uptake: recent studies report ≈70% of German construction firms using BIM in some capacity, mostly among architects and large contractors. The typical maturity level is BIM Level 2 (collaborative sharing of models), with Level 3 beginning in flagship projects. The government provides financial incentives and free digital tools (a national BIM portal) to reduce entry costs [1] [2]. In practice, Germany has integrated BIM into major building and transport works. For example, Deutsche Bahn's infrastructure digitization plans explicitly cite BIM for faster, error-reduced project delivery [2] [7]. Hence, German projects often already capture some BIM efficiencies.

While full quantitative reports on German BIM ROI are still emerging, policy documents underscore expected benefits: the Transport Ministry emphasizes BIM will make construction "faster, more transparent and more cost-effective" [2]. Expert analyses note that although German contractors incur extra design effort upfront, they gain early clarity and

schedule assurance. In one study, early BIM use led to shorter schedules on average, reducing capital costs [6]. Moreover, federal plans expect lifecycle data integration (e.g., energy use, maintenance) will yield sustainability gains [2]. In summary, Germany's environment features high BIM utilization with structured ROI tracking, unlike Pakistan's nascent stage.

4 Economic Metrics

In both countries, there are measurable economic payoffs to BIM, but in different magnitudes. Numerous studies across the world have analyzed the monetary effects of BIM. In a survey carried out by Stanford University (CIFE, 2007) on 32 projects, it was noted that BIM had the potential to remove ~40% of unbudgeted change orders and save up to 10% of contract costs through clash detection while shortening schedules by ~7% [5]. According to more recent reviews, identify time savings, RFIs, and rework reductions as leading factors, with BIM most likely to decrease the total cost of business by 10-20% on large construction projects [6]. On the scale, Autodesk calculated relatively small savings on the ROI model of Revit (~2% average) by including only direct expenditures [6], thereby indicating that greater returns are derived indirectly.

4.1 Pakistan

Empirical cost data from Pakistan are scarce, but surveys hint at large potential. For instance, respondents in one study predicted BIM could cut project costs and durations by more than half [3]. If implemented, these savings would derive from avoiding rework, clashes, and late changes. A local project case (the Nespak office) modeled with BIM showed qualitatively that clashes would be detected early, improving accuracy and schedule. While that study did not list exact savings, it noted large reductions in coordination problems [8]. Another benchmark study (Hong Kong public housing) found BIM design effort increased by 45.9% but reduced construction cost by 8.61%, yielding a net ~6.92% total saving [7]. We can conservatively extrapolate: even a single-digit total cost saving would be significant for Pakistani budgets. Importantly, much of Pakistan's construction waste (material/labor inefficiencies, errors) could be mitigated by BIM data sharing [8]. In practice, any ROI must offset Pakistan's BIM setup costs. Public projects could catalyze ROI by standardizing BIM use in tenders. Anecdotally, Pakistani builders note that BIM's schedule certainty can lower financing costs – a non-cash benefit.

4.2 Germany

In Germany, BIM savings are already realized, although they are increasing. Industry reporting indicates that 5-10 percent reductions in costs can be what can be achieved when BIM workflows have matured. To illustrate, Switzerland (geographically near, same practice) compared two equal-height high-rise buildings: the one built with the use of BIM had higher initial costs but had 10% cheaper additional (extra) costs as opposed to the other traditional high-rise building [6]. This implies net savings on the construction phase. In Germany, transport schemes also give figures of a few per cent reductions in planning costs: Cable-grid infrastructure case estimated that its planning costs would be 25% cheaper due to the support of BIM coordination [6]. These small savings indicate that the non-BIM in Germany is already effective, the savings made by removing the small mismatches and enhance the accuracy of quantities. Interestingly, Germany's public BIM mandates force even the previously uninterested firms to invest, and a review of a government study cited its initial ramp-up phase with investment before ROI is realized [6]. After that, planners will be able to bid more reliably.

Statistically, surveys of German (and European) BIM users find ~70% report a positive ROI on BIM [9]. In Western Europe, half of the experienced firms measure BIM ROI on most projects. This aligns with Germany's expectations: as Transport Minister Wissing put it, "digitalization is a prerequisite for quick planning and construction. BIM will make construction more efficient, cost-effective, and transparent" [2]. In sum, German data support that BIM yields cost and schedule benefits in the mid- to long-term, although individual savings vary by project type.

5 Economic Metrics Technical Outcomes

The value of BIM can also be measured in dollars beyond, yet the reduction of errors and improved processes is often overlooked. It is the technical consequences that are highlighted by both Pakistani and German sources. BIM means that by allowing clash detection to take place, BIM is able to prevent delays by ensuring barriers in the field do not arise. The CIFE report from Stanford observed that only clash detection could save contract value ~10 percent [5]. The best BIM benefits are reported as reduced coordination, fewer RFIs, and better documentation in other surveys in the industry [7]. Rework is endemic in the case of Pakistan: in one survey, ~61 % of construction mistakes related to communication breakdown [7]. Those gaps are closed with the assistance of BIM, which can share one model. Practitioners claim that BIM automatically causes the information in the design to spread, minimizing drafting errors manually [7].

Germany's projects similarly show quality gains. For example, German rail and road projects using BIM have reported more stable timelines – each BIM project tends to meet its milestones more reliably than non-BIM ones [6]. Moreover, BIM's environmental modeling allows early energy and life-cycle analysis [2]: planners can estimate carbon footprints and reuse potential before breaking ground. This was demonstrated in a Pakistan case study of the Nespak building: using BIM energy analysis, annual energy use was estimated to drop from 80 to 50 tons/year by adding green design features [7]. Such efficiency analyses are rare in Pakistan today, but the example shows BIM's potential.

In sum, both countries see BIM as a quality and efficiency enhancer. Pakistan's surveys conclude that even if the direct cost impact is "least" (perceptions in 2014 [4]), BIM decisively improves design and reduces rework. Germany's detailed planning yields more quantifiable benefits: fewer RFIs, consistent data handover from design to construction, and eventual maintenance. A German transport master plan explicitly notes that improved planning quality (less uncertainty) yields immediate savings [6]. Thus, BIM drives error reduction and process integration in both settings; the difference is whether those gains have been fully monetized yet.

6 Comparative Summary

The comparative picture is thus: Pakistan – very low BIM usage today, meaning most buildings are designed and built with traditional 2D CAD and manual coordination [3] [4]. This represents a baseline with high waste and risk. BIM's introduction would first raise design costs but promises huge payoffs (survey respondents suggest halving overruns) [3]. Germany – high and growing BIM adoption, supported by policy. Here, BIM is no longer novel; cost/time savings from BIM are more marginal but more certain. Germany's large projects already use BIM data to cut change orders and speed approvals. The German model suggests that early BIM investments are amortized across a long project pipeline, whereas in Pakistan, each project must individually prove ROI.

Both countries value the same core benefits (fewer clashes, better forecasts), but operate at different maturity levels. Pakistani professionals need convincing case studies and government encouragement. German agencies prioritize standardization and life-cycle analysis (e.g., integrating BIM with facility management). Economically, we can illustrate the gap with representative figures: Pakistan reports 11% BIM adoption [3], whereas Germany reports ~70% [1]. Cost reductions of 10–20% are achievable in Europe [6], while Pakistan's optimistic survey suggests up to 57% savings are possible once BIM is implemented [3]. Time savings range similarly. The figure data below shows sample metrics for charting these contrasts.

Table 1. Comparative BIM Performance Metrics: Pakistan vs Germany

Country	BIM Adoption Rate (%)	Cost Savings (%)	Time Reduction (%)
Pakistan	~11% (limited early-stage adoption)	~57% (theoretical/pilot potential)	~57% (estimated from case studies)
Germany	~70% (mandated for public works)	~10% (realized average)	~7% (realized average)

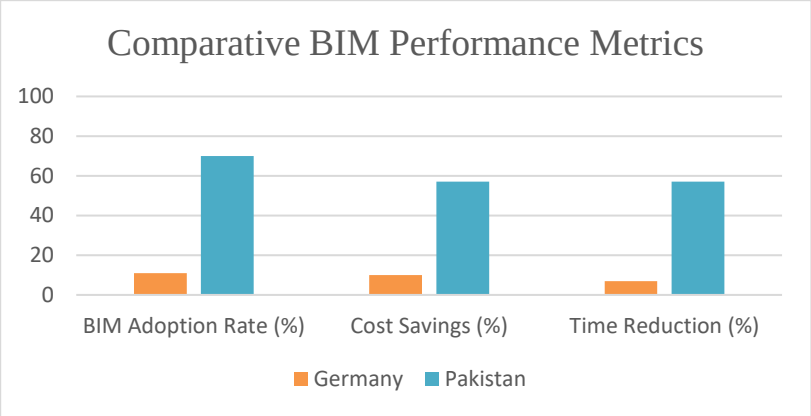


Fig. 2. Building Information Modeling (BIM) performance metrics

The bar chart in Fig. 2 visualizes key Building Information Modeling (BIM) performance metrics—adoption rate, cost savings, and time reduction—for Pakistan and Germany. The data reflect both realized and projected outcomes based on recent studies. Germany, with an established and policy-driven BIM framework, shows a 70% adoption rate, modest but consistent cost savings (~10%), and observed time reductions of around 7%, indicating a mature ecosystem that yields incremental improvements. In contrast, Pakistan's adoption rate is only 11%, but surveys and pilot case studies suggest potential cost and time savings as high as 57% each, if BIM is implemented optimally. These projections highlight Pakistan's significant untapped potential. The disparity in these metrics underscores how maturity and standardization influence measurable outcomes. Germany reaps smaller but dependable gains, while Pakistan has yet to unlock its larger estimated benefits.

7 Discussion

BIM offers clear cost and technical benefits in large construction projects, but realizing those gains depends on context. In Pakistan, the technology is at an early adoption stage: once barriers (cost, training, standards) are addressed, BIM could transform project delivery and yield substantial ROI. In Germany, BIM is maturing into the new norm: significant upfront and learning costs have mostly been absorbed, so the current focus is on leveraging BIM data across project lifecycles. In both settings, research shows positive returns: e.g., Stanford's study projects ~10% cost savings and 7% schedule compression with BIM [5], and even conservative estimates indicate multi-percent improvements on whole-project cost [6]. The German federal BIM initiative expects that by 2025, such improvements will be systematic [2]. For Pakistan, targeted pilot projects and policy frameworks could help capture similar efficiencies. Ultimately, our review finds that BIM yields both economic and technical value in building projects; the difference lies in how fully each country has integrated the technology and measured its results. Germany's BIM adoption was accelerated by institutional enablers like federal mandates and the national BIM portal, which offered free tools and standard guidelines. Pakistan could adopt similar scalable solutions, such as launching a national BIM hub, mandating BIM in select public projects, and offering training incentives to drive broader uptake and standardization. Pakistan should mandate BIM in public projects, establish a national task force, and develop standard protocols. Embedding BIM in curricula and supporting public-private training can further institutionalize adoption.

While this study focuses on Pakistan and Germany, the comparative insights have broader relevance for other Global South countries facing similar infrastructure challenges and digitalization gaps. The stark difference in adoption and outcomes highlights how policy support, training investment, and industry incentives can accelerate BIM uptake. Countries with low adoption rates could leverage Pakistan's early lessons, such as the potential for large gains despite a low baseline, and Germany's structured rollout strategies. This comparative model offers a foundation for policy borrowing, scalability planning, and potential regional collaborations across Asia, Africa, and Latin America, where BIM adoption remains limited but highly beneficial.

References

[1] A. Hasek, "BIM adoption in Europe: 7 countries compared," 21 June 2021. [Online]. Available: https://www.planradar.com/gb/bim-adoption-in-europe/. [Accessed 27 June 2025].

[2] B. f. D. u. V. (BMDV), "Volker Wissing: BIM portal to be expanded into a digital ecosystem," 17 October 2022. [Online]. Available: https://www.bmv.de/SharedDocs/EN/PressRelease/2022/078-wissing-bim-portal.html. [Accessed 27 June 2025].

[3] U. Farooq, S. K. U. Rehman, M. F. Javed, M. Jameel, F. Aslam and R. Alyousef, "Investigating BIM Implementation Barriers and Issues in Pakistan Using ISM Approach," *Applied Sciences*, vol. 10, no. 20, p. 7250, 2020.

[4] R. Masood, M. K. N. Kharal and A. Nasir, "Is BIM Adoption Advantageous for Construction Industry of Pakistan?," *Procedia Engineering*, vol. 77, p. 229–238, 2014.

[5] Alleguard, "BIM Benefits: Efficiency and Cost Savings in Construction," 2023. [Online]. Available: https://alleguard.com/insights/bim-benefits-efficiency-and-cost-savings-in-construction/. [Accessed 27 June 2025].

[6] P. Pick, "Efficiency gains or additional costs – does BIM pay off financially?," 28 October 2024. [Online]. Available: https://www.pom.ch/en/standard-titel/efficiency-gains-or-additional-costs-does-bim-pay-off-financially/. [Accessed 27 June 2025].

[7] W. Lu, A. Fung, Y. Peng, C. Liang and S. Rowlinson, "Cost-benefit analysis of Building Information Modeling implementation in building projects through demystification of time-effort distribution curves," *Building and Environment*, vol. 82, pp. 317-327, 2014.

[8] H. Shinwari, "Building Information Modeling: A Case Study of NESPAK House – Islamabad," Islamabad, 2014.

[9] Autodesk, "The Buisness Valuen of BIM in Europe," 2013.

SPATIAL DOWNSCALING OF GRACE DATASET USING RANDOM FOREST APPROACH FOR A BETTER UNDERSTANDING OF HYDROLOGICAL DROUGHTS IN PAKISTAN

[a] Mustajab Ali, [b] Usman Ali*

a: Department of Civil Engineering, Mirpur University of Science and Technology (MUST), Mirpur Azad Kashmir, Pakistan.
mustajab.ce@must.edu.pk
b: Department of Civil Engineering, Mirpur University of Science and Technology (MUST), Mirpur Azad Kashmir, Pakistan.
aliu70536@gmail.com
*Corresponding author

Abstract- Climate change and increasing urbanization along with anthropogenic activities has intensified the risk of hydrological droughts in a water stressed country like Pakistan. The overall goal of this study; i) to create a Random Forest machine learning framework to downscale GRACE based Terrestrial Water Storage Anomalies (TWSA) from 1° down to 0.25° spatial resolution, and ii) to assess drought frequency and intensity in various regions of Pakistan using an enhanced Terrestrial Water Storage dataset and the TWS-Drought Severity Index (TWS-DSI). A high-accuracy Random Forest model (R^2 = 0.9967) was trained on 1° resolution TWSA data and applied to finer resolution inputs to derive 0.25° TWSA estimates. The downscaled dataset revealed a sharp decline in water storage from 2011 onwards, with extreme drought conditions (TWS-DSI ≤ –1.6) observed post-2020 in regions such as Sindh and southern Punjab. The results obtained highlight the possibilities of ML being used for hydrological monitoring as well as the necessity of cohesive water resources planning that promotes Sustainable Development Goals 6 (Clean Water) and 13 (Climate Action).

Keywords- GRACE, Hydrological Droughts, Random Forest, TWSA, Pakistan

1 Introduction

Terrestrial water storage covers all continental water available in tree canopies, snow, rivers, lakes or reservoirs, wetlands, and groundwater and is a key aspect of the water and energy balance of the world [1]. It is instrumental in influencing the availability of water resources [2] and regulating water flux interactions among diverse components of the Earth system [3]. Additionally, fluctuations in TWS are intrinsically connected to occurrences of droughts [3, 1], floods [4], and variations in global sea levels [5]. In spite of its significance, global TWS has been comparatively under-explored in relation to hydrological fluxes (such as river flows, evapotranspiration, and groundwater flow) due to insufficient large-scale observations and the complexities associated with explicitly delineating all TWS components within hydrological modeling [1]. The Gravity Recovery and Climate Experiment (GRACE) satellite mission, which was specifically designed to enable the comprehensive monitoring of Earth's gravitational field variations. This has consequently provided researchers with enhanced opportunities to refine and substantiate the terrestrial water storage (TWS) simulations that are integral components of these advanced hydrological models [1][2][5]. The GRACE satellite's TWS data, in conjunction with various model simulations, has been employed for an extensive array of applications that encompass diverse fields, including the critical evaluation of water resource availability [2], the thorough examination of

anthropogenic influences on the hydrological cycle [1], the quantification of aquifer depletion rates, the vigilant monitoring of drought conditions, and the thorough assessment of potential flood risks associated with climatic fluctuations [3].

Drought, characterized as a gradually developing phenomenon, ranks among the most expensive natural disasters, directly impacting water resources, agricultural growth, socioeconomic advancement, and ecosystem vitality, and is frequently associated with armed conflicts [6]. A straightforward definition of drought onset involves a decrease in the atmospheric/climatic water balance (commonly referred to as meteorological drought); however, it can evolve into a more intricate natural hazard. For example, a sustained deficit in the climatic water balance may result in diminished streamflow, leading to a hydrological drought [7]; alternatively, it could cause a significant decrease in soil moisture, thereby precipitating an agricultural drought [8]. While meteorological, hydrological, and agricultural droughts are immediate manifestations of reduced water within the hydrological cycle [9]. These droughts subsequently engender numerous detrimental socio-economic, socio-political, and environmental repercussions, including but not limited to water insecurity, food insecurity, economic detriment, and deterioration of water quality, all of which are anticipated to intensify in a progressively warmer future [10].

Anticipated alterations in climatic conditions are expected to exacerbate both the intensity and frequency of droughts globally, driven by transformations in precipitation patterns and rising temperatures [11]. Similar to various other locales, numerous regions in Pakistan face challenges stemming from hydro-meteorological anomalies [12]. Prolonged dry spells may yield catastrophic consequences, negatively affecting water resources and agriculture [13]. Recognized as a region characterized by arid climates, Pakistan experiences scant rainfall coupled with high temperatures [14]. Climate change has precipitated significant repercussions for both the socioeconomic and environmental landscapes in Pakistan [11], as well as in its neighboring regions within Southwest Asia.

An extensive body of literature has emerged focusing on drought assessment utilizing indices such as the standardized precipitation index (SPI), Palmer's drought severity index (PDSI), a standardized runoff index (SRI) and soil moisture drought index (SMI) [10, 1]. These traditional indices were employed to monitor and forecast meteorological, agricultural, and hydrological droughts. Recently, a novel drought index, the TWS drought severity index (TWS-DSI) [15], has been introduced to analyze droughts concerning the vertically available water storage, contrasting with the individual storages or fluxes utilized in conventional indices.

Our research introduces an innovative methodology for assessing drought severity that was previously absent in earlier investigations. The principal objectives of this investigation include (i) the formulation of a Random Forest-based machine learning framework to refine the spatial granularity of GRACE-derived Terrestrial Water Storage Anomalies (TWSA), enhancing its resolution from 1° to 0.25°, and (ii) the application of the improved TWSA dataset to assess drought frequency and intensity across different regions of Pakistan using the TWS-Drought Severity Index (TWS-DSI), in support of the aims outlined in Sustainable Development Goals 6 and 13.

2 Research Methodology

2.1 Study Area

Pakistan is located at latitude 23.5◦–37.5◦ N and longitude 62◦–75◦ E with an area equals to 803,940 km2(Figure 1). Pakistan's hydrology is largely shaped by the Indhetics5 tributary rivers of Indus, Jhelum, Chenab answered, Ravi, and Sutlej, which constitute the Indus Basin and host nearly 90% of irrigated agricultural production [16]. The three main climatic regions of the country are arid, semi-arid, and sub-humid. Rainfall is also irregular, with annual precipitation of less than 200 mm in Balochistan, while in the northern part this surpasses 1,500 mm [11, 14]. Previous episodes of drought especially between 1998-2002 have had catastrophic socio-economic impacts displacing more than 3 million people and generating $2.5 billion in losses [6]. Due to inadequate surface water supplies, farmers are fulfilling their escalating demands through the unregulated overexploitation of groundwater in Pakistan [11]. The concurrent utilization of both groundwater and surface water is occurring on nearly 70% of the irrigated agricultural lands.

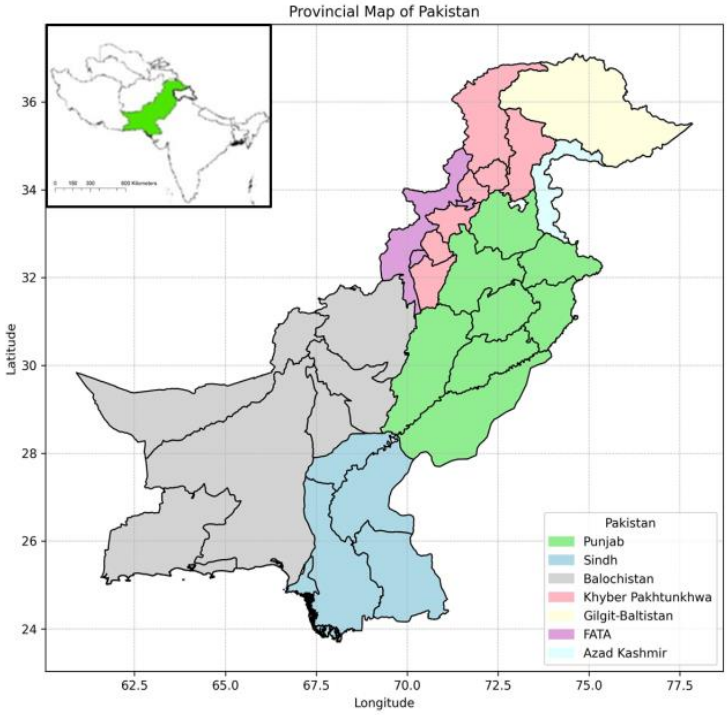


Figure 1 Map of the study area

2.2 Data sources

In the current study, we employed Total Water Storage (TWS) data sourced from the Gravity Recovery and Climate Experiment (GRACE). The GRACE satellite initiative, a collaborative effort between NASA and the German Aerospace Center (DLR), is meticulously structured to evaluate variations in the Earth's gravitational field, thus enabling the monitoring of global changes in the available total water storage. Currently, the gravitational data obtained from GRACE is predominantly disseminated by several processing organizations, including the German Research Center for Geosciences (GFZ), the Jet Propulsion Laboratory (JPL), and the Center for Space Research at the University of Texas (CSR), sustaining a spatial resolution of 1° x 1° [17, 18]. The GRACE data (RL06, level-3) is available at (https://grace.jpl.nasa.gov/data/get-data/) and is presented in terms of equivalent water height, which signifies monthly total water storage [19]. In order to improve the accuracy of the TWSA estimates, we synthesized these three data products. A range of pre-processing techniques were applied to these datasets, including technique called de-stripping filter, Gaussian smoothing, as well as glacier isostatic adjustment (GIA) [20].

2.3 Methodology

2.3.1 GRACE-DSI

For every grid cell, we calculated the GRACE Drought Severity Index (GRACE-DSI) by dividing the GRACE TWS anomaly for month j and year i by the mean of those anomalies represented as $GRACE\text{-}DSI_{i,j} = (TWS_{i,j} - \langle TWS_j \rangle)/\sigma_j$, where i spans from 2002 to 2024, and $\langle TWS_j \rangle$ and $\sigma_j$for the same month and applying the standard deviation [15].

The global GRACE-DSI data follow pseudo-standard normal distribution. Using data from GRACE-DSI, we classified drought into five categories (see

Table 1) indicating that certain levels of drought can be recognized by the magnitude of a TWS deficit in both dry and wet regions.

Table 1 Drought classification on the basis of GRACE DSI [15]

Category	Description	GRACE-DSI
W4	Extremely wet	2.0 or greater
W3	Very wet	1.60 to 1.99
W2	Moderately wet	1.30 to 1.59
W1	Slightly wet	0.80 to 1.29
W0	Near normal	0.50 to 0.79
D0	Abnormally dry	-0.50 to -0.79
D1	Moderate drought	-0.80 to -1.29
D2	Severe drought	-1.30 to -1.59
D3	Extreme drought	-1.60 to -1.99
D4	Exceptional drought	-2.0 or less

2.4 Model Design

For machine learning implementation, a Random Forest model was employed to downscale GRACE TWSA. Initially, the model was trained using coarse-resolution (1°) TWSA as the target and multiple resampled predictor variables the same resolution. Once trained, the model was applied to 0.25° resolution inputs to predict downscaled TWSA [20].The dataset was split into 70% for training and 30% for validation. This means that the model learned patterns from 70% of the data, while its performance was tested on the remaining 30% to ensure generalizability. This split helps to identify whether the model is over fitting or can truly predict on unseen data.

Additionally, 5-fold cross-validation was used to enhance the model's reliability. In this technique, the dataset is divided into five equal parts (folds). The model is trained on four folds and validated on the fifth, and this process is repeated five times so that each fold is used once for validation. The results are then averaged across all five iterations. This approach ensures that the model's performance is stable and not overly dependent on how the data is split, making it ideal for small or noisy datasets. Residuals at the coarse scale were calculated by comparing model predictions with actual GRACE data, and the same trained model was then used to generate downscaled TWSA estimates from high-resolution inputs.

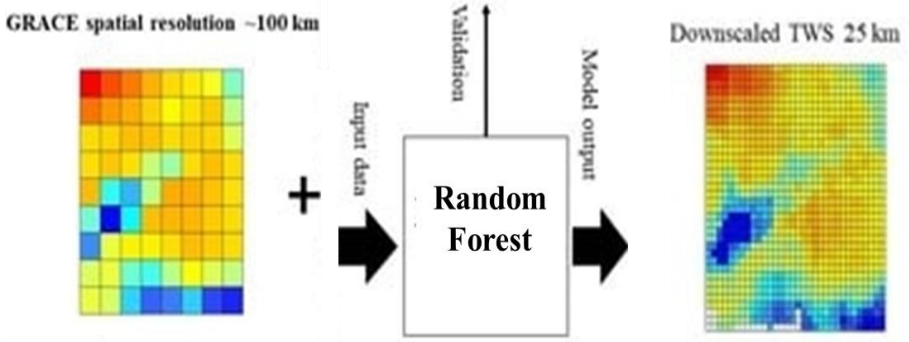


Figure 2 Illustration of the spatial downscaling of GRACE dataset from 1° to 0.25 °

3 Results

3.1 Downscaled GRACE Time Series

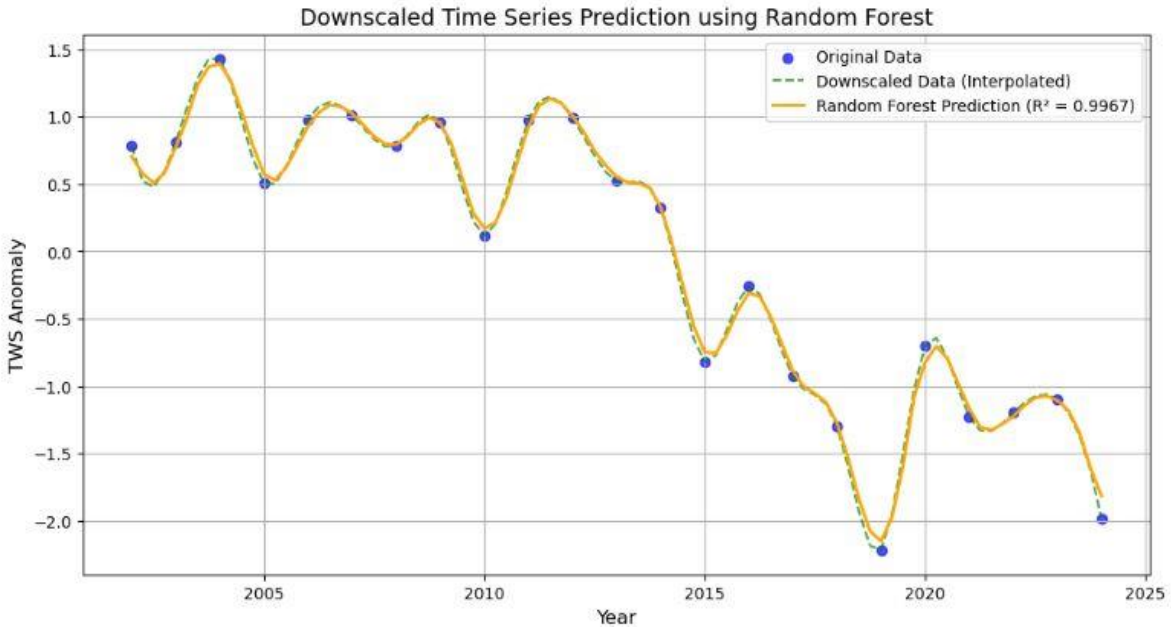


Figure 3Hydrological drought assessment in Pakistan using downscaled GRACE Dataset

The downscaled GRACE Terrestrial Water Storage (TWS) anomaly time series(Figure 3) show interannual to multi-decadal variability from 2002 to 2024 and a clear long-term downward trend as also stated by [1]. The TWS anomaly was characterized by a strong positive signal as seen from the TWS-DSI values (

Table 1) during the first period, from 2002 to approximately 2010, with a recurring seasonality in both peaks and lows that indicates stable conditions that are relatively wet. But, as of 2011 there is a gradual downward trend that indicates a shift to dryer conditions beginning at that date, which could be attributed to lower levels of precipitation as well as more water being drained [19] . The most significant in this regard is the increase in the period 2015-2020 in which TWS anomalies have sharply decreased below -1.0(

Table 1), indicating extreme and constant wetland hydrological drought in this period. This is consistent with GRACE-based studies [15]& [1] on Drought Severity Index, DSI, at the global scale, which also mark relevant drought events in the period. There seems to be a slight and transitory recovery starting around 2020, potentially due to higher precipitations [21] or managed recharge. The anomaly sharply declines again after 2022 and falls under -2.0 (

Table 1) in 2024 indicating that drought conditions are re-establishing and perhaps intensifying [19].

The overall trend is a negative net change of water storage on land in the last two decades, in agreement with recent literature on the subject that highlights the global increase of hydrological droughts. The random forest model reported very high R^2 = 0.9967 which confirms the potential of machine learning to improve temporal resolution and predictions of GRACE TWS data for monitoring water resources.

3.1 Spatial plot

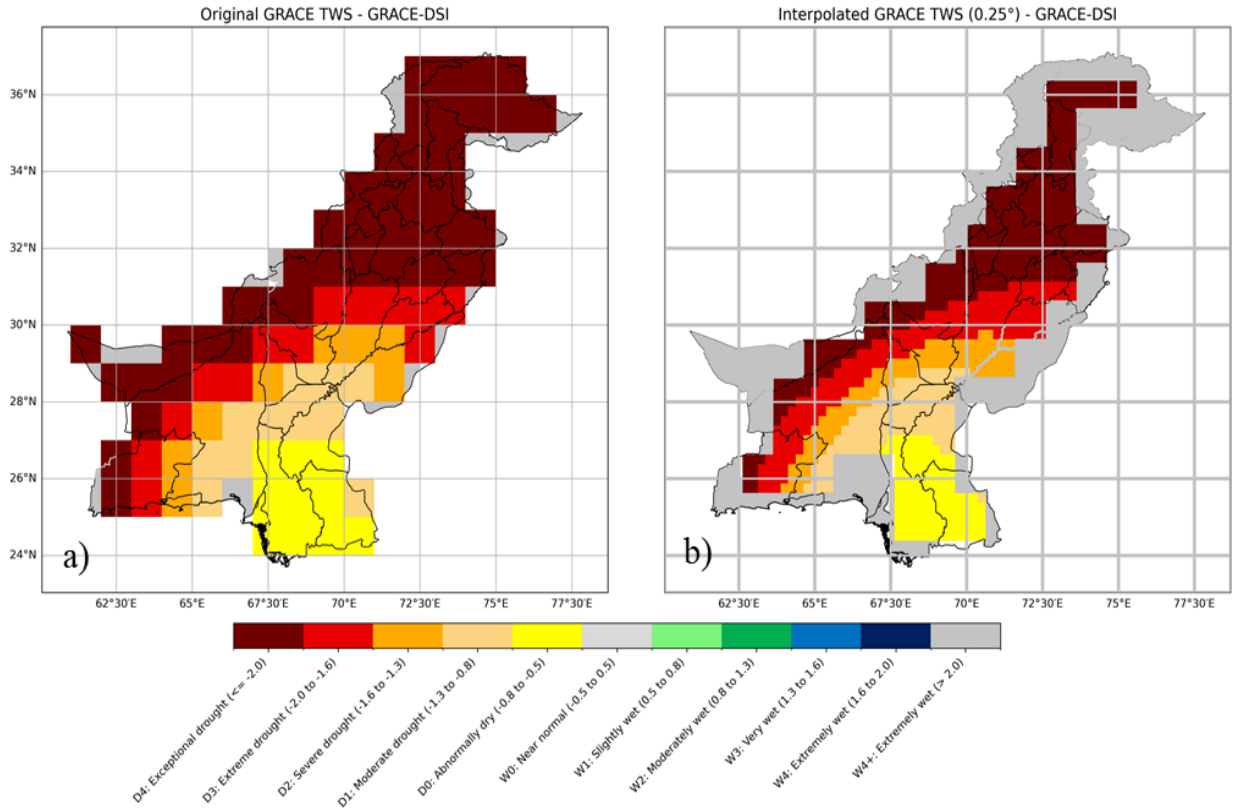


Figure 4 GRACE TWS DSI mapping of Pakistan a) 1º GRACE TWS DSI mapping of Pakistan b) 0.25º downscaled GRACE TWS DSI mapping of Pakistan

GRACE TWS DSI provides a clear perspective on the regional distribution across the country, with areas of significant drought conditions in the northern and western Pakistan contrasting with the south-eastern part of the Indus Basin experiencing significant moisture anomalies [19] as seen in Figure 4. Parts of the north, including Khyber Pakhtunkhwa and Gilgit-Baltistan, have been experiencing severe to exceptional hydrological drought (D3–D4) in reference to

Table 1& Figure 4 largely caused by below normal winter precipitation which is typically associated with enhanced western disturbances that are expected to become weaker during years of strong El Niño conditions [22]. Indeed, a strong El Niño pattern prevailed during the 2023-24 winter, coinciding with lower-than-average snowfall and subsequent water storage in the cryosphere across the Hindu Kush-Himalaya, otherwise Pakistan's main water towers [23].

Balochistan in the west experienced similar trends with (D2–D3) in reference to

Table 1& Figure 4 droughts, continuing the pattern of chronic susceptibility to winter rainfall failures, and confirming its risky dependence on erratic precipitation [24]. Punjab's role as a transition zone presented as moderate anomalies (D0-D1) in reference to

Table 1& Figure 4 as a result of decreased inputs upstream and continued depletion of groundwater reserves due to high abstraction for agriculture, a pattern already well-established in the literature on based groundwater studies in South Asia [11]. Contrarily, residual wetness (W1-W2) in reference to

Table 1& Figure 4 in the southeast province of Sindh corresponded to the hydrological signature of the 2022 super floods, that saw the recharging of subsurface aquifers and soils with water, as previously detected by GRACE sensors after flooding thresholds . This pattern of TWS anomalies, which is not homogeneous across space, reinforces the

relevance of both short-term atmospheric fluctuations and long-term hydrological memory, and highlights once more the necessity of regionally tailored water management policies.

4 Practical Implementation

By observing the trends, the increased intensity of hydrological droughts can be assessed, and mitigation strategies can be adopted. The results of the current study provide useful information that complements national adaptation efforts in line with the United Nations Sustainable Development Goals (SDGs) of 2030, particularly to SDG 6, Clean Water and Sanitation and SDG 13, Climate Action.

5 Conclusion

The following conclusions can be drawn from the conducted study:

1. Our analysis reveals a significant decreasing trend of TWS after 2011; with the most extreme drought conditions (TWS-DSI $\leq$ -1.6) observed post-2020. This marks a critical hydrological shift, especially for southern regions such as Sindh and southern Punjab, underscoring a growing risk of prolonged water scarcity in already vulnerable areas.
2. The TWS-DSI spatial distribution highlights a stark regional contrast: severe to exceptional drought conditions dominate northern and western Pakistan due to weakened winter precipitation influenced by El Niño patterns, while southeastern Sindh shows residual wetness linked to the long-lasting effects of the 2022 super floods.
3. These trends are closely associated with the multiple drivers of climate extremes and increase in human water extractions, particularly groundwater extraction and river regulation via reservoirs.
4. With an R^2 of 0.9967, the Random Forest model demonstrated a high predictive accuracy and proved the potential of machine learning to improve the resolution of satellite-based tools for the monitoring of hydrology, such as GRACE.
5. Our results represent a transition to a more anthropogenically mediated hydrological system, with a particular focus on the sensitivity of the Indus River basin to climatic stress and provide actionable insights for climate-resilient water governance, directly supporting Sustainable Development Goals 6 (Clean Water and Sanitation) and 13 (Climate Action).

Reference

[1] Pokhrel et al., "Pokhrel, Y., Felfelani, F., Satoh, Y., Boulange, J., Burek, P., Gädeke, A., ... & Wada, Y. (2021). Global terrestrial water storage and drought severity under climate change. Nature Climate Change, 11(3), 226-233.," 2021.

[2] Rodell et al., "Rodell, M., Famiglietti, J. S., Wiese, D. N., Reager, J. T., Beaudoing, H. K., Landerer, F. W., & Lo, M. H. (2018). Emerging trends in global freshwater availability. Nature, 557(7707), 651-659.," 2018.

[3] Tapley et al., "Tapley, B. D., Watkins, M. M., Flechtner, F., Reigber, C., Bettadpur, S., Rodell, M., ... & Velicogna, I. (2019). Contributions of GRACE to understanding climate change. Nature climate change, 9(5), 358-369.," 2019.

[4] Pokhrel et al., "Pokhrel, Y. N., Hanasaki, N., Yeh, P. J., Yamada, T. J., Kanae, S., & Oki, T. (2012). Model estimates of sea-level change due to anthropogenic impacts on terrestrial water storage. Nature Geoscience, 5(6), 389-392.," 2012.

[5] Rodell et al., "Rodell, M., Barnoud, A., Robertson, F. R., Allan, R. P., Bellas-Manley, A., Bosilovich, M. G., ... & Seneviratne, S. I. (2024). An abrupt decline in global terrestrial water storage and its relationship with sea level change. Surveys in Geophysics, 45(6),," 2024.

[6] Ali et al., "Ali, M., Gillani, S. H., & Ali, U. (2024). Flash Drought Monitoring in Pakistan Using Machine Learning Techniques and Multivariate Drought Indices. Technical Journal, 3(ICACEE), 717-729.," 2024.

[7] Wu et al., "Wu, G., Chen, J., Shi, X., Kim, J. S., Xia, J., & Zhang, L. (2022). Impacts of global climate warming on meteorological and hydrological droughts and their propagations. Earth's Future, 10(3), e2021EF002542.," 2022.

[8] Zhang et al., "Zhang, Y., Hao, Z., Feng, S., Zhang, X., Xu, Y., & Hao, F. (2021). Agricultural drought prediction in China based on drought propagation and large-scale drivers. Agricultural Water Management, 255, 107028.," 2021.

[9] Yang et al., "Yang, D., Yang, Y., & Xia, J. (2021). Hydrological cycle and water resources in a changing world: A review. Geography and Sustainability, 2(2), 115-122.," 2021.

[10] Akhtar et al., "Akhtar, T., Mushtaq, H., & Hashmi, M. Z. U. R. (2020). Drought monitoring and prediction in climate vulnerable Pakistan: Integrating hydrologic and meteorologic perspectives. Hydrology and Earth System Sciences

Discussions, 2020, 1-29.," 2020.

[11] Ashraf et al., "Ashraf, S., Ali, M., Shrestha, S., Hafeez, M.A., Moiz, A. and Sheikh, Z.A., (2022). Impacts of climate and land-use change on groundwater recharge in the semi-arid lower Ravi River basin, Pakistan. Groundwater for Sustainable Development, 17, p.100743," 2022.

[12] Amjad., "Amjad, M. (2023). Hydrometeorological Extremes and Climate Profiling of Pakistan. In Water and Environment for Sustainability: Case Studies from Developing Countries (pp. 1-16). Cham: Springer International Publishing.," 2023.

[13] Rehman et al., "Rahman, M. A., Ali, M., Mojid, M. A., Anjum, N., Haq, M. E., Kainose, A., & Dissanayaka, K. D. C. R. (2023). Crop coefficient, reference crop evapotranspiration and water demand of dry-season Boro rice as affected by climate variability: A case study from," 2023.

[14] Otto et al., "Otto, F. E., Zachariah, M., Saeed, F., Siddiqi, A., Kamil, S., Mushtaq, H., ... & Clarke, B. (2023). Climate change increased extreme monsoon rainfall, flooding highly vulnerable communities in Pakistan. Environmental Research: Climate, 2(2), 025001.," 2023.

[15] Zhao et al., "Zhao, M., Velicogna, I., & Kimball, J. S. (2017). Satellite observations of regional drought severity in the continental United States using GRACE-based terrestrial water storage changes. Journal of Climate, 30(16), 6297-6308.," 2017.

[16] Janjua et al., "Janjua, S., Hassan, I., Muhammad, S., Ahmed, S., & Ahmed, A. (2021). Water management in Pakistan's Indus Basin: challenges and opportunities. Water Policy, 23(6), 1329-1343.," 2021.

[17] Landerer et al., "Landerer, F. W., & Swenson, S. C. (2012). Accuracy of scaled GRACE terrestrial water storage estimates. Water resources research, 48(4).," 2012.

[18] Ali et al., "Ali, S., Liu, D., Fu, Q., Cheema, M. J. M., Pham, Q. B., Rahaman, M. M., ... & Anh, D. T. (2021). Improving the resolution of GRACE data for spatio-temporal groundwater storage assessment. Remote Sensing, 13(17), 3513.," 2021.

[19] Ali et al., "Ali, S., Khorrami, B., Jehanzaib, M., Tariq, A., Ajmal, M., Arshad, A., ... & Khan, S. N. (2023). Spatial downscaling of GRACE data based on XGBoost model for improved understanding of hydrological droughts in the Indus Basin Irrigation System (IBIS). Rem," 2023.

[20] Chen et al., "Chen, L., He, Q., Liu, K., Li, J., & Jing, C. (2019). Downscaling of GRACE-derived groundwater storage based on the random forest model. Remote Sensing, 11(24), 2979.," 2019.

[21] You et al., "You, Y., Ting, M., & Biasutti, M. (2024). Climate warming contributes to the record-shattering 2022 Pakistan rainfall. npj Climate and Atmospheric Science, 7(1), 89.," 2022.

[22] Latif et al., "Latif, M., Shireen, H., Adnan, S., Ahmed, R., & Hannachi, A. (2024). Drought variability in Pakistan: Navigating historical patterns in a changing climate with global teleconnections. Theoretical and Applied Climatology, 155(8), 8379-8400.," 2024.

[23] Masood et al., "Masood, M. U., Haider, S., Rashid, M., Lodhi, M. U. K., Pande, C. B., Alshehri, F., ... & Sammen, S. S. (2023). The Effect of the El Nino Southern Oscillation on Precipitation Extremes in the Hindu Kush Mountains Range. Water, 15(24), 4311.," 2023.

[24] Ali et al., "Ali, M., Ali, U., & Gillani, S. H. FLASH DROUGHT DETECTION AND RISK EXPOSURE IN PAKISTAN: A MACHINE LEARNING APPROACH WITH MULTIVARIATE INDICES.," 2024.

[25] Modi et al., "29. Modi, P., Hanasaki, N., Yamazaki, D. et al. 2022 Sensitivity of subregional distribution of socioeconomic conditions to the global assessment of water scarcity. Commun Earth Environ 3, 144. https://doi.org/10.1038/s43247-022-00475-w," 2022.

[26] Munir et al., "Munir, M. U., Ahmad, A., Hopmans, J. W., Belgacem, A. O., & Baig, M. B. (2021). Water scarcity threats to National Food Security of Pakistan—Issues, implications, and way forward. Emerging challenges to food production and security in asia, Middle East, a," 2021.

MECHANICAL AND MICROSTRUCTURAL ENHANCEMENT OF EXPANSIVE SOILS VIA SUSTAINABLE WASTE GLASS POWDER AND FLY ASH BLENDS

[a] Muhammad Usama*, [b] Ubaid Ullah, [c] Muhammad Rauf

a: Department of Geodesy and Geoinformatics, Hamburg, Germany. ukhattak999@gmail.com
b: Department of civil Engineering, University of Wah, Wah Cantt, 47040, Pakistan. ubaidkhattak999@gmail.com
c: Department of civil Engineering, University of Wah, Wah Cantt, 47040, Pakistan. engr.roufktk@gmail.com
*Corresponding author

Abstract- Expansive soils, particularly high-plasticity clays, pose significant challenges for construction due to their low shear strength, poor compaction, and shrink-swell behavior. `. Conventional stabilizing methods, such as those using lime or cement, are often associated with high costs and significant environmental impacts. This study investigates the use of two industrial byproducts, waste glass powder (WGP) and fly ash (FA),as sustainable stabilizers for expansive soils. Laboratory tests were conducted using varying contents of WGP (5–30%) and FA (5–17%) to assess improvements in compaction, strength, plasticity, and swell potential. The optimal blend of 25% WGP and 11% FA yielded significant enhancements: UCS increased by 178% to 401.29 kPa, plasticity index reduced by 69% to 11.13%, swell potential dropped by 76% to 6%, and dry density increased to 1.92 g/cm³. Shear strength improvements were also observed, with the angle of internal friction rising by 103% to 35.94° and cohesion reduced to 9 kPa. SEM and XRD analyses confirmed the formation of dense cementitious compounds, validating the microstructural improvement. These findings indicate that WGP and FA provide a sustainable and cost-effective alternative for stabilizing expansive soils in civil engineering applications.

Keywords- Soil Stabilization, Waste Glass Powder, Fly Ash, Expansive Soils, High-Plasticity Clays, Sustainability

1 Introduction

Expansive soils, known for their shrink-swell behaviour, pose substantial challenges in construction due to their low shear strength, poor compaction characteristics, and significant volumetric changes in response to moisture fluctuations [1], [2] Such soils are prevalent in various regions globally, especially in high-plasticity clays, making them unsuitable for engineering projects without proper treatment. With the ongoing rise in urbanization, the use of expansive soils in construction has become unavoidable, which drives the need for sustainable and efficient soil stabilization methods. High-plasticity clay and other expansive soils are often inappropriate for construction purposes, as they result in failure of the structure in terms of settlement, etc [3], [4] Therefore, construction on such types of soil cannot be ignored due to the increasing population and demand for land. So, an effort has been made to provide a feasible and economical approach via the use of waste products as soil stabilizers [5], [6]. Many wastes are discharged each year due to the absence of factories that can reuse waste materials, presenting severe environmental pollution. As a result, using these waste products to improve the geotechnical qualities of soils can provide realistic and cost-effective solutions for such a worst soil . The conventional techniques of soil stabilization may include the utilization of cement, lime, etc., which may cause environmental degradation [7][8].

WGP and FA's cooperative action on soil stability has attracted interest in its combined application. Combining the two pozzolanic materials with the clay minerals in expansive soils results in cementitious compounds that lower

swelling potential and fluidity and boost strength. Combining WGP with FA significantly reduces the swell potential of expansive soils while concurrently boosting the UCS and shear strength, claims research by Hawkar et al. and Ibrahim et al [9] [10]. While the appropriate ratio depends on the kind of soil and environmental conditions, WGP content up to 25% and FA content up to 20% generally show the best results in terms of strength increase and expansibility reduction.

Techniques like scanning the microstructural alterations has been made easier by X-ray diffraction (XRD) and scanning electron microscopy (SEM) in soils treated with WGP and FA [11], [12] .XRD investigations indicate that pozzolanic compounds such C-S-H are produced when WGP reacts with clay minerals, therefore reducing soil expansivity and increasing soil strength [13]. Further verifying the densification of soil samples after treatment are SEM images, which show a more coherent and stable microstructure. These microstructure changes produce better compaction and lower porosity, two improved mechanical properties of the stabilized soils that come from which soil stability is raised [14], [15].

Local stakeholders' settlement issues led to the sample for this study being taken from an Islamabad, Pakistan's developing sector B-17 site. The soil was investigated (of site as shown in Figure 1 in the lab in order to assess certain properties. Tests conducted on both untreated and treated samples included swell potential, Compaction characteristics; unconfined compressive strength; direct shear testing; The limits of Atterberg (also known as the plastic limit (PL), liquid limit (LL), and index of plasticity (PI). The soil and additives (fly ash and waste glass powder) were also subjected to X-ray diffraction (XRD) and SEM (scanning electron microscopy) was employed to evaluate the microscopic characteristics of the two treated and untreated specimens. The initiative aims to maximize fly ash and residual glass powder use in order to improve soil properties.



Figure 1:(a,b) Jacks are used to prevent settling in both freshly built and older homes, as well as fissures caused by expansive soils' volume change behaviour .

2 Research Methodology

2.1 Materials

The high-plasticity clay (CH classification) was sourced from Islamabad, Pakistan, exhibiting a liquid limit of 51.36% and plasticity index of 26.36%. Waste glass powder (WGP) was obtained from Gunj Glassworks (63.99% SiO_2, angular particles), while fly ash (FA) was procured from Fecto Cement Factory (37.81% SiO_2, spherical particles).Figure 2 shows the physical samples of soil, WGP, and FA. Key properties of untreated soil are summarized in Table 1.



Figure 2:Samples of Fly Ash, WGP, and Soil

2.2 Methodology

The experimental program comprised three phases. Phase I involved characterizing untreated soil and additives through sieve analysis, Atterberg limits, compaction tests, UCS, and shear testing (Figure 5a–c). Phase II optimized WGP content (5–30%), while Phase III evaluated synergistic effects by blending optimal WGP (25%) with varying FA (5–17%). Advanced microstructural analysis using XRD, and SEM elucidated stabilization mechanisms. Sieve analysis per ASTM D6913 confirmed the untreated soil's composition (73% clay, 17.8% silt, 9.2% sand), while WGP (90% <0.075 mm) and FA (85% <0.045 mm) exhibited finer gradations, enabling optimal void filling and pozzolanic reactivity for soil stabilization.

3 Results and Discussion

3.1 Phase I: Soil and Additive Characterization

Phase I characterization of untreated soil revealed a high-plasticity clay (CH classification) with liquid limit=51.36%, plasticity index=26.36%, free swell index=25.5%, and specific gravity=2.73; compaction tests showed maximum dry density=1.60 g/cm³ at 19.64% optimum moisture content, while unconfined compressive strength increased from 77.42 kPa (1 day) to 144.25 kPa (28 days), and direct shear testing measured cohesion=22.14 kPa with friction angle=17.74° as shown in Table 1. These results demonstrate the soil's highly expansive nature, low inherent strength, and poor engineering properties – confirming significant susceptibility to moisture-induced volume changes, structural settlement, and shear failure, which necessitates stabilization for construction applications.

3.2 Phase II. Optimization of Waste Glass Powder (WGP)

In Phase II, the soil is treated with Waste Glass Powder (WGP) by varying its percentages to optimize the treatment. The percentages used for WGP were 5%, 10%, 15%, 20%, 25%, and 30%. The effects of these varying percentages were assessed using several tests to determine the optimal level of WGP for improving soil properties as shown in Table 2 .plasticity index decreased by 51% (to 12.81%), maximum dry density increased by 15% (to 1.84 g/cm³), unconfined compressive strength (UCS) surged 166% (to 383.7 kPa at 28 days), and friction angle improved to 26.34°—though cohesion decreased by 33% (to 14.77 kPa) due to WGP's non-cohesive nature; however, exceeding 25% (up to 30% WGP) caused UCS to decline by 23% (to 294.28 kPa) and maximum dry density to reduce to 1.80 g/cm³, while swell potential reduction plateaued and friction angle marginally increased to 27.02°, indicating diminished returns due to insufficient pozzolanic binder-clay interaction and disrupted moisture distribution from excessive granular filler. This threshold behaviour confirms WGP's dual role: optimal at 25% for densification and strength gain through void-filling and pozzolanic reactions, but counterproductive beyond due to particle segregation, reduced cohesion, and inhibited cementitious gel formation.

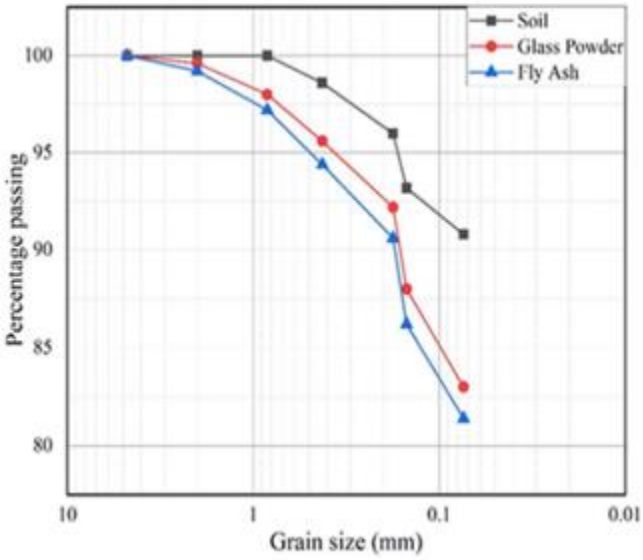


Figure 3:Grain size distribution of untreated soil, WGP, and FA

Table 1:Expanding soil characteristics and the corresponding ASTM standards

Properties of Expansive Soil	Values	Standards
Sieve Analysis	90.80%(Totally Fine i.e silt + clay)	ASTM D7928
Specific gravity of soil	2.74	ASTM D854
Liquid limit	51.36%	ASTM D4318
Plastic Limit	25%	ASTM D4318
Plasticity Index	26.36%	ASTM D4318
Sand	9.20%	ASTM D6913
Silt	17.80%	ASTM D6913
Clay	73%	ASTM D6913
Modified Free swell Index	25.5%,	ASTM D5890-19
USCS Classification	CH	ASTM D2487
Maximum Dry Density	1.60 g/cc	ASTM D698
Optimum Moisture Content	19.64%	ASTM D698
UCS1d (untreated)	77.42 kPa	ASTM D2166
UCS3d	92.8 kPa	ASTM D2166
UCS7d	102.94 kPa	ASTM D2166
UCS14d	132.27 kPa	ASTM D2166
UCS28d	144.25 kPa	ASTM D2166
Cohesion	22.14 kPa	ASTM D2166
Angle of Internal Friction	17.74°	ASTM D6528

Table 2:Summary of phase II Optimization of WGP

Percentage of WGP	Unit	5%	10%	15%	20%	25%	30%
Specific Gravity		2.36	2.32	2.26	2.25	2.23	2.18
Swell Potential		21	19	17	16	14	13
LL(%)	(%)	44.8	40.76	37.23	33.17	27.31	20.145
PL(%)	(%)	22	18	17	16	15	10
PI(%)	(%)	22.8	22.26	22.23	17.17	12.81	9.64
OMC(%)	(%)	19.5	18.6	17	15.66	13	11.6
MDD(%)	(%)	1.71	1.73	1.78	1.79	1.84	1.8
UCS 1st day	(kPa)	87.05	98.67	106.3	112.36	117.6503	108.69
UCS 3rd day	(kPa)	100.74	138.76	156.4	163.65	170.9125	161.26
UCS 7th day	(kPa)	108.28	147.13	167	180.7	190.3344	168.53
UCS 14th day	(kPa)	144.65	148.93	190.9	233.07	287.6731	245.04
UCS 28th day	(kPa)	283.26	328.8	341	360.58	383.7021	294.28
Cohesion	(kPa)	22.93	20	19.1	17.83	14.77	10.91
Angle of Internal Friction	(Degree)	19.29	21.32	23.26	26.01	26.34	27.02

3.3 Phase III

Combining the optimal 25% waste glass powder (WGP) with fly ash (FA) further enhanced soil stabilization, peaking at **11% FA as shown in** Table 3: unconfined compressive strength (UCS) reached 401.29 kPa (178% higher than untreated soil), maximum dry density increased to 1.92 g/cm³, and swell potential dropped to a minimal 6%. Plasticity index reduced to 11.13%, while shear strength shifted toward frictional resistance (friction angle: 35.94°) with reduced cohesion (9 kPa). Beyond 11% FA (e.g., 17% FA), UCS declined by 16% (to 336.72 kPa), density decreased slightly (1.89 g/cm³), and cohesion further diminished (8 kPa), though friction angle rose to 41°. This synergy stems from FA's ultra-fine particles (<0.045 mm) filling micropores and amplifying pozzolanic reactions with WGP's silica, forming dense calcium silicate hydrate gels that strengthen the soil matrix—but excessive FA dilutes reactive surfaces, weakening binding efficiency. The 25% WGP + 11% FA blend thus represents the ideal equilibrium for maximizing strength, density, and swell control.Hence, with 25% WGP + 11% FA, the soil transitions from CH (high-plasticity clay) to CL (low-plasticity clay) per ASTM D2487, with LL=24.3% (<50%) and PI=11.13% (above A-line: PI=0.73×(LL-20)=3.14%). This confirms the reduction in expansivity and validates the efficacy of stabilization using a standardized classification

3.4 XRD Analysis of Clay, Waste Glass Powder, and Fly Ash

X-ray diffraction (XRD) analysis elucidated the mineralogical foundations of stabilization efficacy, revealing that the untreated expansive soil contained quartz, kaolinite, illite, and highly expansive montmorillonite as show in Figure 4,the latter explaining its pronounced shrink-swell behaviour. Waste glass powder (WGP) exhibited a dominant quartz crystalline structure, while fly ash (FA) featured complex crystalline phases including mullite, hematite, goethite, anorthite,

and magnesium hydroxide. Critically, after blending 25% WGP and 11% FA with the soil, XRD detected calcium silicate hydrate (C-S-H) formation—a key pozzolanic reaction product alongside reduced montmorillonite peak intensity.

Table 3:Summary of Phase III: Synergistic Effect of WGP and Fly Ash (FA)

FA WGP	Unit	5% 25%	8% 25%	11% 25%	14% 25%	17% 25%
Specific Gravity		2.33	2.28	2.22	2.2	2
Free Swell Index		18	15	13	9	6
LL	(%)	26.46	25.04	24.3	22.46	19.56
PL(%)	(%)	14.67	13.7	13.17	11.5	9.83
PI(%)	(%)	11.79	11.34	11.13	10.96	9.73
OMC(%)	(%)	13.33	12.66	11.66	11	10.33
MDD(%)	(%)	1.86	1.88	1.92	1.91	1.89
UCS (kPa) 1st day	(kPa)	117.33	142.43	166.97	154.38	125.49
UCS (kPa) 3rd day	(kPa)	161.26	192.73	218.92	199.73	178.68
UCS (kPa) 7th day	(kPa)	198.37	232.32	272.97	225.29	190.33
UCS (kPa) 14th day	(kPa)	229.63	285.38	329.22	291.34	265.5
UCS (kPa) 28 day	(kPa)	232.12	310.45	401.29	366.35	336.72
Cohesion(kpa)	(kPa)	12.48	9.42	9	8.7	8
Angle of Internal Friction	(Degree)	32.3	34.13	35.94	37	41

This mineralogical evolution confirms WGP's quartz-enhanced particle interlocking and shear resistance, while FA's mullite and hematite reinforced mechanical strength, collectively transforming the soil into a stabilized matrix with diminished expansivity and heightened durability.

3.5 The Effect of Clay Content, FA, and WGP on Microstructural Behaviour (SEM)

Scanning electron microscopy (SEM) revealed transformative microstructural changes induced by WGP and FA treatment. Untreated soil exhibited a loose, porous matrix with visible voids and minimal particle bonding (Figure 5a), explaining its low strength and high swell potential. With 25% WGP addition (Figure 5b), pozzolanic reactions generated dense, gel-like structures that entrapped glass particles, reducing porosity and forming incipient cementitious bonds. The synergistic 25% WGP + 11% FA blend (Figure 5c–d) produced a radically densified microstructure where fly ash's spherical particles embedded uniformly within cementitious gels, transforming flaky clay into cohesive, blocky aggregates. Notably, FA's spherical morphology complemented WGP's angular particles, enhancing interlocking and creating a continuous binding framework that minimized voids. This microstructural evolution directly correlated with macro-scale improvements: the homogeneous, cemented matrix increased unconfined compressive strength by 178% and reduced swell potential by 76%, confirming that WGP-FA synergy effectively restructures expansive clays into stable, load-bearing materials.Both WGP and FA are pozzolanic materials, meaning they contain high amounts of amorphous silica (SiO_2) and alumina (Al_2O_3). While they are not cementitious on their own, they react chemically with calcium hydroxide ($Ca(OH)_2$)—either naturally present in clay or added externally (from lime or portlandite in soil minerals)—in the presence of moisture to form cementitious compounds.

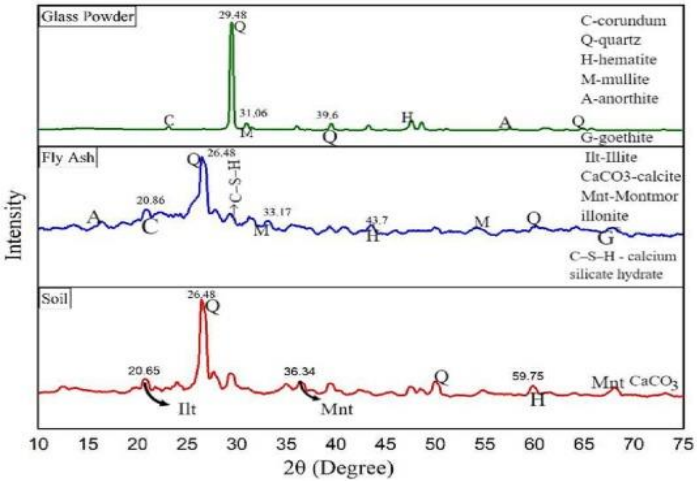


Figure 4:XRD of Clay, WGP, and FA

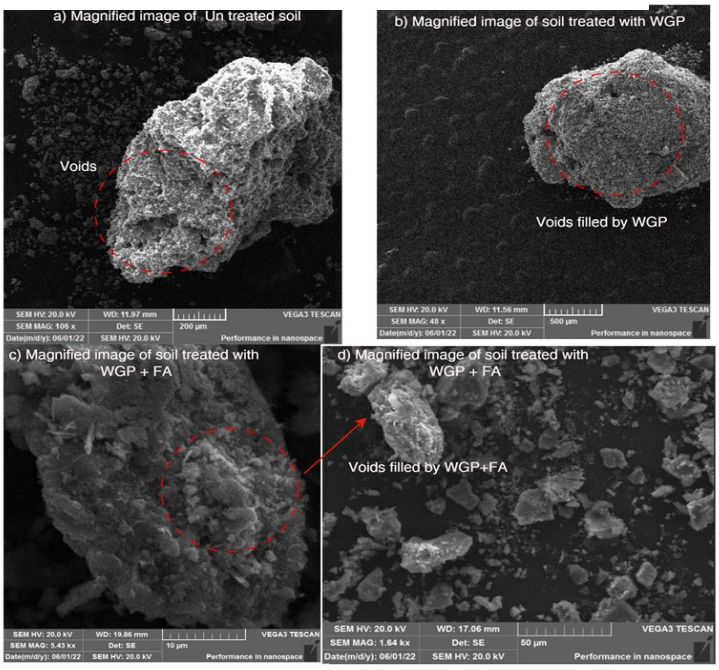


Figure 5:Untreated expansive soil (a), WGP-treated soil (b), and WGP and FA-treated soil (c,d) were all subjected to SEM examination.

4 Practical Implementation

This stabilization method can be effectively applied in road construction and foundation work by blending 25% waste glass powder (WGP) and 11% fly ash (FA) with expansive soils. Using standard mixing equipment and compacting the mixture at approximately 11.7% moisture content achieves the target dry density of 1.92 g/cm³. The materials, sourced from local glass recycling facilities and power plants, reduce material costs by 30–40% compared to traditional cement stabilization, while diverting over 36 tons of waste per kilometer of road. Field validation conducted in Pakistan's Potohar region demonstrated a 35% cost reduction and eliminated seasonal maintenance caused by swelling-related cracking, confirming the method's viability for infrastructure projects in expansive clay regions. For shallow, high-plasticity soil layers (less than 1 meter), soil removal or basement construction may be more cost-effective than stabilization. However,

for deeper deposits, such as at the B-17 site, with an expansive layer depth of 2.5 meters, stabilization using 25% WGP and 11% FA reduces costs by 35–40% compared to cement-based methods and eliminates the need for long-term maintenance. A preliminary cost-benefit analysis further confirmed savings of approximately 30% compared to removal and replacement strategies for road sections with expansive strata exceeding 1 meter in depth.

Conclusion

- The optimal mix of 25% Waste Glass Powder (WGP) and 11% Fly Ash (FA) increased Unconfined Compressive Strength (UCS) by 178%, reaching 401.29 kPa, and reduced swell potential by 76%, down to 6%.
- The Plasticity Index was reduced by 69%, from 26.36% to 11.13%, improving soil workability and reducing volumetric instability.
- The maximum dry density improved from 1.60 g/cm³ to 1.92 g/cm³, while optimum moisture content decreased from 19.64% to 11.66%, enhancing compaction efficiency.
- Shear strength behavior shifted from cohesive to frictional dominance, with the angle of internal friction increasing from 17.74° to 35.94°, and cohesion decreasing to 9 kPa.
- Microstructural (SEM/XRD) analysis confirmed the formation of dense C-S-H gels, validating the strength and stability improvements achieved through the WGP–FA stabilization.

References

[1] D. Barman and S. K. Dash, "Stabilization of expansive soils using chemical additives: A review," *J. Rock Mech. Geotech. Eng.*, vol. 14, no. 4, pp. 1319–1342, 2022.
[2] A. H. Alsabhan and W. Hamid, "Innovative thermal stabilization methods for expansive soils: mechanisms, applications, and sustainable solutions," *Processes*, vol. 13, no. 3, p. 775, 2025.
[3] S. J. Abbey, E. U. Eyo, and S. Ng'ambi, "Swell and microstructural characteristics of high-plasticity clay blended with cement," *Bull. Eng. Geol. Environ.*, vol. 79, no. 4, pp. 2119–2130, 2020.
[4] M. Usama *et al.*, "Predictive modelling of compression strength of waste GP/FA blended expansive soils using multi-expression programming," *Constr. Build. Mater.*, vol. 392, p. 131956, 2023.
[5] S. Fateh, Y. Mansourkiaei, M. M. Shalchian, M. Arabani, M. Payan, and P. Z. Ranjbar, "A comparison of temperature and freeze-thaw effects on high-swelling and low-swelling soils stabilized with xanthan gum," *Results Eng.*, vol. 25, p. 103719, 2025.
[6] H. R. Manaviparast, N. Cristelo, E. Pereira, and T. Miranda, "A Comprehensive Review on Clay Soil Stabilization Using Rice Husk Ash and Lime Sludge.," *Appl. Sci.*, vol. 15, no. 5, 2025.
[7] H. Afrin, "A review on different types soil stabilization techniques," *Int. J. Transp. Eng. Technol.*, vol. 3, no. 2, pp. 19–24, 2017.
[8] H. Gardezi *et al.*, "Predictive modeling of rutting depth in modified asphalt mixes using gene-expression programming (GEP): A sustainable use of RAP, fly ash, and plastic waste," *Constr. Build. Mater.*, vol. 443, p. 137809, 2024.
[9] H. Ibrahim and C. Q. Hassan, "Post-traumatic stress disorder symptoms resulting from torture and other traumatic events among Syrian Kurdish refugees in Kurdistan Region, Iraq," *Front. Psychol.*, vol. 8, p. 241, 2017.
[10] S. Narendra and V. Vasugi, "Development of sintered artificial coarse aggregate by employing the Taguchi optimization technique," *Case Stud. Constr. Mater.*, p. e04724, 2025.
[11] Y. Ordoñez Muñoz, A. J. E. Villota-Mora, F. Perretto, and R. L. dos Santos Izzo, "Eco-friendly stabilization of clayey soil with waste glass powder-based geopolymer," *Geomech. Geoengin.*, vol. 20, no. 3, pp. 557–586, 2025.
[12] A. Minhajuddin and A. Saha, "Performance evaluation of geopolymer concrete with waste granite powder as a sustainable alternative to sand," *J. Mater. Sci. Mater. Eng.*, vol. 20, no. 1, p. 20, 2025.
[13] A. U. Ndaiji, M. Abdullahi, B. A. Abbas, and M. Abubakar, "EFFECTS OF WASTE GLASS POWDER AND CASSAVA PEEL ASH ON COMPRESSIVE STRENGTH OF CONCRETE," Proceeding of the 3rd International Civil Engineering Conference (ICEC 2024), 2025.
[14] Y. Hong, X. Xu, C. Zhang, Z. Cheng, and G. Yang, "Microscopic Mechanism and Reagent Activation of Waste Glass Powder for Solidifying Soil," *Buildings*, vol. 14, no. 5, p. 1443, 2024.
[15] P. Manikandan, V. P. Kumar, and V. Vasugi, "Strength and microstructural characteristics of sustainable aluminosilicate binder using waste glass powder and ground granulated blast furnace slag," *Innov. Infrastruct. Solut.*, vol. 10, no. 3, p. 105, 2025.

FINITE ELEMENT STUDY ON THE ROLE OF SAND RELATIVE DENSITY ON LATERAL LOAD DISTRIBUTION IN PILED RAFT SYSTEMS

[a] Hamad Khan*, [b]Qazi Khurshid Ahmad, [c]Abdullah Khan Jadoon

a: Department of Civil Engineering, UET Peshawar. 20pwciv5445@uetpeshawar.edu.pk
b: Department of Civil Engineering, GIK Institute of Engineering Sciences and Technology, Swabi. gcv2445@giki.edu.pk
c: Department of Civil Engineering, UET Peshawar. 20jzciv0405@uetpeshawar.edu.pk
* Corresponding author

Abstract- Combined Pile Raft Foundation (CPRF) has emerged as a widely adopted foundation system, particularly suitable for high-rise structures and sites with weak subsoil conditions. Previous research has extensively examined the influence of parameters such as pile spacing-to-diameter ratio, raft dimensions, and pile configurations on the load-sharing behavior of CPRF. However, the effect of relative density of sand on the lateral load contribution of piles and raft remains underexplored. This study presents a numerical investigation using small-scale CPRF models in *PLAXIS 3D*, a finite element software known for its capability in simulating soil–structure interaction. Relative density was modeled indirectly by varying the modulus of elasticity (E) and the internal friction angle (ϕ) of sand. The findings indicate that the raft's contribution to lateral load resistance increases with higher relative density, while the pile's share in lateral resistance decreases. Furthermore, both vertical settlement and horizontal displacement were observed to reduce as relative density increased. Specifically, settlement decreased by 71% (from 0.62 mm to 0.18 mm), and horizontal displacement reduced by 50% (0.40 mm to 0.2 mm). The shift in lateral load resistance from front piles to back piles was attributed to increased stiffness in the soil surrounding the rear piles. Understanding the role of relative density in CPRF systems can contribute significantly to their optimized and cost-effective design, reinforcing their potential as a sustainable foundation solution in geotechnical engineering.

Keywords- CPRF, Plaxis-3D, Finite Element Modelling (FEM), Relative Density

1 Introduction

During earthquakes, both vertical and lateral loads act simultaneously on pile raft foundations. CPRFs are advanced geotechnical systems that combine piles and a raft to collectively support structural loads. This system is particularly beneficial for high-rise buildings and sites with weak or compressible soils, where traditional foundations may fall short in terms of bearing capacity and serviceability [2], [5]. The interaction between the raft and piles allows for an effective redistribution of loads, leading to reduced settlement and enhanced lateral load resistance [1], [6], [8]. Extensive research, both experimental and numerical, has been conducted to assess the behavior of CPRF under different loading and soil conditions. For example, studies have shown that vertical loading can improve lateral load resistance; however, excessive vertical loads may destabilize the system [4]. Investigations using small-scale physical models [6], [8] and finite element simulations [2], [4], [7] have highlighted the role of pile spacing, pile configuration, raft geometry, and pile length in optimizing CPRF performance under lateral and vertical loading conditions. Seismic performance has also been explored, with findings indicating that pile group arrangement and load combinations significantly affect the system's response during dynamic events [4]. Moreover, soil parameters such as the modulus of elasticity (E), internal friction angle (ϕ), and Poisson's ratio (ν) have been shown to influence the interaction between the pile, raft, and surrounding soil, affecting

overall foundation behaviour [7], [3]. Recent studies have compared the behavior of connected and disconnected pile raft systems and demonstrated that strategic pile placement can reduce total and differential settlement, while disconnection may help mitigate differential displacements [10]. Theoretical models developed by earlier researchers emphasized the importance of stiffness interaction and load-sharing mechanisms within CPRF systems, under both service and ultimate load conditions [9]. However, despite these advances, the effect of relative density (D_r) of sand—a key indicator of soil compactness on the lateral load distribution between the raft and piles in CPRF remains inadequately studied. D_r plays a critical role in defining the mechanical behaviour of sandy soils and thus significantly affects CPRF performance. As noted by Walter et al. [13]. A better understanding of how D_r affects the lateral load transfer in CPRF is essential for the safe and cost-effective design of foundations in sandy soils.

Additionally, lateral loading on piles induces complex soil-structure interaction phenomena such as gapping behind piles and non-uniform stress distribution along the pile shaft [8]. Though the actual relationship is nonlinear, a simplified linear approach using the modulus of subgrade reaction is often adopted in design practice [12]. This research aims to fill the existing gap by numerically evaluating how variations in the relative density of sand influence the lateral load behavior of CPRF using PLAXIS 3D. By altering sand stiffness and strength parameters to simulate different relative densities, this study contributes to a deeper understanding of CPRF behavior and offers guidance for more optimized, reliable, and sustainable foundation designs in sandy soils.

2 Research Methodology

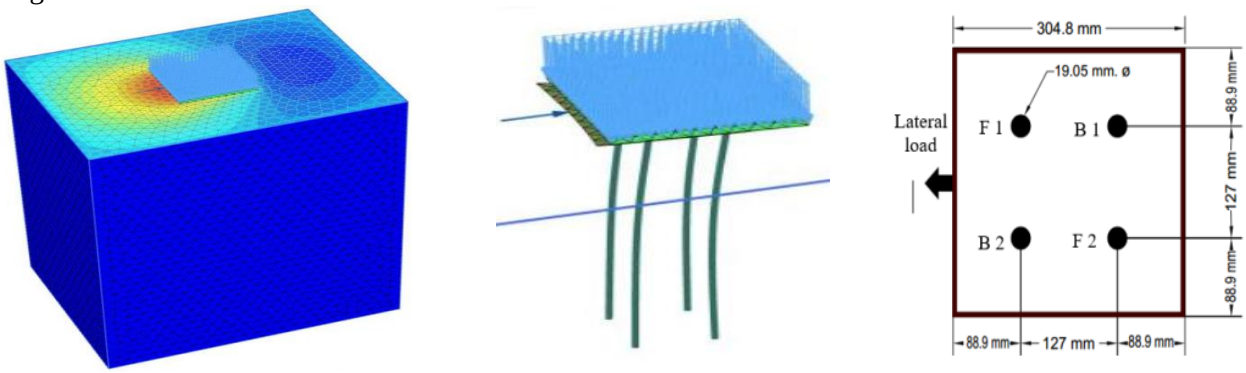
2.1 Finite Element Modelling (FEM) in Plaxis3D

CPRF with four number of piles are modelled in Plaxis3D under combined vertical and horizontal loading. Properties of soil, raft, piles, outer soil box and loading are same as that of experimental and numerical study conducted by [3] and [8] respectively. In Plaxis3D, relative density is varied by varying the value of soil stiffness (E) and phi (ϕ). Correlation between E and phi is taken from the study conducted by[3], shown in Table 1. Hardening Soil Model is used in Plaxis-3D.

Table 1 Correlation of elastic modulus with friction angle [3]

Model	Elastic Modulus E(Mpa)	Friction angle (phi(ϕ)
1	15	22
2	20	27
3	25	32
4	30	37
5	35	42

Figure 1a shows the complete finite element model of CPRF under vertical and lateral loading. Figure1b, depicts the 4-pile raft system showing piles raft under combined loading and figure 1c shows the 4-pile raft configuration.



a. *FEM of CPRF* ***b.*** *Piles and Raft under combined loading* ***c.*** *4-Pile Raft Configuration*

Figure 1 *Finite Element CPRF model in Plaxis3D*

3 Results

3.1 Effect of Relative density on lateral contribution in CPRF

By increasing the relative density of sand in CPRF, three outcomes arrive, firstly, by increasing the relative density enhances raft contribution (from 14.89% to 40.03%) and reduces pile contribution (from 85.10% to 59.96%) due to increased vertical contact pressure beneath the raft, both settlements and horizontal displacement decreased by 71% (from 0.62 mm to 0.18 mm) and 50% (0.40 mm to 0.2 mm) respectively. As the sand becomes denser(stiffer), the lateral load response gradually shifts from the front piles (from 293.85 N to 203.85 N) to back piles(from 92.25 N to 71.82 N) slowly and gradually, due to the increased stiffness of the soil in front of the back piles.

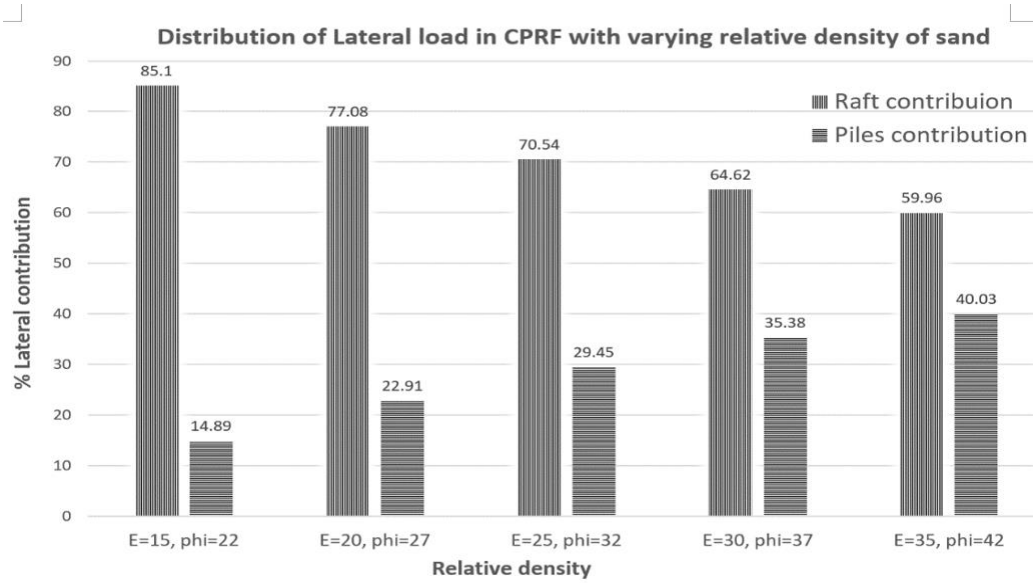


***Figure** 2 Effect of relative density on lateral load distribution in piles and Raft*

Figure 2 presents the effect of relative density of soil on Piles and raft contribution while Table 2 presents the effect on relative density on front and back piles.

Table 2 Effect of relative density on lateral load distribution in front and back piles

Parameters		Front Piles contribution (N)	Back Piles contribution (N)
E(Mpa)	Phi ϕ(degree)		
15	22	293.85	92.25
20	27	279.45	67.86
25	32	249.3	69.93
30	37	225.9	70.29
35	42	203.85	71.82

3.2 Use of Software

Plaxis-3d a finite element software is used in modelling of CPRF.

4 Practical Implementation

In real design, by considering the effect of relative density on lateral contribution of raft and piles, design of CPRF will be economical without the overestimation of shear forces, bending moments and displacements.

5 Conclusion

The following conclusions can be drawn from the conducted study:

1 Raft contribution in response of lateral load is directly proportional to relative density of sand. Greater the relative density of soil, greater will the lateral load response raft and vice versa.
2 By increasing the relative density i.e., stiffness of sand from 15 to 35Mpa, raft lateral contribution was increased from 14.89% to 40.03% and Piles contribution on the other hand, decreased from 85.10 %to 59.96% by increasing the relative density of sand.

At smaller relative density, front piles take more lateral load, as the soil get denser, lateral load contribution shifted from front to back piles gradually, (from 293.85 N to 203.85 N) in front piles and (from 92.25 N to 71.82 N) back piles due to increase in stiffness of soil. As the relative density increases, both settlement and horizontal displacement in piles and raft by 71% (from 0.62 mm to 0.18 mm) and 50% (0.40 mm to 0.2 mm) respectively.

References

[1] Al-Mosawi, Mosa J., Mohammed Y. Fattah, and Abbas A. O. Al-Zayadi. 2011. "EXPERIMENTAL OBSERVATIONS ON THE BEHAVIOR OF A PILED RAFT FOUNDATION." Journal of Engineering 17(04):807–28. doi: 10.31026/j.eng.2011.04.13.
[2] Bandyopadhyay, Srijit, Aniruddha Sengupta, and Yogita Parulekar. 2020. "Behavior of a Combined Piled Raft Foundation in a Multi-Layered Soil Subjected to Vertical Loading." Geomechanics and Engineering 21:379–90. doi: 10.12989/gae.2020.21.4.379.
[3] Khitrov, E. G., et al. "Interrelations of various soil types mechanical properties." Journal of Physics: Conference Series. Vol. 1177. No. 1. IOP Publishing, 2019.
[4] Deb, Plaban, and Sujit Kumar Pal. 2021. "Nonlinear Analysis of Lateral Load Sharing Response of Piled Raft Subjected to Combined V-L Loading." Marine Georesources & Geotechnology 39(8):994–1014. doi: 10.1080/1064119X.2020.1766607.
[5] Hussien, Mahmoud N., Ebraheem H. Ramadan, Mohamed H. Hussein, AbdelAziz A. A. Senoon, and Mourad Karray. 2017. "Load Sharing Ratio of Pile-Raft System in Loose Sand: An Experimental Investigation." International Journal of Geotechnical Engineering 11(5):524–29. doi: 10.1080/19386362.2016.1236224.
[6] Jamil, Irfan, Irshad Ahmad, Irshad Khan, Wali Ullah, Aqeel Ur Rehman, and Shahid Ali Khan. 2023. "Factors Affecting the Lateral Contribution of a Raft in a Piled Raft System." Ain Shams Engineering Journal 14(5):101968. doi: 10.1016/j.asej.2022.101968.
[7] Jamil, Irfan, Irshad Ahmad, Muhammad Shoaib Khan, Shahid Ali Khan, and Alam Khan. 2022. "A Parametric Study on the Interaction Factors of Pile-Raft System." Journal of Himalayan Earth Sciences Volume 55:14–24.
[8] Jamil, Irfan, Irshad Ahmad, Wali Ullah, Mahmood Ahmad, Mohanad Muayad Sabri Sabri, and Ali Majdi. 2022. "Experimental Study on Lateral and Vertical Capacity of Piled Raft and Pile Group System in Sandy Soil." Applied Sciences 12(17):8853. doi: 10.3390/app12178853.
[9] Katzenbach, R., and J. Turek. 2005. "Combined Pile-Raft Foundation Subjected to Lateral Loads." Pp. 2001–4 in Proceedings of the 16th International Conference on Soil Mechanics and Geotechnical Engineering. IOS Press.
[10] Saady, Semaa Z. Al, and Mahdi Karkush. 2024. "Comparison Review between Behavior of Connected and Disconnected Pile Raft Foundation." in AIP Conference Proceedings. Vol. 2864. AIP Publishing.
[13] Walter, John E., William H. Highter, and Robert P. Vallee. 1982. "Determining Maximum Void Ratio of Uniform Cohesionless Soils." Transportation Research Record (897).
[11] Yenginar, Y., and M. Olgun. 2019. "Designing Piled Raft Foundations Using Simplified Analysis Methods." Eurasian Journal of Civil Engineering and Architecture 1(1):13–24.
[12] Khan, Hamad, et al. "Effect of Vertical Contact Pressure on the Lateral response of Combined Piled Raft Foundation: A Numerical Study." Journal of Himalayan Earth Sciences 58.1 (2025): 60-73.

NUMERICAL ANALYSIS OF LATERALLY LOADED PILES IN FINE GRAINED SOIL

[a] Ahsan Raza Khan*, [b] Abdulllah Khalid

a: Department of Civil Engineering, The University of Lahore. hafizark227@gmail.com
b: Department of Civil Engineering, The University of Lahore. Abdullahkhalid7012@gmail.com
* Corresponding author

Abstract- Pakistan is located at the intersection of two plates i.e. Indian and Eurasian plates, had faced various devastated earthquakes in the past. After the catastrophic earthquake of 2005, a group of researchers, academician and practice engineers proposed revision in seismic provision and published Building Code of Pakistan (BCP) in 2021. BCP 2021 provides generic guidelines related to soil dynamics, however, doesn't address the soil-pile dynamic interaction explicitly. In this study, an effort is made to examine the behavior of laterally loaded large diameter piles constructed in Islamabad using numerical method, a framework proposed in already published research studies. Two numerical methods were employed and dynamic characteristics of pile is examined. The result indicated higher displacement at the top and at natural frequency of the pile. Similar trends were noticed for bending moment and shear force variation.

Keywords- Bending Moment, Winkler Model, Finite Element Method, Shear Force, Stiffness

1 Introduction

Pile foundation is characterized as deep foundation is considered appropriate foundation type in the areas having problematic soil. Also in the presence of lateral load, the capacity of shallow foundation may became inadequate to provide resistance leading to adoption of piles as best choice of foundation. Although fundamental function of the pile is to provide resistance to axial loading in the form of skin resistance and end bearing, however, they withstand significant lateral loading coming from earthquakes, wind loading, wave action etc. during their design life. Therefore, a comprehensive understanding of the dynamic response of piles becomes vital for safe design. The design of piles subjected to lateral loading is challenging due to several factors including reliable estimation of soil dynamic properties, precision in numerical modeling, data analysis and interpretation. Ignoring underestimation or inaccuracy in the aforementioned factors may lead to catastrophic results.

Based on the published literature, numerical methods for lateral load analysis can be classified into three groups including (i) Winkler model; (ii) Closed form solutions and (iii) Finite element method. In Winkler model, spring are adopted to model the soil resistance whereas piles are modeled as elastic beam. The empirical relationship between dynamic soil stiffness by modeling soil as spring was first proposed in 1967 which opened the door for researchers to explore in this area [1]. The same idea was extended by considering harmonic loading and a set of equations were proposed to evaluate pile head displacement responses [2], [3], [4]. The first attempt to consider soil as nonlinear material was conducted by Nogami et al, in which formal introduction of p-y curves was presented [5]. With enhanced computational efficiency, the researchers also employed Finite Element Method (FEM) for lateral load analysis. Various finite elements such as 8 node brick element, triangular elements etc. were presented to model the soil [6-9]. Nominal experiment studies were performed in order to verify the accuracy of the aforementioned finite element methods [10-13]. Another disadvantage of the FEM is its high computational cost. The solution to this was proposed by introduction of reduced dimension FEM (RDFEM), in which soil and pile vertical displacement were ignored, as they don't contribute toward the lateral load analysis [14]. The experimental verification of RDFEM was also performed and the obtained results shows excellent matching, hence providing researcher a new framework to anticipate performance of laterally loaded piles [15].

In this study, a research framework proposed by Suhail S.A, and Thammarak, P [15], was employed to perform analysis of laterally loaded large diameter pile embedded in fine grained soil using two numerical methods i.e. Winkler model and finite element method. The dynamic characteristics such as natural frequency and dynamic pile displacement were first obtained, followed by determination of the bending moments and shear force by using theory of elasticity.

2 Research Methodology

2.1 Soil Data Collection

Data of 56 boreholes were collected from different areas of Islamabad and Rawalpindi region. The collected data includes SPT N field values along with soil classification. Based on the field values, corrected standard penetration test SPT N values were determined. Soil dynamic characteristics such as shear and compression wave velocity, dynamic modulus, poison ratio and density of the soil were then evaluated on the corrected SPT N values. The soil spring stiffness to be used for Winkler model was obtained by using the empirical equations proposed by Novak et. al. [3]. Since soil dynamic stiffness is frequency dependent, a code in MATLAB is written in order to obtain resistance at variable frequencies. The soil parameters employed in the present study is presented in Table 1

Table 1 Soil Parameters Used in Numerical Modeling

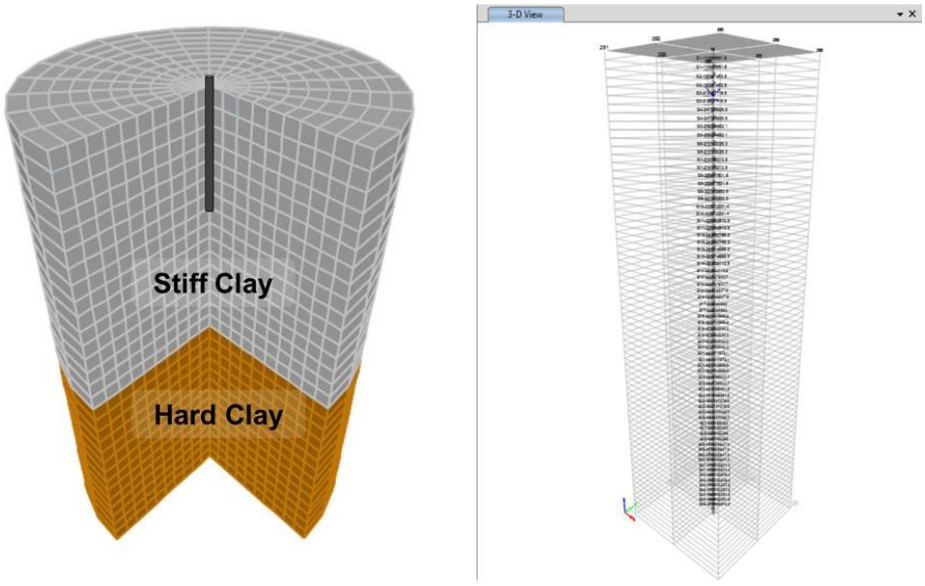
Depth	**V_s**	**UW**	**Elasticity**
(m)	**(m/s)**	**KN/m3**	**(MPA)**
0-3	139	11	3.67
3-11	224	18	8
11-45	249	20	14
45-60	300	21	25

2.2 Numerical Modelling

In Winkler Beam on Spring Foundation (WBSF) model beam elements are used to model pile whereas 1D discrete springs represent soil strength. Soil strength is obtained from the solution proposed by Novak et. al. [3]. WBSF analysis is performed on the commercially available software ETABS. RDFEM analysis was carried out using computer code written in FORTRAN. In RDFEM, Euler's beam element is used to model pile whereas 3D ring element represents soil. An appropriate mesh size and soil boundary were used that is obtained based on shear and compressional wave velocities. The pictorial view of numerical models is shown in Figure 1. A huge pile cap, having mass moments of inertia of 802,623 kg-m^2, is also modelled using area elements to represent superstructure. The input parameters for RDFEM models are given in Table 2.

Table 2: Input Parameters of RDFEM Model

Applied Frequency	1 - 10 Hz
Time Stepping Size	0.01 sec
No. of Time Steps	2000
Analysis Time	20 sec
$V_{s(min)}$	139 (m/sec)
V_p	141 (m/sec)
Smallest Wavelength	0.86 m
Element Size	0.5m
Calculated Outer Boundary Size	3440 m
Boundary Size Used	4000 m



(a) *(b)*

Figure 1: Numerical Models (a) RDFEM (b) WBSF Model

3 Results

The result of the present study indicates that natural frequency of pile is obtained from RDFEM is 2.5 Hz, whereas WBSF gives natural frequency of 2.0 Hz. The corresponding pile head displacements are 4.07E-5m and 5.37E-5m respectively. Based on the results of modal analysis, other dynamic characteristics including deformation, bending moment and shear force variation along the length of the piles were obtained using theory of elasticity for various frequencies including natural frequencies, pre-natural frequencies and post natural frequencies, and are presented in Figure 2, 3 and 4.

From figure 2, it can be observed that maximum deflection is observed at the pile top and at natural frequency of the pile. The amplitude of deflection at frequencies before and after natural frequency is less than what is recorded at natural frequency. The variation of bending moment and shear forces as shown in Figure 3 and 4 showed similar trends as that of pile deflection. This is generally because the dynamic pile responses are primarily governed by stiffness of the infrastructure. As the intersection of pile and superstructure represented by pile cap is modelled at the pile head therefore, the stiffness of the overall system becomes extremely high at the pile top level. As a result, deformation, bending moment and shear force amplitudes become maximum at the pile top. These results align with observations recorded by previous research studies [15].

The results of deflection, bending moment and shear force variation along the pile length also highlighted that these characteristics become zero at pile tip level. This clearly showed that the lower part of the pile (i.e. below the active length, doesn't contribute towards resistance lateral loads.

4 Conclusion

The following conclusions can be drawn from the conducted study:

1 Both numerical methods RDFEM and WBSF can simulate dynamic response of piles.
2 The dynamic head displacement, bending moment and shear will be higher at the pile top level, at the location of intersection of pile and superstructure.

The WBSF method overestimates the pile lateral response in fine-grained soil

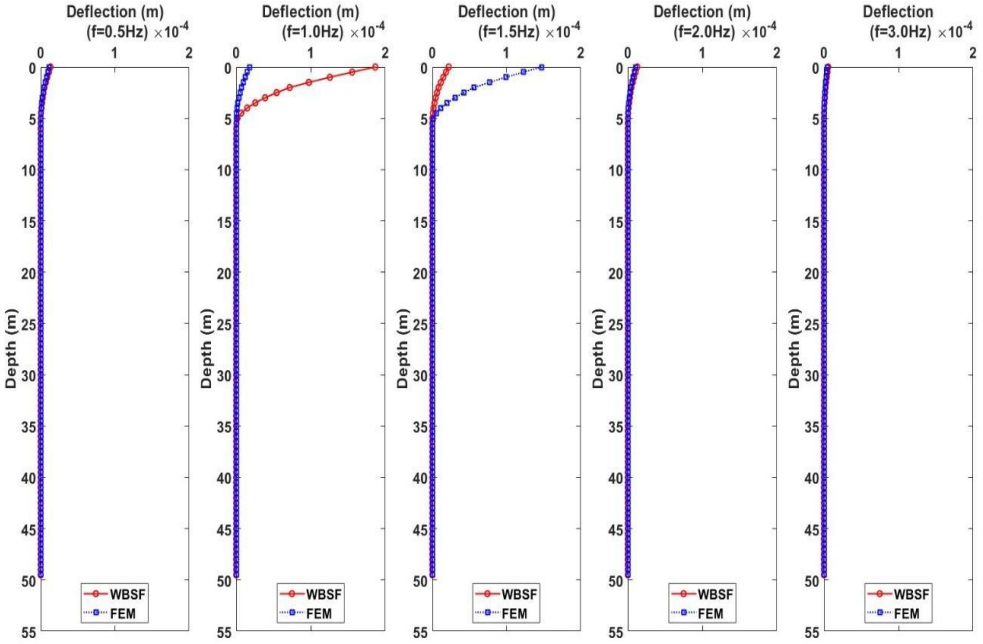


Figure 2: Deformation Pattern along Pile Length

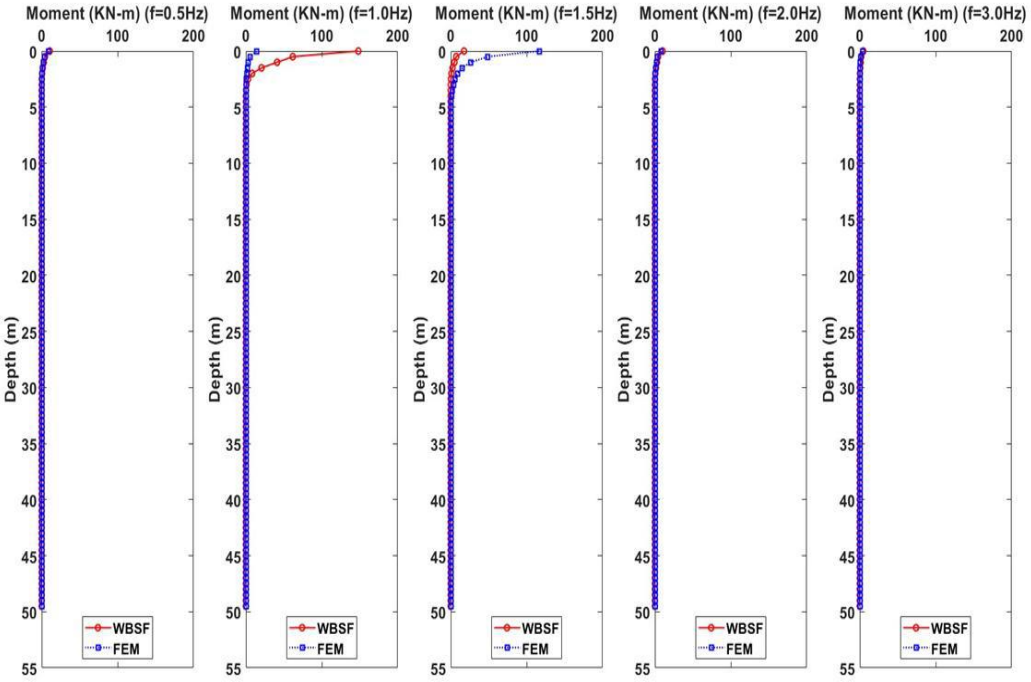


Figure 3: Bending Moment Pattern along Pile Length

.

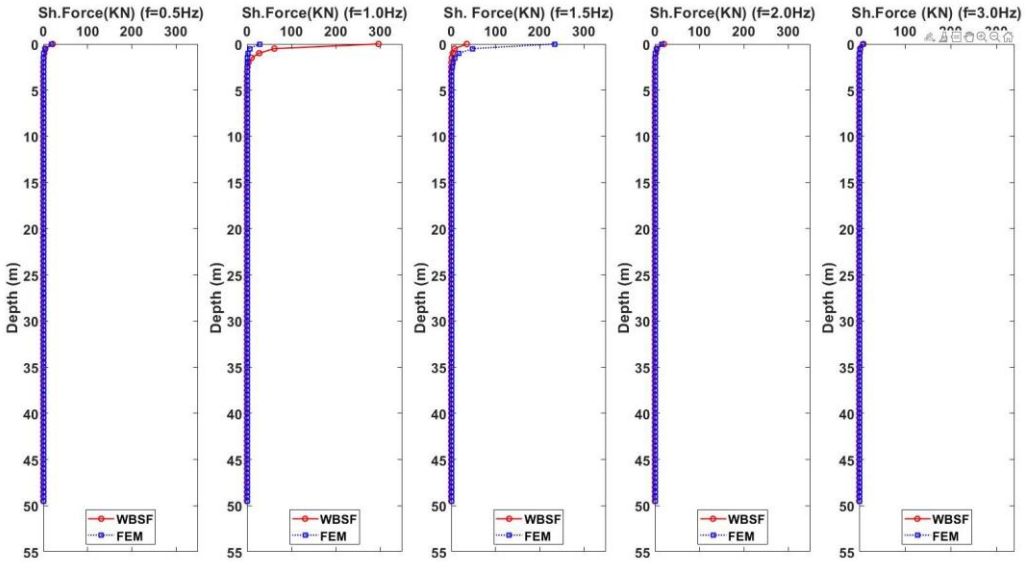


Figure 4: Shear Force Pattern along Pile Length

Acknowledgment

The authors would like to thank Engr. Dr Salman Ali Suhail for his supervision and support during this final year project.

References

[1] Baranov VA, "On the calculation of an embedded foundation," J. Earthq. Eng., no. 14, pp. 195–209, 1967.
[2] T. Nogami and M. Novak, "Resistance of soil to a horizontally vibrating pile," Earthq. Eng. Struct. Dyn., vol. 5, no. 3, pp. 249–261, 1977, doi: 10.1002/eqe.4290050304.
[3] M. Novak and A.-E. Toyoaki, "Dynamic Soil Reaction for Plane Strain Case," J. Eng. Mech., vol. 104, no. 4, pp. 953–959, 1978.
[4] M. Novak and M. Sheta, "Dynamic response of piles and pile groups," 2nd Int. Conf. Numer. Method …, pp. 1–18, 1982,
[5] B. T. Nogami, J. Otani, K. Konagai, and H. Chen, "Nonlinear s o i l - p i l e interaction m o d e l for dynamic lateral m o t i o n," vol. 118, no. 1, pp. 89–106, 1992.
[6] R. Krishnan, G. Gazetas, and A. Velez, "Static and dynamic lateral deflexion of piles in non-homogeneous soil stratum," Geotechnique, vol. 33, no. 3, pp. 307–325, 1983, doi: 10.1680/geot.1983.33.3.307.
[7] G. Wu and W. D. L. Finn, "Dynamic elastic analysis of pile foundations using finite element method in the frequency domain," Can. Geotech. J., vol. 34, no. 1, pp. 34–43, 1997, doi: 10.1139/cgj-34-1-34.
[8] Y. X. Cai, P. L. Gould, and C. S. Desai, "Nonlinear analysis of 3D seismic interaction of soil-pile-structure systems and application," Eng. Struct., vol. 22, no. 2, pp. 191–199, 2000, doi: 10.1016/S0141-0296(98)00108-4.
[9] T. Kishishita, E. Saito, and F. Miura, "Dynamic-Response Charactaristics Of Structures With Micropile Foundation System," 12th World Conf. Earthq. Eng. Auckland, New Zeal., pp. 1–8, 2000.
[10] M. Novak and R. F. Grigg, "Dynamic Experiments With Small Pile Foundations.," Can. Geotech. J., vol. 13, no. 4, pp. 372–385, 1976, doi: 10.1139/t76-039.
[11] G. W. Blaney and M. W. O'Neill, "Measured lateral response of mass on single pile in clay," J. Geotech. Eng., vol. 112, no. 4, pp. 443–457, 1986, doi: 10.1061/(ASCE)0733-9410(1986)112:4(443).
[12] V. K. Puri, "Observed Natural Frequency Pile," proceeding 2nd Int. Conf. Case Hist. Geotech. Eng., 1988.
[13] B. H. El-marsafawi, Y. C. Han, and M. Novak, "Dynamic experiments on t w o p i l e groups," vol. 118, no. 4, pp. 576–592, 1992.
[14] P. Thammarak, "Dynamic response of laterally-loaded piles," 2009.
[15] Suhail S. A., & P. Thammarak, "Evaluation of dynamic behavior of single floating piles embedded in soft clay layer under lateral harmonic and impulse loading," Innov. Infrastruct. Solut., vol. 12, no. 110, 2021.

EXAMINING FREQUENCY-DISPLACEMENT RELATIONSHIP OF PILES IN FINE GRAINED SOIL

[a] Muaaz Duera*, [b] Hamza Shabir

a: Department of Civil Engineering, The University of Lahore, Lahore, Pakistan. muaazdeura019@gmail.com
b: Department of Civil Engineering, The University of Lahore, Lahore, Pakistan. itshamza9282@gmail.com
* Corresponding author

Abstract- This research work focuses on the dynamic response of pile foundations subjected to lateral loading in fine-grained soil by employing Winkler Beam-Spring Foundation model (WBSF) with a Reduced-Dimension Finite Element Model (RDFEM). Three pile diameters (0.76m, 1.2m, 2.0m) were selected for the analysis. The results noted that the WBSF model consistently predicted 20-30% greater displacements and lower natural frequencies) due to its simplified spring-based soil representation. On the contrary, the RDFEM model predicts higher excitation frequencies and reduced displacements as it corporates 3D soil continuity, yielding more realistic soil-pile dynamic interaction. These findings align with already published research, demonstrating that WBSF serves for preliminary analysis, and its limitations in capturing true soil-pile interaction make it unsuitable for critical dynamic loading cases. The RDFEM gives higher accuracy, particularly in simulating seismic effects and soil yielding, provides essential insights for safe foundation design. This work highlights the necessity of advanced modeling techniques for reliable prediction of pile behavior in fine-grained soils subjected to lateral loads, offering practical guidance for geotechnical engineering practice.

Keywords- Pile Foundation, Dynamic Loading, Winkler Method, Pile Response Spectrum

1 Introduction

Pile foundations can be categorized in numerous ways such as by material, construction method, or structural function. However, in geotechnical engineering, the most critical classification is based on how piles behave under certain loads. Generally, piles fall into two main categories. Piles that simply rely on skin friction along their longitudinal direction to support loads are defined as friction piles whereas piles transfer most of the load to a hard stratum at the pile tip, resisting settlement through base reaction is termed as end bearing piles. The load-settlement behavior and axial load transfer mechanism of piles have been extensively studied. However, the response of piles subjected to lateral loading, particularly dynamic lateral loading (particularly generated by earthquakes), remains a complex and less understood phenomenon, due to very limited research on dynamic behavior of pile subjected to lateral load. This lead to an opportunity to explore this area in depth, to mitigate the risk of catastrophic failure in poorly designed foundations, a comprehensive understanding of pile-soil interaction under lateral loading is essential for ensuring structural safety and operational efficiency in geotechnical engineering

According to existing research, lateral load analysis using numerical techniques can generally be grouped into three primary categories: (i) the Winkler-based approach, (ii) analytical or closed-form models, and (iii) the Finite Element Method (FEM). In the Winkler approach, the soil's reaction is modeled through discrete springs, while the pile is considered as a linearly elastic beam. This concept, first introduced in 1967, linked dynamic soil stiffness with spring elements, laying the groundwork for further developments in this field [1]. Later enhancements included the application of harmonic loads,

resulting in mathematical models that estimated displacements at the pile head [2-4]. A significant advancement was made by Nogami and colleagues, who introduced nonlinear soil behavior through the development of p–y curves [5]. With improvements in computing capabilities, FEM became a popular tool for analyzing pile behavior under lateral loads. Soil was represented using various element types, including 8-node bricks and triangular meshes [6-9]. Laboratory experiments were also carried out to validate these FEM-based models [10-12]. However, FEM is often limited by its substantial computational demands. To address this, a simplified approach—Reduced-Dimension FEM (RDFEM)—was introduced, which excludes vertical displacements of both soil and pile, as these have minimal effect on lateral behavior [13]. Subsequent experimental validation of RDFEM confirmed its reliability, offering researchers a refined method for predicting the response of piles subjected to lateral loading[14]. Based upon the already published research, the study utilized two famous methods WBSF and RDFEM for investigating the pile response subjected to lateral loading in fine grained soil. The detailed methodology and results are reported in the proceeding sections

2 Research Methodology

2.1 Data Collection and Selection of Parameters

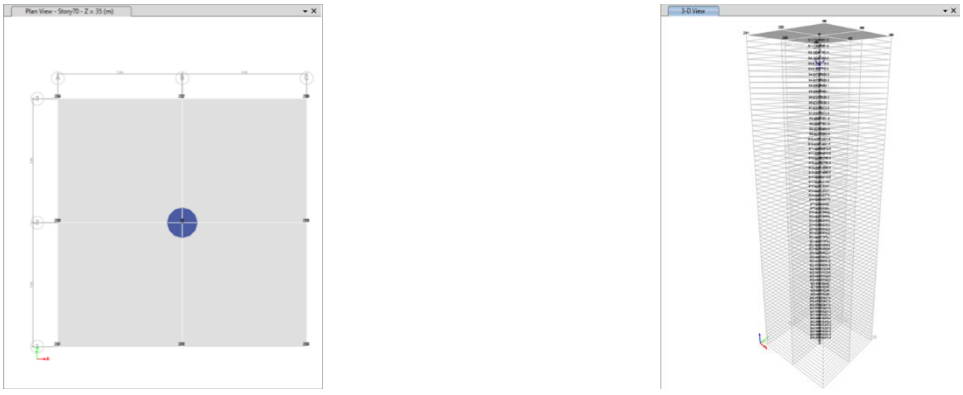
For investigation the data was collected from 56 boreholes distributed over the Rawalpindi-Islamabad region to study soil characteristics for supporting numerical modeling. The soil strata were classified into distinct layers, extending 50 meters deep, based on corrected Standard Penetration Test (SPT-N) results. From these values, crucial parameters like Vs, Vp, unit weight, elastic modulus, Poisson's ratio and shear modulus (G) were estimated using well established empirical co-relations related to fine grained soil [15-17].

2.2 Numerical Modelling Using Winkler Beam Spring Foundation Model

The Winkler Beam-Spring Foundation (WBSF) model is a popular method used to analyze the behavior of piles subjected to lateral load. It reduces the complexity of soil-structure interaction by modeling the soil as a series of independent linear springs. In this case, the reaction from the soil (p) at any point is proportional to the pile's displacement laterally (y), k is modulus of subgrade reaction (force/length), mathematically:

$$p = ky \tag{1}$$

The development of WBSF model includes two main steps. First, is determination of the dynamic spring constant for each individual soil layer, and second is numerical simulation of the soil-pile system. For the first step, a code in MATLAB was written to compute the dynamic stiffness spring constant of soil layers including both components of soil resistance, real (spring stiffness) and imaginary (damping) in the WBSF, following the framework proposed in published study [3]. Next, a numerical model was developed in ETABS to simulate the dynamic response of a pile foundation embedded in layered fine grained. Beam element is employed to represent pile whereas 1D spring element is used for soil. A superstructure is represented by modeling a high pile cap using area elements. WBSF model of pile cap and pile is shown in Figure 1 (a) and (b) respectively.



(a) *(b)*

Figure 1: WBSF Model of Pile Cap and Pile

2.3 Numerical Modelling Using Reduced Dimension Finite Element Model

A computational efficient RDFEM approach was adopted, where the soil was represented as continues ring elements with radial, azimuthal, and axial displacement degrees of freedom (DOFs). The pile was modeled with beam elements whereas pile cap was modelled using area element. The soil boundaries and mesh size was selected on the basis of soil dynamic characteristics

3 Results and Discussion

Frequency displacement relationship of all three piles having diameter of 0.76m, 1.2m and 2.0m is presented in Figure 2, 3 and 4. The pile response spectrum for the 0.76 diameter pile was investigated at frequencies ranging from 1 Hz to 10 Hz. The WBSF method indicated natural frequency of 1 Hz with corresponding displacement of 1.87x10-4 m. The FEM analysis, however, predicted a slightly higher natural frequency of 1.5 Hz and a smaller displacement of 1.47×10^{-4} meters

Due to its ability to capture complex soil-pile interaction behavior, FEM generally produces more results that are accurate. For pile diameter 1.2m. The WBSF method indicated natural frequency of 1.5 Hz with corresponding displacement of 1.87894×10^{-5} m. However, a slightly smaller displacement of 1.51×10^{-5} meters and a higher natural frequency of 2 Hz were found in the FEM analysis. For pile diameter 2.0m, The WBSF method indicated natural frequency of 2.0 Hz with corresponding displacement of 5.37×10^{-6} m. However, a slightly smaller displacement of 4.05×10^{-6} meters and a higher natural frequency of 2.5 Hz were found in the FEM analysis. In particular, the natural frequencies predicted by WBSF were 1 Hz, 1.5 Hz, and 2 Hz for each increasing diameter while FEM provided results of 1.5 Hz, 2 Hz and 2.5 Hz. Likewise, displacements calculated from WBSF were about twenty to thirty percent more than those estimated using FEM. This suggests that the simplified WBSF method exaggerates flexibility whilst underestimating stiffness in soil-pile systems. Due to oversimplification and breaking continuum nature of soil, unlike FEM which captures the true complexity of soil behavior. The comparison of the obtained frequency and displacement values from FEM and WBSF model is presented in Table 1.

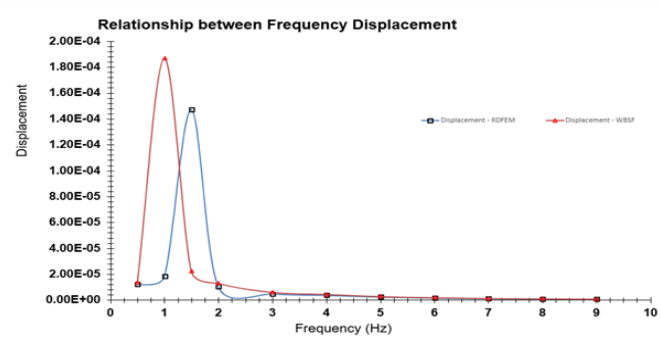


Figure 2: Frequency –Displacement Relationship (Dia. 0.76m)

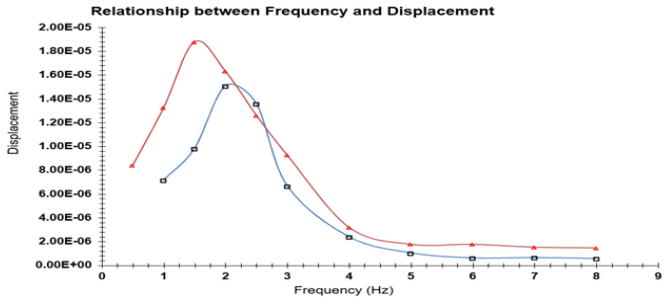


Figure 3: Frequency –Displacement Relationship (Dia. 1.2m)

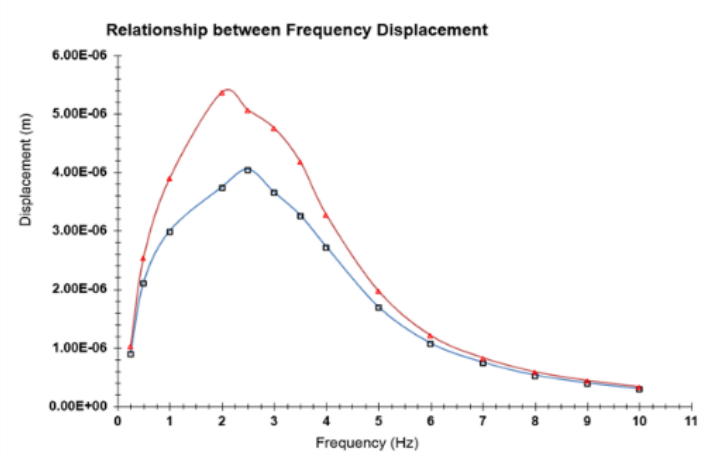


Figure 4: Frequency –Displacement Relationship (Dia. 2.0m)

Table 1: Natural frequencies and Displacement

Diameter	RDFEM		WBSF		% Difference
	Natural frequency	Displacement	Natural frequency	Displacement	
0.76	1.5	1.47E-04	1	1.87E-04	21.39
1.2	2	1.51E-05	1.5	1.87E-05	19.63
2.0	2.5	4.05E-06	2.0	5.37E-06	24.58

The increase in natural frequencies and the corresponding decrease in displacement due to increase in pile size is primarily due to increase in the stiffness of the system (Pile-Soil combined system). The increase in pile size increases its flexural rigidity, which enhanced the stiffness. It is a well-established fact that stiffness governs the overall dynamic response of the pile. The same observation is confirmed in the results of the present study. The inaccurate estimation of dynamic response by WBSF is primarily attributed to its simplification adopted in modeling the soil. As stated above, 1D springs are used in WBSF model to denote soil, which in reality is a 3D continuum material. By doing so, the shear interaction among the soil layers is ignored in WBSF which resulted in higher displacement values along with lower fundamental frequencies. On the contrary, the whole 3D continuum nature of soil can be modelled in FEM. As a result, shear interaction among the soil layers is considered in FEM analysis which helps to produce more accurate results, and the model is close to realistic representation of the soil.

The present study provides useful insights in the dynamic soil-pile characteristics for Islamabad Rawalpindi region. However, the present study is based on the use of empirical co-relation to determine dynamic properties of the soil. Authors recommend examining the pile-soil dynamic behavior by using the actual soil dynamic properties obtained from field experiments to enhance the reliability of the results.

4 Conclusion

The following conclusions are drawn from the present study:

1. Maximum amplitude of displacement, bending moment and shear force are observed at the top of pile at the intersection point of pile and pile cap.
2. WBSF model overestimates the lateral response of piles whereas FEM provides realistic results.
3. The overestimation by WBSF is primarily due to simplification adopted in modeling the soil breaking the continuum nature of the soil.

Acknowledgment

The authors acknowledges the efforts and support of Engr. Dr Salman Ali Suhail as supervisor of our project.

References

[1] Baranov VA, "On the calculation of an embedded foundation," *J. Earthq. Eng.*, no. 14, pp. 195–209, 1967.
[2] T. Nogami and M. Novak, "Resistance of soil to a horizontally vibrating pile," *Earthq. Eng. Struct. Dyn.*, vol. 5, no. 3, pp. 249–261, 1977, doi: 10.1002/eqe.4290050304.
[3] M. Novak and A.-E. Toyoaki, "Dynamic Soil Reaction for Plane Strain Case," *J. Eng. Mech.*, vol. 104, no. 4, pp. 953–959, 1978.
[4] M. Novak and M. Sheta, "Dynamic response of piles and pile groups," *2nd Int. Conf. Numer. Method …*, pp. 1–18, 1982, [Online]. Available: http://scholar.google.co.jp/scholar?cluster=14695026111402290174&hl=ja&as_sdt=2005&sciodt=0,5#0
[5] B. T. Nogami, J. Otani, K. Konagai, and H. Chen, "Nonlinear s o i l - p i l e interaction m o d e l for dynamic lateral m o t i o n," vol. 118, no. 1, pp. 89–106, 1992.
[6] R. Krishnan, G. Gazetas, and A. Velez, "Static and dynamic lateral deflexion of piles in non-homogeneous soil stratum," *Geotechnique*, vol. 33, no. 3, pp. 307–325, 1983, doi: 10.1680/geot.1983.33.3.307.
[7] G. Wu and W. D. L. Finn, "Dynamic elastic analysis of pile foundations using finite element method in the frequency domain," *Can. Geotech. J.*, vol. 34, no. 1, pp. 34–43, 1997, doi: 10.1139/cgj-34-1-34.
[8] G. Wu and W. D. L. Finn, "Dynamic nonlinear analysis of pile foundations using finite element method in the time domain," *Can. Geotech. J.*, vol. 34, no. 1, pp. 44–52, 1997, doi: 10.1139/t96-088.
[9] T. Kishishita, E. Saito, and F. Miura, "Dynamic-Response Charactaristics Of Structures With Micropile Foundation System," *12th World Conf. Earthq. Eng. Auckland, New Zeal.*, pp. 1–8, 2000.
[10] M. Novak and R. F. Grigg, "Dynamic Experiments With Small Pile Foundations.," *Can. Geotech. J.*, vol. 13, no. 4, pp. 372–385, 1976, doi: 10.1139/t76-039.
[11] G. W. Blaney and M. W. O'Neill, "Measured lateral response of mass on single pile in clay," *J. Geotech. Eng.*, vol. 112, no. 4, pp. 443–457, 1986, doi: 10.1061/(ASCE)0733-9410(1986)112:4(443).
[12] B. H. El-marsafawi, Y. C. Han, and M. Novak, "Dynamic experiments on t w o p i l e groups," vol. 118, no. 4, pp. 576–592, 1992.
[13] P. Thammarak, "Dynamic response of laterally-loaded piles," 2009.
[14] S. A. Suhail and P. Thammarak, "Evaluation of dynamic behavior of single floating piles embedded in soft clay layer under lateral harmonic and impulse loading," *Innov. Infrastruct. Solut.*, vol. 6, no. 3, pp. 1–25, 2021, doi: 10.1007/s41062-021-00536-7.
[15] S. P. Naik, N. R. Patra, and J. N. Malik, "Spatial Distribution of Shear Wave Velocity for Late Quaternary Alluvial Soil of Kanpur City, Northern India," *Geotech. Geol. Eng.*, vol. 32, no. 1, pp. 131–149, 2014, doi: 10.1007/s10706-013-9698-3.
[16] A. S. Daag, O. P. C. Halasan, A. A. T. Magnaye, R. N. Grutas, and R. U. Solidum, "Empirical Correlation between Standard Penetration Resistance (SPT-N) and Shear Wave Velocity (Vs) for Soils in Metro Manila, Philippines," *Appl. Sci.*, vol. 12, no. 16, 2022, doi: 10.3390/app12168067.
[17] P. Muley, B. K. Maheshwari, and B. Kirar, "Liquefaction Potential of Sites in Roorkee Region Using SPT-Based Methods," *Int. J. Geosynth. Gr. Eng.*, vol. 8, no. 2, pp. 1–13, 2022, doi: 10.1007/s40891-022-00374-2.

7th Conference on Sustainability in Civil Engineering (CSCE'25)
(An International Conference)
Department of Civil Engineering
Capital University of Science and Technology, Islamabad Pakistan

ECO-FRIENDLY SOLUTION FOR UTILIZATION OF RECLAIMED ASPHALT PAVEMENT MATERIAL

[a] Hamza Afzal*, [b] Imran Hafeez

a: Civil Engineering, University of Engineering and Technology, Taxila, Pakistan. engr.hamza38@gmail.com
b: Civil Engineering, University of Engineering and Technology, Taxila, Pakistan. imran.hafeez@uettaxila.edu.pk
* Corresponding author

Abstract- Although Reclaimed Asphalt Pavement (RAP) is commonly used in road construction, research on its detailed laboratory and field performance is still limited. This study focused on evaluating the fundamental properties of RAP and identifying the optimal content for sustainable asphalt mixtures through a two-phase experimental approach. Key performance aspects such as rutting, cracking resistance, and moisture susceptibility were assessed. Results indicated that mixtures containing 40% RAP achieved the best balance of durability and sustainability. The Cooper wheel tracking test showed rut depths under 2.5 mm after 10,000 cycles, and the SCB test confirmed good fracture resistance at various temperatures. Moisture tests, including rolling bottle and boiling water methods, showed strong binder-aggregate adhesion with coverage above 85%. These findings suggest that with proper design, RAP can enhance pavement performance, reduce environmental impact, and lower the need for virgin aggregates by up to 40%.

Keywords- Fracture Resistance, Recycled Asphalt Pavement, Permanent Deformation, Moisture Damage

1 Introduction

Reclaimed Asphalt Pavement (RAP), obtained through the milling of aged pavements, has gained widespread use in road construction due to its durability and environmental advantages [1], [9], [15]. Though RAP naturally degrades over time from environmental exposure and traffic loads, its reuse in new asphalt mixtures significantly reduces the need for virgin aggregates and bitumen, contributing to lower material consumption, reduced landfill waste, and a more sustainable circular economy [9], [10], [15]. The RAP used in this study was sourced from the M-2 Motorway and had been in service for 15 years, highlighting its potential for reuse in infrastructure projects while decreasing greenhouse gas emissions and energy demands associated with material production and transportation.
Previous studies have demonstrated that RAP improves stiffness and load-bearing capacity due to the presence of aged binder [1], [5], [22]. However, excessive RAP content can compromise flexibility and increase the likelihood of cracking [6], [13], [21]. Optimal RAP content is often recommended in the range of 30–40% to achieve a balance between performance and sustainability [5], [12], [13]. To mitigate the adverse effects of aged binder, various rejuvenators such as sunflower oil, used cooking oil, and Cereclor have been successfully employed to restore flexibility, fatigue resistance, and aging durability in RAP binders [2]–[4]. Recent advancements in machine learning have further supported the optimization of mechanical properties like Indirect Tensile Strength (ITS) in rejuvenated RAP mixtures [18], [19].

Despite these developments, high RAP contents continue to present challenges such as incomplete blending with virgin binder and reduced coating efficiency, leading to inconsistent performance [20], [21]. Therefore, a performance-based approach is essential to optimize RAP dosage and binder properties for reliable pavement design. This study aims to evaluate the physical and mechanical characteristics of RAP through proper mix design and a series of laboratory tests—including wheel tracking, Semi-Circular Bend (SCB), boiling water, and rolling bottle tests—to identify the optimal RAP content for cost-effective, durable, and environmentally friendly asphalt pavement mixtures.

2 Research Methodology

2.1 Laboratory Testing Program

A detailed laboratory program was conducted in two phases to assess RAP suitability, as outlined in Table 1 and illustrated in Figure 1. In Phase 1, RAP from the M-2 Motorway was tested for binder content (3.8%) using the Centrifuge Extraction Method (ASTM D2172) and analyzed for gradation under NHA Class B limits. It was blended with 80/100-grade virgin bitumen, and trial mixes were designed to meet Marshall criteria for stability, air voids, VMA, VFA, and flow. Mixtures with 0%, 25%, 50%, and 100% RAP were prepared to determine the optimum bitumen content. Phase 2 involved performance-based testing of these mixtures, summarized in Table 2, to evaluate mechanical behavior and durability. Using a softer 80/100 binder effectively restored aged RAP binder properties, enhancing flexibility and blending without chemical rejuvenators. Results showed that moderate RAP levels (25–50%) maintained good moisture resistance and durability, while higher RAP contents increased stiffness, reduced binder coating, and raised moisture susceptibility.

Table 1: Laboratory Tests Matrix

Test Name	Standard	Input Parameters	Output Parameters
Bitumen Extraction Test	ASTM D 2172	Solvent: 1000 mL CCl_4, Extraction time: 45-60 minutes, Temperature 120 °C	Optimum Bitumen Content
Marshall Stability	ASTM D-6927	Loading rate: 50 mm/min, Test temperature 60 °C, Core Diameter: 4 inches, Height: 2.5 inches,	Stability values (kg)
Bulk Specific Gravity	ASTM D-2726	25 °C, Weight measurement nearest to 0.01 g in water, air and SSD states	Bulk specific gravity (Gmb)
Cooper Wheel Tracker Test	EN 12697-22	10000 passes, Frequency: 26.5 rpm Load: 720 N, Terminal Rut Depth: 12.5 mm	Permanent Deformation/Rutting Depth
Rolling Bottle Test	EN 12697-11	Temperature:50°C, 60°C, 70°C, Rotation Speed15 rpm, 20 rpm	Durability
Semi Circular Bend	ASTM D 8044-16	Temperature: 40°C to 50°C; Frequency: 1 Hz	Cracking resistance under repeated loading.
Boiling Water Best	ASTM D3626	Temperature (around 100°C or 212°F).Time up to 10 minutes.	Moisture damage

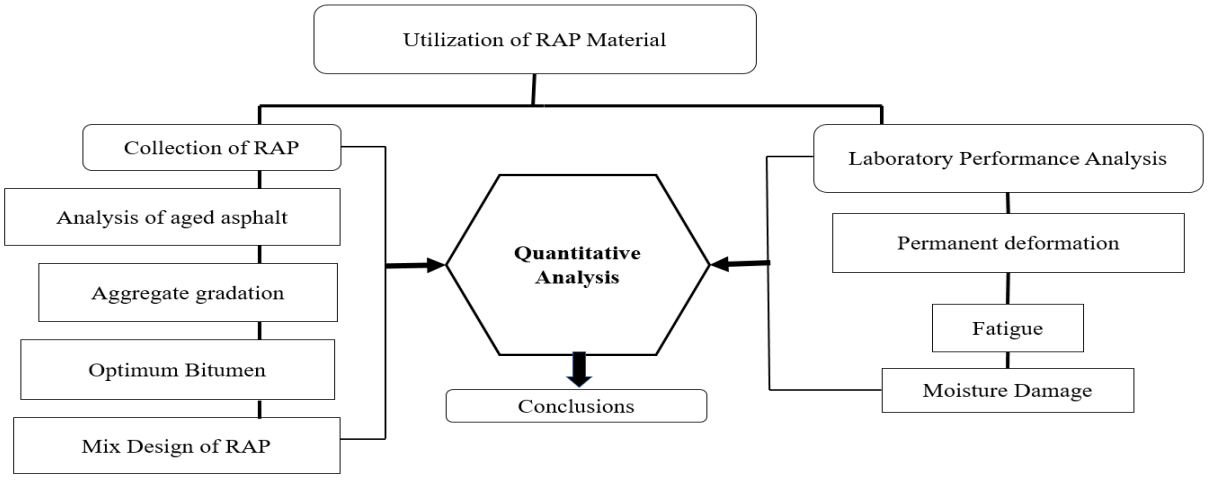


Figure 1: Flow chart of the experimental plan

Table 2: Marshal Parameters Determined For RAP Mix

RAP Contents (%)	Stability (Kg)	Flow (mm)	Unit Weight (Kg/m^3)	VA (%)	VMA (%)	VFA (%)
0	1150	12.7	2340.1	5.60	14.90	68.20
25	1121	11.2	2351.2	5.20	14.40	70.20
50	1230	10.77	2363.0	4.20	13.30	72.40
100	1280	9.2	2336.5	4.00	12.96	73.90

2.2 Aggregate Gradation

Aggregate gradation was performed on RAP aggregate under the NHA class B limitations, and a gradation curve was obtained by plotting the percentage passing versus the corresponding sieve size, as shown in Figure 2.

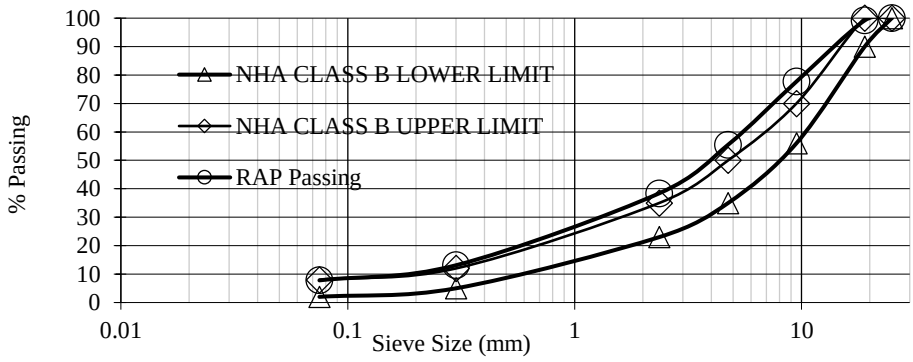


Figure 2: Gradation Curve for RAP Aggregates

2.3 Performance Testing of Asphalt Mixtures

These tests, aligned with international standards, provided a comprehensive understanding of the rutting, cracking, and moisture resistance performance of RAP-containing mixtures.

i. Cooper Wheel Tracking Test (BS EN 12697-22): Used to evaluate rutting resistance under simulated traffic loading. Rectangular slab specimens were tested at 50°C with 10,000 cycles, and rut depths were recorded at predefined intervals.
ii. Semi-Circular Bend (SCB) Test (ASTM D8044-16): Assessed fracture resistance and cracking potential at low temperatures. Semi-circular specimens (150 mm diameter, 62 mm thick) with a notch depth of 19–20 mm were tested to determine fracture energy from load-displacement behavior.
iii. Rolling Bottle Test (EN 12697-11): Evaluated binder-aggregate adhesion under moisture conditioning. 150 g of aggregate (6.3–8 mm) was rotated in 400 ml of water at 60 rpm, and binder coverage was visually assessed after 24, 48, and 72 hours.
iv. Boiling Water Test (ASTM D3626): Measured moisture susceptibility by immersing 250 g of loose asphalt mixture in boiling water for 10 minutes, followed by visual evaluation of binder stripping.

3 Results

3.1 Cooper Wheel Tracking Test

The test results show valuable insights from Cooper Wheel Tracking into the rutting resistance of the RAP material under repeated traffic load at high temperature. The curves show that higher RAP contents show higher resistance to permanent deformation after 10,000 wheel cycles. Mixture with (0% RAP) showed that the rut depth of 5.8mm, and the RAP material with 100% showed a rut depth of 1.9 mm. The RAP of 25% and 50% showed 4.1 mm and 2.2 mm, respectively, as shown in Figure 4.

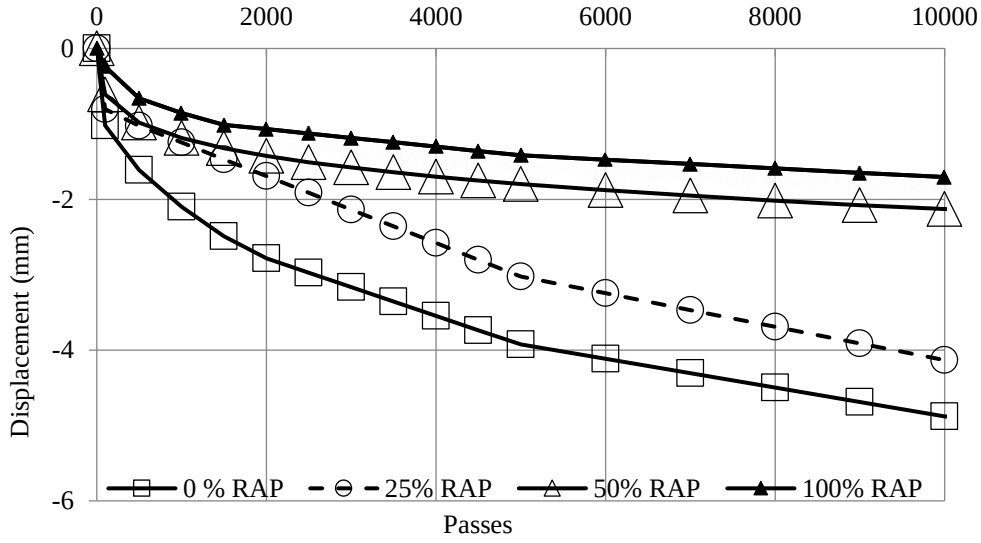


Figure 4: Influence of wheel passes on rut depth at different RAP percentages

Figure 4 demonstrates that rutting decreased as RAP content increased. The mix with 0% RAP showed a displacement of 5.88 mm, exceeding the AASHTO limit of 4 mm, whereas mixtures with 25%, 50%, and 100% RAP recorded rut depths of 4.13 mm, 2.25 mm, and 1.91 mm, respectively—all within acceptable limits. These results align with previous findings that attribute improved rutting resistance to the stiffness of aged binder in RAP mixtures [22], [18]. However, excessive RAP content can compromise flexibility, increasing the risk of cracking [21].

3.2 Semi-Circular Bend Test

The Semi-Circular Bend (SCB) test, conducted according to ASTM D8044, evaluated the fracture resistance of RAP mixtures. At intermediate temperatures, mixes with 25–40% RAP showed fracture energy comparable to or slightly exceeding the control (510 N), with 25% and 50% RAP yielding 570 N and 350 N, respectively. However, at 100% RAP, fracture energy dropped to 242 N, indicating increased brittleness and a higher risk of cracking at elevated RAP levels, as shown in Table 3.

Table 3: Fracture Resistance (N) of asphalt mixtures at different RAP percentages.

Sample	0% RAP	25% RAP	50% RAP	100% RAP
Fracture Resistance N	510 N	570 N	350 N	242 N

3.3 Rolling Bottle Test

This test is used to assess the stripping or loss of adhesion between asphalt binder and aggregate in the presence of water. It provides insight into the moisture damage that may occur in asphalt mixtures under wet conditions. Figure 5 shows the percentage of binder coverage remaining after different conditioning periods (24, 48, and 72 hours) for various RAP percentage

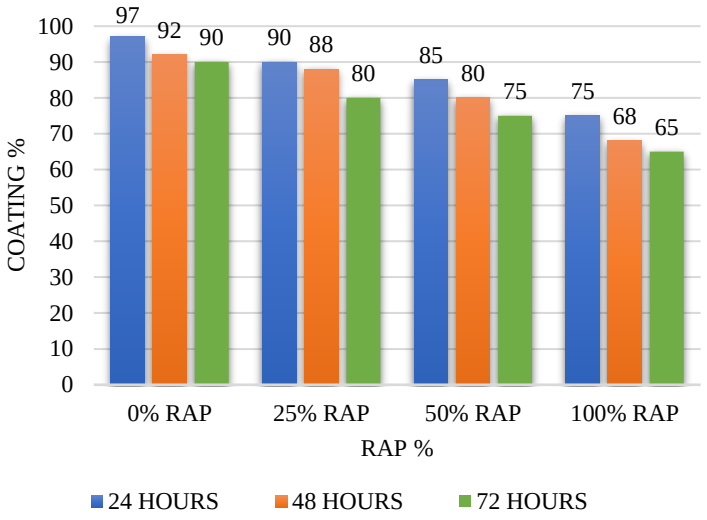


Figure 5: Effect of conditioning time and RAP percentages on binder coating

3.4 Boiling Water Test

The Boiling Water test (ASTM D3626) showed over 90% coating retention for RAP contents up to 40%, and 80–85% for higher RAP levels. This indicates good moisture resistance at moderate RAP use, but potential durability concerns at higher contents, as shown in Figure 6.

3.5 Equations

The aged binder in RAP improves stiffness and rutting resistance but reduces flexibility, increasing cracking risk. Poor blending at high RAP levels can weaken bonding and performance. To achieve balanced properties, RAP content was optimized using a performance-based method.

$$\text{Performance Index} = \frac{\text{Fracture Resistance} \times \text{Moisture Resistance}}{\text{Rut Depth}} \quad (1.0)$$

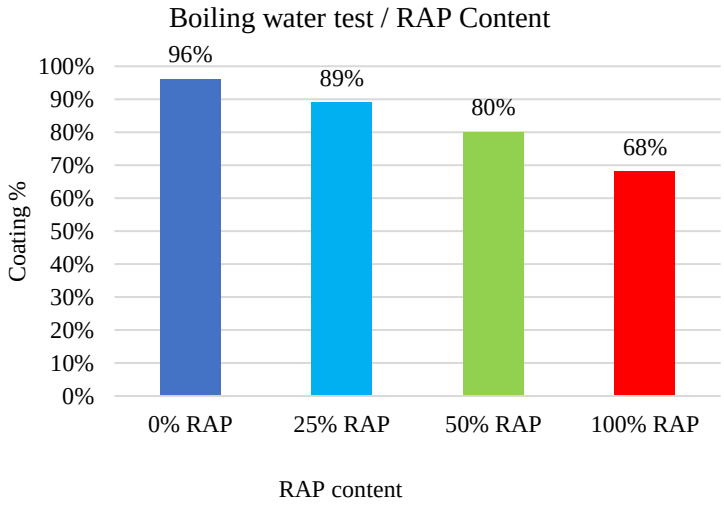


Figure 6: Effect of RAP percentage on binder coating

Table 4: Performance testing results of asphalt mixtures

Permanent Deformation test Rut Depth mm	0% RAP	25%RAP	50%RAP	100%RAP
Rut Depth mm	5.8	4.1	2.2	1.9
Fracture Resistance N	510	570	350	242
AVG OF Boiling Water and Rolling Bottle test	95%	90%	82%	70%

Table 5: Performance index for optimum asphalt content

0% RAP	25% RAP	50%RAP	100%RAP
83.5	125.1	130.5	89.2

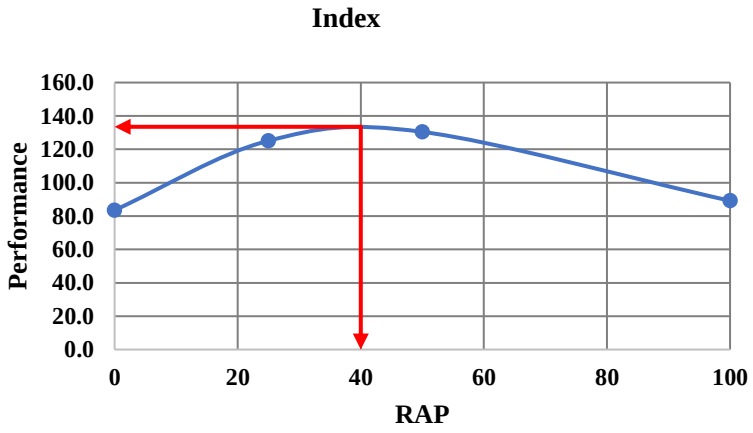


Figure 6: Optimum asphalt content based on performance index

4 Conclusion

This study identified 40% RAP as the optimal content for balanced asphalt performance, offering good rutting resistance, fracture energy, and binder coating. Mixes with 25–50% RAP showed strong durability and moisture resistance, while higher contents improved rutting but reduced fracture strength due to aged binder. The findings support cost-effective, eco-friendly pavement design and quality control through performance testing. However, results are based on lab conditions, excluding long-term factors like traffic and climate. Future research should include field trials and binder analysis. Challenges such as binder variability, limited blending at high RAP levels, and inconsistent standards hinder widespread adoption. Performance-based design and methods like Super pave are recommended for better control.

Acknowledgment

I gratefully acknowledge the Taxila Institute of Transportation Engineering and the Department of Civil Engineering for their financial assistance and support throughout my research. I am also grateful for the valuable technical input, laboratory facilities, and collaborative efforts that greatly enhanced the depth and quality of the research. The careful review and constructive suggestions by the anonymous reviewers are gratefully acknowledged.

References

[1] M. Abdel-Jaber, R. A. Al-shamayleh, R. Ibrahim, T. Alkhrissat, and A. Alqatamin, "Mechanical properties evaluation of asphalt mixtures with variable contents of reclaimed asphalt pavement (RAP)," *Results in Engineering*, vol. 14, 2022. Doi: 10.1016/j.rineng.2022.100463.

[2] *Zakir, Usama &* I. Hafeez, *Enhancement of Self-Healing Tendency of Reclaimed Asphalt Using Different Additives*, 2023. Available: https://www.researchgate.net/publication/373556266.

[3] G. Yaseen and I. Hafeez, "Effect of Cereclor as rejuvenator to enhance the aging resistance of reclaimed asphalt pavement binder," *Materials*, vol. 13, no. 7, 2020. doi: 10.3390/ma13071582.

[4] U. Zakir and I. Hafeez, "Enhancement of the self-healing tendency of reclaimed asphalt using different additives," 2022.

[5] M. Abdel-Jaber, R. A. Al-shamayleh, R. Ibrahim, T. Alkhrissat, and A. Alqatamin, "Mechanical properties evaluation of asphalt mixtures with variable contents of reclaimed asphalt pavement (RAP)," 2022.

[7] K. Akatsu, Y. Kanou, and S. Akiba, "Technical approaches to the recycling of reclaimed asphalt pavement into aggregate and binder," 2022.

[8] A. Bieliatynskyi, S. Yang, V. Pershakov, M. Shao, and M. Ta, "Performance of high-dose reclaimed asphalt mixtures (RAPs) in hot in-place recycling based on balanced design," 2024.

[9] Copeland, A. Reclaimed Asphalt Pavement in Asphalt Mixtures: State of the Practice; No. FHWA-HRT-11-021; United States Federal Highway Administration, Office of Research, Development, and Technology: McLean, VA, USA, 2011. Sapkota, K.; Yaghoubi, E.; Wasantha, P.L.P.; Van Staden, R.; Fragomeni, S. Mechanical Characteristics and Durability of HMA Made of Recycled Aggregates. Sustainability 2023, 15, 5594.

[10] L. Porot and V. Gomes, "Multi-recycling of asphalt mix with reclaimed asphalt and rejuvenator," 2020.

[11] I. Markja, K. Dhoska, M. Fraholli, G. Mustafa Raj, B. Ahmetaj, and D. Elezi, "Asphalt pavement recycling technology with reclaimed asphalt pavement (RAP) according to the standards EN 13108-8 and EN 13108-1," 2024.

[12] S. Kumar, P. Patil, and Assistant Professor, "Experimental investigation on HMA by using RAP material (BC Roads)," *International Research Journal of Engineering and Technology*, 2023.

[13] P. Patil, "Experimental investigation on HMA by using RAP material (BC Roads)," *International Research Journal of Engineering and Technology*, 2020.

[14] M. S. Jameel, H. M. Abubakar, A. Raza, S. Iqbal, and R. A. Khalid, "Effect of aging on adhesion and moisture damage of asphalt: A perspective of rolling bottle and bitumen bond strength test," *International Journal of Pavement Research and Technology*, vol. 15, no. 1, pp. 233–242, 2022. doi: 10.1007/s42947-021-00021-5.

[15] H. Nasir, M. Kaur, and S. Faheem, "A statistical review on the usage of reclaimed asphalt pavement waste as a recyclable material," 2024.

[18] M. K. Islam, U. Gazder, A. Al Mamun, M. Arifuzzaman, H. I. Al-Abdul Wahhab, and M. M. Rahman, "Predicting and optimizing the mechanical properties of rejuvenated asphalt mix with RAP content," *Neural Computing and Applications*, pp. 1–17, 2024.

[19] A. Al Mamun, U. Gazder, M. K. Islam, M. Arifuzzaman, H. A. A. Wahhab, and M. M. Rahman, "Predicting Indirect Tensile Strength of Rejuvenated Asphalt Mixes Using Machine Learning with High Reclaimed Asphalt Pavement Content," *Processes*, vol. 13, no. 5, p. 1489, 2025.

[20] J. K. Thakur and J. Han, "Recent development of recycled asphalt pavement (RAP) bases treated for roadway applications," *Transportation Infrastructure Geotechnology*, vol. 2, pp. 68–86, 2015.

[21] G. Tarsi, P. Tataranni, and C. Sangiorgi, "The challenges of using reclaimed asphalt pavement for new asphalt mixtures: A review," *Materials*, vol. 13, no. 18, p. 4052, 2020.

[22] X. Ma, J. Wang, and Y. Xu, "Investigation on the effects of RAP proportions on the pavement performance of recycled asphalt mixtures," *Frontiers in Materials*, vol. 8, p. 842809, 202

ASSESSING THE ENVIRONMENTAL IMPACT OF BUILDING MATERIALS: A LIFE CYCLE APPROACH TO SUSTAINABLE BUILDING SOLUTIONS

[a] Ruqia Asad, [b*] Fayyaz Ullah

a: Research Student, Civil Engineering Department, UET, Peshawar, Pakistan. 20pwciv5406@uetpeshawar.edu.pk
b: Research Student, Civil Engineering Department, UET, Peshawar, Pakistan. 20pwciv5563@uetpeshawar.edu.pk
* Corresponding author

Abstract- Climate change, driven by carbon emissions and greenhouse gases, is a major global challenge. In Pakistan, rapid urbanization and growing construction activities are key contributors to these emissions, further intensifying global warming. Cement production is one of the most emission-intensive processes, making the need for sustainable construction practices critical. This research explores the Life Cycle Assessment (LCA) of building materials used in affordable housing in Pakistan, focusing on identifying eco-friendly alternatives to reduce carbon footprints. Using a single-story residential unit in Peshawar as a case study, this research quantifies the embodied carbon emissions associated with traditional construction materials. Results demonstrate that alternative materials like rammed earth bricks, fly ash, and blast furnace slag significantly reduce carbon emissions compared to conventional materials. Scenario-based analysis shows that up to 70% reductions in carbon emissions are possible by integrating these sustainable materials into construction practices, highlighting the potential for low-carbon affordable housing in Pakistan. This study contributes to the Sustainable Development Goals (SDGs) by providing practical solutions for reducing carbon emissions in the construction industry.

Keywords- Life Cycle Assessment (LCA), Sustainable Construction, Climate Change, Carbon Emissions

1. Introduction

Global climate change, largely driven by carbon emissions and greenhouse gases, has emerged as a pressing challenge worldwide. These emissions, increased by rapid urbanization and the pursuit of higher living standards, have far-reaching consequences such as global warming, glacial melting, ocean acidification, and severe health risks [1]. Carbon emissions, including chlorofluorocarbons (CFCs), also contribute to ozone layer depletion, allowing harmful ultraviolet (UV) rays to reach the Earth, exacerbating environmental and health problems [2].

Building industry is one of the main contributors to the increase in carbon emissions and is a key source of contributing to the degradation of the environment. The growth in human activities for diverse goals has raised the pace of carbon emissions leading to an increase in global warming and increase in the risks of ocean acidification, eutrophication, health difficulties, lower agricultural development [3]. The construction sector is a major contributor to carbon emissions, with cement production being a particularly high-emission process. Cement manufacturing ranks as the third largest industrial source of pollution, releasing over 500,000 tons of sulfur dioxide, nitrogen oxides, and carbon monoxide annually [4].
LCA is a methodology that evaluates the environmental impact of a product or process from raw material extraction through manufacturing, use, and disposal. It provides insights into reducing carbon footprints and enhancing sustainability. The application of LCA in construction can reveal opportunities to minimize the environmental impacts of materials, as demonstrated in studies such as those by Hurt, Franklin, and Bulle [5] [6].

GHG emissions, covering carbon dioxide (CO2), methane (CH4), and nitrous oxide (N2O), play a vital role in estimating the impact of climate change [7]. LCA provides for the assessment and quantification of these emissions throughout different stages of the product's life cycle. By quantifying these emissions in carbon dioxide equivalents (CO2e), which

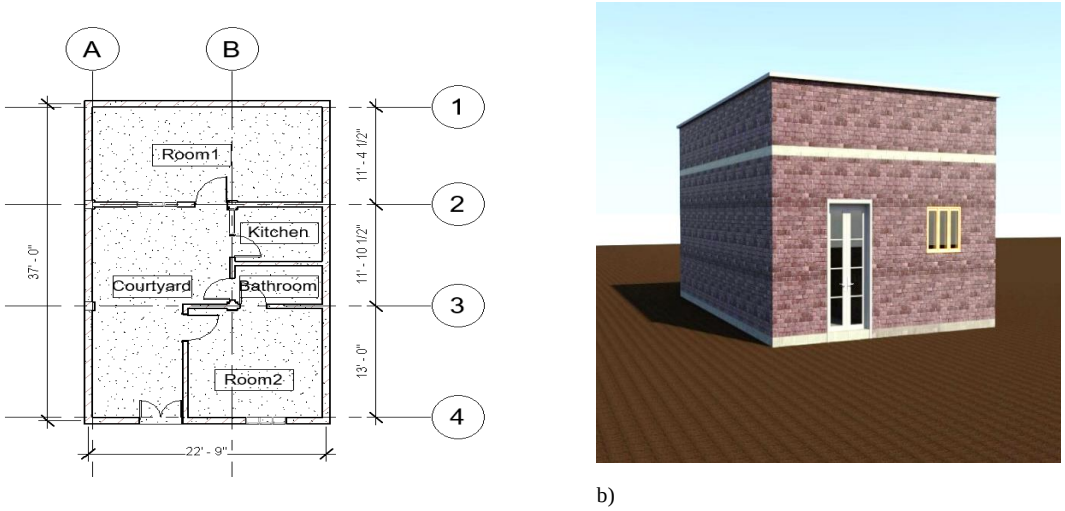
accounts for their varying global warming potentials, LCA provides a full evaluation of the carbon footprint and global warming potential of the system under consideration. This enables decision-makers to identify and mitigate the climate change impact associated with the assessed system, supporting the creation of policies to minimize GHG emissions and promote sustainability [8].

Despite its limitations, LCA is a valuable tool for sustainable construction. It enables comparisons of environmental impacts among different materials, promoting sustainable design and innovation. The approach helps reduce carbon emissions, as demonstrated by case studies across Europe and the work of researchers like Brooks, Cho, Na, and Liu, which show significant reductions in emissions through the use of low-carbon materials and construction techniques [9]. To enable an efficient and cost-effective solution, new construction techniques were investigated by various researchers in last decade [10]. Structures consisted of mortar-free interlocking blocks. Mortar-free blocks used in structure played an important role during strong ground motion. These blocks dissipated more energy during seismic event, because of the relative movement at the block interfaces [11].

2. Research Methodology

2.1 Case Study

This research focuses on an Isolated single-story residential building that typifies most residential units in the Peshawar Saddar area, consisting of two bedrooms, one bathroom, a kitchen, and a courtyard, as depicted in Figure 1 . The structure encompasses a total gross area of 68.25 square meters, with exterior and interior walls measuring 0.22 meters and 0.15 meters in thickness, respectively.



a) b)

Figure 1 Residential Building Model Selected a) Plan view b) Three-Dimensional view

The study involves quantifying the amounts of bricks, concrete, mortar, and steel reinforcement used in the structure. These quantities are crucial for evaluating the carbon intensity of the building, thereby facilitating an accurate assessment of its environmental impact and enabling measures to mitigate its carbon footprint. Table 1 presents the estimated volumes of bricks, mortar, concrete, and the total weight of steel used in the building.

Table 1 Quantities of Building Materials Used in the Single-Story Residential Structure

Category	Volume (m^3)	Wet Volume (m^3)	Dry Volume (m^3)
Bricks	46.38	46.38	46.38
Mortar	19.87	19.87	30.61
Concrete	34.14	34.14	52.57
Steel Quantity in Kilograms	2012.1 kg		

2.2 Work Procedure

This research intends to decarbonize the building by introducing alternative low carbon building materials. The approach of the research work contains a series of assessments on different building materials and examines their impact on the environment till the construction phase of the structure. To investigate the materials based on their carbon emissions, ISO (International Organization for standardization) standards belonging to ISO 14000 family of environmental management standards are followed. A systematic and transparent study is provided by ISO 14044's well-defined life cycle assessment (LCA) procedure, which contains several phases: aim and scope, inventory analysis, impact assessment, and interpretation. GHG quantification accuracy is improved by IPCC techniques. The findings are given context and legitimacy when constraints like data uncertainty and boundary settings are acknowledged. [12].

2.3 Data Analysis

To effectively quantify the carbon footprints of materials, it is vital to monitor the energy use throughout the various stages of the material life cycle. The following stages are involved in the calculation of Embodied Carbon from building construction.

2.4 Production Stage(A1-A3)

Carbon emissions during production stage are given in Equation 1. Database for this stage is provided by ICE (Inventory of Carbon and Energy) its version V3.0 – 10Nov, 2019 [13].

$$\text{Total Carbon emissions } (kgCO_2e) = \text{Quantity } (kg) \times \text{Carbon factor } (kgCO_2/kg) \quad (1)$$

2.5 Transportation Stage(A4)

Transportation stage includes carbon emissions from the transportation of building materials from batching plant to the construction site. Carbon emissions during transportation stage are calculated in Equation 2

$$\text{ECF (A4), i} = \sum_{mode}(TD \times Li \times TEF) \quad (2)$$

Here. TD = Transport Distance, Li = Liters consume per kilometers, TEF = Emission Factors provided by ISO 14064
Table 2 shows carbon intensity factors for transportation Stage and distances of different materials categories from their batching plant to the construction site taken as Peshawar Saddar. The carbon factors for the transportation stage are calculated using the RICS guidelines.

Table 2 Transportation Intensity Factors and Distances for Different Building Materials

Material Category	Distances (km)	A4 ($kgCO_2/kg$)
Bricks	10	0.001
Mortar and Concrete	12	0.0012
Steel Reinforcement	6	0.0006
Distance From Construction site to Disposal Site	12	0.0012

2.6 Construction Stage(A5)

This stage involves carbon emissions from the construction activity of the building. It mainly includes the emissions generated from construction machinery.

2.7 Materials Wastage on site (A5w)

This stage refers to those carbon emissions from the materials that are brought to site but are not used in building construction. Materials wastage on site are calculated in equation 3.

$$\text{ECF (A5w), i} = Wfi\ (\text{ECF (A1-3i)} + \text{ECF (A4i)} + \text{ECF (C2i)} + \text{ECF (C3-4i)}) \quad (3)$$

Here: Wfi = Waste factor for materials are calculated in equation 4.

$$\text{Which is, WFi} = \frac{1}{1-\text{WRi(waste rate in \%)}} - 1 \qquad (4)$$

Where.

ECF = Embodied Carbon Footprints for

1 Production (A1-3i)
2 Transportation to site (A4i)
3 Transportation away from site (C2i)
4 Waste processing disposal (C3-4i) (According to RICS guide, it is suggested that in the absence of better data, emissions for processing and disposal of the waste material is 0.013 $kgCO_2/kg$ [14])

2.8 Data Analysis

Table 3 provides the carbon emission values for each type of material when multiplied by the specific quantity utilized in a single-story building. The materials used in the research work are readily available from the selected site. They are selected for their applicability and cost-effective substitutes of conventional materials in residential buildings.

Table 3 Data Analysis on Building Materials

No.	Material	Material Quantity (kg)	Total Carbon Factor from A1-A5 ($kgCO_2/kg$)	Total Carbon Emissions (kg)	Total Carbon Emissions (tons)	Percent Reduction (%)
Bricks and Block Masonry Units						
1	Engineering Bricks	69106.2	0.271	18731.24	18.73	--
2	Concrete Blocks	92760	0.121	11228.6	11.23	40.05
3	Rammed Earth Bricks	83484	0.037	3113.953	3.11	83.38
Cement Used in Mortar						
1	General	6294.86	0.878	5525.63	5.52	--
2	Portland Cement	6294.86	0.962	6055.72	6.05	--
3	Blast furnace Cement (88%)	6294.86	0.156	986.70	0.98	82.1
4	Pozzolanic Cement (46%)	6294.86	0.529	3332.36	3.33	39.7
Concrete						
1	General	126181.4	0.111	14067.23	14.06	--
2	Portland Concrete	126181.4	0.121	15262.64	15.26	--
3	30% Replacement by Fly Ash	126181.4	0.098	12340.54	12.34	12.3
4	75% Replacement by Blast Furnace	126181.4	0.054	6894.819	6.89	51
Steel Reinforcement						
1	Steel Rebar	1907.615	2.096	4000	4.00	--
2	Recycled Rebar	1907.615	1.264	2413	2.41	40

3. Results and Discussion

3.1 Bricks and Block Masonry Units

Various types of bricks were compared with traditional engineering bricks. The results of this comparison are illustrated in Table 3. The results highlight that the CO_2 emissions of building materials are directly linked to the energy required for their production and transportation. The more energy-intensive a material is to produce and transport, the higher its carbon footprint [15].

3.2 Mortar and Concrete

Cement contributes significantly more to carbon emissions compared to sand and aggregates used in mortar and concrete [16]. To address this, the results examine the replacement of cement with alternative cementitious materials, such as natural

pozzolana, Fly Ash and blast furnace slag as shown in Table 3. Ordinary Portland Cement (OPC) and normal concrete are used as benchmarks, with their CO_2 emissions set at 100% for comparison purposes. Table 3 illustrates that as the proportion of cement replacement increases, carbon emissions decrease, aligning with the findings of Maddalena et al [17].

3.3 Steel Reinforcement

Table 3 illustrates that the use of recycled steel can reduce carbon emissions by approximately 40% compared to virgin steel bars. According to Shaymsteel's research, recycling steel saves up to 74% of the energy required for primary steel production, significantly lowering carbon emissions [18].

3.4 Embodied Carbon Emissions in a Single-Story Unit: Different Scenarios

Three scenarios were developed to assess the embodied carbon emissions of a single-story unit using various building materials, as outlined in Table 4. Each scenario compares the carbon emissions of alternative materials with those of traditional ones.

Scenario 1: Conventional materials such as Portland concrete, Portland cement, steel bars, and engineering bricks are used, resulting in total carbon emissions of 44.05 tons.
Scenario 2: In this case, 30% of the cement used in concrete is replaced with fly ash, 46% of cement used in mortar is replaced with pozzolana, while steel bars and concrete blocks are also used. This reduces the total carbon emissions to 30.90 tons, a 29.85% decrease compared to Scenario 1.
Scenario 3: This scenario employs alternative materials with the highest potential for carbon reduction, including a 75% replacement of cement with blast furnace slag in concrete, an 88% replacement in mortar, recycled steel bars, and rammed earth bricks. Total carbon emissions in this scenario are 13.4 tons, representing 69.56% reduction compared to Scenario 1.

As shown in Table 4, Scenario 3, which uses the lowest-carbon materials from Table 3, achieves a 70% reduction in embodied carbon compared to conventional materials. These findings are consistent with the research of moghayedi et al., where a similar scenario resulted in a 75% reduction in carbon emissions [19].

Table 4 Embodied Carbon Emissions Comparison from Cradle to Practical Completion Stage

Scenarios	Concrete	Cement used in Mortar	Steel	Bricks	Total Emissions(tons)	Percent Reduction
Conventional Materials	Portland Concrete	Portland Cement	Steel bars	Engineering Bricks	44.05	--
Alternative Materials case II	30% replacement of cementitious materials with Fly Ash	46% Cement Replacement by Pozzolana	Steel bars	Concrete Block	30.90	29.85
Alternative Materials Case III	75% Replacement of cement by blast furnace slag	88% Replacement of Cement by Blast Furnace	Recycled Steel bars	Rammed Earth Bricks	13.4	69.56

4. Conclusions

The findings of this study underscore the critical role that material selection plays in reducing carbon emissions in the construction sector, particularly for affordable housing in Pakistan. By applying the Life Cycle Assessment (LCA) methodology, this research has identified that traditional materials, such as Portland cement and engineering bricks, are significant contributors to carbon emissions. In contrast, alternative materials like rammed earth bricks, fly ash, and blast furnace slag offer substantial carbon savings without compromising structural integrity. Because building data are limited, carbon factors have been assumed, especially for the C3–C4 incineration phase and can marginally influence outcomes. The absence of consideration for doors, windows, and frames may have affected total emissions. However, the study's primary goal "material comparison" remains unaltered. The scenario analysis revealed that adopting these low-carbon materials can reduce embodied carbon by as much as 70%, contributing to both environmental sustainability and cost-effectiveness. As Pakistan faces rising urbanization and increasing housing deficits, transitioning to sustainable building

materials is imperative for mitigating climate change impacts. Future policies and construction practices should prioritize the use of low-carbon alternatives to foster sustainable development and resilience against climate challenges.

Acknowledgment

The authors would like to thank the Civil Engineering Department, UET Peshawar, and Professor. Dr. Khan Shahzada for his valuable guidance and support throughout this research work. The detailed review and constructive suggestions by the anonymous reviewers are gratefully acknowledged.

References

[1] S. Bolan *et al.*, "Impacts of climate change on the fate of contaminants through extreme weather events," *Science of the Total Environment*, vol. 909, no. 168388, Jan. 2024, doi: 10.1016/j.scitotenv.2023.168388.

[2] "(PDF) AN ENVIRONMENTAL STUDY OF GLOBAL WARMING AND CLIMATE CHANGE," ResearchGate. Accessed: Jun. 17, 2025. [Online]. Available: https://www.researchgate.net/publication/377767313_AN_ENVIRONMENTAL_STUDY_OF_GLOBAL_WARMING_AND_CLIMATE_CHANGE

[3] "The effect of carbon dioxide emissions on the building energy efficiency | Request PDF." Accessed: May 23, 2024. [Online]. Available: https://www.researchgate.net/publication/362986040_The_effect_of_carbon_dioxide_emissions_on_the_building_energy_efficiency

[4] "(PDF) The Greenhouse Gas Emissions Produced by Cement Production and Its Impact on Environment: A Review of Global Cement Processing." Accessed: Jun. 17, 2025. [Online]. Available: https://www.researchgate.net/publication/319292238_The_Greenhouse_Gas_Emissions_Produced_by_Cement_Production_and_Its_Impact_on_Environment_A_Review_of_Global_Cement_Processing

[5] E. Matsinos and G. Rasche, "Analysis of the Low-Energy π[±]p Elastic-Scattering Data," *JMP*, vol. 03, no. 10, pp. 1369–1387, 2012, doi: 10.4236/jmp.2012.310174.

[6] "(PDF) IMPACT World+: a globally regionalized life cycle impact assessment method," *ResearchGate*, doi: 10.1007/s11367-019-01583-0.

[7] "Greenhouse gases emissions and global climate change: Examining the influence of CO2, CH4, and N2O | Request PDF," *ResearchGate*, doi: 10.1016/j.scitotenv.2024.173359.

[8] "Advances and challenges of Life Cycle Assessment (LCA) of Greenhouse Gas Removal Technologies to Fight Climate Changes | Request PDF," *ResearchGate*, doi: 10.1016/j.jclepro.2019.118896.

[9] "The Reduction of CO2 Emissions by Application of High-Strength Reinforcing Bars to Three Different Structural Systems in South Korea." Accessed: Jun. 17, 2025. [Online]. Available: https://www.mdpi.com/2071-1050/9/9/1652

[10] "(PDF) Effectiveness of the Modern Methods of Construction in Terms of Cost and Time: A Case Study of the United Kingdom." Accessed: Jun. 17, 2025. [Online]. Available: https://www.researchgate.net/publication/351591994_Effectiveness_of_the_Modern_Methods_of_Construction_in_Terms_of_Cost_and_Time_A_Case_Study_of_the_United_Kingdom

[11] "Dynamic response of mortar-free interlocking structures | Request PDF," *ResearchGate*, doi: 10.1016/j.conbuildmat.2013.01.010.

[12] J. S. Pechsiri *et al.*, "Exploring the use of a machine assisted goal and scope in a Life Cycle Studies to understand stakeholder interest and priorities," *Cleaner Environmental Systems*, p. 100288, Jun. 2025, doi: 10.1016/j.cesys.2025.100288.

[13] "Embodied Carbon Footprint Database - Circular Ecology." Accessed: Jun. 17, 2025. [Online]. Available: https://circularecology.com/embodied-carbon-footprint-database.html

[14] "RICS Guide.pdf."

[15] H. Sasana and A. Eka Putri, "The Increase of Energy Consumption and Carbon Dioxide (CO2) Emission in Indonesia," *E3S Web Conf.*, vol. 31, p. 01008, 2018, doi: 10.1051/e3sconf/20183101008.

[16] A. Petek Gursel, E. Masanet, A. Horvath, and A. Stadel, "Life-cycle inventory analysis of concrete production: A critical review," *Cement and Concrete Composites*, vol. 51, pp. 38–48, Aug. 2014, doi: 10.1016/j.cemconcomp.2014.03.005.

[17] R. Maddalena, J. Roberts, and A. Hamilton, "Can Portland cement be replaced by low-carbon alternative materials? A study on thermal properties and carbon emissions of innovative cements," *Journal of Cleaner Production*, vol. 186, Feb. 2018, doi: 10.1016/j.jclepro.2018.02.138.

[18] Shyamsteel, "The Benefits of Using Recycled Steel in Construction: Environmental and Economic Advantages - Shyamsteel." Accessed: Jun. 17, 2025. [Online]. Available: https://shyamsteel.com/blogs/the-benefits-of-using-recycled-steel-in-construction-environmental-and-economic-advantages/

[19] A. Moghayedi, M. Massyn, K. L. Jeune, and K. Michell, "Evaluating the impact of building material selection on the life cycle carbon emissions of South African affordable housing," *IOP Conf. Ser.: Earth Environ. Sci.*, vol. 1101, no. 2, p. 022021, Nov. 2022, doi: 10.1088/1755-1315/1101/2/022021.

PERFORMANCE ANALYSIS OF LIGHTGBM, XGBOOST, RANDOM FOREST, AND GRADIENT BOOSTING IN PHOTOVOLTAIC ENERGY FORECASTING WITH HYPERPARAMETER OPTIMIZATION

[a]Muhammad Ehtsham*, [b] Marianna Rotilio, [c]Federica Cucchiella

a: Department of Civil, Construction-Architectural and Environmental Engineering, University of L'Aquila, 67100 L'Aquila, Italy.
muhammad.ehtsham@graduate.univaq.it
b: Department of Civil, Construction-Architectural and Environmental Engineering, University of L'Aquila, 67100 L'Aquila, Italy.
marianna.rotilio@univaq.it
c: Department of Industrial and Information Engineering and Economics, University of L'Aquila, 67100, L'Aquila, Italy.
federica.cucchiella@univaq.it
* Corresponding author

Abstract- Accurate photovoltaic (PV) energy forecasting is crucial for effective grid integration and for predictive usage at residential and industrial levels, especially under increasing climatic variability. This study evaluates and compares four machine learning (ML) models, LightGBM, XGBoost, Random Forest, and Gradient Boosting, for hourly PV energy forecasting using real-time data from numerical weather model (NWM), PVGIS, and historical production data from operational PV plant in Southern Italy. Three hyperparameter strategies, namely default settings, Optuna optimization, and Grid Search, were tested. Results show that LightGBM achieved the best performance with Grid Search tuning, yielding an MAE of 2.85 kWh, RMSE of 5.45 kWh, and R^2 of 0.71 over an 8-day forecasting horizon. Comparatively, XGBoost with Grid Search attained an MAE of 3.00 kWh, RMSE of 5.82 kWh, and R^2 of 0.67. The findings highlight that hyperparameter tuning significantly improved forecast accuracy and provide actionable insights for selecting ML models and optimization techniques in PV management systems. Findings are specifically of interest for practitioners, researchers, and organizations associated with PV management and operations.

Keywords- Gradient Boosting, LightGBM, Machine Learning, PV Management

1 Introduction

Extreme climatic phenomena have hugely impacted various parts of the globe in the recent past, and the consequences of environmental change are more evident than ever before. Encouraging communities and policymakers to adopt sustainable and clean practices, including green energy resources [1], [2]. Photovoltaic (PV) energy is one of the most sustainable types of energy sources, and in recent years, the reliance on it has increased notably [3]. In Figure 1, a comparative analysis of the increase in PV and wind energy in Italy as compared to hydro energy, which was previously considered as most green source of energy. However, the most challenging phenomenon related to PV energy is its uncertainty and difficulty in prediction at various parts of the globe, and specifically in diverse terrains and climatic conditions. In this regard, various researchers have adopted, evaluated, and reported the latest technologies. Many researchers nowadays are exploring and reporting the potential of machine learning in different scientific applications.[4], [5], [6]. Similarly, many researchers have exploited the potential applications of machine learning and deep learning technologies in PV-related challenges, including efficiency analysis, forecasting, predictive maintenance, faults and diagnosis, feasibility reports, etc. However,

the inherent shortcoming of machine learning models is a continuous need to evaluate and assess the effectiveness of different techniques for hyperparameter optimization. Some researchers have studied the effects of hyperparameter optimization in different fields. However, literature lacks a comprehensive study that evaluates notable models like LightGBM [7], XGBoost [8], Random Forest [9], and Gradient Boosting [10] for PV forecasting and specifically provides a holistic overview of these models in terms of various hyperparameter optimization techniques with real-time data from numerical weather model (NWM), PVGIS [11], and already operational PV plant.

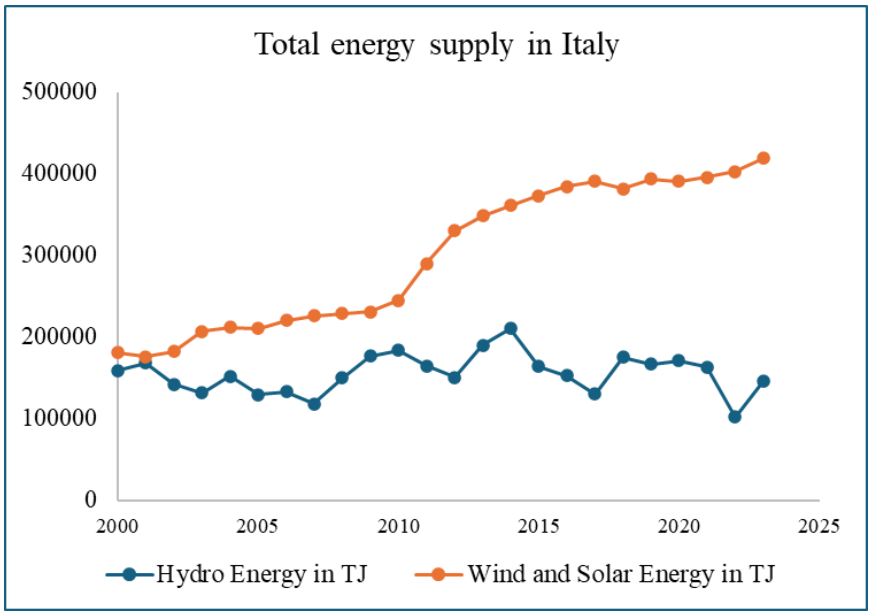


Figure 1: Share of solar, wind, and hydropower energy in Italy. Source: IEA [12].

This study not only provides a framework for utilizing the PVGIS and NWM for hourly PV energy forecasting but also provides a comparative analysis of machine learning models: LightGBM, XGBoost, Random Forest, and Gradient Boosting. In addition, the study tests and evaluates three hyperparameter approaches, namely, Default hyperparameters, Optuna tuning technique [13], and the Grid Search tuning technique [14]. Results of this study can be utilized by the organizations and researchers associated with the management and operation of PV facilities and can provide a clearer path in terms of choosing and deploying of specific hyperparameter techniques.

2 Research Methodology

2.1 PV, NWM, and PVGIS Data

The dataset was constructed by integrating meteorological and PV production data to enable robust machine learning model development for PV energy forecasting. Initially, the PV energy production data of a PV plant, located in southern Italy, were collected. the dataset was accessed from a MySQL database, using specifically tailored queries to convert the 5-minute data recorded by data loggers to hourly cumulative values. Meteorological variables were collected from the OpenWeather [15] NWM, providing high-resolution hourly weather forecasts and reanalysis data. The weather-related features include atmospheric pressure, relative humidity, wind speed, cloud cover, maximum and minimum temperature, as well as solar irradiance components, including direct beam irradiance Gb(i), diffuse irradiance Gd(i), and ground-reflected irradiance Gr(i), along with sunshine duration (hours of sun per day), air temperature measured at 2 meters above ground level (T2m), and wind speed measured at 10 meters (WS10m).

To complement the weather data, hourly data for the same location were retrieved from the PV Geographical Information System (PVGIS), which provides reliable PV performance estimates based on solar radiation and system characteristics. The dataset thus captures both the environmental predictors and the corresponding PV output, facilitating supervised learning. In addition, temporal features were engineered to reflect daily and diurnal patterns, including the full timestamp,

date-only fields (to capture day-to-day variability), and time-only fields (to account for intra-day dynamics). This enriched dataset allows the models to learn complex interactions between weather conditions, time-of-day, and PV output, providing a comprehensive basis for evaluating forecasting performance under realistic operational scenarios.

2.2 Data Validation and Outlier Removal

Before using the dataset for model training and evaluation, a thorough data validation and cleaning process was carried out to ensure data quality and consistency. The PV production data extracted from the MySQL database were checked for completeness and alignment with the meteorological and PVGIS datasets. Any missing or duplicated records were identified and removed. To address potential measurement errors and anomalous values in the PV and meteorological variables, an outlier detection procedure was applied. For continuous variables such as PV output, irradiance components, and temperature, statistical thresholds were defined based on domain knowledge and descriptive statistics (e.g., interquartile range and physical plausibility limits). Observations falling outside these acceptable ranges were flagged as outliers.

Specifically, PV output values were constrained to be non-negative and not to exceed the rated capacity of the PV plant. Irradiance components were limited to their respective theoretical maxima under clear-sky conditions. Meteorological variables such as temperature, humidity, and wind speed were also cross-checked against climatological norms for the location and time of year. Outliers were treated by either removing the affected records entirely or imputing them with more plausible values based on temporal neighbors or climatological averages, depending on the nature and extent of the anomaly. This validation and cleaning step ensured that the dataset fed into the forecasting models was reliable and representative of real-world operational conditions.

2.3 Machine Learning Models and Optimization Techniques

For the PV energy forecasting task, four machine learning models were employed: Random Forest, Gradient Boosting, Extreme Gradient Boosting, and Light Gradient Boosting Machine. These tree-based ensemble methods are well-suited for capturing complex, nonlinear relationships in high-dimensional datasets such as the one constructed for this study.

Each model was initially trained using default hyperparameters, as implemented in their respective Python libraries (scikit-learn, xgboost, and lightgbm), to establish baseline performance. To improve forecasting accuracy and assess the sensitivity of the models to hyperparameter settings, two optimization techniques were applied:

- Grid Search: A systematic, exhaustive search over a predefined set of hyperparameter values, combined with 5-fold cross-validation to select the best configuration based on validation performance.
- Optuna: An advanced, efficient hyperparameter optimization framework based on a Bayesian approach, which automatically explores the hyperparameter space and prunes unpromising trials to accelerate convergence to an optimal set of parameters.

2.4 Efficiency Analysis

These optimization techniques were applied individually to each machine learning model. The objective function in both cases was to minimize forecasting error, evaluating using metrics such as Root Mean Squared Error (RMSE), Mean Absolute Error (MAE), and Correlation Coefficient (R^2). The inclusion of both traditional Grid Search and modern Optuna optimization in addition to default settings provided a comprehensive analysis of model performance and robustness under different tuning strategies. By comparing the default, Grid Search optimized, and Optuna-optimized versions of each model, this study highlights the benefits of hyperparameter tuning in improving PV energy forecasting accuracy.

3 Results

3.1 Application of Machine Learning Models for Hourly Forecasts

All the selected machine learning models were deployed for the forecasting of PV energy production of the selected PV plant for the next 8 days. The models were trained with the hourly meteorological records as training features and hourly

PV production as the target variable. In the initial phase, the models were deployed for real-time data, and forecasts were generated using the default hyperparameters of the models. In the successive stages, the hyperparameter tuning was performed with Optuna and Grid Search techniques, and forecasts were generated for the same forecasting horizon. The generated forecasts were compared with the actual recorded data by data loggers. Figure 2 provides an overview of the difference between the actual and recorded forecasts generated by models using default hyperparameters. Figures 3 and 4 provide an overview of the forecasting efficiency of the models using the Optuna and Grid Search methods, respectively.

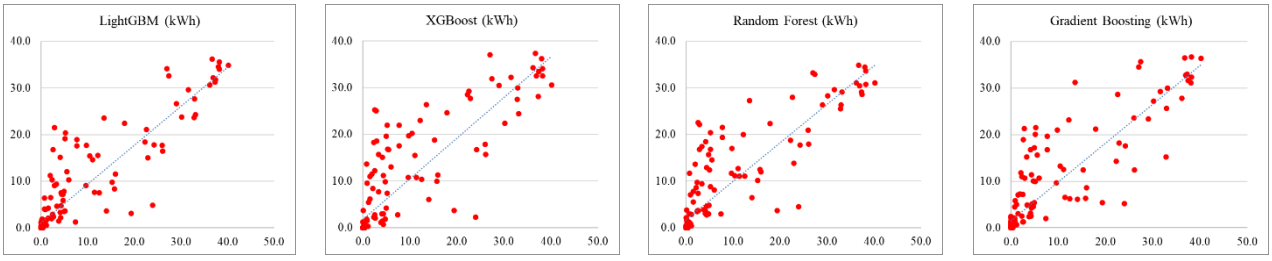


Figure 2: Comparison of forecasted vs recorded values using default hyperparameters

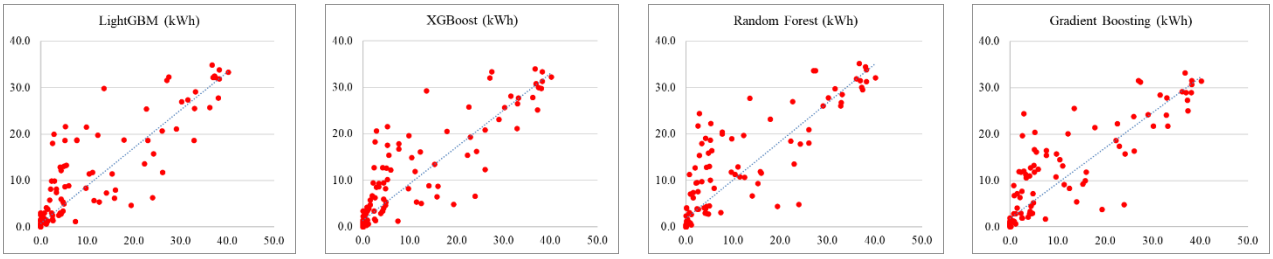


Figure 3: Comparison of forecasted vs recorded values using Optuna hyperparameters

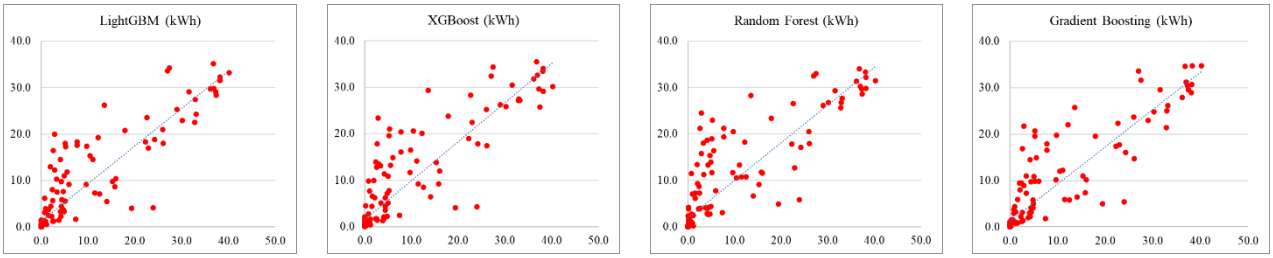


Figure 4: Comparison of forecasted vs recorded values using Grid Search hyperparameters

3.2 Performance of Various Models and Techniques

The performance of models needs to be assessed based on universally accepted and well-known performance metrics. In this regard, the authors decided to calculate MAE, R2, and RMSE of all the models and forecasts generated. Table 1 provides an overview of the estimated performance metrics, creating an opportunity for the readers to assess the accuracy of various models and techniques using the same dataset and forecasting horizon.

Table 1 Evaluation Metrics using all the techniques

Model	MAE (kWh)	R^2	RMSE (kWh)
Default Hyperparameters			
LightGBM	2.81	0.70	5.54
XGBoost	3.68	0.57	6.70

Model	MAE (kWh)	R^2	RMSE (kWh)
Random Forest	3.01	0.66	5.85
Gradient Boosting	3.41	0.64	6.06
Optuna Hyperparameter Optimization			
Model	**MAE (kWh)**	**R^2**	**RMSE (kWh)**
LightGBM	3.25	0.70	5.63
XGBoost	3.20	0.70	5.62
Random Forest	3.09	0.65	6.00
Gradient Boosting	3.19	0.69	5.66
Grid Search Hyperparameter Tuning			
Model	**MAE (kWh)**	**R^2**	**RMSE (kWh)**
LightGBM	2.85	0.71	5.45
XGBoost	3.00	0.67	5.82
Random Forest	3.15	0.65	6.06
Gradient Boosting	2.92	0.72	5.48

The deployed optimization techniques, Optuna and Grid Search, automatically tuned key hyperparameters for each model to improve their predictive performance. The optimal parameter configurations identified through these methods are summarized in Table 2. Optuna generally favored lower learning rates and higher numbers of estimators, with shallower tree depths for controlling overfitting. Grid Search, on the other hand, selected more conservative settings, balancing model complexity and generalization. These tuned hyperparameters highlight the differences in search strategies and their impact on model configuration

- n_estimators: Specifies the number of boosting rounds or trees in the ensemble. A higher value can improve learning but may increase computation and risk overfitting if not combined with regularization.
- learning_rate: Controls how much each tree contributes to the overall prediction. Lower learning rates (e.g., 0.0138 for Gradient Boosting with Optuna) slow down learning, often requiring more estimators but improving generalization.
- max_depth: Limits the maximum depth of each tree, helping to prevent overfitting by reducing model complexity. Optuna tended to choose shallower depths (e.g., 3) compared to Grid Search.
- num_leaves (LightGBM): Defines the maximum number of leaves per tree. A higher number allows more complex splits, while lower values improve regularization.
- subsample (XGBoost): Specifies the fraction of the training data to use when growing each tree, acting as a regularization mechanism to prevent overfitting by introducing randomness.
- min_samples_split (Random Forest): Sets the minimum number of samples required to split an internal node, which controls the granularity of splits and impacts overfitting.

Table 2 Optimized hyperparameters of the machine learning models using Optuna and Grid Search optimization techniques.

Optuna Hyperparameter Tuning	
	Selected Parameters
LightGBM	'n_estimators': 52, 'learning_rate': 0.114, 'max_depth': 3, 'num_leaves': 23
XGBoost	'n_estimators': 185, 'learning_rate': 0.025, 'max_depth': 3, 'subsample': 0.806
Random Forest	'n_estimators': 173, 'max_depth': 15, 'min_samples_split': 5
Gradient Boosting	'n_estimators': 214, 'learning_rate': 0.0138, 'max_depth': 5
Grid Search Hyperparameter Tuning	
	Selected Parameters
LightGBM	'n_estimators': 100, 'learning_rate': 0.05, 'max_depth': 6, 'num_leaves': 31

XGBoost	'n_estimators': 100, 'learning_rate': 0.05, 'max_depth': 6, 'subsample': 1.0
Random Forest	'n_estimators': 200, 'max_depth': 8, 'min_samples_split': 5
Gradient Boosting	'n_estimators': 100, 'learning_rate': 0.05, 'max_depth': 4

4 Practical Implementation

The findings of this study evaluate and report the effectiveness of machine learning models, particularly tree-based ensemble methods, for forecasting PV energy production using meteorological and temporal features. Among the evaluated models, LightGBM and Gradient Boosting consistently achieved the best performance across all optimization strategies, with MAE as low as 2.76 kWh and R^2 reaching up to 0.72, a similar trend was reported by [16], [17]. This level of accuracy highlights the feasibility of integrating such models into real-world PV system management and energy planning applications. Specifically, grid operators and energy managers can utilize these models for short-term PV generation forecasts to optimize grid balancing, reduce reliance on fossil fuel-based backup generation, and improve scheduling of energy storage systems. Furthermore, the ability to tune models using optimization techniques such as Grid Search and Optuna enhances forecasting robustness, ensuring that models can be adapted to specific sites and operational requirements. The findings also underscore the importance of using high-resolution weather forecasts and properly engineered time-based features to capture the variability inherent in solar energy production, making these approaches highly applicable for smart grid and sustainable energy initiatives, in different parts of the globe.

5 Conclusion

The following conclusions can be drawn from the conducted study:

- The study highlights the potential of machine learning, particularly tree-based ensemble models, in effectively forecasting PV energy production using remotely sensed meteorological and historical PV production data.
- By comparing default settings with two hyperparameter optimization techniques, the study demonstrates that tuning significantly improves model performance, with LightGBM and Gradient Boosting showing the most promising results.
- The findings offer a practical framework for PV operators and researchers to select fine-tune models for more reliable hourly energy forecasts, supporting better planning and integration of renewable energy into the grid and for energy usage optimization at residential and industrial levels.

Future work can explore incorporating additional data sources, like more advanced NWM, satellite imagery, IoT sensors, and applying advanced deep learning models to capture complex patterns. Researchers can also explore the latest hybrid models and incorporate long-term climatic trends. Developing adaptive algorithms to handle climate anomalies and creating practical tools for PV operators.

Acknowledgment

This research is carried out as part of the XXXVIII Cycle of the PhD programme in Civil, Building-Architecture and Environmental Engineering at the University of L'Aquila. The research topic is "Monitoring System for the Production of Renewable Energy and Data Acquisition System" co-financed by the company Solis SpA. The authors express their gratitude to Solis SpA for their invaluable cooperation in this study. This encompasses providing technical and production data for BIPVs and BAPVs, supplying the necessary computer processing system and required software, as well as the contributions of the monitoring team and the company's technical head in validating the research findings. The authors would also like to express their gratitude to the developers of OpenWeather for providing the meteorological data. We would like to express our sincere appreciation to PVGIS (Photovoltaic Geographical Information System) and European Commission's Joint Research Centre for providing data resources. The research supervisor is Prof. Marianna Rotilio, co-supervisors are Prof. Federica Cucchiella and Prof. Gianni Di Giovanni, and the industrial tutor is Massimo Innaurato. The Ph.D. student in charge of the research is Eng. Muhammad Ehtsham

References

[1] F. Cucchiella, M. Rotilio, L. Capannolo, and P. De Berardinis, "Technical, economic and environmental assessment towards the sustainable goals of photovoltaic systems," *Renewable and Sustainable Energy Reviews*, vol. 188, p. 113879, 2023.

[2] F. Cucchiella *et al.*, "Renovation Wave: a bioeconomy panel produced with waste.," *J Clean Prod*, p. 142868, 2024.

[3] M. Ehtsham, M. Rotilio, and F. Cucchiella, "Deep learning augmented medium-term photovoltaic energy forecasting: A coupled approach using PVGIS and numerical weather model data," *Energy Reports*, vol. 13, pp. 4299–4317, Jun. 2025, doi: 10.1016/J.EGYR.2025.03.058.

[4] G. Di Giovanni, M. Rotilio, L. Giusti, and M. Ehtsham, "Exploiting building information modeling and machine learning for optimizing rooftop photovoltaic systems," *Energy Build*, p. 114250, 2024.

[5] Y. Li *et al.*, "A machine-learning approach for regional photovoltaic power forecasting," in *2016 IEEE Power and Energy Society General Meeting (PESGM)*, IEEE, 2016, pp. 1–5.

[6] T. S. Qaid, H. Mazaar, M. Y. H. Al-Shamri, M. S. Alqahtani, A. A. Raweh, and W. Alakwaa, "Hybrid deep-learning and machine-learning models for predicting COVID-19," *Comput Intell Neurosci*, vol. 2021, no. 1, p. 9996737, 2021.

[7] G. Ke *et al.*, "LightGBM: A Highly Efficient Gradient Boosting Decision Tree," *Adv Neural Inf Process Syst*, vol. 30, 2017, Accessed: Jul. 14, 2025. [Online]. Available: https://github.com/Microsoft/LightGBM.

[8] T. Chen and C. Guestrin, "XGBoost: A scalable tree boosting system," *Proceedings of the ACM SIGKDD International Conference on Knowledge Discovery and Data Mining*, vol. 13-17-August-2016, pp. 785–794, Aug. 2016, doi: 10.1145/2939672.2939785/SUPPL_FILE/KDD2016_CHEN_BOOSTING_SYSTEM_01-ACM.MP4.

[9] L. Breiman, "Random forests," *Mach Learn*, vol. 45, no. 1, pp. 5–32, Oct. 2001, doi: 10.1023/A:1010933404324/METRICS.

[10] A. Natekin and A. Knoll, "Gradient boosting machines, a tutorial," *Front Neurorobot*, vol. 7, no. DEC, p. 63623, Dec. 2013, doi: 10.3389/FNBOT.2013.00021/BIBTEX.

[11] "Photovoltaic Geographical Information System (PVGIS) Available at: https://joint-research-centre.ec.europa.eu/photovoltaic-geographical-information-system-pvgis_en, Last accessed on: Feb. 15 2025."

[12] "International Energy Agency (IEA). Finland. Available at: https://www.iea.org/countries/finland. Accessed: 03 March 2025."

[13] T. Akiba, S. Sano, T. Yanase, T. Ohta, and M. Koyama, "Optuna: A Next-generation Hyperparameter Optimization Framework," *Proceedings of the ACM SIGKDD International Conference on Knowledge Discovery and Data Mining*, pp. 2623–2631, Jul. 2019, doi: 10.1145/3292500.3330701.

[14] H. Alibrahim and S. A. Ludwig, "Hyperparameter Optimization: Comparing Genetic Algorithm against Grid Search and Bayesian Optimization," *2021 IEEE Congress on Evolutionary Computation, CEC 2021 - Proceedings*, pp. 1551–1559, 2021, doi: 10.1109/CEC45853.2021.9504761.

[15] "OpenWeatherMap. Available at: https://openweathermap.org/ Last accessed on January 16, 2025.".

[16] S. Rezashoar, E. Kashi, and S. Saeidi, "A hybrid algorithm based on machine learning (LightGBM-Optuna) for road accident severity classification (case study: United States from 2016 to 2020)," *Innovative Infrastructure Solutions*, vol. 9, no. 8, pp. 1–22, Aug. 2024, doi: 10.1007/S41062-024-01626-Y/METRICS.

[17] K. Ng and P. Lei, "A Lightweight Method using LightGBM Model with Optuna in MOOCs Dropout Prediction," *ACM International Conference Proceeding Series*, pp. 53–59, Jul. 2022, doi: 10.1145/3551708.3551732;TAXONOMY:TAXONOMY:CONFERENCE-COLLECTIONS;WGROUP:STRING:ACM.

Annexure A

Photo Gallery


7TH CONFERENCE ON SUSTAINABILITY
IN CIVIL ENGINEERING

A







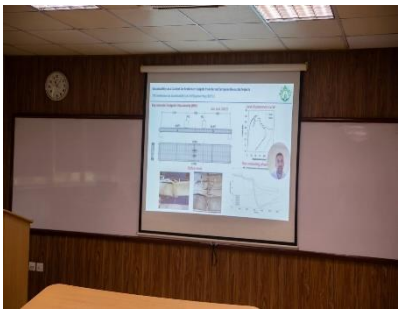













Line stabilization – HS2 embankments

Eco-Innovation in Construction:
Harnessing Industrial Waste for



RECYCLED XPLOS FIBERS FOR CRACK CONTROL IN
HIGH STRENGTH CONCRETE- A USE CASE IN



PRACTICAL IMPLEMENTATIONS

COTTON FIBERS FOR IMPROVED
CONCRETE TENSILE STRENGTH
AND CRACK RESISTANCE IN SLABS






EXPERIMENTAL INVESTIGATION ON THE
FLEXURAL BEHAVIOR OF STEEL FIBER IN
CONCRETE


Introduction

Introduction

Background: Gen Z Pedagogical Challenges





Crack Detection Optimization in
BIM













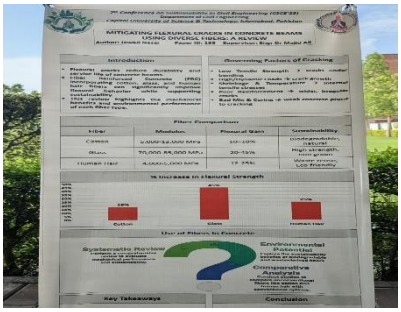




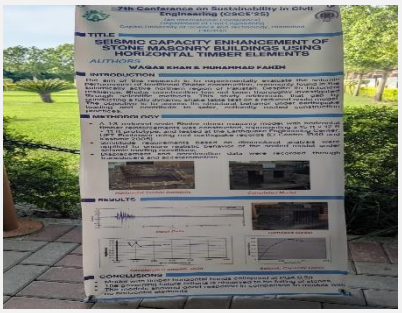


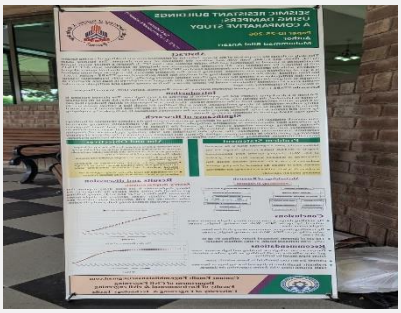





MITIGATING FLEXURAL CRACKS IN CONCRETE BEAMS USING DIVERSE FIBERS: A REVIEW
Introduction
Governing Factors of Cracking
Fiber Comparison
Fiber
Modulus
Flexural Gain
Considerability
Cotton
Glass
Human Hair
% increase in flexural strength
Use of Fibers in Concrete
Systematic Review
Environmental Potential
Comparative Analysis
Key Takeaways
Conclusion




7th Conference on Sustainability in Civil Engineering (CSCE'25)
TITLE
SEISMIC CAPACITY ENHANCEMENT OF STONE MASONRY BUILDINGS USING HORIZONTAL TIMBER ELEMENTS
AUTHORS
WAQAS KHAN & MUHAMMAD FAHIM
INTRODUCTION
METHODOLOGY
RESULTS
CONCLUSIONS









Authors Index – CSCE'25

A
Ahmad, N. **(15)**
Asim, M.Z. **(23)**
Arslan, R. **(51)**
Anwar, M. **(98)**
Awais, M. **(151)**
Anwar, M. **(167)**
Ajwad, A. **(192)**
Ansari, M.B. **(211)**
Azhar, S. **(234)**
Anwar, S. **(242)**
Akbar, C.M.S. **(259)**
Ali, M. **(266)**
Ali, U. **(266)**
Ahmad, Q.K. **(282)**
Afzal, H. **(296)**
Asad, R. **(303)**

B
Baloch, S. **(01)**
Bahar, N.R **(15)**
Bakar, A. **(45)**
Bilal, M.Q. **(259)**

C
Cheema, E. **(105)**
Cucchiella, F. **(309)**

D
Duera, M. **(291)**

E
Ejaz, A. **(146)**
Ehtesham, M. **(309)**

F
Fahim, M. **(204)**
Fahim, M. **(218)**
Farooq, U. **(251)**

G
Gul, F. A. **(85)**
Gul, F. A. **(113)**

H
Haider, M.A. **(23)**
Haq, R.U. **(29)**
Hasan, B. **(118)**
Hasan, B. **(124)**
Hanif, M.A. **(146)**
Hafeez, I. **(296)**

I
Irshad, N. **(71)**
Irum, S. **(139)**

J
Jalal, M.Y. **(180)**
Jahangir, M.A. **(251)**
Jadoon, A.K. **(282)**

K
Khan, H. **(45)**
Khalid, U. **(71)**
Khan, A. **(90)**
Khan, S.S. **(98)**
Khalid, U. **(105)**
Kareem, A. **(159)**
Khan, S.S. **(167)**
Khattak, M.H.M. **(174)**
Khan, R.W.Z. **(188)**
Khan, R.S.Z. **(188)**
Khan, W. **(218)**
Khan, H. **(282)**
Khan, A.R. **(286)**
Khalid, A. **(286)**

L
Latour, M. **(192)**

M
Mateen, F. **(09)**
Muthusamy, K. **(15)**
Munir, K. **(63)**
Mursaleen, M. **(78)**
Mehboob, S.S. **(159)**
Medley, G. **(226)**

N
Naz, F. **(01)**
Naeem, A.B. **(37)**
Naeem, A.B. **(56)**
Nasar, J. **(90)**
Nasar, J. **(174)**
Najeeb, A. **(180)**

Q
Qamar, F. **(196)**

R
Rashid, M.U. **(151)**
Raza, A. **(46)**
Raheel, H.B. **(242)**
Rauf, M. **(274)**
Rotilio, M. **(309)**

S
Shahzad, U. **(01)**
Sajid, M.Z. **(09)**
Shafique, S. **(23)**
Shah, S.I.A. **(37)**
Shah, S.I.A. **(56)**
Sikandar, A. **(85)**
Sikandar, A. **(113)**
Shabbir, F. **(139)**
Salahuddin, H. **(139)**
Shaukat, K. **(204)**
Salman, A. **(226)**
Shao, G. **(234)**
Sultan, A. **(251)**
Shabir, H. **(291)**

T
Turab, A. **(78)**
Tariq, Q.M. **(118)**
Tariq, Q.M. **(124)**

U
Usama, M. **(274)**
Ullah, U. **(274)**
Ullah, F. **(303)**

W
Wadood, A. **(51)**

Y
Yaqub, M. **(188)**
Yaqub, M. **(211)**
Yucel, B. **(234)**

Z
Zakria, U. **(29)**
Zakria, U. **(63)**
Zulqarnain, M. **(151)**
Zwain, M. **(196)**
Ziyad, M. **(259)**